



FRICTION MACHINES

Eng.D. Jarosław Mikołajczyk

RADA WYDAWNICZA:

Donat Mierzejewski (przewodniczący), Joanna Kryza (sekretarz), Paweł Dahlke, Małgorzata Lesińska-Sawicka, Katarzyna Orfin-Tomaszewska, Przemysław Frąckowiak, Jarosław Kołodziej, Sylwester Sieradzki

RECENZENT:

prof. dr hab. inż. Bogdan Żółtowski



ANS

Akademia Nauk Stosowanych
im. Stanisława Staszica w Pile

© Copyright by Wydawnictwo Akademii Nauk Stosowanych im. Stanisława Staszica w Pile

Sto dziewięćdziesiąta dziewięć publikacja Akademii Nauk Stosowanych im. Stanisława Staszica w Pile

In memory of prof. Ryszard Marczak

Piła 2022

e-ISBN

978-83-62617-96-8

TABLE OF CONTENTS

SYMBOLS AND ACRONYMS FREQUENTLY USED IN THIS PUBLICATION.....	9
1. PREFACE.....	10
2. CHARACTERISTICS OF BASIC FACTORS RELATED TO TRIBOLOGICAL TESTS.....	11
2.1. SURFACE LAYER	11
2.1.1. SURFACE LAYER MODELS.....	13
2.1.2. QUANTITIES DESCRIBING THE CONDITION OF THE SURFACE LAYER.....	14
2.1.2.1. PHYSICOCHEMICAL CHARACTERISTICS OF THE SURFACE LAYER.....	15
2.1.2. 2.FEATURES OF THE GEOMETRICAL STRUCTURE OF THE SURFACE.....	16
2.2. TYPES OF TRIBOLOGICAL WEAR PROCESSES.....	25
2.3. LUBRICANTS AND IMPROVERS.....	29
2.4. LUBRICANT AGENTS.....	33
2.4.1. PREPARATIONS OF A CHEMICAL ACTION.....	34
2.4.2. PREPARATION WITH PARTICLES OF SOLID LUBRICANTS.....	35
2.4.3. PREPARATIONS ENABLING LUBRICATION ON THE BASIS OF THE SO-CALLED SELECTIVE TRANSFER (SEL).....	37
3. TYPES OF COMBINATIONS OF FRICTION CONTACTS.....	38
4. TRIBOLOGICAL TEST RIGS.....	46
4.1. GROUP 1 (SLIDING PAIRS).....	47
4.1.1. 77MT-1 TEST RIG.....	47
4.1.2. TRIBOLOGICAL TEST RIG FOR TESTING THE EFFECT OF VIBRATION ON A LUBRICANT.....	48
4.1.3. FALEX TEST RIG WITH THE ROLLER-VEE BLOCKS PAIR.....	50
4.1.4. TIMKEN TEST RIG.....	52
4.1.5. TEST RIG FOR DETERMINING THE FRICTION FACTOR BY UPSETTING A CYLINDER.....	56
4.1.6. TEST RIG FOR TESTING FRICTIONAL RESISTANCE IN MODEL CONDITIONS OF SHEET METAL EXTRUSION PROCESSES.....	58
4.1.7. TEST RIG FOR DETERMINING FRICTIONAL RESISTANCE IN THE PROCESS OF UPSETTING A CYLINDRICAL SAMPLE BASED ON A CONTINUOUS MEASUREMENT OF FORCES.....	60
4.1.8. TEST RIG FOR TESTING CHANGES IN TRIBOLOGICAL PROPERTIES OF CONNECTOR JOINTS DURING THEIR MULTIPLE CONNECTION AND DISCONNECTION.....	62
4.1.9. TRIBOLOGICAL TEST RIG DESIGNED FOR TESTING KINEMATIC PAIRS WITH CONFORMAL CONTACT.....	63
4.1.10. TEST RIG FOR DETERMINING FRICTIONAL RESISTANCE BASED ON THE METHOD OF RINGS UPSETTING.....	85
4.1.11. TEST RIG FOR TESTING THE WEAR OF METALS AND THEIR ALLOYS AT ELEVATED TEMPERATURES ACCORDING TO THE PATENT PL 193 429.....	88
4.1.12. HEAD FOR TESTING FRICTION AND WEAR ACCORDING TO	

THE PATENT PL 113 646.....	91
4.1.13. TRIBOLOGICAL TEST RIG WITH ADJUSTABLE FRICTIONAL RESISTANCE ACCORDING TO THE PATENT PL 171 768.....	93
4.1.14. TEST RIG FOR TESTING ABRASIVE WEAR ACCORDING TO THE PATENT PL 117 763.....	95
4.1.15. FRET III TEST RIG.....	98
4.1.16. SMOK TEST RIG.....	101
4.1.17. SOOG TEST RIG.....	104
4.1.18. SON TEST RIG.....	106
4.1.19. TEST RIG FOR TRIBOLOGICAL TESTING OF LUBRICANTS AND CONSTRUCTION MATERIALS ACCORDING TO THE PATENT No. PL 160 594.....	109
4.1.20. TEST RIG FOR TESTING THE ABRASION OF CONSTRUCTION MATERIALS ACCORDING TO THE PATENT PL 160 596.....	111
4.1.21. TEST RIG WITH A BALL-DISC OR SPINDLE-DISC FRICTION CONTACT FOR TESTING WEAR RESISTANCE AND RESISTANCE TO MOTION, ESPECIALLY FOR SOLID CERAMIC ELEMENTS AND CERAMIC SURFACE LAYERS ACORDING TO THE PATENT PL 176 145.....	113
4.1.22. TEST RIG WITH A ROLLER-V BLOCKS PAIR FOR TESTING RESISTANCE TO THE WEAR AND SEIZURE OF CONSTRUCTION MATERIALS ACCORDING TO THE PATENT PL 177 205.....	117
4.1.23. TEST RIG FOR TESTING WEAR AND RESISTANCE TO MOTION OF LUBRICATED AND NON-LUBRICATED ELEMENTS ACCORDING TO THE PATENT PL 177 201.....	120
4.1.24. TEST RIG FOR TESTING FRICTION AND WEAR OF LUBRICATED AND NON-LUBRICATED ELEMENTS ACCORDING TO THE PATENT PL 177 192.....	123
4.1.25. TEST RIG FOR TESTING THE WEAR RESISTANCE AND FRICTIONAL RESISTANCE OF LUBRICATED AND NON- LUBRICATED ELEMENTS ACCORDING TO THE PATENT PL 160 590.....	126
4.1.26. TEST RIG FOR TESTING THE FRICTION AND WEAR CONTAINING A ROTATING COUNTER-SAMPLE AGAINST WHICH STATIONARY BLOCK SAMPLES OR MOVING ROLLER SAMPLES ARE PRESSED, ACCORDING TO THE PATENT No. PL 160 597.....	129
4.1.27. TPZ TEST RIG (RECIPROCATING TRIBOMETER).....	131
4.1.28. TPZ-1 TEST RIG (PROTOTYPE).....	133
4.1.29. ALMEN-WIELAND TEST RIG DESIGNED FOR BOUNDARY FRICTION TESTS.....	135
4.1.30. SKODA-SAVIN TYPE TEST RIG.....	143
4.1.31. KEWAT-1 TYPE TEST RIG.....	145
4.1.32. KEWAT-2 TYPE TEST RIG.....	146
4.1.33. KEWAT-3 TYPE TEST RIG.....	147
4.1.34. KEWAT-4 (KEWA-4) TYPE TEST RIG.....	149
4.1.35. KEWAT-5 TYPE TEST RIG.....	154
4.1.36. KEWAT-6 TYPE TEST RIG.....	155
4.1.37. KRWAT-1 TEST RIG.....	157

4.1.38. TEST RIG FOR TRIBOLOGICAL TESTING OF THE CAM-PUSHER TYPE.....	159
4.1.39. STRIKER TEST RIG WITH A VIBRATION EXCITER DESIGNED FOR PITTING TESTS (FOUR-SPRING).....	161
4.1.40. STRIKER TEST RIG WITH A VIBRATION EXCITER DESIGNED FOR PITTING TESTS (TWO-SPRING WITHOUT A SPRING TENSION ADJUSTMENT).....	163
4.1.41. STRIKER TEST RIG WITH A VIBRATION EXCITER DESIGNED FOR PITTING TESTS (TWO-SPRING WITH A ONE-SIDED SPRING TENSION ADJUSTMENT).....	164
4.1.42. STRIKER TEST RIG WITH A VIBRATION EXCITER DESIGNED FOR PITTING TESTS (TWO-SPRING WITH A TWO-SIDED SPRING TENSION ADJUSTMENT).....	165
4.1.43. STRIKER TEST RIG WITH A VIBRATION EXCITER DESIGNED FOR PITTING TESTS (SINGLE SPRING – LOWER SPRING – WITHOUT A SPRING TENSION ADJUSTMENT).....	166
4.1.44. STRIKER TEST RIG WITH A VIBRATION EXCITER DESIGNED FOR PITTING TESTS (SINGLE SPRING – UPPER SPRING – WITHOUT SPRING TENSION ADJUSTMENT).....	167
4.1.45. SINGLE-CONTACT TEST RIG WITH A UNIVERSAL COUPLING	168
4.1.46. TEST RIG FOR TESTING EROSION RESISTANCE.....	169
4.1.47. TWT-500N TRIBOTESTER DESIGNED FOR FRICTION AND WEAR TESTS.....	171
4.1.48. MUJ TYPE FATIGUE TEST RIG USED FOR FRETTING WEAR TESTS.....	173
4.1.49. TEST RIG FOR FRETTING TESTS WITH AN ELECTROMAGNETIC INDUCTOR AS A COMPONENT THAT FORCES DISPLACEMENT.....	177
4.1.50. TEST RIG FOR FRETTING TESTS WITH AN ECCENTRIC SYSTEM FORCING DISPLACEMENT WITH A RELATIVE MOTION OF SAMPLES: ROTATING, OSCILLATING.....	185
4.1.51. TEST RIG FOR FRETTING TESTS WITH AN ECCENTRIC SYSTEM FORCING DISPLACEMENTS WITH A RELATIVE MOTION OF SAMPLES: LINEAR, RECIPROCATING.....	187
4.1.52. TEST RIG FOR FRETTING TESTS WITH A HYDRAULIC SYSTEM FORCING DISPLACEMENTS AND HYDRAULIC LOADING OF SAMPLES.....	189
4.1.53. TEST RIG FOR FRETTING TESTS IN WHICH THE COMPONENT FORCING THE DISPLACEMENT IS AN ELECTROMAGNETIC VIBRATOR.....	191
4.1.54. FRETTING TEST RIG IN WHICH THE COMPONENT THAT FORCES THE DISPLACEMENT IS A SCREW MECHANISM.....	194
4.1.55. TEST RIG FOR FRETTING TESTS WITH A PIEZOELECTRIC SET FORCING DISPLACEMENT.....	195
4.1.56. MANDREL-DISC TEST RIG IN WHICH A BRAKE DISC IS THE COUNTER-SAMPLE, AND A BRAKE BLOCK IS THE SAMPLE.....	196
4.1.57. TEST RIG FOR TESTING THE COEFFICIENT OF STATIC FRICTION OF METAL-POLYMER FRICTION CONTACTS.....	198
4.1.58. TEST RIG FOR TESTING THE WEAR OF PISTON RINGS	

ACCORDING TO THE PATENT PL 154 209.....	201
4.1.59. TEST RIG FOR TESTING THE STATIC AND KINETIC COEFFICIENT OF FRICTION FOR FRICTIONAL PAIRS.....	204
4.1.60. TEST RIG FOR TESTING ABRASIVE WEAR IN THE CONDITIONS OF INDUSTRIAL SUSPENSIONS ACCORDING TO THE PATENT PL 207 139.....	206
4.1.61. TEST RIG FOR TESTING ABRASIVE WEAR UNDER COMPLEX STRESS CONDITIONS IN THE TESTED MATERIAL ACCORDING THE PATENT PL 211 447.....	208
4.1.62. TEST RIG FOR TESTING THE DYNAMIC LOAD CAPACITY OF THRUST SLIDE BEARINGS LUBRICATED WITH MAGNETIC LIQUID, CONSTRUCTED ACCORDING TO THE PATENT PL 222 239.....	210
4.1.63. TEST RIG FOR TESTING THE SLIDING FRICTION IN A TEMPERATURE-CONTROLLED LUBRICANT ACCORDING TO PATENT PL 95 008.....	213
4.1.64. TEST RIG FOR TESTING FRICTIONAL RESISTANCE AND WEAR OF PLASTICS ACCORDING TO THE PATENT PL 119 178.....	216
4.1.65. THE MEASURING SYSTEM OF FRICTIONAL RESISTANCE OF THE TEST RIG FOR TESTING SLIDING FRICTION IN A TEMPERATURE-CONTROLLED LUBRICANT ACCORDING TO PATENT PL 132 896.....	218
4.1.66. AUTOMATIC UNIT DESIGNED TO THE FRICTION CONTACT ACCORDING TO THE PATENT RU 2 165 077.....	220
4.1.67. TEST CHAMBER OF A FRICTION TEST RIG WITH A RING- BLOCK FRICTION CONTACT ACCORDING TO THE PATENT RU 2 163 013 C2.....	232
4.1.68. TEST RIG FOR TRIBOLOGICAL TESTS OF MATERIALS ACCORDING TO THE PATENT SU 1 219 962 A.....	237
4.1.69. TRIBOMETER FOR MANDREL-DISC FRETTING TESTS ACCORDING TO THE PATENT APPLICATION 396 512.....	239
4.1.70. SKMR-2 FATIGUE TEST RIG.....	240
4.1.71. TEST RIG FOR TRIBOLOGICAL TESTS WITH ACOUSTIC EMISSION SIGNALS RECORDING.....	242
4.1.72. TEST RIG FOR ACCELERATED WEAR TESTING OF THE PISTON-CYLINDER GROUP OF COMBUSTION ENGINES.....	245
4.1.73. T-07 ABRASION TEST RIG.....	248
4.1.74. T-20 BALL-DISC TRIBOTESTER.....	260
4.1.75. "ROTATING BOWL" TEST RIG FOR TESTING WEAR IN SOIL.....	273
4.1.76. TEST RIG FOR TESTING THE WEAR OF WORKING ELEMENTS IN SOIL USING THE "GROUND TUNNELING" METHOD.....	279
4.1.77. TEST RIG WITH AN ABRASIVE CLOTH.....	280
4.1.78. TEST RIG FOR HIGH-TEMPERATURE ABRASIVE TESTS OF HT-ET TYPE.....	283
4.1.79. TEST RIG BUILT ON THE BASIS OF THE HAWORTH METHOD.....	284
4.1.80. MILLER TEST RIG.....	286
4.1.81. TEST RIG FOR MEASURING THE ABRASIVE WEAR	

RESISTANCE USING MWT METHOD.....	287
4.1.82. CIAT TYPE TRIBOTESTER.....	288
4.1.83. SOIL BIN TYPE TRIBOTESTER.....	290
4.1.84. CENRTIFUGAL PARTICLE ACCELERATOR.....	295
4.1.85. TRIBOTESTER WITH A FRICTION CONTACT: PISTON RING- CYLINDER LINER SURFACE.....	296
4.1.86. KRAUSS TRIBOTESTER.....	297
4.1.87. TRIBOTESTER FOR INERTIAL TESTING TecSA TT 2400EL.....	300
4.1.88. FAST TRIBOTESTER.....	302
4.1.89. TEST RIG FOR TESTING THE DEGREE OF WEAR OF HYDRAULIC ELEMENTS OR SYSTEMS ACCORDING TO PATENT PL 187 552.....	303
4.1.90. TEST RIG FOR TESTING HIGH-SPEED HEADSTOCKS ACCORDING TO THE PATENT PL 55 370.....	305
4.1.91. TEST RIG FOR TETING IMPACT AND GRINDING WEAR ACCORDING TO THE PATENT PL 210 732.....	307
4.1.92. TEST RIG FOR COMPARATIVE TESTING OF THE WEAR RESISTANCE OF FRICTION MATERIALS ACCORDING TO PATENT PL 123 756.....	309
4.1.93. TEST RIG FOR TESTING THE WEAR OF BODIES IN AN ABRASIVE MASS ACCORDING TO THE PATENT PL 150 471.....	311
4.1.94. TEST RIG FOR TESTING THE WEAR OF BODIES IN AN ABRASIVE MASS ACCORDING TO THE PATENT PL 96 503.....	313
4.1.95. TEST RIG FOR TESTING THE ABRASION RESISTANCE OF THE MATERIAL FOLD EDGES ACCORDING TO THE PATENT PL 107 388.....	314
4.1.96. TEST RIG FOR TESTING ELEMENTS IN SLIDING INTERACTION ACCORDING TO THE PATENT PL 215 116.....	318
4.1.97. TEST RIG FOR DETERMINING FRICTIONAL RESISTANCE.....	320
4.1.98. TEST RIG FOR DETERMINING FRICTIONAL RESISTANCE IN THE STAMPING PROCESS ACCORDING TO F. TYCHOWSKI AND Z. WIŚNIEWSKI.....	324
4.1.99. TEST RIG FOR DETERMINING THE COEFFICIENT OF FRICTION OCCURRING BETWEEN THE PUNCH AND THE DEFORMED SHEET ACCORDING TO JU. P. KAZAKOV	326
4.1.100. TEST RIG FOR DETERMINING THE FRICTION COEFFICIENT BASED ON THE PRINCIPLE OF FORCING A SEMICIRCULAR PUNCH INTO A SHEET METAL STRIP ACCORDING TO BILGIN	331
4.1.101. TRIBOLOGICAL TEST RIG FOR TESTING THE STICK PHASE AND SLIP PHASE.....	335
4.2. GROUP 2 (ROLLING PAIRS).....	337
4.2.1. AMSLER FRICTION TEST RIG.....	337
4.2.2. T-05 TEST RIG.....	341
4.2.3. TABER-ABRASER TEST RIG.....	343
4.2.4. STBL-02 TRIBOLOGICAL TEST RIG.....	344
4.2.5. PAVLOV TEST RIG FOR DETERMINING THE FRICTIONAL RESISTANCE DURING THE ROLLING PROCESS USING THE FORCED BRAKING METHOD OR CLAMPING METHOD.....	345
4.2.6. T-02 FOUR-BALL TEST RIG.....	348
4.2.7. T-03 FOUR-BALL TEST RIG DESIGNED FOR TESTING THE	

PITTING.....	351
4.2.8. TEST RIG FOR MEASURING THE RESISTANCE AND COEFFICIENT OF ROLLING RESISTANCE OF MOTOR VEHICLE WHEELS ACCORDING TO THE PATENT PL 74 682....	352
4.2.9. MWO TEST RIG (TEST RIG WITH ROTATING LOAD).....	355
4.2.10. FOUR-BALL TEST RIG ACCORDING TO THE PATENT PL 160 591.....	358
4.2.11. FOUR-BALL TEST RIG ACCORDING TO THE PATENT PL 160 592.....	360
4.2.12. FOUR-BALL TEST RIG ACCORDING TO THE PATENT PL 177 200.....	362
4.2.13. FOUR-BALL TEST RIG ACCORDING TO THE PATENT PL 177 203.....	364
4.2.14. TEST RIG FOR FATIGUE TESTS ACCORDING TO THE PATENT PL 160 595.....	366
4.2.15. FOUR-BALL TEST RIG FOR TRIBOLOGICAL TESTS.....	368
4.2.16. AN OLDER TYPE OF A FOUR-BALL TEST RIG DESIGNED FOR TRIBOLOGICAL TESTS.....	370
4.2.17. ROLLER TEST RIG (WITH CYLINDRICAL ROLLERS) DESIGNED FOR TESTING PITTING.....	372
4.2.18. ROLLER TEST RIG (WITH CONICAL ROLLERS) DESIGNED FOR TESTING PITTING.....	374
4.2.19. THREE-CONTACT TEST RIG WITH A VARIABLE CYCLIC SLIP DESIGNED FOR TESTING PITTING.....	376
4.2.20. TEST RIG WITH THREE ROLLERS IMITATING THE MESHING OF TOOTHED WHEELS WITH STRAIGHT AND OBLIQUE TEETH	377
4.2.21. ROLLER-DISC TEST RIG DESIGNED FOR TRIBOLOGICAL TESTS.....	379
4.2.22. SBOP TYPE TEST RIG DESIGNED FOR TRIBOLOGICAL TESTS	381
4.2.23. TEST RIG DESIGNED TO TEST SLIDE BEARINGS.....	383
4.2.24. TEST RIG FOR TESTING THE ROLLING RESISTANCE OF DISCS ACCORING THE PATENT PL 223 986.....	385
4.2.25. TEST RIG FOR MODELING THE FRICTION PROCESS IN NEEDLE BEARINGS ACCORDING TO THE PATENT PL 219 650 (SMT-1 TEST RIG).....	387
4.2.26. TEST RIG FOR TESTING JOURNAL BEARINGS LUBRICATED WITH A CONTAMINATED MEDIUM, ACCORDING TO THE PATENT PL 103 942.....	390
4.2.27. TEST RIG FOR TESTING THE MESHING DURABILITY OF AN EPICYCLIC CYCLOIDAL GEAR.....	393
4.2.28. TEST RIG FOR TRIBOLOGICAL TESTS OF MATERIAL, IN PARTICULAR LUBRICANTS, ACCORDING TO THE PATENT SU 1 670 520 A1.....	401
4.2.29. TEST RIG FOR TESTING RADIAL SLIDE BEARINGS PG 2-1 Ł	403
4.2.30. PRESSURE RING OF THE TEST RIG FOR TESTING LUBRICATING PROPERTIES AND FRICTION PHEONOMENA ACCORDING TO THE PATENT PL 125 950.....	417
4.2.31. TEST RIG FOR TESTING ROLLING BEARINGS ACCORDING TO PATENT PL 129 957.....	418
4.2.32. TRIBOLOGICAL TEST RIG FOR TESTING STARTER BEARINGS	421

4.3. GROUP 3 (UNIVERSAL RIGS).....	423
4.3.1. FOUR-BALL TEST RIG.....	423
4.3.2. TEST RIG FOR TESTING SLIDING AND ROLLING FRICTION OF FRICTION WHEELS TM.260.1.....	431
4.3.3. SMC-2 TRIBOTESTER.....	434
4.3.4. UNIVERSAL TEST RIG FOR TESTING WEAR AND FRICTION COEFFICIENT OF MZiWT-1 TYPE.....	467
LITERATURE.....	479

SYMBOLS AND ACRONYMS FREQUENTLY USED IN THIS PUBLICATION

Symbols

F	– loading force, N,
L	– friction path, m,
P	– power, kW,
Ra	– arithmetic mean of profile ordinates, μm ,
Rpk	– reduced height of the roughness profile peak, μm
Rq	– RMS mean of profile ordinates, μm ,
Rt	– total profile height, μm ,
Spk	– reduced height of the roughness surface peaks, μm ,
Sq	– mean square deviation from the mean plane, μm ,
St	– total surface height, μm ,
T	– temperature, K,
v	– relative motion speed, m/min,
α	– the angle of association (intersection) of the characteristic traces after processing (structure lay direction), $^{\circ}$,
Δl	– linear wear, μm ,
Δm	– mass wear, mg,

Abbreviations and acronyms

2 D	– two-dimensional layout,
3 D	– three-dimensional layout,
WSL	– wear surface layer,
AGE	– lubricant agents,
SEL	– selective transfer,
ST	– surface texture,
LUB	– lubricating composition - type,
TSL	– technological surface layer,
SL	– surface layer.

1. PREFACE

Basically all wear processes are inherently connected with the existence of technical objects. They have a destructive effect on their technical condition and lead to observable damages. As most of these damages occur in the surface layer (SL) of the mating elements, it is this layer that is provided with characteristics which increase resistance to the destructive effects of excitations during the operation of machines and test rigs. Therefore, the surface layer is the subject of research conducted in many national and foreign research centers. It was found that the mechanism and intensity of the wear process depend on the features of the surface layer formed as a result of the implementation of the assumed technological process, e.g. [166, 178, 193]. Therefore, it is justified to undertake research aimed at better understanding of the mechanism of this process, and in particular the methods of controlling it, because it allows reducing its undesirable effects.

The basic method that reduces the intensity of the wear process is to lubricate the mating surfaces. For this purpose lubricants are used which are usually a mixture of base oil and lubricating additives. Finding to the broadest extent the rules and mechanisms that occur during the wear of the friction contact elements one can select lubricant additives in such a way so that during operation they ensure minimal changes in the surface layer, and at the same time the longest working time with unchanged, structurally assumed features of the friction contact.

In principal every technical object is characterized by a certain set of functional features. When we think about test rigs, their performance and technical capabilities, such as reliability and durability, result from certain features represented by units that form a constructional structure of a given object. These units form a set of kinematic pairs, thus one can conclude that a given set of functional features is determined by certain features assigned to given kinematic pairs. The characteristics of given objects also depend on the condition of the surface layer. The surface layer (SL) which is formed in the manufacturing process undergoes further changes during the operation of the object. Lubrication is used to minimize its unfavorable changes over time. Research has been conducted for many years and in many centers inter alia on the influence of lubricating additives on the wear process of kinematic pairs with tribological criteria, e.g. [84, 87, 88, 193, 196]. In general, this research can be divided into theoretical and practical work. Theoretical work presents various hypotheses and theories, while practical work either confirms or rejects them. To conduct practical research test rigs are required. This publication is devoted to these test rigs - tribotesters. Although it presents only a small fraction of all types of tribotesters in the world it might be an inspiration for further work on the development of tribological test rigs.

2. CHARACTERISTICS OF BASIC FACTORS RELATED TO TRIBOLOGICAL TESTS

2.1. Surface layer

There are many definitions of SL in the literature on the subject. Although they sometimes differ, the essence of SL remains the same. The definitions presented below may confirm this observation.

According to the fundamental position [15], the surface layer of an element is understood as: '... a set of material points between its external surface and a certain conventional surface, which is the boundary of changes in the characteristics value of the subsurface zone resulting from various external excitations: pressure, temperature, chemical factors, electrical factors, charged particle bombardment and others. The remaining part of the object material, except for the surface layer - is the core.'

The actual surface of test rig elements which is characterized by a very complex stereometric structure – there is unevenness of various dimensions, shapes and positions - is the outer part of the material layer called the surface layer (SL).

In the Polish standard referring to the surface layer [170] it is defined as: '... a layer of material bounded by the actual surface of the object, including this surface and that part of the material further down from the actual surface that shows altered physical and sometimes chemical characteristics in relation to the characteristics of that material in the depth of the object.' Changes in SL properties as a function of the distance from the surface, in accordance with the above-mentioned definition, are schematically shown in Figure 2.1. The values presented there, which are characteristic features of SL, are only examples.

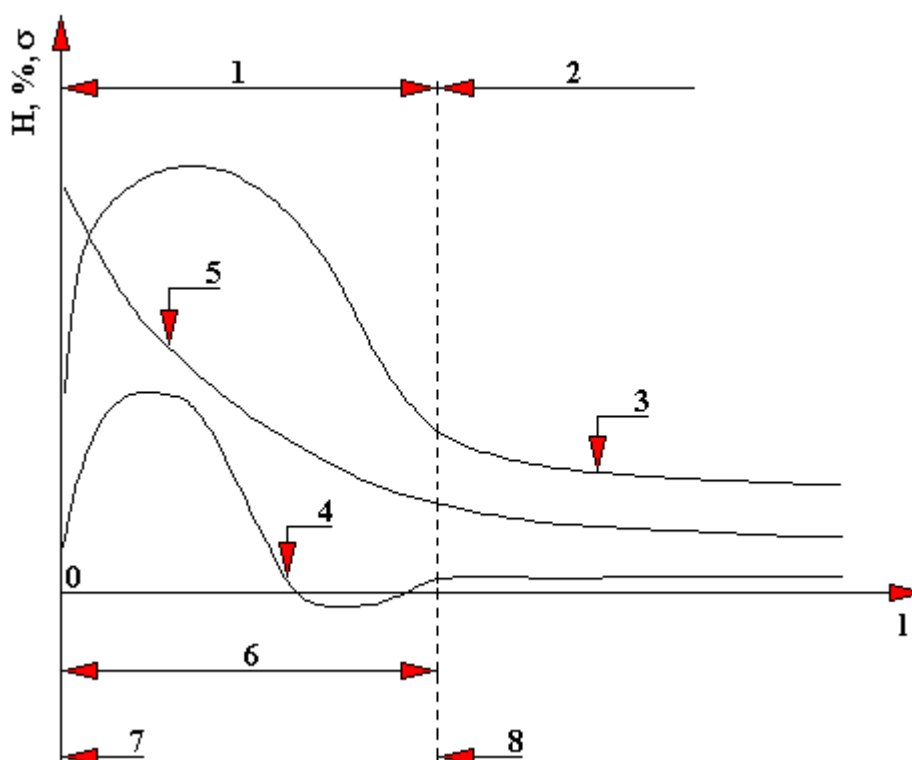


Fig. 2.1. Distribution of exemplary distribution curves of the surface layer features [170]
 1 - surface layer; 2 - core; 3 - hardness (H); 4 - internal stress (σ); 5 - element content (%); 6 - thickness of the surface layer; 7 - external border (actual surface); 8 - internal border (conventional surface); l - distance from the actual surface

The definition of SL, a very similar one to that contained in the quoted standard, was also presented in an earlier study [41].

The increased interest and intensification of research on SL of machine elements has been observed since the turn of the 19th and 20th centuries. Initially, the only characteristic of the surface obtained as a result of machining was its smoothness (roughness). Later, the research was extended to surface layers obtained by other techniques. The set of quantities that describe the state of SL has also been extended. This research work allows us to find and develop the knowledge about surface characteristics obtained as a result of various processes of machining, mainly finishing.

Numerous studies, e.g. [6, 19, 20, 21, 55, 61, 64, 65, 66, 166, 183, 184, 192, 200, 213] showed a close relationship between the state of SL of machine elements and tribological features of these elements, e.g. seizure resistance, wear resistance, friction coefficient, tribological durability. Therefore, one can conclude that the state of SL decisively determines the functional features of the entire test rig. It was also found that the course of wear - its intensity, mechanism and effects - depends on the state of the SL formed as a result of the implementation of the assumed technological process [36, 166, 167, 178, 182, 183, 183 193]. For this reason, SL is the subject of research carried out in many research centers - foreign and national. This interest is sustained by the ever-expanding sets of constructional plastics and techniques of SL forming, as well as increasing research possibilities, both in the field of test rigs and methods used.

The surface layer of test rig elements formed during the manufacturing process is called the technological surface layer (TSL) [9, 10, 11, 12, 13, 66]. Its features, i.e. characteristics, properties and structure, depend largely on the parameters and type of finishing applied, and on the type of construction material from which the mating elements are made.

The technological features obtained in the manufacturing process are not constant. Under the influence of external operational excitations, e.g. load, temperature, environmental impact, etc., they undergo changes. Changes can also occur spontaneously, without the involvement of external factors, e.g. as a result of aging or stress relieving. The surface layer at this stage of the test rig existence is called the wear surface layer (WSL) [9, 10, 11, 12, 13, 14, 15, 65, 66].

Taking into account the phases of existence ('life') of the test rig, the two above-mentioned varieties of SL occur in the following phases:

- manufacturing of test rig elements and assembling them - TSL, with its features already defined at the construction and design stages,
- operation of the test rig - WSL.

In the literature, one can find various information on how to qualify SL of elements in the transition phase, i.e. during storage and transport - to the WSL or TSL. The study [13] proposes to include it into the WSL, while the author of the study [96] includes it into the TSL. It should be stressed that the authors support their proposals by substantive arguments. It is important because in this phase of existence of the element the features of its surface layer may also undergo changes spontaneously, especially if this period is long, or under the influence of external excitations, e.g. the influence of active ingredients of maintenance substances or vibrations of the substrate. When referring SL in this phase to its existing varieties, i.e. TSL and WSL, such surface is called a post-technological or pre-operation surface layer.

2.1.1. Surface layer models

In the literature on the subject one can find various models of the surface layer structure. They usually differ in the degree of adopted simplifications. All SL models assume its zonal structure: starting from the 3-zone model proposed in [55] to the most developed 9-zone model [33]. Each of these zones has a specific depth (thickness) and is determined by the area of occurrence of specific SL features.

In models with a greater number of zones, new ones were created by dividing the existing zones or introducing additional ones [47, 60, 200]. In a big number of cases the boundaries of individual zones are not clear. Some zones may be absent or interpenetrate creating areas of smooth fading of the characteristics of one zone with a parallel appearance of features of another zone.

The simplest Kolman model distinguishes the following zones [55]:

- outer - made of particles of foreign origin, covered with a gas coating (adsorbed gases), its thickness is $0.001 \div 0.02 \mu\text{m}$, including the gas coating - approx. $(2 \div 3) \cdot 10^{-4} \mu\text{m}$,
- middle - consisting of strongly crushed grains of the core material, its thickness is $0.5 \div 500 \mu\text{m}$ (it determines functional properties),
- inner - this is a layer consisting of grains not plastically deformed but having a structure different from the core material, its thickness reaches several thousand micrometers.

The most developed model consists of 9 zones [33]:

- I - an electric field above the surface of the metal ("over-surface"),
- II - formed as a result of adsorption of organic polar particles on the surface of metals (fats - lubricants, sweat, etc.)
- III - formed as a result of adsorption of water molecules (usually from vapors),
- IV - formed as a result of gas adsorption (nitrogen, sulfur vapors, phosphorus),
- V - a layer of core metal oxides formed as a result of a chemical reaction of oxygen with the core material,
- VI - formed as a result of damage to the core metal grains by the cutting tool,
- VII - covers the area of plastically deformed metal, it is distinguished by a distinct fibrousness and sometimes even texturization,
- VIII - covers the area of metal only plastically deformed (non-textured),
- IX - covers the area of elastic strains and tensile stresses.

Depending on the research purpose and necessary detailed analyzes related to it, models with a larger or smaller number of zones are adopted in these considerations.

Tribological phenomena depend primarily on the condition of the surface layer of the contact areas of rubbing test rig elements. The wear of these components is in fact SL wear which is caused by all types of friction.

For the purpose of this study, with reference to its goal (observation of the effects of the WSL transformation), a standardized 5-zone model [170] - which is not overly complex and, at the same time, is sufficiently detailed - was adopted in further considerations. The zones which occur in it are shown in Figure 2.2.

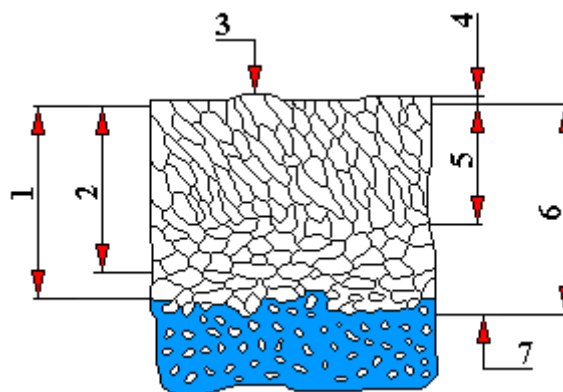


Fig. 2.2. Diagram of the 5-zone model of the surface layer [170]

1 - textured zone; 2 - zone of thermal effects; 3 - actual surface; 4 - near-surface zone; 5 - orientation zone; 6 - strain zone; 7 - material core boundary

The following zones are identified in this model:

- Near-surface zone – it constitutes a part of the SL directly adjacent to the actual surface, it has no characteristic own structure, it is built of ions adsorbed or chemically bound to the substrate, coming from the surrounding medium or other elements mating with the object
- orientation zone - lying under the near-surface zone, there is an orientation of the material grains in it, e.g. due to plastic deformation,
- zone of thermal effects - this is a zone in which, as a result of thermal processes, there have been, e.g. phase changes, physical changes, changes in grain dimensions, chemical reactions, etc.,
- textured zone - this is a zone in which crystalline texture occurs.

2.1.2. Quantities describing the condition of the surface layer

The functional features of test rigs are, inter alia, a function of values of quantities determining the condition of the surface layer caused by processing and operation. The durability of test rig elements and reliability of technical objects should therefore be described by the SL features of the elements of the kinematic pairs participating in the friction process, taking into account the anticipated external excitations. For this reason, it is advisable to try to create a set of significant parameters of the SL condition of test rig elements on the basis of which it will be possible to conclude about the condition of the technical object and predict possible damage. These tasks constitute basic activities of technical diagnostics, and they include respectively: diagnosing and forecasting. They are aimed at improving the functional quality of test rigs and all test rigs by enabling control of durability and reliability features.

The condition of the surface layer is determined by a set of features that can be described by parameters: stereometric, physicochemical and stereometric-physicochemical [9, 10, 11, 12, 13, 14, 15, 20, 21, 45, 199, 200].

The properties and characteristics of SL are determined to the greatest extent by the parameters describing the stereometric structure of the surface, more commonly referred to as the surface structure (ST) [9, 10, 11, 12, 13, 14, 15].

The group of parameters describing the ST includes the following parameters [15, 40, 41, 100, 101, 102, 108, 110, 213, 214]:

- roughness,
- lay direction,

- ST defects,
- waviness.

The physicochemical parameters that define the state of SL include quantities that describe the following features [10, 15, 44]:

- structural features of the material (its structure),
- mechanical features (brittleness, internal stress, hardness),
- chemical features (chemical composition, chemical adsorption, absorption),
- physical (physical adsorption, adhesion),
- magnetic (permeability, coercivity),
- electrical (resistance, conductivity).

As stereometric and physicochemical parameters accepted are [45]:

- surface energy,
- surface tension,
- emissivity,
- reflectivity.

In each of the aforementioned groups of parameters there are quantities which are to a greater or smaller degree important for the operation process, and thus for the wear process. Moreover, their importance is not the same under all operating conditions of the kinematic pair.

From the point of view of the tribological properties of the elements of friction contacts, the most important quantities describing the state of SL should include [15, 41, 163]:

- stereometric:
 - roughness;
 - structure lay direction;
- physicochemical:
 - type of engineering material,
 - its structure,
 - internal stress,
 - hardness.

2.1.2.1. Physicochemical characteristics of the surface layer

The type of structural material of the kinematic pair elements and their microstructure (metallographic structure) affect the properties of the surface layer of these elements. The microstructure is defined as the structure of SL including the arrangement of the constituent elements (crystals, grains, the arrangement of atoms in the crystal lattice) and a set of relations between these elements [15, 41].

Microstructure of constructional material

Metals and most non-metals have a crystalline structure, i.e. an internal structure composed of crystals, with a strictly defined arrangement of ions, atoms or molecules in the crystal unit cells.

The surface layer may have the following microstructure:

- primary - formed during the transition of the metal liquid phase into the solid phase,
- secondary - formed from the primary microstructure after recrystallization in the solid state as a result of various phase changes or plastic working.

The primary microstructure in the surface layer is rather rare, e.g. during melting (electron, laser, plasma), while the secondary microstructure occurs almost always, however microstructure

transformations may occur repeatedly, either during the manufacturing process or during operation.

Internal stress

Internal stresses reflect the state of internal forces resulting from the interaction in a given place of two parts of the material located on both sides of the conventional material cross-section, related to a given cross-section unit.

The result of external loads is a change in the position of atoms of the crystal lattice of the material. This disrupts the construction of the network. These disturbances lead to the formation of internal stresses in the material. After cessation of external influences, the first part of changes disappears in the form of elastic deformations (reversible changes) and the stress caused by them, while the second part remains in the material in the form of e.g. plastic deformations (irreversible changes) and the resulting stresses, which from that moment constitute the internal stress of the material [45, 201].

Internal stresses can be classified according to the following criteria [15, 41]:

- due to the balancing area - micro-, macro- and internal sub-stresses (balancing respectively: in the area of the entire object or surface layer, in the grain area or within the crystal),
- due to the cause of formation - mechanical (plastic deformation), thermal (thermal expansion) and structural (changes in the specific volume of structural components),
- due to the impact - compressive and tensile,
- due to the machining operations that trigger them - foundry, hardening, welding.

Due to the fact that the internal stresses add up to the stresses resulting from external loads, it is very advantageous for the strength to have compressive stresses (with a negative sign) in the surface layer of the material. Then these stresses are subtracted from the stresses coming from external forces.

Hardness

Hardness is a property of a solid characterized by resisting plastic deformation or cracking with local, strong action of another harder material on its surface.

Hardness cannot be defined by other physical quantities. It is therefore a conventional feature that allows comparing the resistance of different materials to surface damage.

In general, the hardness of SL of the elements of kinematic pairs should be the greater the greater the pressure it will transmit. Hardness, however, is often associated with brittleness - most often a negative feature - which is the reciprocal of hardness, therefore, assuming a specific hardness of elements the permissible fragility of the material should also be taken into account.

2.1.2.2. Features of the geometric structure of the surface

The quantities characterizing the geometric structure of the surface are shown in Figure 2.3.

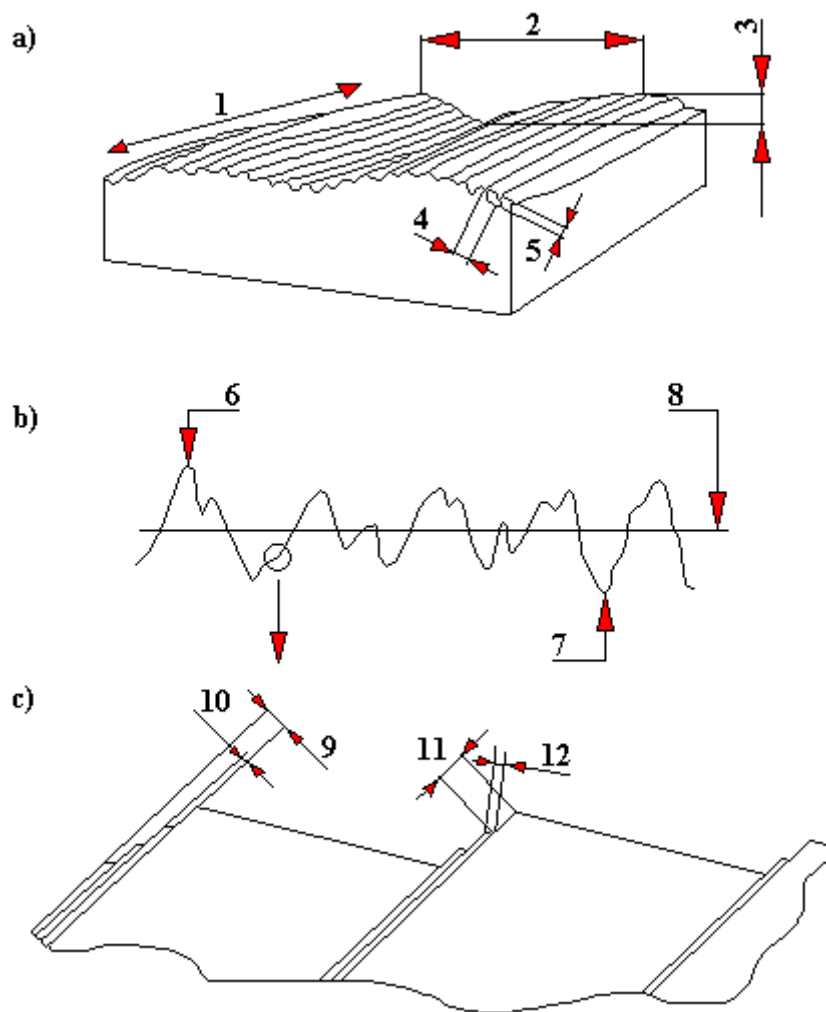


Fig. 2.3. Surface texture: a) pattern of waviness and roughness orientation, b) roughness profile, c) submicro-roughness [201]
 1 - lay direction; 2 - waviness interval; 3 - wave height; 4 - roughness distance; 5 - roughness; 6 - line of profile peaks; 7 - line of profile valleys; 8 - profile mean line; 9 - slip band; 10 - glide line; 11 - ~ 1000 atomic diameters; 12 - ~ 100 atomic diameters

With reference to the scale of observation, ST features can be classified as [Wiśniewski 1995]:

- macroscopic (waviness),
- microscopic (lay direction and roughness parameters),
- submicroscopic (submicroscopic roughness - unevenness less than 0.01µm in height).

Among the quantities describing the surface texture, the parameters of surface lay direction and its roughness are taken as basic [15, 41, 100, 101, 108, 110, 116, 117, 163, 202, 203].

This view can also be confirmed by the ST classification presented in the works [105, 106, 107, 108, 109, 110, 111, 112, 169]. The criteria for its classification adopted were:

- finishing method,
- lay direction of machining marks (ST lay),
- roughness parameter values.

Surface roughness

According to the definition, the surface roughness is defined in the Polish Standard [169], as a set of actual surface unevenness, conventionally defined as deviations of the profile measured from the reference line within the segment where waviness and shape deviations are not taken into account.

The roughness is determined by the surface profile. Therefore, one can conclude that the surface profile (roughness profile) is the basic element of the surface roughness characteristics. The measured surface profile is a profile obtained by cutting the surface of an object with a plane with a specific position in relation to the nominal surface (Fig. 2.4). Very often the intersection is perpendicular to the surface of the object or to a plane tangent to it, and it is made in the direction that is likely to give the greatest profile deviation (right angle to the lay direction of the surface structure) [10, 15, 41, 213, 214, 215].

The line that describes the roughness profile is denoted by the function:

$$z = f(x)$$

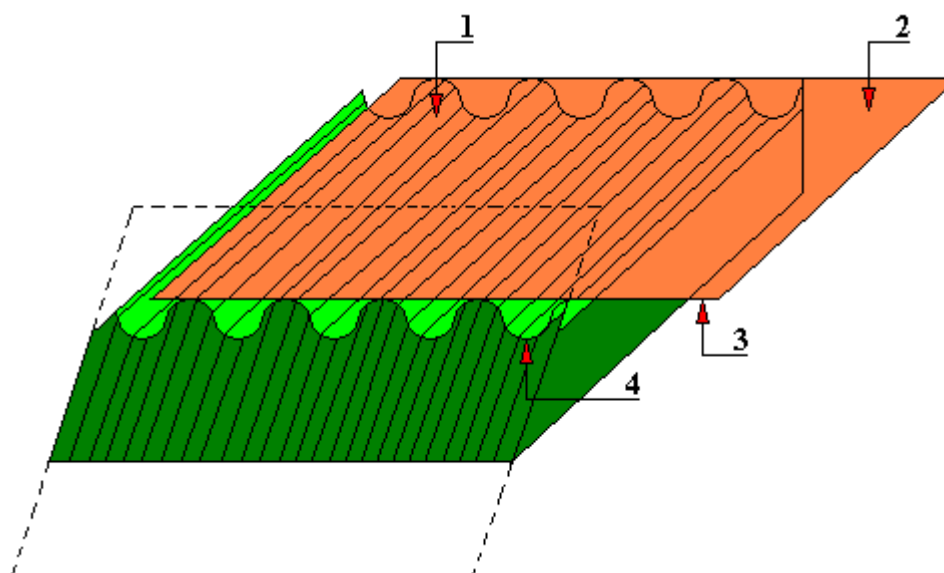


Fig. 2.4. Surface profile with roughness elements [169]

1 - observed surface; 2 - nominal surface; 3 - nominal profile (outline); 4 - profile (outline) observed

Such an approach to the problem reduces it to the determination of roughness parameters in a two-dimensional (2D) system.

The roughness parameters defining the ST in a two-dimensional system are included in the standard [169]. They are classified in the following groups [116, 117, 163, 169, 213, 214]:

- vertical (amplitude) parameters,
- horizontal (distance) parameters,
- hybrid parameters (mixed),
- characteristic curves.

Among the vertical parameters, there are those whose value can be read directly from the profile and those that are calculated from the measurement results.

The first group includes the following parameters:

- R_c – average height of profile elements,
- R_v – depth of the lowest profile valley,
- R_p – height of the highest peak of the profile,
- R_t – total profile height.

On the other hand, the vertical parameters, calculated on the basis of the profilogram (average values of ordinates) are:

- R_{ku} – profile slope coefficient,
- R_a – arithmetic mean of profile ordinates,
- R_q – quadric mean of profile ordinates,
- R_{sk} – profile asymmetry factor,

The other roughness parameters according to the standard [169] include, among others:

- the distance parameter (horizontal) is:
 - R_{Sm} – average width of grooves of elements of a given profile,
- the hybrid (mixed) parameter is:
 - $R_{\Delta q}$ – mean square profile height,
- characteristic curves include:
 - R_{mr} – material share of the profile,
 - profile material share curve – load capacity curve (Abbott-Fireston),
 - $R_{\delta c}$ – differences between the two cutting levels,
 - amplitude density curve.

The characteristics of surface unevenness in the form of curves are introduced in order to better evaluate the surface properties. The material proportion curve - the load capacity curve (distribution of the relative load length) is the most widely used. This curve is also called the Abbott-Firestone plot and describes the material distribution in the profile [1, 115, 116]. Since this curve informs about the profile course, it is possible to read the properties of a given profile in terms of surface function [1, 24, 103, 104, 108, 109, 110, 115]. The parameters that we obtain from the profile load capacity curve, which are at the same time characterizing this curve, include [1, 24, 115, 116]:

- R_k – reduced roughness height, μm ,
- R_{pk} – reduced height of the roughness profile peak, μm ,
- R_{vk} – reduced height of the roughness profile valleys, μm ,
- Mr_1 – bearing surface of peaks, %,
- Mr_2 – bearing surface of valleys, %.

Graphical interpretation of the above-mentioned parameters is shown in Figure 2.6.

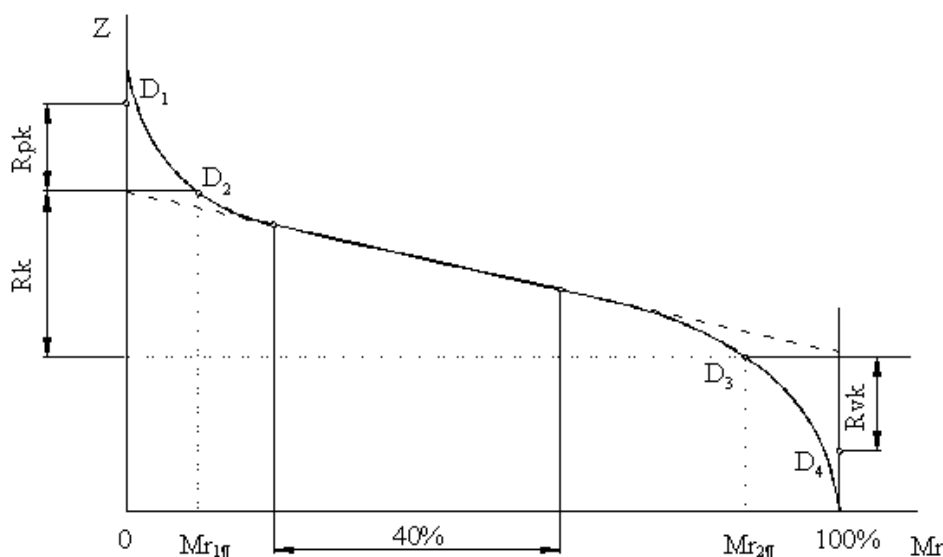


Fig. 2.6. Typical load-bearing curve diagram [169]

The frequency structure of the profile is described by the autocorrelation function and the related with it the Fourier transform power spectral density function. In research, depending on its purpose, one of the above functions is assumed. Mostly, however, the power spectral density function is used, on the basis of which it is possible to assess the influence of the components of the cutting force [8] and the condition of the cutting blade [57, 71] on ST or changes occurring in it during operation.

In the literature on the subject also other classifications of parameters and their sets are proposed, e.g. in the works [99, 100, 101, 102] the following division of parameter groups was introduced:

- height: Ra , Rq , Rp , Rv , Rt ,
- length: Sm , S , Swm , λq ,
- slope: $\Delta\alpha$, Δq , θ , γ ,
- defining the radii of rounding the roughness peaks,
- constituting functions of autocorrelation and power spectral density,
- load capacity and peaks distributions.

Modern measuring test rigs (profilographometers) enable the measurement and registration of many parameters of roughness. Some of them are related and dependent on each other. This often leads to a situation where the user has to decide for themselves which parameters to choose for the surface evaluation.

In the work [100, 101] its author presented 39 parameters, and ISO standards contain 57 parameters [22]. Various roughness indicators are also presented in the works [30, 48, 115, 216, 217, 219].

Currently, there is a tendency in the world to standardize and reduce the number of privileged parameters in national standards.

The authors of the work [53] warn against using an excessive number of parameters. Introducing new parameters should be very thoughtful and it should be preceded by a thorough research. The authors also propose the division of parameters into two groups of parameters: scientific and industrial. However, such division may be difficult to implement and raises some doubts.

In the industrial practice, the roughness parameter most often used in measurements is Ra . Other parameters necessary for the roughness assessment are selected on the basis of the analysis of the tasks to be performed by a given surface.

All roughness parameters presented above are in a two-dimensional (2D) system. Due to a limited area of profiling, random selection of the measurement site, difficulties in accurate reading of values and the difficulty of profiling surfaces with complex shapes, the 2D method is characterized by a limited accuracy of surface assessment. For this reason, roughness measurement in the three-dimensional (3D) system is increasingly used [48, 71, 103, 104, 105, 106, 107, 108, 109, 110, 111, 112, 190, 191, 204], despite the fact that there is still no standard for measurements in this system. According to the draft of such standard [190, 191] ST can be characterized by parameters classified in the following groups:

- Group I - amplitude parameters - correlating with vertical 2D parameters included in the standard [169]:

- Sa – arithmetic mean deviation from the mean plane,

$$Sa = \frac{1}{NM} \sum_{x=0}^{N-1} \sum_{y=0}^{M-1} |Z_{x,y}|,$$

- Sq – mean square deviation from the mean plane,

$$Sq = \sqrt{\frac{1}{NM} \sum_{x=0}^{N-1} \sum_{y=0}^{M-1} Z_{x,y}^2},$$

- St – total surface height,
- Sp – height of the highest peak,
- Sv – depth of the lowest valley,

- Ssk – symmetry of the depth distribution curve,

$$Ssk = \frac{1}{NMSq^3} \sum_{x=0}^{N-1} \sum_{y=0}^{M-1} Z_{x,y}^3,$$

- Sku – flatness of the depth distribution curve,

$$Sku = \frac{1}{NMSq^4} \sum_{x=0}^{N-1} \sum_{y=0}^{M-1} Z_{x,y}^4,$$

- Group II - volumetric parameters:

- STp – relative load capacity,
- $SHTp$ – relative load capacity height,
- $Smvr$ – average void volume,
- $Smmr$ – average volume of the filled space (material),

- Group III - spatial parameters:

- SPc – peak density between the two levels,
- Sds – peaks density,
- Sal – the length of the fastest fall,
- Str – relative structure ratio,
- Std – lay direction,

– hybrid parameters:

- Sdq – mean square slope,
 - Ssc – arithmetic mean of the peaks curve,
 - Sdr – surface development,
 - Sfd – fractal dimension,
- parameters characterizing the load capacity curve (similar to 2D):
- Sk – reduced roughness height,
 - Spk – reduced height of the roughness surface peaks,
 - Svk – reduced height of the roughness surface valleys,
 - $Sr1$ – bearing surface of peaks,
 - $Sr2$ – bearing surface of valleys,
 - Sbi – load capacity index,
 - Sci – fluid retention index (core),
 - Svi – fluid retention index (valley).

The three-dimensional characterization of surface roughness cannot be complete without the function of autocorrelation and power spectral density. Based on the graphs of these functions - more often autocorrelation - one can determine whether the surface is anisotropic or isotropic.

The autocorrelation function is more useful for assessing a random structure, while the spectral power density function is more useful for assessing a determinate structure [35, 212].

Lay direction

ST lay direction is characterized by the mutual location of traces formed on the surface in the following processes: machining or wear. For this reason, all surfaces can be broadly divided into directed, mixed and non-directed (Figure 2.7).

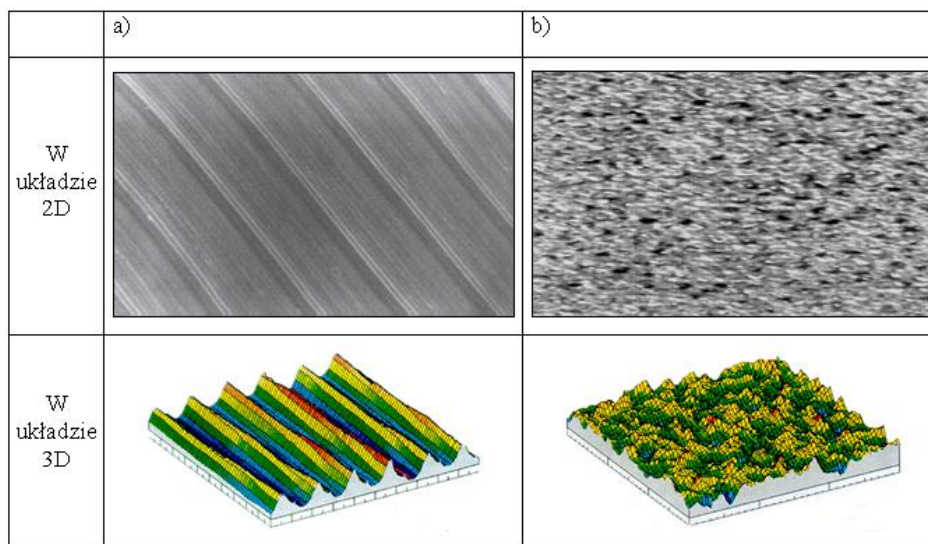


Fig. 2.7. Surface texture: a) directed, b) non-directed [108]

The nature of ST lay is governed by national and international standards [24, 168]. Table 2.1. presents the ST lay classifications according to the above mentioned standards.
Table 2.1. ST lay obtained by various machining methods according to [168]

Type of lay	Lay variety	Symbol	Traces of machining and marking methods	Examples of machining giving a given structure
unidirectional	perpendicular (a), parallel (b) – to the edge on which the mark is given	\perp =		longitudinal turning, planing, chiselling, cylindrical milling, pull broaching, grinding
	concentric	C		face turning, face milling
multidirectional	cross	X		face milling, honing (honing process)
	radial	R		face grinding
	disordered	M		scraping, lapping, superfinishing
non-directional	point	P		EDM, abrasive blasting, ultrasonic

Structures with privileged directions are called anisotropic structures, and structures that do not have privileged marks - isotropic structures. If the structure has straight, parallel machining marks, it is called an orthotropic structure.

In general, the isotropy of the properties of a given medium is characterized by the fact that it exhibits the same geometrical or physical properties in each direction. Therefore, the isotropy of ST means the structure is the same in all directions. One can say that it is a perfectly symmetrical structure with respect to all possible axes of symmetry [108, 110].

The isotropy (or anisotropy) measure in the 2D system is usually taken as the ratio of the selected roughness parameters measured for two typical mutually complementary directions. The assessment is based on longitudinal or vertical parameters [18, 19, 106, 110, 111, 112, 116, 117].

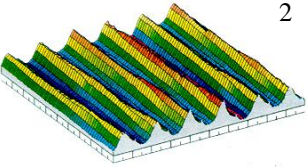
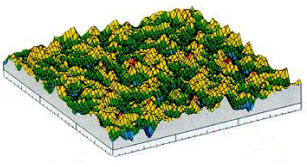
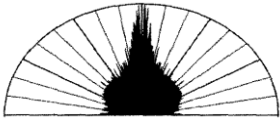
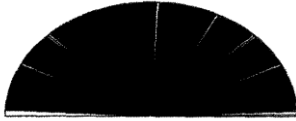
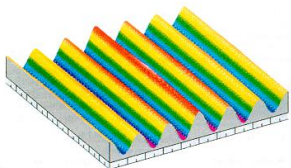
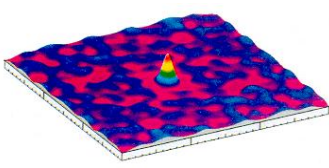
The isotropy index (I_z) can be expressed as a percentage from 0% to 100%, or in the range of values from 0 to 1. Sometimes, instead of the isotropy index, its inverse, i.e. the anisotropy index, is taken. In the work [108] the authors define the isotropy index expressed in %, while the authors of the papers [30, 31, 69] determine the anisotropy index ranging from 0 to 1.

Isotropy index values close to zero mean a completely anisotropic structure, and values close to one or 100% mean a completely isotropic structure. The nature of the structure described by the anisotropy index is determined analogously. The isotropy level is conventionally divided as follows [108]:

- $I_z < 20\%$ (0.2) – anisotropic structure,
- $20\% \leq I_z \leq 80\%$ - mixed structure,
- $I_z > 80\%$ (0.8) – isotropic structure.

Table 2.2. shows examples of structures after various treatments, their isotropy diagrams and the form of autocorrelation function in the 3D system.

Table 2.2. Examples of ST isotropy: 1 – finishing turning, 2 – ball peening [108]

1 Surface image		2 
Isotropy diagram	 180° Isotropy – 3,02 %° 0°	 180° Isotropy – 90,1 %° 0°
Autocorrelation function in a 3D system		

The analysis of the surface topography in a 3D system shows this positive feature in relation to the possibility of the analysis of the roughness profiles (2D) that it is possible to calculate the parameters characterizing the isotropy. There are many ways to determine the level of ST isotropy [3, 41, 71, 213, 214]. The most justified method seems to be the analysis of the autocorrelation function (or spectral power density), the shape of which is slender, elongated and asymmetrical in one direction in the case of anisotropic surfaces, and symmetrical and circular for isotropic surfaces. [30, 31, 108, 109, 111].

2.2. Types of tribological wear processes

As a result of the impact of operational forces on the elements of a kinematic pair, the wear process takes place. When this process is accompanied by friction: sliding or rolling, this is called a tribological wear - Fig. 2.8.

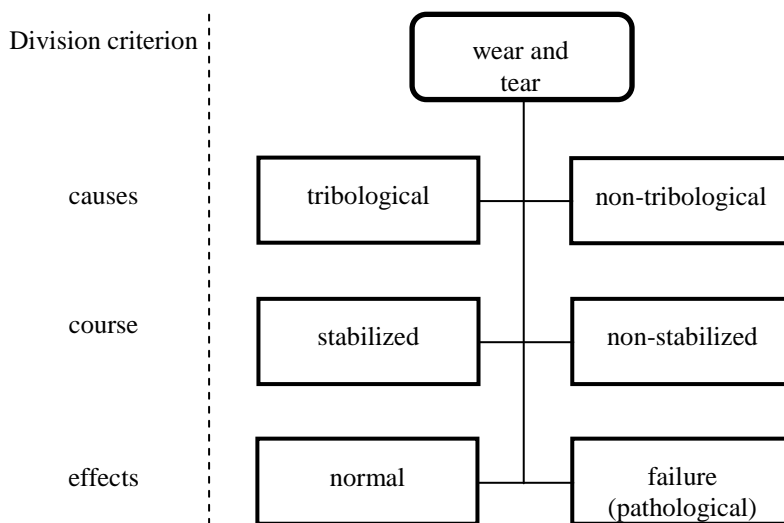


Fig. 2.8. Classification of wear processes of test rig elements for various criteria [65]

Tribological wear includes abrasive, fatigue, adhesive and oxidation wear, while non-tribological wear includes the effects of corrosive and erosive processes. Regarding the scope of work, only tribological wear will be considered in the further part of this work.

The wear of elements of kinematic pairs is a continuous process of changes occurring in their surface layer leading to unfavorable changes in SL characteristics. These changes are caused by the interaction of the mating surfaces of the elements forming pairs and may be intensified by the working environment neighborhood [45, 47, 187, 199, 215].

The wear process is the result of destructive changes in the working surface layer. Changes in WSL can be quantified by using parameters that describe wear.

Wear is the result of the wear process. Various absolute or relative measures are used to evaluate the intensity of the wear processes, and thus the wear values [65, 182, 183, 184].

The absolute wear measure (Z) is either the volume V_z or the mass m_z of the material separated from the surface layer of the element or the thickness h_z of the separated or deformed part of SL. These measures can be described by the following relationships:

$$V_z = L_t \cdot b_t \cdot h_z$$

where: L_t – friction path length,

b_t – friction path width,

h_z – thickness of the separated or deformed zone of SL;

and:

$$m_z = V_z \cdot \rho$$

where: ρ – material density.

A relative measure of wear is the wear intensity I which is the reference of the volumetric (ΔV_z), mass (Δm_z) or linear (Δl_z) loss to time (τ_t), friction work (P_t) or the friction path (L_t). The wear intensity can therefore be written as follows:

$$I_\tau = \frac{Z}{\tau_t};$$

$$I_L = \frac{Z}{L_t};$$

$$I_P = \frac{Z}{P_t};$$

where: Z can take the forms: ΔV_z , Δm_z , Δl_z .

The inverse of the wear intensity is called wear resistance [65, 182, 183, 184]. This quantity can also be interpreted in an energetic way as the specific work of wear, that is the ratio of the work of friction to the mass of wear products [182, 183, 184] or the friction energy density, that is the ratio of the friction work to the volume of the material removed [36].

When the wear intensity is constant over time, the process is taken as stabilized, otherwise – non-stabilized (Fig. 2.9).

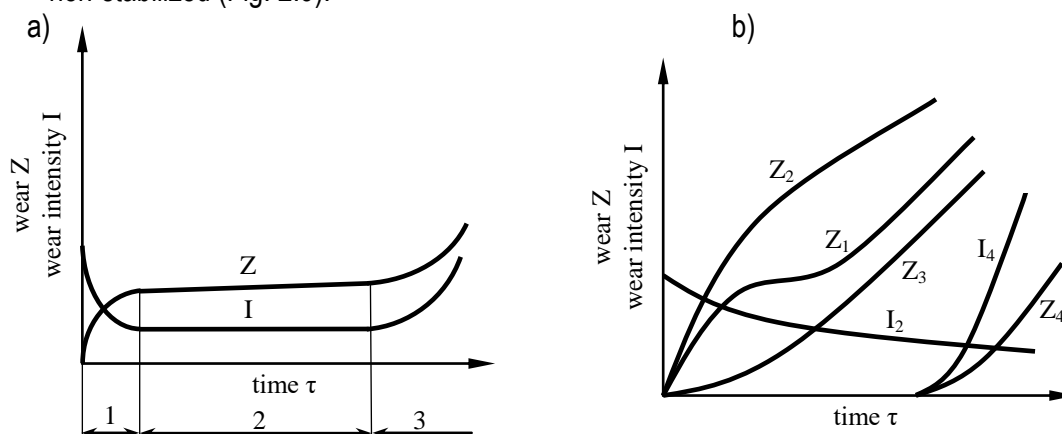


Fig. 2.9. Characteristics of wear processes [65]: a) stabilized, b) non-stabilized

Figure 2.9a shows that three periods can be distinguished with stabilized wear. The first period (1) of variable, but decreasing wear intensity - this is the period of grinding-in (adjusting) the elements, which takes place with increased wear intensity. After running-in, a second (2) period of stable operation follows, in which the wear intensity is almost constant. Completion of this stage and commencement of the third (3) is revealed by a significant increase in wear intensity, e.g. due to an increase in the clearance in the tribological pairs, or as a result of wear of the hardened surface layer zone. Work during this period should not be allowed, because the intensity of damage to test rig elements increases very rapidly, thus significantly increasing the costs of removing the effects of such damage.

In some tribomechanical systems, stabilized wear does not occur after the running-in period (Fig. 2.9.b). The reasons for this may be, for example: wear products contained in unchanged and unfiltered oil - curve with index 1, hardening of metals under normal loads - curve with index 2 (decreasing wear intensity), wear of the anti-wear surface layer - curve with index 3 (increasing wear intensity), cyclic contact stresses - curves with index 4 (some operating time with almost no wear).

The visible effects of wear in the second period occur when there is no decohesion (loss of cohesion) in the area of the core of the parent material, and plastic deformation and decohesion occur only in thin layers of secondary structures and when there is a dynamic equilibrium between the formation of these structures and their wear. Emergency effects - the third period occurs when there is cohesion and the friction contact is no longer suitable for further work. Continuing the wear process under such conditions may cause extensive damage to the entire test rig.

The causes of wear are purely mechanical or mechanical combined with the chemical effect of the surrounding medium, and the basic ones are [15, 45, 47]:

- elastic and plastic deformations of peaks of unevenness and their strain,
- formation of oxide films on the friction surface, though preventing seizure and deep tearing out of the material particles, but because the oxides are brittle, they flake and spall, the exposed areas undergo re-oxidation, etc.,
- embedding of SL particles of one rubbing material into the surface of the other material, which, during sliding, causes cracks and scratches on the surface, and as a result, wear of the less hard surface,
- adhesion of joints in contact with surfaces, which leads to accelerated wear, material transfer from one SL to another,
- accumulation of hydrogen in the surface layers of steel and cast iron parts causing hydrogen wear [188].

The classification of tribological wear, taking into account the mechanism of the surface layer wear process, is shown in Figure 2.10.

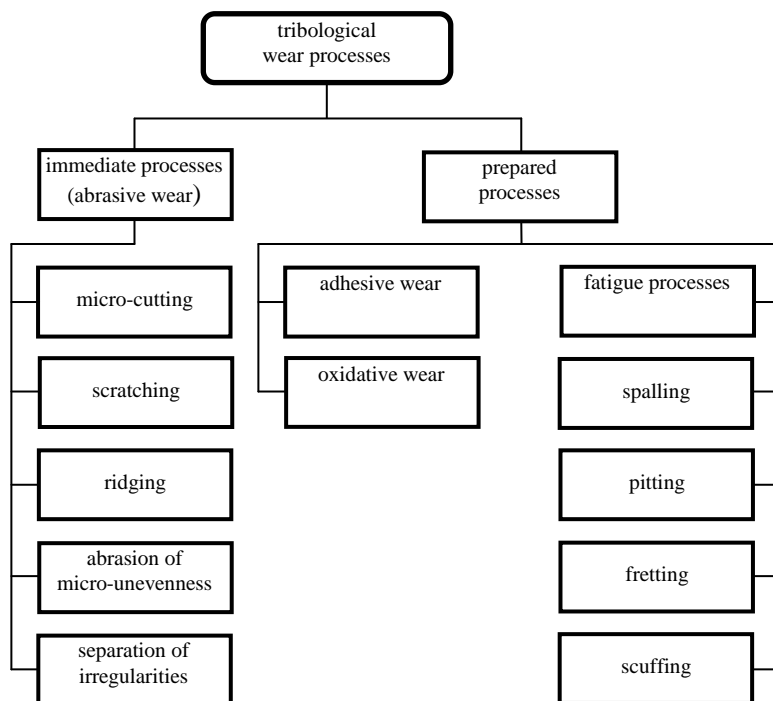


Fig. 2.10. Classification of tribological wear [45, 65]

The state of ST of friction elements has the greatest influence on tribological wear, both in conditions of dry friction and with a lubricant. Among parameters describing the ST condition, the course of wear pattern is most influenced by the surface roughness and mutual orientation of the roughness of friction surfaces - the cooperation (intersection) angle between the characteristic lay direction of a given surface [15, 75, 76, 77, 192, 193, 194].

Tribological wear occurs as a result of the co-acting of elements of a kinematic pair rubbing against each other, and is understood as the process of destroying and removing material from the surface of solid bodies as a result of friction, manifested by a continuous change in the dimensions and shapes of rubbing elements.

The separation of material in the wear process is a result of the immediate, mechanical impact of the contacting elements, or it is preceded by other phenomena that cause or facilitate the mechanical separation of the element material. With these mechanisms in mind, the material wear processes can be divided into [65]:

- prepared,
- immediate.

Abrasive wear occurs when the process of the surface layer wear takes the form of: scratching, micro-cutting, ridging, shearing of irregularities, separation of surface irregularities or reeling of abrasive grains. The loss of SL material in the process of abrasive wear results mainly from a mechanical effect. Hard particles of foreign bodies get into the friction area or areas of the co-acting elements and behave like micro-cutting blades. The same role can be fulfilled by protruding irregularities of the harder material of the mating surfaces [45].

Micro-cutting consists in cutting a specific micro-volume in the material as a result of the cutting action of the abrasive element. The separated material is in the form of chips.

Scratching consists in creating a scratch in the element material by a moving protrusion of the mating element or abrasive grain, partly by cutting, and partly by moving the material to the sides. It is an intermediate phenomenon between micro-cutting and micro-ridging.

Micro-ridging consists in sinking the protrusion of the element into the material of the mating element and plastic extruding of micro-grooves in it under the influence of a relative motion.

Shearing of irregularities occurs when the value of the force necessary to shear the projection is lower than the value of the deformation resistance of the co-acting projection or lower than the value of the resistance of its displacement in the mating element. The fulfillment of these conditions depends on the shape of the surface irregularities, the height of projections and the mechanical properties of the materials.

Separation of irregularities occurs when the projections of friction contact elements engage in rubbing, when the material of projections (one or both) has a non-homogeneous structure.

Reeling of abrasive grains occurs when abrasive particles of appropriate shape and high compressive strength enter the space (clearance) between mating elements, and then their reeling may occur. It will result in the formation, due to plastic deformation, of micro-valleys with material flashes at the edges. Due to repeated deformation causing fatigue, these flashes are separated in the form of wear particles.

Abrasion is the most common type of wear, accounting for approximately 80÷90% of all tribological wear [15, 65]. It dominates when the friction contact is not lubricated - dry friction, or when the lubrication is insufficient - mixed friction. Under fluid friction conditions, it can occur when the lubricant contains abrasive particles (e.g. dirt or wear products).

Abrasive wear depends on the type, structure and properties of the materials of mating elements, e.g. it is assumed that the wear resistance increases with the increase of hardness [9, 10, 11, 12, 13, 14, 15].

Adhesive wear is the result of breaking the adhesive joints formed at the points of real contact of surfaces at their relative movement. The condition for the occurrence of bonding is the approximation of the mating surfaces to a distance shorter than the range of bond strength between atoms, and the absence of adsorbed or oxide layers with non-metallic bonds [15, 45, 65].

This process occurs at low relative velocities and high unit pressures, with insufficient lubrication - mixed friction, or no lubrication - dry friction.

The principle of oxidative wear consists in the adsorption of oxygen to the friction area and its diffusion into plastically and elastically deformed metal micro-volumes and then removal of oxide layers formed in this way due to friction. Thus, it is a chemical and mechanical form of wear.

Oxidative wear is a predominant process if the speed rate of continuous oxide layers formation and their subsequent removal is faster than other wear processes (e.g. abrasion).

Fatigue wear consists in the destruction of the surface layer of elements as a result of cyclic contact stresses (elastic-plastic). Multiple-cycle contact stresses in SL cause material fatigue and then a local loss of cohesion, which causes the formation and development of micro cracks, and consequently cracks and material losses.

The fatigue process may take place in the entire volume of the element or only in its surface layer. In the first case, there is volumetric fatigue wear, and in the second - surface (contact) wear. In this work elaboration, due to its subject matter, the considerations are limited to the second case.

Surface fatigue wear occurs with the co-action of elastic bodies with straight and curvilinear friction surfaces or with curvilinear surfaces, in point or linear contact, where sliding with rolling friction occurs. [Burakowski at al. 1992; Burakowski, Wierzchoń 1995; Łunarski 1989, Marczak 2002].

The following types of wear can be classified as fatigue wear [9, 10, 11, 12, 13, 14, 15, 45, 65, 75, 76, 77]:

- spalling,
- pitting,
- fretting,
- scuffing.

Spalling is the detachment of scale material as a result of cyclic contact stresses. It occurs when there is no lubrication (dry friction) and sometimes also when there is insufficient lubrication (mixed friction) during turning. This process is usually accompanied by the oxidation of material in the near-surface layer.

Pitting is the destruction of the surface layer as a result of cyclic contact stresses due to the physico-chemical interactions of the lubricant manifested in the form of local material losses.

Fretting (abrasive-corrosive wear) is the destruction of the surface layer in the form of local losses of elements material exposed to vibrations or slight sliding during a to-and-fro motion, as a result of cyclic contact stresses and intense influence of the corrosive environment.

Scuffing (abrasive-adhesive wear) is the combined effect of the abrasive and adhesive wear processes that lead to seizure.

2.3. Lubricants and improvers

Lubricants are substances introduced between co-acting friction surfaces in order to reduce the effects of the wear process, e.g. frictional resistance. Their main task is to eliminate dry friction from rubbing associations. Lubricants are made of a lubricating base, which is a kind of foundation, and improvers. The type of additives and their proportions are determined by the intended use of a given lubricant. The group of improvers includes:

- anti-corrosion additives,
 - corrosion inhibitors,
 - oxidation inhibitors,
 - rust inhibitors,
 - metal deactivators,
- depressants,
- anti-aging additives,
- anti-foam additives,
- lubricity additives,
- dispersing additives,
- washing additives (detergents),

- viscose additives (improving the viscosity index).

In the group of anti-corrosion additives there are four types of additives mentioned above, which -although they belong to the same group - differ in their mechanism of action. Two of them are described below.

Oxidation inhibitors - prevent chain and catalytic oxidation reactions, reduce organic peroxides, inhibit the processes of acid, resin, sediment and sludge formation. They are used more widely than other improvers. Their task is to slow down the breakdown of the base oil by oxidation. They work by decomposing hydroperoxides formed by the reaction of oxygen with hydrocarbons, or free peroxide radicals.

Lubricating oil or plastic grease is in contact with the air oxygen during operation, and the high temperature and catalytic properties of the metal of the friction surface create good conditions for oil oxidation. There are complex oxidation reactions that are autocatalytic. Oxidation products increase the viscosity of the oil, create acidic impurities with corrosive properties, and deposits such as resins, varnishes and polymers. Oxidation inhibitors counteract the formation of the above-mentioned products.

Rust inhibitors - polar particles of these additives which adhere tightly to the metal surface form a water-resistant film; reacting with metal under friction conditions they create a new surface layer, more resistant to wear.

Examples of the types of these chemical compounds are: amine, sodium, calcium phosphates, petroleum sulfonates, alkylated succinic acids, fatty acids, zinc dialkyl diphosphates, tricresylphosphates.

Depressants - they reduce the freezing temperature by surrounding the nuclei of paraffinic hydrocarbon crystals with depressant molecules. During their crystallization, they form closed, lattice three-dimensional structures that adsorb the polymer and form a gel-like mass. Depressants coat small paraffin crystals with a thin film, preventing them from aggregating into larger clusters, thus creating a skeletal structure that obstructs the flow of oil. Depressants do not inhibit the crystallization of solid hydrocarbons but produce extremely small and non-cohesive crystals that do not form large conglomerates. Molecular weights of depressants according to [65] are much smaller than those of viscosity additives, usually in the range of 500 to 100 000 Da.

Anti-aging additives - their task is to stabilize as much as possible the positive properties of the lubricant.

Examples of the types of these chemical compounds: phenol derivatives, phenylamines.

Anti-foam additives - prevent the formation of foam by changing the surface tension. These additives create a thin layer on the surface of the oil not allowing the foam to stay in the oil. Silicone oils are used as anti-foam additives added in the amount of thousandths of a percent.

Examples of the types of these chemical compounds: silicone polymers.

Lubricating additives - under the conditions of friction they decompose and react with the metal creating new compounds (sulfides, chlorides) which are easier to shear than the base metal. They participate in the widest range of tribochemical reactions among all improvers. These improvers are divided into:

- a) anti-seize,
- b) anti-wear,

c) friction modifiers.

Anti-seize additives, called EP (Extreme Pressure) additives, are organic chemicals that counteract excessive wear of the friction surface during lubrication. These additives contain one or more heteroatoms in their molecule, such as sulfur, phosphorus or chlorine. The carboxyl group also has anti-seize functionality, be it in acid or salt form. All these compounds, under severe boundary and mixed friction conditions react with the metallic surface of the friction to form a simple inorganic compound. The formed inorganic compounds (sulfide, phosphate, thiophosphate, chloride) have a shear strength lower than that of metal and prevent the adhesive bonding of the friction surface (welding of the frictional contact surface).

Chemical compounds that effectively act as EP additives are sulfurized: fats, hydrocarbons, methyl esters of unsaturated fatty acids and terpenes. They also include aliphatic and aromatic silylphides, organic phosphites and phosphates, ammonium phosphates, phosphorus sulfurized hydrocarbons, dialkyl(aryl)dithiophosphates and dialkyl dithiocarbamates of metals as well as chlorinated paraffins, chlorosulfurized fatty oils and lead naphthenate.

Sulfurized chemicals have sulfide bonds in their molecule that consist of one or more sulfur atoms. They include mono-, di-, tri- (and more) sulfides. With an increase in the number of sulfur atoms in the sulfide bond above two, the chemical reactivity of these substances with the friction surface increases significantly and they become corrosive. As a result of sulfurization of hydrocarbons, sulfur bridges are formed in the compound molecule.

Among organic disulfides, the best EP properties are shown by dibenzyl disulfide, and anti-wear properties - by diphenyl disulfide.

Synthetic oil of the phosphoric acid ester with phenols is also used as an anti-wear EP additive.

Phosphites are also used as anti-seize additives. Good anti-seize additives are also multifunctional additives - lead or antimony dialkyl dimithio carbamates.

Anti-wear additives reduce the wear of the friction surface under moderate loads. The most widely used are zinc dialkyl (aryl)-dithiophosphates, tricresol phosphates, phosphates, thiophosphites, sulfurized hydrocarbons, zinc dialkyldithiocarbamates and thioxomolybdenum dual core complexes.

Anti-wear additives in contact and reaction with the metal of the friction surface create adsorption layers and reactive compounds, reduce frictional resistance, as a result of which wear is also reduced.

Additives reducing the friction factor work by increasing the durability of the physically adsorbed surface layer. High-polar additive particles are adsorbed on the friction surface and remain there during the friction process, preventing metal-to-metal contact. The additives reducing friction (friction modifiers) include mainly fatty acids and amines, fats and some dithiophosphate salts, N-acylsarcosides and their derivatives, mixtures of organophosphoric and fatty acids.

Examples of the types of these chemical compounds: sulfurized vegetable or animal oils, chlorinated hydrocarbons, lead salts of organic acids, chlorinated sulfur, fatty acid esters, phosphorus compounds [61, 62, 63, 65].

Dispersing additives - they inhibit the formation of sludge, surround dirt particles, prevent their agglomeration and separation. These additives have good dissipating (dispersing) properties. Their molecules, like detergents, consist of a long hydrocarbon chain ensuring good solubility of the additive in the oil to which a polar group is attached. The polar group contains one or more nitrogen, oxygen, and sometimes phosphorus heteroatoms, it is metal free and thus

these additives are ashless. Most widely used are additives with a nitrogen heteroatom, such as alkyl mono- and bis-succinimides.

The dispersing additives, by adsorbing with a polar group on the surface of the solid oil contaminants, prevent them from aggregating into larger agglomerates and thus create their permanent suspension.

Examples of the types of these chemical compounds: succinimides, methacrylates, nitrogen-containing polymers, polymethacrylates, high-molecular amines, amides, barium, calcium sulfonates.

Washing additives (detergents) - they regulate the processes of sludge agglomeration, prevent sludge accumulation, keep them, e.g. in the form of suspension. They are organic compounds with surface-active properties. Detergents used in oils reduce their surface tension and decomposition temperatures of some improvers. They are also anti-wear additives and rust inhibitors, and sodium salts are used as emulsifiers of oil in water in the production of cutting-tool lubricants.

The chemical structure of washing additives is typical for surface-active agents. A detergent molecule consists of a hydrophobic long hydrocarbon chain and a polar end of the molecule.

The most commonly used washing additives are neutral and basic metal sulfonates and phenates (calcium and magnesium).

Additives improving the viscosity index (viscose additives) - their task is to reduce the influence of temperature on viscosity change.

All viscosity additives are macromolecular compounds. The most common are:

- polyisobutylenes;
- polymethacrylates and polyacrylates (esters of alcohols with 4 to 8 carbon atoms in the molecule);
- olefin copolymers (ethylene-propylene copolymers, ethylene, propylene and hexadiene copolymers);
- polystyrene;
- styrene-diene copolymers.

At low temperatures, the helically twisted polymer molecules are suspended in the oil and are in a colloidal state. At higher temperatures they dissolve in oil and their chains are stretched to their full length. This increases the additive-oil contact surface, inhibiting the mobility of the oil and increasing the internal friction between its particles, which increases the viscosity and viscosity index.

The effect of viscosity additives depends on their content in the oil, the molecular weight and the properties of the base oil. The molecular weight of the additives is in the range 50 000÷1000 000 Da. As the molecular weight of the additive increases, the efficiency of increasing the oil viscosity index grows, while its shear resistance decreases. The reduction of dimensions of polymer molecules as a result of their shear and the presence in frictional contact of:

- oxidation processes,
- increased temperature,
- hydrolysis,

worsens the properties of the additive. Therefore, some polymers, as viscous additives, are used in the presence of other additives that increase their chemical stability.

Copolymers containing carboxyl ester groups and one or more polar groups, such as:

- amide,
- ether

- hydroxy,
- amine,
- epoxy,
- phosphoroester,
- carboxylic acid,
- carboxylic - anhydride or nitrile,

have dispersing and viscous properties. Viscous additives can also lower the solidification point of metal [61, 62, 63, 65].

2.4. Lubricant agents

In the operation of test rigs and equipment efforts are made to ensure that friction contacts operate in the conditions of fluid friction or at least boundary friction.

Lubricants - commercial oils, despite their numerous advantages, which include the ability to remove heat and wear products from the friction zone, damping vibrations, protection against corrosion and others, do not solve the problems of lubrication under conditions of extreme loads or temperatures, do not eliminate the so-called cold start (cold start of the engine, transmission, friction contact). Thus, the idea arose to introduce with oil, into a given friction contact, a lubricant agent (AGE) which could alleviate such conditions by improving the quality of the boundary layer capable of carrying higher loads and being resistant to breaking. AGE is a complex substance in its structure. It usually contains an oil base with a complex of various additives, incl. lubricating, anti-aging and others [9, 10, 11, 12, 13, 14, 15, 50, 51, 58, 113, 114, 174]. The mechanism of AGE action can be broadly presented as follows. AGE particles are transported by the liquid lubricant to the friction contacts where as a result of the adsorption process - physical or chemical they permanently bond with the metallic surfaces co-acting with each other. A new lubricating film or a replacement boundary layer is thus formed on the surfaces of the friction contact. In the case of under-lubrication at the points of local contact of metallic surfaces, AGE particles take over the role of the lubricating film. At this point, the friction factor is rapidly reduced to the values characteristic for fluid friction. The effectiveness of interaction of the substitute boundary layer in the micro-contact areas of the mating surfaces depends on the intensity of the adsorption processes in the micro-contact areas. The model of a friction contact with the use of AGE is shown in Fig. 2.11.

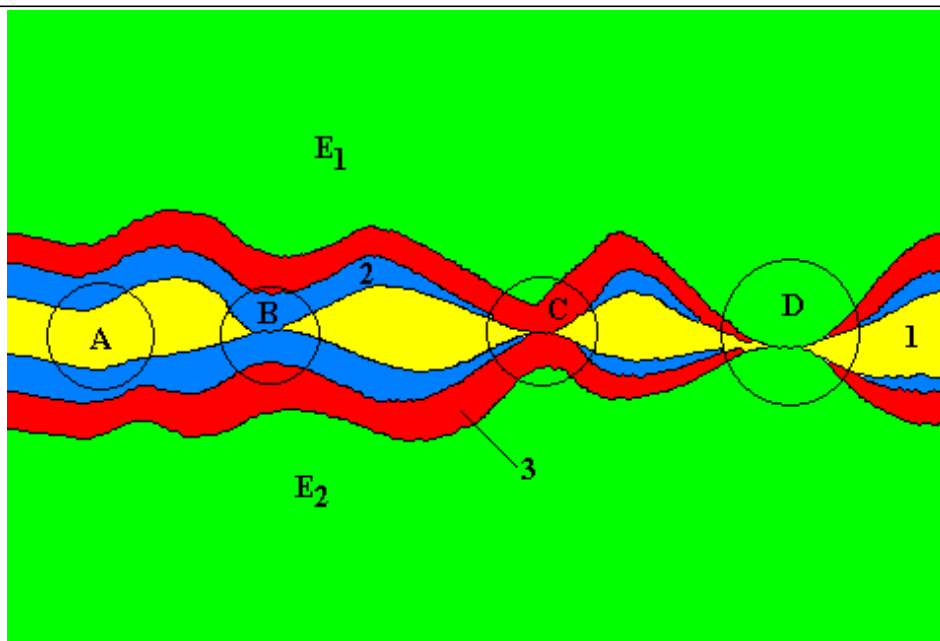


Fig. 2.11. Model of a friction contact with the use of lubricant agents:
 E1, E2 - elements of the friction contact; 1 - lubricant enriched with an agent, 2 - proper boundary layer (created as a result of using a lubricant), 3 - substitute boundary layer; A - fluid friction phase, B - boundary friction phase, C - boundary friction phase with the participation of a substitute boundary layer, D - dry friction phase [62, 63]

Due to the fact that CON have different mechanisms of action they can be classified according to this mechanism. In the work [63] the author divides them into three main groups:

- of a chemical action,
- containing in its composition specific particles of solid lubricants such as Teflon, soft metals, graphite and others,
- enabling the formation in the friction contact of the so-called selective transfer lubrication (SEL).

2.4.1. Preparations of a chemical action

These preparations include compounds containing, among others sulfur, chlorine, additionally enriched with oxygen, zinc, boron and selenium. They react with the metallic substrate. Due to the diffusion of the components of these additives into the surface layer, protective layers of phosphates, sulphides, etc. are formed on the metal surface. In this way obtained is both a 'strong' oil boundary layer due to chemisorption, and additional protection in the form of a diffusion layer. The surface layer formed in this way which is regenerating during the operation of the friction contact, is characterized by high resistance to the transmission of mechanical loads, a reduced coefficient of friction and increased resistance to wear (seizure). The model of the friction contact lubricated with oil containing AGE additive of a chemical action is shown in Fig. 2.12.

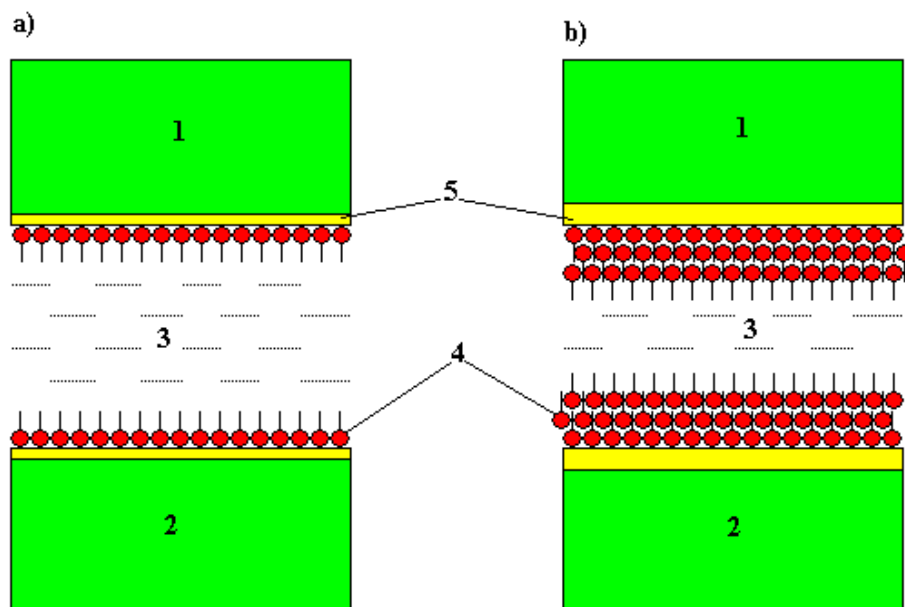


Fig. 2.12. Model of the friction contact lubricated with: a) base oil, b) oil enriched with an agent of a chemical action; 1, 2 - rubbing elements, 3 - lubricant, 4 - boundary layer formed as a result of physical sorption, 5 - boundary layer formed as a result of chemisorption [62, 63]

2.4.2. Preparations with particles of solid lubricants

Solid lubricants include inter alia graphite or molybdenum disulfide, the structure and operation of which are discussed below. Due to the difficulties of their effective application, these substances are most often used in preparations as lubricating additives.

Graphite is an example of a structure in which there are bonds of various types. The existence of strong covalent bonds between the carbon atoms in the layers and weak - metallic bonds between the layers facilitate sliding in the graphite cohesion planes - Fig. 2.13.

The essence of graphite lubrication is explained by two theories: structural and adsorption. Structural theory attributes lubricating properties to the layered lattice structure, while the adsorption theory attributes them to lubricant adhesion to the metal surface. The presence of large distances between the layers of carbon is the cause of a weak interatomic interaction (low van der Waals forces). As a result of this facilitated is the mutual displacement of these films in the crystals along the slip planes (structural theory). At the same time graphite shows good lubricating properties due to water adsorption. The adsorbed water molecules on the main slip planes reduce the adhesion between them and thus reduce the friction coefficient during their movement (adsorption theory). However, it should be assumed that good lubricating properties are obtained when both conditions are met, i.e. the lubricant has a layer structure and, moreover, it has good adhesive properties.

Molybdenum disulfide also has a layer structure. There are three-layer packages - layers of molybdenum atoms and two layers of sulfur. The existence of strong covalent bonds between Mo - S atoms and weak (van der Waals) bonds between S - S sulfur atoms allows for an easy slide of sulfur-sulfur layers. The lubricating mechanism of molybdenum disulfide is similar to that of graphite. The difference is that the formation of a thin film adhering directly to the metal surface occurs not only as a result of physical adsorption but also chemisorption caused by the chemical reaction of sulfur ions with metal atoms. After this layer is formed, the cavities are then filled in with molybdenum disulfide molecules until a slip occurs between the MoS₂ layers.

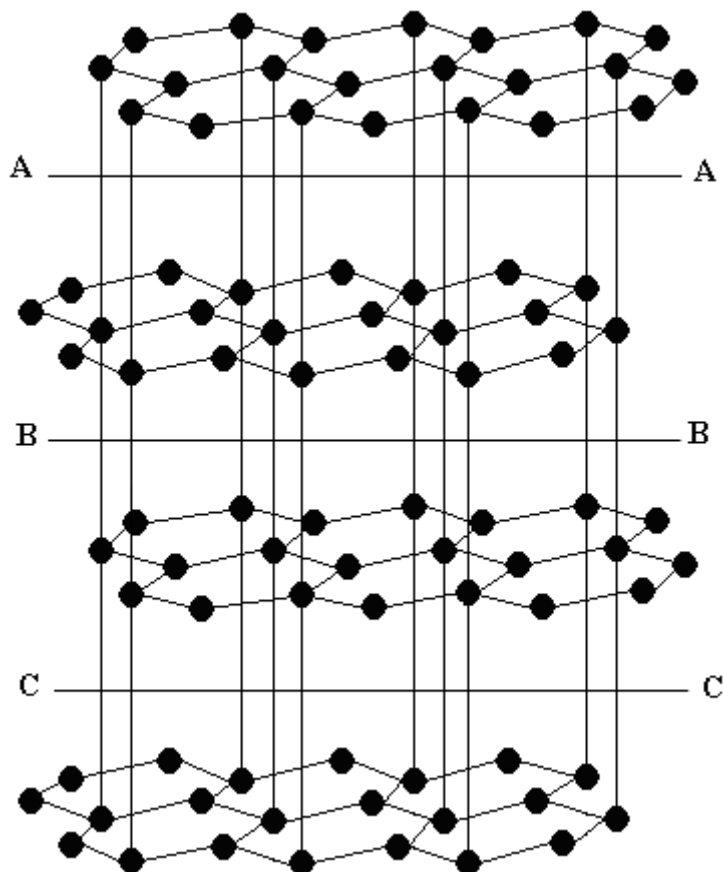


Fig. 2.13. Graphite structure, A-A, B-B, C-C - traces of slip planes [61]

The reduction of friction and wear of mating surfaces can also be obtained by introducing into the friction contact spherical particles of Teflon (PTFE) - a solid lubricant with low internal cohesion. PTFE may be permanently positively electrically charged or it may be electrically neutral. In the first case, as a result of electrostatic interaction, PTFE preparations are attracted to a metal surface and a physico-chemical bond between PTFE and metal occurs. PTFE particles, adsorbed in the form of films on the surface of metals, usually have larger sizes than the micro-irregularities of these surfaces of elements. When the distance between the surfaces of the mating elements is reduced, the PTFE particles are rolled. The so-called 'filling' of the surface takes place. The resulting layers have a very high adhesion to the mating surfaces.

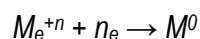
In the second case - when the PTFE particles are electrically neutral - observed is the lack of ability to form metal layers on the mating surfaces of the previously described durability.

2.4.3. Preparations enabling lubrication on the basis of the so-called selective transfer (SEL)

The selective transfer effect is based on a tribological phenomenon as a result of which a plastic, thin, non-oxidizing film, with a specific structure, is formed on the friction surfaces. It is produced when there is no fluid friction in the friction contact under given conditions, and yet the value of the friction coefficient and the wear intensity decrease by 2÷3 orders.

The essence of the selective transfer mechanism is explained by two hypotheses:

- a mechanism based on micro-adhesive bonding of soft metal particles with the friction surface of hard metal. In the initial stage, the formed protective layer has a soft metal composition. This composition may change if conditions favoring the selective transfer process are created. The film may be enriched with cathode components as a result of selective dissolution of, e.g. copper, when its alloys are the soft metal [61, 37];
- the mechanism according to which the formation of a metallic protective layer is the result of an electrochemical process such as:



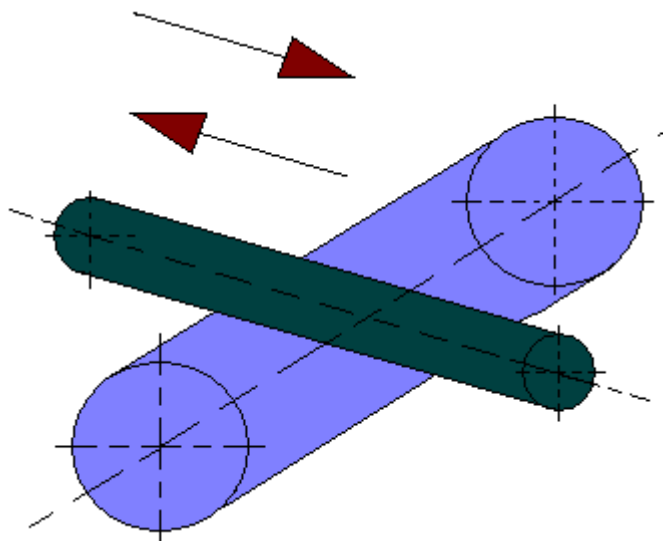
The formed film contains only one metal introduced in the form of a metallizing additive to the lubricant or applied to the friction surface as a result of the reaction of the components of the lubricant with the surface containing this metal - in the form of alloy components, coating or films. In the case of copper alloys - copper is transferred [61, 75, 76, 77, 37].

3. TYPES OF COMBINATIONS OF FRICTION CONTACTS

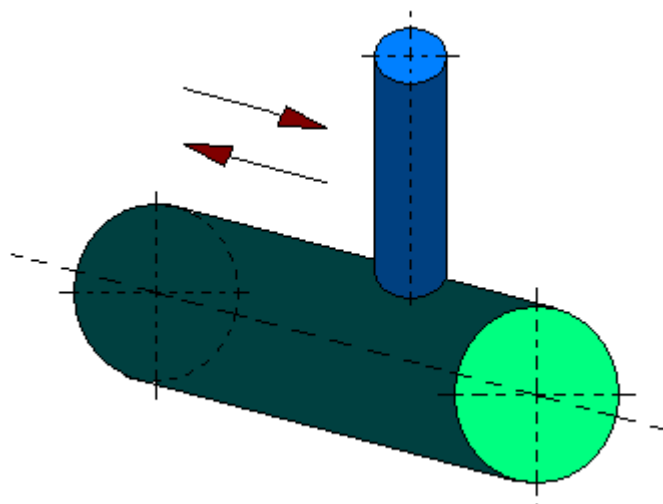
The number of types of friction test rigs in the world today can be around one thousand. This number is constantly growing due to the great interest in this subject. Some of them are commercial test rigs, some are original non-commercial test rigs. However, the main types of combinations of friction contacts are only a dozen, which are presented below, based on ÖNORM M 8122 (Austria).

1. Point contact, reciprocating movement

1.1. Cylinder/cylinder (outside); ÖNORM M 8122 designation CCE - *cylinder/cylinder* (extern)

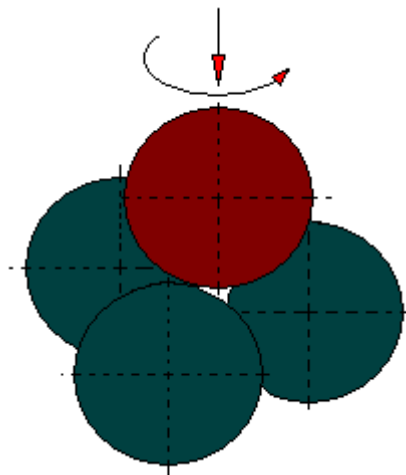


1.2. Cylinder/cylinder; ÖNORM M 8122 designation SC - *sphere/cylinder*

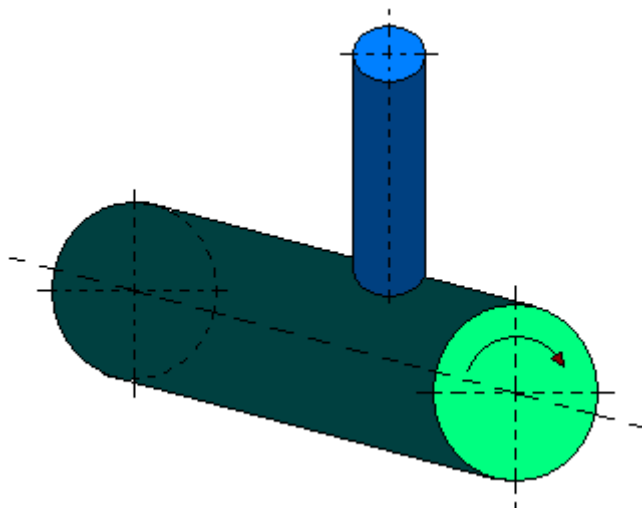


2. Point contact, continuous movement

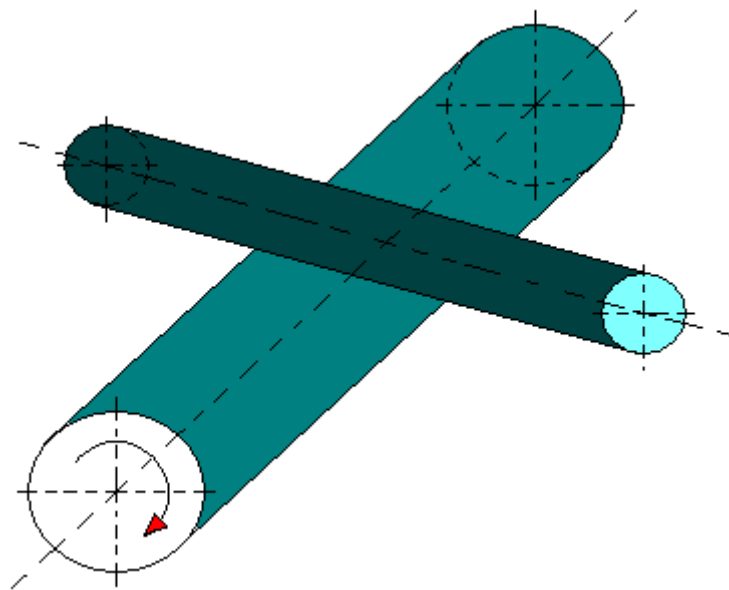
2.1. Sphere/sphere; ÖNORM M 8122 designation SS - sphere/sphere



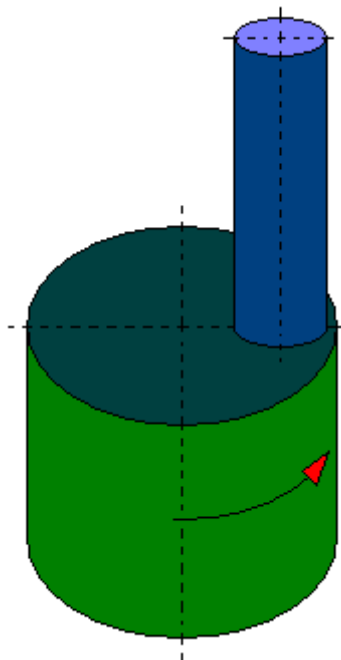
2.2. Sphere/cylinder; ÖNORM M 8122 designation SC - sphere/cylinder



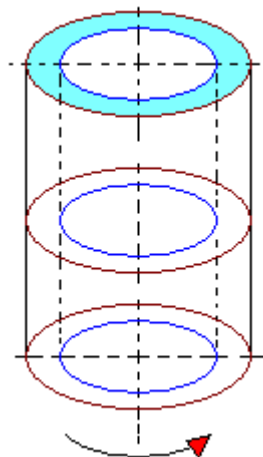
2.3. Cylinder/cylinder (outside); ÖNORM M 8122 designation CCE - cylinder/ cylinder (extern)



2.4. Sphere/plane; ÖNORM M 8122 designation SP

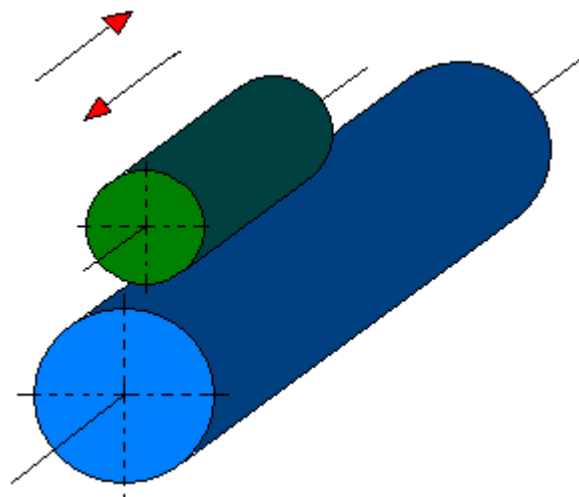


2.5. Ring / ring; ÖNORM M 8122 designation RR

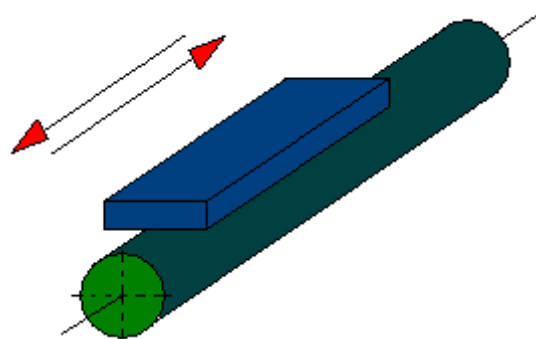


3. Line contact, reciprocating movement

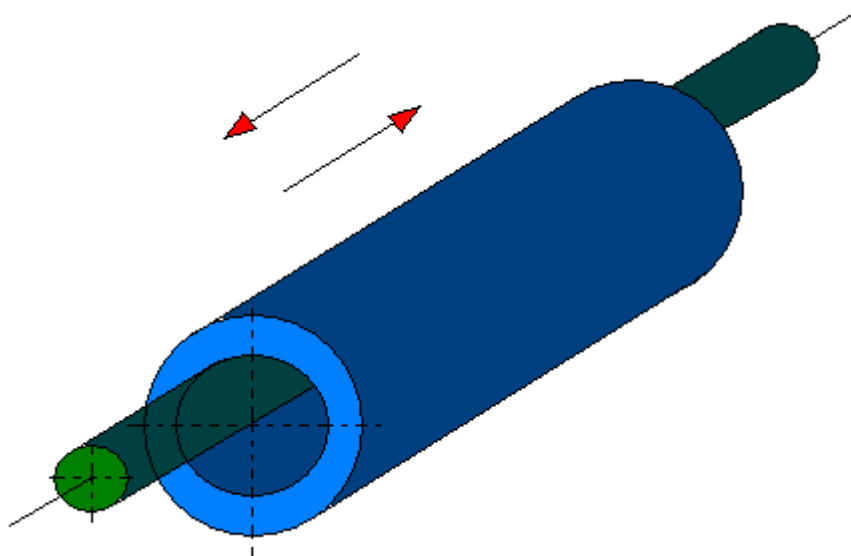
3.1. Cylinder / cylinder (outside); ÖNORM M 8122 designation CCE - cylinder/cylinder (extern)



3.2. Plane/cylinder; ÖNORM M 8122 designation PC

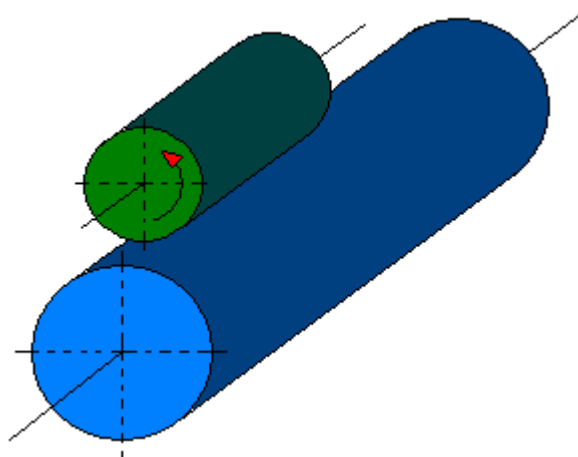


3.3. Cylinder/cylinder (inside); ÖNORM M 8122 designation CCI - cylinder/cylinder (intern)

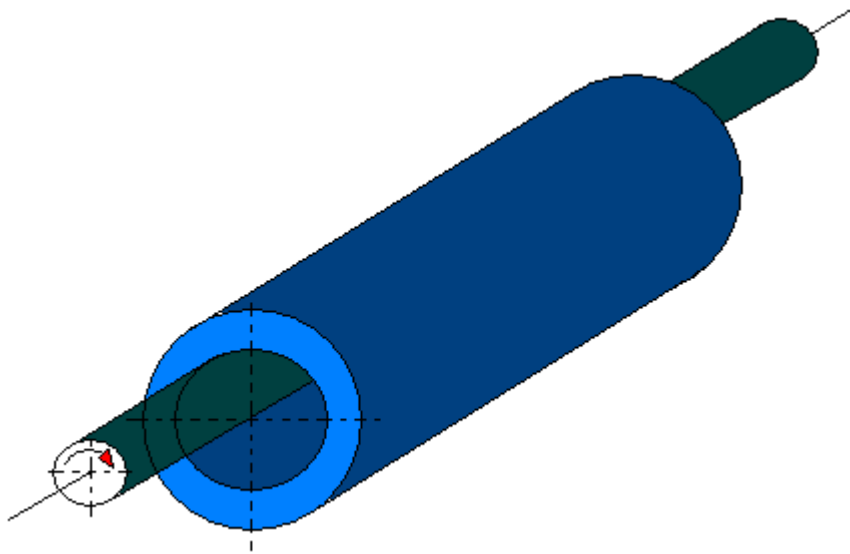


4. Line contact, continuous movement

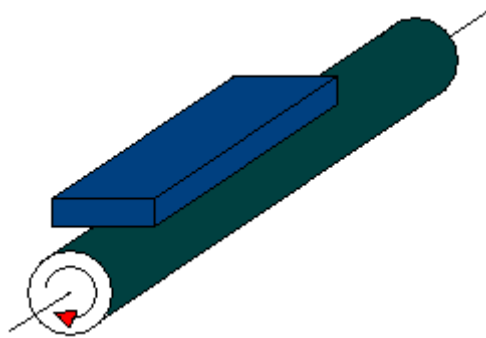
4.1. Cylinder/cylinder (outside); ÖNORM M 8122 designation CCE – cylinder/cylinder (extern)



4.2. Cylinder/cylinder (inside); ÖNORM M 8122 designation *CCI* – cylinder/cylinder (*intern*)

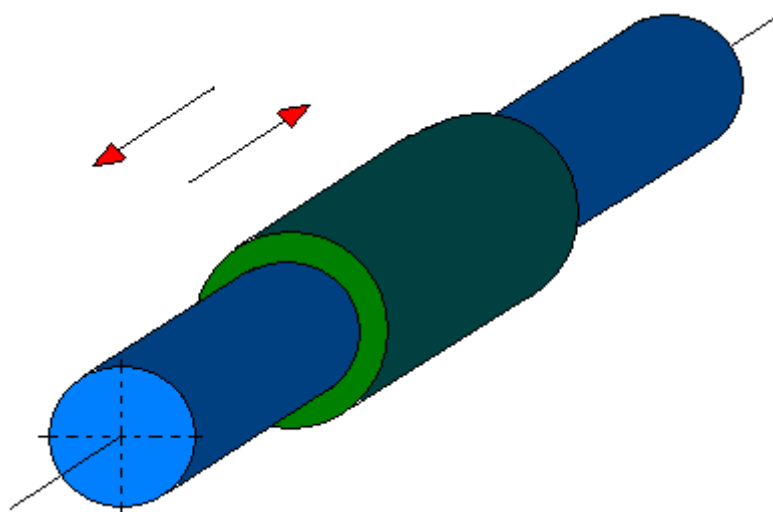


4.3. Plane/cylinder; ÖNORM M 8122 designation *PC*

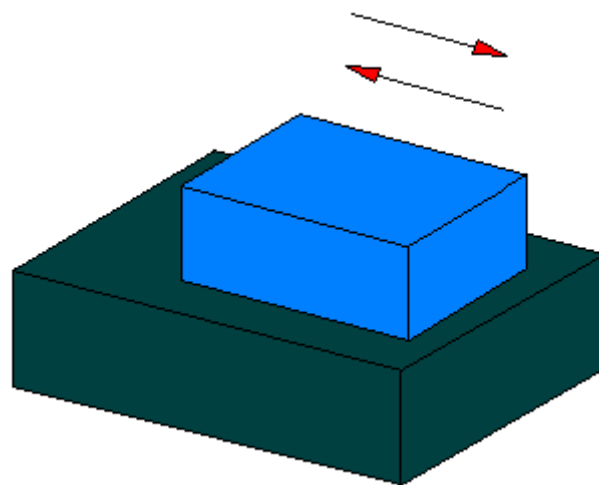


5. Surface contact, reciprocating movement

5.1. Cylinder/cylinder (inside); ÖNORM M 8122 designation *CCI* – cylinder/cylinder (*intern*)

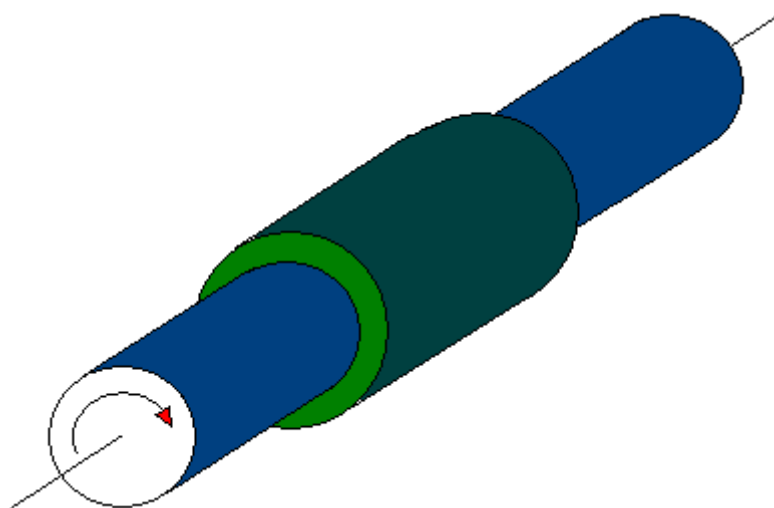


5.2. Plane /plane; ÖNORM M 8122 designation PP

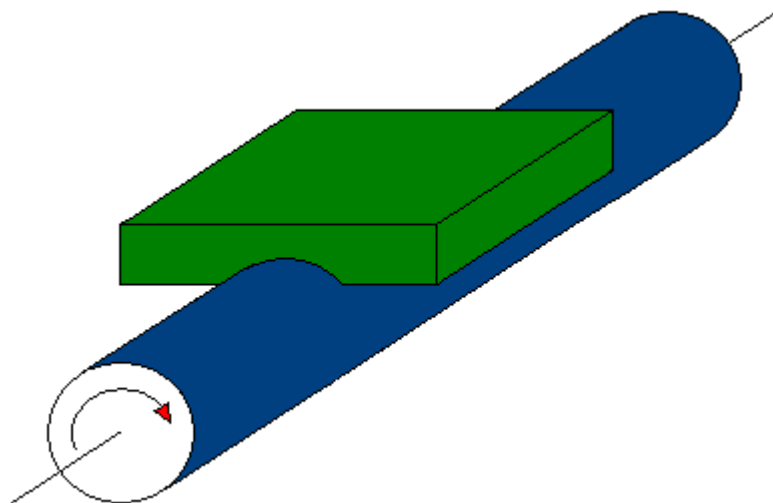


6. Surface contact, continuous motion

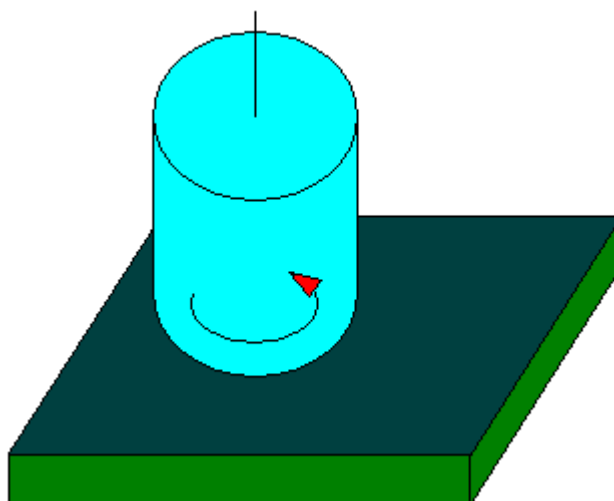
6.1. Cylinder/cylinder (inside); ÖNORM M 8122 designation CCI – cylinder/cylinder (intern)



6.2. Cylinder/cylinder (inside); ÖNORM M 8122 designation CCI – cylinder/cylinder (intern)



6.3. Plane /plane; ÖNORM M 8122 designation *PP*



4. TRIBOLOGICAL TEST RIGS

Presented below is the structure, operation and intended use of tribotesters, mainly non-commercial ones. These tribotesters can be found in many Polish research centers, mainly universities and polytechnics.

Tribological test rigs are divided in the following way (Fig. 4.1). If it is possible to perform tests on a given rig only for sliding pairs, then these rigs are included in group 1. If it is possible to perform tests on a given rig only for rolling pairs, then these rigs are included in group 2. If it is possible to perform tests on a given test rig for both sliding pairs and rolling pairs, then these rigs are included in group 3 (universal rigs).

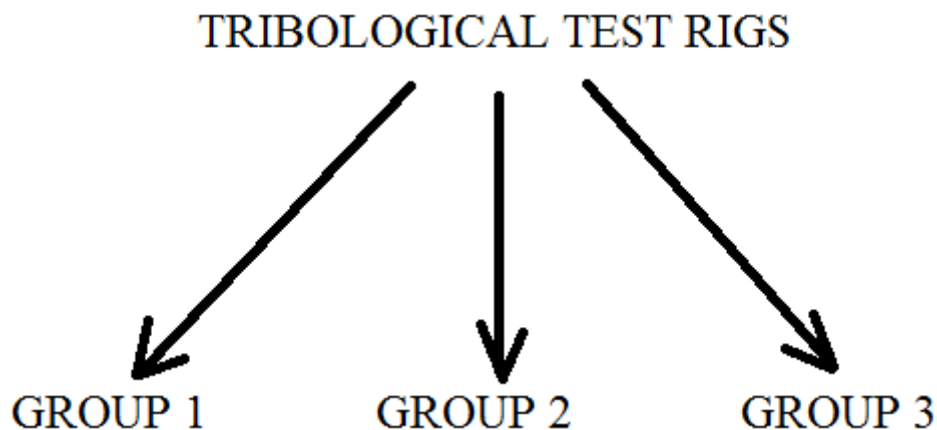


Fig. 4.1. Division of tribological test rigs according to pair combinations

4.1. Group 1 (sliding pairs)

4.1.1. 77MT-1 test rig

The 77MT-1 test rig is used to carry out tribological tests simulating the co-action of a pair: sleeve-piston ring of the combustion engine. This test rig can also be used to test the constituting process of the working surface layer (WSL) during a reciprocating motion.

The drive of the 77MT-1 tribotester is an electric motor 12 connected to the reducer by a clutch 11. The rotational motion of the engine is converted into a reciprocating motion by means of a crank system 9 connected by catches 8 with a working slide 3. The counter-sample 2 is attached to the working slide. The reciprocating motion is performed by the counter-sample which is co-acting with the stationary sample 1. The sample 1 is fixed in the holder of the heating element 14 and pressed against the counter-sample 2 by means of a spring. The pressure on the spring is exerted by the load lever 7 on which the variable load 15 is suspended. The tribotester is additionally equipped with a lubricator 13. Thanks to this, it is possible to carry out wear tests with different oils and with different additives to them. During the tests sample 1 and counter-sample 2 are immersed in the lubricant reservoir 16. By changing the gear ratio of the reducer it is possible to change the relative velocity of the mating elements. Adjusting the temperature of the heating element 14 makes it possible to make the test conditions resemble the actual operating conditions, e.g. in the combustion engine. Figure 5.1.1.1 shows the kinematic diagram of the 77MT-1 friction test rig. This test rig does not enable current archiving and visualization of data collected from this test rig.

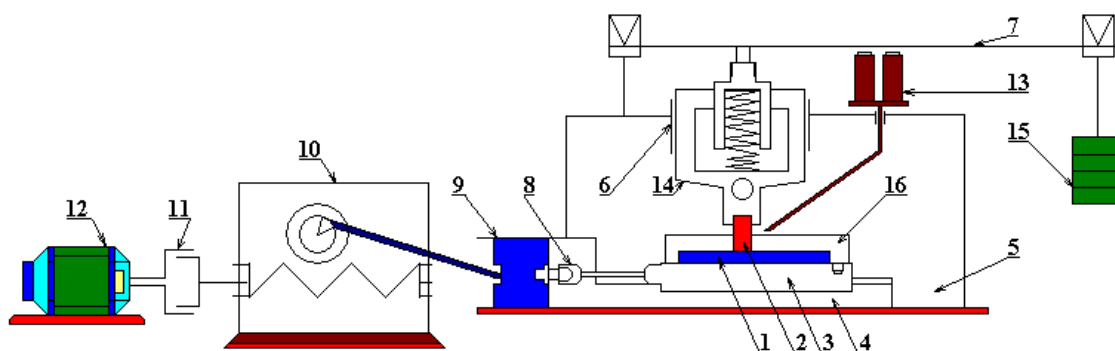


Fig. 4.1.1.1. Kinematic diagram of the friction test rig 77MT-1

1 - sample, 2 - counter-sample, 3 - working slide, 4 - guide, 5 - head, 6 - working cylinder, 7 - load lever, 8 - catch, 9 - crank system, 10 - reducer, 11 - clutch, 12 - drive motor, 13 - lubricator, 14 - heating element, 15 - weight, 16 - lubricant reservoir [77]

The 77MT-1 friction test rig is not a commercial test rig, and the reason for its creation was the need to conduct research on the sleeve-piston ring friction contact type of combustion engines.

4.1.2. Tribological test rig for testing the effect of vibration on a lubricant

The operation of test rigs and mechanisms is usually accompanied by vibrations which are components of the load on friction contacts. The vibrations transform the physico-chemical and mechanical characteristics of materials and reveal a significant influence they have on the operation of the tribological connection. The nature and degree of this influence depends mainly on the type of friction contact, type of lubricant, lubrication system, kinematic factor and others. The research on vibro-resistance of lubricants used in friction contacts is the main topic of a complex problem of the influence of vibrations on lubricating materials and the longevity of friction contacts. Presented below (Figure 4.1.2.1) is a test rig for testing the impact of vibrations on the operation of lubricants described in [82]. The surface of the inner ring of the bearing 1 is covered with the tested lubricant 6. This ring is fixed on a support, a pin 2, which in turn is rigidly connected to the vibrator table 3 by means of fixing screws 8. And the outer ring 4 of the bearing is mounted in the body 5 of a 1 kilogram weight. The tested lubricant in the form of a thin film is distributed between rings 1 and 4.

The test rig allows to carry out tests at a vibrating motion with frequency regulation every 1 Hz in the range from 0 to 200 Hz, with a turning angle of $\pm 30^\circ$ and a radial load on the bearing up to 10 000 [N].

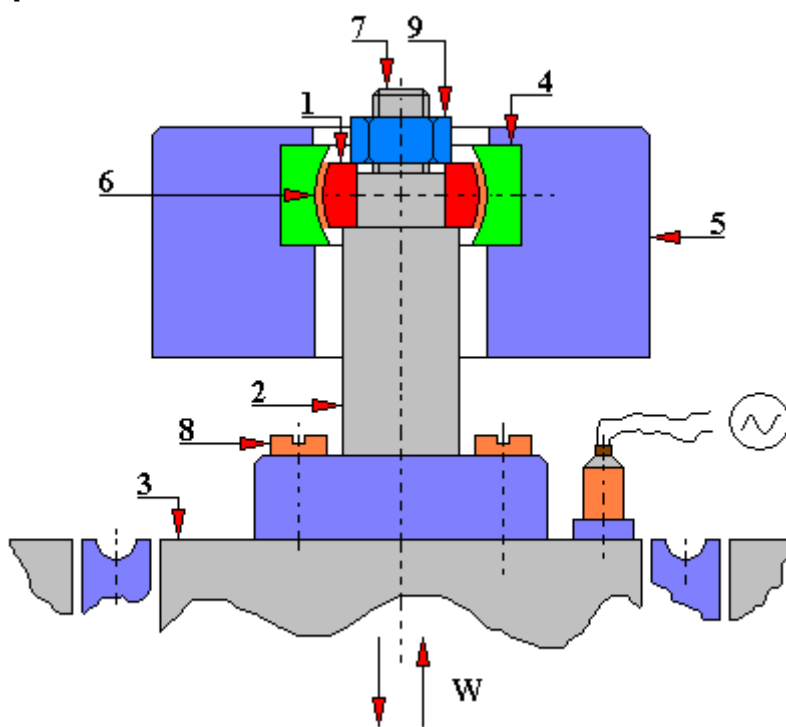


Fig. 4.1.2.1. Diagram of the test rig for vibro-machining of the friction contact with or without lubrication

1 - sample, 2 - pin, 3 - vibrator table, 4 - counter-sample, 5 - body of 1 kg weight, 6 - lubricant, 7 - threaded end of the pin, 8 - fixing screw, 9 - nut, W - vibration direction [82]

Generally, this tribological test rig is intended to define:

- changes in the degree of dispersion of the lubricant as a whole;
- changes in the mobility degree of the tested friction contact;
- changes in color and consistency of the lubricant;
- changes in the migration activity of components making up the tested lubricant;
- the volume of separation of base oil from improvers;

- evaluation of the resistance of the tested lubricant to vibrations.

It is also possible to test on this test rig the influence of vibrations on the friction contact without the use of a lubricant.

4.1.3. Falex test rig with the roller-vee blocks pair

Test rigs of this type are designed to measure the durability of the oil layer between the friction elements as well as to measure the value of the pin wear and the value of the coefficient of friction. The diagram of co-action of the tested elements of the Falex test rig is shown in Figure 4.1.3.1. Rotary motion is performed by a shaft (pin). And V-blocks undergo a compression. The contact with this pair is immersed in the tested fluid. The angle of the V-block is:

- $90^\circ \pm 0.5^\circ$ acc. PN-75/M-04308 or
- $96^\circ \pm 1^\circ$ acc. ASTM D 2625-83, ASTM D 2670-81, ASTM D 3233-73.

The roughness parameter R_a of a V-block sample and a cylindrical sample is, however:

- $0.63 \mu\text{m}$ acc. PN-75/M-04308 or
- $0.13 \div 0.25 \mu\text{m}$ acc. ASTM D 2625-83, ASTM D 2670-81, ASTM D 3233-73.

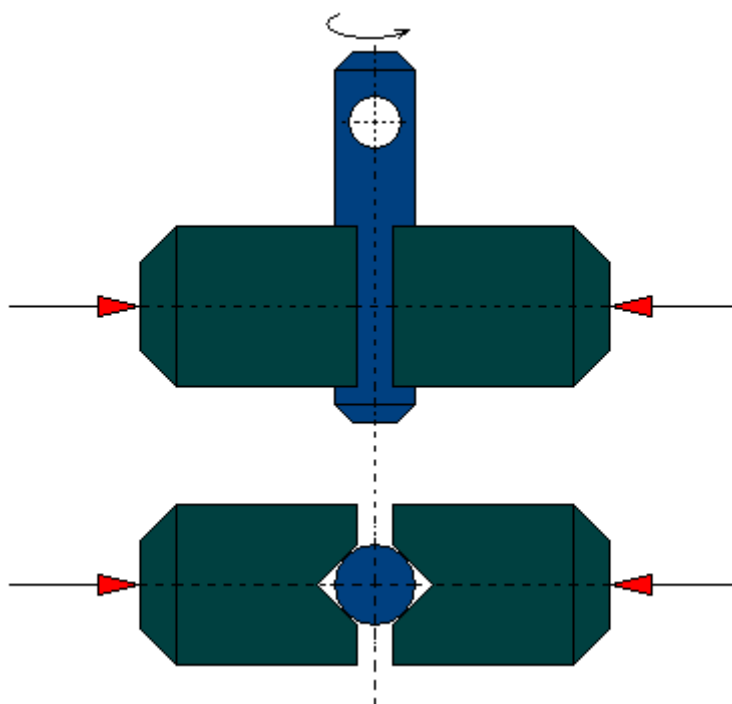


Fig. 4.1.3.1. The friction contact roller-vee blocks used, inter alia, in the Falex test rig and the T-09 tribotester

Two jaws (V-blocks) are pressed against the rotating pin (shaft) with a force from 0 to 20400 [N]. The rotational speed of the shaft is constant and equals to 300 [rpm]. This speed corresponds to the friction speed of 0.1 [m/sec]. The rubbing surfaces are lubricated with the tested lubricant composition. The durability of the layer is tested gradually by increasing the load pressing the rubbing elements.

The test of resistance to wear by metal friction can be performed on the Falex test rig according to the standard PN-75/M-04308 or according to ASTM D 2670-81 standard. *Measuring Wear Properties of Fluid Lubricants (Falex Pin and Vee Block Method)*.

Testing the lubricating properties of fluids in concentrated linear contact on the Falex test rig is also the object of the American standard ASTM 3233 which defines two test methods. Both of these methods consist in determining the load for which seizure of the friction contacts of the object immersed in the tested fluid will occur with increasing load on the samples. The first method provides for a linear increase in load, while the second method provides for a stepwise

increase in load by a constant value (1112 N every 1 minute). The seizure force value is the result of this test. If seizure does not occur, then the test result is the highest sample load value.

4.1.4. Timken test rig

A Timken test rig is a test rig which, depending on the friction contact used, can be either a roller-block test pair or a ring-block pair, and belongs to the group of test rigs with linear, concentrated or distributed contact, depending on the shape of the block, used among others for scuffing tests, assessment of lubricating properties of lubricants in, for instance, a concentrated linear contact. In Poland the methods of assessing lubricants on this test rig are standardized and they are included in the standard PN-86/C-04073 *Przetwory naftowe [Petroleum products]. Badanie własności smarnych olejów i smarów metodą Timkena [Examination of lubricating properties of oils and greases by Timken method]*. A general view of Timken test rig is shown in Figure 4.1.4.1. And Figure 4.1.4.2 shows the roller - block friction contact with a distributed contact. And the types of friction contacts applied in this test rig are shown in Figure 4.1.4.3. Figure 4.1.4.4 shows a diagram of a Timken test rig lever, and Figure 4.1.4.5 presents a cross-section of this test rig.

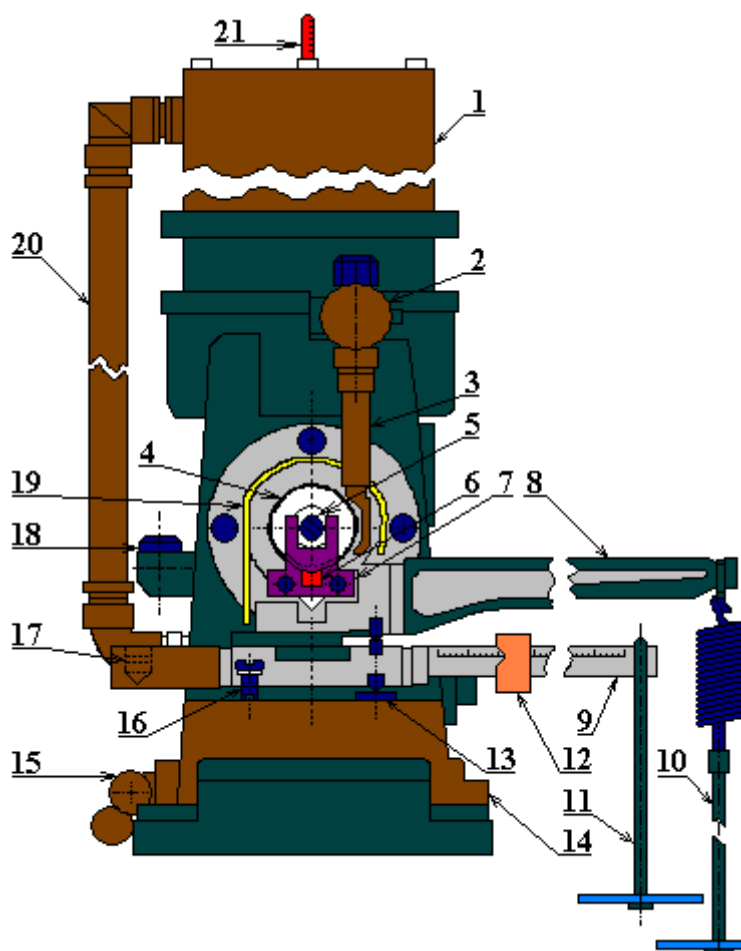


Fig. 4.1.4.1. Timken test rig. General view

1 - oil tank, 2 - three-way valve, 3 - stub pipe supplying oil or grease to the friction contact, 4 - test ring, 5 - locknut, 6 - test block, 7 - block holder, 8 - main lever, 9 - measuring lever, 10 - spring holder with the main lever pan, 11 - measuring lever pan, 12 - sliding weight, 13 - cross support, 14 - drip pan, 15 - hose connecting the drip pan with the pump, 16 - stop screw, 17 - liquid level, 18 - oil level control screw in the driveshaft bearings, 19 - cover, 20 - pipe connecting the pump with the oil tank, 21 - thermometer.

The essence of the assessment of the lubricating properties of lubricants tested on the Timken test rig consists in introducing the tested product (oil, grease) into the friction contact and performing test runs with successively changing set loads until changes occur on the rubbing surfaces of the test elements which indicates a break of the lubricating film. The conditions under which the test runs are carried out are specified in detail in the standard PN-86/C-4073.

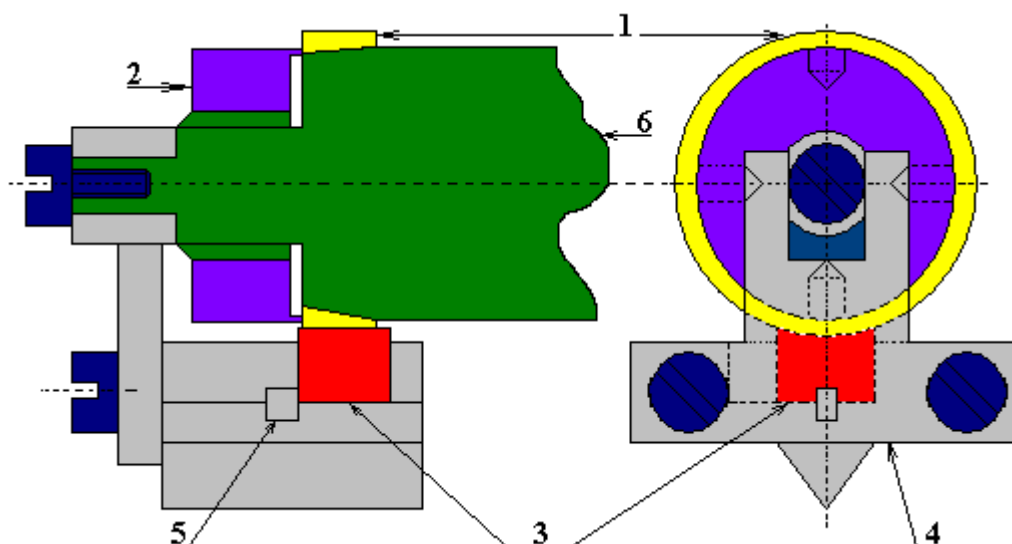


Fig. 4.1.4.2. Timken test rig. Roller-block friction contact with distributed contact.
1 - test ring, 2 - locknut, 3 - test block, 4 - block holder, 5 - wedge, 6 - drive shaft

The test rig is powered by an electric motor driving the shaft of the test rig. A test ring which performs a rotary motion is mounted on the shaft. The test ring mates with a stationary test block fixed to the holder. Between the mating surfaces, oil or grease is fed to the friction contact through a stub pipe. The amount of lubricant supplied is regulated by a three-way valve. The pressing force of the test block against the rotating test ring is regulated by means of the main lever. This test rig does not enable current archiving and visualization of the data collected from this test rig. The test elements on this test rig, as already mentioned above, are a ring and a block measuring 12.7 mm x 12.7 mm x 19 mm which are made of steel with hardness of $60 \div 62$ HRC. The rotational speed of the ring can be 500 rpm, 750 rpm, 1000 rpm or 1500 rpm. The corresponding sliding velocities of the friction contact are then 0.92 m/sec, 1.37 m/sec, 1.84 m/sec or 2.74 m/sec. The plate is pressed against the rotating ring with a force in the range $50 \div 1000$ [N]. The friction surfaces are coated with a lubricant in which the bearing is immersed. The measure of lubricity of the tested oil (grease) is the wear (loss) of the block material in a given test period. On this test rig measured simultaneously is the value of the moment of friction and on this basis conclusion is made about the durability of the lubricating layer. The obtained results can be used for a preliminary evaluation of the oil used, e.g. for lubrication of gears. Much more accurate test results for the quality of oil used, for example, to lubricate a gear transmission, are obtained on special test rigs that reflect the operation of a given gear transmission, such as SBOP test rig. The Timken test rig is one of the first tribotester test rigs, therefore, its equipment and adjustment possibilities are limited as for nowadays. Despite all this, its design or variations have many followers today.

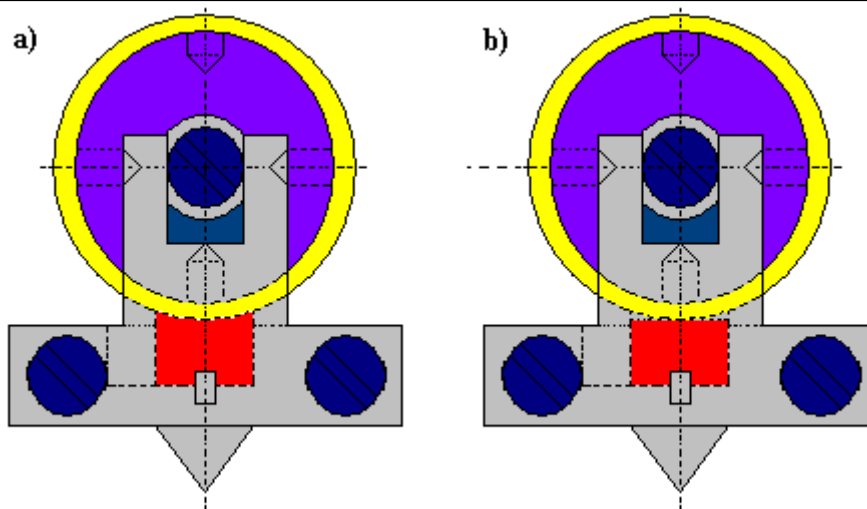


Fig. 4.1.4.3. Friction contact of the roll – block Timken test rig with a contact:
a) distributed, b) concentrated

The test of lubricating properties of oils and greases using the Timken method may be performed in accordance with the standard PN-86/C-04073.

The standardized test parameters on the Timken test rig include: determination of the load capacity of the lubricating layer of lubricants [PN-86 / C-04078]; determination of the load capacity of the lubricating layer of plastic greases [ASTM D 2509]; determination of the load capacity of the lubricating layer of lubricating fluids [ASTM D 2782] ; determination of the load-bearing capacity of the lubricating layer as well as anti-friction and anti-wear properties of lubricating fluids [IP 240/82]; determination of the load capacity of the lubricating layer as well as anti-friction and anti-wear properties of plastic greases [IP 326/80].

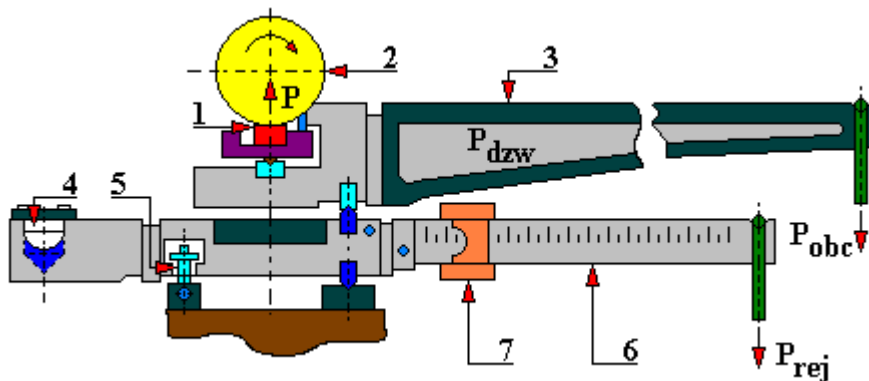


Fig. 4.1.4.4. Timken test rig designed to test friction and wear; lever system
1 - sample, 2 - counter-sample (ring), 3 - loading lever, 4 - liquid level, 5 - locating pin, 6 - moment of friction recording lever, 7 - sliding weight, P_{dzw} - weight of loading lever, P_{obc} - load on the loading lever, P_{rej} - load on the lever recording the moment of friction [45]

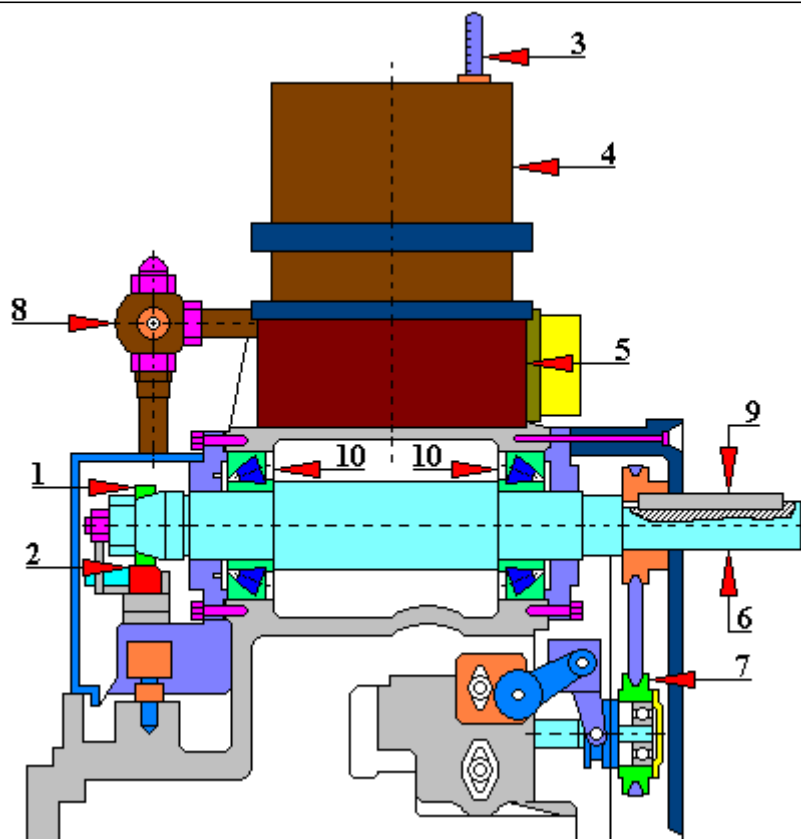


Fig. 4.1.4.5. Cross-section of the Timken test rig [45]

1 - test ring, 2 - test block, 3 - thermometer, 4 - oil tank, 5 - electric heater, 6 - spindle, 7 - oil pump drive clutch, 8 - oil flow control valve, 9 - key, 10 - bearing

4.1.5. Test rig for determining the friction factor by upsetting a cylinder

A test rig for determining the coefficient of friction by upsetting (Fig. 4.1.5.1) is based on the measurement of barrelling. The essence of the method consists in upsetting a cylindrical sample 6 between two flat anvils. The author of the method determines the coefficient of friction μ from the formula:

$$\mu = \frac{6.25 \cdot (\delta + 2\delta^2)}{1 - \varepsilon} \cdot \left(\frac{d_0}{h_0} \right)^{1.5}$$

where: δ – sample barrelling; ε - true strain

$$\delta = \frac{(D_z - D_w)}{D_w}$$

$$\varepsilon = \frac{\Delta h}{h_0}$$

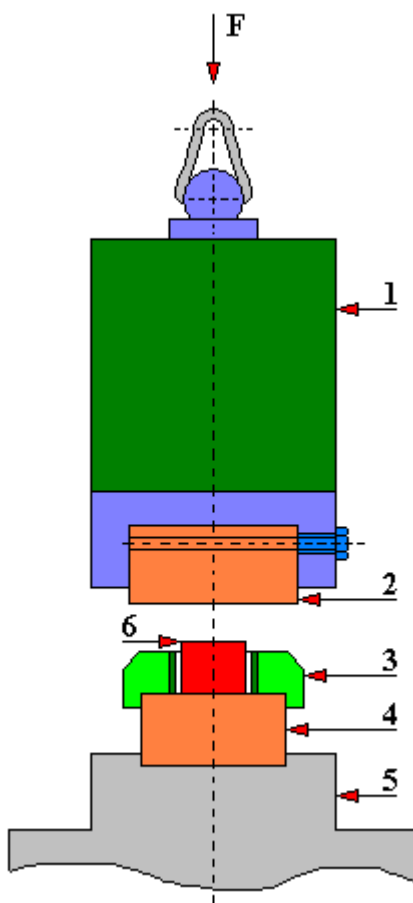


Fig. 4.1.5.1. Diagram of the test rig for determining the frictional resistance according to S. I. Gubkina [42]

1 – beater; 2 – hammer block; 3 – spacer ring; 4 – lower anvil; 5 – cast of the anvil; 6 – upset sample

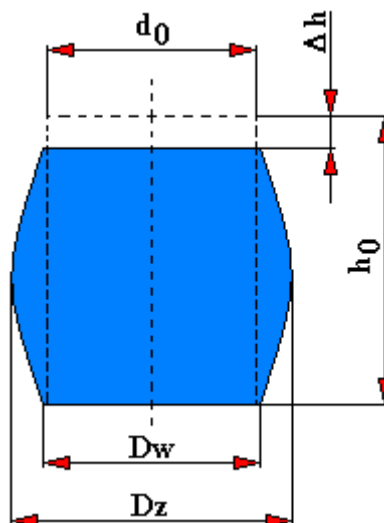


Fig. 4.1.5.2. A cylindrical sample after upsetting D_w - inside diameter; D_z - outer diameter; h_0 - initial height of a cylindrical sample; Δh - height difference before and after upsetting

4.1.6. Test rig for testing frictional resistance in model conditions of sheet metal extrusion processes

This is a test rig based on the patent No. PL 170088 created by Klaudiusz Lenik, Czesław Kajdas, Gabriel Borowski. This tribotester is designed to test the frictional resistance of metals, especially when one of the elements of the friction contact undergoes elastic deformation.

This test rig (shown in Figure 4.1.6.1) consists of two plates: (1) and (2). Exchangeable plates (6) and (7) are fastened to the plates between which fitted is a sample (3) of the tested material. The sample (3) is surrounded by a clamping ring (8) connected by a replaceable tension member (5) with two bolts (4) connected to the rod (5) and plates (1) and (2). Extensometers are stuck on the tension member (5) and the plate (2).

The principle of operation of this test rig is that two plates, the upper (1) and the lower (2), are axially compressed in a press (hydraulic or mechanical). At this time, in the case of modeling the extrusion process, the sample (3) of the tested material - placed between the plates (6) and (7) - is ejected. The measurements of the normal and tangential force are carried out by means of a system of extensometers (9) and (10), and a measuring equipment. The speed of ejection of the sample (3) of the tested material during compression is regulated by means of two screws (4), and the fixing of the tension member (5). A set of plates (6) and (7) fixed in the plates: upper (1) and lower (2), allows to make measurements for materials of a tool and samples with different physical properties.

A tribological test rig based on the patent number PL 170088 allows to:

- test the frictional resistance in conditions similar to those prevailing in the processes of volumetric machining, e.g. upsetting, drawing or sheet-metal forming,
- test the frictional forces under the normal pressure of material deformation - upsetting,
- test the friction forces under normal pressure and material sliding along the tool - upsetting forces and tangential forces acting on the contact surface,
- control the real pressures and displacements under the action of normal and tangential forces,
- change the speed of horizontal material movement in modeled plastic working processes.

The authors of this original test rig state that it can be widely used for testing and selecting lubricants as well as for evaluating and selecting tool materials and the condition of their surfaces for sheet-metal forming processes.

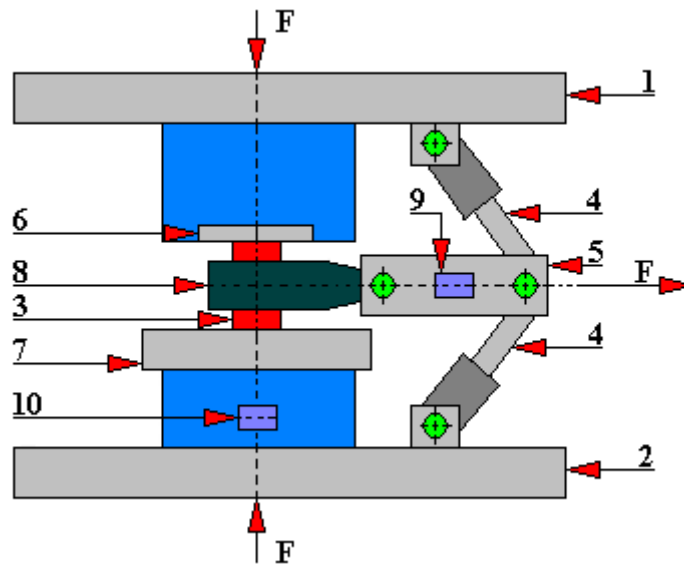


Fig. 4.1.6.1. Tribological test rig as per the patent No. PL 170088

1 - upper plate, 2 - lower plate, 3 - sample of the tested material, 4 - fixing screws, 5 - replaceable tension member, 6 - replaceable plate, 7 - replaceable plate, 8 - clamp, 9 - extensometer , 10 - extensometer.

4.1.7. Test rig for determining frictional resistance in the process of upsetting a cylindrical sample based on a continuous measurement of forces

In [95] presented is a method for determining the coefficient of friction in the process of upsetting a cylindrical sample based on the continuous measurement of the normal force and tangential force, which enables the tracking of changes in the friction force during the process of plastic deformation. Figure 4.1.7.1 shows the principle of operation of an instrument used for measuring using this method. The test rig is built of a rigid frame 6 in which the hammer 1 is guided, pressing on the wedge 2 with a mounted cylindrical sample 3. As a result of moving the wedge 2 along a plane inclined at an angle of 45° , the sample 3 undergoes upsetting and at the same time moves along the surface of the counter-sample 4 usually made of tool steel. The counter-sample 4 transmits the normal pressure N through the sensor 5, while the friction force T is measured by the sensor 7 with the affixed extensometers. By connecting the outputs of sensor signals 5 and 7 to the recording unit (measurement card, computer) obtained is the monitoring of force changes during sample upsetting. Based on the measured forces N and T it is possible to determine the coefficient of friction from the following formula (assuming the correctness of Amontons's law):

$$\mu = \frac{T}{N}$$

Of course, it is possible to program in such a way that both the measured parameters (N , T) and calculated parameters (μ) are displayed on the monitor in real time.

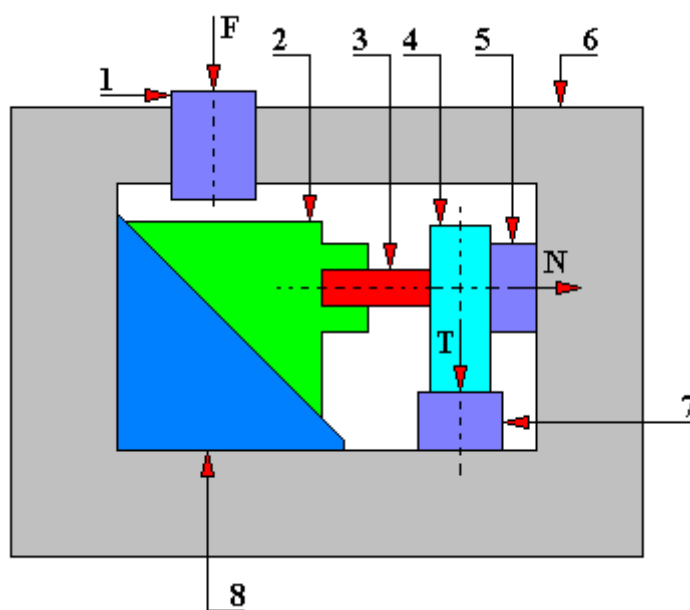


Fig. 4.1.7.1. A diagram of the test rig for determining frictional resistance in the process of upsetting a cylindrical sample based on a continuous measurement of forces [95]
 1 - hammer; 2 - wedge; 3 - cylindrical sample; 4 - counter-sample; 5 - measuring sensor; 6 - frame; 7 - strain gauge; 8 - wedge

The author in his research used samples with a diameter of $d = 20$ mm, height $h = 30$ mm, and the gripping part of the sample was 10 mm, then the quotient $h/d = 1$.

The above-mentioned test rig can be mounted on a press (hydraulic or screw) or on a hammer. Thanks to this, it is possible to determine the coefficient of friction for low strain rates (press) or high strain rates (hammers). The advantage of this test rig is, of course, the simplicity of its construction. The disadvantages, however, include difficulties in determining additional frictional resistances occurring, for example, in the guide planes, and the displacement of the normal force N during the measurement (the need to construct special sensors).

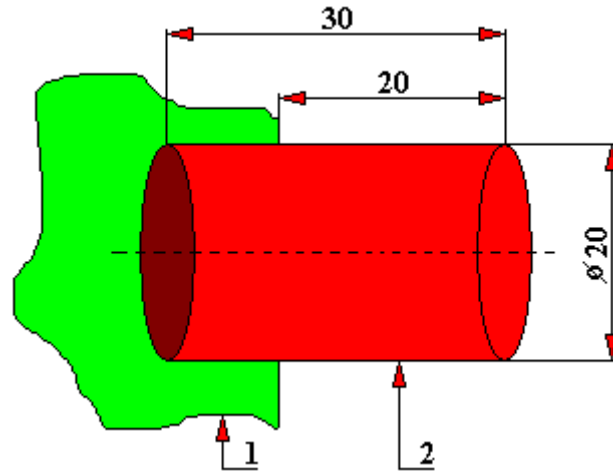


Fig. 4.1.7.2. Sample mounting scheme
1 - wedge (gripping part); 2 - test sample

4.1.8. Test rig for testing changes in tribological properties of connector joints during their multiple connection and disconnection

This is an original non-commercial test rig built at Katedra Eksploatacji Pojazdów Samochodowych Politechniki Śląskiej w Katowicach (Department of Motor Vehicle Operation of the Silesian University of Technology in Katowice) [218]. It is designed to study the effect of multiple connection and disconnection of a pair of electric slide-in connector joints on the friction force between them. This test rig has a servo drive that causes the male connector to oscillate cyclically at a preset speed. The amplitude of the reciprocating motion is also adjustable, so it is possible to carry out tests with different types of connectors. The female connector was mounted on the station in a fixed stationary position to enable the measurement of the friction force using the UTICELL M240 strain gauge force sensor with a measuring range of ± 100 [N]. The applied analog-to-digital converter made it possible to measure the friction force with an accuracy of 0.01 [N]. The measurement and control system was based on a single-circuit microcontroller controlling the servo drive. The data collected from the system was sent to the computer via the RS-232 port. Figure 4.1.8.1 shows a pair of slide-in connector joints, and Figure 4.1.8.2 shows a diagram of the test rig for slide-in connector joints. The duty cycle for testing 6.3 mm wide crimp-mount connector joints for 5 mm² (10 AWG) conductors. The amplitude of the reciprocating motion was 8.5 mm.

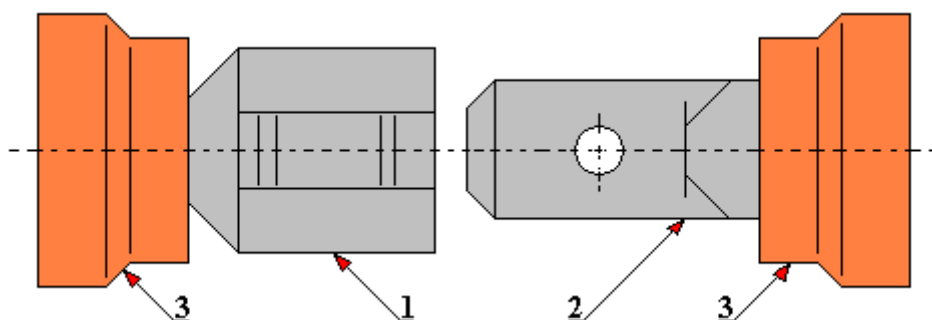


Fig. 4.1.8.1. Exemplanary slide-in connector joint
1 - female joint, 2 - male joint, 3 - insulation

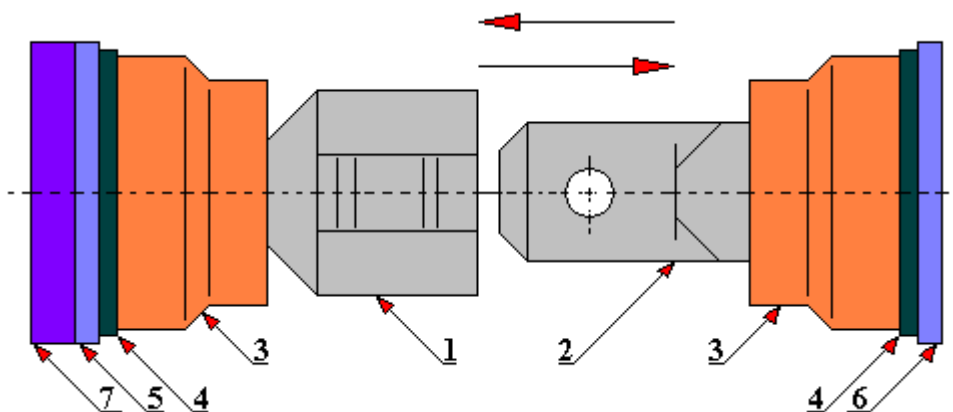


Fig. 4.1.8.2. Diagram of the test rig for slide-in connector joints [218]
1 - female joint, 2 - male joint, 3 - insulation, 4 - handle, 5 - servo drive, 6 - friction force sensor, 7 - displacement sensor

4.1.9. Tribological test rig designed for testing kinematic pairs with conformal contact

An original test rig was designed and built in the laboratory of the Department of Production Engineering at the Faculty of Mechanical Engineering of the University of Science and Technology in Bydgoszcz. The mechanical part of the test rig is shown in Figure 4.1.9.1.

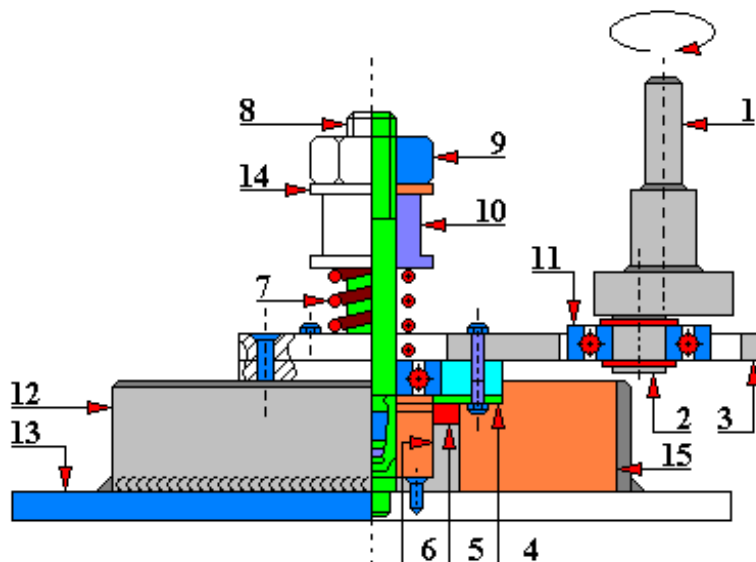


Figure 5.1.9.1. Structural form of the test rig

1 – eccentric handle, 2 – eccentric, 3 – lever, 4 – counter sample, 5 – tested samples, 6 – samples stabilizing bush, 7 – spring, 8 – central screw, 9 – nut, 10 – distance bush, 11 – single-row ball bearing, 12 – pipe jacket, 13 – steel plate of the base, 14 – washer, 15 – tested lubricating compound

The tested samples 5 are mounted in three grooves made every 120° on the face of the sample holding sleeve 6. In this way, a reliable and even three-surface pressure of the mating elements is obtained by means of a spring 7. The samples are placed immobile in the sleeve, and the counter-sample 4 performs a relative, oscillating motion. The oscillating motion transmitted to the bearing counter-sample is obtained by changing the rotational motion into a linear motion using the lever 3 and the eccentric 2. The change in the length of the relative displacements of the sample and counter-sample (elementary friction path) is obtained by means of an eccentric with different values of its axis shift. In order to minimize the wear of the stand elements the eccentric acts on the lever through a rolling bearing. Successive load values are obtained as a result of a change in the tension of the spring 7 or as a result of using springs with different characteristics. Due to the use of a spring the pressure value is constant. Figure 5.1.9.2 shows the general principle of co-action of the kinematic pair of conformal contact - the sample with the counter-sample during the tests carried out on the mentioned test rig. On the end face of the sample holding sleeve 3, the test samples 2 are fixed immobile in three grooves made every 120° . In this way, a three-surface, evenly distributed pressure of the mating elements is obtained, which is realized by the spring tension. The counter-sample 1 performs a relative oscillating motion.

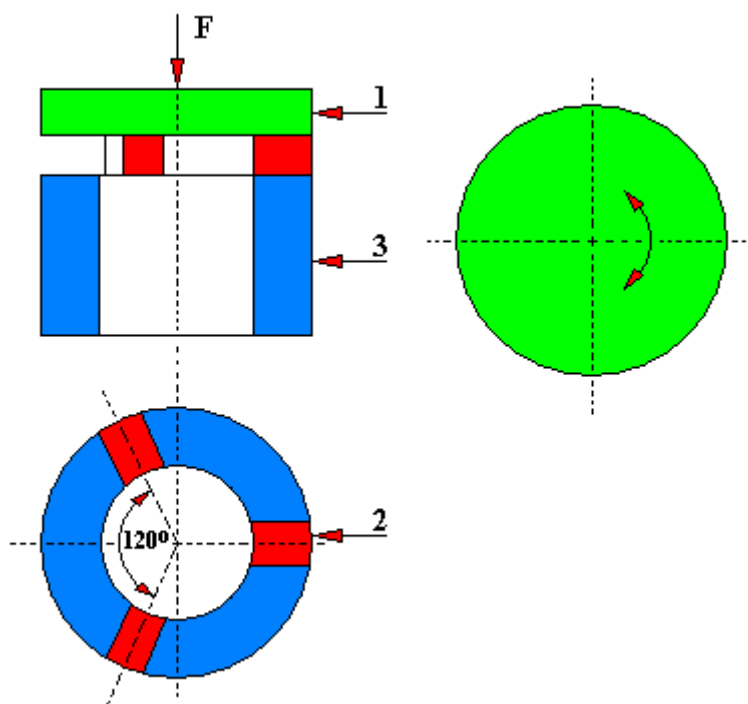


Fig. 4.1.9.2. Scheme of co-action of samples with a counter-sample:
1 - counter-sample, 2 - sample, 3 - sample fixing base

A number of different studies were carried out on this test rig, including tests which were to give an answer to the question whether the angle of intersection of the characteristic lines of traces after machining affects the course of the SL transformation and whether these changes depend on other mating conditions.

Examples of conditions for tests carried out on this test rig:

- sample material steel C45 with hardness 40 HRC,
- counter-sample material steel 102Cr6 with hardness 60 HRC,
- external load value: 300 [N] and 600 [N],
- the contact surface of samples with the counter-sample 300 mm², the speed of relative motion during the tests was 3 m/min (0.05 m/sec),
- the samples worked in a test rig oil lubricating medium (L - AN 68),
- the angle of mating between the characteristic traces after machining was 0° and 60°.

Because of many advantages, including construction ones, and the resulting test needs, this test rig was modernized; its modernization consisted in the construction of a system of current visualization and archiving of data collected during the tests. The description of the modernized test rig is presented below.

The system shown in Figure 4.1.9.3 allows, among others, to take a four-point temperature measurement (three points in oil, fourth point - ambient temperature), its recording, rotational speed setting, measurement and recording of the current, frequency, voltage and power consumed by the drive.

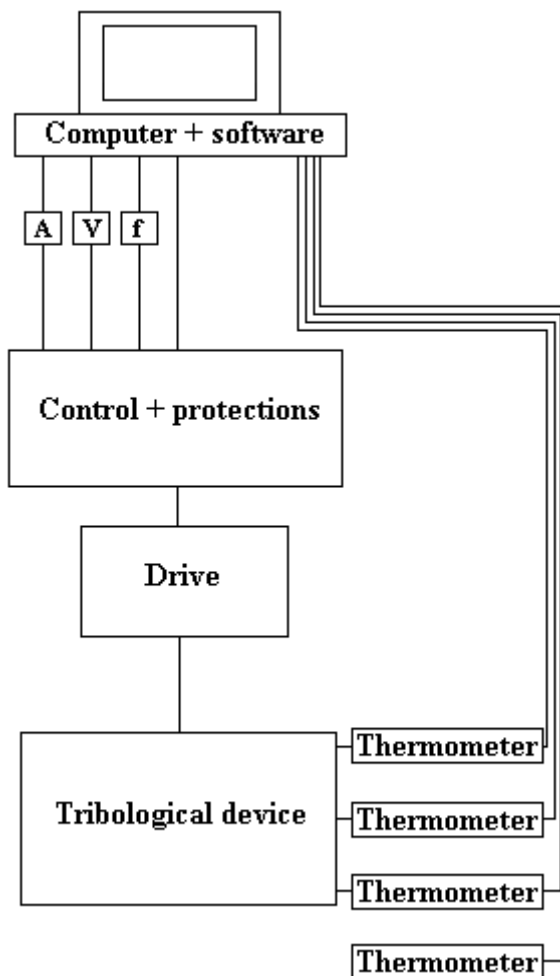


Fig. 4.1.9.3. A block diagram of the modernized tribological test rig [84, 85, 86, 87, 88, 89, 91, 92]

The computer is connected to the ADAM 4019+ concentrator module via the ADAM-4520 converter (RS 485 - RS 232). Using the ADAMView software, data is read from the concentrator and sent to the computer. The system can have several types of boards for data visualization depending on the user's needs. The system does not have a torque meter or a tachometer. By collecting current and frequency data from the inverter via the S + / S- communication output, it is possible to determine the moment of samples seizure. Additionally, by determining the total power consumption of a tribological test rig drive during testing a given lubricating composition under the same operating conditions, it is possible to determine which of the tested compositions is better in terms of lubricating properties. Generally, that type of composition is better for which less energy is consumed by the drive. Figure 4.1.9.4 shows a block diagram of connections between individual elements of the system.

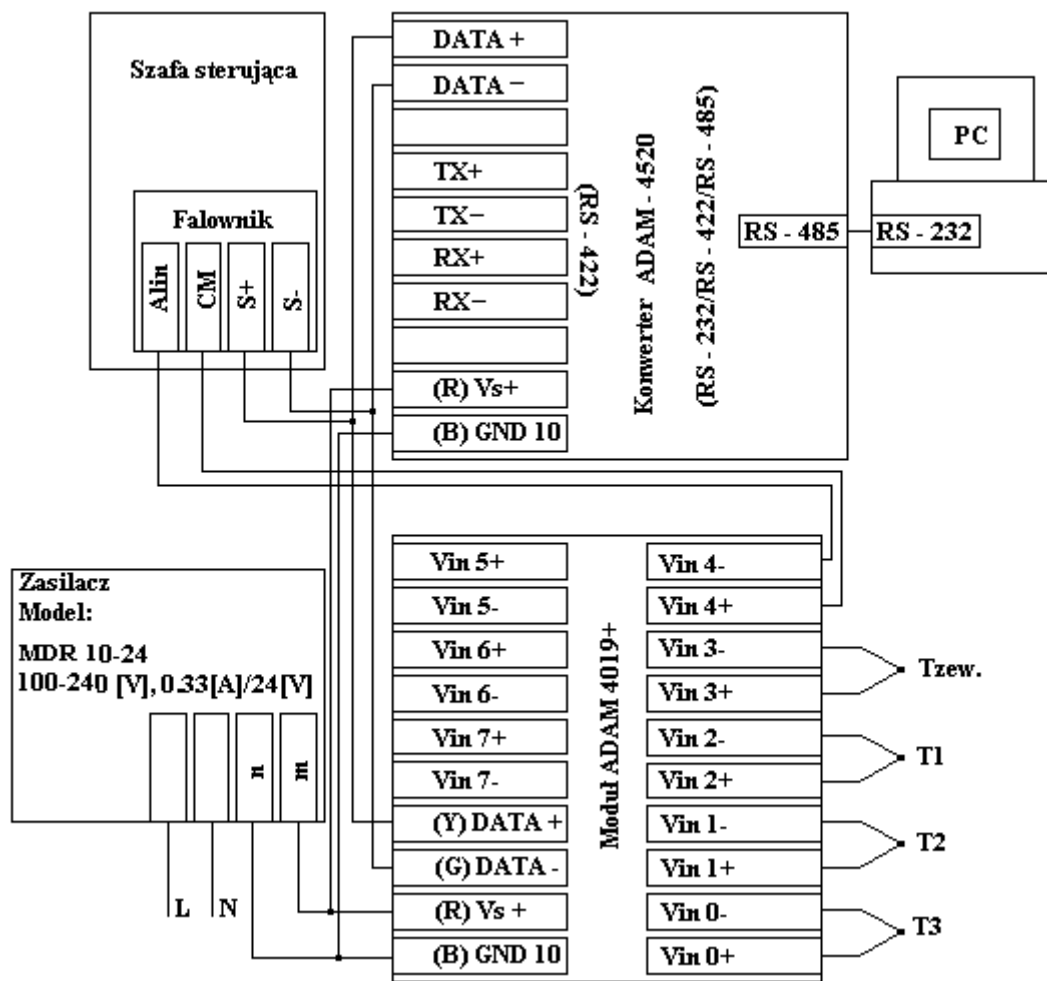


Fig. 4.1.9.4. A block diagram of the system connections [84, 85, 86, 87, 88, 89, 91, 92]

The designed and manufactured system consists of the following parts:

- a tribological test rig,
- a drive for the tribological test rig,
- a control cabinet for the drive,
- ADAM 4019+ module with ADAM - 4520 converter by Advantech,
- PC with DriveView 3.3 software (for communication with the inverter) and ADAMView software.

Both the ADAM 4019+ module and the converter are powered from the same 240/24 [V] power supply. Four K-type thermocouples are connected to ADAM 4019+ ports with numbers from 0 to 3. Port number 4 is connected to the analog input of the inverter. Its S+/S- communication output and the DATA +/DATA- module port are connected to the DATA +/DATA- converter port. And the converter is connected to the PC via RS-232 / RS-485 ports. The module ports 5, 6 and 7 are not used in this study. The tribological test rig is driven by a three-phase bench drill. The control cabinet, which is shown in Figure 4.1.9.5, consists mainly of the inverter and protections.

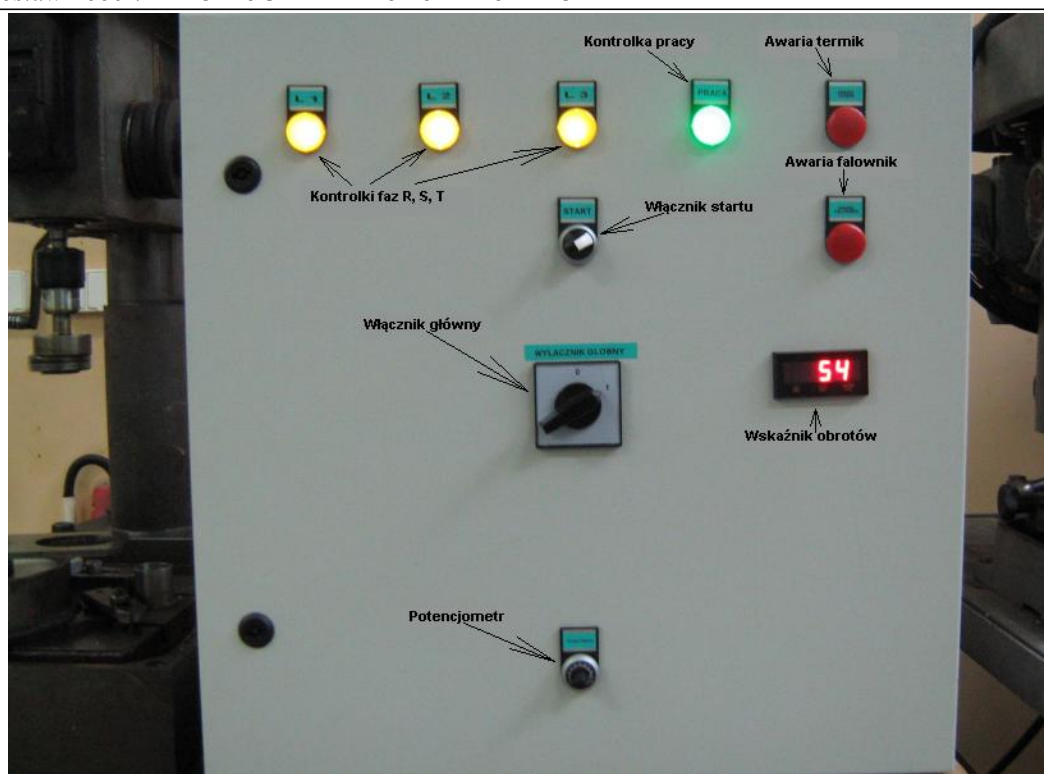


Fig. 4.1.9.5. View of the front panel of the control cabinet [84, 85, 86, 87, 88, 89, 91, 92]

Its purpose is to enable a steady control of the rotational speed of the drive (drill) in the frequency range from 0 to 50 [Hz]. The inverter of the company LS type SV 022iG5A-4 was used here. This inverter has only one analog input $0 \div 10$ [V] used for measuring the frequency and rotational speed, and an RS 485 interface. This interface allows communication with the computer using DriveView 3.3 or ADAMView software. The diagram of electrical connections of the control cabinet is shown in Figure 4.1.9.6.

The cabinet consists of the following elements:

- S1 - main switch (type 4G25-10-U manufactured by APATOR),
- F1 – protection of phase indicator light, phase failure sensor,
- H1, H2, H3 - phase indicator light of R, S, T,
- H4 - thermal cutoff failure indicator light,
- H5 - operation indicator light,
- H6 - inverter failure indicator light,
- S2 - start switch,
- F2 - inverter protection,
- T1 - thermal protection (thermal cutoff),
- V3 - phase failure sensor,
- K1 - contactor,
- Z1 - WSK-N2 rotation indicator (manufactured by COBI ELEKTRONIC),
- V1 - potentiometer (enables frequency setting without entering the inverter menu),
- Z2 - CRT - V1 - clock - running time programmator,
- N1 - VMC line filter, FEE 3006 type (manufactured by LS).

The cabinet is made of metal. Its dimensions are 600x600x250 [mm] – manufactured by the company 'Meller'.

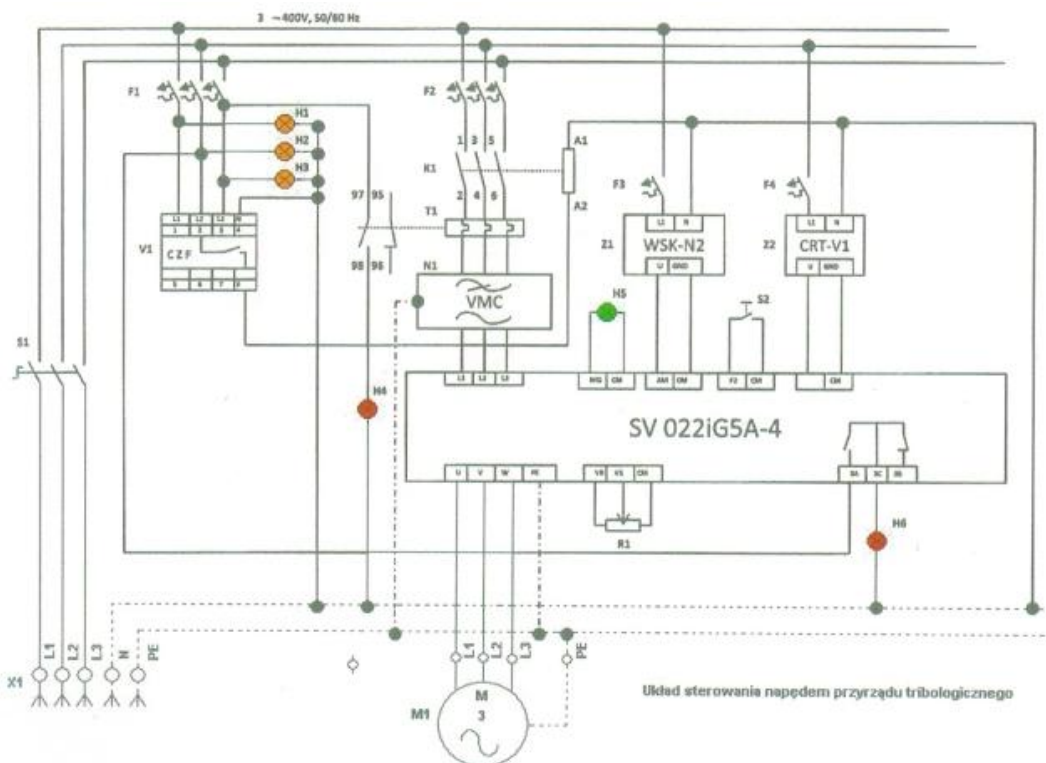


Fig. 4.1.9.6. Diagram of electrical connections of the control cabinet for the tribological test rig [84, 85, 86, 87, 88, 89, 91, 92]

The module 4019+ has eight analog inputs, four of which are used for the temperature sensors. The thermocouples are placed near the contact surface of the samples with the counter-sample (3 thermocouples). The fourth thermocouple measures the ambient temperature. Port 4 of this module is connected to the analog output of the inverter. The module 4019+ is connected to the computer via the ADAM-4520 converter.

Due to the fact that ADAM-4520 converter has only one pair of DATA +/DATA- (RS-485) terminals to which ADAM 4019+ module and the inverter (S+/S- terminals) are simultaneously connected, it is necessary to have the OPC Server software. It enables communication between the module, inverter and computer using the MODBUS protocol.

The operation of the system intended for recording and visualization of the working conditions of the tribological test rig is based on the program created in ADAMView environment and on the ADAM 4019+ data concentrator module with thermocouples along with the inverter connected to its inputs.

The ADAM 4019+ module has two operating modes: INIT and NORMAL. The NORMAL mode is only used to set the parameters of individual ports. The INIT mode is used to set the parameters of the module to run alone or together with other modules (inverters) - depending on the user's needs. Both solutions are used in this study. Each program in ADAMView in any mode consists of two main parts:

- the user panel which acts as an integrated front panel of units that make up a virtual instrument (e.g. a front panel of a tribological test rig),
- a block diagram with the icons of functional blocks and connections between functional blocks of the virtual test rig. The block diagram is the source code of the control software for the virtual test rig.

Creating a software in ADAMView language consists in assembling a block diagram by moving (by drag and drop) to the panel of icons, objects or function icons collected on the top menu bar. Next, the module should be configured to perform the set function.

Figure 4.1.9.7. shows the view of the main panel of the module during the off-line operation. In this case, data is collected only from the ports connected to the ADAM 4019+ module. These are four thermocouples (ports 0 ÷ 3) and the inverter analog input (port 4).

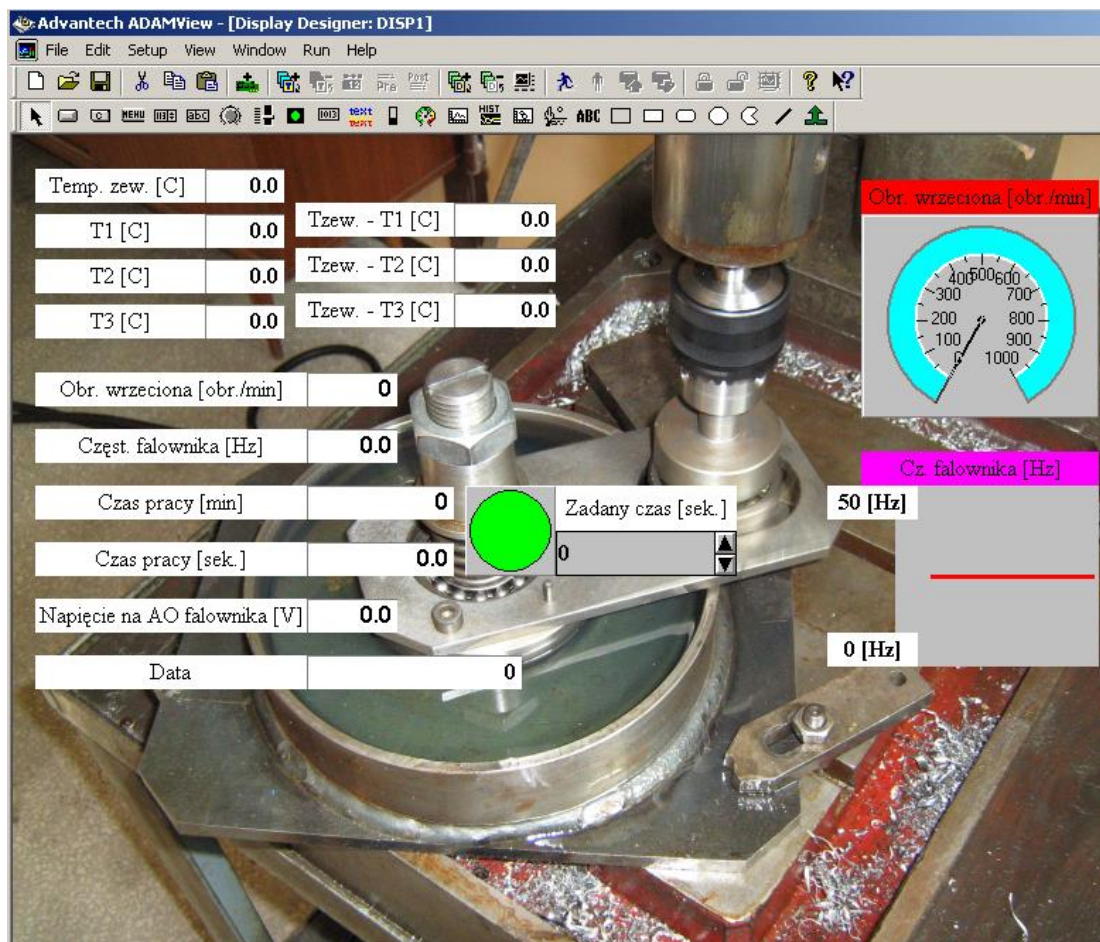


Fig. 4.1.9.7. The main panel of the tribological test rig built on the basis of the ADAMView software for off-line operation [84, 85, 86, 87, 88, 89, 91, 92]

The screen (Figure 4.1.9.7) shows the following values:

- ambient temperature T_{zew} , t
- emperature $T1$ (measurement near the first point of support, sample/counter-sample),
- temperature $T2$ (measurement near the second point of support, sample/counter sample),
- temperature $T3$ (measurement near the third point of support (sample/counter-sample),
- temperature difference between $T_{zew} - T1$,
- temperature difference between $T_{zew} - T2$,
- temperature difference between $T_{zew} - T3$,
- voltage value at the analog input of the inverter AO (from 0 to 10 [V]),
- current operating frequency of the inverter,
- drill spindle revolutions determined on the basis of the inverter operating frequency,
- operating time in minutes,

- operating time in seconds,
- current date, visual indicator of spindle rotation,
- visual frequency indicator,
- indicator of elapsed time set.

Not all data backed up to the computer need to be displayed on the desktop and vice versa. The data displayed on the control panel does not have to be saved on the computer.

Due to the fact that the applied ADAM 4019+ module does not have analog outputs, it cannot be connected to external signaling units, e.g. a bell, indicator lights on the control cabinet indicating the end of the running time set. Therefore, the elapse of the set time indicator available in ADAMView was used here. Visual speed and frequency indicators allow the user to control parameters from a greater distance. The parameters of running time and dates possible for different recordings are also possible thanks to the ADAMView software used here.

The only analog input of the inverter is used here in three ways. First, to determine the operating frequency of the system. This input has a voltage range from 0 to 10 [V]. The frequency equal to 0 [Hz] corresponds to the value 0 [V]. The frequency equal to 50 [Hz] corresponds to the value 10 [V]. And this current voltage value can also be displayed. This is the second way to use the analog input of the inverter. The third way is to convert the inverter frequency into the spindle revolutions. It was assumed here that the spindle revolutions are linearly proportional to the frequency, and the slip on the V-belts between the motor and spindle is negligible small. Knowing the spindle revolutions for the frequency of 50 [Hz] from the tachometer measurement, it is possible to determine the spindle revolutions for each lower frequency because only one straight line can pass through two points, as shown in Figure 4.1.9.8, therefore this relationship was used to determine the rotational speed of the spindle. The second point is the origin of the coordinate system - point 0.

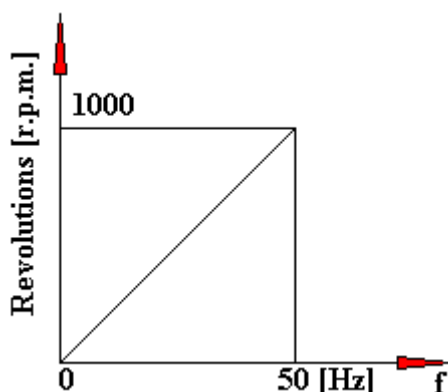


Fig. 4.1.9.8. The dependence of the rotation speed on the frequency for an induction motor and a given gear ratio (slips were omitted).

Figure 5.1.9.9 shows the connection diagram for the module operation in the off-line mode. We see here four thermocouples marked with TMP1, TMP2, TMP3 and TMP4 respectively. Logic blocks SOC1, SOC2, and SOC3 are responsible for computing the temperature difference between individual thermocouples. The AI1 analog input is used for downloading data from the inverter. In addition, there are five scripts on the diagram: SCR1, SCR2, SCR3, SCR4 and SCR5 used for the visualization of indicators of revolutions, frequency, elapsed time and for converting frequency into revolutions.

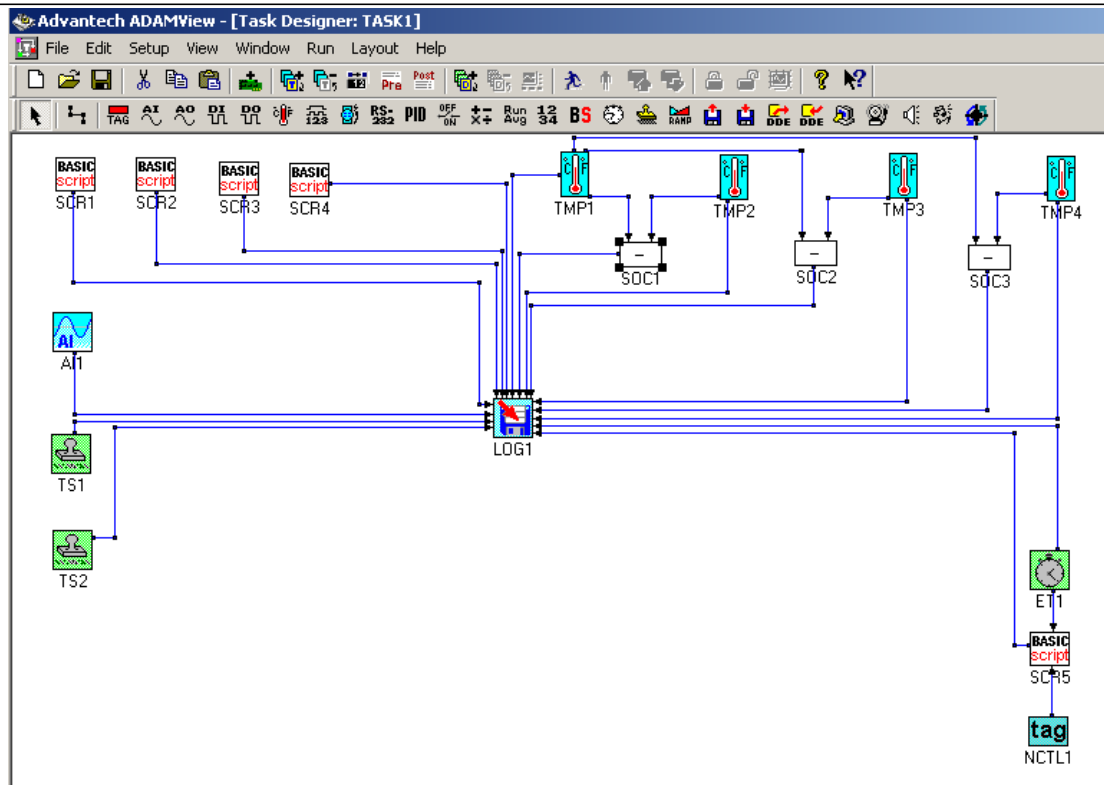


Fig. 4.1.9.9. Diagram of the main panel connections for a lonely work of ADAM 4019 + module.

The TS1, TS2 and ET1 program blocks are used to calculate the time in seconds, minutes and to insert the date in the appropriate format in the file. The LOG1 program block is used for saving on the file the data downloaded from units connected to the module. The NCTL1 block causes the change of the semaphore light icon color after a preset time, e.g. from green to red.

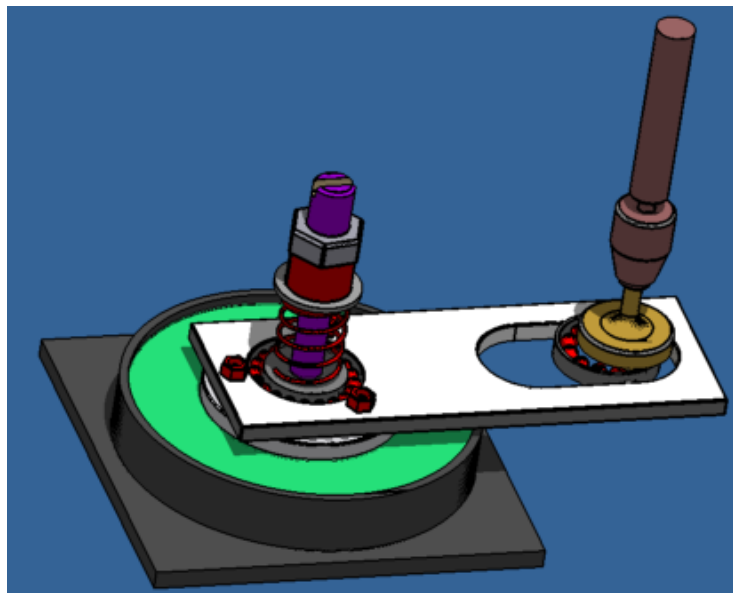


Fig. 4.1.9.10. A bitmap of the test rig for tribological tests of kinematic pairs with conformal contact, created on the basis of a drawing made in the Solid Works software. This bitmap may be the background for the main panel.

The background of the main panel shown in Figure 5.1.9.7 does not have to be a photograph of the test rig. It can also be a bitmap created from a drawing made in any program as shown in Figure 4.1.9.10.

Data obtained from ADAM 4019+ module during the test is saved in a txt file. Figure 4.1.9.11 shows a fragment of such a file for ADAM 4019+ module operation in the off-line autonomous mode. The file is structured as follows (in the following columns put are): date of the measurement, measurement time in minutes and seconds, semaphore mode status (0 means red, 1 means green), voltage value on the analog output of the inverter (in Figure 4.1.9.16 this value is 0 because the inverter was turned on only after some time), measurements of temperatures and differences between Tzew and T1, T2, T3.

Data	Czas pracy [sek]	stan semafora	Cz. fał.	Tz - T1	T1	Tz-T2
Mon Oct 17 16:22:46 2011	0:00:00.00	0	0	-3.300	18.100	-0.300
Mon Oct 17 16:22:47 2011	0:00:00.98	1	0	-1.300	15.500	3.100
Mon Oct 17 16:22:48 2011	0:00:02.02	2	1	-2.700	18.400	-2.400
Mon Oct 17 16:22:49 2011	0:00:02.97	3	1	-4.800	17.700	-1.700
Mon Oct 17 16:22:50 2011	0:00:04.02	4	1	-3.200	16.100	-1.300
Mon Oct 17 16:22:51 2011	0:00:04.97	5	1	-2.800	19.500	-2.800
Mon Oct 17 16:22:52 2011	0:00:05.96	6	1	-4.700	16.800	-1.700
Mon Oct 17 16:22:53 2011	0:00:07.02	7	1	-16.700	23.800	-8.800
Mon Oct 17 16:22:54 2011	0:00:07.99	8	1	-22.200	16.300	-2.700
Mon Oct 17 16:22:55 2011	0:00:08.98	9	1	-4.900	27.100	-1.700
Mon Oct 17 16:22:56 2011	0:00:09.97	10	1	-1.700	30.200	-0.400
Mon Oct 17 16:22:57 2011	0:00:10.97	11	1	-10.100	49.100	-17.000
Mon Oct 17 16:22:58 2011	0:00:11.96	12	1	7.500	30.400	3.800
Mon Oct 17 16:22:59 2011	0:00:12.96	13	1	-15.400	51.200	-24.100
Mon Oct 17 16:23:00 2011	0:00:13.99	14	1	-3.400	43.900	-1.900
Mon Oct 17 16:23:01 2011	0:00:15.02	15	1	5.200	36.000	13.300
Mon Oct 17 16:23:02 2011	0:00:15.98	16	1	-10.700	24.700	7.500
Mon Oct 17 16:23:03 2011	0:00:16.97	17	1	-4.700	26.400	3.800
Mon Oct 17 16:23:04 2011	0:00:17.97	18	1	-2.400	33.000	-1.300
Mon Oct 17 16:23:05 2011	0:00:18.97	19	1	0.600	33.000	7.100
Mon Oct 17 16:23:06 2011	0:00:19.96	20	1	-7.700	33.100	-5.000
Mon Oct 17 16:23:07 2011	0:00:20.98	21	1	-4.500	32.700	-4.600
Mon Oct 17 16:23:08 2011	0:00:21.97	22	1	-3.600	50.300	-10.900
Mon Oct 17 16:23:09 2011	0:00:23.03	23	1	11.400	43.500	1.600
Mon Oct 17 16:23:10 2011	0:00:23.97	24	1	2.300	38.800	-10.100
Mon Oct 17 16:23:11 2011	0:00:24.97	25	1	-7.200	43.000	3.000

Fig. 4.1.9.11. Fragment of the test data file for the operation of ADAM 4019+ module in the off-line autonomous mode.

During the autonomous operation of the ADAM 4019+ module one can use the DriveView 3.3 software dedicated only to this type of inverters manufactured by Samsung LS. In this way it is possible to obtain more information about the operating status of the inverter. In order to start the softawer that records the inverter parameters, select the Graph Monitor icon, which opens the window shown in Figure 4.1.9.12. In this way, it is possible to register additional four parameters selected in any combination from the drop-down list of inverter operation parameters. The maximum recording time is one hour. The displayed values of selected parameters are instantaneous values. The following parameters can be selected from the drop-down list:

- **Fault** - error number/type,
- **3 ABC** - relays operation status,
- **MO** - ground terminal (it can be defined),
- **P1 ÷ P8** - multifunctional outputs,
- **RPM** - motor rotational speed for a specified number of pole pairs,
- **I** - analog current output of the inverter,
- **V2** - analog voltage output of the inverter,
- **V1** - analog voltage output of the inverter,
- **Output Power** - output power,
- **DC - Link Volt.** - voltage of the inverter intermediate circuit,
- **Output Volt.** - effective phase-to-phase output voltage,
- **Output Freq.** - output frequency,
- **Freq. Command** – inverter frequency setpoint.

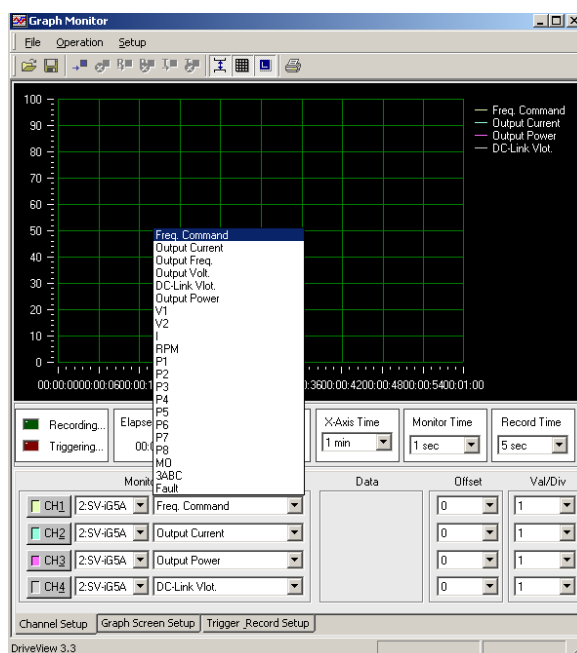


Fig. 4.1.9.12. Selection of the recorded parameters of the inverter operation. DriveView software 3.3

Figure 4.1.9.13 shows an example of selected parameters for a time of 1 minute with a record every 5 seconds.

The second mode of operation of ADAM 4019+ module is the mode of parallel operation with other units. In this case ADAM 4019+ module must be properly programmed. In the INIT mode, select the MODBUS mode of operation. ADAMView software has a built-in OPC Server. Thus, it is possible to recognize various units by their addresses. When starting this application one should remember that OPC Server gives Advantech units lower numbers than numbers given to units made by other companies. Address conflicts often arise here. The inverter used in the study has a factory-set value of the inverter number for network operation via RS 485 equal to 1 (manufactured by Samsung LS). The 4019+ module has the identical setting given by the OPC Server (prod. Advantech). Therefore, this parameter must be changed in the inverter menu. The maximum number of inverters from this manufacturer that can work in this way is 251. However, the maximum number of logical blocks created in ADAMView cannot exceed 75.

Figure 4.1.9.14 shows ADAM 4019+ module in MODBUS mode and the state of its ports. K-type thermocouples are assigned to ports 0 ÷ 3, which can be seen in the form of the current temperature value displayed. Ports 4 ÷ 7 can be used e.g. for voltage measurement within ± 10 [V]. After starting the OPC Server software, catalogues of co-acting units were created and addresses were assigned to them. In this case, there are two units. Figures 4.1.9.15 and 4.1.9.16 show the successive steps of OPC Server programming. ADAM module is assigned address 1, inverter is assigned address 2. Then, parameter subcategories with their addresses were created. Inverter operating parameter addresses, such as acceleration time, stop time, output frequency, output power, DC bus voltage and others are in its user manual.

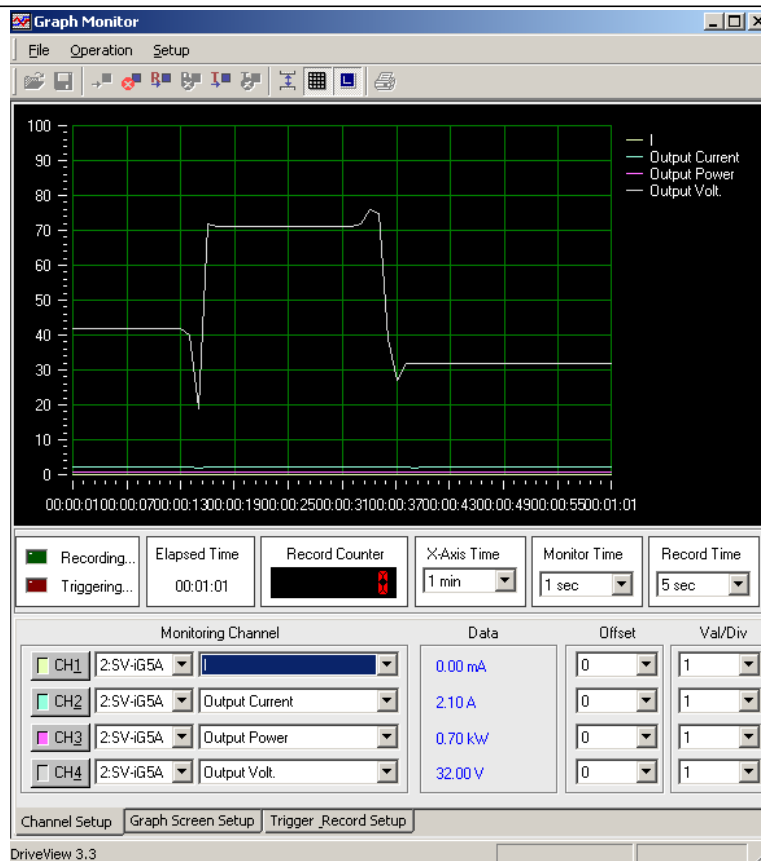


Fig. 4.1.9.13. An exemplary course of selected inverter operating parameters. DriveView 3.3. software

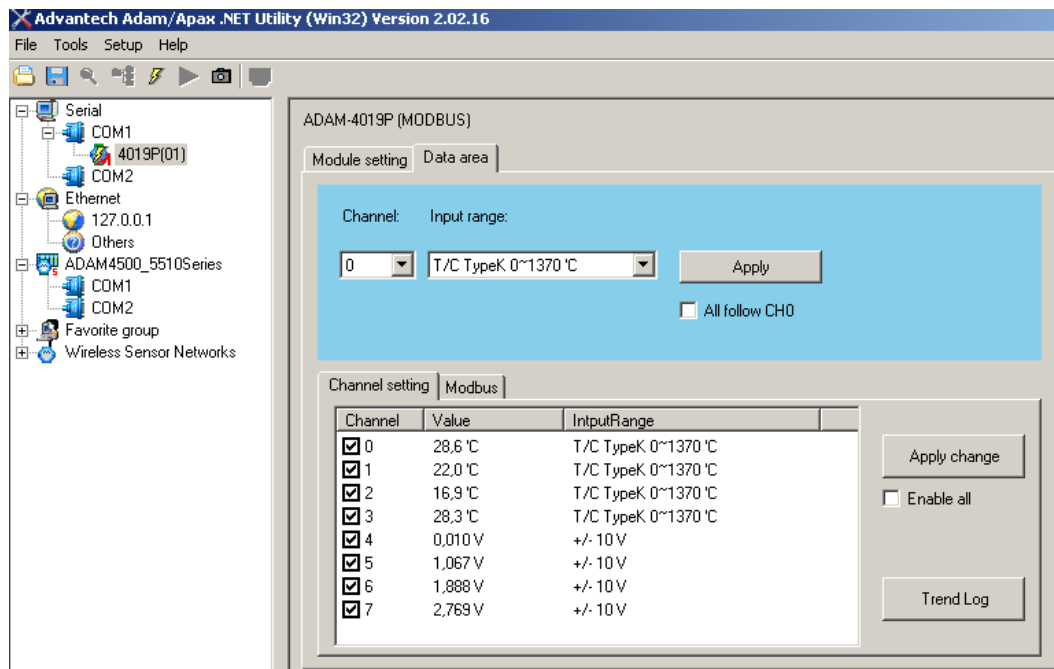


Fig. 4.1.9.14. Exemplary use of ADAM 4019+ ports

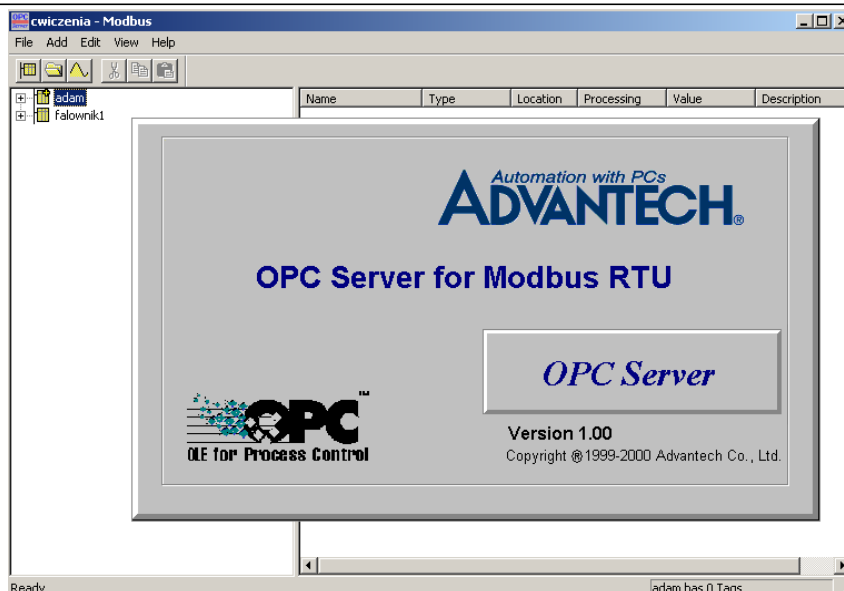


Fig. 4.1.9.15. Created catalogues in OPC Server

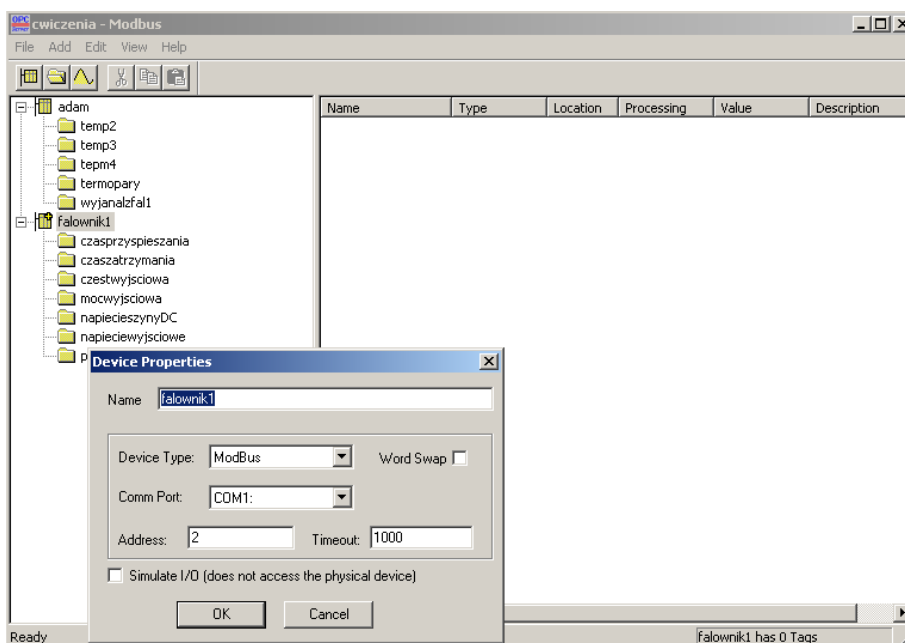


Fig. 4.1.9.16. View of the created subcatalogues

This type of inverter has 21 addressable parameters. A very useful parameter in tribological tests is the output power. This parameter makes it possible to compare the power consumed by the drive when testing different oil lubricating compositions, lubricants working in the same operating conditions. The second important parameter is the value of the consumed current. A sudden increase in the consumed current (appropriately calibrated) may correspond, for example, to the moment of seizure. Other parameters include, inter alia: inverter DC link voltage, RMS output voltage, output frequency, stop time, acceleration time and more. The structure shown in Figure 4.1.9.17 was built from units configured in this ways.

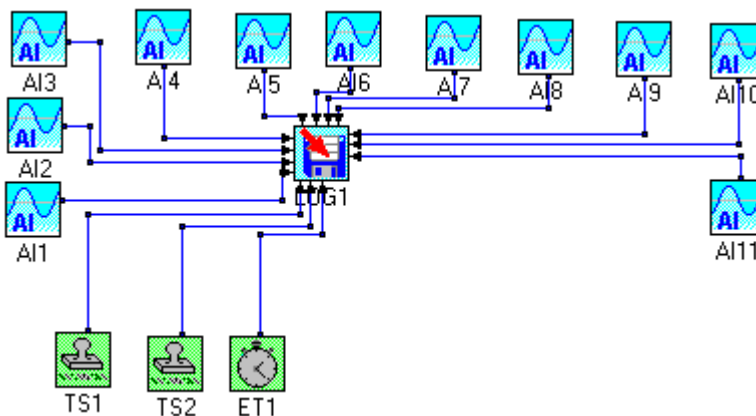


Fig. 4.1.9.17. Structure designed for OPC Server

The structure shown in Figure 4.1.9.17 contains 11 analog inputs (four thermocouples, one analog input of the inverter, six address parameters). The TS1, TS2 and ET1 program blocks are used to calculate the time in seconds, minutes and to insert the date in the appropriate format in the file. The blocks AI1, AI2, AI3 and AI4 get data from thermocouples. The remaining blocks AI5, AI6, AI7, AI8, AI9, AI10 and AI11 define the following inverter operation parameters: acceleration time, stop time, output current, output frequency, output voltage, DC bus voltage, output power. Figure 4.1.9.18 shows the view of the main panel for the parallel operation of ADAM 4019+ module. This panel contains graphs of the course of three selected temperatures and a graph of power consumption. The motor load is not dynamic here, therefore, the power is kept constant (only the lost motion of the drill).

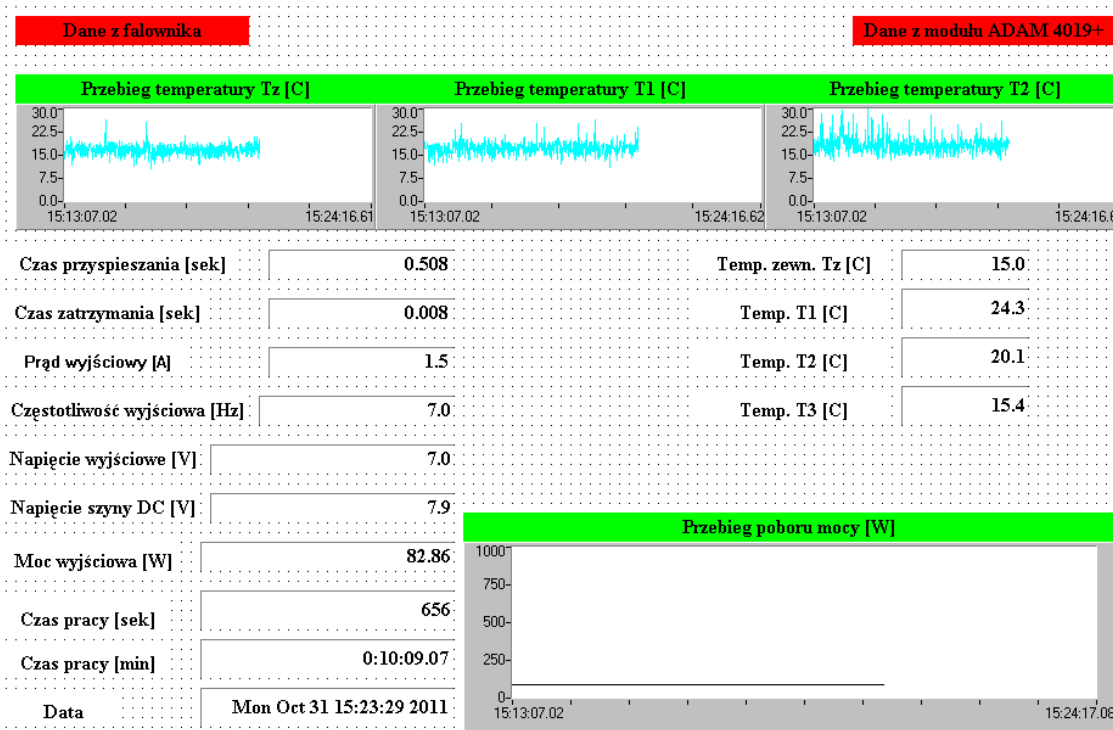


Fig. 4.1.9.18. The view of the main panel for the module operation in a parallel mode

Inverter parameters displayed include: acceleration time, stop time, output current, output frequency (necessity of calibration), output voltage (necessity of calibration), DC bus voltage, output power.

Temperature measurement is possible thanks to thermocouples connected to the module ports. A certain difficulty here is the calibration (re-scaling) of parameters in such a way that the displayed values reflect the actual state. The form of recording the registered data in the parallel operation mode is shown in Figure 4.1.9.18, and Figure 4.1.9.19 shows the arrangement of K-type thermocouples in the tribotester oil chamber.

Below is a fragment of the results of tests carried out on a modernized tribological test rig for testing kinematic pairs with conformal contact and described are conditions under which the tests were carried out.

The average speed of relative motion during the tests was: 4.8 m/min (0.08 m/s) i 9.6 m/min (0.16 m/s). The samples with counter-sample co-acted at the external load of 600 N, which - with the contact area of the samples and counter-sample of 300 mm² - corresponds to the theoretical pressures in the contact zone of 2.0 MPa.

Taking into account the material of the samples and counter-sample, the following hardness of samples was assumed: 40 HRC, for the counter sample: 60 HRC.

PE Motor Life and Mind M were selected as additives to the SN-150 base oil. The following criteria were used when selecting them: availability, mechanism of action, purpose. Besides, in the analyzed literature no research was found on a lubricating composition consisting of the above-mentioned operating preparations. Producers of the above-mentioned preparations recommend their 5% concentration in the oil base. In this study, concentrations both lower than this value and higher were adopted in order to better see their effects. Thus, the following concentrations were adopted: 0% (pure oil base); 0.5%; 1%; 2%; 5% and 7% of the tested additive in the oil base. The third CON was a composition consisting of Motor Life and Mind M in the ratio 1: 1 in the above concentrations - the designation 'Komp'.

The tests were carried out for improved C45 steel with a hardness of 40 HRC, the counter-sample was made of 102Cr6 steel hardened to hardness 60 HRC. The hardness of the counter-sample largely exceeds (by 50%) the hardness of the samples, so that the changes in ST condition occur mainly in the SL of the samples. In order not to take conclusions out of the context, I refer the reader to the literature [84, 85, 86, 87, 88, 89, 91, 92].

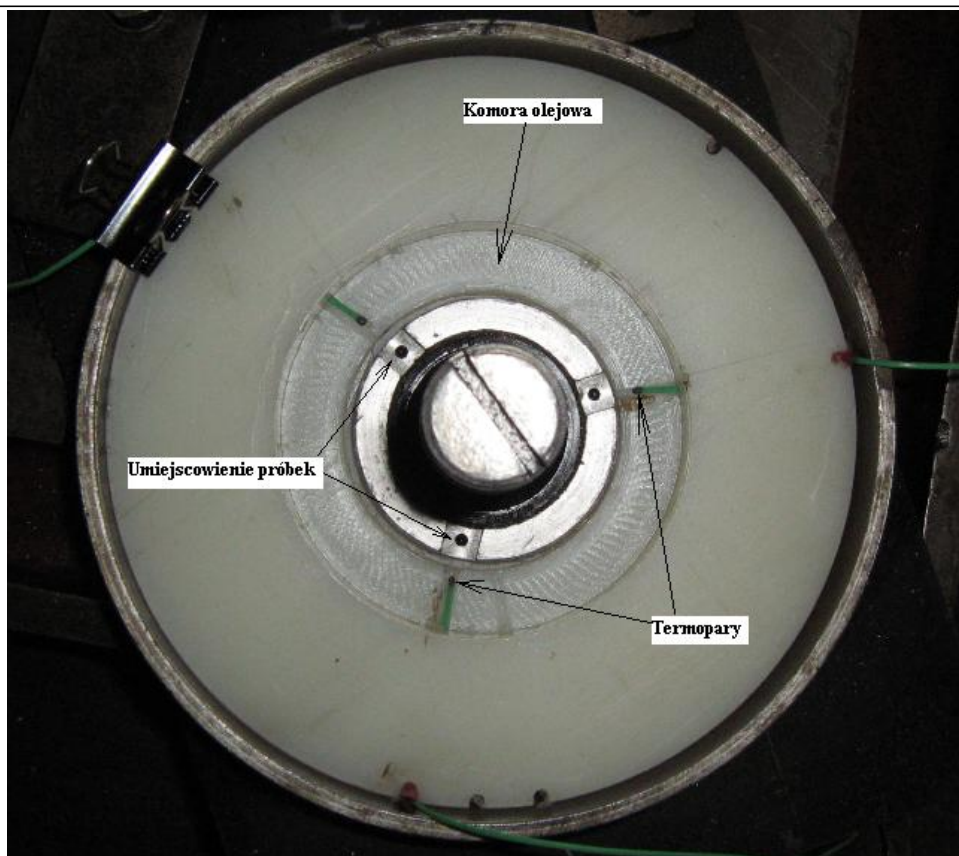


Fig. 4.1.9.19. Arrangement of K-type thermocouples in the tribotester oil chamber [84, 85, 86, 87, 88, 89, 91, 92]

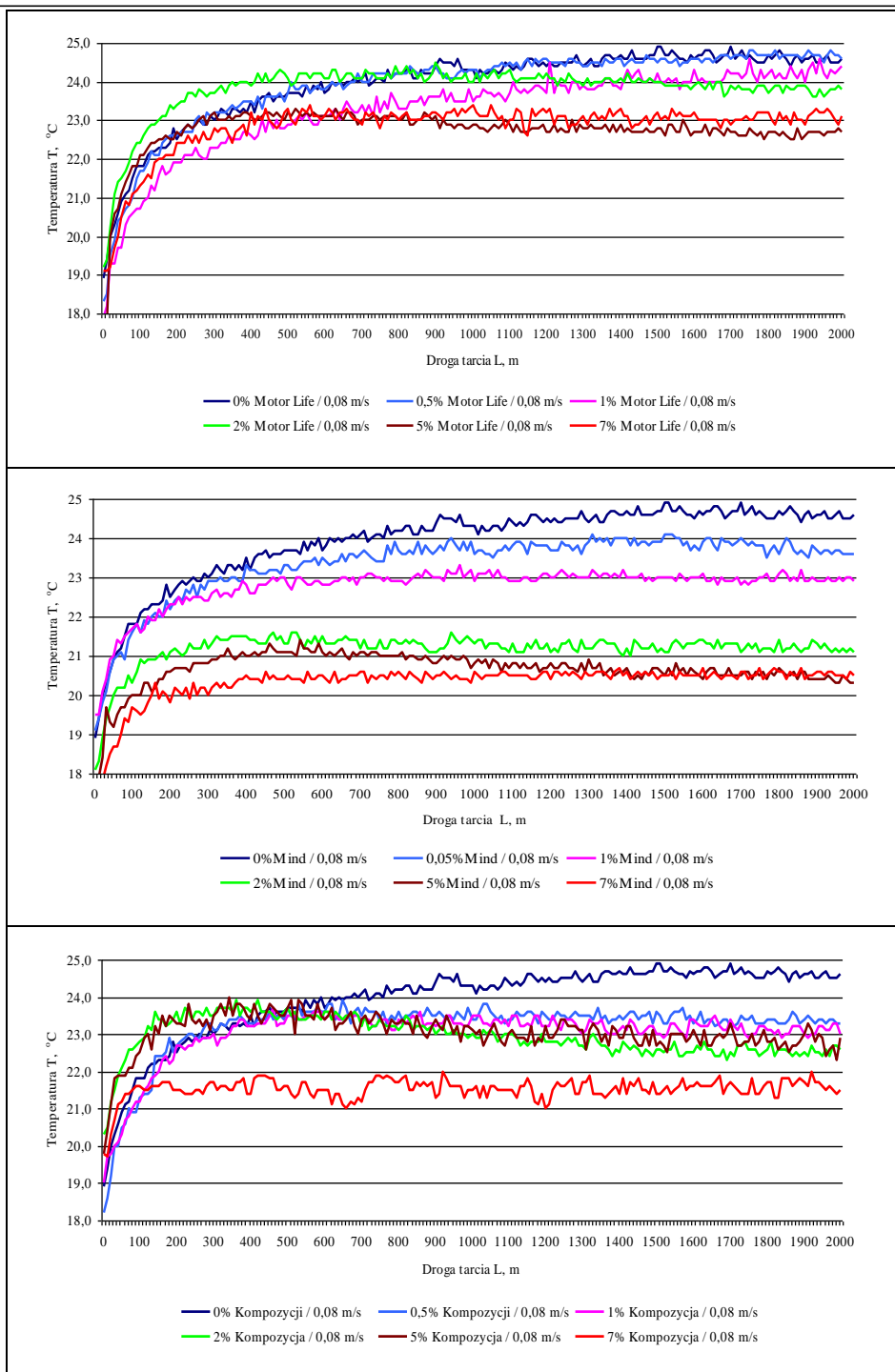


Fig. 4.1.9.20. The change in temperature T in the function of the path of friction L for various concentrations of tested AGE at the velocity $v_1 = 0.08$ m/s obtained on the basis of tests carried out on this test rig

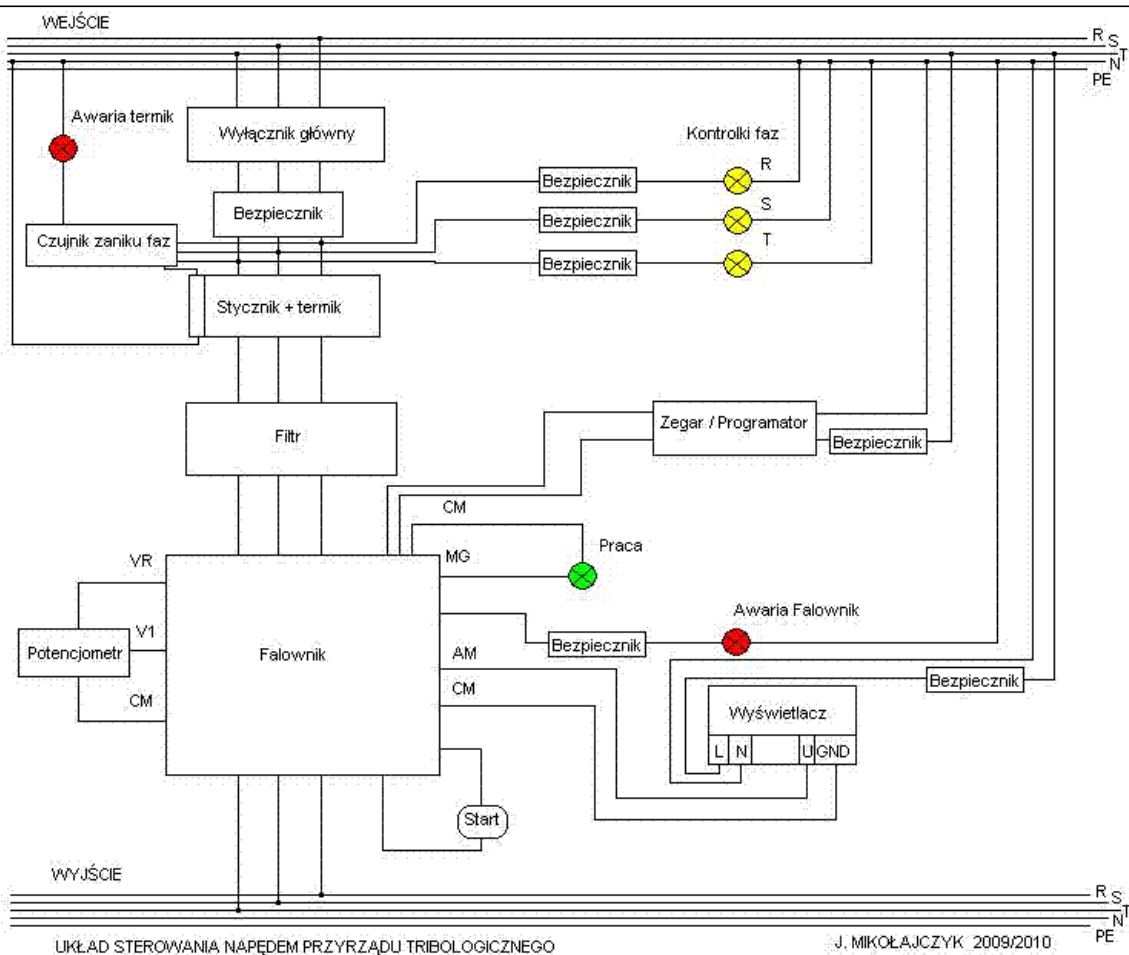


Fig. 4.1.9.21. Drive (engine) control system for a tribological test rig with a friction contact of conformal contact



Fig. 4.1.9.22. Prepared test rig for tribological tests with a friction contact of conformal contact. Side view.



Fig. 4.1.9.23. The base plate of the test rig for tribological tests with a friction contact of conformal contact with visible 3 samples immersed in the oil chamber



Fig. 4.1.9.24. The base plate of the test rig for tribological tests with a friction contact of conformal contact with visible three millings for samples

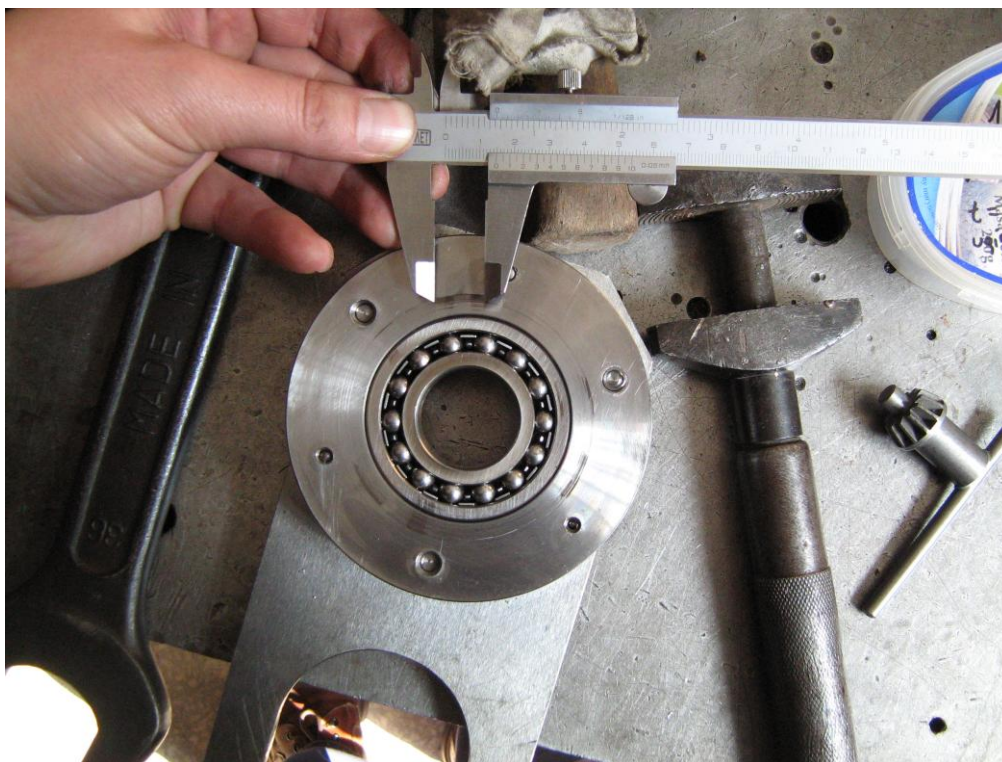


Fig. 4.1.9.25. The arm of the test rig for tribological tests with a friction contact with conformal contact with a disc-shaped counter-sample in which the bearing is mounted. Visible traces of wear of the counter-sample

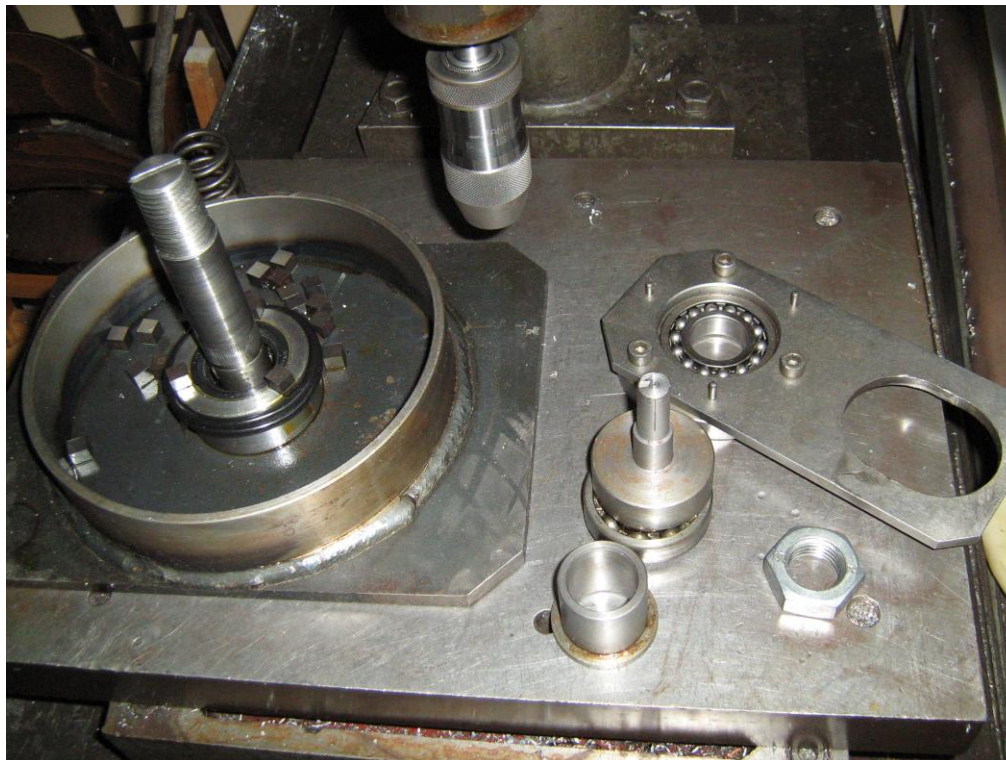


Fig. 4.1.9.26. Dismantled test rig for tribological tests with a friction contact of conformal contact



Fig. 4.1.9.27. A partially assembled test rig for tribological tests with a friction contact of conformal contact (mechanical part)



Fig. 4.1.9.28. A test rig during work

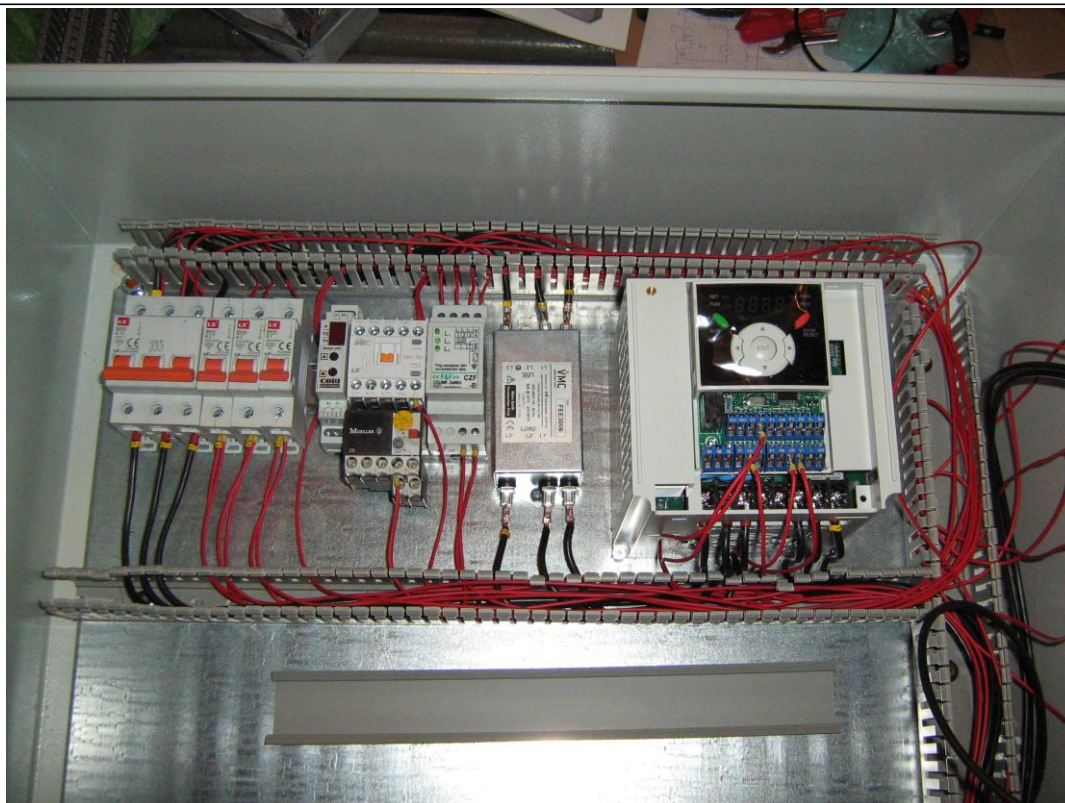


Fig. 4.1.9.29. A fragment of the interior of the cabinet controlling the tribological test rig

4.1.10. Test rig for determining frictional resistance based on the method of rings upsetting

A test rig for determining frictional resistance based on the method of rings upsetting (Fig. 4.1.10.1) is made of two plates 1, usually made of steel, placed e.g. in a press. Between the plates 1 there is the tested upset ring 2. Under the influence of the compressive forces F , the upset ring 2 is deformed. The essence of this method is based on the observation that there is a certain correlation between the frictional resistance and the change in the dimensions of the hole in the upset ring 2. During upsetting without frictional forces, the displacement of individual ring sections would be proportional to their distance from the symmetry axis. And the friction occurring in the contact zone disturbs an even flow of the metal (or other construction material), which is reflected in the change of dimensions of the inner and outer diameter of the upset ring 2.

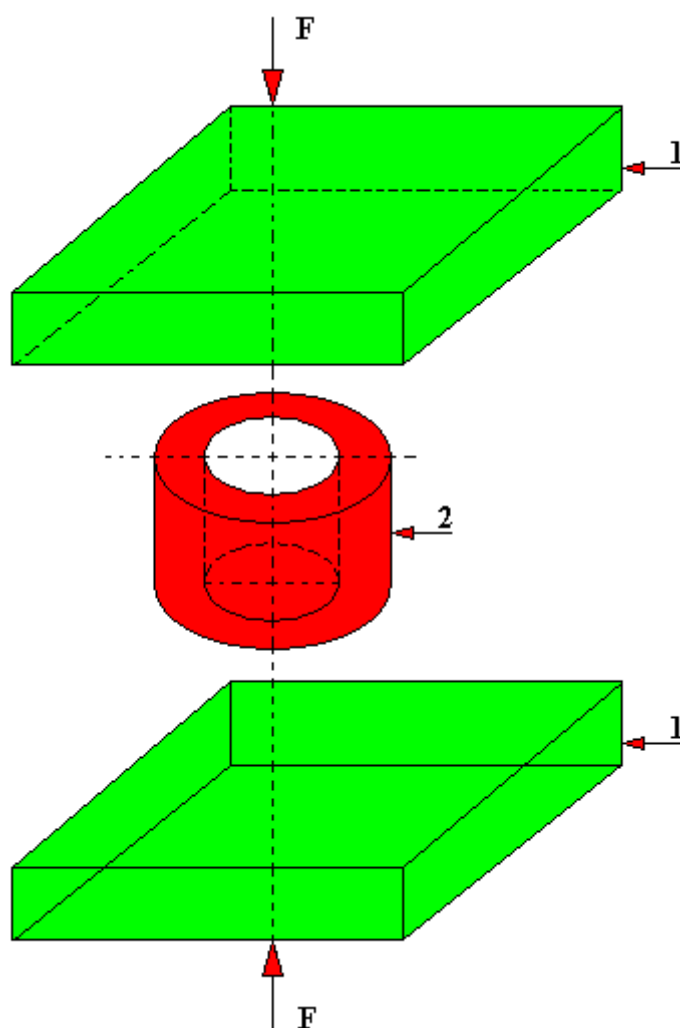


Fig. 4.1.10.1. Test rig for determining frictional resistance based on the method of rings upsetting
1 – steel plate; 2 - ring

With high resistance of frictional forces (Fig. 4.1.10.2) the internal diameter of the upset ring is reduced ($d_1 < d_0$). At a certain limit value of the friction forces, the hole diameter may remain unchanged ($d_1 = d_0$). With moderate frictional resistances there is a slight increase in the hole diameter ($d_1 > d_0$). Unfortunately, the disadvantage of this method is an uneven distribution of pressures and tangential forces on the contact surface. A graphic interpretation of this drawback

is the non-linear dependence of the pressures on the contact forces [17, 27, 28, 74]. Nowadays, of course, the nonlinear dependence of any variables (if they are not fast-changing) with the use of computers is not a major problem for their analysis.

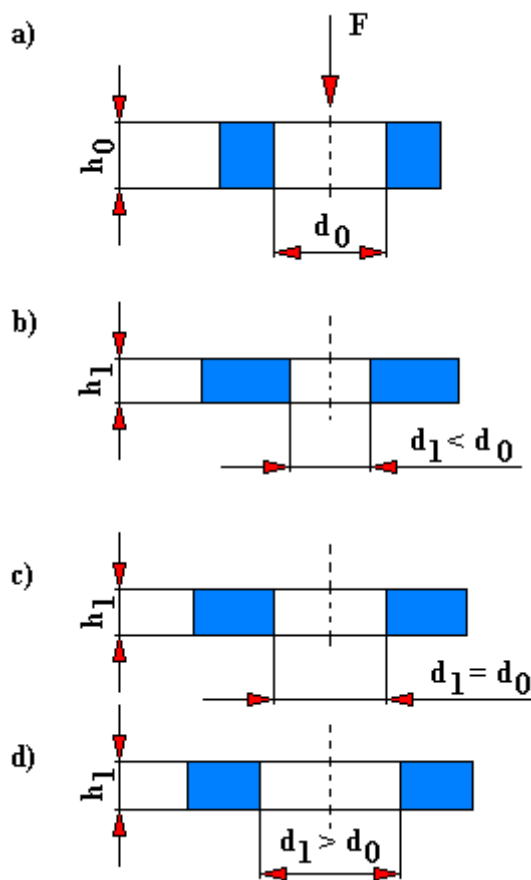


Fig. 4.1.10.2. Changing the dimensions of rings upset under different friction conditions [17]

Fig. 4.1.10.3 presents a Nomogram for determining the frictional resistance in the ring upsetting method [17].

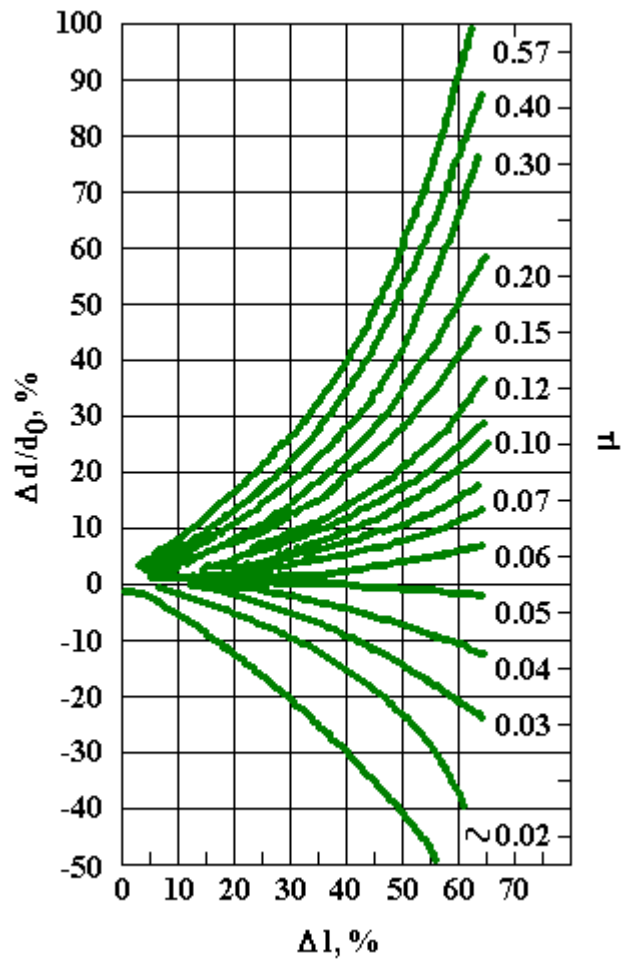


Fig. 4.1.10.3. Nomogram for determining the frictional resistance in the ring upsetting method [17]
 $\Delta d/d_0, \%$ - increase in the internal diameter of the upset ring; $\Delta l, \%$ - deformation; μ - coefficient of friction

4.1.11. Test rig for testing the wear of metals and their alloys at elevated temperatures according to the patent PL 193429

The originator of the test rig (Fig. 4.1.11.1 and 4.1.11.2) for testing the wear of metals and their alloys at elevated temperatures according to the patent number PL 193429 is Tadeusz Hejwowski.

The essence of the operation of the above-mentioned test rig is that a rectangular sample 1 embedded in the holder 2 of the bearing arm 3 is pressed against the counter-sample 4 in the shape of a roller with a horizontal axis of rotation. The pressure of the sample 1 against the counter-sample 4 is performed by a set consisting of a horizontal shaft 5 ending with a ball that touches the bearing arm 3. The horizontal shaft 5 is slidingly mounted in the ball bearing guide 7. The other end of the horizontal shaft 5 ends with a stop flange 8 against which the compression spring 9 rests.

The stop flange 8 is fixed axially to the horizontal shaft 5. This test rig has a strain gauge 11 mounted on a helical gear. This gear consists of a nut No.13 secured against rotation by a roller No. 14. Screwed into this nut is the bolt No. 15 which is based in a bearing pair and is connected with the stepper motor No. 18 by means of a clutch.

A pipe 19 is led from the bottom of the abrasive material tank 20 to the contact area of the sample 1 and counter-sample 4. The abrasive material tank 20 is equipped with a metering valve 21 for dosing the abrasive material and a thermocouple 23. The metering valve 21 for abrasive material is enclosed in an electric resistance heater 22.

The counter-sample 4 is mounted on a horizontal hollow shaft 24 connected by a belt transmission 26 to a stepping motor 27. The horizontal shaft 24 is hollow for delivering the cooling water. This water is drained through the collector 29.

The horizontal hollow shaft 24 is supported in a bearing contact with a housing 25.

In the lower and upper part of the bearing arm 3 there are cooling inserts 31. Similar cooling inserts are located in the body 30 mounted near the axis of rotation of the bearing arm 3.

An additional electric heater was installed above sample 4 and a thermocouple was brought in between. The space under the counter-sample 4 is closed with the abrasive material chute 34.

The following elements are attached to the base plate 35 of the above-mentioned test rig:

- body 30;
- guide housing;
- housing of the bearing contact 16;
- stepper motor 18;
- housing of the bearing contact 25;
- a stepper motor housing 36.

This test rig is characterized by a compact structure and easy operation. The maximum pressure force of the sample 1 against the counter-sample 4 is 200 [N]. The maximum test temperature is up to 600°C. The maximum rotational speed of the counter-sample 4 is 1 [rpm]. The time needed to stabilize the set temperature does not exceed 15 minutes. This test rig has a data recording and visualization system.

The samples holder 2 enables mounting the tested cuboidal samples 1 of the thickness in the range of 3 ÷ 8 [mm]. After fixing the sample in the holder the electric resistance heater 32 is turned on which heats the tested sample 1 to the preset temperature. The temperature is controlled by a thermocouple. After reaching the set temperature, the stepper motor 18 is turned on.

The value of the pressure exerted on the sample 1 is set on two-way comparator co-acting with a strain gauge bridge measuring the force by means of a strain gauge 11.

The comparator causes the stepper motor 18 to rotate in a direction depending on the current value of the pressing force. After reaching the preset pressing force the stepper motor 27 is turned on causing the rotation of counter-sample 4.

It is possible to carry out tests on this test rig with or without the use of abrasive material. When abrasive is used the metering valve 21 is opened.

The rate of rotation of the counter-sample 4 is given by the function generator. After a preset path of friction (or preset operating time) has been passed, electric resistance heaters 22 and 32 are turned off, stepper motors 18 and 27 are turned off, and the abrasive metering valve 21 (if used) is closed.

After completion of tests, the housing of the electric resistance heater 32 is removed together with the thermocouple 33. Stepper motor 18 is turned on for a moment in order to relieve (remove the load) the friction contact. Closed is the cooling water flow and sample 1 is disassembled.

As disadvantages of this test rig one should include the need to use softened or at least demineralized water for cooling, otherwise lime scale will be deposited in the cooling inserts, effectively hindering both the water flow and heat transfer (heat exchange/removal).

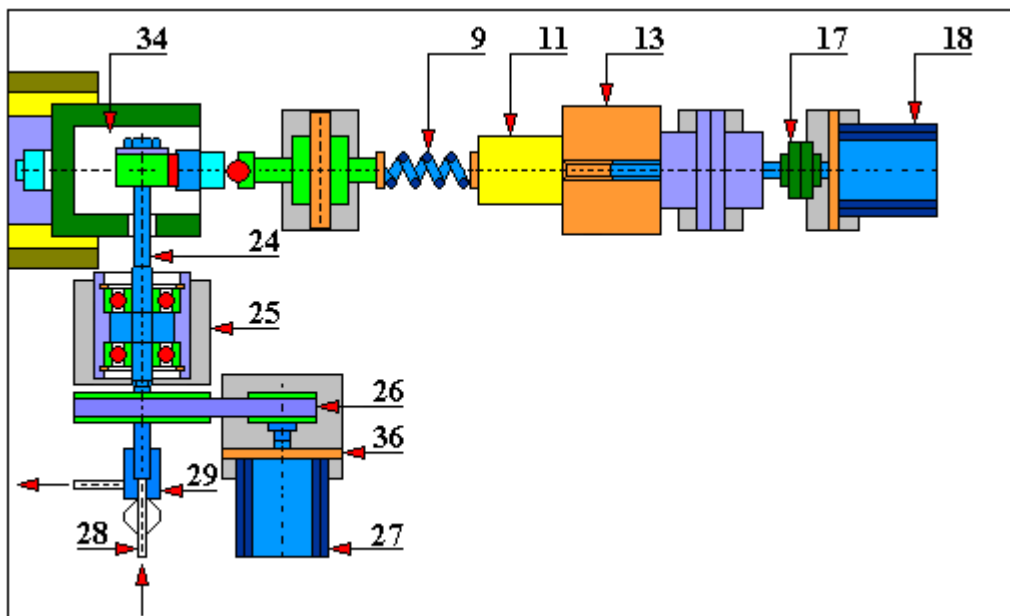


Fig. 4.1.11.1. General view of the test rig for testing the wear of metals and their alloys at elevated temperatures according to the patent PL 193429

1 - test sample; 2 - sample holder; 3 - bearing arm; 4 - counter-sample; 5 - horizontal roller; 6 - a ball; 7 - ball bearing guide; 8 - limiting flange; 9 - compression spring; 10 - flange; 11 - strain gauge sensor; 12 - single row ball bearing; 13 - nut; 14 - roll; 15 - screw; 16 - bearing contact housing; 17 - clutch; 18 - stepper motor; 19 - pipe; 20 - abrasive material tank; 21 - abrasive material metering valve; 22 - electric resistance heater; 23 - thermocouple; 24 - horizontal hollow shaft; 25 - bearing contact housing; 26 - belt transmission; 27 - stepping motor; 28 - cooling water supply; 29 - cooling water drain; 30 - body; 31 - cooling inserts; 32 - electric resistance heater; 33 - thermocouple; 34 - abrasive material chute; 35 - base plate; 36 - stepper motor housing (description applies to figures 4.1.11.1 and 4.1.11.2)

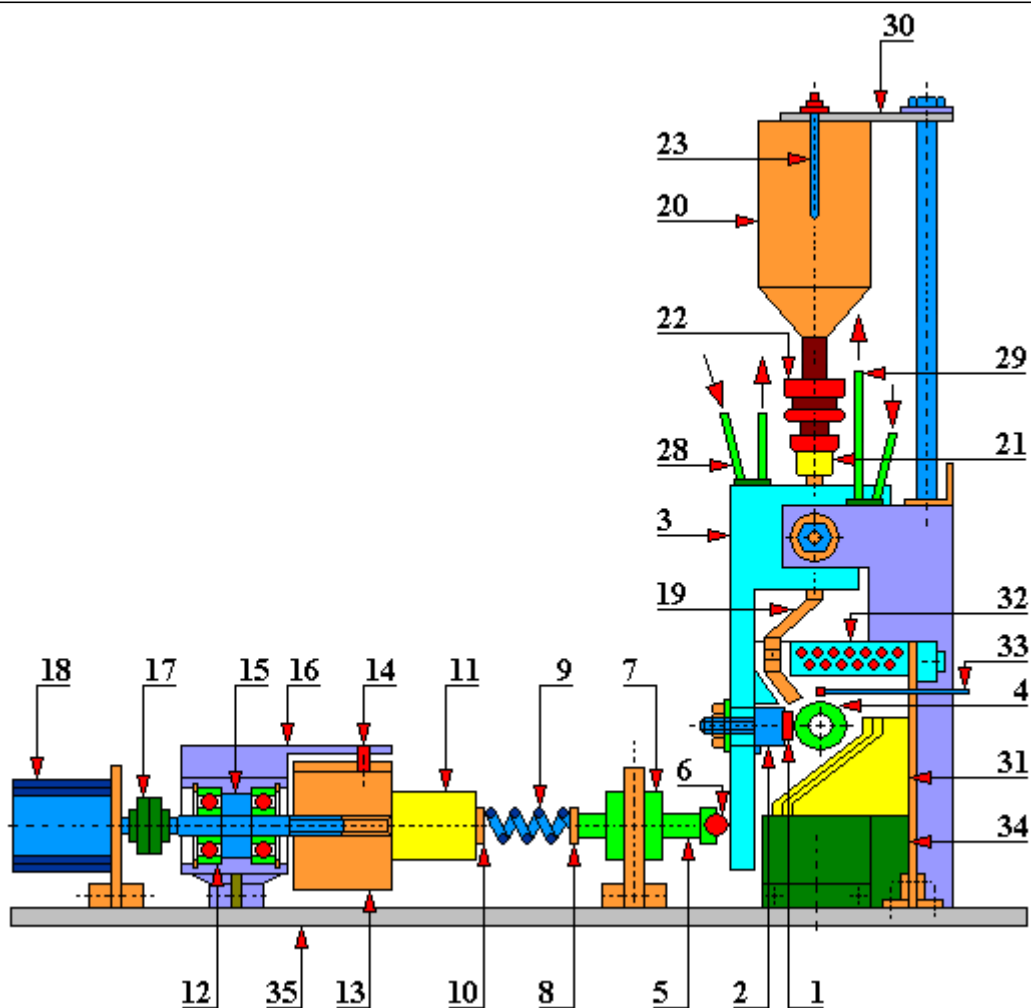


Fig. 4.1.11.2. General view of the test rig for testing the wear of metals and their alloys at elevated temperatures according to the patent PL 193429

1 - test sample; 2 - sample holder; 3 - bearing arm; 4 - counter-sample; 5 - horizontal roller; 6 - a ball; 7 - ball bearing guide; 8 - limiting flange; 9 - compression spring; 10 - flange; 11 - strain gauge sensor; 12 - single row ball bearing; 13 - nut; 14 - roll; 15 - screw; 16 - bearing contact housing; 17 - clutch; 18 - stepper motor; 19 - pipe; 20 - abrasive material tank; 21 - abrasive material metering valve; 22 - electric resistance heater; 23 - thermocouple; 24 - horizontal hollow shaft; 25 - bearing contact housing; 26 - belt transmission; 27 - stepping motor; 28 - cooling water supply; 29 - cooling water drain; 30 - body; 31 - cooling inserts; 32 - electric resistance heater; 33 - thermocouple; 34 - abrasive material chute; 35 - base plate; 36 - stepper motor housing (description applies to figures 4.1.11.1 and 4.1.11.2)

4.1.12. Head for testing friction and wear according to the patent PL 113646

The object of the present invention (Fig. 4.1.12.1) according to the patent PL 113646, whose originator is Lucjan Kocjan, is a head for testing friction and wear used primarily for testing sliding pairs made of plastics.

The essence of the operation of this test rig is as follows. The head contains a counter-sample 1, in the shape of a rotational cylinder, located in the opening of the disc 2. To both sides of the disc 2, which is shaped like a ring, are radially mounted hydraulic motors 3 and 4, three on each side. Each motor 3 mounted on one side of the disc 2 is located between two adjacent motors 4 mounted on the other side of the disc 2. Moreover, beams 5 and 6 are attached to the disc 2, parallel to the horizontal plane, protruding beyond the disc 2. On these beams, symmetrically with respect to the vertical plane of disc 2, ball-shaped supports 7 are mounted, coupled with bar dynamometers 8.

Each bar dynamometer 8 is at a distance equal to three radii of the counter-sample 1. At the free end of the first beam 5, a weight 9 is slidably mounted for static balancing of the head. In the free ends of the pistons 10 of the hydraulic motors 3 and 4, there are seats for samples 11.

During the operation of this test rig the friction forces on the sliding surfaces of samples 11 and a counter-sample 1 create a torque moment of friction balanced by the anti-torque of the bar dynamometers 8. On the basis of the pressing force of samples 11 against the counter-sample 1 and the values of forces read on the dynamometers of the bar force gauges 8, the equation of equilibrium of moments is made from which the value of the coefficient of friction is calculated. On the other hand, the value of the abrasive wear of samples is measured with a micrometer or using the method of artificial bases measuring the value of the chord of the artificial base with a workshop microscope.

In another design of a similar head for testing friction and wear, presented in the study [Janusz Jarecki, Michał Hebda, „Tarcie, smarowanie i zużycie części maszyn”, WNT Warszawa 1969, s. 343, rys. 5.36] the moment of frictional in the head is balanced only by the moment derived from one reaction force applied at the disc suspension point, shifted relative to the axis of rotation of the counter-sample. This causes an additional load or relief of the sample during the head operation and thus an error in the measurement of the coefficient of friction. This design solution for the head for testing friction and wear, according to the patent PL 113646, eliminates the above-mentioned defect. In addition, the advantage of this design is a high reliability and ease of measurements and the possibility of loading samples continuously from 0 to 500 kG, as well as a high reliability and durability of the head.

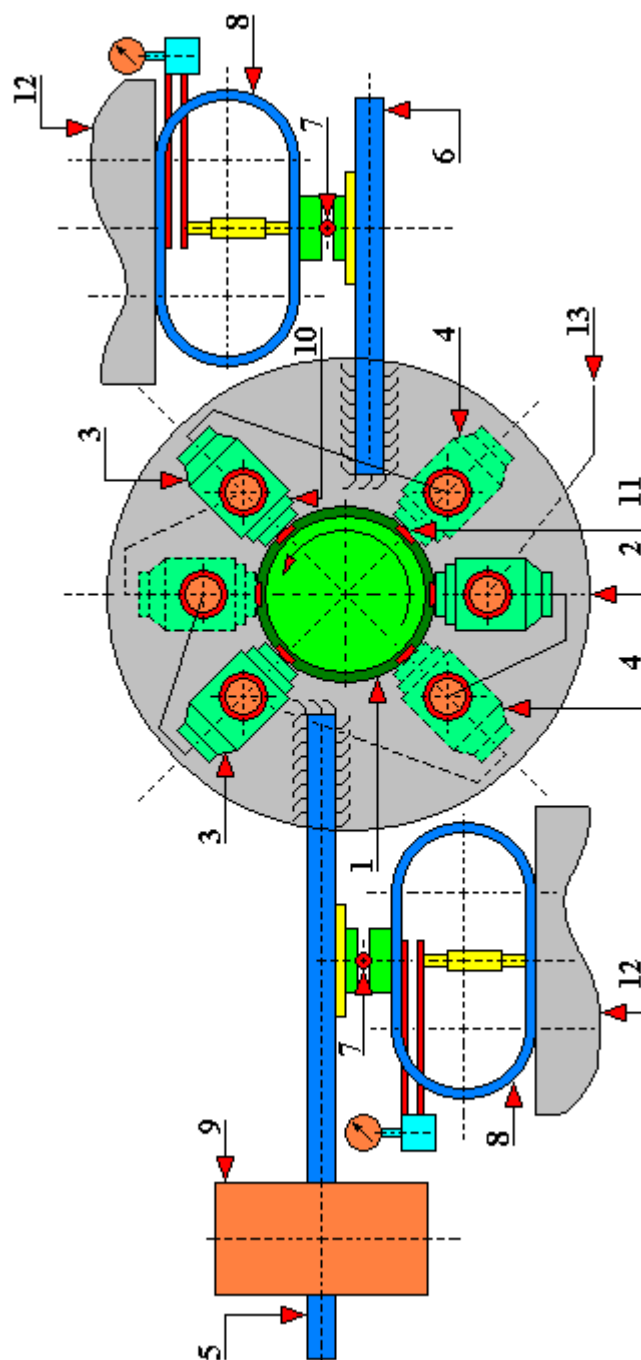


Fig. 4.1.12.1. General view of the head for testing friction and wear according to the patent PL 113646

1 - counter-sample in the shape of a rotational cylinder; 2 - ring-shaped disc; 3 - hydraulic motor; 4 - adjacent hydraulic motors; 5 - first beam; 6 - second beam; 7 - ball-shaped support; 8 - bar dynamometer; 9 - slidably weight; 10 - free end of the piston of the hydraulic motor; 11 - sample; 12 - base; 13 - power supply for hydraulic motors

4.1.13. Tribological test rig with adjustable frictional resistance according to the patent PL 171768

This position, whose authors are Jan Sadowski and Jan Ciecieląg, concerns a method of adjusting the sliding frictional resistance occurring in the rotational motion between the co-acting elements of a friction contact, especially in test rigs intended for testing friction and material wear.

The previously known methods of adjusting the frictional resistance are realized e.g. by changing the value of the pressing force of rubbing elements. The friction force T is the product of the coefficient of friction μ and the aforementioned pressing force N .

$$T = N \cdot \mu$$

In the case of a specific kinematic contact, e.g. consisting of a disc (counter-sample) and block (sample) the value of the coefficient of friction μ slightly changes with the change of the pressing force. Thus, by increasing this force, we obtain a proportional (approximately) increase in the friction force. This effect occurs in friction clutches and brakes. It is often accompanied by the following features (disadvantages):

- instability of frictional resistance;
- generating mechanical vibrations;
- increased wear of the materials of the mating friction contact.

This test rig enables the adjustment of frictional resistance with the omission of the above-mentioned disadvantages and is intended mainly for the cases of friction contacts in test rigs for testing friction and wear of plastic and metals.

It was surprisingly found that the value of the coefficient of friction μ can be changed and adjusted in a controlled manner, in a wide range of values, if during the friction process the tribological wear products are removed from the friction contact. It was found that during a technically dry friction of a standardized steel sample, grade 45, against the surface of a counter-sample of steel grade NC 6 with a hardness of 60 HRC, it is possible to change the degree of coefficient of friction μ , in the range from 0.3 to 0.6, by adjusting the level of contact surface cleaning. As a consequence, it becomes possible to change the value of frictional resistance with a constant, set load of the friction contact, even by 100%. At the same time, it turned out that such regulated friction resistances can be completely independent of other friction parameters, especially the sliding speed and the friction contact temperature.

The essence of the operation of this test rig consists in the fact that during the friction of two (many) elements in the rotational motion, one of which is stationary, the degree of cleaning the friction surface from wear products of the friction elements is continuously regulated. This adjustment is made by changing the value of the force pressing the surface cleaning element of the rotating element of the friction contact against this element. According to this invention the degree of cleaning of the friction surfaces of the rotating element is controlled by changing the degree of absorption of the wear products by the forcefully pressed down, with adjustable force, cleaning element made of a soft, porous material, preferably made of felt.

The method of adjusting the frictional resistance according to this invention is carried out during the friction process of two (many) elements of the mating frictional pair in the friction testing rig, of which the element 1 (sample) is stationary and pressed with a constant force N against the element 2 rotating at speed ω (counter-sample). By means of the measuring system 3, the frictional resistance T in this friction contact is continuously measured.

At the same time, by means of a cleaning element 4 made of felt, pressed against the friction surface of the element 2 (counter-sample) with force P , the friction products formed in the process of friction and deposited on the friction surface of the friction elements are removed.

Changing the value of the force P causes a change in the value of frictional resistance measured by the system 3, and this is due to the change in the amount of wear products of friction elements absorbed by the cleaning element 4 (felt). The more of these products are absorbed, the greater the degree of cleanliness of the friction surface and the lower the friction coefficient μ . Thus, the adjustment of the frictional resistance is made by continuously adjusting the cleaning of the friction surface by changing the value of force P pressing the cleaning element against the cleaned surface.

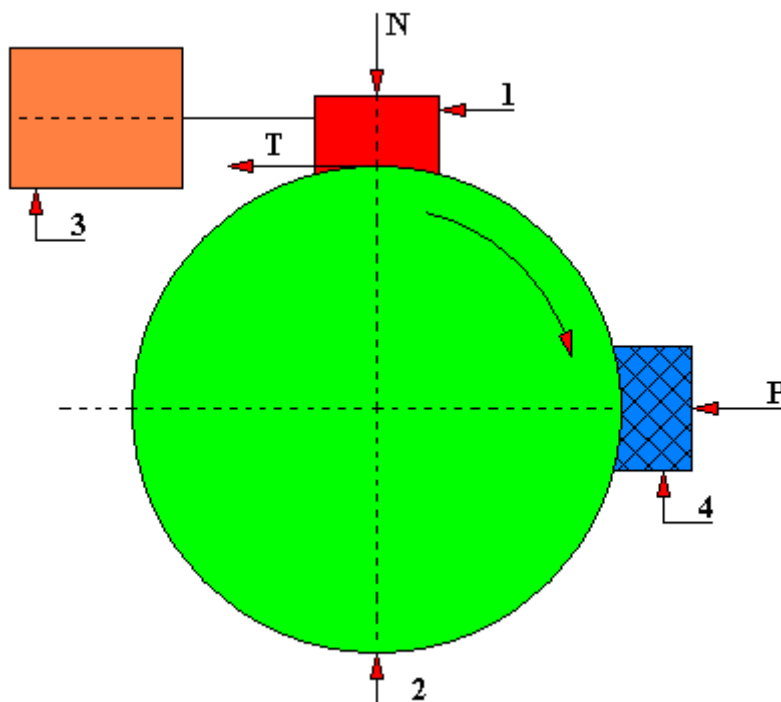


Fig. 4.1.13.1. General view of a tribological test rig with adjustable frictional resistance according to the patent PL 171768

1 - sample; 2 - counter-sample (cleaned element); 3 – meter circuit; 4 - cleaning element (felt); N - force pressing the sample against the counter-sample; P - force pressing the cleaning element (felt) against the counter-sample surface; T - friction force

4.1.14. Test rig for testing abrasive wear according to the patent PL 115763

A test rig according to the patent PL 115763, created by Franciszek Rudol, Elżbieta Elman and Alicja Maj, is designed to test abrasive wear during sliding friction in laboratory conditions using the peripheral abrasion method.

Known are test rigs for testing abrasive wear using the method of peripheral abrasion. For example, the Skoda-Savina test rig has an individual drive with a continuous change of rotational velocity, but it is characterized by a big weight - about one ton, and large dimensions (height: 1500 mm, width: 500 mm). The abrasion length is measured using a special microscope installed in the test rig. However, in order to measure the abrasion it is necessary to change the position of the sample, which unfortunately makes it impossible to precisely position the sample in the same place for further wearing out. This is especially important with different friction paths of metallized or coated samples.

Another test rig for abrasive wear testing using the peripheral abrasion method is the Amsler type test rig. Its construction is complicated and very expensive as for that time. Its advantage is that it is a universal test rig.

MZIWT-1 test rigs - designed to test wear and the coefficient of friction using the peripheral abrasion method - are characterized by interesting technical solutions [Czasopismo Techniczne, Wydawnictwo Politechniki Krakowskiej, z. 6 – M/1972, PWN Warszawa-Kraków]. These test rigs have an individual drive, a lever-loading system and are equipped with a number of instruments for carrying out tests in different conditions. Because these test rigs have an extensive instrumentation they are also universal.

There is also a test rig made according to the patent PL 102802, known as a test rig for tribological tests, in which an engine lathe is used as a drive unit. In the test chamber of this test rig, attached to the lathe bed, there is a mandrel with material samples, located rotationally, to which the samples of co-acting materials are pressed. The tests are performed in a similar way as on the Amsler test rig.

And this design (according to the patent PL 115763), which is designed to test abrasive wear using the method of peripheral abrasions, enables cooperation with a universal test rig tool (e.g. with a lathe) and it uses its drive. This goal was reached because the base 1 is provided with projections 4 in which a tank 6 with samples holder 9 is mounted rotationally. The extension of the tank bottom 6 is the arm of the sample loading lever. The counter-sample 18 is mounted on a mandrel provided with driver pins by means of a nut. This test rig can be adapted to many types of machine tools. The tests can be carried out under various conditions:

- dry running;
- running with water cooling or other cooling lubricants;
- running at elevated temperatures (with the use of appropriate instrumentation).

This test rig ensures that the sample is positioned in the same abrasion point after the measurement is made in order to continue the tests.

The essence of the operation of this test rig is as follows. The base 1 of the test rig is attached to the lathe bed with 2 set screws 3. The bottom 5 of the tank 6 for lubricating and cooling liquids is mounted in the projections 4 of the base 1 by means of pins 7. In the bottom 5 of the tank 6 there are pins 8 for setting the holder 9 of the sample 10, the position of which is fixed by means of a washer 11 and a pressure plate 12, and then clamped by springs 13 after their positioning by means of bolts 14 and nut 15. The mandrel 16, with the Morse taper B22 with the mounted counter-sample 18, is inserted into the lathe spindle, and the end is supported by the tooth with the tail of the lathe. The driver pins 19 are designed to transmit the torque to the counter-sample 18.

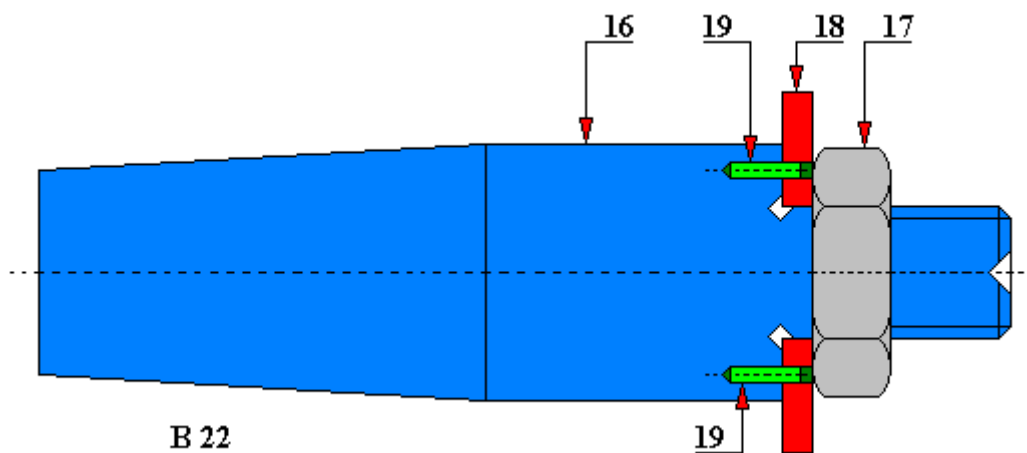


Fig. 4.1.14.1. A spindle with Morse B 22 taper with the attached counter-sample
 1 - test rig base; 2 - lathe bed; 3 - set screws; 4 - projections; 5 - extension of the bottom; 6 - tank; 7 - pins; 8 - pins; 9 – holder for samples fixing; 10 - sample; 11 - washer; 12 - pressure plate; 13 - springs; 14 - bolts; 15 - nuts; 16 - spindle with Morse taper; 17 - nut; 18 - counter-sample; 19 - driver pins; 20 - lever arm; 21 - weights; 22 - lock screw (description applies to Fig. 4.1.14.1, 4.1.14.2 and 4.1.14.3)

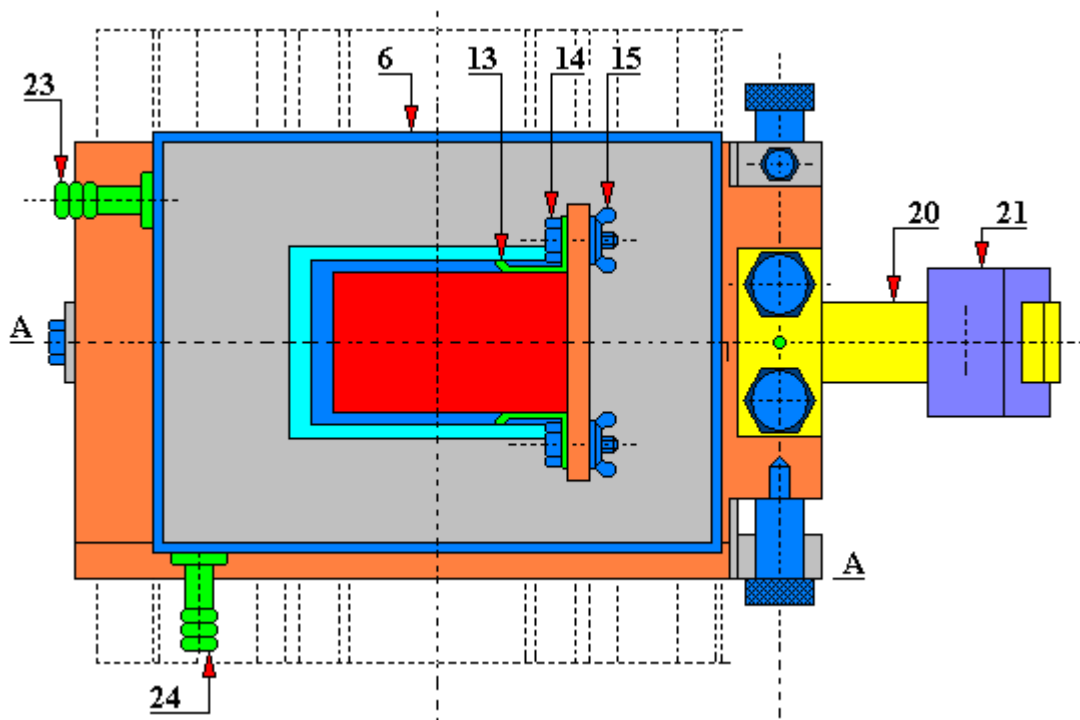


Fig. 4.1.14.2. Top view of the test rig according to the patent 115763
 1 - test rig base; 2 - lathe bed; 3 - set screws; 4 - projections; 5 - extension of the bottom; 6 - tank; 7 - pins; 8 - pins; 9 – holder for samples fixing; 10 - sample; 11 - washer; 12 - pressure plate; 13 - springs; 14 - bolts; 15 - nuts; 16 - spindle with Morse taper; 17 - nut; 18 - counter-sample; 19 - driver pins; 20 - lever arm; 21 - weights; 22 - lock screw; 23 - stub that supplies the tank with a lubricant (oil); 24 - lubricant drain stub from the tank (description applies to Fig. 4.1.14.1, 4.1.14.2 and 4.1.14.3)

A weight 21 is placed on the lever 20 constituting an extension of the bottom 5 of the tank 6 and secured with a screw 22 against a spontaneous shifting during the test rig operation.

After setting the selected load, friction conditions and spindle rotation, the lathe drive is turned on. After a specified time corresponding to the desired friction path, the lathe is turned off and measured is the length of the abrasion constituting a basis for the relative determination of the wear resistance of the friction contact under test.

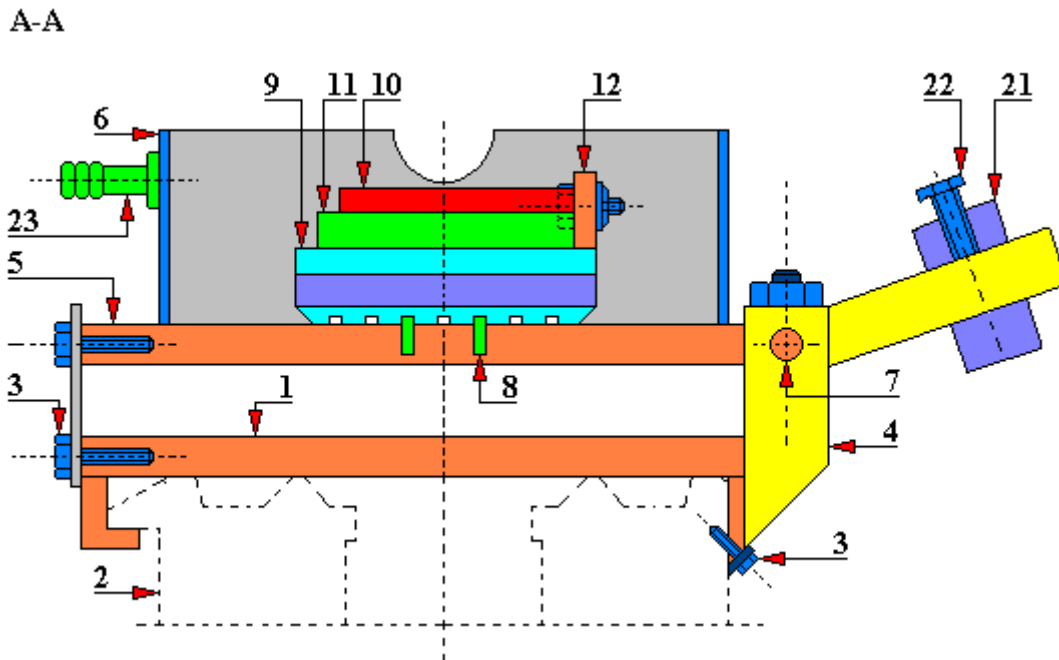


Fig. 4.1.14.3. Top view of the test rig according to the patent 115763

1 - test rig base; 2 - lathe bed; 3 - set screws; 4 - projections; 5 - extension of the bottom; 6 - tank; 7 - pins; 8 - pins; 9 - holder for samples fixing; 10 - sample; 11 - washer; 12 - pressure plate; 13 - springs; 14 - bolts; 15 - nuts; 16 - spindle with Morse taper; 17 - nut; 18 - counter-sample; 19 - driver pins; 20 - lever arm; 21 - weights; 22 - lock screw; 23 - stub that supplies the tank with a lubricant (oil); 24 - lubricant drain stub from the tank (description applies to Fig. 4.1.14.1, 4.1.14.2 and 4.1.14.3)

4.1.15. FRET III test rig

FRET III test rig (Figures 4.1.15.1, 4.1.15.2, 4.1.15.3 and 4.1.15.4) is intended for testing fretting wear. It is a non-commercial original test rig built by the Laboratory of the Department of Construction and Operation of Machines at Gdańsk University of Technology. Tests on this test rig are most often carried out for a concentrated contact. The tests are based on the fact that a cylindrical or ball-shaped sample is set in motion by an electromagnetic vibrator. This sample is pressed against a stationary counter-sample and moved tangentially in relation to it.

This test rig enables, among others, the examination of the following quantities:

- friction force between mating surfaces,
- number of cycles,
- oscillation amplitudes,
- linear or volumetric samples wear.

The technical parameters of this tribological test rig are as follows:

- load up to 50 [N],
- oscillation amplitude: 0 ÷ 500 [Hz],
- typical dimensions of a cylindrical sample: diameter \varnothing 10 [mm], thickness of the cylinder $b=2$ [mm],
- typical dimensions of a ball-shaped sample: diameter \varnothing 10 [mm].

Laboratory exercises performed by students on the FRET III test rig are carried out on samples made of mild carbon steel with the following parameters:

- vibration frequency 180 [Hz],
- vibration amplitude 60 [μ m],
- samples load 50 [N],
- the duration of tests is approximately 20 minutes.

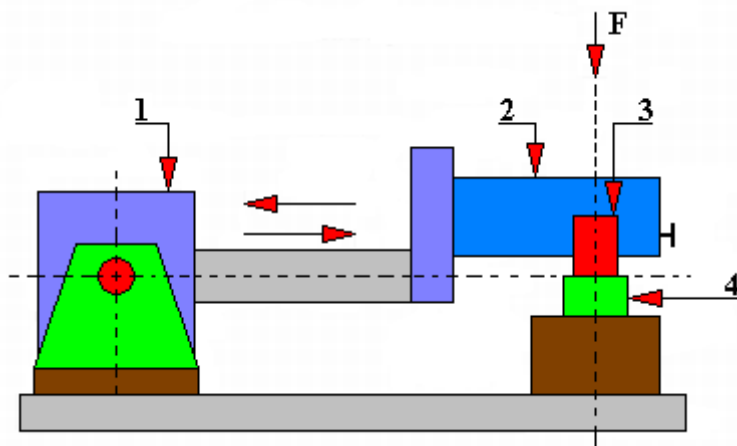


Fig. 4.1.15.1. Diagram of the FRET III test rig (tests of the fretting process)

1 - electromagnetic vibrator, 2 - sample holder, 3 - movable cylinder-shaped or ball-shaped sample, 4 - stationary counter-sample.

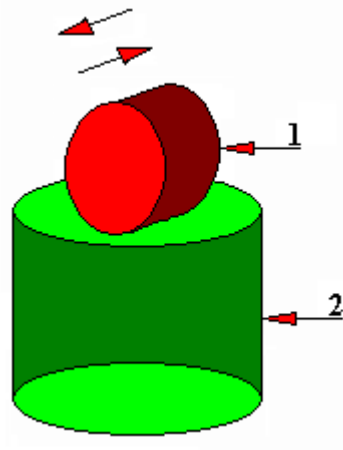


Fig. 4.1.15.2. Diagram of the co-action of the friction contact of FRET III test rig (fretting process tests)
1 - cylinder-shaped or ball-shaped movable sample, 2 - stationary counter-sample.



Fig. 4.1.15.3. FRET III test rig built at the Department of Construction and Operation of Machines, Faculty of Mechanical Engineering of Gdańsk University of Technology - visible, among others, displacement sensors, exciter

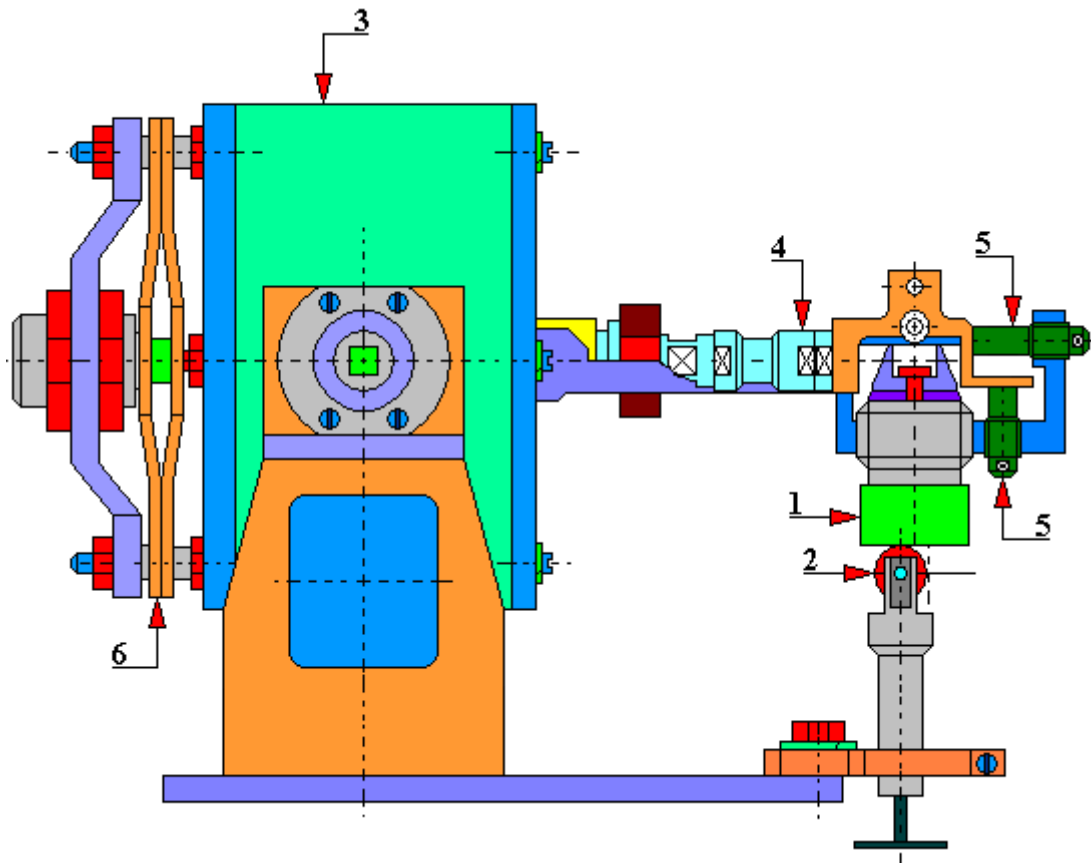


Fig. 4.1.15.4. FRET III test rig The design solution applied by the Department of Construction and Operation of Machines, Faculty of Mechanical Engineering of Gdańsk University of Technology
1 - movable sample, 2 - stationary sample, 3 - exciter, 4 - dynamometer, 5 - displacement sensors, 6 - set of tension springs.

4.1.16. SMOK test rig

SMOK test rig is designed to determine the characteristics of dynamically loaded radial slide bearings. It is a non-commercial original test rig built by the Laboratory of the Department of Construction and Operation of Machines, Faculty of Mechanical Engineering of Gdańsk University of Technology. The test rig is built (Figures 4.1.16.1 and 4.1.16.2) of the test shaft (1) driven by an electric motor. The test shaft (1) is seated in the supports (2). Between supports (2), the shaft has got an eccentric on which the tested bearing (3) is mounted. The bearing (3) is mounted in the housing (4) which is located in the connecting rod (6). The assembly of the test shaft (1) and supports (2) is attached to the head plate (13). The head plate (13) is attached to the support frame (12) with foundation bolts (14). The head plate (13) is attached in the top part of the cylinder (15). The piston (9) moves in the cylinder. The piston (9), in its upper part, has a connecting rod (11) which is connected to the connecting rod (6) by means of a connecting pin (10). SMOK test rig is equipped with a double-acting hydraulic actuator facilitating the exertion of pendulum loads on the tested bearing (3) as well as unilaterally and bilaterally variable loads in a wide range of excitation frequencies. The actuator chambers are supplied from two independent branches with regulated supply pressure. As a result of the rotation of the eccentric test shaft (1) and the resulting reciprocating motion of the piston (9) in the cylinder (15), as well as due to the outflow of oil from the cylinder chambers (15), the pressure in the chambers changes, and the generated variable load is transferred by the connecting rod (11) to the tested bearing (3). The actuator can operate using both chambers (7 and 8) or one of them (7 or 8), which makes it possible to change the character of the applied load. The upstream valves (17) and the downstream nozzles (18) are used to control the pressure in the chambers.

SMOK test rig has the following technical data:

- load of the tested bearing up to 200 [kN],
- frequency of load changes: 20 ÷ 70 [Hz],
- length of the tested bearing: 29.6 [mm],
- diameter of the tested bearing: \varnothing 52.7 [mm].

SMOK test rig enables the measurement of the following parameters:

- force loading the tested bearing,
- the number of load cycles,
- supply pressure of the tested bearing and support bearings,
- supply pressure of the actuator chambers,
- temperature of the tested bearing,
- temperature of the support bearings,
- oil temperature on the upstream to the tested bearing.

On SMOK test rig carried out were, among others, tests of fatigue cracks in hydrodynamic bushings of radial bearings - estimators of the fatigue strength of sliding layers.

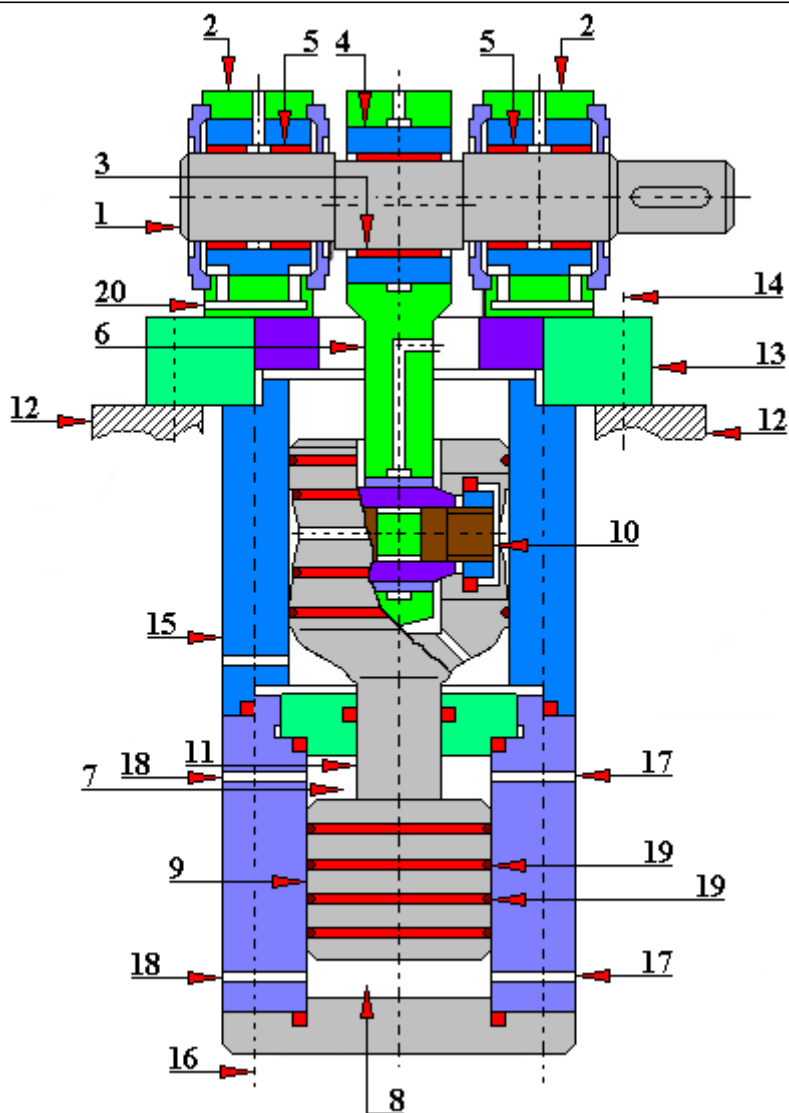


Fig. 4.1.16.1. Diagram of the construction of SMOK test rig

1 - test shaft, 2 - supports, 3 - tested bearing, 4 - tested bearing housings, 5 - support bearings, 6 - connecting rod, 7 - upper chamber, 8 - lower chamber, 9 - piston, 10 - connecting pin, 11 - connecting rod, 12 - supporting frame, 13 - head plate, 14 - foundation bolts, 15 - cylinder, 16 - tie rods, 17 - oil inlet valves, 18 - oil outlet nozzles, 19 - sealing rings, 20 - lubrication system of bearing contacts.

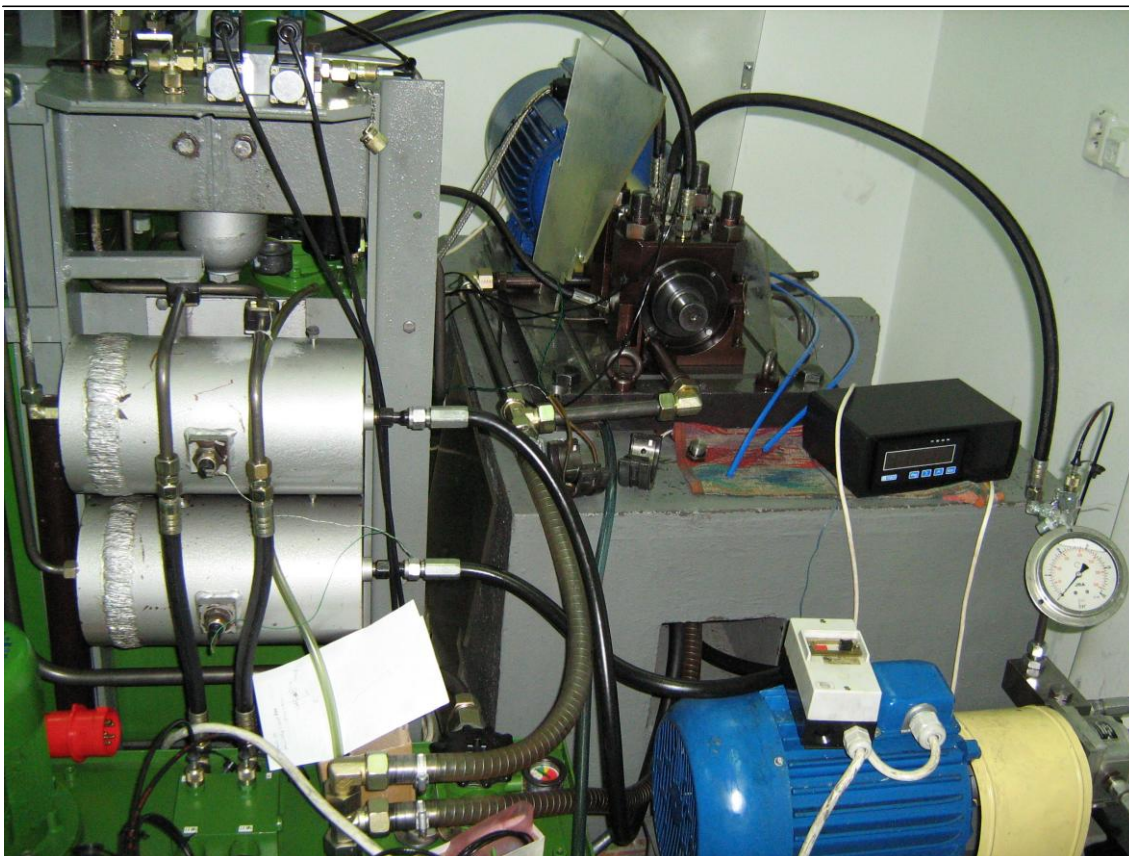


Fig. 4.1.16.2. SMOK test rig

4.1.17. SOOG test rig

SOOG test rig (Figures 4.1.17.1, 4.1.17.2 and 4.1.17.3) is intended for tribological tests of lubricant-free bearing materials for the conditions of rectilinear micro-oscillations in the sliding plane. It is a test rig built by the Laboratory of the Department of Construction and Operation of Machines of Gdańsk University of Technology. The tested samples (1 and 3, Figure 4.1.17.1) have a flat sliding surface. They can be made of the same or different materials. These samples are pressed with the same loading force F against the counter-sample (4) made of stainless steel. It is possible to make a counter-sample (4) from a different construction material. The samples (1 and 3) are fixed in the holder (2). The counter-sample (4) performs a reciprocating motion of low amplitude and high frequency. The source of the motion is the drive shaft (7) which has an eccentric e . The shaft is driven by an electric motor. During the eccentric rotation of the shaft (7), the pusher (6) adheres to its surface with a spherical (or disc) surface. The pusher (6) exerts direct pressure on the counter-sample (4) moving it to the right. The return motion of the counter-sample (4) - to the left - is achieved by means of the return spring (5) which at the same time ensures a continuous pressure of the pusher (6) against the shaft surface (7).

This rig makes it possible to determine:

- temperature of the middle of the counter-sample,
- surrounding temperature of the test contact,
- number of cycles,
- friction coefficient (static or kinetic),
- linear or total sample wear intensity (nominal and actual),
- friction force (its value and time course).

The technical data of the rig are as follows:

- sample dimensions: 10x10x6 [mm],
- frequency of micro-oscillations: 0 ÷ 93 [Hz],
- micro-oscillation amplitude: 80 ÷ 120 [μm],
- load with a force of up to 90 [kN].

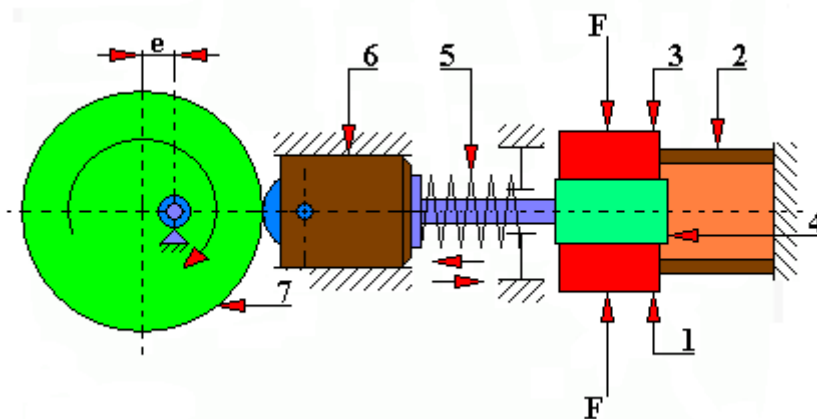


Fig. 4.1.17.1. Diagram of the construction of SOOG test rig

1 - lower sample, 2 - sample holder, 3 - upper sample, 4 - counter-sample, 5 - return spring, 6 - pusher, 7 - drive shaft with eccentric e , F - loading force, e - size of the eccentric (adjustable)

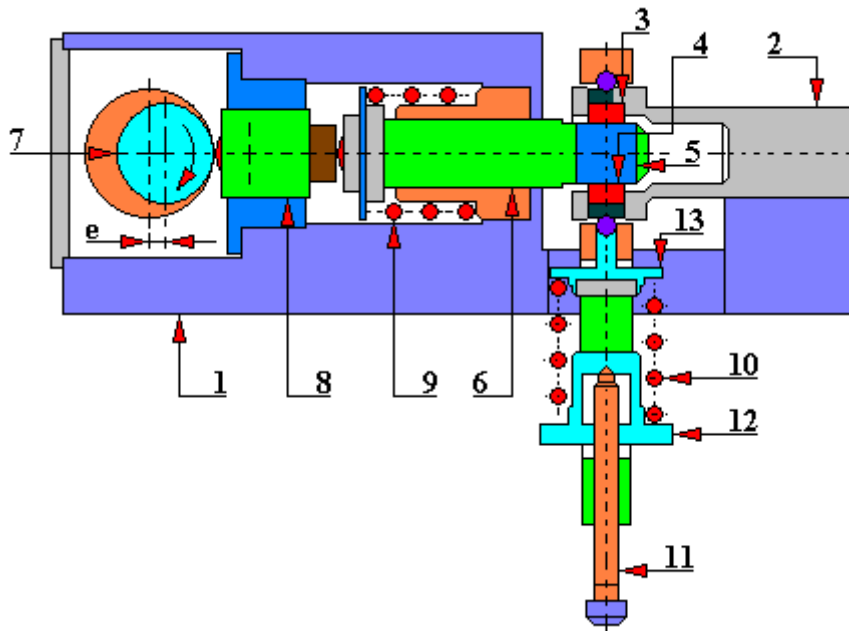


Fig. 4.1.17.2. SOOG test rig for testing abrasive wear in micro-oscillation conditions in the sliding plane. The design solution applied by the Department of Construction and Operation of Machines, Faculty of Mechanical Engineering of Gdańsk University of Technology
 1 - body, 2 - sample holder, 3 - upper sample, 4 - lower sample, 5 - counter sample, 6 - pusher, 7 - drive shaft with eccentric e , 8 - roller pusher, 9 - spring, 10 - load spring, 11 - adjusting screw, 12 - spring cup, 13 - spring plate, e - size of the eccentric (adjustable)

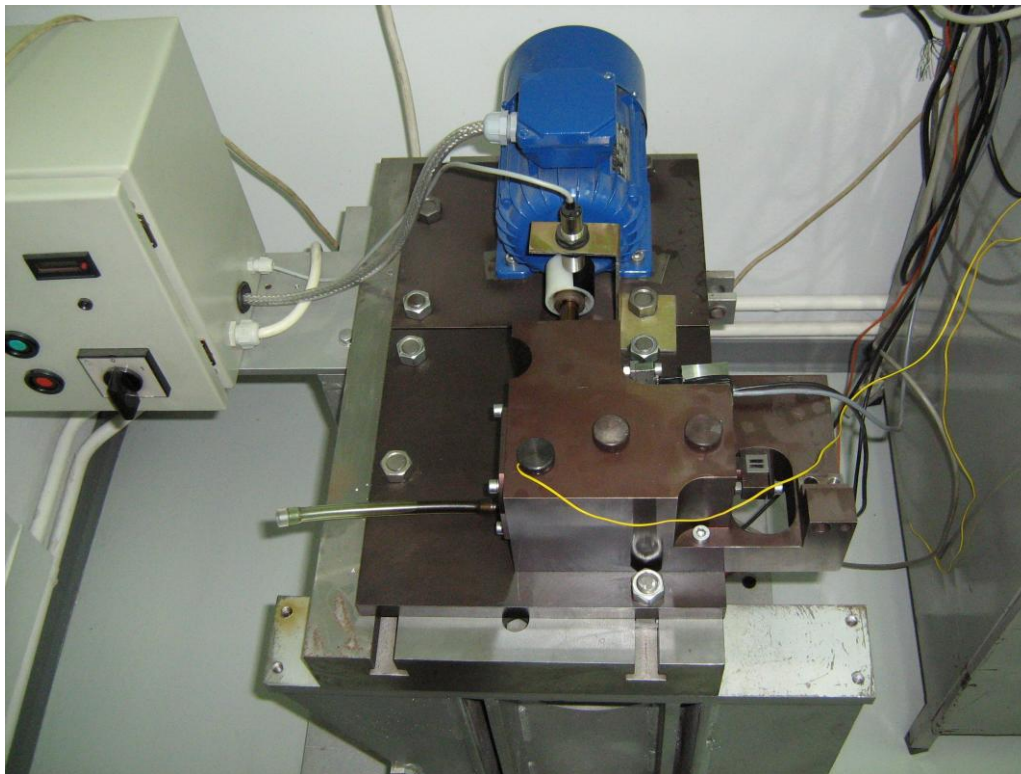


Fig. 4.1.17.3. General view of the SOOG test rig

4.1.18. SON test rig

The SON test rig (Figures 4.1.18.1, 4.1.18.2, 4.1.18.3, 4.1.18.4 and 4.1.18.5) is intended for testing hydrodynamic thrust bearings, e.g. ceramic bearings with self-aligning blocks. It is a non-commercial rig built by the Laboratory of the Department of Construction and Operation of Machines, Faculty of Mechanical Engineering of Gdańsk University of Technology.

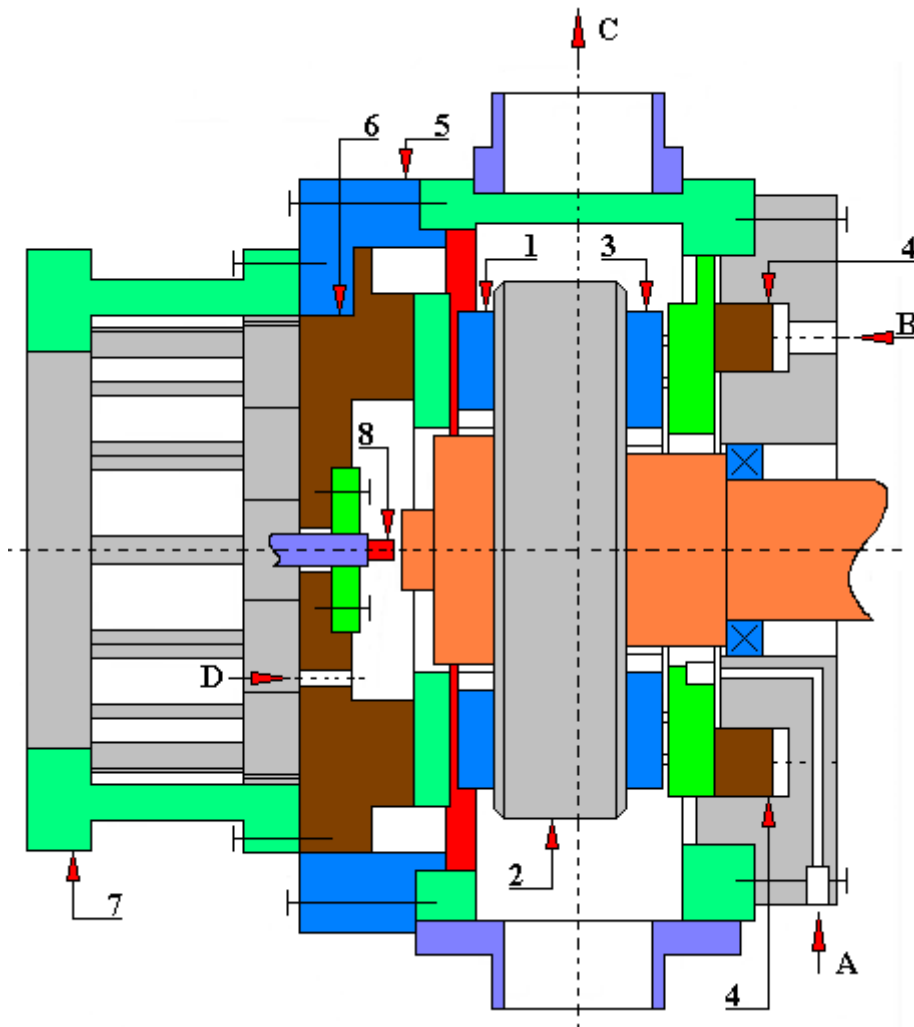


Fig. 4.1.18.1. General diagram of the construction of SON test rig

1 - front bearing, 2 - collar, 3 - rear bearing, 4 - load pusher, 5 - bearing housing, 6 - bearing plate, 7 - torque gauge, 8 - distance sensor, A - regulated supply of lubricating oil, B - adjustable load pusher oil supply, C - cooling oil (or coolant) outlet, D - adjustable lubricating oil supply.

The quantities that can be tested at the SON rig include:

- moment of friction
- load,
- deformation of bearing elements,
- temperature in bearings,
- minimum thickness of the lubricating film,
- lubricating oil temperature,
- rotational speed of the shaft.



Fig. 4.1.18.2. The main panel of the hydraulic unit of the SON test rig



Fig. 4.1.18.3. The main panel of the hydraulic unit of the SON test rig with the visible disassembled thrust bearing tested

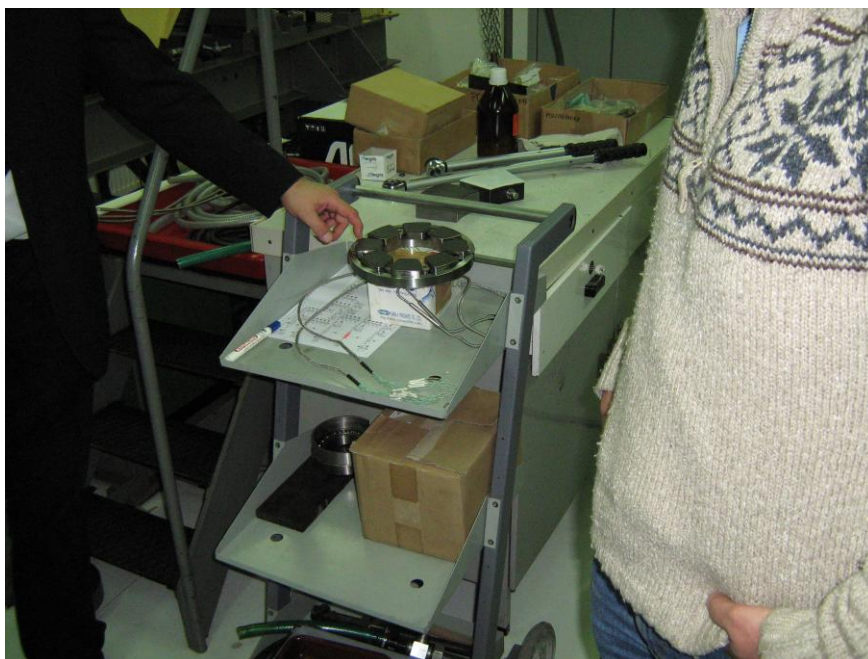


Fig. 4.1.18.4. Dismantled tested thrust bearing



Fig. 4.1.18.5. General view of the SON test rig (source: www.pg.edu/web/katedra-konstrukcji-maszyn-i-pojazdow/son).

A - housing of tested bearings, B - drive shaft, C - drive gear, D - electric motor, E - hydraulic unit.

The technical data of the SON rig are as follows:

- axial bearing load up to 90 [kN],
- rotational speed of the shaft: 20 ÷ 5000 [rpm],
- outer diameter of the tested bearings up to \varnothing 200 [mm],
- adjustable lubricating oil flow (A + D) up to 45 [liter/min].

4.1.19. Test rig for tribological testing of lubricants and construction materials according to the patent No. PL 160594

A tribological test rig (Fig. 4.1.19.1) according to the patent No. PL 160594, created by Stanisław Koziół, Marian Szczerek, Witold Piekoszewski, is designed for tribological tests of lubricants and construction materials. This test rig consists of a drive motor (9) which rotates the spindle (14) through a reducer (11). The spindle ends with a handle (3) with a roller counter-sample (2) attached to it, against which the block sample (1) is pressed. The pressure of the sample against the counter-sample is exerted by means of loading levers (6) with weights (13). In the drive system between the electric motor (9) and reducer (11) there is a belt transmission (10) with a toothed belt. And on the reducer shaft transmitting the drive onto the counter-sample (2) mounted is the impulse transmitter (12) of the revolution counter and of the rotational speed indicator. A strain gauge (8) of force is coupled to the holder (3) of the sample (1) and the sample loading system (1) forms the aforementioned set of levers (6) in the shape of open quadrilateral.

This tribotester has a control and measurement system consisting of three circuits: C1, C2 and C3.

The first circuit is used to measure and record the friction force between the sample (1) and the counter-sample (2). This circuit consists of a strain gauge (8), amplifier (15), voltage/frequency converter (16), frequency counter (17), digital readout panel (24), interface (19) and a computer interface (20).

The second circuit measures the rotational speed of the counter-sample spindle (2). This circuit consists of a pulse amplifier (21), pulse doubler (22), frequency counter (23), digital readout panel (24), interface (25) and a computer interface (26).

The third circuit is used to measure and record the temperature of the lubricant supplied to the friction contact. This circuit consists of a thermostat (27), push-pull amplifier (28), voltage/frequency converter (29), frequency counter (30), digital readout panel (31), interface (32), computer interface connector (33), temperature controller (34) and a heater (35).

The disadvantages of this test rig in this version include the inability to smoothly adjust the rotational speed of the spindle. This inconvenience, however, is easily eliminated by using, for example, a frequency converter (inverter) in the drive system. However, then this rig will be more expensive.

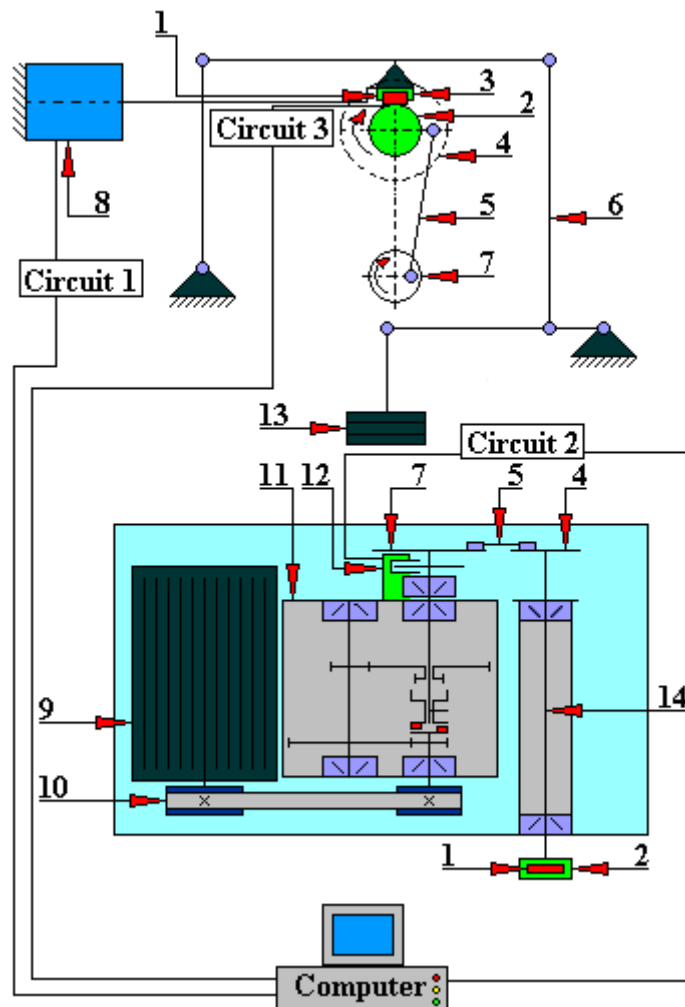


Fig. 4.1.19.1. Test rig for tribological testing of lubricants and construction materials according to the patent No. PL 160594

1 - block sample, 2 - counter-sample, 3 - sample holder, 4 - eccentric disc, 5 - connecting rod, 6 - set of levers in the shape of an open quadrilateral, 7 - eccentric disc, 8 - force strain gauge, 9 - drive motor, 10 - belt transmission with toothed belt, 11 - reducer, 12 - pulse transmitter, 13 - load, 14 - spindle.

Circuit 1 consists of: a strain gauge (8), amplifier (15), voltage/frequency converter (16), frequency counter (17), digital readout panel (24), interface (19) and a computer interface (20).

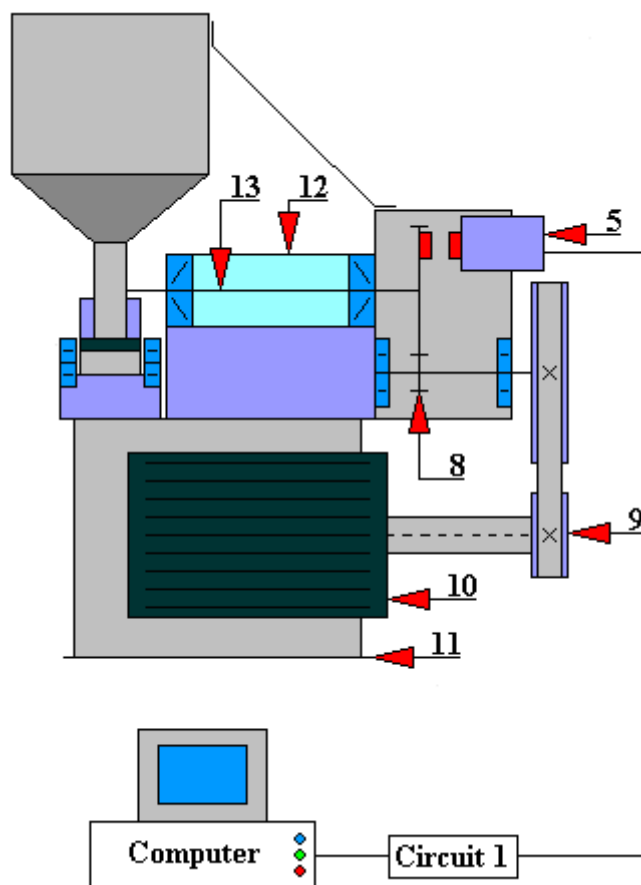
Circuit 2 consists of: a pulse amplifier (21), pulse doubler (22), frequency counter (23), digital readout panel (24), interface (25) and a computer interface (26).

Circuit 3 consists of: a thermostat (27), push-pull amplifier (28), voltage/frequency converter (29), frequency counter (30), digital readout panel (31), interface (32), computer interface connector (33), temperature controller (34) and a heater (35).

4.1.20. Test rig for testing the abrasion of construction materials according to the patent PL 160596

A test rig for testing the abrasion of construction materials (Fig. 4.1.20.1), according to the patent PL 160596, created by Jan Wulczyński and Witold Piekoszewski, is designed to assess the wear resistance of metal materials and coatings when rubbing against loose abrasive. This rig consists of a base (11) to which a motor (10) is attached. The drive from the engine (10) is transmitted through the gear with a toothed belt (9) and toothed gear (8) to the main shaft (13) mounted in the body (12). At the end of the main shaft (13) a counter-sample (2) is mounted which forms a friction contact with a stationary sample block (1). This sample (1) is mounted in the loading lever (6). The weight (7) is suspended on the loading lever (6). This test rig has a tank (4) installed for abrasive with an opening near the friction contact. The tank (4) has a dispenser (3) regulating the amount of abrasive supplied to the friction contact. The motion of the abrasive towards the friction contact goes under the gravitational force. The revolutions counter sensor (5) is mounted in the gear housing (8).

The tribotester is additionally equipped with a control and measurement system for counting the number of revolutions and for tripping the drive motor (10) after a preset number of revolutions. This circuit consists of a pulse amplifier (14), digital readout panel (15), interface (16) and a computer interface (17).



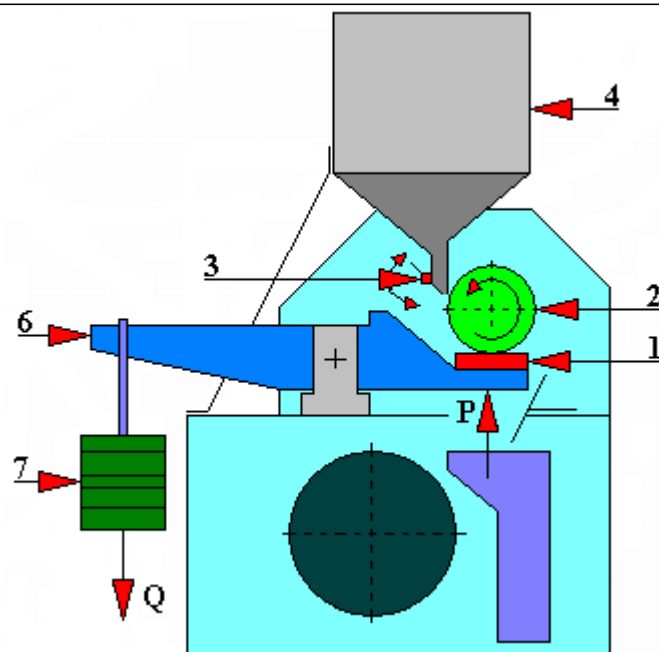


Fig. 4.1.20.1. A test rig for tribological abrasion tests of construction materials according to the patent No. PL 160 596

1 - stationary block sample, 2 - counter-sample, 3 - dispenser, 4 - abrasive tank, 5 - rev counter sensor, 6 - loading lever, 7 - weight, 8 - gear transmission, 9 - belt transmission with a toothed belt, 10 - engine drive, 11 - base, 12 - body, 13 - main shaft.

Circuit 1 consists of: a pulse amplifier (14), digital readout panel (15), interface (16), and computer interface (17).

4.1.21. Test rig with a ball-disc or spindle-disc friction contact for testing wear resistance and resistance to motion, especially for solid ceramic elements and ceramic surface layers according to the patent PL 176145

A test rig with a ball-disc or spindle-disc friction contact – according to the patent No. PL 176145 created by Stanisław Koziół, Witold Piekoszewski, Marian Szczerek, Marek Wiśniewski – is designed for testing wear resistance and resistance to motion, especially for solid ceramic elements and ceramic surface layers. In this tribotester (Figure 4.1.21.1) a spherical or pin-shaped sample (8) is fixed in a tilting lever (7) which is rotationally set in the head (6) mounted on columns (9a) and (9b). The displacement transducer (18) is rigidly mounted in the holder (23) on the column (9a). On the column (9b) installed is by means of the bracket (20) a loading lever (10) on which a weight (11) is mounted. The string (12) is articulated to the lever (10). This string is articulated with the strain gauge (13). The strain gauge (13) is rigidly connected to the head (6).

The loading lever (10) consists of two arms rigidly connected to each other at right angles. A weight (11) is slidably mounted on the outer arm of this lever (10). This design allows for the horizontal positioning of the counter-sample axis.

The drive from the electric motor (2) to the spindle (5) with the counter-sample (3) mounted on it is transmitted through a belt transmission (4) with a toothed belt and through a flexible coupling (19). The drive motor (2) is rigidly connected to the plate (21) which is elastically connected to the body (1) through flexible washers (22).

The impulse transmitter (25) of the rotation sensor (24) and the rotational speed sensor (14) are located on the spindle (5). On the head (6) there is - in the plane of the friction force - a strain gauge transducer (15) of the friction force. And on the surface of the body (1) mounted is a vibroacoustic transducer (17) of the body vibrations. On the side surface of the tilting lever (7), in the plane passing through the sample axis (8), a vibroacoustic transducer (16) of the sample vibrations (8) is fixed.

The control and measurement system of this tribotester consists of seven circuits.

The circuit 1 consists of an amplifier (26), analog-to-digital converter (27) and impulse counter (28). This circuit is connected to the strain gauge (13). Circuit 1 is designed to measure and record the force applying a load on the test friction contact.

The circuit 2 consists of an amplifier (29), analog-to-digital converter (30) and impulse counter (31). This circuit is connected to the strain gauge (15). The circuit 2 is designed to measure and record the friction force between the sample (8) and the rotating counter-sample (3).

The circuit 3 consists of a receiver (32), amplifier (33) and a pulse counter (34). This circuit is connected to the rotational speed sensor (14). Circuit 3 is designed to measure and record the rotational speed of the counter-sample (3).

This circuit 4 consists of a receiver (26) and impulse counter (35). This circuit is connected to the rotation sensor (24). The circuit 4 is designed to count and record the number of revolutions of the counter-sample (3) in order to measure the path of friction.

The circuit 5 consists of an amplifier (36), analog-to-digital converter (37) and impulse counter (38). This circuit is connected to the displacement transducer (18). The circuit 5 is designed to measure and record the linear wear of the friction contact elements.

Circuit 6 consists of a charge amplifier (39), analog-to-digital converter (40) and a pulse counter (41). This circuit is connected to the vibration sensor (17). The circuit 6 is designed to measure and record the vibration level of the test rig body.

Circuit 7 consists of a charge amplifier (42), analog-to-digital converter (43) and a pulse counter (44). This circuit is connected to the vibration sensor (16). The circuit 7 is designed to measure and record the vibration level of the sample (8).

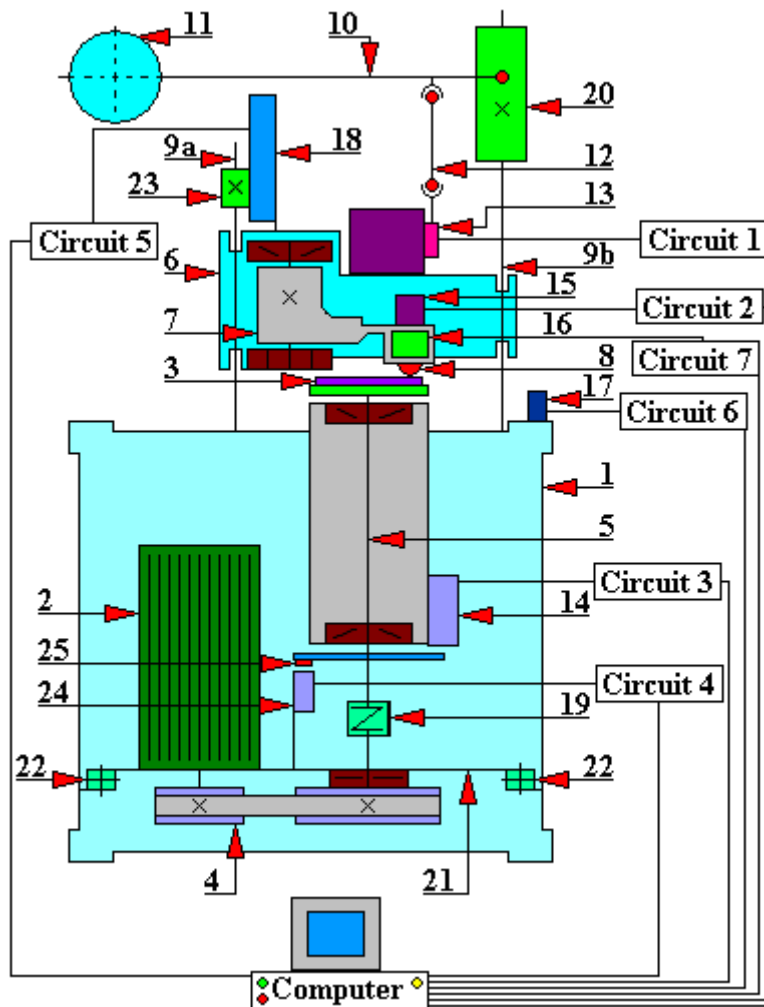


Fig. 4.1.21.1. A tribological test rig with a ball-disc or spindle-disc friction contact according to the patent No. PL 176145 for a variant of the test rig with a vertical axis of counter-sample rotation

1 - body, 2 - electric motor, 3 - counter-sample, 4 - belt transmission with a toothed belt, 5 - spindle, 6 - rotary head, 7 - tilting lever, 8 - spherical or pin-shaped sample, 9a, 9b - columns, 10 - loading lever, 11 - weight, 12 - string, 13 - strain gauge transducer, 14 - rotational speed sensor, 15 - friction strain gauge transducer, 16 - vibroacoustic transducer of sample vibrations, 17 - vibroacoustic transducer of body vibrations, 18 - displacement transducer, 19 - flexible coupling, 20 - bracket, 21 - base plate, 22 - flexible washers, 23 - displacement transducer holder, 24 - rotation sensor, 25 - pulse transmitter.

Circuit 1 consists of: amplifier (26), analog-to-digital converter (27) and impulse counter (28).

Circuit 2 consists of: amplifier (29), analog-to-digital converter (30) and impulse counter (31).

Circuit 3 consists of: receiver (32), amplifier (33) and impulse counter (34).

Circuit 4 consists of: receiver (26) and impulse counter (35).

Circuit 5 consists of: amplifier (36), analog-to-digital converter (37) and impulse counter (38).

Circuit 6 consists of: charge amplifier (39), analog-to-digital converter (40) and impulse counter (41).

Circuit 7 consists of: charge amplifier (42), analog-to-digital converter (43) and impulse counter (44).

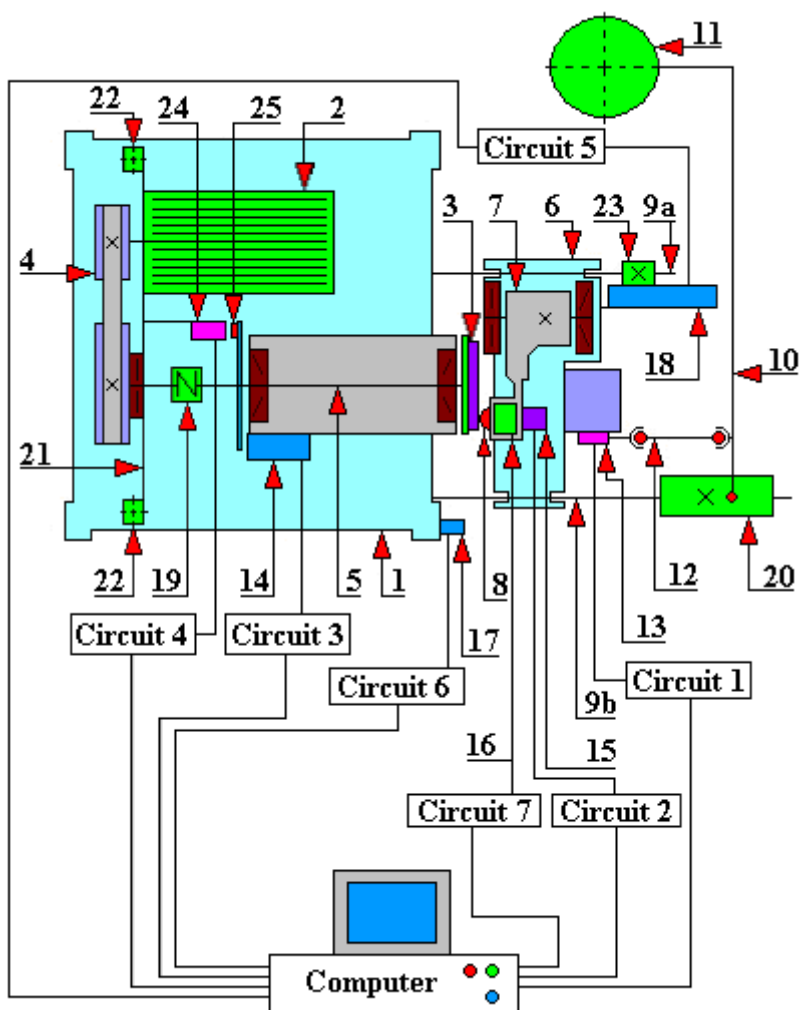


Fig. 4.1.21.2. A tribological test rig with a ball-disc or spindle-disc friction contact according to the patent No. PL 176 145 for the variant of the test rig with a horizontal axis of counter-sample rotation

1 - body, 2 - electric motor, 3 - counter-sample, 4 - belt transmission with a toothed belt, 5 - spindle, 6 - rotary head, 7 - tilting lever, 8 - spherical or pin-shaped sample, 9a, 9b - columns, 10 - loading lever, 11 - weight, 12 - string, 13 - strain gauge transducer, 14 - rotational speed sensor, 15 - friction strain gauge transducer, 16 - vibroacoustic transducer of sample vibrations, 17 - vibroacoustic transducer of body vibrations, 18 - displacement transducer, 19 - flexible coupling, 20 - bracket, 21 - base plate, 22 - flexible washers, 23 - displacement transducer holder, 24 - rotation sensor, 25 - pulse transmitter.

Circuit 1 consists of: amplifier (26), analog-to-digital converter (27) and impulse counter (28).

Circuit 2 consists of: amplifier (29), analog-to-digital converter (30) and impulse counter (31).

Circuit 3 consists of: receiver (32), amplifier (33) and impulse counter (34).

Circuit 4 consists of: receiver (26) and impulse counter (35).

Circuit 5 consists of: amplifier (36), analog-to-digital converter (37) and impulse counter (38).

Circuit 6 consists of: charge amplifier (39), analog-to-digital converter (40) and impulse counter (41).

Circuit 7 consists of: charge amplifier (42), analog-to-digital converter (43) and impulse counter (44).

This test rig is built in two variants:

- a) with the vertical axis of rotation of the counter-sample (Figure 4.1.21.1),
- b) with the horizontal axis of rotation of the counter-sample (Figure 4.1.21.2),

Two design solutions of this rig enable the testing of contact for two different operating conditions. In the case of a test rig with a vertical axis of rotation of the counter-sample the wear products remaining on the disc may enter the contact zone again. And in the case of a test rig with a horizontal axis of rotation of the counter-sample, the wear products are removed from the disc under the gravity force. Thus, they should not re-enter the contact zone of the mating surfaces. For these two design solutions there are different wear intensities of the test elements with the same operating parameters (load, rotational speed of the counter-sample disc, sample material, counter-sample material, etc.).

4.1.22. Test rig with a roller- V blocks pair for testing resistance to wear and seizure of construction materials according to the patent PL 177 205

The tribological test rig (Figures 4.1.22.2a and 4.1.22.2b) according to the patent No. PL 177 205, created by Stanisław Koziół, Witold Piekoszewski, Marian Szczerek, is designed to test the wear resistance of construction materials mating in the roller-V blocks test friction contact. In this tribotester the rotating counter-sample has the shape of a roller (3). This roller is mounted in the spindle seat (13) by means of a pin. The spindle (13) is driven by the electric motor (1) through a set of two belt transmissions (2) with toothed belts. At the other end of the spindle (13) mounted is an eccentric pin (15). A ratchet (16) is slidingly mounted on the eccentric pin (15) and it engages with the ratchet-wheel (7). The ratchet-wheel (7) is rigidly connected with the turnbuckle (8) screwed into the nuts (17) and (18). The nut (18) presses down the spring (9). The spring (9) presses the lever (6) through the friction contact load transducer (20) and self-adjusting inserts. The lever (6) loads the jaws (4) mounted in the head (25). In the cylindrical jaw seats (4) there are loosely placed samples (11) and (12) pressing down the counter-sample (3). Attached to the head (25) is the arm (21) contacting the transducer of resistance to motion (10).

This test rig has two control and measurement systems: 1 and 2. The meter circuit 1 consists of four circuits: circuit 1, circuit 2, circuit 3, and circuit 4. The meter circuit 2 consists of two circuits: circuit 5 and circuit 6.

The circuit 1 consists of an amplifier (26), analog-to-digital converter (27) and impulse counter (28). This circuit is connected to the friction contact load transducer (20). Circuit 1 is designed to measure the force applying a load on the friction contact.

Circuit 2 consists of an amplifier (29), analog-to-digital converter (30) and impulse counter (31). This circuit is connected to the strain gauge (10). Circuit 2 is designed to measure the frictional resistance.

This circuit 3 consists of a receiver (32) and impulse counter (33). This circuit is connected to the rotation sensor (22). Circuit 3 is designed to measure the path of friction by counting revolutions of the counter-sample (3).

The circuit 4 consists of an amplifier (34), analog-to-digital converter (35) and impulse counter (36). This circuit is connected to the temperature transducer (23). Circuit 4 is used to measure the temperature of the liquid lubricant or the surroundings of the friction contact in the case of testing non-lubricated contact.

Circuit 5 consists of relay (37) and protection (38) actuators. This circuit is attached to the heater (24). Circuit 5 is used to control the temperature of the lubricant.

Circuit 6 consists of relay (39) and protection (40) actuators. This circuit is attached to the drive motor (1). Circuit 6 is used for turning the electric motor power on / off (1).

The design of this test rig allows, among others, to test the wear of structural materials and diffusion layers obtained as a result of thermo-chemical treatment, working with or without a lubricant, with constant or increasing pressure in conditions of a sliding friction. This tribotester can also be used for:

- assessment of the degree of resistance to the scuffing of materials and diffusion layers,
- measurement and recording of the force loading the tested contact,
- measurement and registration of resistance to motion,
- measurement and registration of lubricant temperature changes,
- measurement and registration of the friction path,
- controlling the course of the test process.

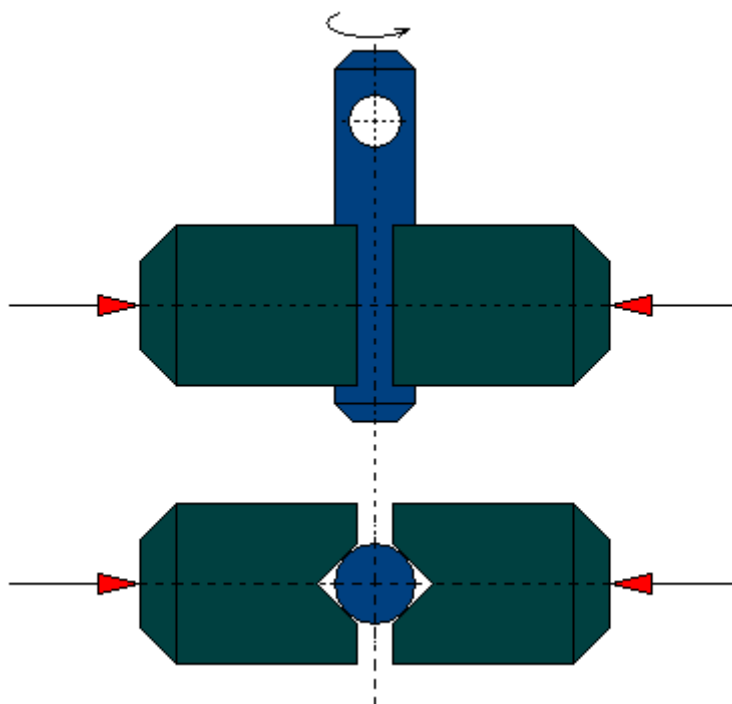


Fig. 4.1.22.1. The roller-vee blocks friction contact used in the test rig according to the patent No. PL 177 205

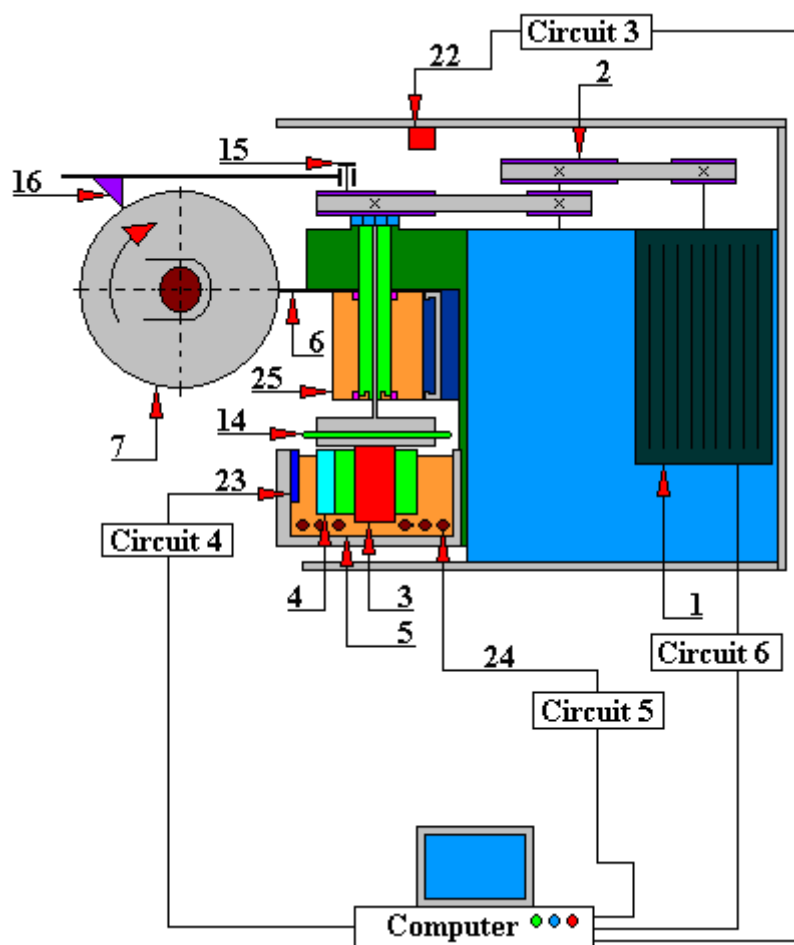


Fig. 4.1.22.2a. A tribological test rig with a roller-vee blocks mating designed to test the resistance to wear and scuffing of construction materials according to the patent No. PL 177 205 - side view

1 - electric motor, 2 - set of two belt transmissions, 3 - roller-shaped counter-sample, 4 - jaws, 5 - lubricant, 6 - loading lever, 7 - ratchet wheel, 8 - turnbuckle, 9 - spring, 10 - resistance to motion transducer, 11 - sample, 12 - sample, 13 - spindle seat, 14 - pin, 15 - eccentric pin, 16 - ratchet, 17 - nut, 18 - nut, 19 - self-adjusting inserts, 20 - force transducer, 21 - arm , 22 - rotation sensor, 23 - temperature transducer, 24 - heater, 25 - head.

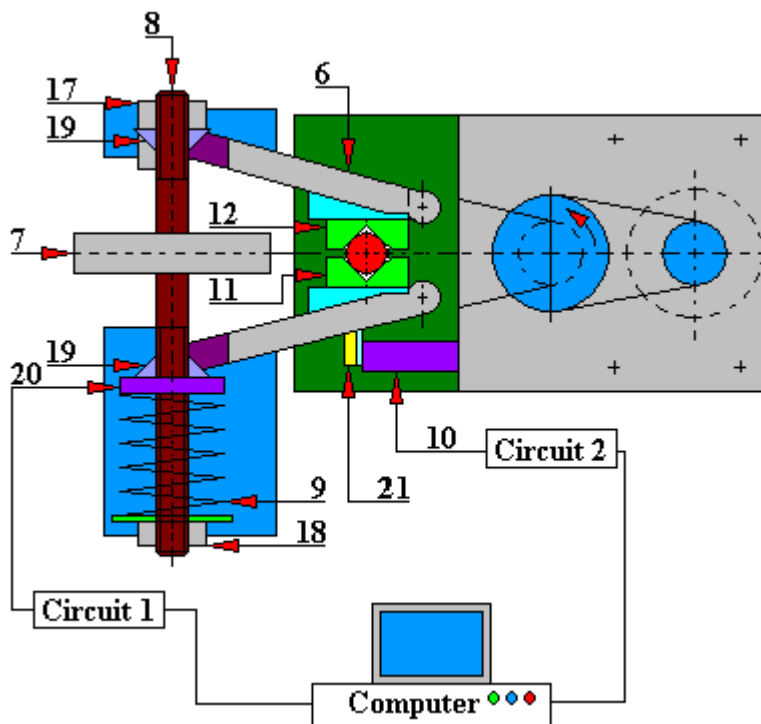


Fig. 4.1.22.2b. A tribological test rig with a roller-vee blocks mating designed to test the resistance to wear and scuffing of construction materials according to the patent No. PL 177 205 – top view

1 - electric motor, 2 - set of two belt transmissions, 3 - roller-shaped counter-sample, 4 - jaws, 5 - lubricant, 6 - loading lever, 7 - ratchet wheel, 8 - turnbuckle, 9 - spring, 10 - resistance to motion transducer, 11 - sample, 12 - sample, 13 - spindle seat, 14 - pin, 15 - eccentric pin, 16 - ratchet, 17 - nut, 18 - nut, 19 - self-adjusting inserts, 20 - force transducer, 21 - arm , 22 - rotation sensor, 23 - temperature transducer, 24 - heater, 25 - head.

4.1.23. Test rig for testing wear and resistance to motion of lubricated and non-lubricated elements according to the patent PL 177201

The test rig (Fig. 4.1.23.1) according to the patent No. PL 177201, created by Stanisław Koziół, Witold Piekoszewski, Marian Szczerek, Jan Wulczyński, is designed to test wear and resistance to motion of elements operating in lubricated and non-lubricated contact.

The test rig is characterized in that the pin-shaped or ball-shaped sample (14) is pressed against the rotating disc-shaped counter-sample (15) with weights (13). The load direction coincides with the sample axis which is perpendicular to the counter-sample face, and the direction of the friction force coincides with the axis of the pusher (20) and the measuring transducer (19) mounted on the bracket (18) slidably fixed on the support (7). The sample (14) is placed immobile in the lever (11) by means of the holder (22) and it is pressed against the counter-sample (15) with weights (13) placed on the tilting bracket (12) whose axis coincides with the vertical axis of the sample (14). On the opposite side, the load lever (11) has a counterweight (9) and balance weights (8). The lever (11) is rotationally fixed in the vertical and horizontal planes on the support (7) linked with the body (1) through a bracket (18) bolted behind the shaft (10) and the axis (24).

The electric motor (2) is powered by the controller. This motor drives the spindle (6) through a belt transmission (3) with a toothed belt. On the spindle (6) mounted in the sleeve (5) rigidly connected to the body (1), at its one end there is an impulse transmitter (21) of the rotation sensor (25) and the rotational speed sensor (4) installed. And on its other end, the spindle (6) has a pressure plate (17), fitted on key, on which a counter-sample (15) is mounted with a nut (16). Both the rotation sensor (25) and the rotational speed sensor (4) are permanently attached to the sleeve (5).

This test rig for tribological testing is equipped with a control and measurement system consisting of five circuits: circuit 1, circuit 2, circuit 3, circuit 4, and circuit 5.

The circuit 1 consists of an amplifier (27), analog-to-digital converter (28) and impulse counter (29). This circuit is connected to the measuring transducer (19). Circuit 1 measures the friction force.

Circuit 2 consists of a receiver (30), amplifier (31) and a pulse counter (32). This circuit is connected to the rotational speed sensor (4). Circuit 2 measures the rotational speed of the disc (counter-sample).

This circuit 3 consists of a receiver (33) and impulse counter (37). This circuit is connected to the rotation sensor (25). Circuit 3 is designed to measure the path of friction by counting revolutions of the counter-sample.

Circuit 4 consists of an amplifier (35), analog-to-digital converter (36) and impulse counter (37). This circuit is connected to the temperature sensor (26). Circuit 4 is designed to measure the sample temperature or the surrounding temperature of the friction contact.

Circuit 5 consists of a digital-to-analog converter (38) and a power supply controller (39). This circuit is attached to the electric motor (2). Circuit 5 is designed to control the operation of the tribotester drive motor.

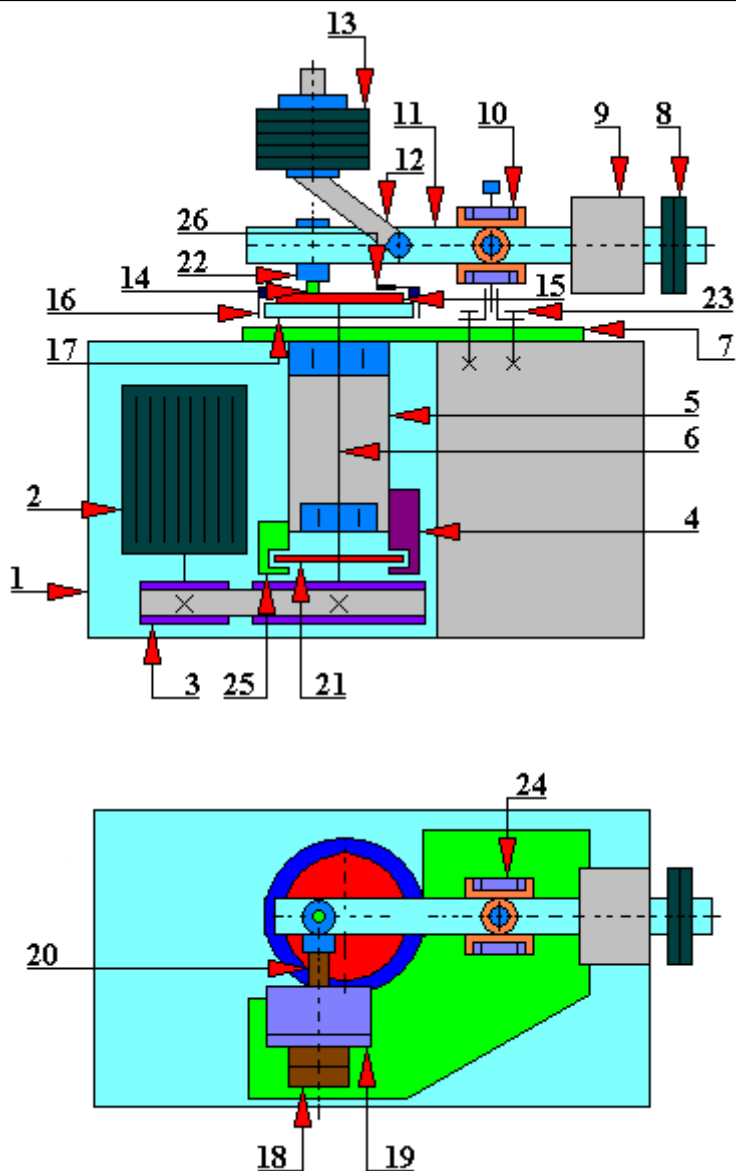


Fig. 4.1.23.1. A test rig for testing wear and resistance to motion of lubricated and non-lubricated elements according to the patent No. PL 177201; construction scheme
 1 - body, 2 - motor, 3 - belt transmission with a toothed belt, 4 - rotational speed sensor, 5 - sleeve, 6 - spindle, 7 - test rig, 8 - balancing weights, 9 - counterweight, 10 - shaft, 11 - lever 12 - tilt bracket, 13 - weights, 14 - pin or ball-shaped sample, 15 - disc-shaped counter-sample, 16 - nut, 17 - pressure plate, 18 - brackets, 19 - measuring transducer, 20 - pusher, 21 - pulse transmitter, 22 - handle, 23 - bracket, 24 - axis, 25 - rotation sensor, 26 - temperature sensor.

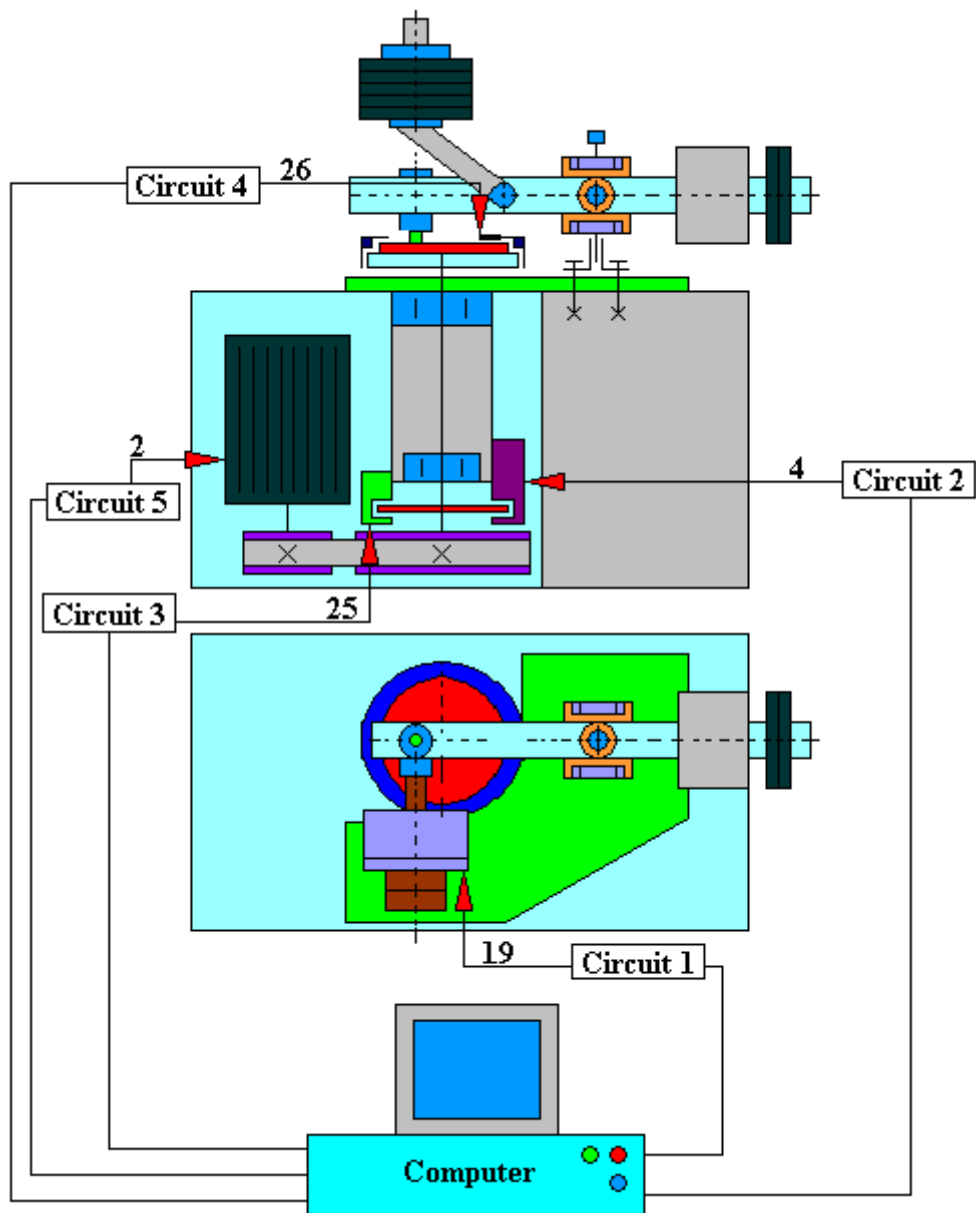


Fig. 4.1.23.2. Test rig for testing wear and resistance to motion of lubricated and non-lubricated elements according to the patent No. PL 177201; connection diagram of the control and measurement system

2 - engine, 4 - rotational speed sensor, 19 - measuring transducer, 25 - rotation sensor, 26 - temperature sensor.

Circuit 1 - measurement of the friction force.

Circuit 2 - measurement of the rotational speed of the disc.

Circuit 3 - measurement of the path of friction.

Circuit 4 – measurement of the sample temperature or surrounding temperature of the friction contact.

Circuit 5 - drive motor control.

4.1.24. Test rig for testing friction and wear of lubricated and non-lubricated elements according to the patent PL 177192

The test rig (Fig. 4.1.24.1 and 4.1.24.2) according to the patent No. PL 177192, created by Stanisław Koziół, Witold Piekoszewski, Marian Szczerek, Jan Wulczyński, is designed to test the friction and wear of various construction materials operating in the conditions of sliding friction with or without a lubricant. This test rig enables simultaneous measurements and recording of the friction force, mass temperature of the sample or the surrounding area of the friction contact and the path of friction, and also enables the control of the testing process.

In this test rig, the pin-shaped or ball-shaped sample (12) is pressed against the face of the rotating disc-shaped counter-sample (13). The sample (12) is fixed immobile in the lever (9) by the holder (20). And the counter-sample (13) is pressed with weights (11) placed on the tilting bracket (10) whose axis coincides with the vertical axis of the sample (12), and the direction of the friction force coincides with the axis of the pusher (18) and the measuring transducer (17) mounted on the bracket (16) slidably attached to the test rig (7). The lever (9) is permanently attached to the shaft (8). The lever (9) is mounted slidably in the vertical plane and rotationally in the horizontal plane in the bracket (21) which is connected with the base (7) and body (1) with the screws. The shaft (8) in the lower part is supported by the lever unit (24) and weights balancing the lever (9) together with the fixed sample (12).

The electric motor (2) is powered by the controller (38). This motor drives the spindle (6) through a belt transmission (3) with a toothed belt. On the spindle (6) mounted in the sleeve (5) rigidly connected to the body (1) there is installed at one end an impulse transmitter (19) of the rotation sensor (22) and the rotational speed sensor (4). And on its other end, the spindle (6) has a keep plate (15), fitted on key, on which a counter-sample (13) is mounted with a nut (14). The rotation sensor (22) and the rotational speed sensor (4) are permanently attached to the sleeve (5).

The control and measurement system consisting of five circuits: circuit 1, circuit 2, circuit 3, circuit 4, and circuit 5.

The circuit 1 consists of an amplifier (26), analog-to-digital converter (27) and an impulse counter (28). This circuit is connected to the measuring transducer (17). Circuit 1 is designed to measure the friction force.

Circuit 2 consists of a receiver (29), amplifier (30) and a pulse counter (31). This circuit is connected to the rotational speed sensor (4). Circuit 2 is designed to measure the rotational speed of the disc.

Circuit 3 consists of a receiver (32) and impulse counter (33). This circuit is connected to the rotation sensor (22). Circuit 3 is designed to measure the path of friction by counting revolutions of the counter-sample.

The circuit 4 consists of an amplifier (34), analog-to-digital converter (35) and an impulse counter (36). This circuit is connected to the temperature sensor (23). Circuit 4 is designed to measure the mass temperature of the sample or the surrounding temperature of the friction contact.

Circuit 5 consists of a digital-to-analog converter (37) and a power supply controller (38). This circuit is attached to the electric motor (2). Circuit 5 is designed to control the operation of the electric motor of the test rig drive.

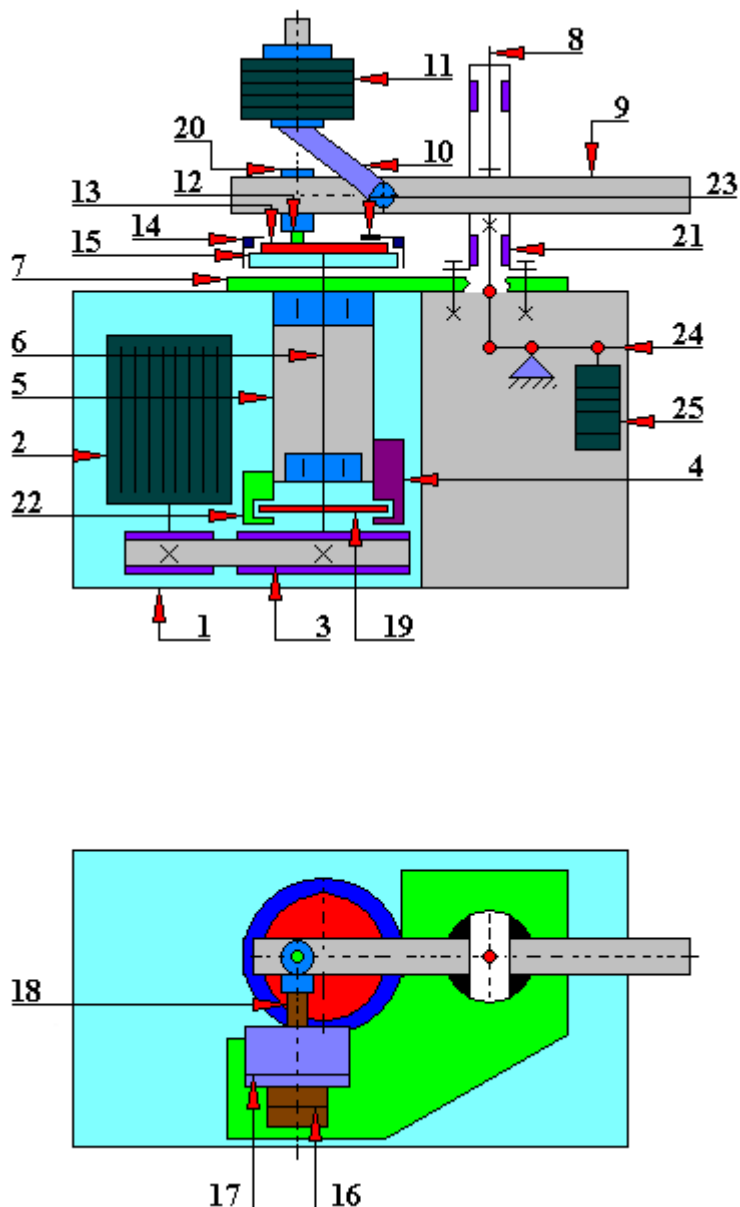


Fig. 4.1.24.1. A test rig for testing friction and wear of lubricated and non-lubricated elements according to the patent PL 177192; construction scheme

1 - body, 2 - motor, 3 - belt transmission with a toothed belt, 4 - rotational speed sensor, 5 - sleeve, 6 - spindle, 7 - test rig, 8 - shaft, 9 - lever, 10 - tilting bracket, 11 - weights, 12 - spindle or ball-shaped sample, 13 - disc-shaped counter-sample, 14 - nut, 15 - pressure plate, 16 - bracket, 17 - measuring transducer, 18 - pusher, 19 - pulse transmitter, 20 - handle, 21 - bracket, 22 - rotation sensor, 23 - temperature sensor, 24 - lever unit, 25 - weights.

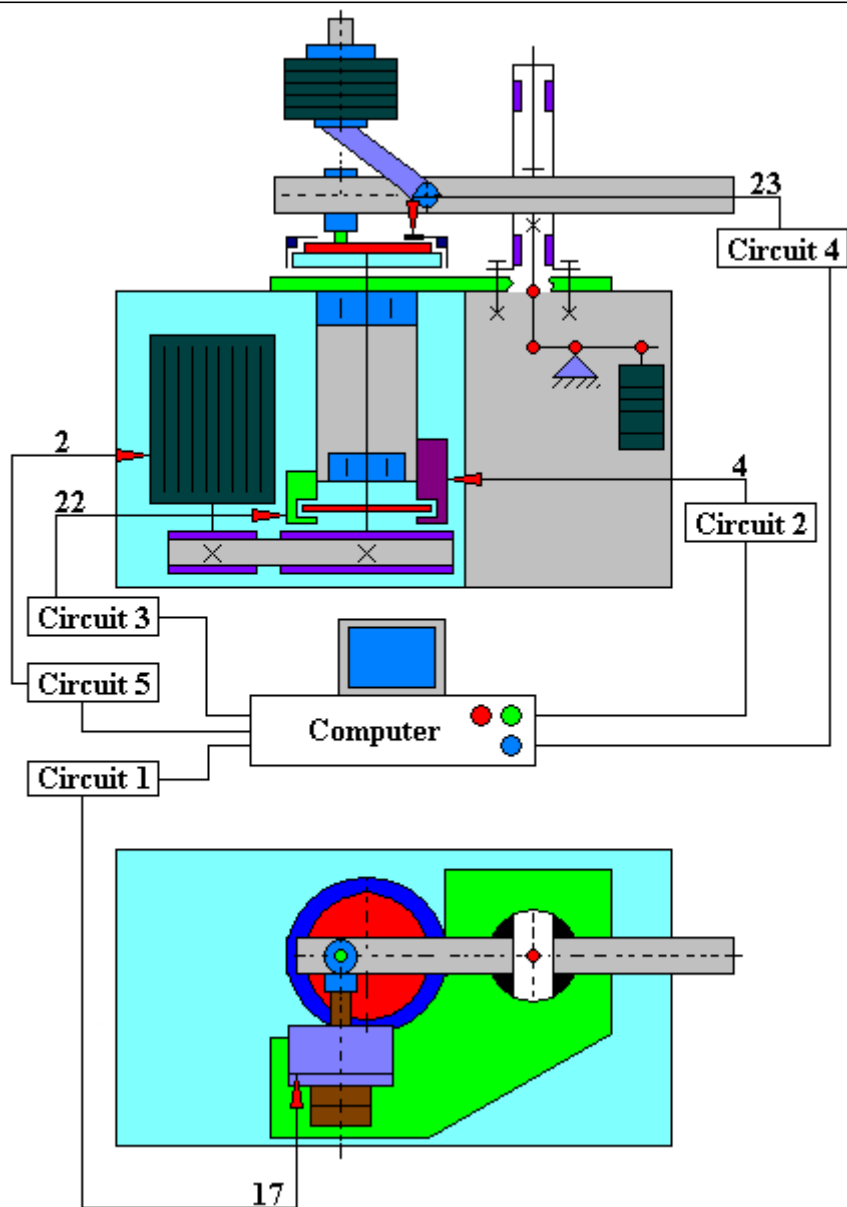


Fig. 4.1.24.2. A test rig for testing friction and wear of lubricated and non-lubricated elements according to the patent No. PL 177192; connection diagram of the control and measurement system

2 - engine, 4 - rotational speed sensor, 17 - measuring transducer, 22 - rotation sensor, 23 - temperature sensor.

Circuit 1 - measurement of the force of friction.

Circuit 2 - measurement of the rotational speed of the disc.

Circuit 3 – measurement of the path of friction by counting revolutions of the counter-sample.

Circuit 4 – measurement of the sample temperature or ambient temperature of the friction contact.

Circuit 5 - control of the electric motor operation of the test rig drive.

4.1.25. Test rig for testing the wear resistance and frictional resistance of lubricated and non-lubricated elements according to the patent PL 160590

The test rig (Fig. 4.1.25.1 and 4.1.25.2) according to the patent No. PL 160590 created by Marek Wiśniewski, Witold Piekoszewski, Marian Szczerek, Ryszard Reizer, is designed to test the wear resistance and frictional resistance of lubricated and non-lubricated elements with a friction contact of the spindle-disc type.

In this test rig the friction contact is formed by three pins (1) pressed against the disc-shaped moving counter-sample (2). The pins (1) are fixed immobile in the sample holder (3) and positioned every 120° at the same distance r from the center of the holder (3). The drive from the electric motor (9) to the gear (8) and from the gear (8) to the counter-sample spindle (2) is transmitted through belt transmissions with a toothed belt (7). The strain gauge (10) is rigidly fixed on the housing (11) and connected to the sample holder (3) by means of a pusher (12). The holder (3) is centered in relation to the counter-sample (2) through the pin (13) mounted in the loading lever (4). The weights (5) are suspended on the loading lever (4). On the counter-sample spindle (2) there is a pulse transmitter (6) for revolutions counter and rotational speed indicator.

The control and measurement system consisting of four circuits: circuit 1, circuit 2, circuit 3, and circuit 4.

Circuit 1 consists of a strain gauge (10), amplifier (14), voltage/frequency converter (15), frequency counter (22), digital readout panel (17), interface (18) and a computer interface (19). This circuit is connected to a strain gauge (10). Circuit 1 is designed to measure and record the friction force between the pins (1) and a counter-sample (2).

Circuit 2 consists of a pulse amplifier (20), pulse doubler (21), frequency counter (22), digital readout panel (23), interface (24) and a computer interface (25). This circuit is connected to the pulse transmitter (6). Circuit 2 is designed to measure the rotational speed of the counter-sample (2).

Circuit 3 consists of a thermostat (26), push-pull amplifier (27), voltage/frequency converter (28), frequency counter (29), digital readout panel (30), interface (31), and computer interface connector (32). This circuit is designed to measure and record the temperature of the lubricant supplied to the tested friction contact.

Circuit 4 consists of a transformer displacement sensor (33), push-pull amplifier (34), voltage/frequency converter (35), frequency counter (36), digital readout panel (37), interface (38) and a computer interface (39). Circuit 4 is designed to identify the type of friction at the pin (1) – counter-sample (2) contact.

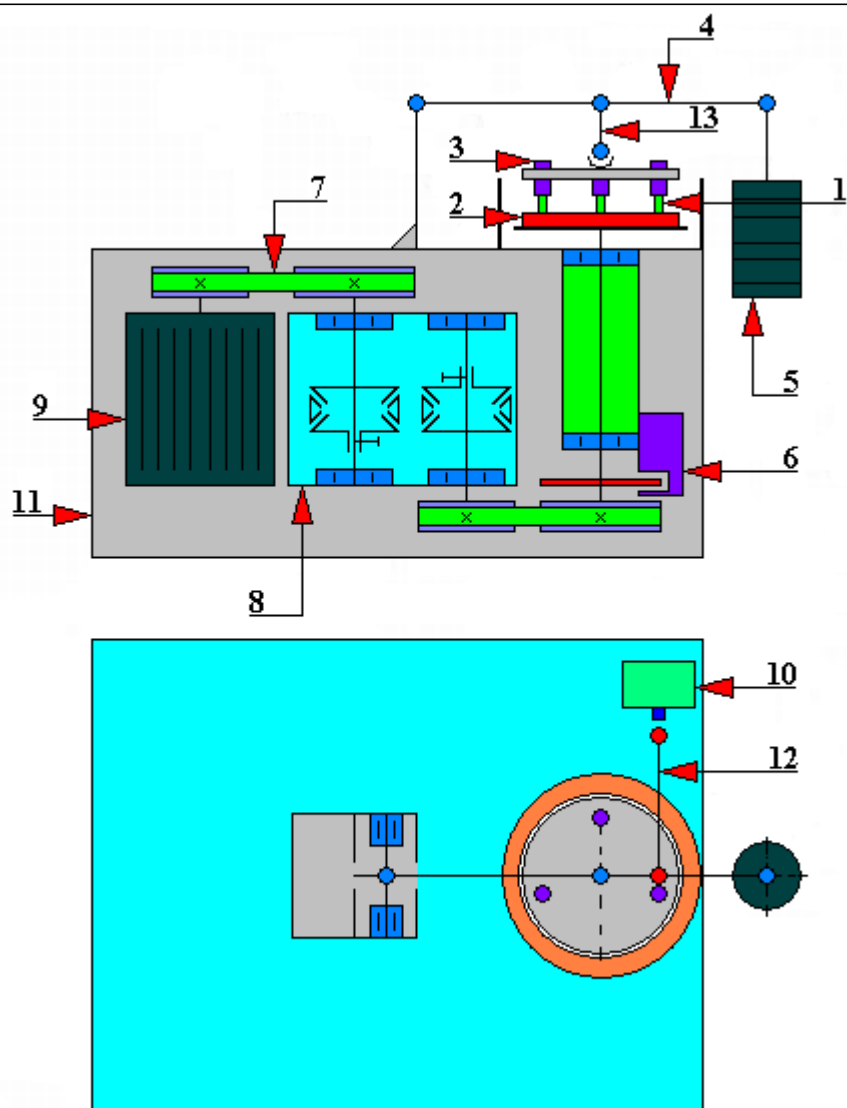


Fig. 4.1.25.1. A test rig for testing the wear resistance and frictional resistance of lubricated and non-lubricated elements according to the patent PL 160590; construction scheme
 1 - immobile samples (three pins), 2 – moving disc-shaped counter-sample, 3 - sample holder, 4 - loading lever, 5 - weights, 6 - pulse transmitter for revolutions counter and rotational speed indicator, 7 - belt transmission with a toothed belt, 8 - gear, 9 - electric motor, 10 - strain gauge, 11 - housing, 12 - pusher, 13 - pin.

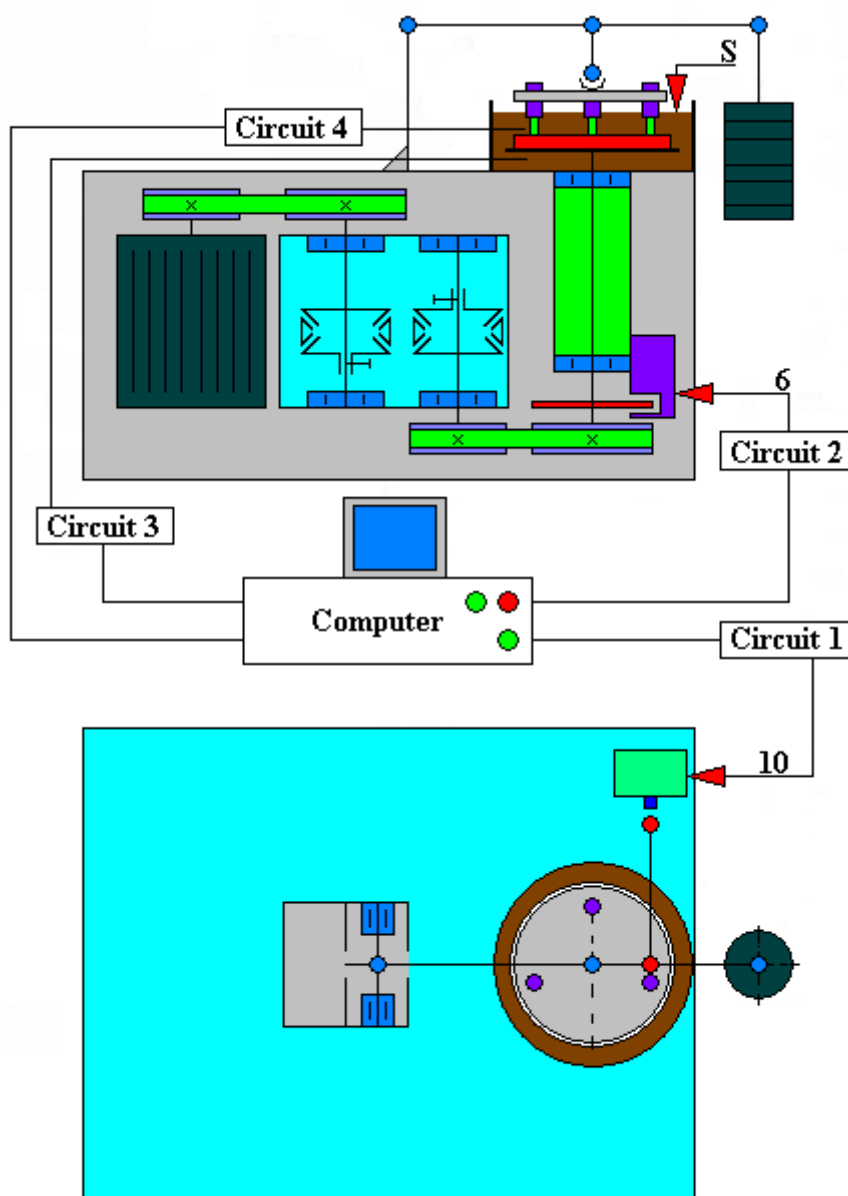


Fig. 4.1.25.2. A test rig for testing the wear resistance and frictional resistance of lubricated and non-lubricated elements according to the patent PL 160590; connection diagram of the control and measurement system

6 - pulse transmitter for rev counter and rotational speed indicator, 10 - strain gauge, S - lubricant.

Circuit 1 - measurement and recording of the friction force between the pins and a counter-sample.

Circuit 2 – measurement of the rotational speed of the counter-sample.

Circuit 3 – measurement and recording of the temperature of the lubricant supplied to the tested friction contact.

Circuit 4 - Identification of the type of friction at the pin/counter-sample contact.

4.1.26. Test rig for testing the friction and wear containing a rotating counter-sample against which stationary block samples or moving roller samples are pressed, according to the patent No. PL 160597

The test rig (Fig. 4.1.26.1 and 4.1.26.2) according to the patent No. PL 160597, created by Marek Wiśniewski, Witold Piekoszewski, Marian Szczerek, Ryszard Reizer, is designed for friction and wear tests; it contains a rotating counter-sample against which stationary block samples or moving roller samples are pressed. In this test rig the samples pressing system (1) is the arm (8) applying load on the strain gauge (9). The arm (8) is attached to the lever (3) pressing the sample (1). The ends of both levers (3) are bent towards each other on one side and are articulated on the crank (7). The crank (7) is mounted rotationally and coaxially in relation to the counter-sample (2). At the other end, the ends of both levers (3) are slidably connected by a rod (10) ended with a screw (5) on which a load spring (4) and nut (6) are mounted ensuring the required pressure of samples (1) against the counter-sample (2). The quantity of the desired pressure is controlled by the strain gauge (11) coupled with the rod (10).

The control and measurement system consisting of five circuits: circuit 1, circuit 2, circuit 3, circuit 4, circuit 5.

Circuit 1 is designed to measure the force applying load on the samples (1). This circuit consists of a strain gauge (11), amplifier (12), voltage/frequency converter (13), frequency counter (14), digital readout panel (15), interface (16) and a computer interface (17).

Circuit 2 is designed to measure the friction force between samples (1) and a counter-sample (2). This circuit consists of a strain gauge (9), amplifier (18), voltage/frequency converter (19), frequency counter (20), digital readout panel (21), interface (22) and a computer interface (23).

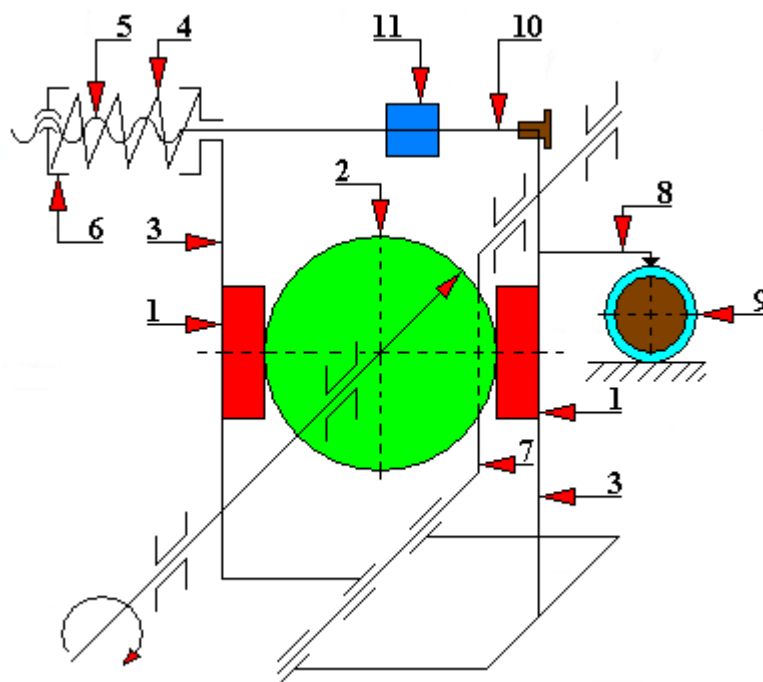


Fig. 4.1.26.1. A test rig for testing the friction and wear containing a rotating counter-sample against which stationary block samples or moving roller samples are pressed, according to the patent No. PL 160 597; construction scheme.

1 - samples, 2 - counter-sample, 3 - levers, 4 - loading spring, 5 - screw, 6 - nut, 7 - crank, 8 - loading arm, 9 - strain gauge, 10 - rod, 11 - strain gauge.

Circuit 3 is designed to measure the rotational speed of the counter-sample (2). This circuit consists of a pulse amplifier (24), pulse doubler (25), frequency counter (26), digital readout panel (27), interface (28) and a computer interface (29).

Circuit 4 is designed to measure and record the temperature of the lubricant supplied to the tested friction contact. This circuit consists of a thermostat (30), push-pull amplifier (31), voltage/frequency converter (32), frequency counter (33), digital readout panel (34), interface (35), computer interface connector (36), temperature controller (37) and a heater (38).

Circuit 5 is designed to identify the type of friction which occurs between mating samples (1) and a counter-sample (2). This circuit consists of a sensor/converter (39) of effective resistance and voltage of the sample (1)/counter-sample (2) contact, input amplifier (40), threshold discriminator block (41), gating circuit block (42), frequency counter (43), digital reading panel (44), interface (45), and a computer interface connector (46).

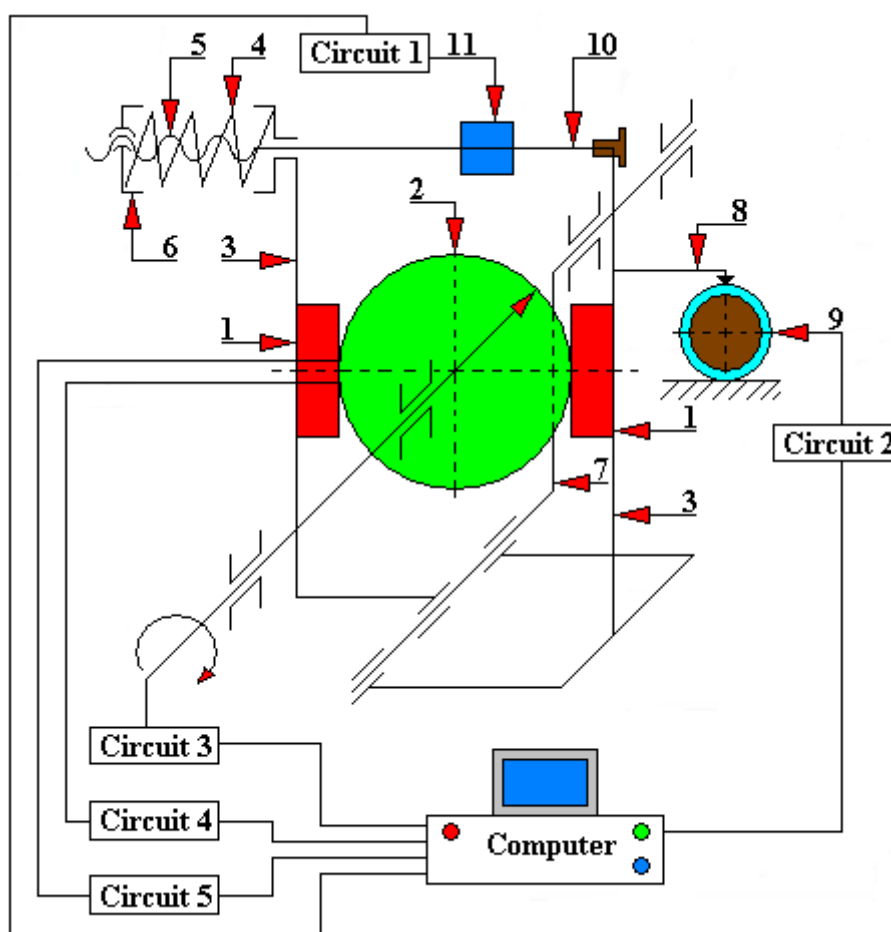


Fig. 4.1.26.2. A test rig for testing the friction and wear containing a rotating counter-sample against which stationary block samples or moving roller samples are pressed, according to the patent No. PL 160 597 Connection diagram of the control and measurement system.

1 - samples, 2 - counter-sample, 3 - levers, 4 - loading spring, 5 - screw, 6 - nut, 7 - crank, 8 - loading arm, 9 - strain gauge, 10 - rod, 11 - strain gauge.

Circuit 1 - measurement and recording of the force loading the samples.

Circuit 2 – measurement of the friction force between samples and a counter-sample.

Circuit 3 – measurement and recording of the rotational speed of the counter-sample.

Circuit 4 – measurement and recording of the temperature of the lubricant supplied to the tested friction contact.

Circuit 5 – identification of the type of friction which occurs between mating samples and a counter-sample.

4.1.27. TPZ test rig (reciprocating tribometer)

The TPZ tribotester (Fig. 4.1.27.1) is a non-commercial original tribological test rig built in the Department of Construction and Operation of Machines at Gdańsk University of Technology. This test rig is designed to test sliding friction that is technically dry or working in a lubricated contact. The design of this test rig enables testing with an adjustable level of excitation and different stiffness of the passive sample mounting system and the load setting system.

The structure of this test rig is as follows. The upper sample (2) is mounted in the lower part of the pusher (1) guided by linear roller bearings which are mounted in the body (5). This sample is a passive sample. The body (5), on the other hand, is connected by means of elastic elements to the rig frame (6). The elastic elements are in the form of rectangular frames with the stiffness for the vertical direction by several orders of magnitude greater than for the horizontal direction. By using different frames one can obtain changes in the dynamic properties of this test rig. The provided load can be realized in two ways:

- by tensioning the spring,
- with weights acting on the pusher (1) via a springy lever.

Reciprocating motion (working motion) is performed by the slide (4). The lower sample (3) is mounted in the slide (4). This sample is an active (moving) sample. The slide (4) moves on the rolling guides placed in the frame (6) of the test rig. The TPZ tribotester is driven by an electric motor (induction, squirrel-cage). This motor is powered by an AC frequency converter (inverter). The electric motor drives the crank through the belt transmission thus forcing the reciprocating movement of the slider (4). The use of an inverter in the drive system allows the motor speed to be controlled by a computer in the frequency range from 0 to 50 [Hz] while maintaining a constant power. The computer control of the drive motor also enables the programming of changes in the sliding speed of the mating samples. This feature makes the test rig a useful tool for testing the dynamics of friction. In the slide (4) there are semiconductor elements (operating on the basis of the Peltier effect) designed to heat or cool the samples in order to stabilize the temperature of the tested friction contact mating.

The heat generated as a result of the friction process flows through the exchanger which flows around the stream of air forced by the fan. The temperature of samples and/or grease is measured by means of thermocouples.

The friction force is indirectly measured by measuring the displacement of the upper sample (2). The measurement of the displacement of this sample (2) is made by means of strain gauges placed on elastic frames connecting the body (5) with the frame (6); in the body a pusher (1) is guided. The total wear of both mating samples during the test is determined by measuring the displacement of the pusher (1) - value "z".

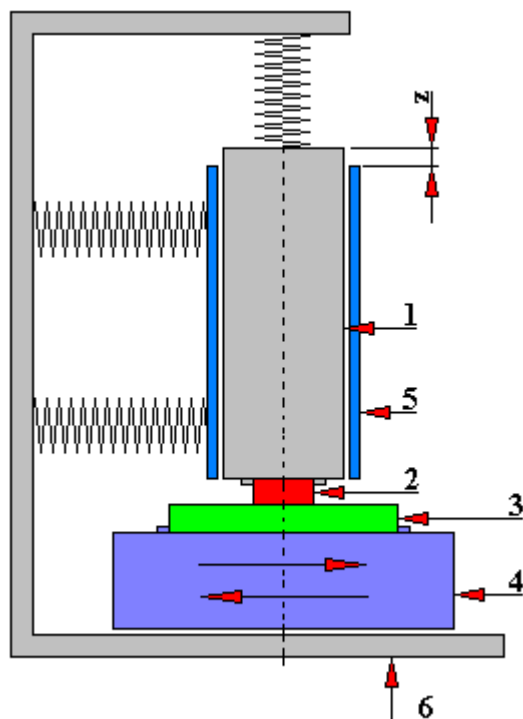


Fig. 4.1.27.1. Schematic diagram of the test head of the TPZ rig intended for testing the wear resistance in dry friction conditions or in a lubricated contact
1 - pusher, 2 - upper (passive) sample, 3 - lower (active) sample, 4 - reciprocating slide, 5 - body guiding the pusher, 6 - rig frame, z - total wear of both mating samples during the testing

4.1.28. TPZ-1 test rig (prototype)

The TPZ-1 tribotester (Figures 4.1.28.1 and 4.1.28.2) is intended for testing the materials of friction and sliding pairs at both positive (<math> < 200^{\circ}\text{C}</math>) and negative temperatures (up to minus a dozen or so $<^{\circ}\text{C}</math>). The authors of this construction design are Krzysztof Druet and Marian Król (patent application P-275 860). This test rig serves in particular, inter alia, to determine:$

- lubricant destruction temperature;
- characteristics of sliding pairs for fixed or adjustable excitations of temperature, speed and pressure;
- limiting pressures of scuffing of different material mating for different values of the product of speed and temperature.

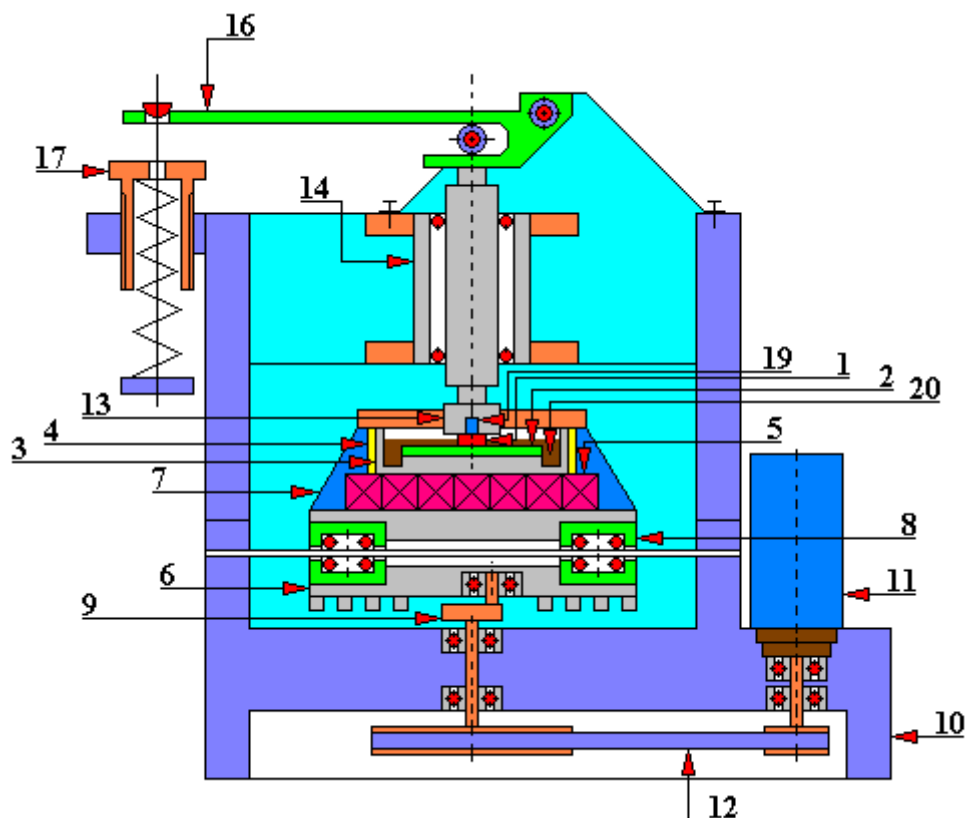


Fig. 4.1.28.1. General longitudinal diagram of the TPZ-1 tribotester (prototype) [32]

1 - upper sample (fixed), 2 - lower sample (moving), 3 - lubricant reservoir, 4 - housing, 5 - thermoelectric module, 6 - movable body, 7 - thermal insulation, 8 - rolling guides, 9 - crank mechanism, 10 - test rig body, 11 - DC motor, 12 - belt transmission, 13 - pusher handle, 14 - sleeve, 15 - spring elements, 16 - lever, 17 - screw-elastic tensioner, 18 - inductive displacement sensor, 19 - thermocouple, 20 - lubricant; the description refers to Figures 4.1.28.1 and 4.1.28.2

The TPZ-1 tribotester (prototype) is made of an upper sample 1 with a cross-section of 5x2 [mmxmm] and a lower (moving) sample with dimensions of 50x (4 ÷ 6) x (2 ÷ 4). The lower (moving) sample is placed in the lubricant reservoir 3 which is embedded in the housing 4. This housing is in contact with a set of thermoelectric modules 5 which are arranged on a moving body 6. The housing 4 is covered with thermal insulation 7.

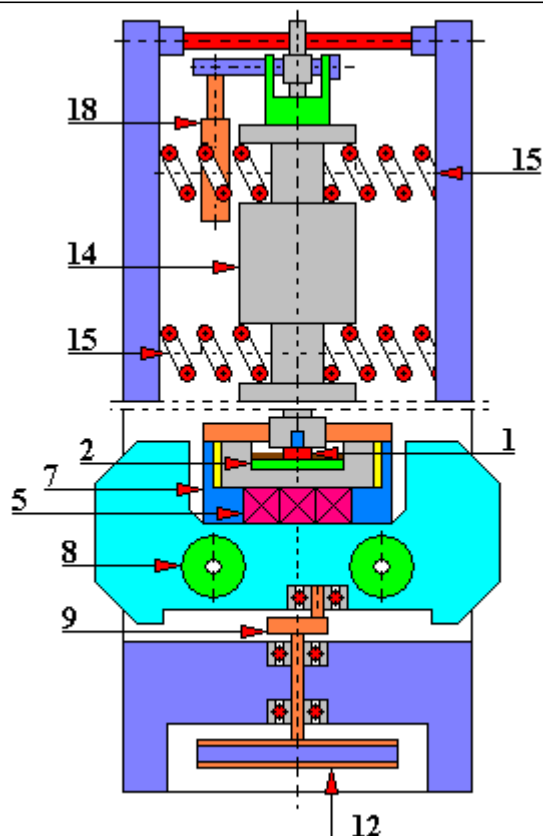


Fig. 4.1.28.2. General transverse diagram of the TPZ-1 tribotester (prototype) [32]

1 - upper sample (fixed), 2 - lower sample (moving), 3 - lubricant reservoir, 4 - housing, 5 - thermoelectric module, 6 - movable body, 7 - thermal insulation, 8 - rolling guides, 9 - crank mechanism, 10 - test rig body, 11 - DC motor, 12 - belt transmission, 13 - pusher handle, 14 - sleeve, 15 - spring elements, 16 - lever, 17 - screw-elastic tensioner, 18 - inductive displacement sensor, 19 - thermocouple, 20 - lubricant; the description refers to Figures 4.1.28.1 and 4.1.28.2

The body 6, which is moving, reciprocates on the rolling guides 8 and is driven by a crank mechanism 9 embedded in the body of the test rig 10. The change of speed of the moving body is achieved by means of a DC motor 11. This motor drives the crank mechanism via a belt transmission 12. The upper (fixed) sample 1 is mounted in the self-aligning pusher holder 13. The pusher is guided in a sleeve 14 attached to the body of the test rig 10. As a fixing solution, elastic elements 15 are used here which enable the use of strain gage measurement of the friction force. The adjustable pressure of samples 1 and 2 is obtained by means of a lever 16 which is loaded by means of a helical-elastic tensioner 17.

The measurement of the total linear wear of both mating samples is carried out by means of an inductive displacement sensor 18 whose movable tip is influenced by the moving pusher 13.

Temperature measurement is carried out using a thermocouple 19.

4.1.29. Almen-Wieland test rig designed for boundary friction tests

This type of a test rig is designed to measure the value of the boundary friction coefficient and to measure the durability of the oil layer between the rubbing elements. The mating of the tested elements is shown in Figure 4.1.29.1. The tested elements include:

- a shaft with a diameter of $\varnothing 6.35$ mm (some sources say $\varnothing 6.30$ mm);
- two bearing halfshells pressed with a force of $500 \div 30000$ [N] against a rotating shaft at a speed of 200 [rpm]. The slip speed is then 0.066 m/sec.

Bearing halfshells are pressed with the force increasing every 30 seconds by a value of 500 [N]. Rubbing surfaces are covered with the tested lubricating composition. Breaking of the boundary layer is accompanied by the seizure of the tested pair. This results in the increase of the value of the moment of friction causing the twisting of the tested shaft in the place of the notch cut on it.

On the basis of the value of the halfshells loading at which the coupling seizes one can draw conclusion on the durability of the boundary layer of the tested lubricant composition.

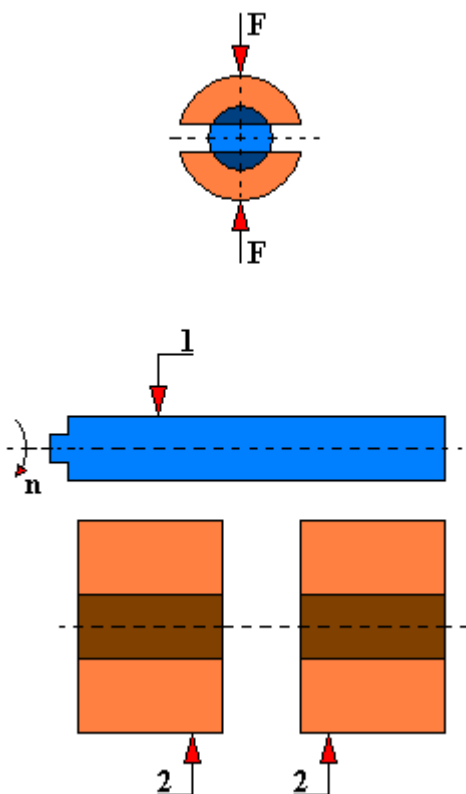


Fig. 4.1.29.1. The friction contact of the Almen-Wieland test rig
1 - rotating shaft, 2 - two halfshells

The test rig from Max Wieland (Wieland Schmiermittel-Prüfmaschine), generally known as the Almen-Wieland test rig, is intended, inter alia, for testing the durability of the oil film. The basic part of this test rig is a bearing consisting of two halfshells and a roller rotated by a belt transmission at a constant speed $n = 20.944$ [rad/sec] (200 rpm).

In the original version during the tests the bearing is immersed in the oil contained in an appropriate reservoir, which is also a holder for the lower halfshell. The oil can be in a continuous

flow thanks to an appropriate supply and discharge installation. During the test the halfshells may be hydraulically pressed against the roller with infinitely variable adjustment to the maximum value of approx. $5.884 \cdot 10^5$ [N/m²] (6000 kG cm²). In principle, only the friction force can be measured on this test rig, as measured by the stator angle of the self-aligning electric motor rotating the roller. It is possible to calculate the coefficient of friction from the measurement.

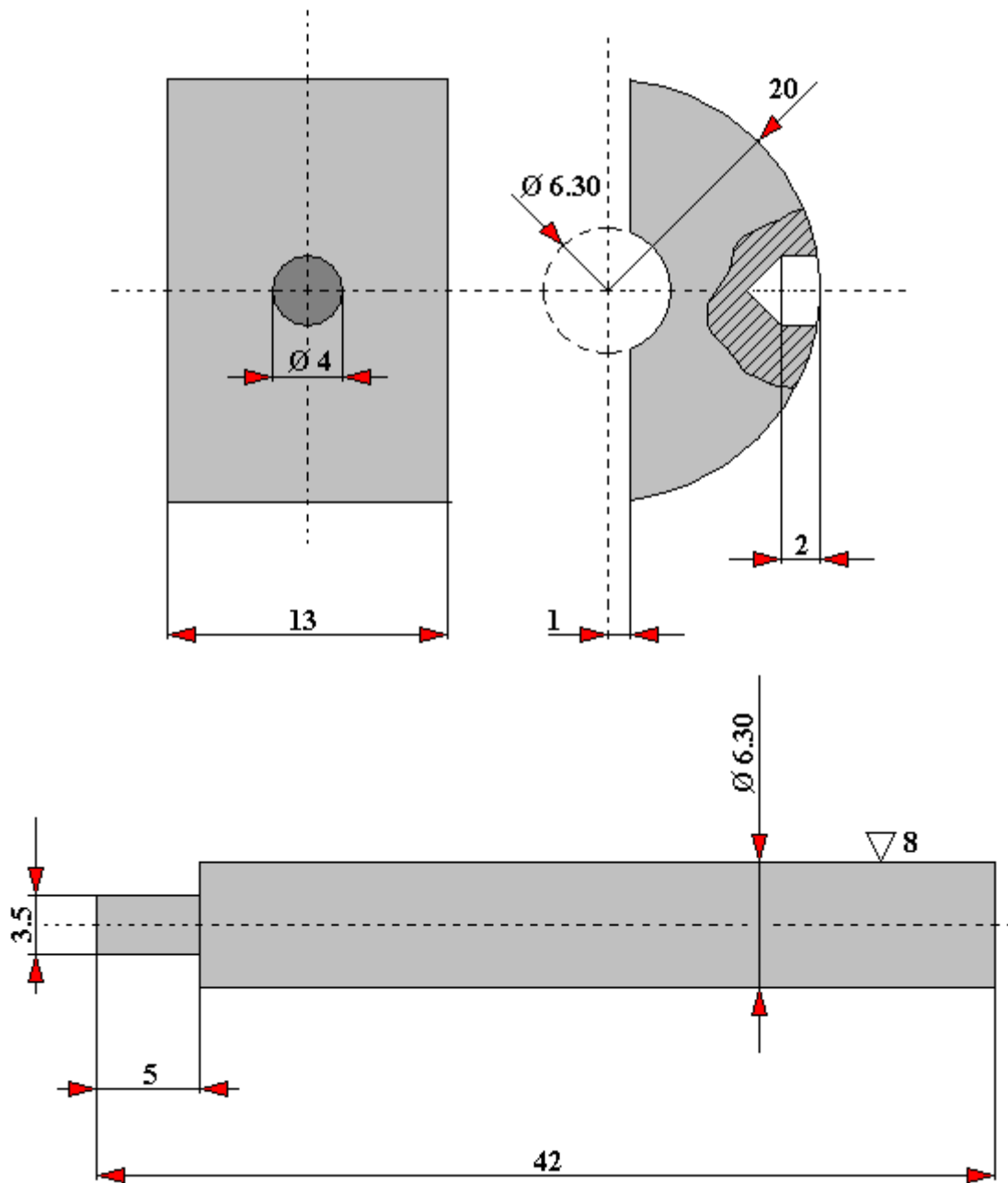


Fig. 4.1.29.2. The bearing (friction contact) of Almen-Wieland test rig with given factory dimensions
below - a rotating shaft; above - halfshell (2 pieces)

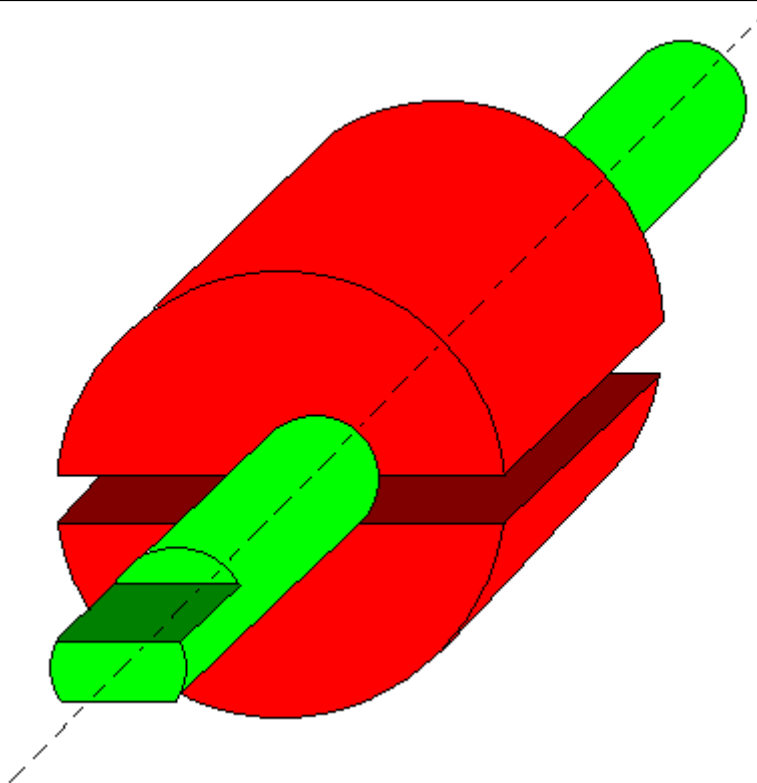


Fig. 4.1.29.3. A sample for the Almen-Wieland test rig

Many users of this test rig have upgraded this test rig to meet their research needs. For example, Jerzy Magiera and Marian Pieczarka [73] in order to determine the durability of the oil film during the mating of the pin and bush they have equipped the Almen-Wieland test rig with an appropriate electrical measuring system (Fig. 4.1.29.4). In addition, from the mechanical point of view, their modernization consisted in making the oil tank made of plastic (dielectric) in which the bearing-sample is working. In addition, the oil supply system was cut off. Before carrying out the tests (when assembling the bearing in the holders for the roller), a strictly defined amount of oil is dosed.

To determine the behavior of the oil film 2 (Fig. 4.1.29.4), formed in the tested bearing, an original method was used consisting in measuring the voltage drop across the resistance of this film. Along with the loss of the oil film the transition resistance between the bushings in which the shaft rotates decreases for the electric current. As a result, the tension on the oil film also decreases. A transformer with an output voltage of $U = 24$ [V] was used as a source of alternating current with a constant RMS value $I = 1$ [A] and frequency $f = 50$ [Hz]. This transformer was supplied with stabilized voltage of 220 [V] and frequency of 50 [Hz].

This measurement method is characterized by very small changes in the transition resistance between the bushings, which are also defined measurement points, which is its unquestionable advantage. The disadvantages of this method, however, were the technical difficulties in solving the amplifying circuit, controlled by variable voltage drop increments on the transition resistance. The amplification circuit used here had to be characterized by appropriate sensitivity and a high gain factor.

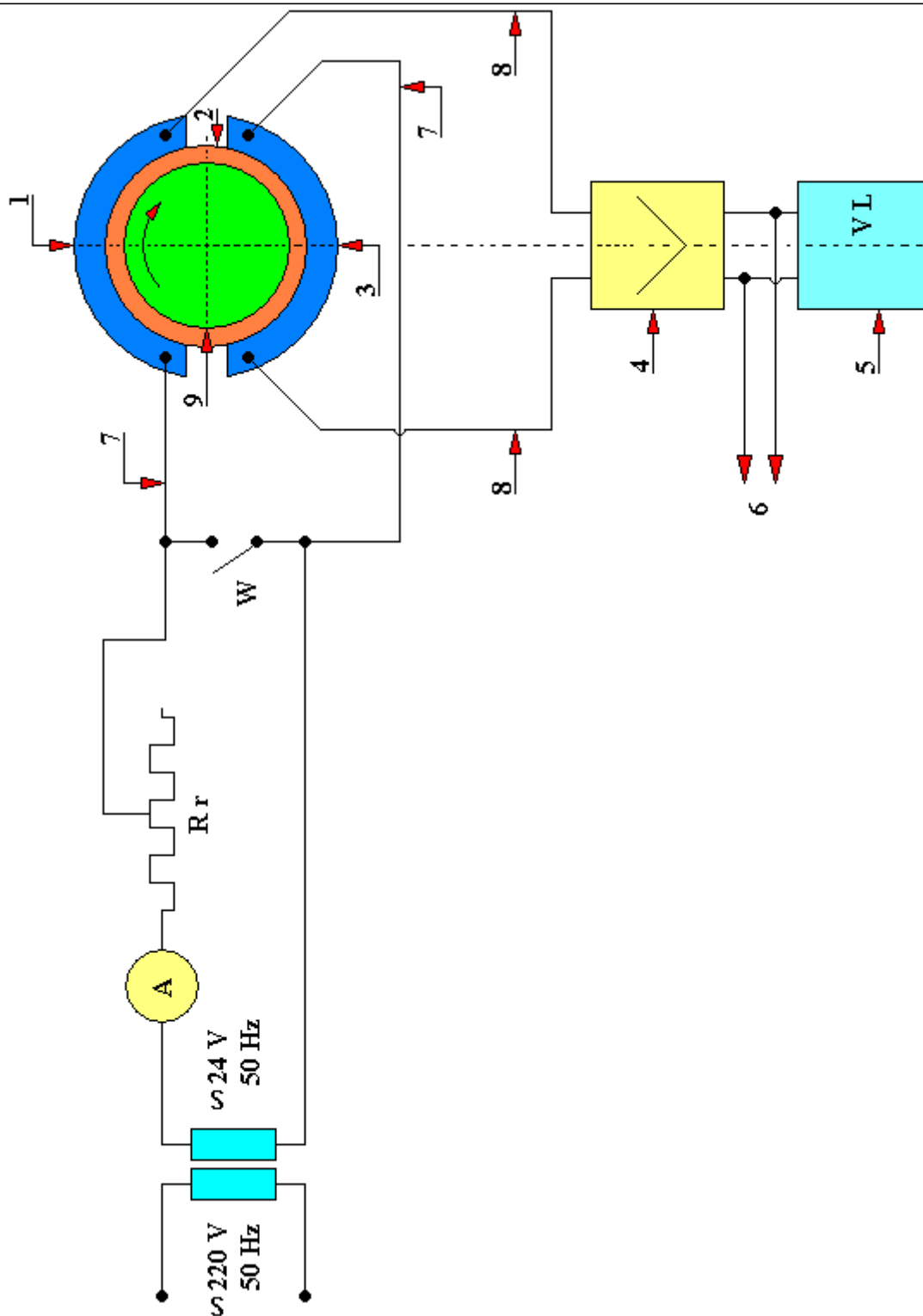


Fig. 4.1.29.4. A diagram of electrical installation for testing the oil film on the Almen-Wieland test rig by Jerzy Magiera and Marian Pieczarka

R r - slide resistor (variable resistance resistor); W - safety switch; A - ammeter; 1 - upper bushing; 2 - oil film; 3 - lower bushing; 4 - measuring amplifier; 5 - voltmeter (the author used a tube voltmeter here in the original version); 6 - for switching on the recorder or oscilloscope; 7 - power terminals; 8 – gauging points; 9 - shaft

The description of the applied measuring wiring diagram is as follows. A transformer is connected to the electric network with the frequency $f = 50$ [Hz] and voltage $U = 220$ [V] through the voltage stabilizer at the output of which the voltage is 24 [V]. This voltage is supplied to an electric circuit composed of:

- ammeter "A" - used to determine the selected current value and its control during the measurement;
- regulating resistor R_r (variable resistance resistor) - enabling the change of the current value in the electric circuit and protecting the current source against short-circuit conditions;
- the arrangement of bushings 1 and 3 (Fig. 4.1.29.4) with power-gauging points;
- shaft 9 (Fig. 4.1.29.4).

The power-gauging points 7 and 8 are made of copper wire with an appropriate cross-section and carefully soldered to the bushings in such a way so that the voltage drop across the resistance of the terminals, including the soldering points, is negligibly small in relation to the voltage drop on the transition resistance (voltage drop across the oil film). This circuit is closed by the oil film transition resistance 2 (Fig. 4.1.29.4) between the shaft 9 and the upper 1 and lower 3 bushings (Fig. 4.1.29.4).

In the electric circuit there is also a special switch "W" which is designed to protect the amplifier against over control and the voltmeter against damage when the bushings are replaced. Thanks to "W" switch it is possible to replace the bushings without disconnecting the power from the circuit.

The voltage drop on the transition resistance (on the oil film) is applied to the measuring amplifier with dynamic characteristics, and then to the voltmeter (the authors originally used a WL-2c tube voltmeter of Polish production) which is the actual measuring instrument.

The built-in measuring amplifier has a step-adjustable gain factor. An alternating current was selected to supply the measuring circuit in order to avoid the influence of possible electromotive forces (EMF) arising at the 'metal-oil-metal' contact. In addition, the use of AC current eliminates the need for a DC amplifier in the circuit.

The power transformer can be treated as a current source with a low internal resistance. As the transition resistance (through the oil filter) changes insignificantly, it does not have a significant effect on the changes in the voltage and current supplying the measuring circuit. The effective value of this current was determined experimentally being guided by:

- the necessity to obtain a voltage drop, that can be amplified, on the transition resistance (through the oil film);
- avoiding the development of heat on this resistance originating from the supply current (the heat generated will be the result of the friction force only).

It is possible to connect an oscillograph or a recorder in the measuring system.

Ideally, the transition resistance (through the oil film) is only dependent on the oil film itself. In fact, it depends, inter alia, on:

- film thickness;
- pressure of the bushings;
- roughness of mating surfaces;
- geometric symmetry of the bushing-shaft system;
- rotational speed of the shaft;
- temperature of mating surfaces.

The thickness of the oil film layer has a direct impact on the transition resistance. And the thickness of the oil film layer, at least partially, depends on the pressure of the bushings, roughness of the mating surfaces and their temperature, and the rotational speed of the shaft.

The greater the roughness of the mating surfaces, which is confirmed by the measurements of the above-mentioned authors, the faster the electric short circuit between the bushings and the shaft will occur. This condition indicates the presence of a mixed friction as in the cavities of the unevenness there will still be grease.

The eccentric position of the shaft and bushings also causes an early short circuit. The state of the electrical short circuit significantly reduces the transition resistance (through the oil film) which in this case depends mainly on the forces of pressing the bushings against the shaft.

The above-mentioned authors in their research used Ł10As bearing alloy as the bushing material, and P35 steel as the roller material.

The universal U oil was used as a lubricant, which is applied for slide bearings of freight wagons - new and used (sourced from axle-boxes of wagons). This oil has been enriched with anti-seizure additives.

Before starting the tests each set (two halfshells and a shaft) was ground in with a pressure of $98068.5 \text{ [N/m}^2\text{]}$ (1 kg/cm^2) during $n=500 \text{ rpm}$. During this period a correct fitting of elements was found.

After placing the lower halfshell and the shaft, and placing the insulating inserts on the flat surfaces of the halfshell, 3 drops of oil were placed on the roller with the use of a dropper. This method of dosing ensured that the weight of individual drops (and thus their volume) for all tested oils differed insignificantly. Then the upper halfshell was fitted and the whole was subjected to a pressure of $F=49033.25 \text{ [N/m}^2\text{]}$ (0.5 kG/cm^2). After connecting the ends of wires led from the halfshells to the appropriate terminals on the switchboard, the shaft was rotated several times in order to distribute the oil. After the circuit was closed, the measurements were carried out.

The testing was conducted in two versions, as:

- static (motionless roller and increasing pressure on the bushings);
- moving (a roller rotating at a speed of $n=20,944 \text{ [rad/sec]}$ (200 rpm); pressure on the bushings is constant).

In this way the dependence of the voltage drop on the oil film resistance as a function of pressure or as a function of time was determined (at $F=\text{const}$). Indirectly also the thickness of the oil film was determined in this way.

On the basis of the conducted tests the above-mentioned authors confirm the usefulness of the described method for measuring the oil film layer in the slide bearing-sample, both in static and running conditions. Thanks to this it is possible to determine the durability of the oil film under assumed operating conditions. The decrease in voltage drop on the transition resistance indicates the improvement of conditions of the current flow, i.e. the disappearance of the film layer or even a direct contact of the pin surface with the bushing (e.g. as a result of local melting of bushings due to excessive heat input).

Knowing the specific resistance of the appropriate type of oil (lubricant) it is also possible to determine the thickness of the oil film for individual pressures, which of course is conditioned

primarily by the compliance with the requirements for the roughness of the co-acting surfaces of the shaft and bushings.

It is worth mentioning here that Almen-Wieland test rig is very well suited for testing slide bearings of any design and materials dedicated to these bearings.

Slide bearings, though they are displaced from test rigs by rolling bearings, have a number of advantages thanks to which they are still used inter alia as crankshaft bearings or axle bearings for freight wagons. The advantages of slide bearings include:

- resistance to shock loads;
- the ability to dampen vibrations;
- high durability (in liquid friction conditions);
- small transverse dimensions;
- resistance to corrosion;
- good thermal conductivity (when using metal materials).

Slide bearings disadvantages usually include:

- the difficulty of maintaining fluid friction under changing operating conditions;
- frictional resistance higher than in rolling bearings.

The service life of a slide bearing depends mainly on the observance of the rules of their proper operation, which means:

- proper selection of the lubricant;
- ensuring the appropriate amount of the lubricant used;
- preventing the inflow of contaminants with unfiltered oil or grease.

Additionally, the accelerated wear of slide bearings is influenced by the difficulty in maintaining continuous fluid friction, the conditions under which the pin should co-act with the bushing. At startup, slide bearings most often operate in the mixed friction range. For a quick assessment of whether a given slide bearing is currently operating in a fluid or mixed friction range, the so-called Sommerfeld parameter k is used (Fig. 4.1.29.5). This parameter is expressed as the following relationship:

$$k = \frac{\eta \cdot n}{p_{sr}}$$

where:

η – oil body [0.001 Nsec/m²] or (cP);

n -pin rotational speed [rad/sec] or [rpm];

p_{sr} – average pin pressure on the bushing [N/mm²] or (kG/cm²)

Fuller [D. Fuller: Teoria i praktyka smarowania, PWN, Warszawa 1960] states that for the parameter

$$k > 420 \div 570$$

we are dealing with a liquid lubrication. It is well known that fluid friction occurs when mating surfaces are separated by a layer of lubricant that prevents from a direct contact of the peaks of

the unevenness of both co-acting surfaces. Some sources additionally state that the thickness of this layer of lubricant used should be at least the thickness of its a dozen or so molecules.

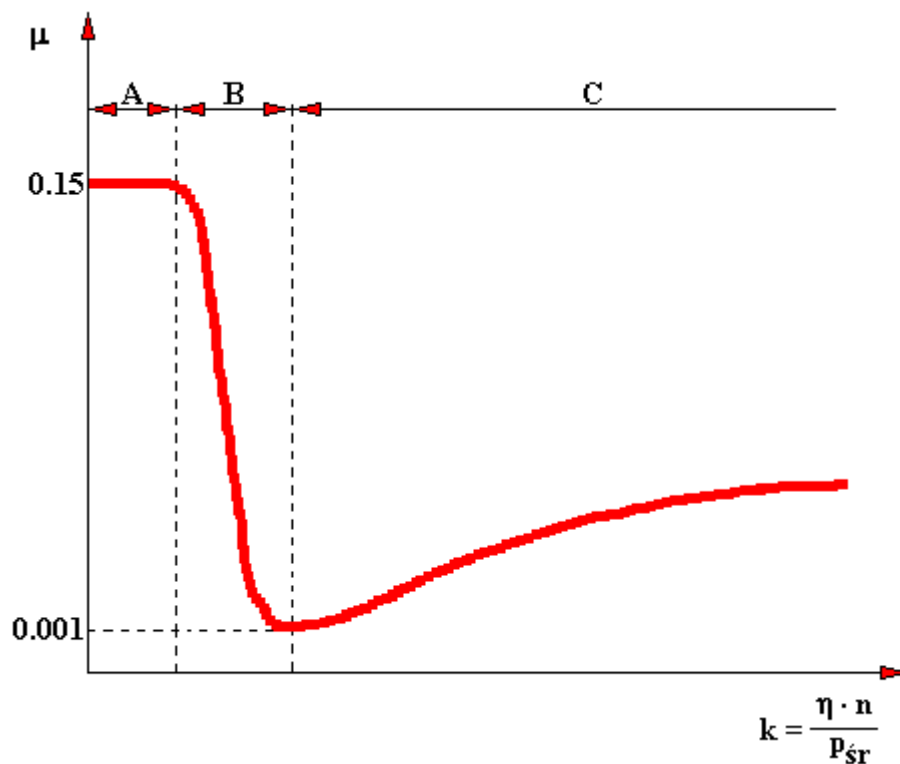


Fig. 4.1.29.5. Dependence of the friction coefficient μ on the Sommerfeld parameter k [73]
 A – boundary lubrication; B - mixed lubrication; C - liquid lubrication; η - oil body; n – pin rotational speed; p_{sr} - average pressure of the pin on the bushing

4.1.30. Skoda-Savin type test rig

This type of a test rig is designed to carry out quick abrasion tests. A schematic diagram of this type of test rig is shown in Figures 4.1.30.1 and 4.1.30.2. This test rig has the following features:

- adjustable rotational speed of the motor driving the rotating counter-sample;
- unit pressures adjustable with weights;
- loading weight system;
- variable (increasing with the increase of wear) friction face of the sample;
- constant nature of the load;
- liquid coolant;
- does not have a measuring system of the moment of friction;
- the medium of friction is potassium dichromate.

This type of test rig can be used to test a flat or cylindrical sample with a wide disc of the diameter of $\varnothing 30$ mm and thickness of 2.5 mm. The disc is pressed with a constant load and mounted in the guiding yoke by means of levers in the guides. A speed-controlled electric motor drives a wide disc via a shaft. The wear is measured using an optical microscope (reading of the width of one groove).

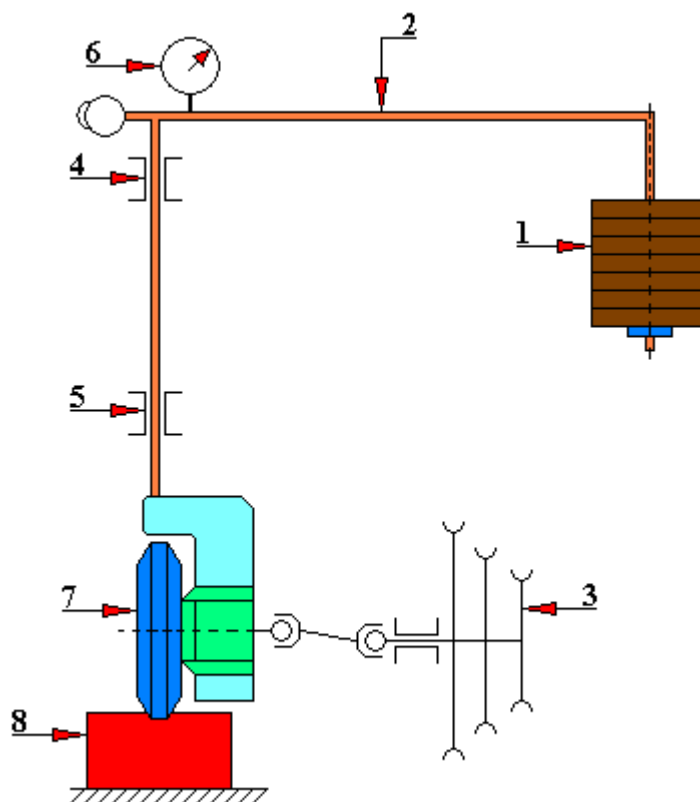


Fig. 4.1.30.1. Schematic diagram of the Skoda-Savin test rig

1 - load, 2 - lever, 3 - pulleys of the drive shaft, 4 - bearing in the guiding yoke, 5 - bearing in the guiding yoke, 6 - dynamometer, 7 - wide disc (counter-sample), 8 - tested cylindrical or flat sample

The lubricating and cooling agent is potassium dichromate ($K_2Cr_2O_7$) dissolved in distilled water (for cast iron, bronze and steel: 0.5% solution). The peripheral speed, the total number of revolutions (testing time) and the pressure of the disc on the tested material are determined individually for each test case. A greater speed and a low pressure on the disc, as well as a shorter testing time, are taken for materials with low hardness [45].

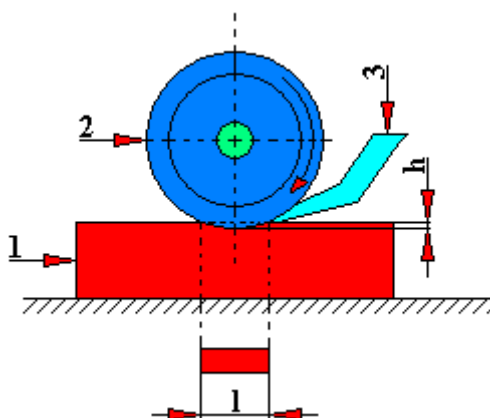


Fig. 4.1.30.2. A diagram of the Skoda-Savin test rig. View from the side of the widia disc.
1 - tested sample, 2 - widia disk (counter-sample), 3 - lubricant dispensing nozzle,
l – length of the wear trace, h – depth of the wear trace

4.1.31. KEWAT-1 type test rig

In test rigs of this type (Figure 4.1.31.1) a flat sample is rubbed against a flat counter-sample (conformal contact). The working motion is a reciprocating motion here. The sample load during one stroke of work may be constant or variable. The variable load is obtained through the appropriate cam profile. KEWAT-1 test rig is characterized by the following features:

- the counter-sample speed ranges from 0.25 to 4 [m/sec];
- the stroke of the slide is 150 [mm];
- friction environment: practically any lubricant composition (water, water solutions, oils);
- friction torque measuring system: strain gauge;
- loading system: spring;
- the sample controlled by the cam profile of the eccentric mechanism is pressed perpendicularly to the counter-sample surface;
- unit pressure is from 0.02 to 100 [MPa];
- the friction face ranges from 2 to 6 [cm²];
- sample temperature measurement: thermistor sensor, thermocouple;
- nature of the load: constant, sinusoidal or other variable.

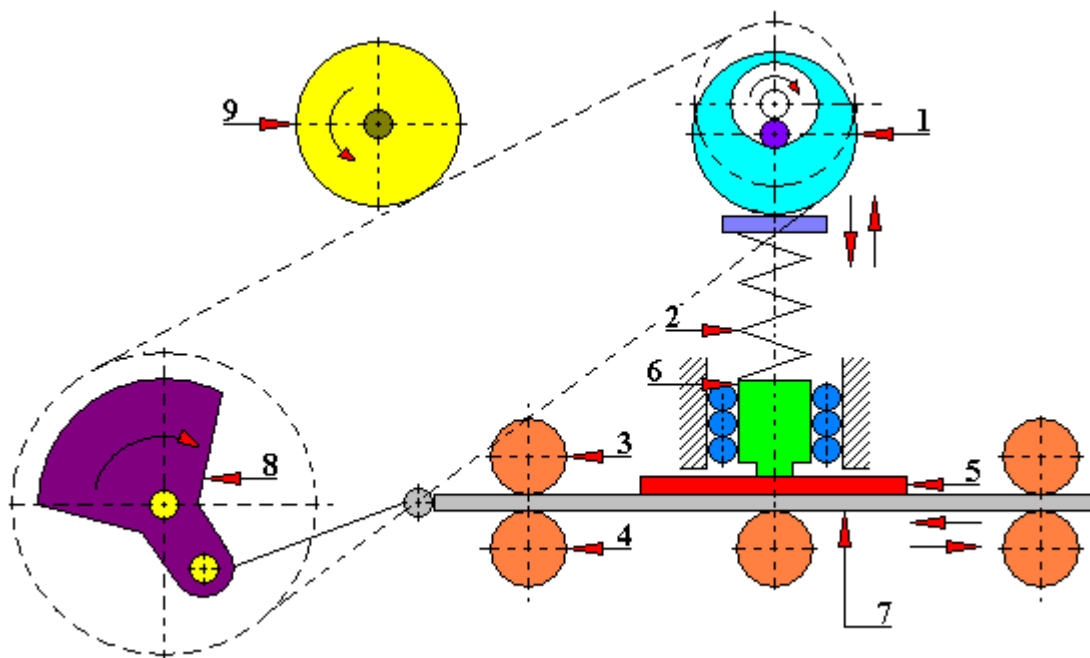


Fig. 4.1.31.1. Scheme of KEWAT-1 test rig [45]

1 - eccentric mechanism for adjusting the normal pressure of the tested sample, 2 - compression spring, 3 - upper slide bearing, 4 - lower slide bearing, 5 - counter-sample, 6 - sample, 7 - slide table, 8 - crank drive, 9 - chain tensioner

4.1.32. KEWAT-2 type test rig

This test rig performs a rotational motion, and the friction of two rectangular samples against a rotating counter-sample is performed under a constant load (Figure 4.1.32.1).

The principle of operation of this test rig is based on the fact that a rotating counter-sample, driven by an electric motor with adjustable rotational speed, is pressed against two rectangular samples with a defined normal force. Friction is generated in the area of contact between the two samples and the rotating counter-sample. The value of this friction force is measured by means of a strain gauge system. This test rig is characterized by the following parameters:

- the friction face is 2 [cm²];
- loading system: spring;
- friction environment: any oil composition;
- samples temperature measurement by means of thermocouples;
- nature of the load: fixed, stepped;
- friction torque measuring system: strain gauge;
- unit pressure is from 0 to 7.0 [MPa];
- rotational speed of samples from 300 to 3000 [rpm];
- friction velocity from 2.5 to 25 [m/min].

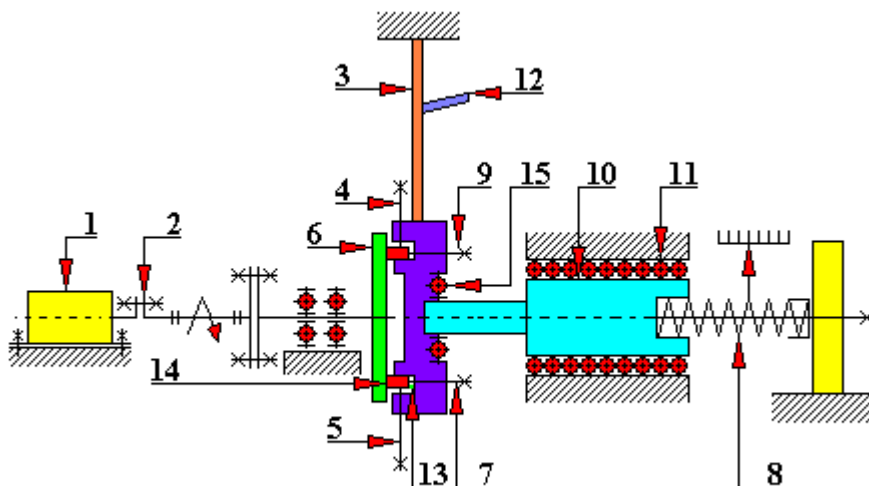


Fig. 4.1.32.1. Scheme of KEWAT-2 test rig [45]

1 - revolution counter, 2 - revolution counter clutch, 3 - strain gauge beam, 4 - sample setting adjustment, 5 - sample setting adjustment, 6 - counter-sample, 7 - sample setting adjustment, 8 - strain gauge, 9 - sample compression spring, 10 - guide, 11 - guide bearing, 12 - strain gauge, 13 - thermocouple, 14 - sample, 15 - self-aligning bearing

4.1.33. KEWAT-3 type test rig

This test rig is designed for tribological tests at swinging motion and programmable pressing force (Figure 4.1.33.1). Its design reflects the kinematics of the motion and dynamics of the load of the link and vehicle caterpillar pin. The counter-sample and sample are cylindrical and touch along the generatrices. The sample has a negative and the counter-sample has a positive radius of curvature. The cam is chain driven from the electric motor. The motor also drives (by direct connection) the crank shaft of the pendulum mechanism causing the pin to swing. The sample eye is connected by a loading spring, strain gauge beam and a roller with a cam whose rotational speed is reduced by 2.5 times in relation to the rotational speed of the drive motor. The mating surfaces can be lubricated with any oil composition, or contaminated with sand, in order to faithfully reproduce the actual operating conditions of the caterpillar link of the vehicle.

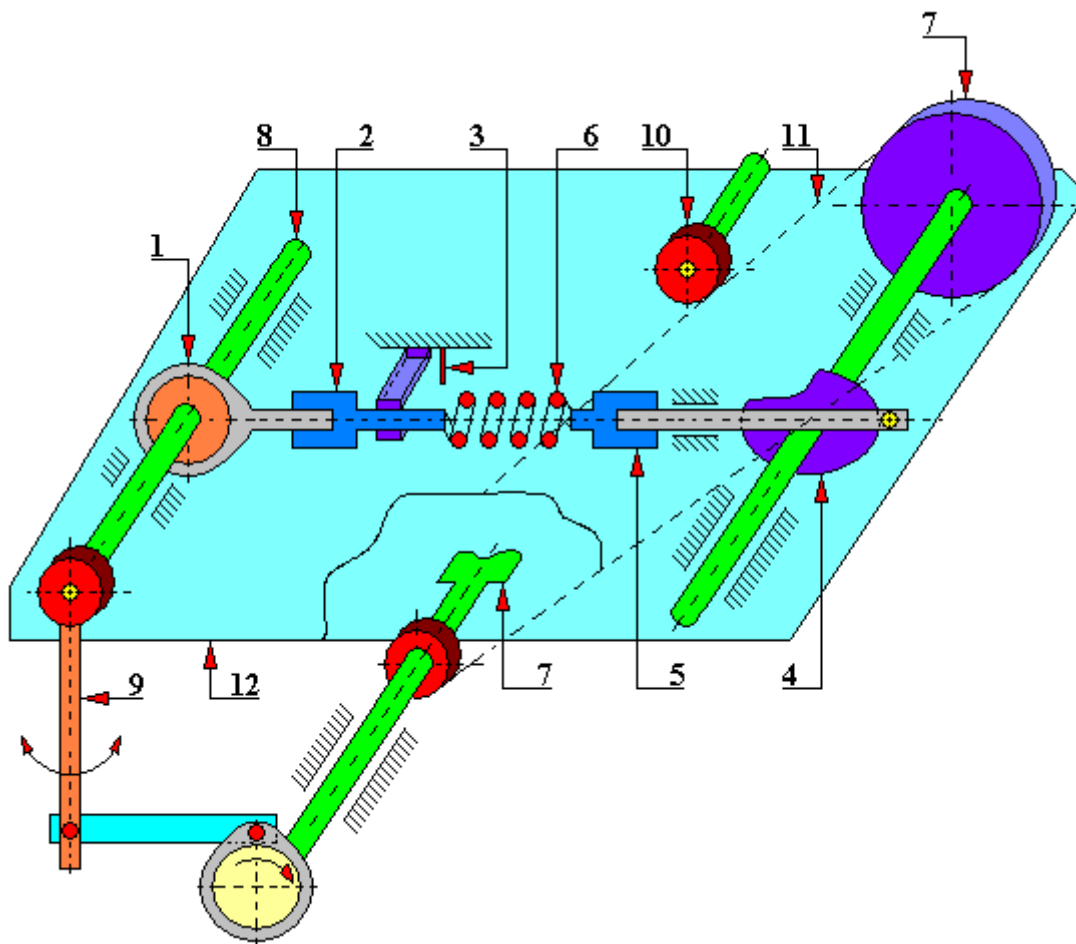


Fig. 4.1.33.1. Scheme of KEWAT-3 test rig [45]

1 - eye, 2 - strain gauge beam, 3 - thermometer, 4 - cam, 5 - strain gauge beam, 6 - loading spring, 7 - drive shaft, 8 - sample shaft, 9 - pendulum crank, 10 - chain tension, 11 - chain, 12 - base plate

This design is characterized by the following parameters:

- friction environment: dry friction with an abrasive;
- friction velocity: $0.03 \div 0.57$ [m/sec];
- nature of the load: variable or fixed;
- friction face: 4 [cm²];
- unit pressure: $0 \div 15.0$ [MPa];
- load periodicity: $1 \div 10$ [cycles/sec];

- loading system: eccentric and spiral spring;
- cooling: water;
- friction torque measuring system: strain gauge.

4.1.34. KEWAT-4 (KEWA-4) type test rig

This test rig is designed to test the friction force in the pin-bushing pair. The sample rotates simultaneously with the drive shaft. The shaft is driven by a stepped belt transmission and an electric motor. The counter-sample, attached to the 'stationary' measuring lever, is pressed onto the sample through the pressure plate and a rolling bearing. The pair is loaded by means of a lever system. As a result of the frictional resistance between the test sample and counter-sample forces arise which act on the dynamometer through the lever. This dynamometer records the value of the friction force. (Fig. 4.1.34.1 and 4.1.34.2).

The design of this tribotester is characterized by the following parameters:

- sample length: $15 \div 30$ [mm];
- normal load: $0 \div 800$ [N];
- measurement of the friction force: using a spring dynamometer;
- measurement of the rotational speed: using a manual revolution counter;
- counter-sample temperature measurement: thermistor, thermocouple;
- friction environment: any lubricant composition;
- sample rotational speed: $20 \div 2000$ [rpm];
- internal diameter of the sample: $20 \div 30$ [mm].

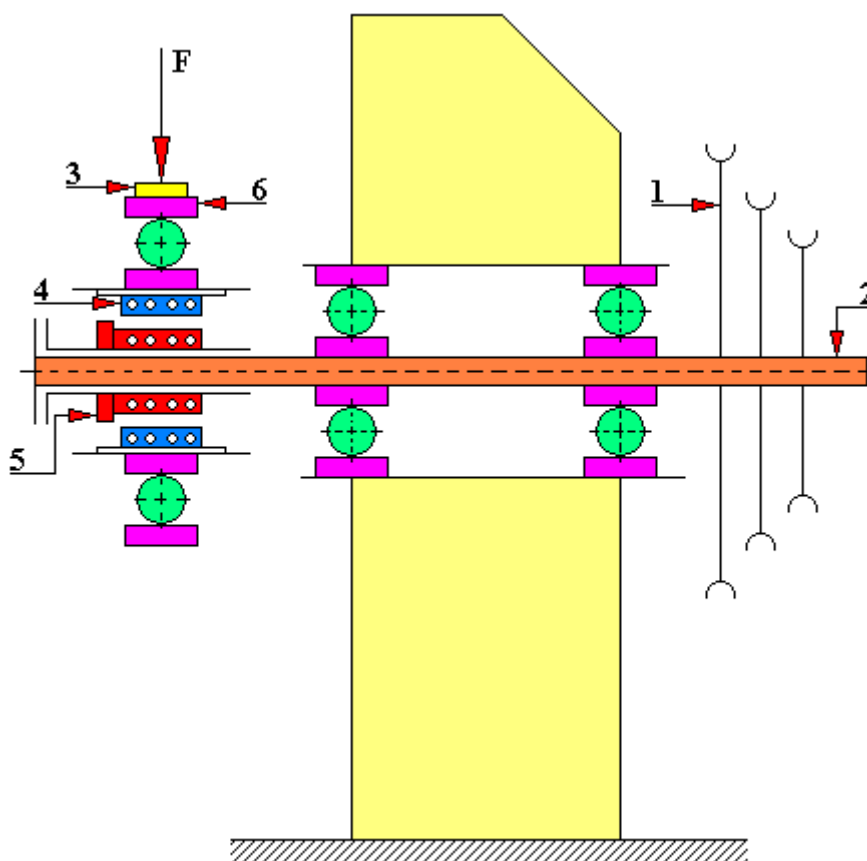


Fig. 4.1.34.1. Scheme of KEWAT-4 test rig (side view) [45]

1 - stepped belt transmission, 2 - drive shaft, 3 - pressure plate, 4 - counter-sample, 5 - sample, 6 - rolling bearing, F - force of pressure of the sample against the counter-sample

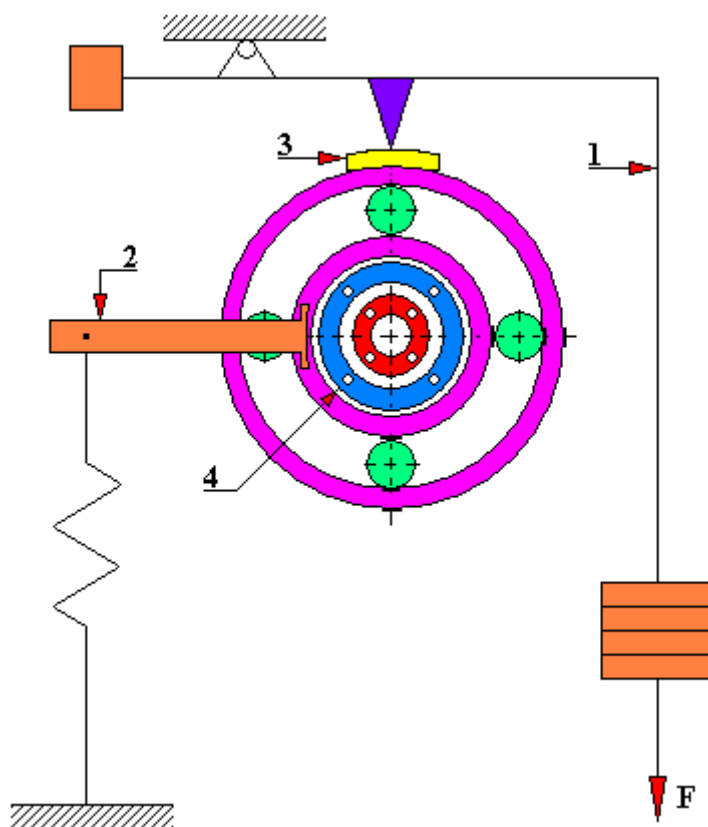


Fig. 4.1.34.2. Diagram of the KEWAT-4 test rig (view from the drive shaft side) [45]

1 - loading lever, 2 - friction torque measuring lever, 3 - pressure plate, 4 - spring dynamometer, F - load

In the work [Michał Hebda, Ryszard Moraczewski: Niektóre zagadnienia materiałów niemetalowych na łożyska ślizgowe samosmarowne. Zeszyt 8, 1979] presented is the design of 'KEWA-4' test rig (Fig. 4.1.34.3 and 4.1.34.4). This test rig is very similar to 'KEWAT-4' test rig. Probably one of them is a development of the other.

The 'KEWA-4' test rig imitates the operation of a slide bearing and it is intended, inter alia, for:

- laboratory and comparative tests on the values of the coefficient of friction and wear resistance of various materials (mainly non-metallic) that may be used for slide bearings;
- laboratory tests on the permissible values of friction velocity and normal loads of self-lubricating bearings made of various materials, including non-metallic materials;
- laboratory research on the durability of slide bearings made of various materials;
- research on some phenomena in the areas of frictional contact of a slide bearing;
- research on the influence of temperature and the working environment of a bearing (metal or non-metal) on the stability of its dimensions.

The object of tests performed on the 'KEWA-4' test rig are samples in the form of a sleeve or disc which can be made, for example, of the following non-metallic materials co-acting with steel counter-samples (e.g. steel 45):

- compressed wood (pressed and bentwood, e.g. birch or beech);
- compressed wood (pressure glued wood);
- polyamide;

- polyamide with different fillers (e.g. MoS₂; HAF (carbon black); graphite).

In addition, 'KEWA-4' test rig enables model testing of a slide bearing in which the bushing is, for example, a compressed wood bushing or polyamide bushing co-acting with a steel pin. The tests can be carried out during a dry friction, with water cooling or with oil lubrication (tested with the lubricant composition).

In the case of a technically dry friction, the scuffing of the co-acting materials usually takes place in a short time. Of course, the more the bushing has fillers, such as MoS₂, graphite, Teflon, carbon black, the longer is this scuffing time. At a certain limiting concentration of a given filler (or fillers), seizure may not occur, even with a dry friction.

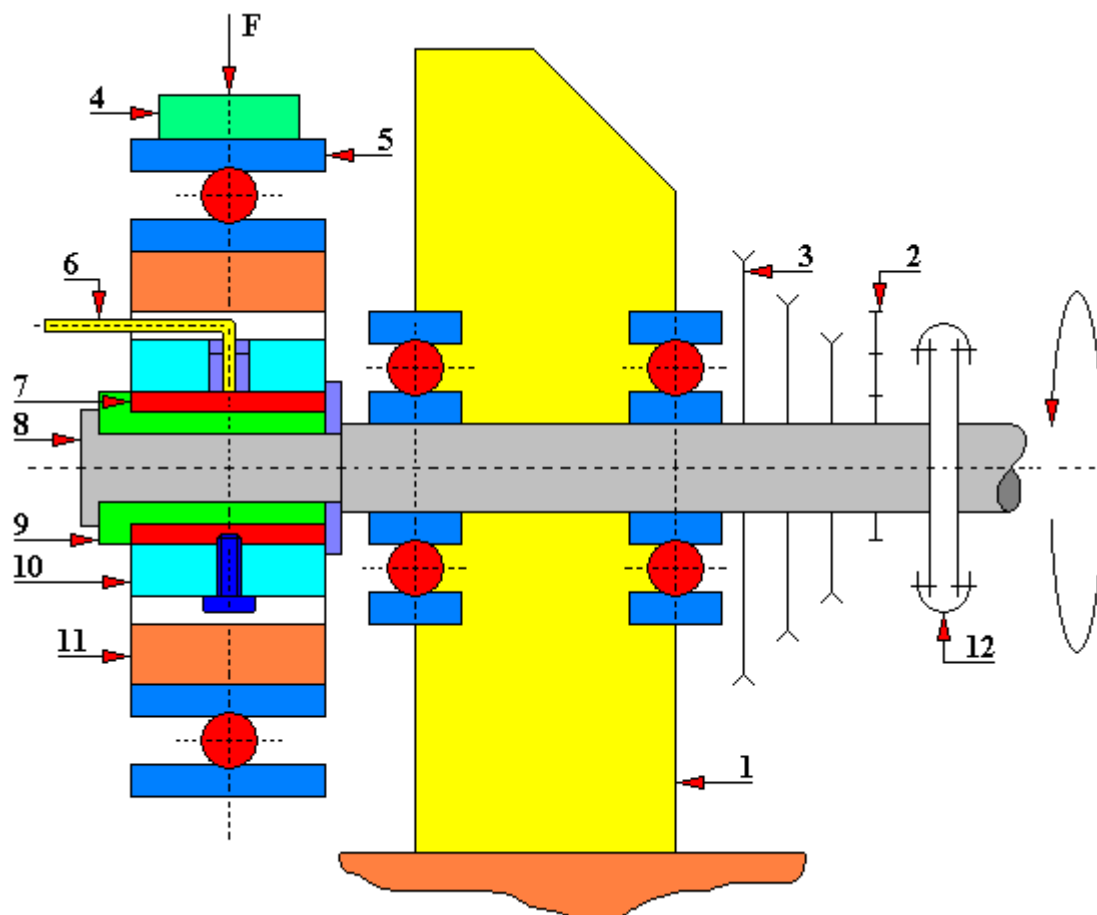


Fig. 4.1.34.3. Scheme of KEWA-4 test rig

1 - test rig frame; 2 - rev counter drive; 3 - belt gear wheel; 4 - plate; 5 - bearing; 6 - thermocouple; 7 - test sample; 8 - spindle; 9 - counter-sample; 10 - clamping ring; 11 - bearing holder; 12 - clutch

Bearing sleeves for this type of test rig were made, inter alia, by Warszawska Fabryka Tworzyw Sztucznych in Warszawa.

It is worth mentioning here that, for example, thermoplastics can work as sliding elements in principle only when the macromolecular compounds are improved either by modifiers and stabilizers or by adding lubricant fillers. Then, the most commonly used are polyethylene and polyamide filled with e.g. graphite, carbon black, molybdenum disulphide or tungsten disulphide.

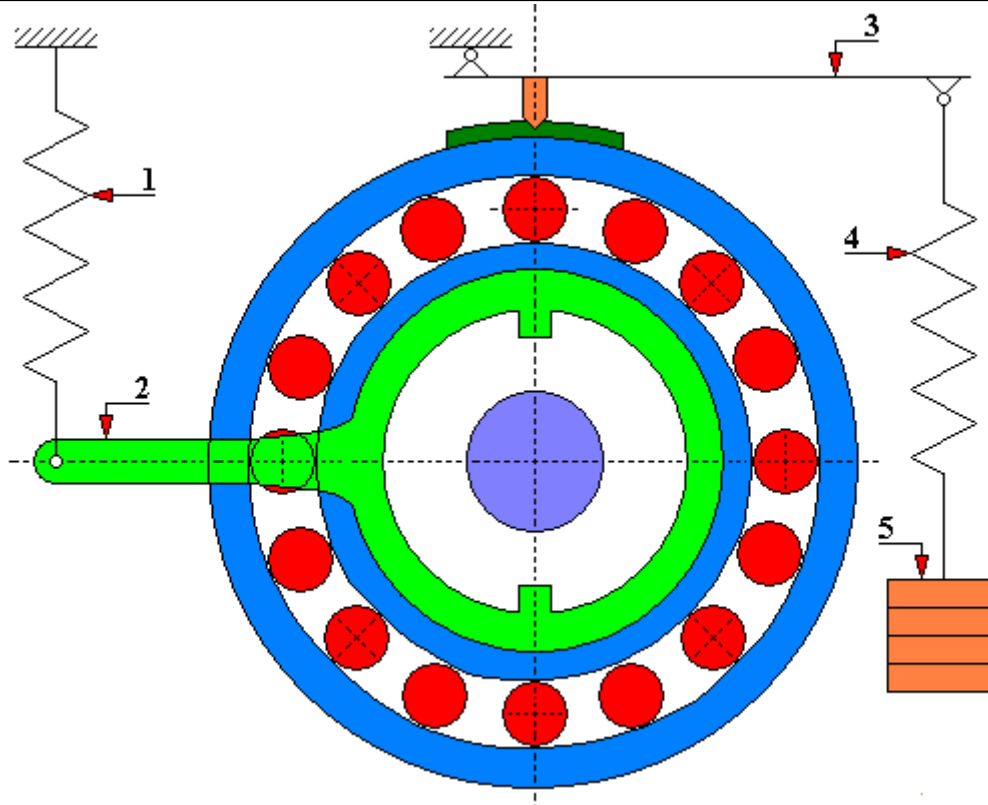


Fig. 4.1.34.4. Scheme of operation of KEWA-4 slide bearing test rig

1 - dynamometer; 2 - lever for measuring the moment of friction; 3 - loading lever; 4 - spring; 5 - load

On the 'KEWA-4' test rig it is also possible to measure the temperature of the surface layer of the mating friction contacts. In the case of determining the friction-wear characteristics of friction materials the problem of measuring the actual temperature of the surface layer is of great importance. Generally, in almost all cases of friction of plastics there is a much greater temperature gradient than in friction of metals due to the low thermal conductivity of the former. Therefore, the reliability of a temperature measurement with a thermocouple placed inside the surface layer of the plastic, even at a distance of a few tenths of a millimeter from the mating surfaces, is very low.

In the work [J. Janecki: Wpływ obróbki cieplnej hamulcowych tworzyw fenoloformaldehydowych na zmiany ich cierności i odporności na zużycie. Biuletyn WITPiS, z. 1, 1968] it was concluded that the most reliable method of measuring the temperature of the surface layer is the measurement with a thermocouple immersed in the material of the surface layer touching the friction surface of the metal with its head (Fig. 5.1.34.5). Thus, with a thermocouple head diameter of a few tenths of a millimeter, there is a real premise for the assumption that the temperature of the surface layer is being measured, and not the temperature of the core. It was also found in the above-mentioned work that the friction of the thermocouple head directly against the metal surface under such light pressure (elasticity of the wires and the friction of the head against the walls of the hole drilled in the sample) resulted in a very slight error in the temperature measurement. Covering with molybdenum disulfide or graphite of the path of friction of the micro thermocouple head on the metal surface (and thus a clear reduction of the coefficient of friction of

the thermocouple against the metal) did not give any differences in temperature indications. This may prove that the thermocouple reflects then quite accurately the temperature of the surface layer of the plastic.

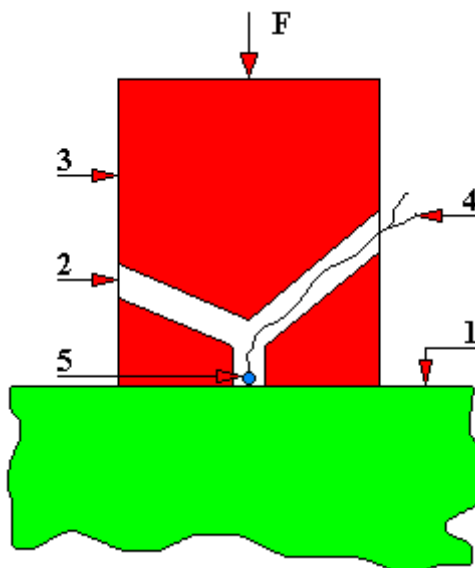


Fig. 4.1.34.5. A diagram of measuring the temperature of the friction surface and the surface layer of the abraded plastic showing the method of mounting the thermocouple to the slide bearing test rig in the KEWA-4 test rig

1 - counter-sample (metal); 2 - drillings; 3 - sample; 4 - the ends of the micro thermocouple; 5 - micro thermocouple head; F - force acting on the sample

Table 4.1.34.1. Comparison of test conditions on 'Amsler' and 'KEWA-4' test rigs

Parameters of the tested object	Symbol	Parameter values during tests on 'KEWA-4' test rig	Parameter values during tests on 'Amsler' test rig
Mating dimensions:			
- nominal diameter of the mating	d	Ø 24 mm	Ø 40 mm
- nominal length	l	20 mm	10 mm
- shape factor	l/d	1.2	4.0
- nominal surface	S	4.8 [cm ²]	2.22 [cm ²]
Friction surface hardness of the counter-sample (steel 45)	HV	140	140
Fit	H11/d11		
Medium radial clearance		0.2 ± 0.03 mm	
Nature of the load		static	static
Test duration		1÷2 hours for each load	1÷2 hours for each load
Analytical unit pressure	p	2.5; 5.0; 7.5 [kG/cm ²]	2; 5; 8 [kG/cm ²]
Rotational speed of the sample	n _p	0	200 [rpm]
Rotational speed of the counter-sample	n	105.286 [rpm]	0

4.1.35. KEWAT-5 type test rig

This test rig reproduces the kinematics and dynamics of operation of clutch plates of motor vehicles (Figure 4.1.35.1). In the body of this test rig there is a shaft mounted, ended with a holder for mounting the tested friction discs made of plastic and two metal discs. The metal discs are pressed against the friction disc by means of a load lever mechanism. A toothed bushing which is slidably mounted on the end of the test disc holder holds the friction disc connected to the drive shaft. The electric motor transmits the drive to the driving shaft through a belt transmission.

KEWAT-5 test rig has the following features:

- lubrication: air or any lubricant composition;
- friction torque measuring system: strain gauge or dynamometric;
- loading system: lever;
- friction face: $27 \div 200$ [cm²];
- unit pressure value: $0 \div 1.5$ [MPa];
- friction face temperature measuring system: using a strain gauge;
- drive shaft rotational speed: 250, 500 or 650 [rpm];
- speed of friction of the sample against counter-sample: 0.95, 1.88 or 2.45 [m/sec];
- type of load: impact (sudden engagement or disengagement of the clutch).

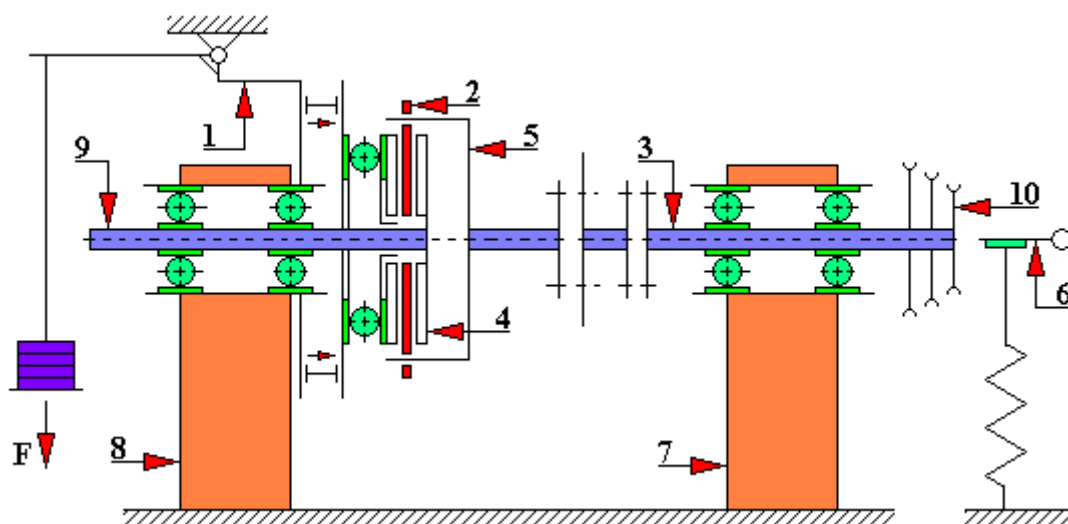


Fig. 4.1.35.1. Scheme of KEWAT-5 test rig [45]

1 - loading lever, 2 - tested disc, 3 - drive shaft with clutches, 4 - metal discs, 5 - toothed bushing of the tested disc, 6 - friction torque measurement mechanism, 7 - drive shaft frame, 8 - frame, 9 - metal disc shaft, 10 - belt transmission, F - load

4.1.36. KEWAT-6 type test rig

This test rig is designed for tribological tests, mainly for testing wear-resistant materials. The diagram of KEWAT-6 drive system is shown in Figure 4.1.36.1. The drive motor 6 drives the test rig spindle by means of a belt transmission and a dog clutch 2. There is a cast iron counter-sample 4 mounted on the spindle. The spindle rolling bearings are pressed into the bearing sleeve mounted on the frame. The bearings of the self-aligning disc 6 are seated on the outer surface of the sleeve (Fig. 4.1.36.2). These bearings enable the rotation of the plate regardless of the rotational speed of the spindle. The sample holders 7 are embedded in the self-aligning disc 6.

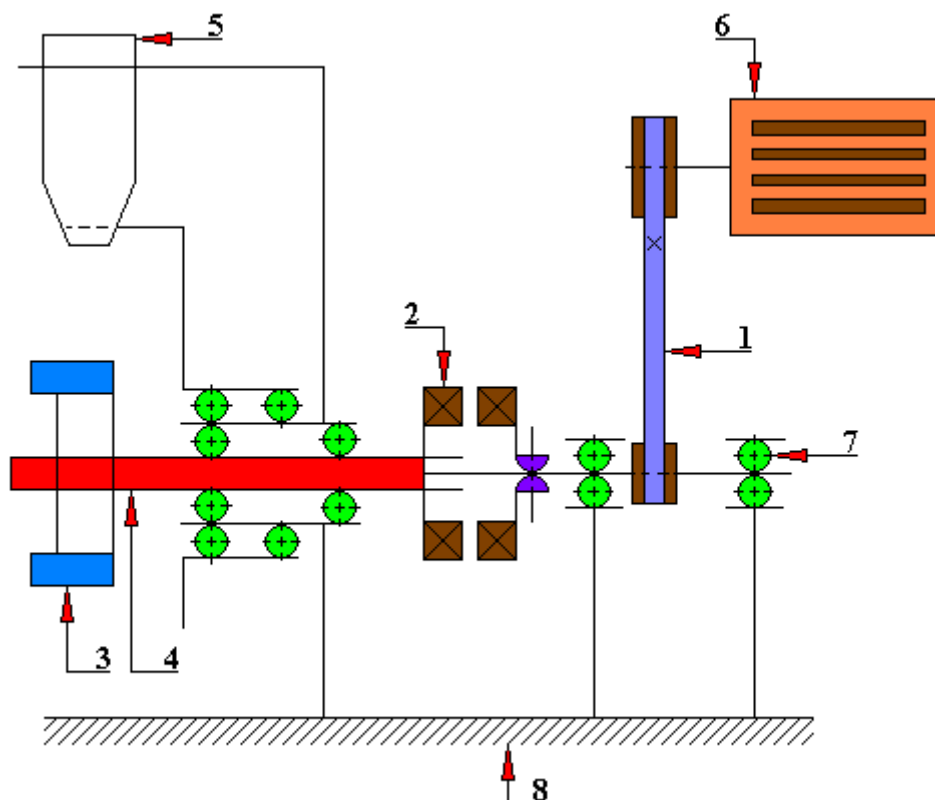


Fig. 4.1.36.1. The diagram of KEWAT-6 drive system [45]

1 - belt transmission, 2 - dog clutch, 3 - spindle, 4 - counter-sample, 5 - friction torque measuring spring, 6 - electric motor, 7 - bearing, 8 - test rig base

The friction force in the contact areas of the samples 7 and counter-sample 4 causes the rotation of the self-aligning disc 6 whose roller rests against a flat spring 5. The deflection of the measuring spring 5 is measured with a dial gauge and recorded on the tape.

The value of the flat measuring spring 5 deflection of the frictional moment is proportional to the value of the friction force between samples 7 and the cast iron counter-sample 4. The pressing force is realized by compressing a compression spring with a known characteristic. The spring deflection is measured with a dial gauge. In the sample (or samples) a thermocouple is placed close to the friction surfaces, connected to the temperature indicator 11. An electric pinch motor 8 with a clutch and gear is fitted to the self-aligning disc 6. This arrangement eliminates the inertia of the motor and allows it to be started and stopped quickly. Depending on the direction of the passage of current through the motor 8, the gear housing may shift to the right or to the left causing the sample 7 to be loaded or unloaded by means of a spring. The direction of the current

depends on the position of the self-aligning disc 6. And the loading or unloading of the sample depends on the direction of the current 7. A lever system with a very high ratio is connected to the self-aligning disc 6. This system controls the operation of mercury contacts 9. At the preset value of the moment of friction both mercury contacts are open. Then, the flow of alternating current controlling the P1 and P2 relays is not possible through them. These relays switch on the direct current flowing to the pinch motor 8 in the appropriate direction. If the moment of friction increases by 10%, then the measuring spring is deflected by 0.1 [mm] and this movement by means of a lever system causes the shorting of one of the mercury contacts and supply of current to the pinch motor 8. The direction of the current in this case is such that the pressure of the sample 7 against the counter-sample 4 is reduced. As a result, the moment of friction returns to its preset value. If the value of the moment of friction is reduced, the second mercury contact closes. This causes the current to flow in the opposite direction. The opposite direction of the current causes the sample 7 to be loaded as a result of which the moment of friction increases to the set value. After reaching the set value of the moment of friction the power is shut off. Then, there is friction at a pressure determined in this way. This state lasts until the next change of the friction torque by 10%, i.e. until the next activation of the pinch motor 8. KEWAT-6 test rig allows obtaining any value of the moment of friction only by changing the position of mercury contacts.

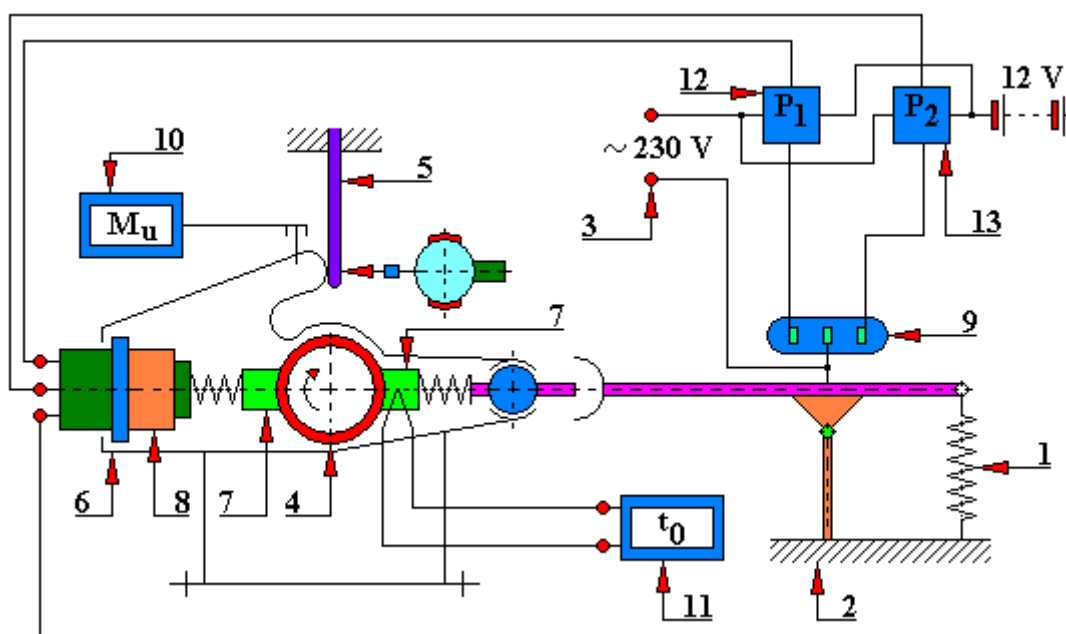


Fig. 4.1.36.2. Scheme of KEWAT-6 test rig [45]

1 - spring, 2 - test rig base, 3 – potential terminal, 4 - rotating counter-sample, 5 - flat friction torque measuring spring, 6 – self-aligning disc, 7 - sample, 8 - pinch motor, 9 - mercury contacts, 10 - recorder of the moment of friction, 11 - temperature gauge, 12 - P₁ relay, 13 - P₂ relay

4.1.37. KRWAT-1 test rig

This test rig (Fig. 4.1.37.1) is designed to test the wear of the pin-bushing friction contact and to record the value of the moment of friction. It is driven by a DC motor 10 which enables a stepless change of the rotational speed. The shaft of this motor 10 is connected on one side by a semi-flexible coupling 9 to the spindle of the ring 8. And on the other side of the shaft of the motor 10, a tachometer 11 with a revolution counter is connected. The spindle of the bracket is ended with a cone with an expansion sleeve intended for mounting the rotating ring constituting the counter-sample 3. Below the rotating counter-sample 3 there is a plate 2 with a fixed sample. The sample 2 is pressed against the rotating counter-sample 3 by means of a lever system 4 with symmetrically suspended weights. One of the arms of the lever system 4 is supported on a balance 5 recording the value of the friction force. The electric motor 10, the bracket with the spindle, and the leverage 4 are placed on the prisms of the common bed in order to maintain coaxiality. The sample 2 imitating a bushing was fixed in the holder by means of two plates tightened with screws. The handle housing, which is hollow inside, has two terminals for supplying and draining the cooling liquid. A spring-loaded thermistor is inserted into the hole. In the lower part, the housing has a spherical recess with which through a ball it rests against a support plate made of insulating material.

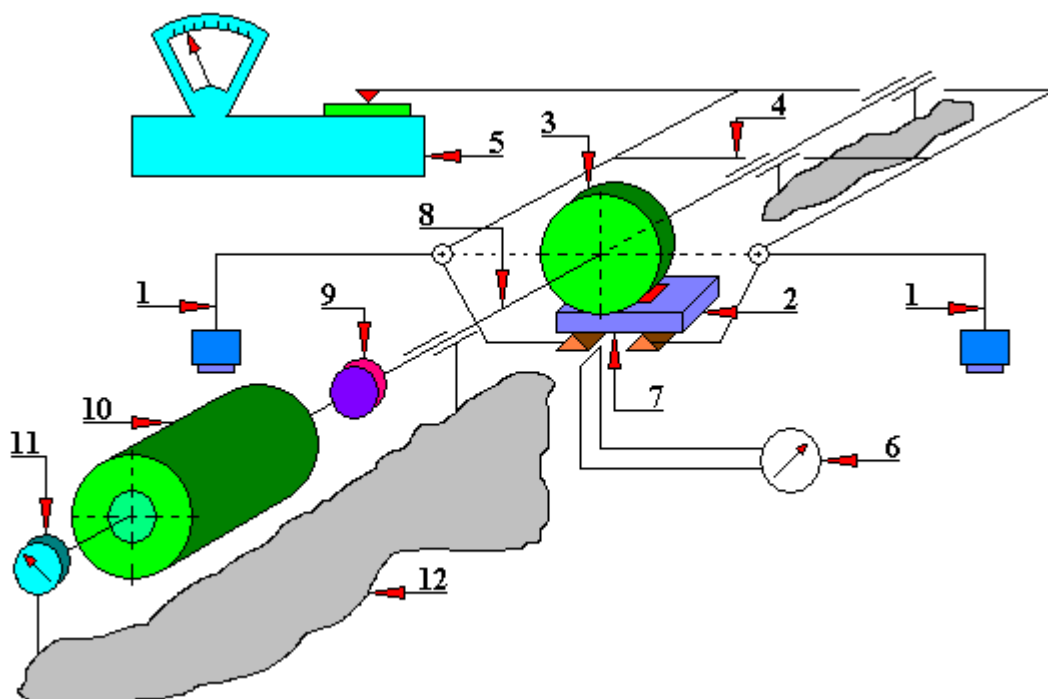


Fig. 4.1.37.1. General diagram of KRWAT-1 test rig designed for tribological tests [45]

1 - lever, 2 - plate with a sample attached, 3 - rotating ring, 4 - lever friction torque transmission, 5 - tangent balance, 6 - galvanometer designed to measure the thickness of the oil layer, 7 - thermocouple, 8 - ring spindle, 9 - semi-elastic clutch, 10 - electric DC drive motor, 11 - rev-counter (tachometer), 12 - base body

This test rig has the following features:

- friction environment - any lubricant composition in a liquid state,
- friction face: 4 [cm²],
- friction torque measuring system: weight,
- rotational speed of the counter-sample: 20÷2000 [rpm],

- sample temperature measuring system: thermistor,
- unit pressure: 0÷25 [MPa],
- loading system: lever, permanent load.

4.1.38. Test rig for tribological testing of the cam-pusher type

This test rig, shown in Figure 4.1.38.1, is designed for testing the wear resistance by scuffing and pitting of timing gear components of combustion piston engines lubricated with the tested lubricant composition. The main element of this test rig is the cam 4 mounted on the camshaft. This shaft is supported by three bearings. The camshaft is driven by a DC motor with infinitely variable speed control. The pusher 3 is co-acting with the camshaft. The pusher is connected to the tappet rod 1 and flat spring lever 9. The pusher 1 is guided in the body 2. A movable support 8 of the spring lever 9 can be shifted in the directions shown by the arrow in order to apply the desired load to the tested friction contact. The pump 7 and thermostatic oil reservoir 5 provide lubrication of the tested friction contact. The lubrication system is closed.

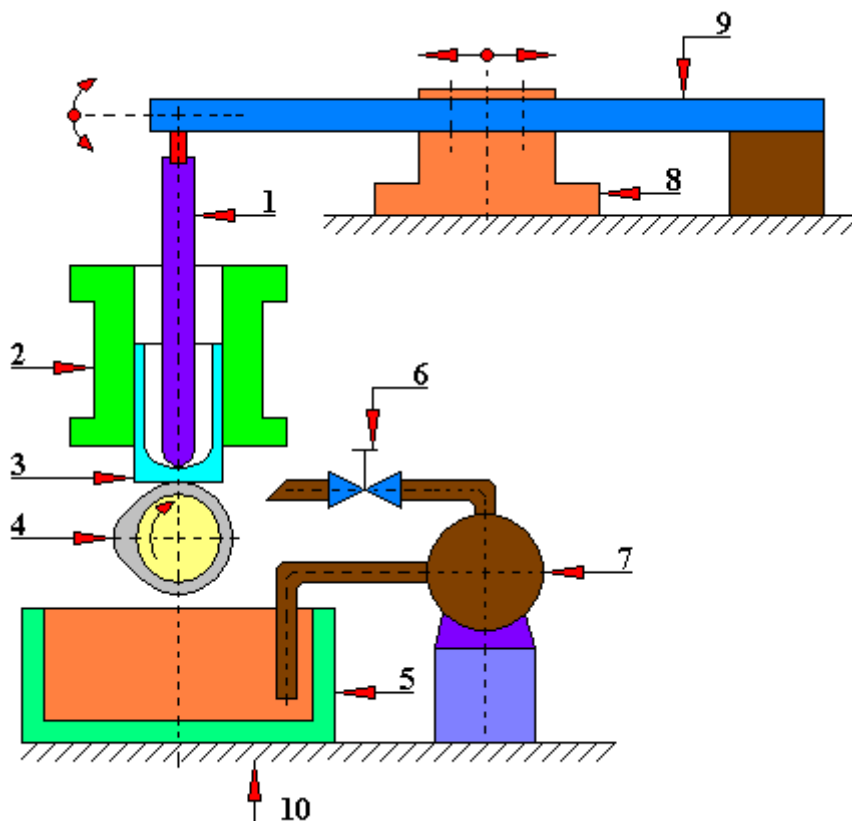


Fig. 4.1.38.1. A general diagram of the cam-pusher type of wear testing rig [45]

1 - tappet rod, 2 - body, 3 - pusher, 4 - cam located on the camshaft, 5 - oil reservoir, 6 - oil outflow control valve, 7 - oil pump, 8 - movable support, 9 - loading lever, 10 - foundation

The test rig of a cam-pusher type has the following features:

- friction torque measuring system - inductive torque meter,
- friction environment - oil,
- load measurement system - with a bow dynamometer,
- oil flow rate - $0 \div 1$ [liter/min],
- oil temperature - $20^{\circ}\text{C} \div 150^{\circ}\text{C}$,
- wear intensity measurement - qualitative or quantitative assessment with the isotope method,
- a system for measuring the number of cycles and rotational speed - frequency,

- camshaft rotational speed: 0÷6000 [rpm],
- response-pulsating load: 0÷3500 [N],
- temperature measurement system in the friction area: by the krypton method.

4.1.39. Striker test rig with a vibration exciter designed for pitting tests (four-spring)

This test rig, shown in Fig. 4.1.39.1, is designed to test pitting wear resistance. The main element of this test rig is a vibration generator 8 which produces sinusoidal vibrations of a certain amplitude and frequency. The amplitude of the output signal from the generator 8 is then amplified by the amplifier 9.

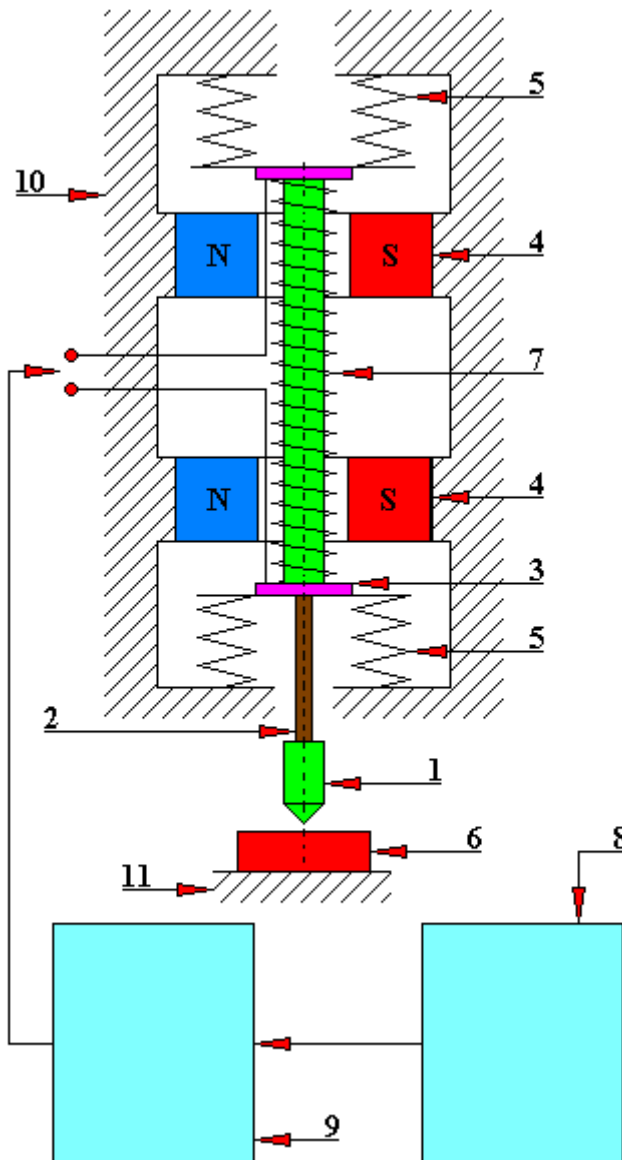


Fig. 4.1.39.1. A general diagram of a striker test rig with a vibration exciter intended for pitting tests [45]

1 - striker, 2 - pin, 3 - carcass, 4 - permanent magnet, 5 - spring, 6 - tested sample, 7 - indicating coil, 8 - vibration generator, 9 - power amplifier, 10 - test rig body, 11 - sample holder

The signal from the power amplifier 9 controls the operation of the excitation coil 7 fitted on the shaft body. The operation of the electromagnetic inductor is based on the effect of the magnetic field of the permanent magnets 4 on the AC powered indicating coil 7 placed therein. The shaft with the indicator coil 7 fixed thereon is suspended, depending on the construction, on two pairs of springs or coaxially on two springs. The vibrations take place around the equilibrium position

resulting from the tension of springs. The vibrating shaft ends with a pin 2 on which mounted is a striker 1. The striker 1 ends with a ball which hits the stationary sample 6 forcing a periodic load. The material of the ball can be selected according to individual needs, e.g. depending on the material of the sample 6, vibration amplitude, impact force, and type of lubricant composition.

The test rig with a vibration exciter for testing pitting is characterized by the following features:

- wear: qualitative or quantitative assessment,
- the amplitude of the striker motion: 0÷5 [mm],
- friction environment: dry or lubricated,
- the amplitude of the exciting force: 0÷30 [N],
- striker ball diameter: 5÷10 [mm],
- frequency of load changes: 1÷1000 [Hz].

4.1.40. A striker test rig with a vibration exciter designed for pitting tests (two-spring without a spring tension adjustment)

This test rig, shown in Figure 4.1.40.1, is very similar in its design to that shown in Figure 4.1.39.1. The difference between them lies in the method of mounting the springs. In the first case we have two springs coaxial to the pin 2. And in the second one there are as many as four springs which are placed symmetrically but not coaxially relative to the pin 2. The structure with two coaxial springs is simpler in its structure and provides more reliable and stable operation than the structure with four springs. However, the disadvantage of the solution with two coaxial springs in this particular case is the inability to adjust the tension of the springs.

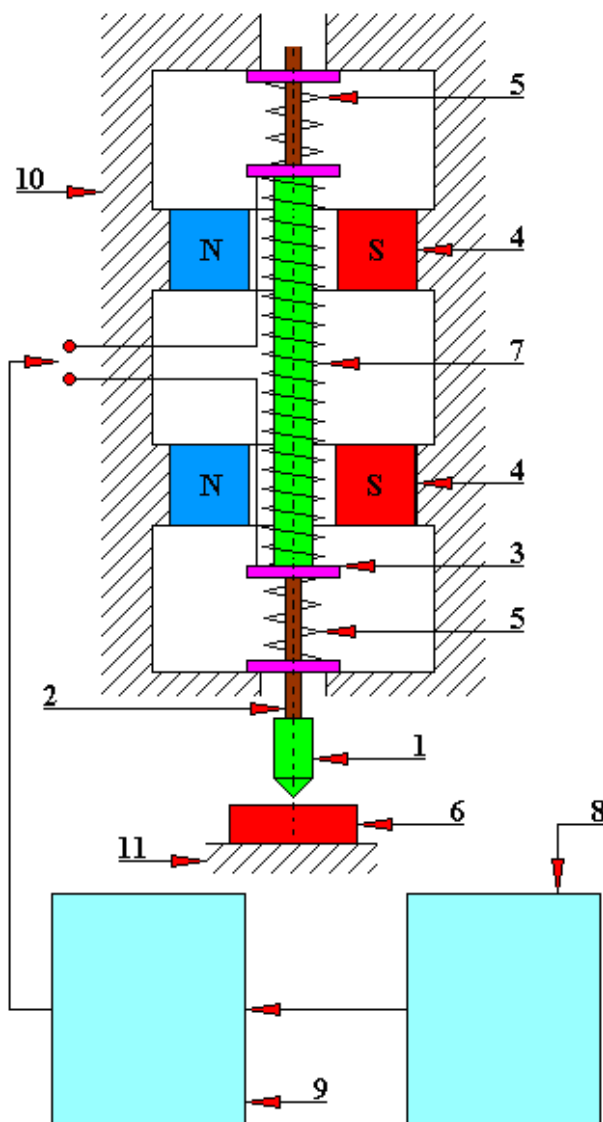


Fig. 4.1.40.1. A general diagram of a striker test rig with a vibration exciter designed for pitting tests (two-spring without a spring tension adjustment)

1 - striker, 2 - pin, 3 - carcass, 4 - permanent magnet, 5 – springs (lower and upper), 6 - tested sample, 7 - indicating coil, 8 - vibration generator, 9 - power amplifier, 10 - test rig body, 11 - sample holder [Wp. 26838 dated 2018-08-10. Applicant: J. Mikołajczyk]

An industrial design registration right was submitted to the Patent Office of the Republic of Poland. Application number: Wp. 26838 dated 2018-08-10. Applicant: J. Mikołajczyk.

4.1.41. A striker test rig with a vibration exciter designed for pitting tests (two-spring with a one-sided spring tension adjustment)

This test rig, presented in Figure 4.1.41.1, is an extension of the structure from the previous drawings: 4.1.40.1 and 4.1.39.1. In this case it is possible to adjust the tension of the springs 5 on one side by means of the adjusting screws 12 screwed to the test rig body 10.

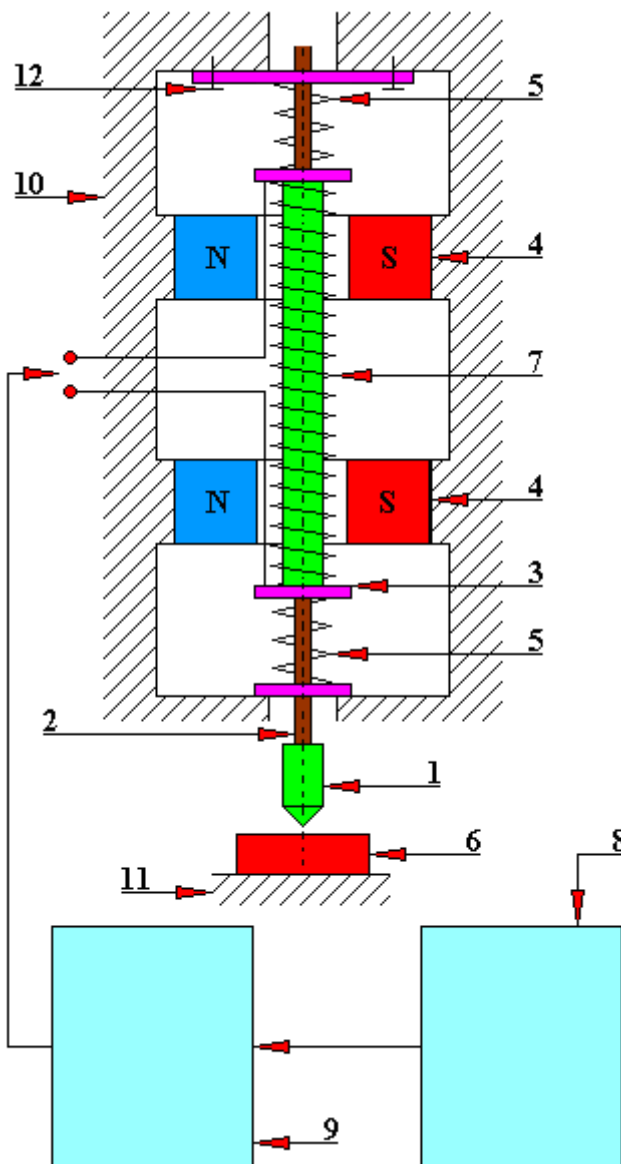


Fig. 4.1.41.1. A general diagram of a striker test rig with a vibration exciter designed for pitting tests (two-spring with a one-sided spring tension adjustment)
 1 - striker, 2 - pin, 3 - carcass, 4 - permanent magnet, 5 – springs (lower and upper), 6 - tested sample, 7 - indicating coil, 8 - vibration generator, 9 - power amplifier, 10 - test rig body, 11 - sample holder, 12 - spring tension adjusting screws [author: J. Mikołajczyk]

An industrial design registration right was submitted to the Patent Office of the Republic of Poland. Application number: Wp. 26838 dated 2018-08-10. Applicant: J. Mikołajczyk.

4.1.42. A striker test rig with a vibration exciter designed for pitting tests (two-spring with a two-sided spring tension adjustment)

This test rig, presented in Figure 4.1.42.1, is a further extension of the structure from the previous drawings: 4.1.41.1, 4.2.40.1 and 4.1.39.1. In this case it is possible to adjust the tension of two springs 5 on two sides by means of the adjusting screws 12 screwed to the test rig body 10.

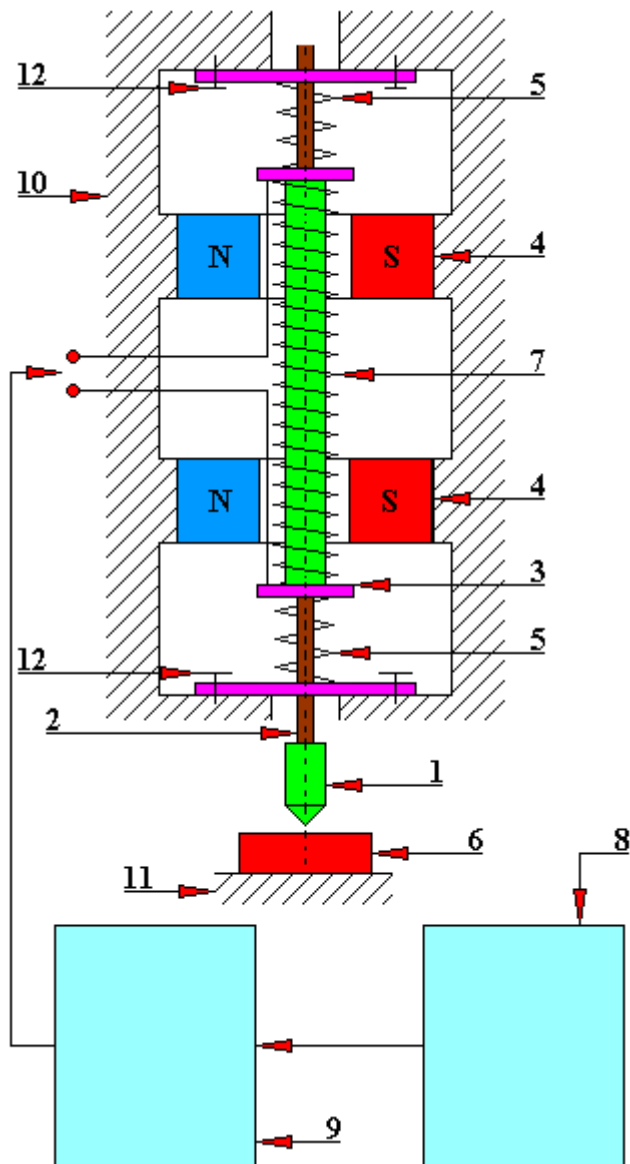


Fig. 4.1.42.1. A general diagram of a striker test rig with a vibration exciter designed for pitting tests (two-spring with a two-sided spring tension adjustment)
 1 - striker, 2 - pin, 3 - carcass, 4 - permanent magnet, 5 – springs (lower and upper), 6 - tested sample, 7 - indicating coil, 8 - vibration generator, 9 - power amplifier, 10 - test rig body, 11 - sample holder, 12 - spring tension adjusting screws [author: J. Mikołajczyk]

An industrial design registration right was submitted to the Patent Office of the Republic of Poland. Application number: Wp. 26838 dated 2018-08-10. Applicant: J. Mikołajczyk.

4.1.43. A striker test rig with a vibration exciter designed for pitting tests (single spring - lower spring - without a spring tension adjustment)

This test rig, presented in Figure 4.1.43.1, is an extension of the structure from the previous drawings: 4.1.42.1, 4.1.41.1, 4.1.40.1 and 4.1.39.1. In this case we have only one spring 5 mounted coaxially on the pin 2. The upper end of the pin 2 is free (not fixed) and it can move in the hole of the washer fastened with screws 12. This hole (both in the lower and upper washer) ensures the coaxial operation of the pin during vibrations (tests).

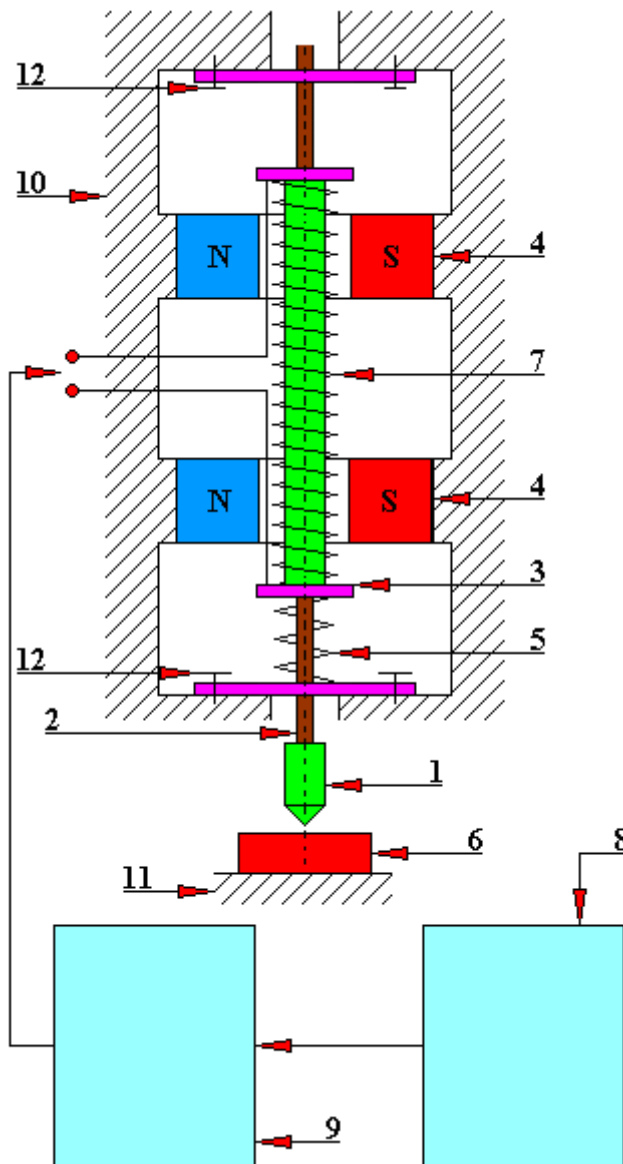


Fig. 4.1.43.1. A general diagram of a striker test rig with a vibration exciter designed for testing pitting (single spring - lower spring - without a spring tension adjustment)
 1 - striker, 2 - pin, 3 - carcass, 4 - permanent magnet, 5 – lower spring, 6 - tested sample, 7 - indicating coil, 8 - vibration generator, 9 - power amplifier, 10 - test rig body, 11 - sample holder, 12 - bolts securing washers to the test rig body [author: J. Mikołajczyk]

An industrial design registration right was submitted to the Patent Office of the Republic of Poland. Application number: Wp. 26838 dated 2018-08-10. Applicant: J. Mikołajczyk.

4.1.44. A striker test rig with a vibration exciter designed for pitting tests (single spring - upper spring - without spring tension adjustment)

This test rig, presented in Figure 4.1.44.1, is an extension of the structure from the previous drawings: 4.1.43.1, 4.1.42.1, 4.1.41.1, 4.1.40.1 and 4.1.39.1. In this case we have only one spring 5 mounted coaxially on the pin 2. The lower end of the pin 2 is free (not fixed) and it can move in the hole of the washer fastened with screws 12. This hole (both in the lower and upper washer) ensures the coaxial operation of the pin during vibrations (tests).

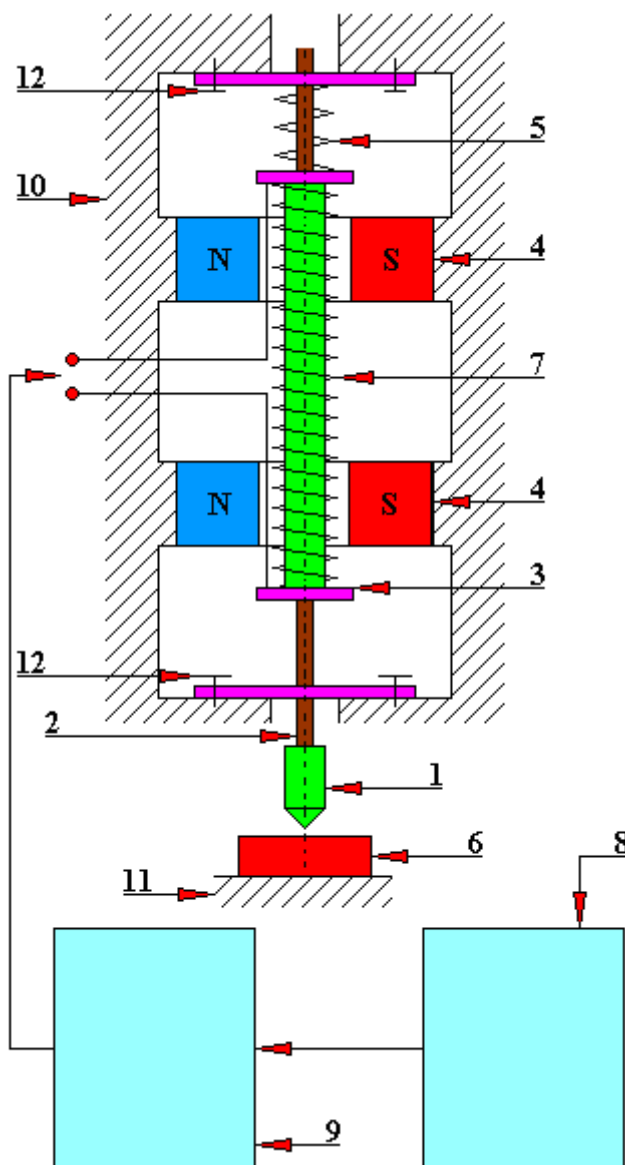


Fig. 4.1.44.1. A general diagram of a striker test rig with a vibration exciter designed for testing pitting (single spring - upper spring - without a spring tension adjustment)
 1 - striker, 2 - pin, 3 - carcass, 4 - permanent magnet, 5 – upper spring, 6 - tested sample, 7 - indicating coil, 8 - vibration generator, 9 - power amplifier, 10 - test rig body, 11 - sample holder, 12 - bolts securing washers to the test rig body [author: J. Mikołajczyk]

An industrial design registration right was submitted to the Patent Office of the Republic of Poland. Application number: Wp. 26838 dated 2018-08-10. Applicant: J. Mikołajczyk.

4.1.45. A single-contact test rig with a universal coupling

This test rig, shown in Figure 5.1.45.1, is designed to test rollers with a variable slip. Variable values of the slip velocities of the tested pulleys 1 and 2 are obtained by using two universal couplings (9 and 10) in the drive which are set in such a way as to cause periodic accelerations and delays of the rotational motion of the pulley 1 at a constant angular velocity of the pulley 2.

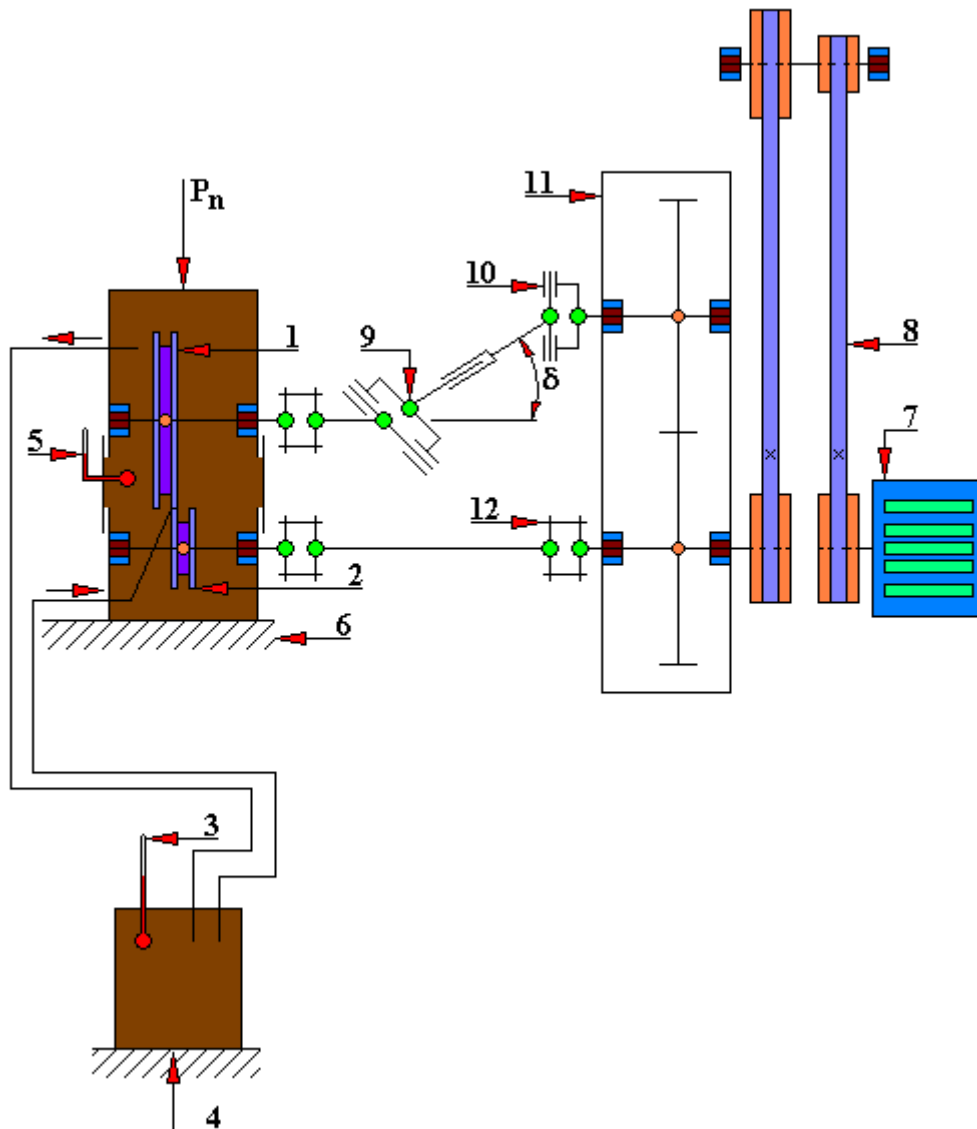


Fig. 4.1.45.1. A general diagram of a single-contact test rig with a universal coupling
 1 - first pulley under test, 2 - second pulley under test, 3 - oil reservoir thermometer, 4 - oil reservoir base, 5 - gear thermometer with tested pulleys, 6 - gear base with tested pulleys, 7 - drive motor, 8 - belt transmission, 9 - second universal coupling, 10 - first universal coupling, 11 - gear body, 12 - semi-flexible coupling, P_n - pressure force of tested pulleys, δ - angle between shafts.

Temporary gear ratio $\pm \omega_1/\omega_2$ varies approximately according to the cosine curve, with its extreme values being:

$$i_{\min} = \cos \delta \qquad i_{\max} = \frac{1}{\cos \delta}$$

4.1.46. Test rig for testing erosion resistance

The contact of solid particles with the elements of fluid-flow test rigs causes their erosion. This phenomenon occurs, inter alia, in rotor mills, in fans, in pneumatic transport test rigs. Erosion is the cause of a progressive loss of mass of elements of the exemplary test rigs listed here. The loss of mass of elements over a longer period of time causes the lack of stability of technological processes. The erosion mechanism is different for plastic materials and different for brittle materials. The test rig presented in Figure 4.1.46.1 enables the testing of erosive wear of both materials. The erosion on this test rig can be evoked by quartz sand carried by a stream of air under a given pressure, e.g. 0.5 MPa. The angle of incidence of the flux α may be variable and it may be, for example: 0° (90°), 30° and 60° . The test time depends on operating parameters, e.g. 5 minutes. The samples are usually weighed every certain period of time, e.g. after 1 minute of the particle flux interaction. Before the test, the weight fractions of individual grain diameters (grain fractions) in the mass of the abrasive are determined. The test rig for testing the erosive wear is presented in the work [70].

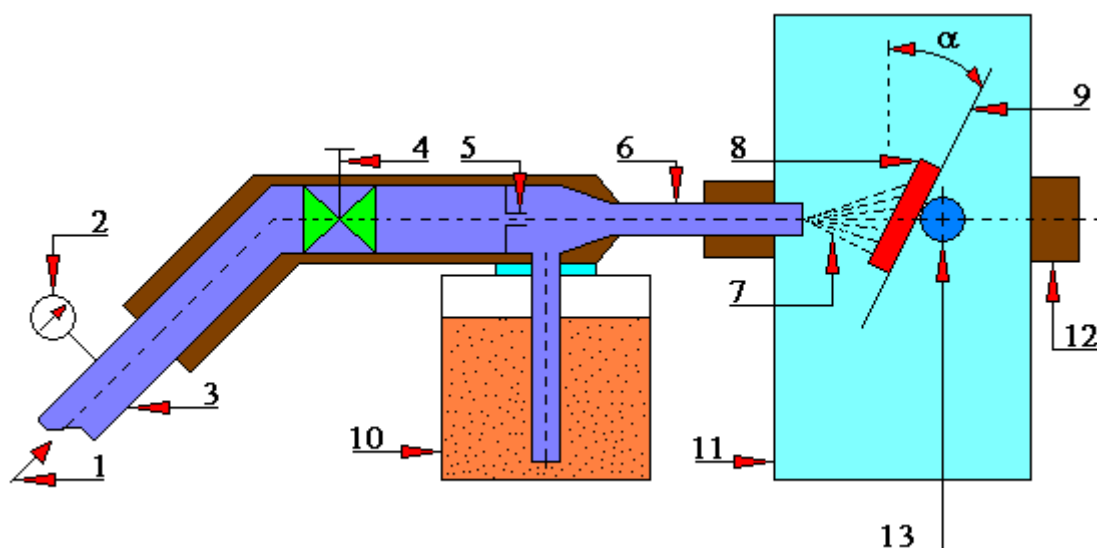


Fig. 4.1.46.1. A general diagram of the test rig for erosive wear tests [70]

1 - compressed air (0.5 MPa), 2 - pressure gauge, 3 – pressure conduit, 4 - closing valve, 5 - air nozzle, 6 - steering wheel, 7 - sand jet, 8 - tested sample, 9 - sample holder, 10 - container with sand (abrasive), 11 - working chamber, 12 - ventilation duct, 13 - shaft of rotation of the handle fixing the tested sample, α - angle of incidence of sand particles (abrasive)

The material of tested samples may be, for example, the following:

- construction tonnage steel as a reference material [S235JR (St3S)],
- material used in rotor mills [51CrV4 (50 HF)],
- material used in rotor mills [42CrMo4 (40HM HF)].

Below, Figure 5.1.46.2 shows a diagram of a similar test rig for measuring wear by sandblasting, shot blasting or glass beads blasting, most often used in tests with constant operating parameters. Because of its simplicity of construction it is a very popular test rig. This type of design provides:

- repeatability of results;
- constant abrasive performance;

- constant kinetic energy of abrasive particles;
- constant distance between the nozzle and the sample;
- constant pressure of the gaseous medium (most often compressed air).

The reader can find information about the impact of the angle α of abrasive particles on the surface of the tested sample for sandblasting/shot blasting /washing, washing-impact or impact glass beads blasting in the work [38]

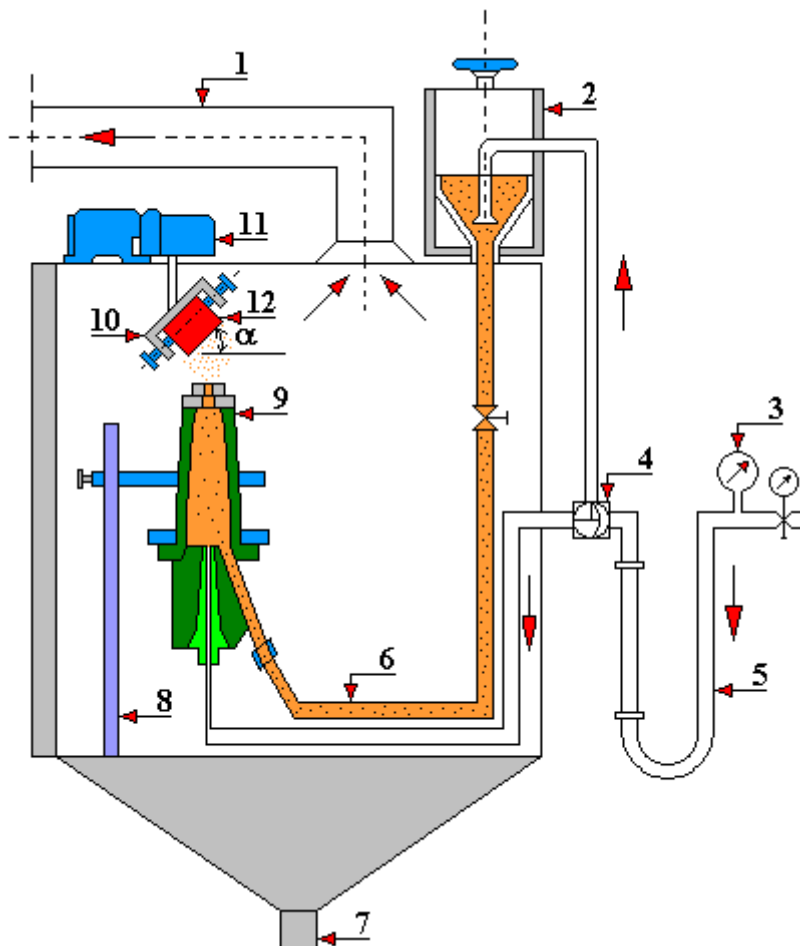


Fig. 4.1.46.2. A classic chamber for sandblasting/shot blasting /glass beads blasting of the sample abraded at the α angle with constant operating parameters

1 - ventilation duct; 2 - abrasive container; 3 - pressure gauge; 4 - three-way valve; 5 - compressed air supply pipe; 6 - abrasive supply duct; 7 - chute for used abrasive; 8 - bracket for mounting the nozzle; 9 - nozzle; 10 - sample holder; 11 - sample holder adjuster; 12 - tested sample; α - angle of incidence of abrasive particles

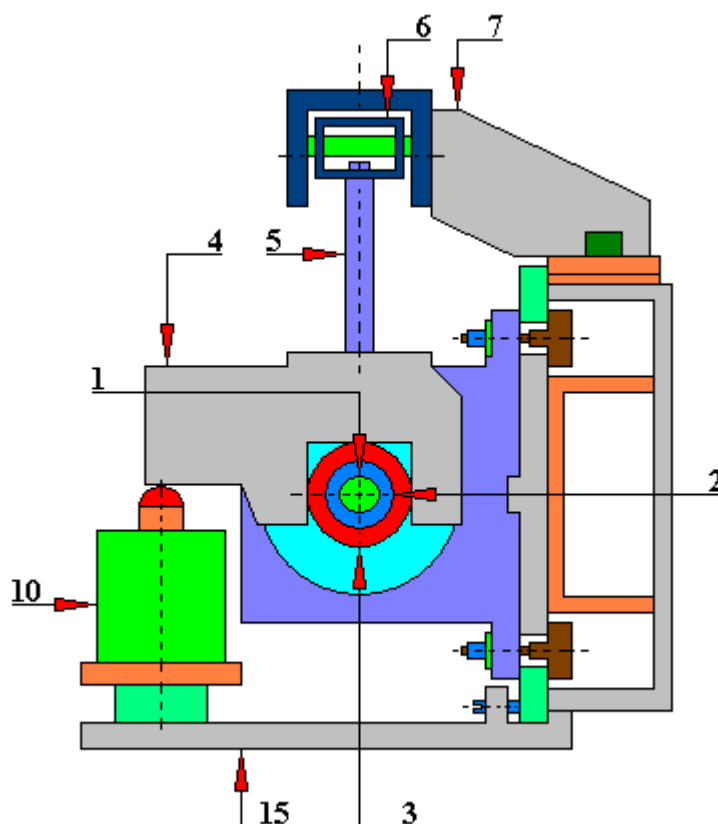
4.1.47. TWT-500N tribotester designed for friction and wear tests

TWT-500N test rig, developed by the Institute of Plastic Forming in Poznań, enables high-temperature tribological tests of elements of slide bearings intended, in particular, for ventilation systems of AIRBUS family airplanes. This tribotester uses a 'sleeve-shaft' friction contact. The maximum value of normal load that can be used on this test rig is 500 [N], with this load being graduated. This test rig is also equipped with a temperature control system that allows carrying out tests up to the temperature value of 600°C. Moreover, this tribotester has a system for smooth speed control up to 120 [rpm] built with the use of a frequency converter. During the tests the temperature in the tested friction contact is measured and the moment at which the friction coefficient is determined from the formula:

$$\mu = \frac{M}{P \cdot r}$$

where: M - moment of force [Nm],
P - pressure force [N],
r - inner sleeve radius [m].

The new sleeve mounting system for the TWT-500N tribotester was designed and manufactured at the Plastic Forming Institute in Poznań.



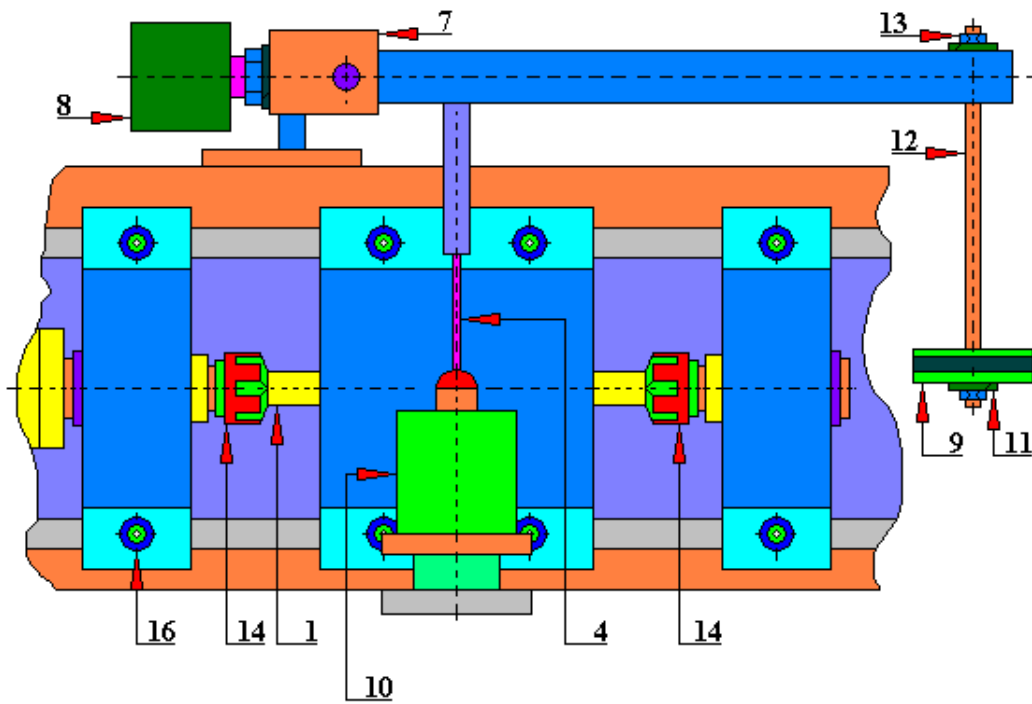


Fig. 4.1.47.1. A general diagram of the TWT-500N tribotester [181]

1 - drive shaft, 2 - shaft (counter-sample), 3 - sample (sleeve), 4 - sample mounting, 5 - clamp, 6 - lever arm, 7 - lever bracket, 8 - counterweight, 9 - given load, 10 - dynamometer, 11 - spring washer, 12 - arm fixing the set load, 13 - nut, 14 - coupling, 15 - base body, 16 - mounting bolts

4.1.48. MUJ type fatigue test rig used for fretting wear tests

The design of the MUJ fatigue test rig enables the achievement of a periodically variable load with pure bending. Thanks to this, it was possible to use it for the fretting wear test in the interference joint shown in Figure 4.1.48.1. The sample (sleeve) 1 was connected by interference with the shaft 2. The application of the periodically changing load Q of the rotating sample 1 causes the amplitude of oscillating tangential displacements between the connected surfaces of the sample 1 and the shaft 2. The oscillation amplitude depends on the normal stresses and the value of the applied bending moment which in turn will determine the deflection value of the sample 1. Thus, there is a close relationship between the deflection of the shaft 2 and the amplitude of the oscillations that occur. On Figure 4.1.48.2 presented is the diagram of the friction contact of the sample (sleeve) 1 and the shaft 2 which is a model of the wheel-axle connection.

To determine the value of the slip amplitude in the tested interference connection, the model of connection shown in Figure 4.1.48.3 was used. Loading the sample (sleeve) 1 with a bending moment will cause the deflection of the shaft 2. And the result of the shaft 2 deflection will be the elongation of its surface at the length of contact with the sleeve by the value Δl. If it is assumed that the shaft deflection is very small and the deformations are elastic, then Hooke's law can be used to determine the elongation value Δl. Then the relative linear elongation can be determined by the formula:

$$\varepsilon = \frac{\Delta l}{l}$$

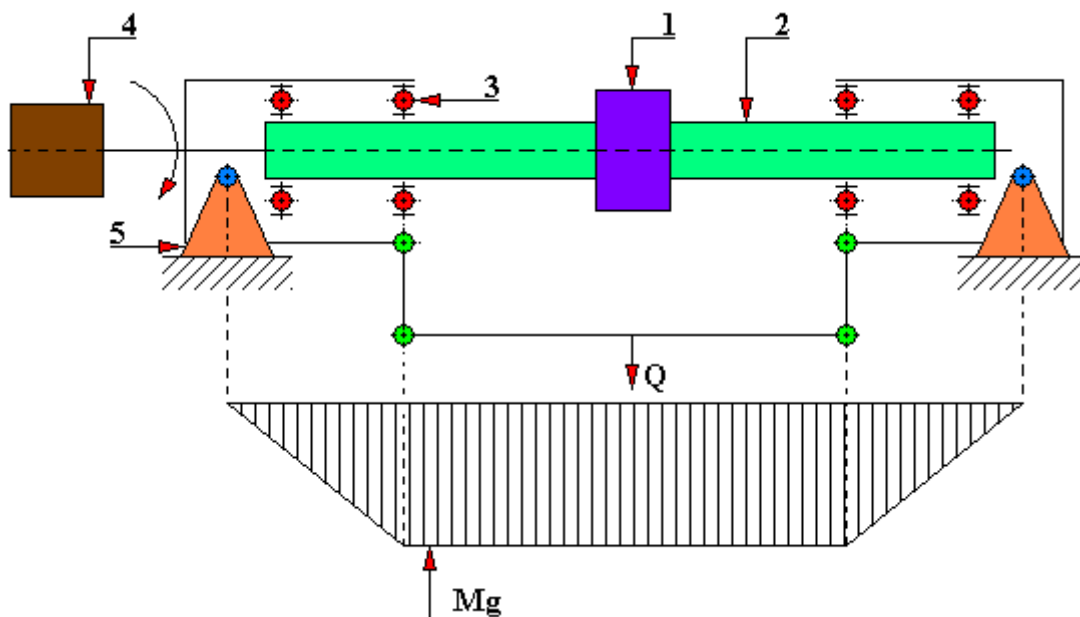


Fig. 4.1.48.1. A diagram of the Q force loading of the sample 1 on the MUJ fatigue test rig used for fretting wear tests [43]

1 - sample (sleeve), 2 - shaft, 3 - bearing, 4 - drive motor, 5 - support, Q - set periodically variable load, Mg - bending moment diagram

The above-described method of determining the value of the slip amplitude gives an estimate value of this amplitude. It is very difficult to measure the actual slip amplitude between the contact surface of the sleeve (sample) 1 and the shaft 2 in rotational-flexure wear tests.

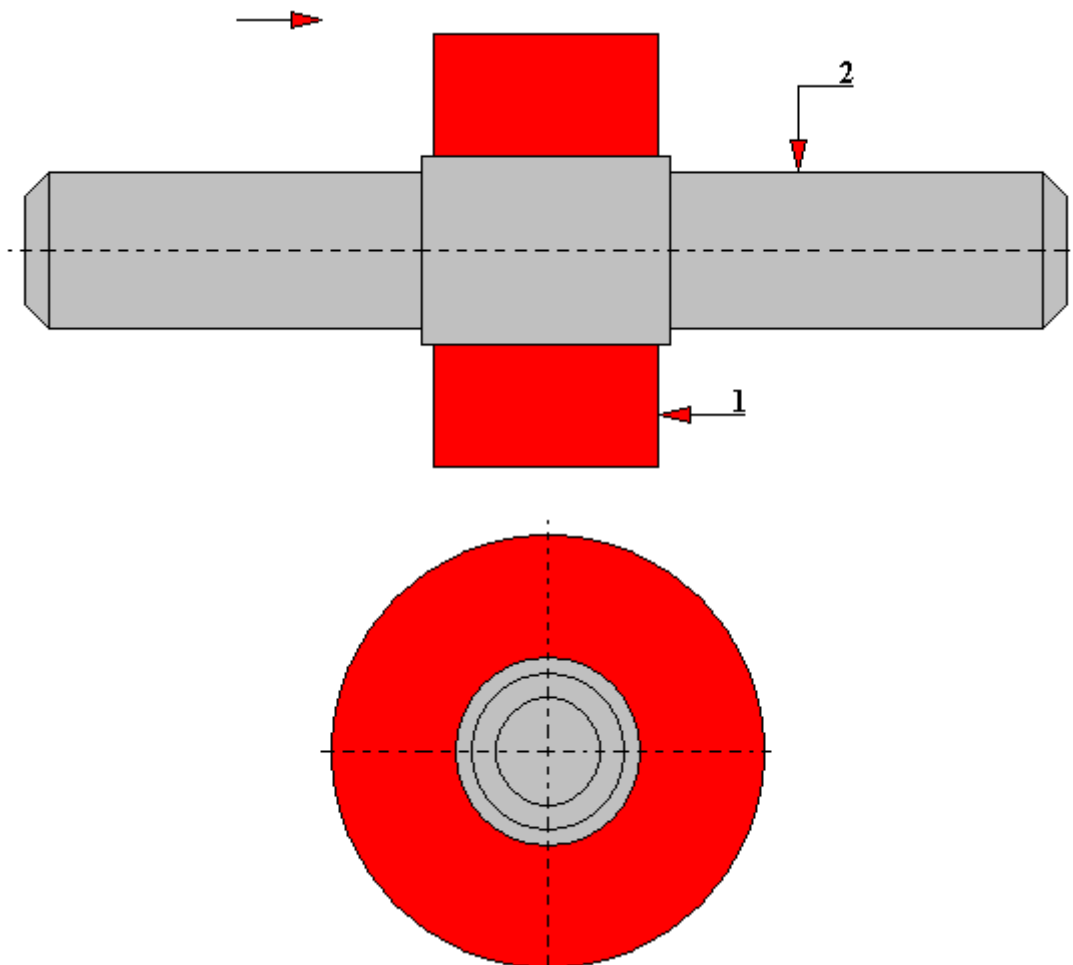


Fig. 4.1.48.2. A diagram of the friction contact of the sample (sleeve) 1 and the shaft 2 being a model of the wheel-axle connection [43]
1 - sample (sleeve), 2 - shaft

Figures 4.1.48.3, 4.1.48.4 and 4.1.48.5 show the scheme of determining the slip between the sleeve (sample) face and the shaft surface.

$$\Delta l = \alpha = 2 \cdot \alpha'$$

Δl - total linear elongation,
 α' - the quantity of displacement of point A_1 (A_2) relative to the sleeve face

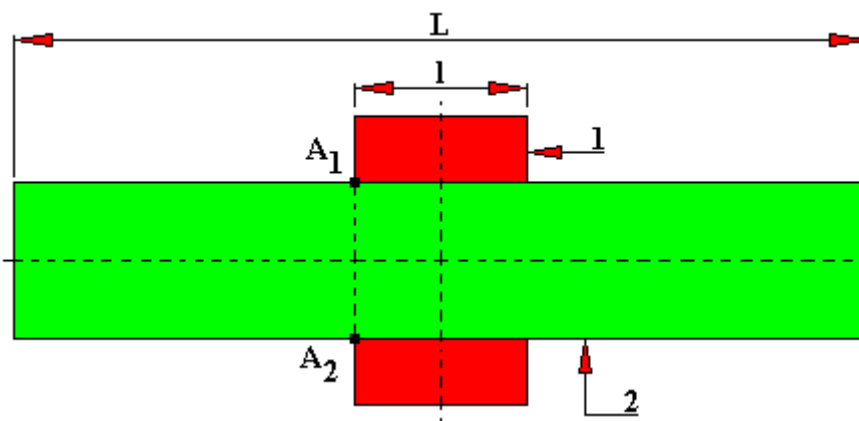


Fig. 4.1.48.3. A shaft/sleeve connection in a free state (without loading with a bending moment). Determination of the slip amplitude between the face of sleeve 1 and the surface of the shaft 2 [43]

1 - sample (sleeve), 2 - shaft, L - total length of the shaft, l - contact length of the interference connection of the shaft with the sleeve, A₁-A₂ - points related to the shaft surface and defining the contact point of the shaft surface and the sleeve face

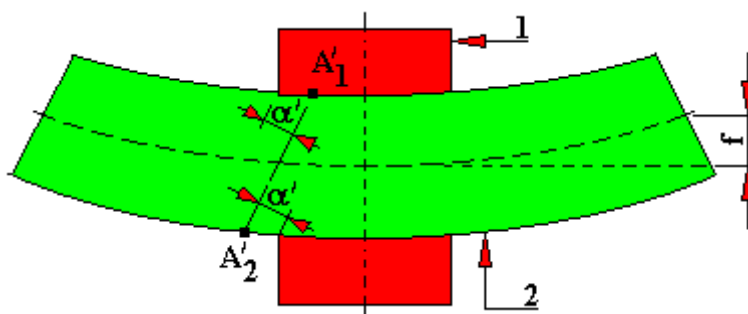


Fig. 4.1.48.4. A shaft/sleeve connection in a state of loading with a bending moment. Determination of the slip amplitude between the face of sleeve 1 and the surface of the shaft 2 [43]

1 - sample (sleeve), 2 - shaft, f - shaft deflection arrow, A'₁-A'₂ - as a result of the shaft deflection (under the influence of the bending moment) the plane originally passing through points A₁-A₂ rotates and takes a new position passing through the points A'₁ -A'₂, A'₁ - point on the compressed surface, A'₂ - point on the tension surface (here the point A₂ was displaced beyond the sleeve face), α_1, α_2 - relative displacements

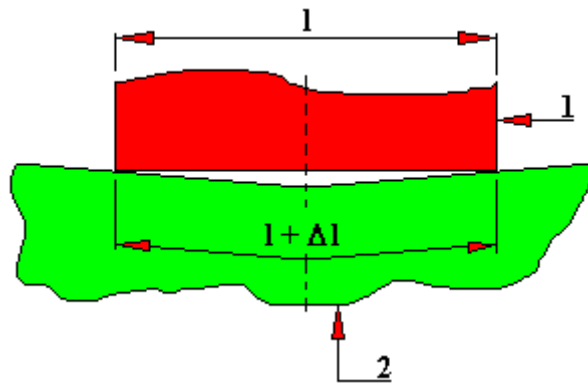


Fig. 4.1.48.5. A scheme of connection of the friction contact of the sample (sleeve) 1 and the shaft 2 for determining the oscillation amplitude [43]

1 - sample (sleeve), 2 - shaft, Δl - elongation of the contact surface of the shaft with the sleeve as a result of loading with the bending moment, l - contact length of the interference connection of the shaft with the sleeve

4.1.49. A test rig for fretting tests with an electromagnetic inductor as a component that forces displacement

Each tribotester designed for fretting testing is made of three main components:

- a component that exerts a load on the tested sample (test samples),
- a component in contact with test samples,
- a component forcing a relative motion of the samples.

It is rare for both samples (or the sample and the counter-sample simultaneously) to be in motion (make relative motion) in a component of test samples. Most often, one of the samples is stationary (attached to the base). And the second one is moved by the component that forces the relative motion. There are two types of sample contact geometry:

- concentrated (Hertzian) contact,
- conformal (unfolded) contact.

At the Hertzian contact the wear of samples is concentrated thanks to which it is possible to measure the wear geometrically (e.g. by profilographing). A negative feature of a concentrated contact is a continuous increase of the contact area occurring with the increase in wear and the associated decrease in pressure.

The following are mainly used as a concentrated contact:

- a) contact of a spherical surface with a flat surface,
- b) contact of a cylindrical surface with a cylindrical surface (crossed rollers),
- c) the contact of a cylindrical surface with a flat surface.

The conformal contact used in real objects is mainly the contact of a flat surface with a flat surface. The disadvantage of a conformal contact (in fretting tests) is that the fretting pits are scattered over the entire surface. This feature prevents or at least makes it very difficult to geometrically measure the wear of the samples.

The following test rigs may fulfil the role of the driving component used to force the relative motion of the samples:

- a) a system of two rotating unbalanced discs,
- b) a special hydraulic actuator,
- c) an eccentric unit,
- d) electromagnetic vibrator.

Hydraulic actuators are mainly used in tribotesters with a conformal contact where high loads are required for the tested samples. The eccentric mechanisms, despite the advantageous wide selection of amplitude, cannot operate at high frequencies. Electromagnetic vibrators, due to the ease of access and the ability to work at high frequencies of excitation, are commonly used as a drive for fretting test rigs.

A relative motion of samples forced by driving units is mainly rotary, oscillating and reciprocating.

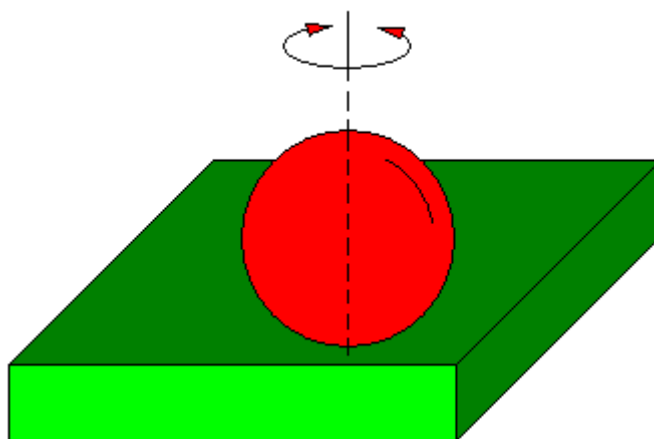
The role of the loading component may be performed by:

- lever system,
- a system with a hydraulic actuator,
- a spring system,
- the weight bob itself.

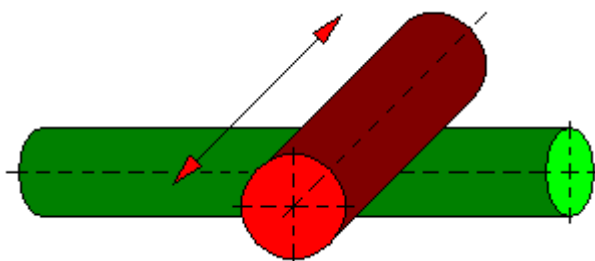
In addition to the above-mentioned basic components of tribotesters intended for fretting tests these test rigs, like every test rig, are equipped with measuring or special components.

In the work [94] the author presents four most frequently used sample contact configurations in fretting tests. These include:

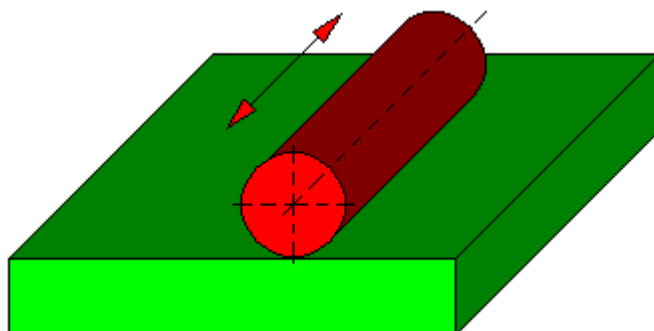
a) ball - flat element



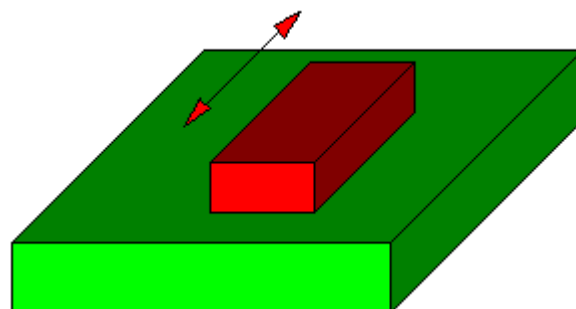
b) roller - roller



c) roller - flat element

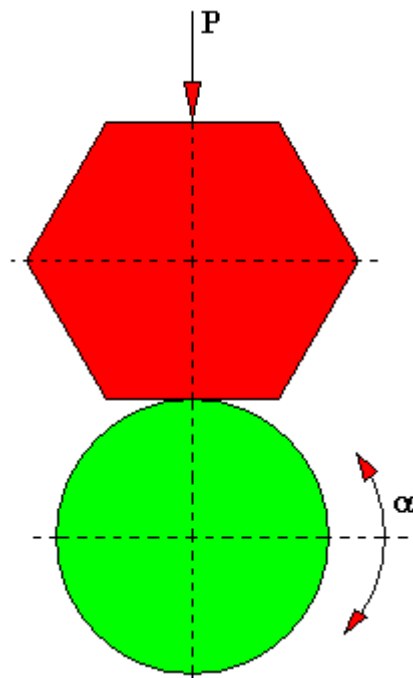


d) flat element – flat element

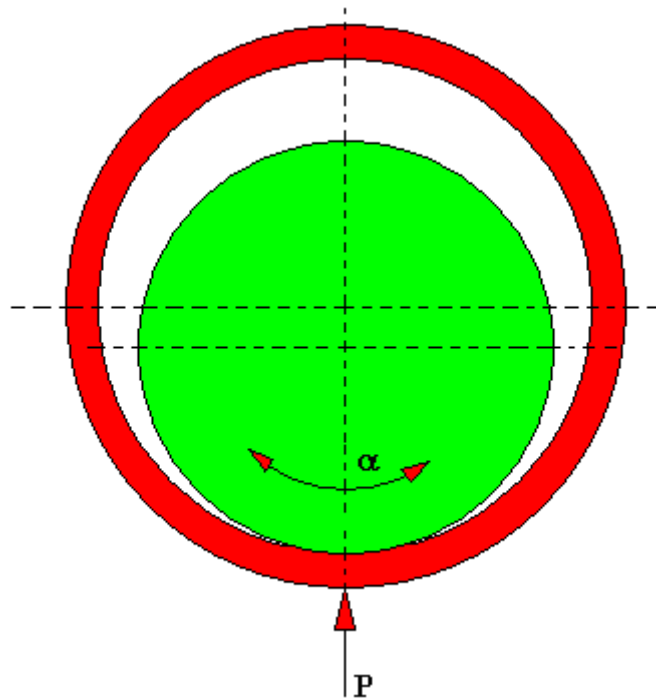


And in the work [2] the authors present the following models of contact types found in fretting wear testing:

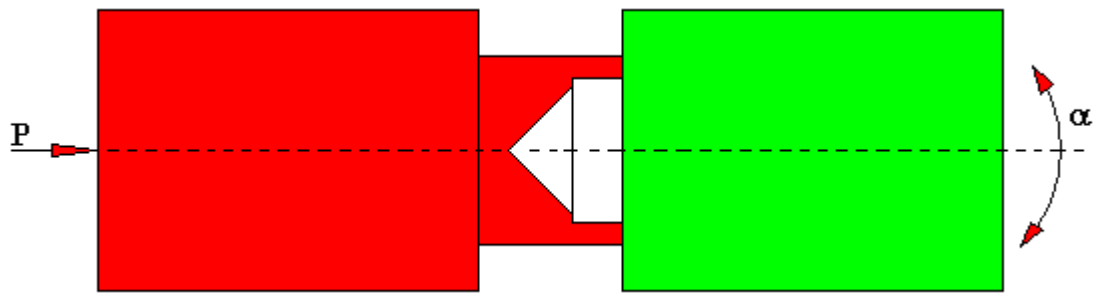
1) roller- plane or ball-plane (point or line contact)



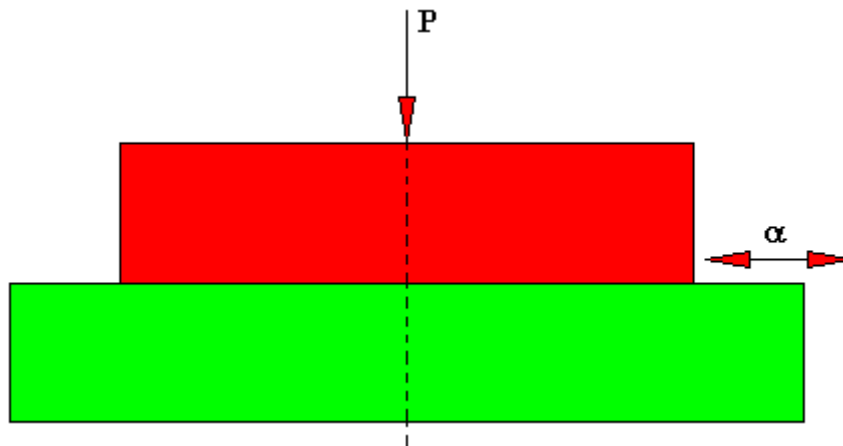
2) roller - bushing or ball - bushing (point or line contact)



3) bushing-plane (flat contact)



4) plane-plane (flat contact)



The measuring components of units for testing fretting are intended mainly for measuring:

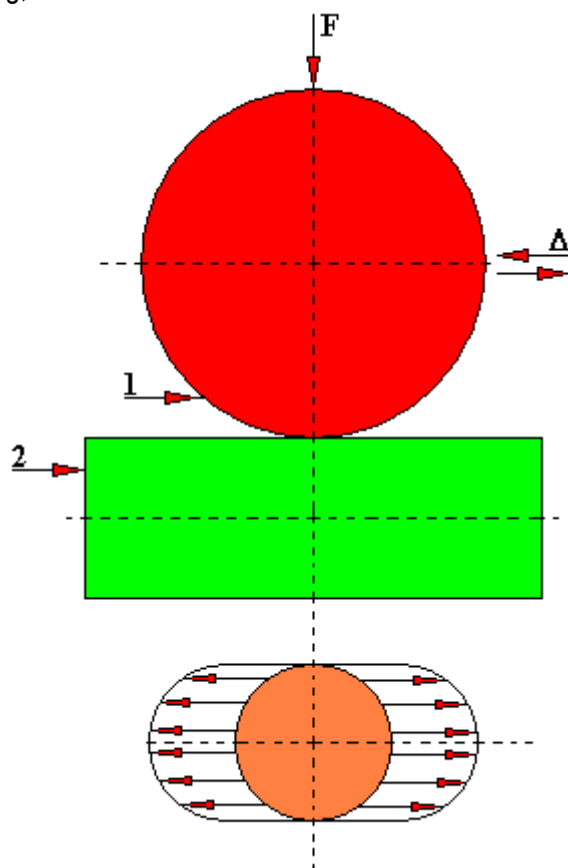
- electrical resistance of the sample contact,
- friction forces,
- oscillation frequency,
- displacement amplitudes,
- temperature of the surface layer of co-acting samples.

Special components can be designed, for example, for:

- creating a vacuum,
- creating an atmosphere with set parameters,
- creating an aggressive environment,
- testing at low / high temperatures.

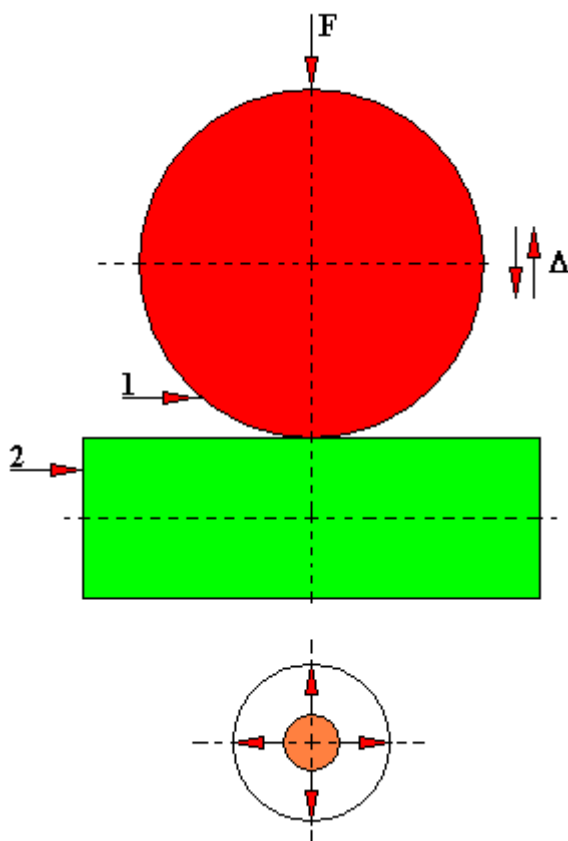
A classic case of fretting is the tangential oscillating relative displacement of elements of a given contact pair. Then, the process of destruction occurs. With regard to the direction of displacements, the authors of the work [222] introduced the following fretting classification for the ball-flat element pair:

a) tangential fretting,

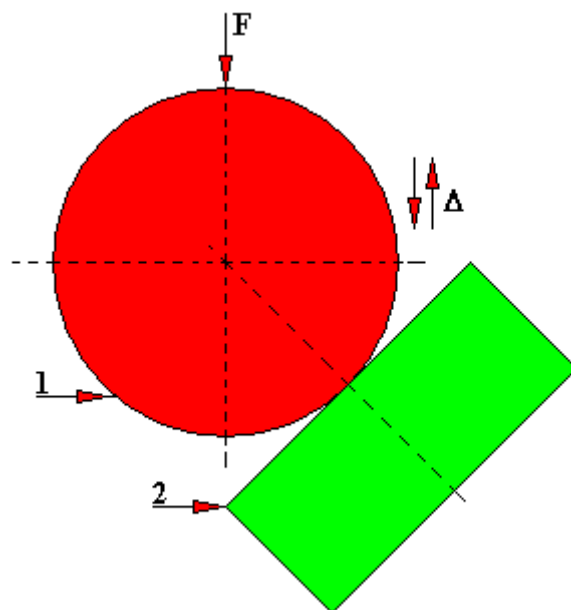


1 - sample, 2 - counter-sample

b) fretting with radial (perpendicular) motion,

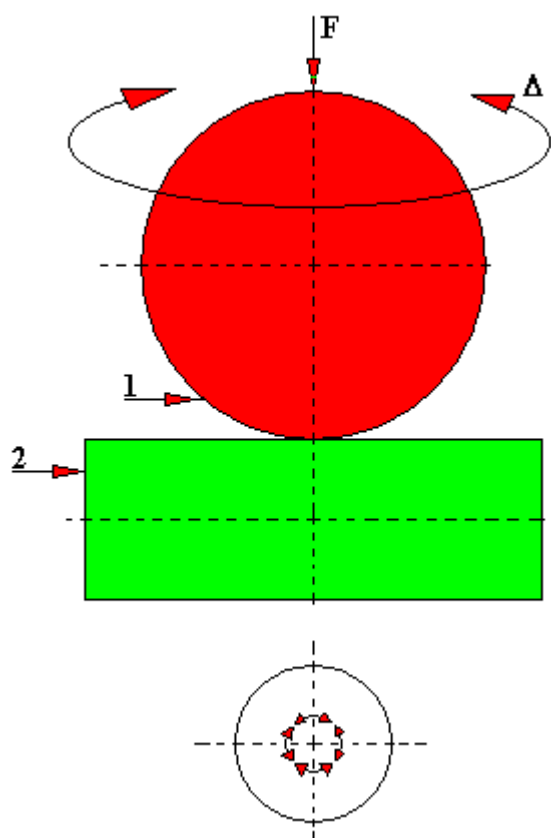


c) complex fretting,

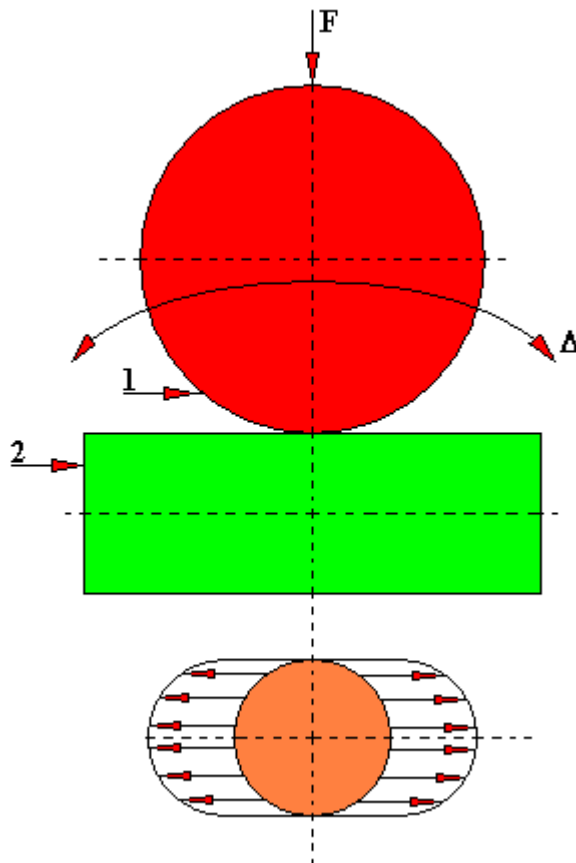


1 - sample, 2 - counter-sample

d) torsional fretting,



e) rotary fretting,



1 - sample, 2 - counter-sample

A similar classification of fretting can be introduced for a pair e.g. a flat element - flat element or a roller-roller. Then one can obtain:

- flat element - flat element, linear tangential motion,
- flat element - flat element, rotational motion,
- roller-bushing, linear motion or bending,
- roller-bushing, rotational motion.

Figure 4.1.49.1 shows a diagram of the test rig intended for fretting tests where the component forcing the displacement of the moving sample 2 is the electromagnetic inductor 8. Fastened to the vibration exciter 8 is the arm 5 which is subject to elastic bending deformations. A movable sample 2 is attached to the end of the bent arm 5. A moving sample 2 co-acts with a stationary sample (counter-sample) 3. The geometry of the sample contact is a ball-plane. Subjected to vibrations, the bent arm 5 heats up. In order to counteract this phenomenon, the arm has cooling liquid inlet and outlet connectors. As a coolant, water was used by the authors in this case. The acceleration sensor 6 and the capacitive sensor 7 were used to measure the magnitude of the displacement amplitude and the oscillation frequency. The construction of this test rig provides a wide selection of the frequency of excitations.

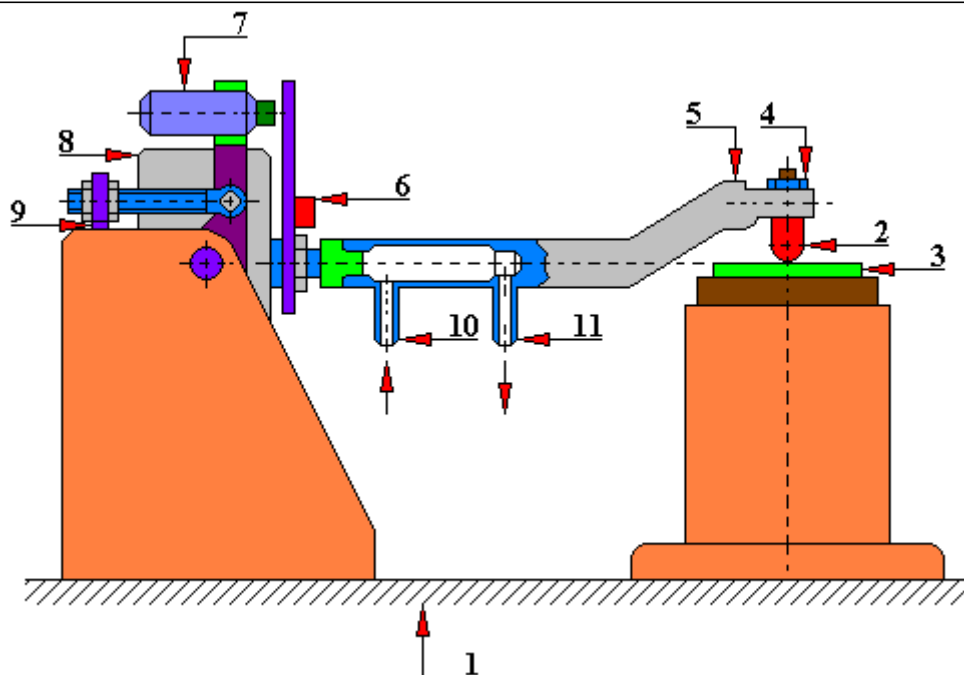


Fig. 4.1.49.1. A test rig for fretting tests with an electromagnetic inductor as a component forcing displacement [210]

1 - base, 2 - moving sample (ended with a ball), 3 - stationary sample (counter-sample), 4 - nut fixing the moving sample, 5 - bent arm, 6 - acceleration sensor, 7 - capacitive sensor, 8 - vibration generator (electromagnetic inductor), 9 - tilting mechanism, 10 – connector supplying cooling water to the bent arm, 11 - a return connector of bent arm cooling water

4.1.50. A test rig for fretting tests with an eccentric system forcing displacements with a relative motion of samples: rotating, oscillating

Tribotesters with eccentric systems forcing displacement are characterized by a limited selection of frequencies, which is their disadvantage, and a wide selection of amplitude. Figure 4.1.50.1 shows a test rig for fretting tests in which the system that forces displacement is the eccentric system.

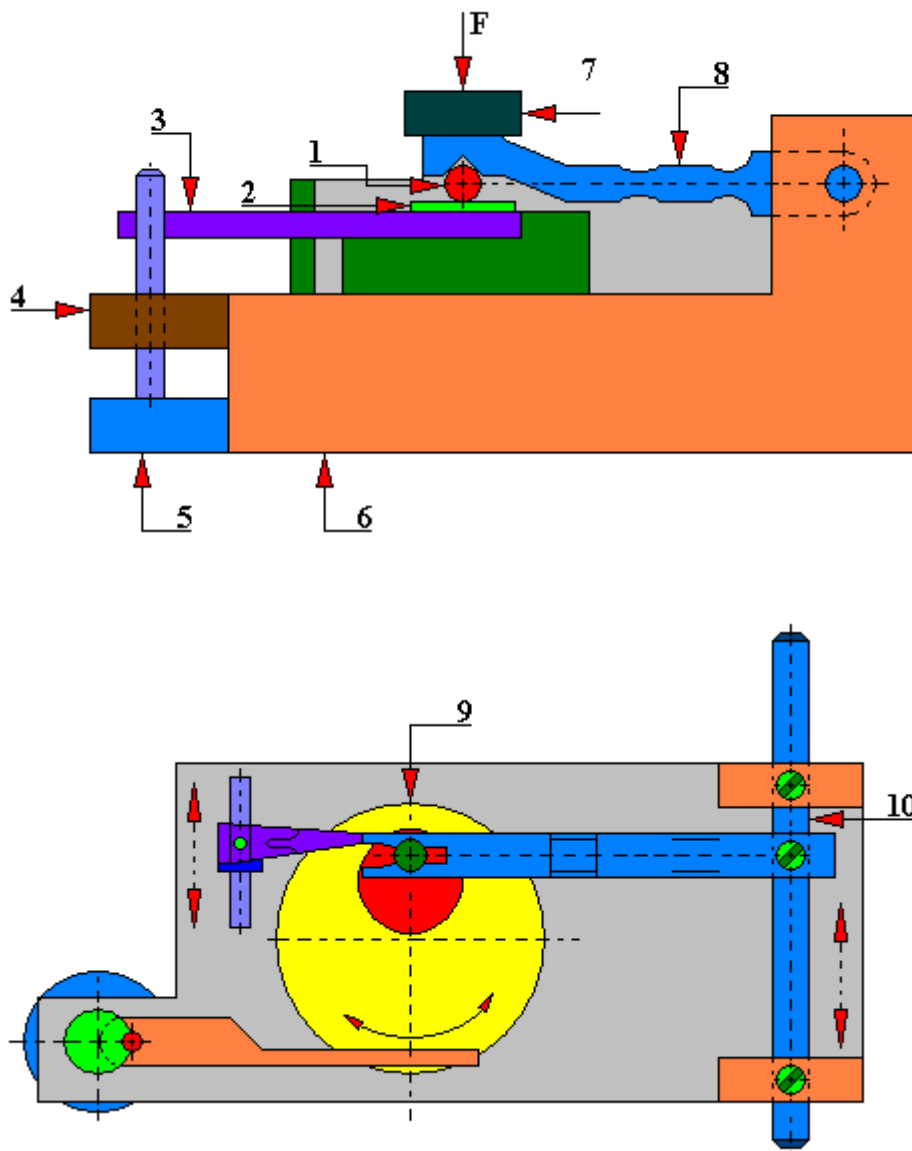


Fig. 4.1.50.1. A test rig for fretting tests with an eccentric system forcing displacements [54]
 1 - upper sample, 2 - lower sample (counter-sample), 3 - eccentric, 4 - support, 5 - drive motor, 6 - test rig body, 7 - load, 8 - pressure arm, 9 - oscillating table, 10 - regulation of amplitude

The body 6 of the test rig has a pressure arm 8 which exerts a direct pressure on the upper sample 1. A weight 7 acts on the pressure arm 8 from the top. Such a solution of applying the load does not enable a smooth (programmable) pressure application, and the quantity of load

depends on the possessed set of weights. The pressure arm 8 does not make working vibrations (working motion) so there is no need to cool it. The upper sample 1 co-acts with the lower sample 2 (counter-sample). The geometry of the sample contact is a roller-plane. A relative motion of co-acting samples: rotating, oscillating. The lower sample 2 (counter-sample) is attached to the oscillating table 9 which forces the relative motion of samples by means of the eccentric 3. The eccentric 3 is driven by an electric motor 5. The current various design solutions of eccentrics make it possible to change the magnitude of the eccentric stroke within a certain range.

4.1.51. A test rig for fretting tests with an eccentric system forcing displacements with a relative motion of samples: linear, reciprocating

Figure 4.1.51.1 presents another design solution of a fretting test rig in which the eccentric system forcing the displacement makes a relative motion of the samples: linear, reciprocating. Attached to the body 4 of the test rig is a holder 5 that holds the lower stationary sample (counter-sample) 2. This counter-sample co-acts with the upper sample 1. The upper sample 1 is a roller and the counter-sample 2 is a plane. The upper sample 1 is mounted in the holder 12. The handle is subjected to the force of the loading lever 7. A weight load 3 is suspended on the loading lever 7. This load may only change discretely by steps, depending on the size of the suspended weights. The handle 12 is connected by means of a tension member 6 to the arm 10 of the eccentric mechanism making a linear, reciprocating motion. Guiding of the arm 10 is provided by a hole in the guide disc 11.

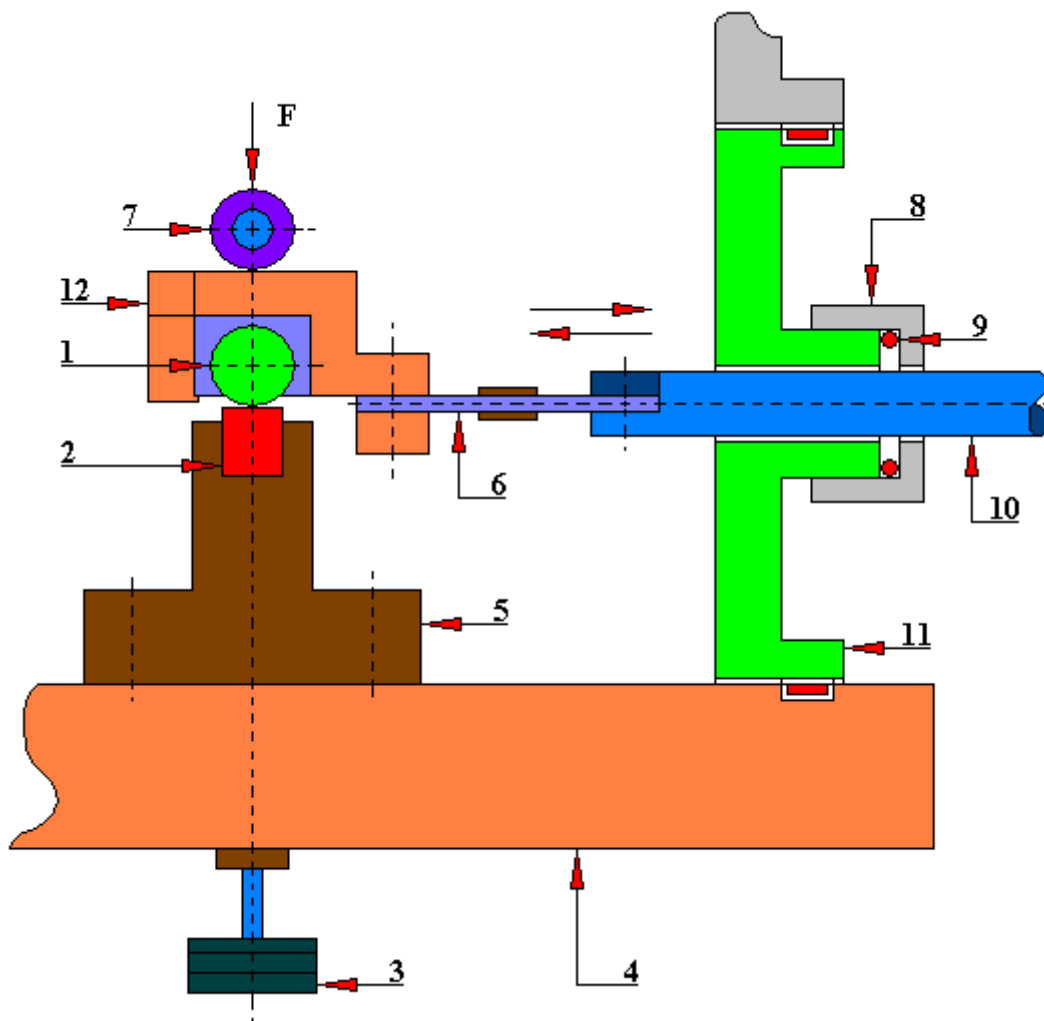


Fig. 4.1.51.1. A test rig for fretting tests with an eccentric system forcing displacements with a linear, reciprocating motion [46]

1 - upper sample (moving), 2 - lower sample, stationary (counter-sample), 3 - weight load, 4 - test rig body, 5 – holder for fixing a stationary sample, 6 - tension member, 7 - loading lever, 8 - nut, 9 - sealing, 10 - arm of the eccentric mechanism with linear, reciprocating motion, 11 - disc guiding the arm of the eccentric mechanism, 12 - holder of the moving sample, F - amount of the loading force

The tension member 6 should be in the symmetry axis of the holder 12 fixing the moving sample 1. At low motion amplitudes and low pressures F , the system should remain stiff. However, with the increase of these parameters, and thus the appearance of wear on the mating surfaces, significant vibrations in the system may appear.

Generally, in tribotesters in which a component that forces a relative motion by means of an eccentric system it is difficult to select the values of excitations, e.g. amplitude of the order of micrometers with an oscillation frequency of several hundred (several thousand) hertz. Often, the essence of the design of this drive does not allow this.

4.1.52. A test rig for fretting tests with a hydraulic system forcing displacements and hydraulic loading of samples

Figure 4.1.52.1 shows the rig intended for fretting tests in which a hydraulic system was used as a component forcing displacements. Additionally, in this test rig, the loading of samples is also carried out by means of a hydraulic system.

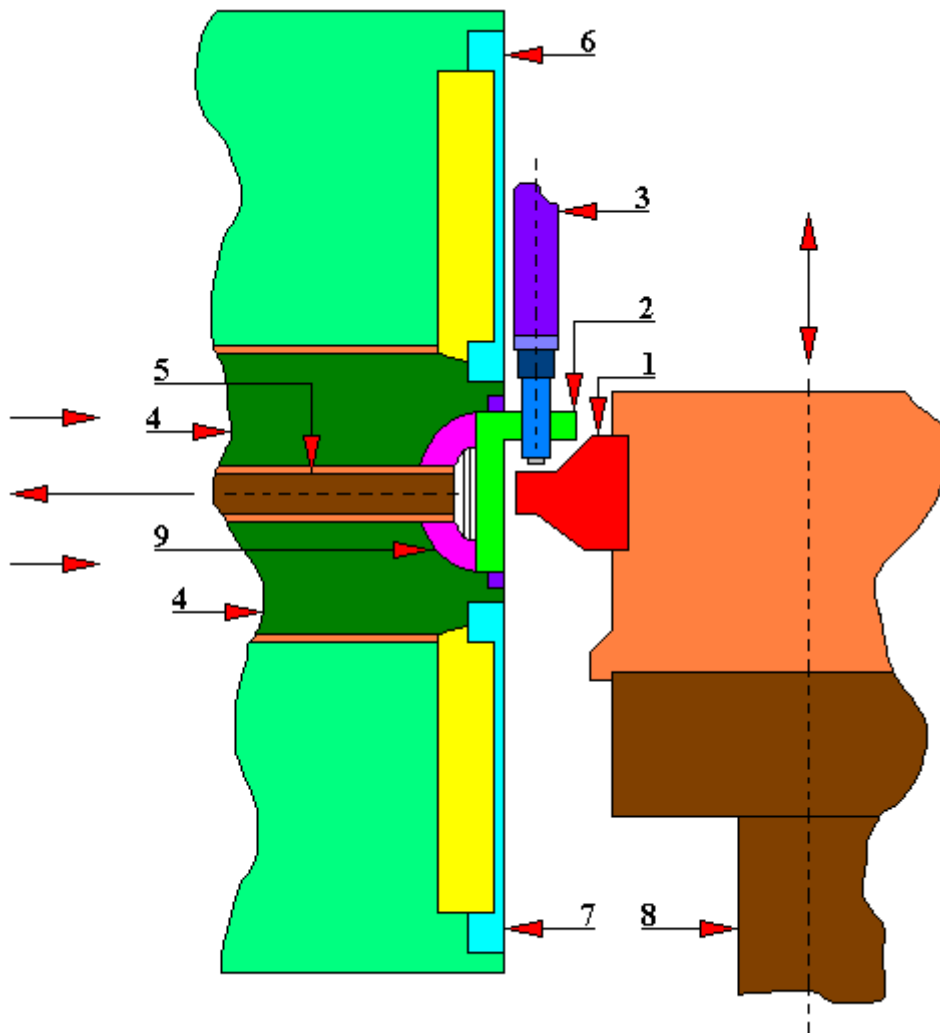


Fig. 4.1.52.1. A Test rig for fretting tests with a hydraulic system forcing displacements and hydraulic loading of samples [211]

1 - moving sample, 2 - stationary sample (counter-sample), 3 - displacement sensor, 4 - hydraulic weight, 5 - spherical support blocking piston, 6 - membrane, 7 - membrane, 8 - hydraulic cylinder forcing a reverse motion, 9 - spherical support

The moving sample 1 is mounted on a movable piston which makes a reciprocating motion. This sample co-acts with the stationary sample 2 (counter-sample) fixed by the spherical support 9 to the hydraulic weight 4. The counter-sample 2 is shaped to allow the installation of the displacement sensor 3. The amount of pressure force between the mating samples is realized by means of a hydraulic weight 4. And the quantity of displacement of the moving sample is determined by the displacement sensor 3. By controlling these two values it is possible to

influence the parameters of the wear process. A big change in the frequency of changing the direction of motion causes the oil in the hydraulic cylinder to heat up. The jumps in the displacement of the moving sample (its amplitude) can be relatively large in this solution, and the load can also reach big values. And the oscillation frequency, with reference to e.g. the temperature of the hydraulic fluid and pulsating changes in the pressure direction, makes it rather impossible to achieve its high values. The type of sample contact geometry used by the author in this design solution: plane – plane.

4.1.53. A test rig for fretting tests in which the component forcing the displacement is an electromagnetic vibrator

Figure 4.1.53.1 shows the rig intended for fretting tests in which an electromagnetic vibrator was used as a component forcing displacements.

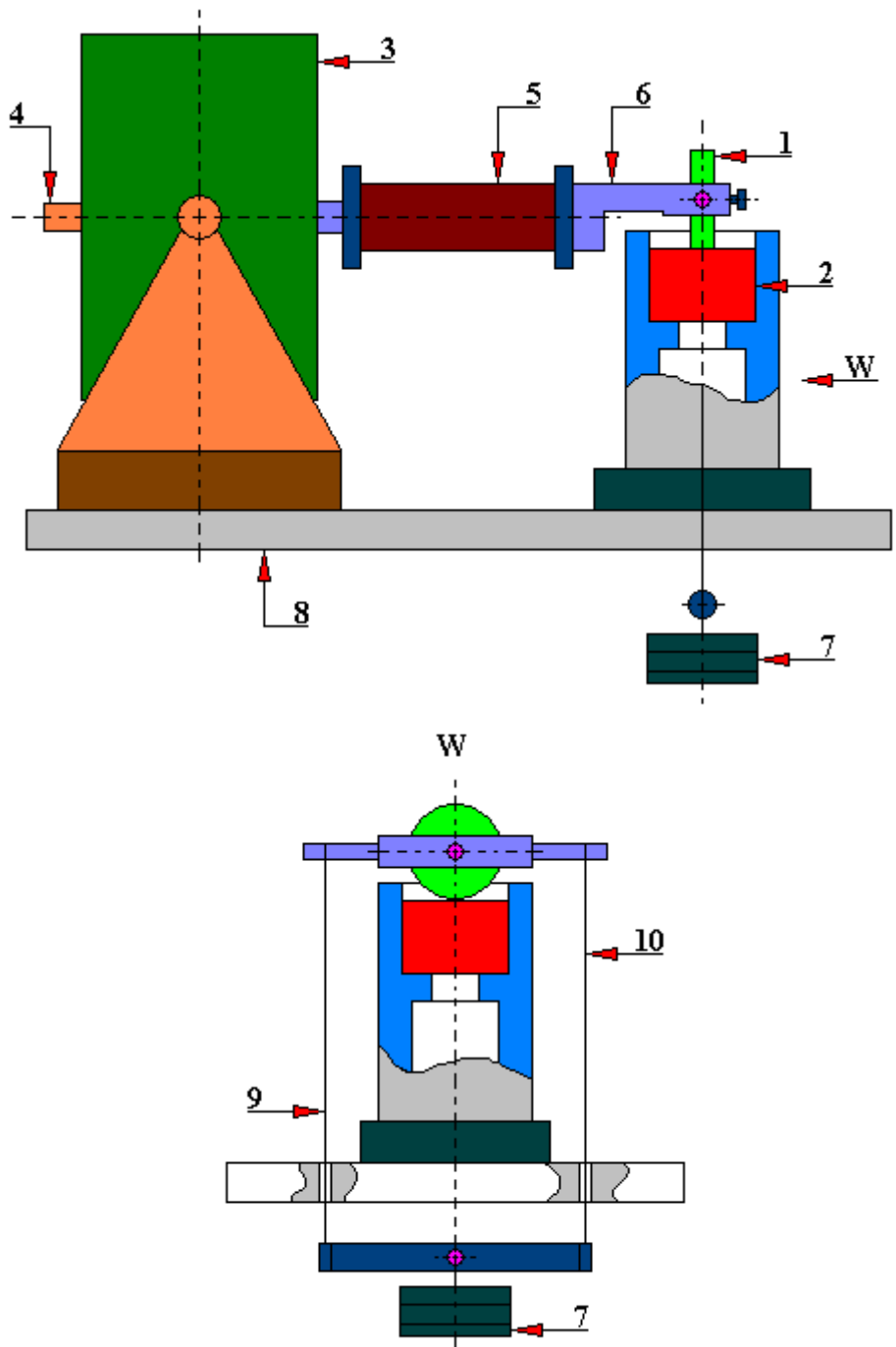


Fig. 4.1.53.1. A general scheme of the test rig for fretting tests by A. Neyman [94]
 1 - cylindrical moving sample, 2 - stationary sample (counter sample), 3 - electromagnetic vibrator, 4 - acceleration sensor, 5 - arm, 6 - moving sample holder, 7 - weight load, 8 - base body, 9 – tension member, 10 – tension member

The design of this test rig uses a movable cylindrical sample 1 which is mounted in a holder 6. The form of a moving test sample is shown in a separate Figure 4.1.53.3. The handle 6

is connected to the arm 5 moved by an electromagnetic vibrator 3. The author used a vibrator type 11076 by VEB RTF Messelektronik which is powered by a vibration generator type PO-24 by KABID ZOPAN. The amplitude of vibrations is measured by a system made of an acceleration sensor 4 (type KD-5 by Bruel & Kjaer), a bridge of the amplifier SM10 type 11013 from VEB RTF Messelektronik and an oscilloscope ST 315 A II manufactured by KABID Wrocław. The amplitude value is stabilized by a feedback system regulating the signal of the vibration generator.

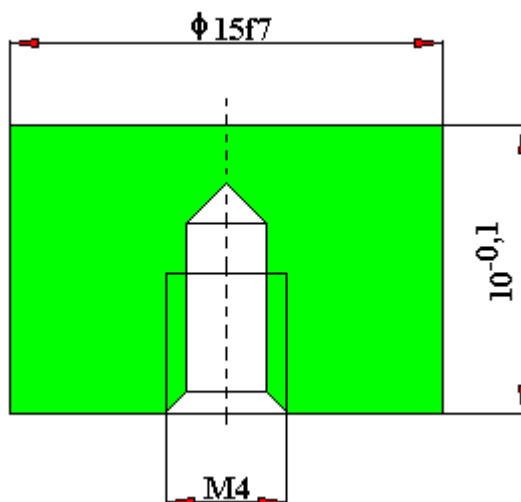


Fig. 4.1.53.2. The form of a stationary sample (counter-sample) [94]

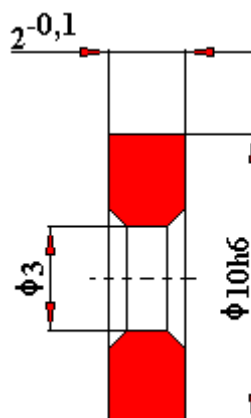


Fig. 4.1.53.3. The form of a moving sample [94]

The load is exerted on the test samples by means of weights 7 suspended on the moving sample holder. The cylindrical moving sample 1 is positioned with a flat surface in the direction of the motion to avoid the hydrodynamic effect when testing the fretting of pairs lubricated by a liquid lubricant composition. Figure 4.1.53.2 shows a stationary sample (counter-sample).

On this test rig there were, inter alia, tests carried out for the following conditions of excitations:

- oscillation amplitude: 60 [μm],
- sample loading: 50 [N],
- oscillation frequency: 200 [Hz],
- test duration: 4 hours (it corresponds to $2.88 \cdot 10^6$ cycles and a path of friction 345.6 meters),

- roughness of working surfaces of samples: $R_a = 0.32 \div 0.64 \text{ } [\mu\text{m}]$.

The volume of sample wear was determined by the author of this test rig by making fretting pit profilographs on the stationary sample, parallel and perpendicular to the direction of a relative motion, three in each direction, at equal intervals. The directions of pitting profiling on the stationary sample 2 (counter-sample) are shown in Figure 4.1.53.4. And for the moving sample 1, the author of the test rig prepared two profilograms for each fretting pit in the circumferential direction.

The sample material was steel: St 3.

The material of a counter-sample: steel St 3.

Types of tested lubricants:

- TU32 turbine oil,
- vaseline oil,
- ŁT 43 plastic grease,
- molybdenum disulfide powder,
- graphite powder.

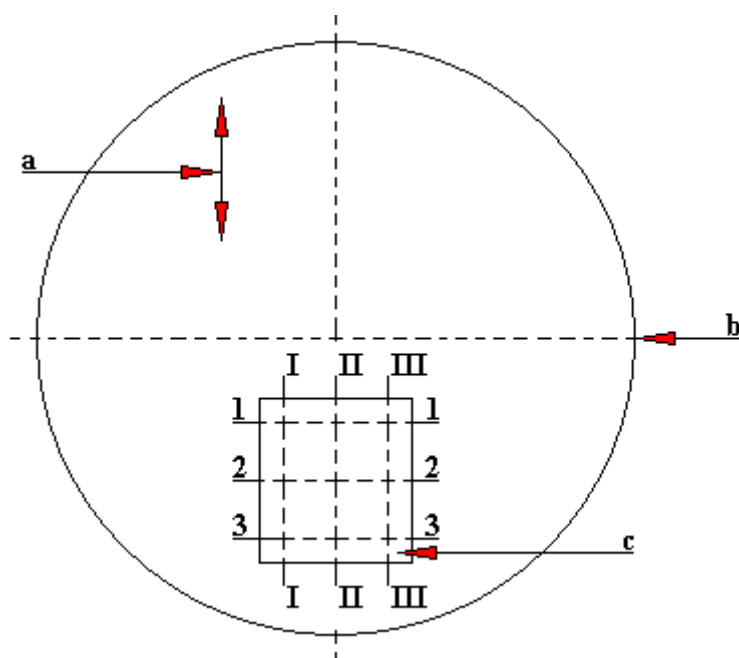


Fig. 4.1.53.4. The directions of profiling on the stationary sample 2 (counter-sample) [94]
 a - direction of motion of the moving sample, b - stationary sample (counter-sample), c - fretting pit, 1-1, 2-2, 3-3 - planes of profiling in the direction perpendicular to the direction of motion, II, II-II, III-III - profiling planes in the direction parallel to the direction of motion

4.1.54. A fretting test rig in which the component that forces the displacement is a screw mechanism

Figure 4.1.54.1 shows the test rig intended for fretting tests with a screw mechanism for inducing displacements. The upper sample 2 (in the form of a ball) is stationary and is placed in the holder 8. The handle is subjected to the load weight force 3. The measurement of the set load is measured by means of a force sensor 6 attached to the support arm. In order to adjust the settings of the support, it has horizontal 10 and vertical 9 motion mechanisms. And the lower sample 1 is attached to a movable table driven by a motor 5 through a spindle 4. The quantity of displacement of the lower sample 1, and thus the movable table, is measured by means of the displacement sensor 7. The entire test rig rests on the body 11. The change of the direction of the shift of the movable table is accompanied by a change in the direction of rotation of the spindle. In this design solution it is difficult to obtain a low value of the displacement amplitude and high oscillation frequencies. There is therefore a problem with this solution, precisely regarding the regulation of both the oscillation frequency and the amplitude.

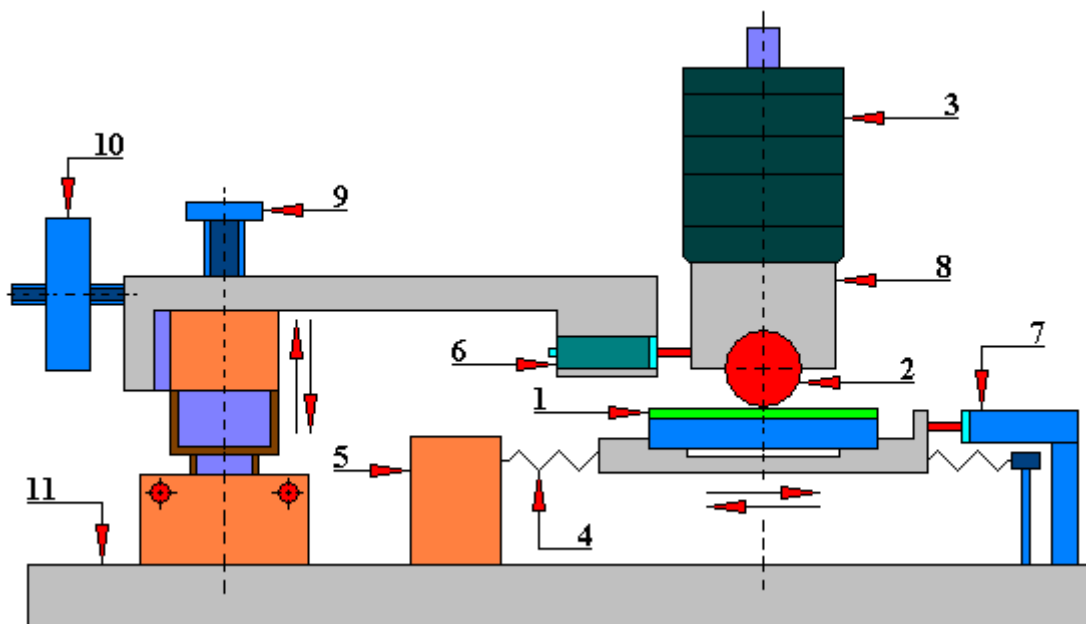


Fig. 4.1.54.1. A fretting test rig in which the component that forces the displacement is a screw mechanism [34]

1 - moving lower sample, 2 - upper sample, 3 - weight, 4 - spindle, 5 - spindle drive motor, 6 - force sensor, 7 - displacement sensor, 8 - stationary sample holder, 9 - mechanism of a vertical support motion, 10 - horizontal support motion mechanism, 11 - test rig body

4.1.55. A test rig for fretting tests with a piezoelectric set forcing displacement

Figure 4.1.55.1 shows a test rig intended for tribological tests in which the component that forces the motion is a piezoelectric set. This solution enables precise adjustment of the frequency and amplitude of oscillation at low displacement values. This test rig is easy to use. The moving sample is a ball 1 which co-acts with two counter-samples 2 which are flat elements. Counter-samples 2 are placed in a sample holder 3. Attached to these holders are weights 6 which ensure the maintenance of an appropriate value of force pressing the sample against the counter-samples. The source of motion is a semiconductor oscillator 5 which acts on the ball sample 1 from below. The quantity of displacement of the moving sample 1 is measured by means of a displacement sensor 7.

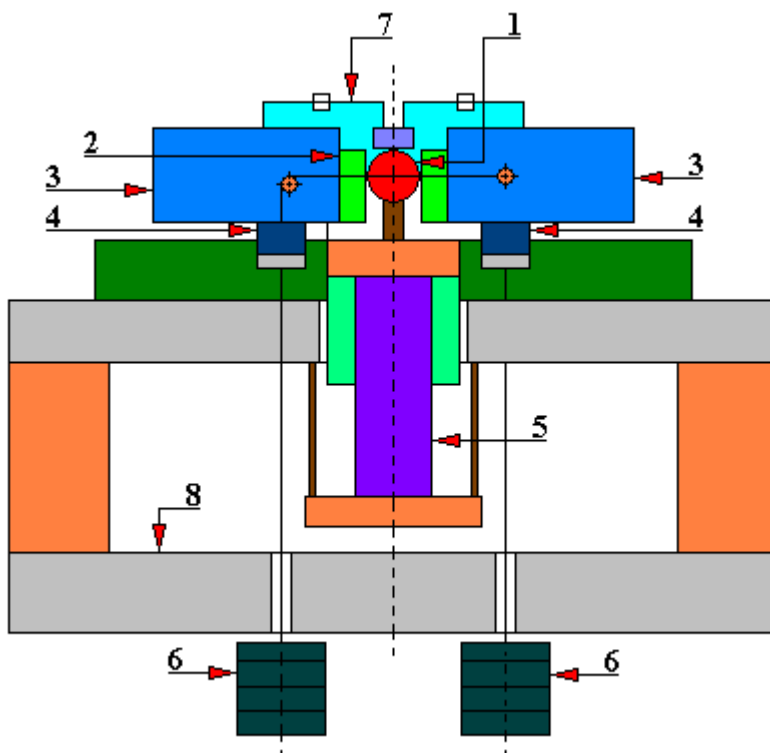


Fig. 4.1.55.1. A test rig for fretting tests in which a component forcing the displacement is a piezoelectric set
 1 - moving sample (ball-shaped), 2 - stationary sample (flat), 3 - sample holder, 4 - linear guides,
 5 - semiconductor oscillator, 6 - set load, 7 - displacement sensor, 8 - test rig body

4.1.56. A mandrel-disc test rig in which a brake disc is the counter-sample, and a brake block is the sample

Figure 4.1.56.1 shows the test rig intended for basic tribological tests with the use of original materials applied in the brake mechanism. The rotating disc 8 is mounted on the drive shaft 4 which rests on the thrust bearing 9. The brake disc 1 is attached to the rotating disc 8 by means of fixing pins 6. An insulating washer 7 is placed between the rotating disc 8 and the brake disc 1. In order to minimize the run-out of the brake disc 1, a centering plate 5 was placed on the shaft. A brake disc 1 co-acts with the sample - brake block 2. The block is placed in a holder 12 on which the set force F is acting.

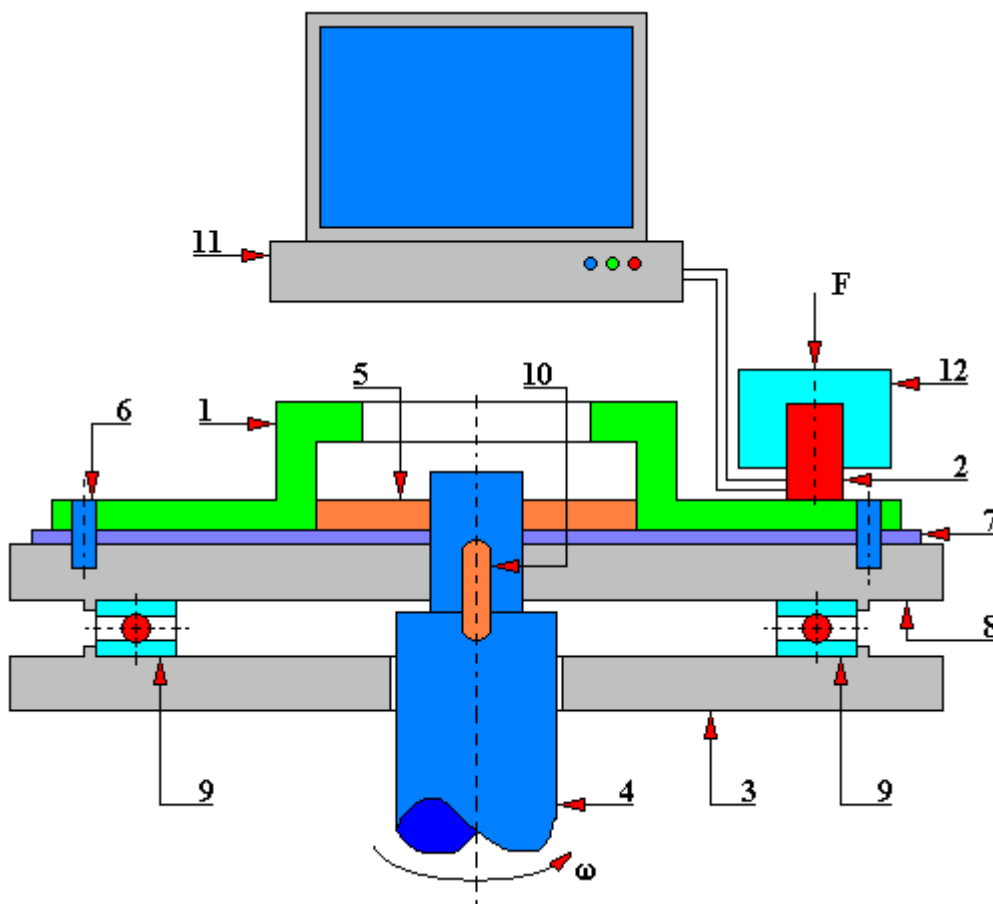


Fig. 4.1.56.1. A diagram of a disc-mandrel test rig where the original brake disc is the counter-sample, and the brake block is the sample [56]

1 - counter-sample, 2 - sample, 3 - test rig body, 4 - drive shaft, 5 - centering plate, 6 - mounting pin, 7 - insulating washer, 8 - disc, 9 - thrust bearing, 10 - keyway, 11 - PC computer, 12 - sample mounting holder, F - pressure force of the brake block sample) to the counter-sample (brake disc), ω - angular velocity of the drive shaft

This test rig enables continuous registration of the value of the friction force and temperature measured near the friction zone. The principle of measurement of the friction force and temperature is shown in Figure 4.1.56.2.

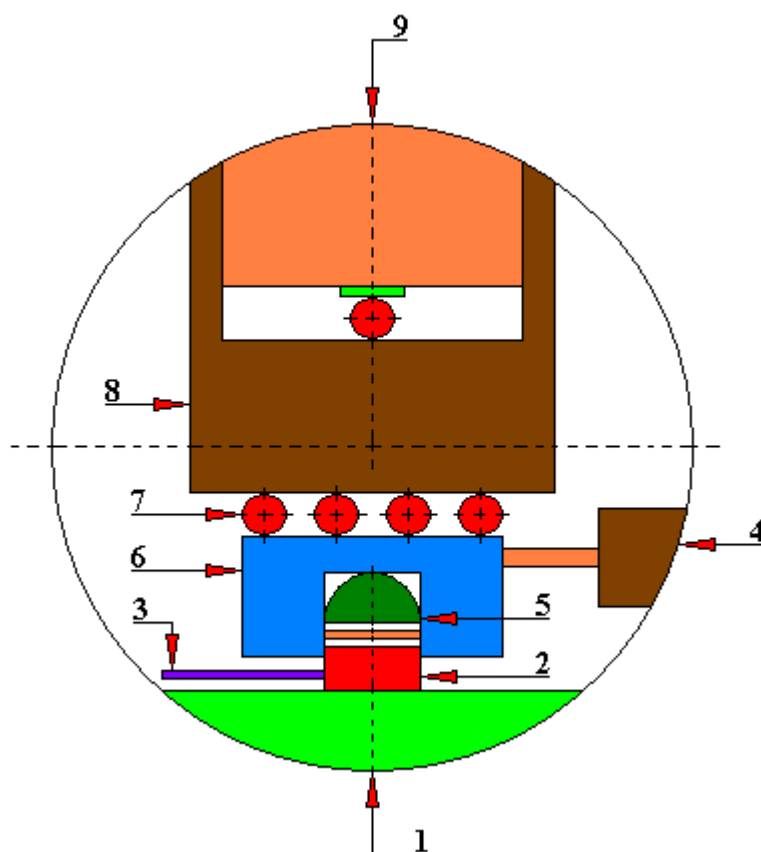


Fig. 4.1.56.2. A diagram of a disc-mandrel test rig where the original brake disc is the counter-sample, and the brake block is the sample. Principle of friction force and temperature measurement [56]

1 - counter-sample (brake disc), 2 - sample (brake block), 3 - thermocouple, 4 - force sensor, 5 - hemispherical element, 6 - sample holder, 7 - balls, 8 - guiding element, 9 - loading mass

4.1.57. A test rig for testing the coefficient of static friction of metal-polymer friction contacts

The general principle of operation of this test rig designed to determine static friction is based on the measurement of the friction angle ρ in accordance with the basic relationships between the forces occurring on the inclined plane. The inclination angle ρ , which is the friction angle, allows determining the value of coefficient of rest friction μ . The general diagram of this test rig is shown in Figure 4.1.57.1, and the design solution is shown in Figure 4.1.57.2.

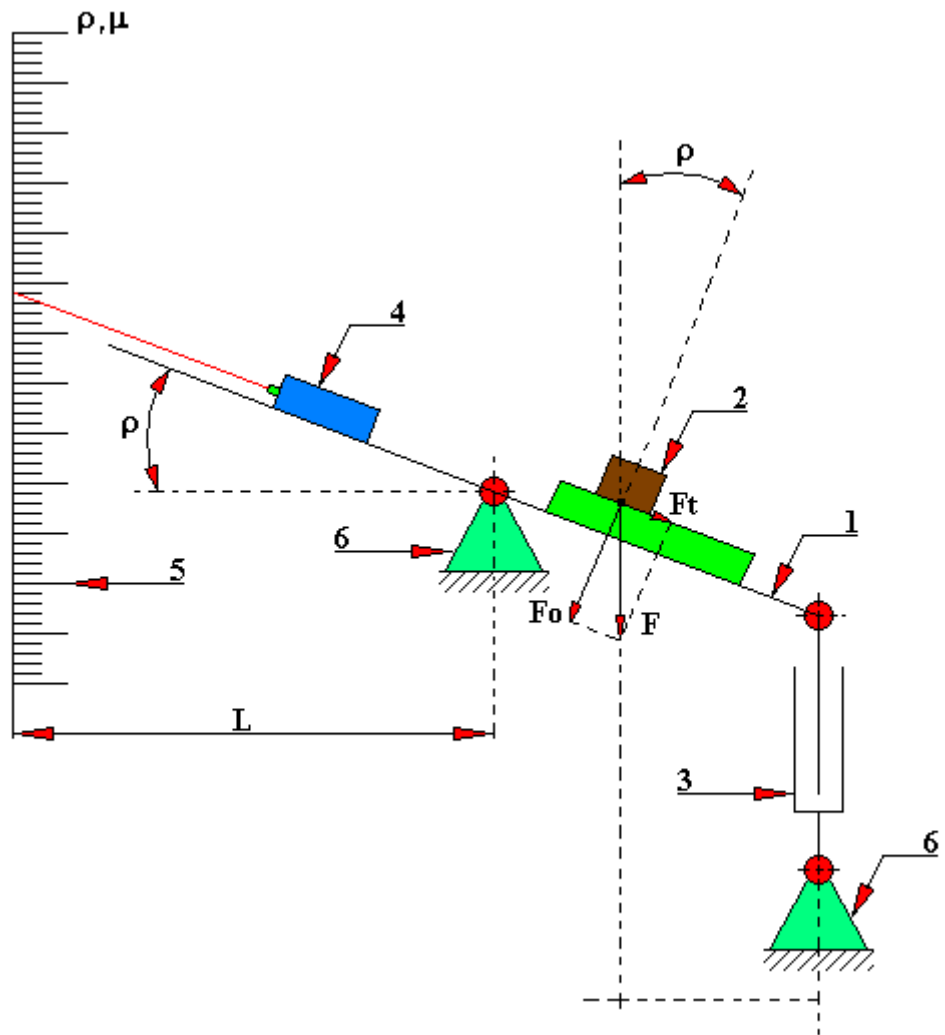


Fig. 4.1.57.1. A diagram of the test rig designed to determine the coefficient of static friction of metal-polymer friction contacts [59]
 1 - tilting arm, 2 - sliding pair, 3 - electric actuator, 4 - laser pointer, 5 - scale bar, 6 - support

The design solution of this test rig is characterized by simplicity and minimization of the influence of external factors. These features are an unquestionable advantage of this test rig.

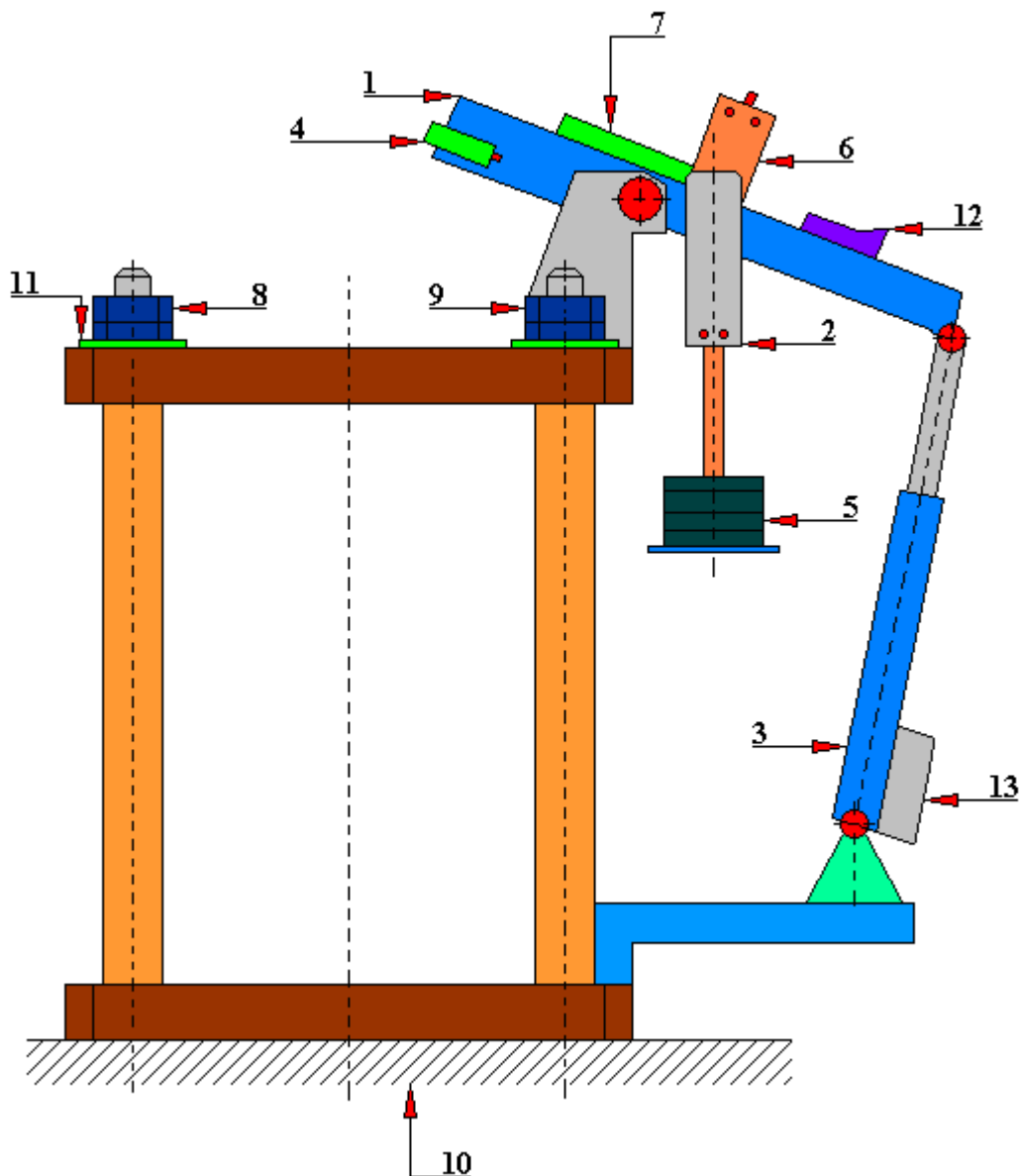


Fig. 4.1.57.2. A design solution of the test rig intended for determining the coefficient of static friction of metal-polymer friction contacts [59]

1 - tilting arm, 2 - rotating pan, 3 - electric actuator, 4 - laser pointer, 5 - weights, 6 - sample holder, 7 - tested sample, 8 - nut, 9 - nut, 10 - base, 11 - washer, 12 - motion sensor connected to the electric actuator control system, 13 - electric terminal box

Materials and friction contacts with conformal contact can be tested on this test rig. The measurement is based on the slow and uniform inclination of the friction contact located on the tilting arm until the motion takes place. The angle at which the relative motion occurs between the sample and counter-sample is the static friction angle ρ .

At the end of the tilting arm 1, which the authors used from the T-01 test rig produced by the Institute of Sustainable Technology in Radom, a laser pointer 4 is attached in the friction plane perpendicular to the axis of rotation. The laser marker indicates the value of the friction coefficient μ and the friction angle ρ read from the scale. The bar with a scale is placed at a constant distance L from the axis of rotation of the tilting arm. According to the authors of this test

rig, such a solution makes it possible to increase the accuracy of the measurement of the friction angle ρ by increasing the distance L .

This test rig allows to load the tested friction contact with additional force (which is not only the weight of the sample) in order to enable friction testing at different values of unit pressure. The force F , which is an additional weight of put weights, is applied by the system of a rotating pan 2. The authors of this test rig designed the pan in such a way that - regardless of the angle of inclination of the tilting arm 1 - the vector of additional loading force is hooked at the height of the sample - counter-sample contact.

For this design solution the maximum load of the sliding contact is 50 kg, which for samples with a diameter of $\varnothing 8$ [mm] gives the pressure $p \approx 10$ [MPa]. The loading pan 2 offers the possibility to test the sliding pairs for inclinations $\rho \leq 45^\circ$ ($\mu \leq 1$).

The drive of the tilting arm 1 is an electric actuator 3 consisting of a DC motor and a screw gear. The tilt speed of the tilting arm 1 is controlled by changing the supply voltage of the actuator motor 3. The control system comprises a motion sensor 12 which stops the movement of the tilting arm 1 when the motion between the sample and the counter-sample occurs.

The whole test rig was placed on a movable base which allows its free movement and adjustment of the distance L .

4.1.58. A test rig for testing the wear of piston rings according to the patent PL 154 209

The test rig for testing the piston rings is an invention developed by Edward Kołodziej and Władysław Śliwiński. Figure 4.1.58.1 shows a cross-section of the cylinder liner mounting assembly, while figure 4.1.58.2 shows a schematic diagram.

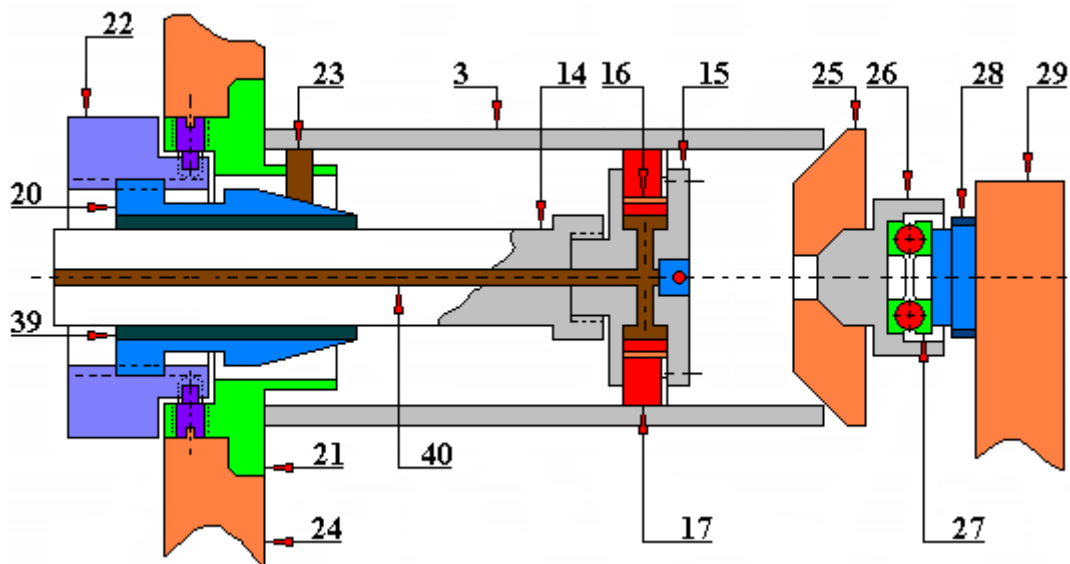


Fig. 4.1.58.1. A cross-section of the assembly of mounting the cylinder liner of the test rig for testing the wear of piston rings according to the patent PL 154 209 (the description below applies to figures 4.1.58.1 and 4.1.58.2).

1 - body, 2 - mounting plate, 3 - cylinder sleeve, 4 - thermal shield, 5 - DC drive motor, 6 - thyristor engine speed control unit, 7 - adjustable temperature regulator stabilizing thermal conditions in the climatic chamber, 8 - oil drain pan, 9 - drive wheel, 10 - adjustable eccentric, 11 - connecting rod, 12 - belt transmission, 13 - joint, 14 - hollow piston rod, 15 - hydraulic clamp (handle), 16 - pistons, 17 - tested ring, 18 - hydraulic flexible hose, 19 - manual pump dispenser, 20 - conical sleeve, 21 - spindle mount, 22 - knob, 23 - expansion bolts, 24 - centering head test rig, 25 - pressure cone, 26 - rotary tip, 27 - thrust bearing, 28 - screw, 29 - support, 30 - oil supply duct, 31 - oil drain duct, 32 - heating element, 33 - temperature sensor, 34 - asbestos thermal insulation lining, 35 - pressure gauge, 36 - special pump, 37 - filter, 38 - oil tank, 39 - conical sleeve seal, 40 - hollow piston rod duct, 41 - washer, 42 - spring

The body 1 of this test rig is an enclosed latticed structure with a mounting plate 2. On this plate there is mounted a two-head assembly of a cylinder liner 3, encased in a removable thermal shield 4. This cover constitutes the climatic chamber of the entire mounting assembly of the tested friction contact. The mounting plate 2 also houses the mechanism of the eccentric drive of the piston holder 15 of the samples of the tested piston ring 17, in the longitudinal axis of the mounting assembly. In the body 1 there is also a DC electric motor 5 with a thyristor unit 6 intended for regulating its rotational speed and an adjustable temperature control 7 which stabilizes thermal conditions in the climatic chamber. The test rig also includes a drip tray 8 for the oil used in co-action with the tested wet friction contact.

The eccentric drive mechanism consists of a drive wheel 9 with an adjustable eccentric 10 and a connecting rod 11. The test rig is powered by the above-mentioned DC electric motor 5 which sets the drive wheel 9 in motion by means of a belt transmission 12. The connecting rod 11 is connected by a joint 13 with a hollow piston rod 14. The piston rod 14 has a hydraulic piston

clamp (holder) mounted at its other end in which the pistons 16 are horizontally guided, holding the tested fragments of the piston ring 17. The piston rod 14 is connected by a flexible conduit 18 to the manual pump dispenser 19.

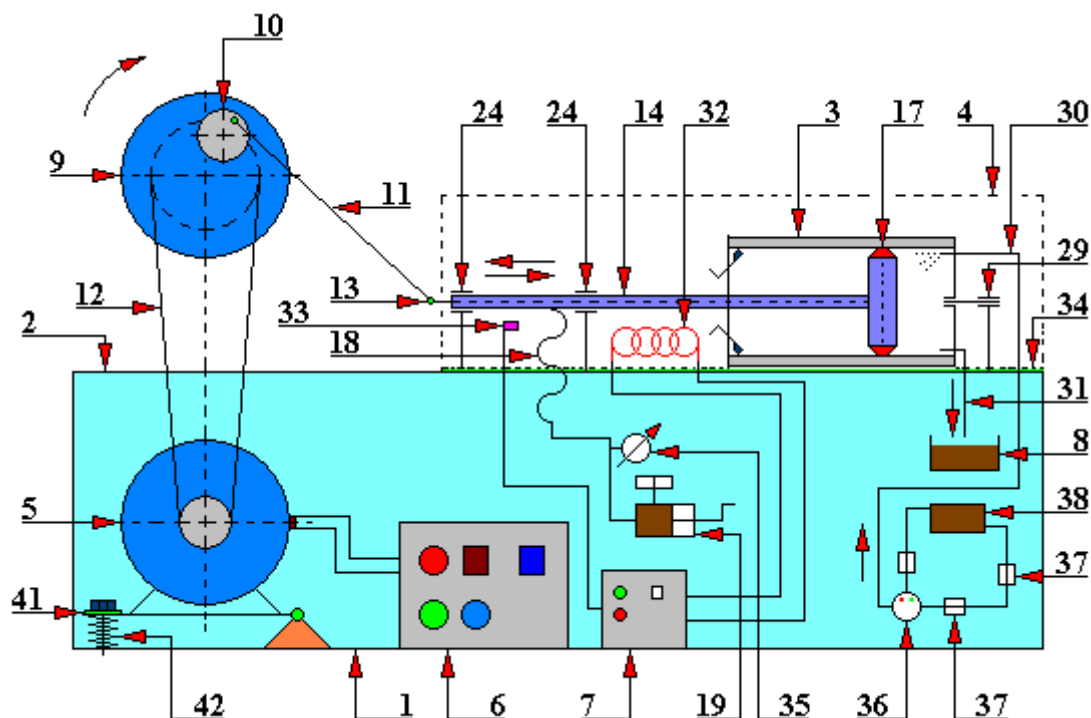


Fig. 4.1.58.2. A schematic diagram of the test rig for testing the wear of the piston rings according to the patent PL 154 209 (the description below applies to figures 4.1.58.1 and 4.1.58.2)

1 - body, 2 - mounting plate, 3 - cylinder sleeve, 4 - thermal shield, 5 - DC drive motor, 6 - thyristor engine speed control unit, 7 - adjustable temperature regulator stabilizing thermal conditions in the climatic chamber, 8 - oil drain pan, 9 - drive wheel, 10 - adjustable eccentric, 11 - connecting rod, 12 - belt transmission, 13 - joint, 14 - hollow piston rod, 15 - hydraulic clamp (handle), 16 - pistons, 17 - tested ring, 18 - hydraulic flexible hose, 19 - manual pump dispenser, 20 - conical sleeve, 21 - spindle mount, 22 - knob, 23 - expansion bolts, 24 - centering head test rig, 25 - pressure cone, 26 - rotary tip, 27 - thrust bearing, 28 - screw, 29 - support, 30 - oil supply duct, 31 - oil drain duct, 32 - heating element, 33 - temperature sensor, 34 - asbestos thermal insulation lining, 35 - pressure gauge, 36 - special pump, 37 - filter, 38 - oil tank, 39 - conical sleeve seal, 40 - hollow piston rod duct, 41 - washer, 42 - spring

The piston rod 14 is slidable in the centering head and is mounted concentrically in the conical sleeve 20. This sleeve is a clamping element of the centering holder in the assembly fixing the cylindrical sleeve 3. The centering holder consists of a spindle mount 21, a knob 22 mounted in it, a conical sleeve 20 threaded with a knob 22 and expansion bolts 23, which are slidably mounted in the holder 21 and co-act with the conical surface of the sleeves 20. The centering holder is fastened to the test rig 24 of the centering head by means of a pin mount 21. The second pressure head of the mounting assembly consists of a replaceable cone 25 mounted on the end 26 rotationally connected by means of a thrust bearing 27, bolt 28, guided support 29. The pressure cone 25 is connected by the oil supply duct 30 and oil drain duct 31. The oil supply duct 30 is connected to a hydraulic system consisting of, inter alia, filters 37, oil tank 38 and a special pump 36. And the oil drain duct 31 is connected to the sump 8. The authors of this test rig used the internal lining of the thermal shield 4 with asbestos (asbestos thermal insulation lining

34). Inside the thermal shield there are: a heating element 32 and temperature sensor 33. Both the heater and the temperature sensor are electrically connected to the temperature controller 7.

Before starting the tests, the stroke and frequency of reciprocating motion of the clamp (holder) 15 are determined. The tested ring is placed in the holder. The cylinder liner to be tested is then clamped between the pressure head and centering head. A thermal shield 4 is put on, temperature conditions are set, the type of friction of the tested friction contact is determined and the force of pressing the rings 17 against the surface of the cylindrical sleeve 3 is determined by controlling it on the pressure gauge 35. After the specified test time, the system is dismantled and the wear of the tested ring 17 is determined.

This test rig can also be used for comparative tests of materials for piston rings carried out at negative temperatures.

A very detailed description of the test rig, presented above by the authors of this invention, proves that they have made a prototype.

4.1.59. A test rig for testing the static and kinetic coefficient of friction for frictional pairs

The test rig for testing the static and kinetic coefficient of friction for friction contacts was built by the Department of Machine Design and Operation of the AGH University of Science and Technology in Cracow in order to conduct research on the friction processes of selected material pairs and to carry out laboratory exercises by students, enabling them to learn about the tribological processes occurring during the operation of friction clutches and brakes. The diagram of this test rig is shown in figure 4.1.59.1.

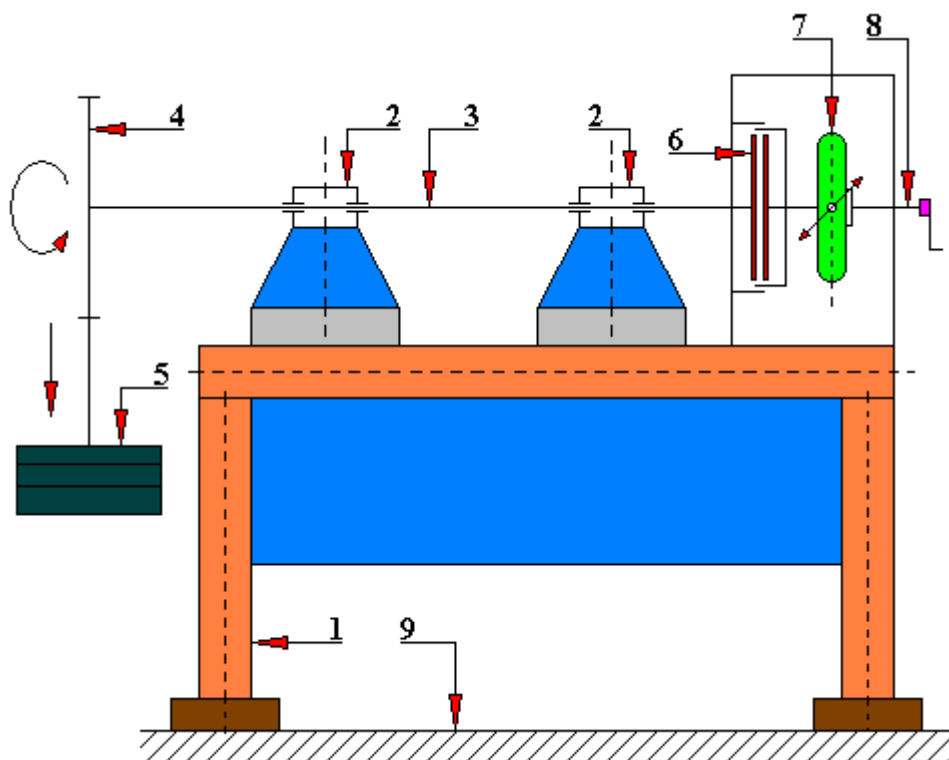


Fig. 4.1.59.1. A general diagram of the test rig for testing friction for frictional pairs [68]

1 - body, 2 - bearing, 3 - shaft, 4 - rope pulley, 5 - weights, 6 - tested friction discs, 7 - sensor measuring the pressure force of the tested friction discs, 8 - adjusting screw, 9 - base (foundation)

This test rig consists of a body 1 on which a rotating shaft 3 is supported on bearings 2. On one side of this shaft, a rope pulley 4 with weights 5 is mounted, and on its other side, the tested friction discs 6 are mounted. These discs are replaceable, thanks to which it is possible to carry out tests for various material combinations, e.g. steel, cast iron, non-ferrous metals, organic materials based on resins and rubber, inorganic materials made of ceramic metals. The pressure on the mating friction plates 6 is exerted by means of an adjusting screw 8. In order to know the value of this pressure, the measuring sensor 7 was installed in the system.

In order to determine the value of the static friction coefficient, unfortunately, it is necessary to simultaneously measure as many as three variables: pressure force, torque value and shaft angle value. Since all these values are dynamic, there was a need to build a system for registering and visualizing data collected from the test rig.

The pressing force of the tested friction discs 6 is measured by strain gauge force sensors glued to the bar force transducer 7.

The value of the twisting moment is determined by means of four strain gauges glued on the surface of the shaft 3 in pairs in mutually perpendicular directions, at an angle of 45° to the generatrix of the shaft 3 on its opposite sides.

The angle of twisting the shaft 3 is measured with a digital angle sensor.

A general scheme of the measuring system of this test rig is presented in Figure 4.1.59.2.

Finally, it is worth mentioning that this test rig is intended only for testing friction elements that work in dry friction conditions for which the friction coefficients reach the highest values.

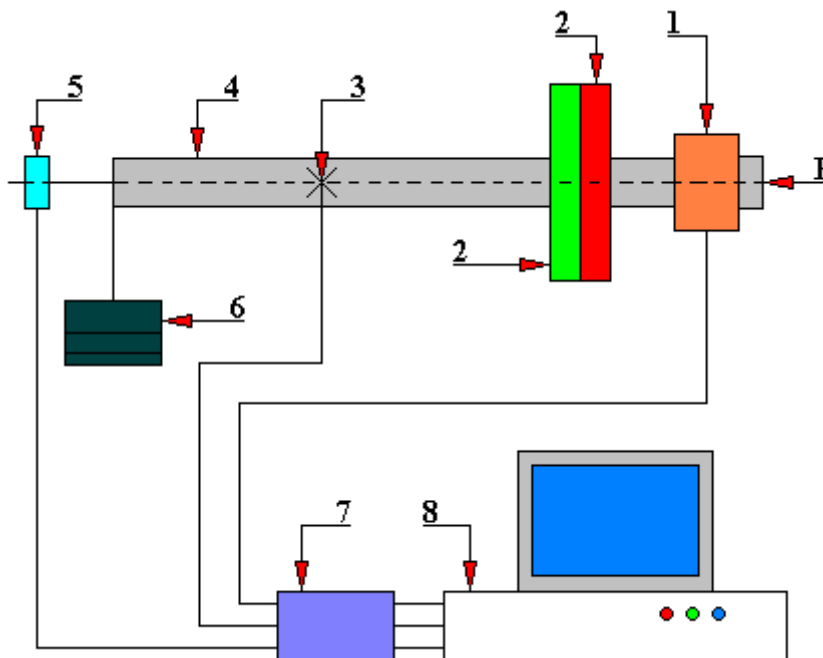


Fig. 4.1.59.2. A general diagram of the measuring system of the test rig for testing friction for friction contacts [68]

1 - sensor for measuring the pressing force of the tested friction discs, 2 - tested friction discs, 3 - torque sensor, 4 - rotating shaft, 5 - angle sensor, 6 - weights, 7 - measuring amplifier, 8 - computer, F - pressing force

4.1.60. Test rig for testing abrasive wear in the conditions of industrial suspensions according to the patent PL 207 139

The test rig is built according to the patent PL 207 139, shown in Figure 4.1.60.1, the authors of which are: Andrzej Weroński and Andrzej Trzciński; it is designed to determine the resistance to abrasive wear the measure of which is the loss of mass of the tested samples on a specific path of friction.

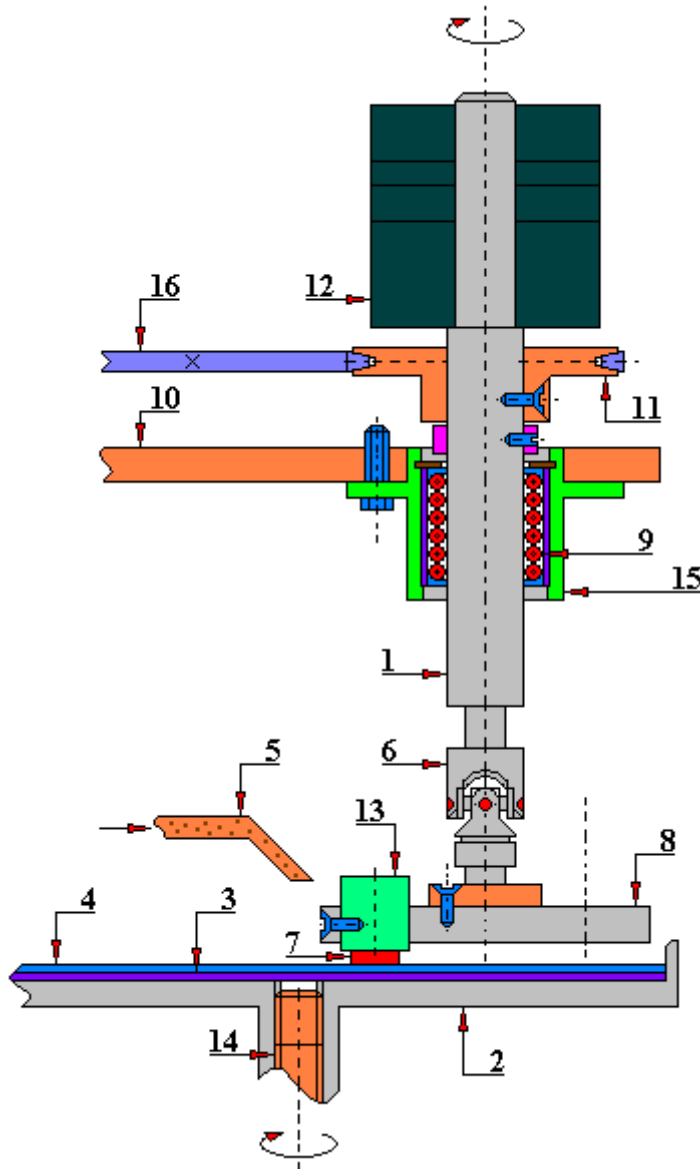


Fig. 4.1.60.1. A general diagram of the test rig for testing abrasive wear in the conditions of industrial suspensions according to the patent PL 207 139.

- 1 - drive shaft, 2 - rotating disc, 3 - washer made of flexible material, 4 - disc, 5 - abrasive suspension feeder, 6 - Cardan joint, 7 - test sample, 8 - guide disc, 9 - linear-rotary bearing, 10 - body, 11 - belt transmission, 12 - mass-adjustable weight, 13 - samples mounting holder, 14 - bearing-mounted shaft, 15 - sleeve, 16 - V-belt

The test rig consists of a drive shaft 1 driven by a belt transmission 11. The drive shaft 1 is loaded with mass-adjustable weights 12 and supported by a linear-rotary bearing 9 mounted in

the sleeve 15. The sleeve 15 is mounted in the body 10. The lower part of the drive shaft 1 is connected to the guide disc 8 through the Cardan joint. In the guide disc there is a holder 13 for holding three samples 7. These samples, making a rotary motion, are pressed by weights 12 to the rotating disc 2. A washer 3 made of elastic material is fastened to the rotating disc 2, and a disk 4 is mounted on this washer. An abrasive suspension 5 is supplied to the surface of the disc 4. As a result of co-acting of three samples 7, the abrasive suspension 5 and the disc 4, the process of their wear takes place, the intensity of which can be adjusted, among others, by means of the direction of rotation of the guide disc 8, rotating disc 2, the value of the set load 12 or the type of abrasive suspension 5.

4.1.61. Test rig for testing abrasive wear under complex stress conditions in the tested material according to the patent PL 211 447

The test rig is built according to the patent PL 211 447, shown in Figure 4.1.61.1, the authors of which are: Andrzej Weroński, Andrzej Trzciński and Tadeusz Hejwowski; it is designed to determine the abrasive wear resistance of the tested material at variable pressure.

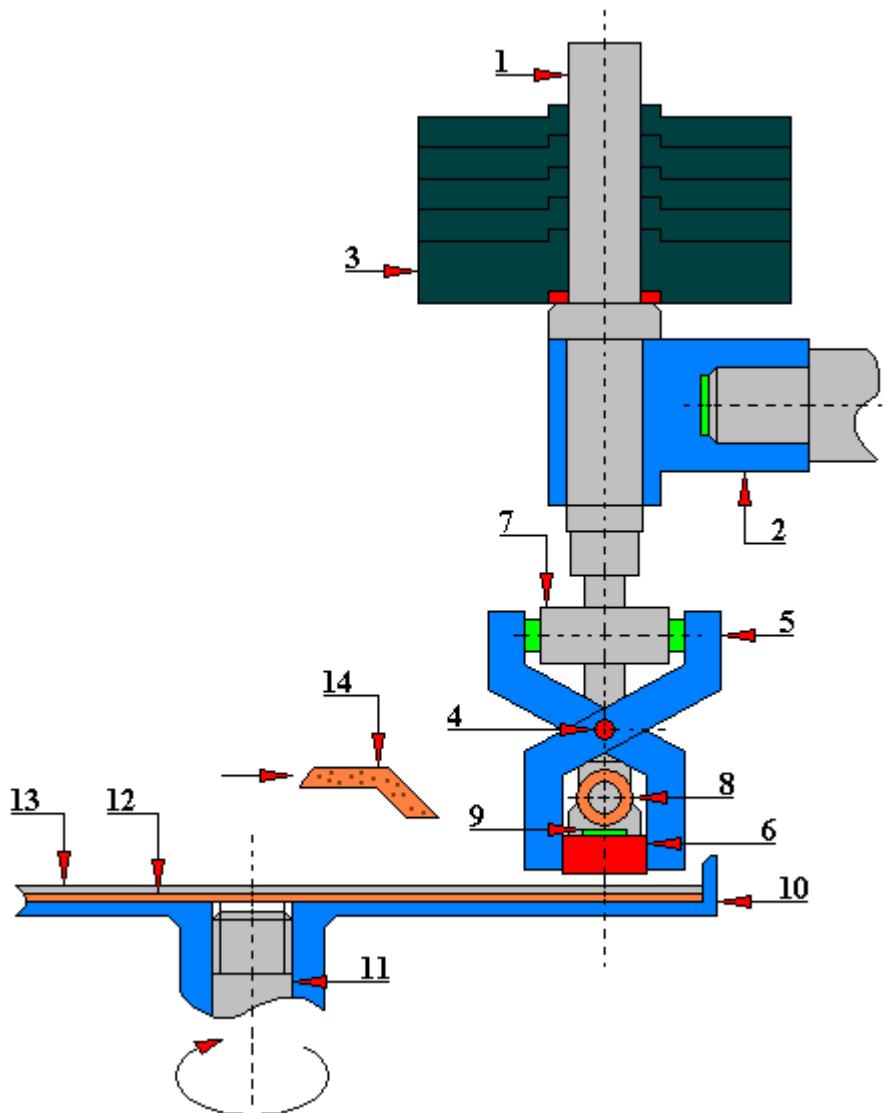


Fig. 4.1.61.1. A general diagram of the test rig for testing abrasive wear under complex stress conditions in the tested material according to the patent PL 211 447

1 - mandrel, 2 - body, 3 - mass-adjustable weight load, 4 - joint, 5 - jaw chuck, 6 - tested material, 7 - hydraulic actuator, 8 - second hydraulic actuator, 9 - strain gauge, 10 - rotating disc, 11 - drive shaft, 12 - washer, 13 - disc, 14 - duct supplying abrasive

The test rig consists of a mandrel 1 which is embedded in the body 2. Weights with an adjustable mass 3 act on the mandrel. In the lower part of the mandrel 1, a jaw chuck 5 is fastened via the joint 4. In this holder the test sample 6 is mounted on which compressive stresses are exerted in mutually perpendicular directions by means of the jaws of the holder 5 and actuators 7 and 8. On the upper surface of the tested sample 6 there are strain gauges 9.

The test sample 6, fixed in the jaw chuck 5, is pressed against the rotating disc 10 which is driven by a bearing-mounted drive shaft 11. On the surface of the rotary disc 10 there is a washer 12 made of elastic material, and there is a disc 13 on it. The abrasive is supplied to the surface of the disc 13 by means of a duct 14. As the disc 10 rotates, the tested material undergoes abrasive wear. The measure of resistance to abrasive wear is the loss of mass of the tested material on a specific path of friction after applying compressive stresses with the use of hydraulic actuators 7 and 8.

4.1.62. A test rig for testing the dynamic load capacity of thrust slide bearings lubricated with magnetic liquid, constructed according to the patent PL 222 239

The test rig is built according to the patent PL 222 239, shown in Figure 4.1.62.1, the authors of which are: Wojciech Horak, Józef Salwiński, Włodzimierz Ochojski, Marcin Szczęch; it makes it possible to test the dynamic load capacity of thrust slide bearings.

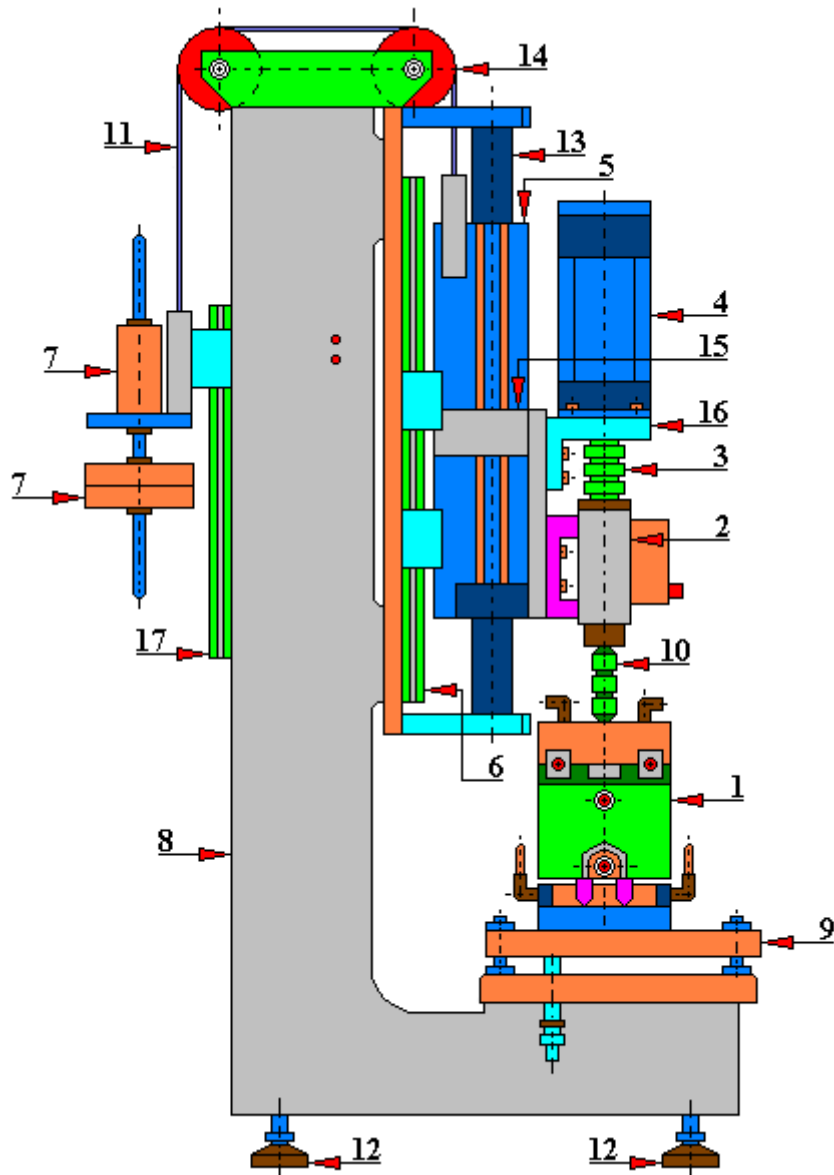


Fig. 4.1.62.1. A general diagram of the test rig according to the patent PL 222 239 (the description below applies to figures 4.1.62.1 and 4.1.62.2)

- 1 - test head, 2 - force and torque sensor, 3 - bellows coupling, 4 - rotary motor, 5 - linear motor, 6 - guide, 7 - balance weights, 8 - body, 9 - setting table, 10 - clamping sleeve, 11 - chain, 12 - foot, 13 - magnetic core of the linear motor, 14 - sprocket wheel, 15 - frame, 16 - flange, 17 - rear guide, 18 - shaft, 19 - rotating plate, 20 - magnetic liquid, 21 - groove, 22 - pressure plate, 23 - electromagnet, 24 - electromagnet core, 25 - head cover, 26 - coil elements, 27 - cover stub, 28 - cooling channels, 29 - head body elements, 30 - lower base connectors, 31 - side connectors, 32 - cooling channels of head body, 33 - locating pin, 34 - hole

The main operating parameter of a thrust bearing lubricated with magnetic liquid is the dynamic load capacity defined by the thrust force that can be maintained by a magnetic liquid when subjected to a magnetic field without metal-metal contact between the sliding surfaces. The size of the dynamic load capacity depends, among others, on:

- the type of magnetic fluid,
- the amount of magnetic fluid,
- the geometry of the sliding surfaces,
- magnetic field strength in the interspace,
- rotational speed of the shaft.

This test rig consists of a body 8 supported by three height-adjustable feet 12. These feet enable precise vertical alignment of the guides 6. The frame 15 moves along the guides 6 together with the linear motor 5. The linear motor 5 moves along the axis of the magnetic core 13 fixed to the cantilevers of the body 8. A flange 16 is attached to the frame 15 on which the rotary motor 4 rests. Mounted on the shaft of the rotary motor 4 is a bellows clutch 3 which is connected to the housing with the force and torque sensor 2. Unit: rotary motor 4 - bellows clutch 3 - frame 15 - force and torque sensor 2, through the clamping sleeve 10 it is connected to the shaft 18 of the tested thrust bearing in the test head 1. This head is placed on the setting table 9. Preferably, the table should have a triaxial position control that allows the force and torque sensor 2 to be aligned with the shaft 18 in the test head 1. The mass of drive components and measuring sensors is balanced by weights 7 suspended on a chain 11 wound around chain wheels 14. Chain wheels 14 are bearing-mounted in the upper part of the body 8. The weights 7 can slide along the rear guide 17 attached to the body 8.

The main element of the test head, shown in Figure 5.1.62.2, is a shaft 18 terminated with a replaceable rotating plate 19 with a given geometry and external diameter, made of a non-magnetic material and constituting, together with the fixed pressure plate 22, the tested thrust bearing. The rotating plate 19, positioned in the test head chamber at an appropriate distance from the pressure plate 22, forms a gap filled with magnetic fluid 2. The head chamber is closed at the top with a cover 25 made of magnetic material which directs the magnetic field in the tested bearing. A groove 21 is made in the pressure plate 22 to accommodate the temperature sensor and the magnetic field strength sensor and to lead by wires their signals through the hole 34. The source of the magnetic field in the test head 1 is an electromagnet 23 mounted in the elements of the coil 26. The top element of the coil 26 is non-magnetic. The element focusing the magnetic field in the measuring head 1 is the electromagnet core 6 on which the electromagnet 23 is mounted. The elements of head 29 are part of the magnetic circuit, and the cooling channels of the head body 29 stabilize the operating temperature of the electromagnet 23. The test head body 1 is supplied with a cooling agent by means of connectors 30, 31, 28, 27. The position of the test head 1 on the setting table 9 is determined by the locating pin 33.

The dynamic load bearing capacity of the tested thrust bearing is determined by measuring the thrust force transmitted by the magnetic fluid 20 in the gap between the faces of the rotating plate 19 and the fixed pressure plate 22. The value of the longitudinal force is determined at a set magnetic field strength and a given rotational speed of the shaft 18.

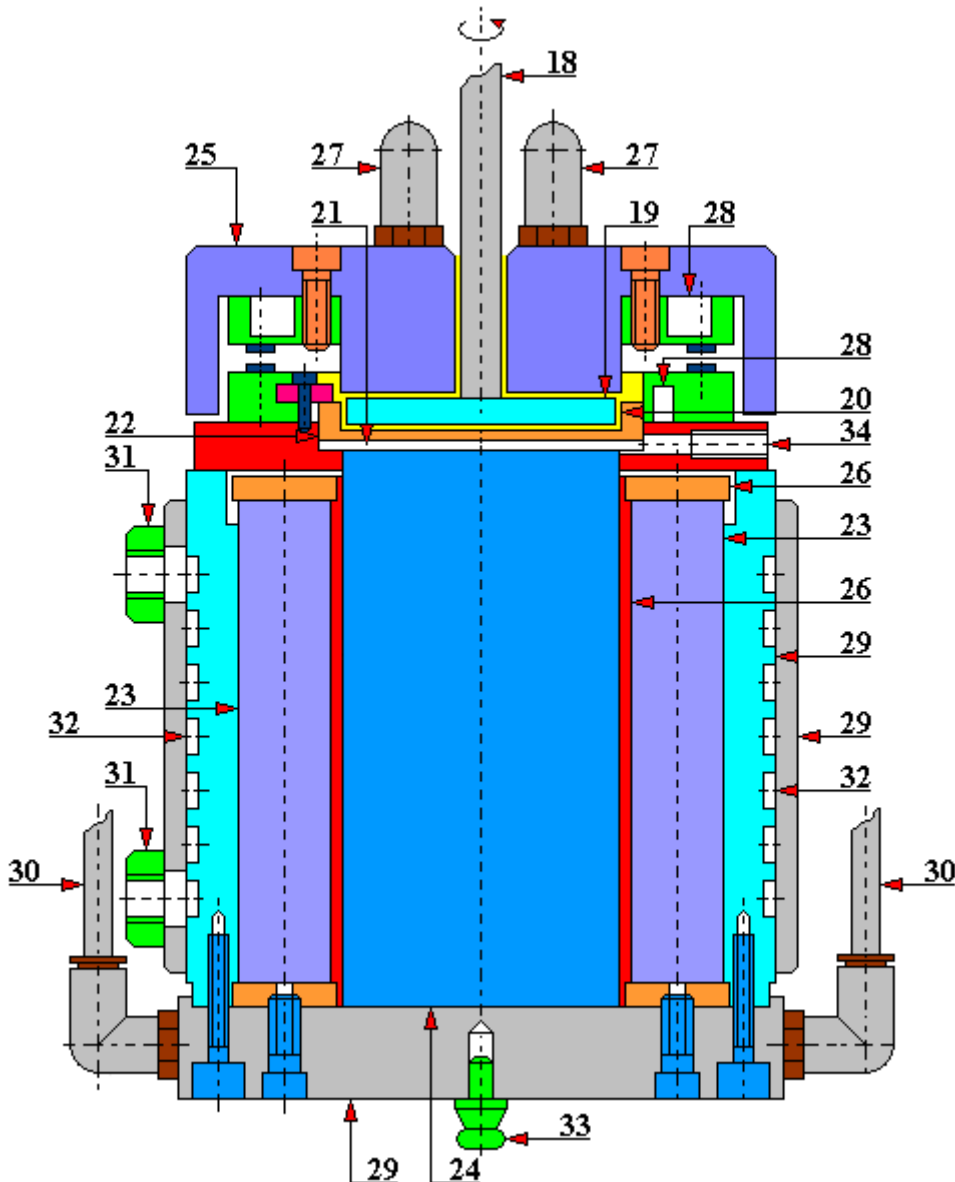


Fig. 4.1.62.2. A general diagram of the test head according to the patent PL 222 239 (the description below applies to figures 4.1.62.1 and 4.1.62.2)

- 1 - test head, 2 - force and torque sensor, 3 - bellows coupling, 4 - rotary motor, 5 - linear motor,
- 6 - guide, 7 - balance weights, 8 - body, 9 - setting table, 10 – clamping sleeve, 11 - chain, 12 -
- foot, 13 - magnetic core of the linear motor, 14 – chain wheel, 15 - frame, 16 - flange, 17 - rear
- guide, 18 - shaft, 19 - rotating plate, 20 - magnetic liquid, 21 - groove , 22 – pressure plate, 23 -
- electromagnet, 24 - electromagnet core, 25 - head cover, 26 - coil elements, 27 - cover stub, 28 -
- cooling channels, 29 - head body elements, 30 - lower base connectors, 31 – side connectors, 32
- cooling channels of head body, 33 - locating pin, 34 - hole

4.1.63. Test rig for testing the sliding friction in a temperature-controlled lubricant according to the patent PL 95 008

The test rig is built according to the patent 95 008, the hydraulic system of which is shown in Figure 4.1.63.1, the authors of which are: Tadeusz Łubiński, Olgierd Olszewski, Jan Kłopotcki and Jerzy Pasiński; it makes it possible to carry out tests on the impact on the character and course of the friction process:

- the temperature of the oil used as a lubricant,
- surface characteristics of the tested materials,
- volumetric characteristics of the tested materials.

This test rig eliminates or limits unfavorable and difficult to determine influences on the course of the friction process of external vibrations, load errors, uneven distribution of surface pressures of the tested elements.

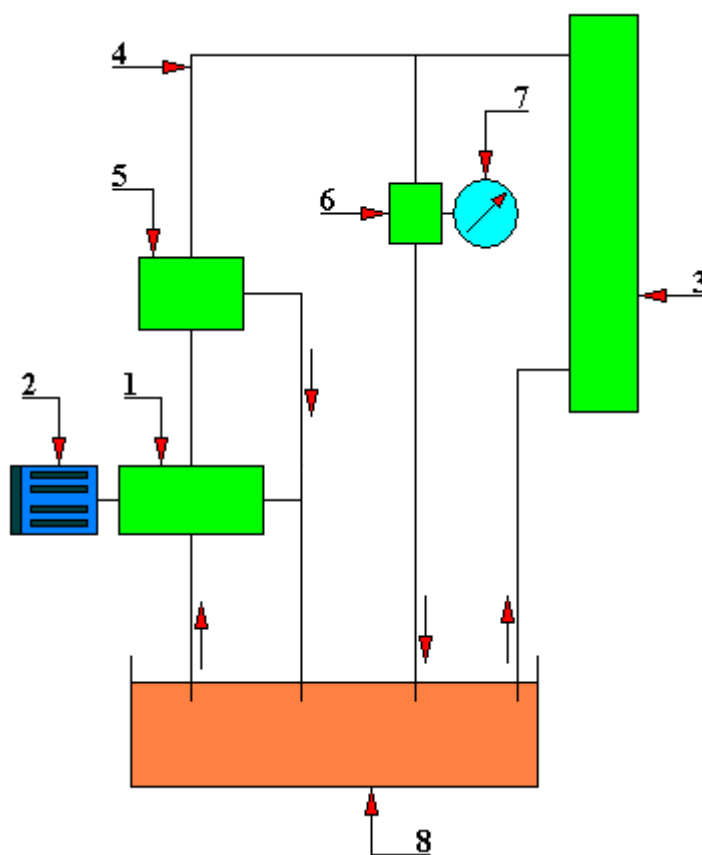


Fig. 4.1.63.1. A diagram of connection of the test head with the hydraulic system of the test rig for testing sliding friction in a temperature-controlled lubricant according to the patent 95 008.

1 - hydraulic pump, 2 - electric motor, 3 - test head, 4 - hydraulic conduit, 5 - overflow valve, 6 - release valve, 7 - pressure gauge, 8 - oil tank

Figure 4.1.63.1 shows the system of a hydraulic pump 1 driven by an electric motor 2 connected by conduits 4 to the test head 3 of this test rig. On conduits 4 there is an overflow valve 5, a release control valve 6 and a pressure gauge 7.

On the body 7 (Figure 4.1.63.2) of the head 3 there is mounted the body of the hydrostatic bearing 8 of the loading piston 9 and the body of the hydrostatic bearings 10 of the rotary spindle 11, and these bearings are mounted as non-slidable.

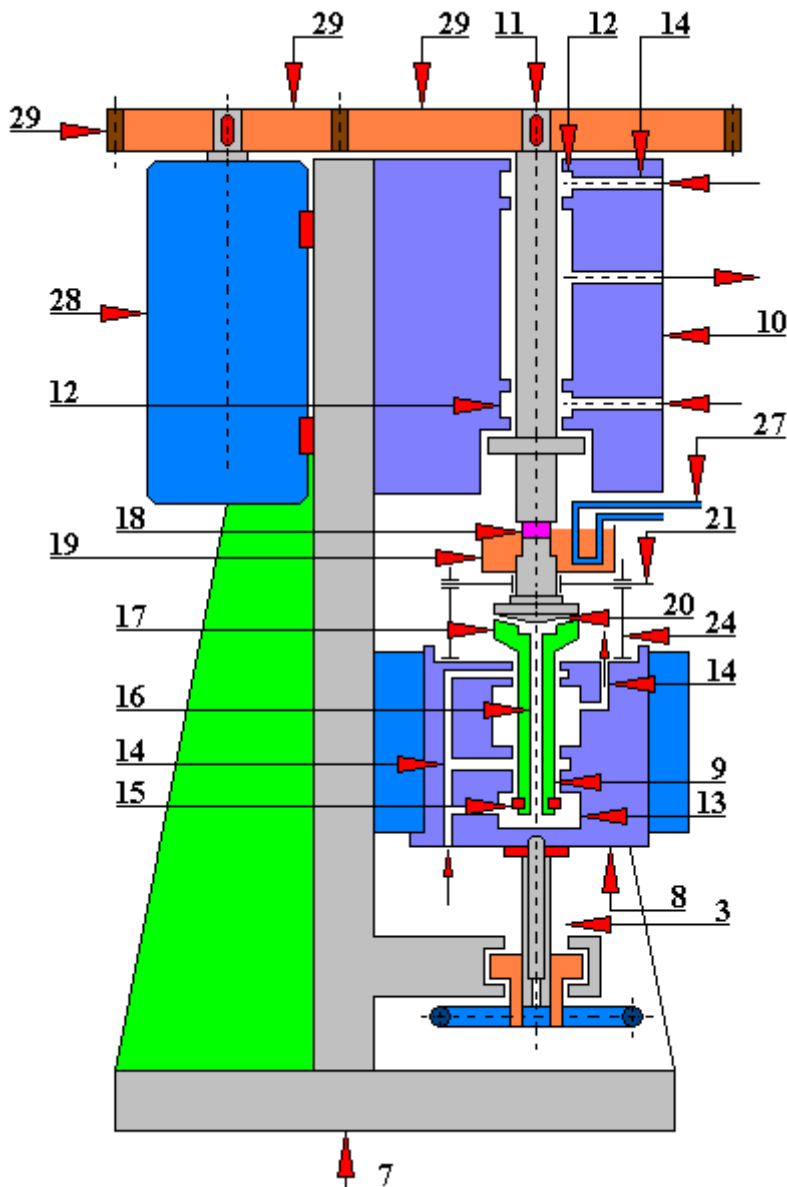


Fig. 4.1.63.2. Axial section of the test rig for testing the sliding friction in a temperature-controlled lubricant according to the patent PL 95 008.

3 - test head, 7 - head body, 8 - hydrostatic bearing body, 9 - loading piston, 10 - spindle hydrostatic bearing body, 11 - rotary spindle, 12 - transverse hydrostatic supports, 13 - oil chamber, 14 - channels, 15 - securing ring, 16 - hole for supplying oil to a spherical or flat bowl, 17 - spherical or flat bowl, 18 - sleeve bottom handle, 19 - lubricant reservoir, 20 - spherical pin, 21 - strain gauge beams, 24 - cantilever bars, 27 - heat exchanger, 28 - drive motor, 29 - gear transmission

The loading piston 9 is guided in the transverse hydrostatic supports 12 and is pushed upwards by the pressure of the oil in the chamber 13. These supports, together with the oil chamber 13, are connected by channels with the hydraulic pump system 4 which maintains the oil pressure in the bearings 8, 12 and in the chamber 13 in a continuous and regulated manner.

The piston 9 is secured against falling out by a ring 15 and has an opening 16 which supplies oil to the bowl 17. This bowl dish can be spherical or flat. In this bowl, the lower handle

18 is loosely mounted on the oil pad, together with the lubricant reservoir 19. The lower handle 18 and the reservoir 19 are fastened by a spherical pin 20. To this holder attached are beams 21 onto which the strain gauge transducers 22 are glued. At the ends of beams 21 there are rolling bearings 23 mounted, which during the measurements rest on the cantilever bars 24.

In order to ensure a continuous contact of the rolling bearings 23 with the beams 21, springs 25 are attached which are connected on one side with these beams and on the other side with the shaft 26 of the intermediate unit.

In the lubricant reservoir 19 there is mounted a heat exchanger 27 made of a shaped tube inside which a fluid flows at a set temperature.

The rotary spindle 11 is also supported on hydrostatic supports 12 connected by channels 14 to the hydraulic pump system 1. The spindle 11 is driven by an electric motor 28 through a gear transmission 29. The spindle has a socket for mounting the tested sample. In the lower part, the bearing 8 of the loading piston 9 is supported by a screw mechanism for lowering the lower sample during sample exchange.

By replacing the lower handle 18 it is possible to use this test rig as a four kilo machine.

The tested samples are immersed in the oil in the tank 19.

Figure 5.1.63.3 shows the mechanical part of the test head measuring system.

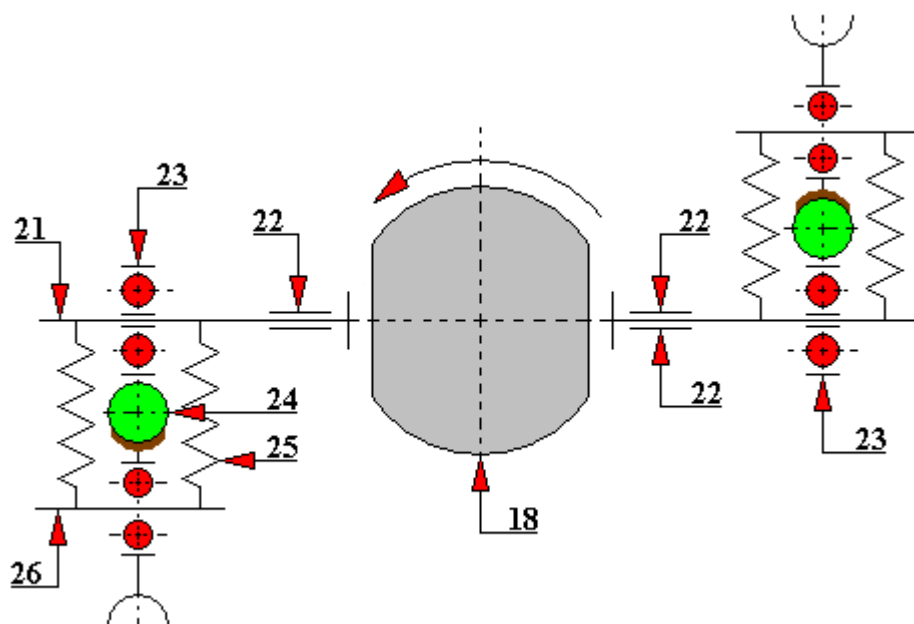


Fig. 4.1.63.3. Fragment of the measuring system of the test head of the test rig for testing sliding friction in a temperature-controlled lubricant according to the patent PL 95 008

18 - lower sleeve holder, 21 - strain gauge beam, 22 - strain gauge transducers, 23 - roller bearing, 24 - cantilever bar, 25 - spring, 26 - shaft

Between the sample (Fig. 4.1.63.2) mounted in the rotary spindle holder 11 and the sample mounted in the lower holder 18, a moment of friction is generated which is balanced by the pair of forces acting on the rolling bearings 23, mounted on dynamometric beams 21, resting on the cantilever bars 24 .

The strain gauge transducers 22, glued at the base of the dynamometer beams 21, are incorporated into a measuring electronic system which is not shown in the drawings. The dynamometric beams are attached to the lower samples holder 18.

4.1.64. Test rig for testing frictional resistance and wear of plastics according to the patent PL 119 178

The test rig for testing the frictional resistance and wear of plastics co-acting with steel at technically dry friction, built according to the patent PL 119 178, created by Kazimierz Ziemiański, is intended to determine the tribological characteristics of any types of plastics mating with steel at any temperature.

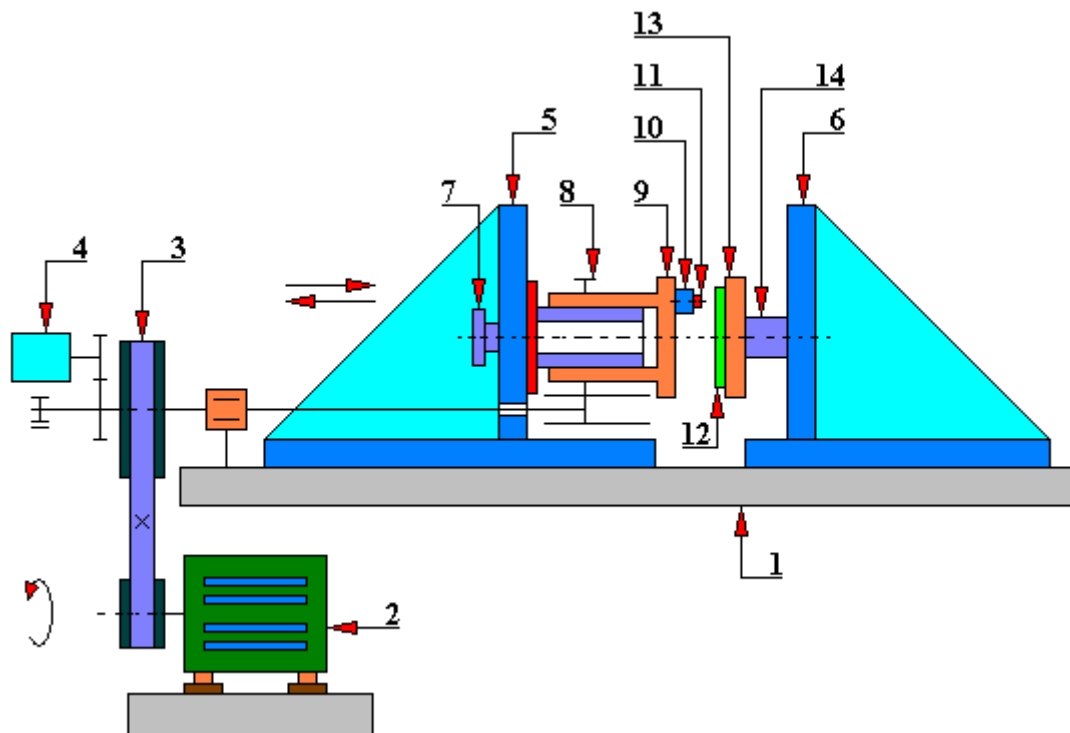


Fig. 4.1.64.1. A diagram of the test rig for testing frictional resistance and wear of plastics according to the patent 119 178.

1 - test rig body, 2 - drive motor, 3 - belt transmission, 4 - tachometer, 5 - pressure head, 6 - fixed head, 7 - cylinder stub pipe, 8 - toothed ring, 9 - rotating sleeve, 10 - tested sample holder, 11 - sample, 12 - counter-sample, 13 - plate holder of the counter-sample, 14 - measuring shaft with glued resistance strain gauges

The tribotester shown in Figure 4.1.64.1 consists of a body 1 to which a drive motor 2 is attached. This motor transmits the drive to the rotating sleeve 9 by means of a belt transmission 3. Two heads are attached to the body: pressure 5 and fixed (measuring) 6. The pressure head 5 is equipped with a cylinder ended with a stub pipe 7 through which air is supplied under pressure.

A toothed ring 8 is attached to the rotating sliding sleeve 9. A holder 10, in which the tested sample 11 is located, is fixed on the front surface of this sleeve. And in the stationary head 6, a counter-sample 12 is mounted in a plate holder 13. The holder 13 is mounted on a measuring shaft 14 on which resistance strain gauges are glued, connected with a measuring system used for determining the value of the twisting moment and the pressure force from which the friction resistance is calculated.

The pressure head 5 is moved pneumatically towards the stationary head 6. This solution provides a smooth pressure, with an adjustable value, of the sample 11 to the counter-sample surface 12.

An interesting solution used in this construction is the transfer of rotational motion from the motor 2 to the sleeve 9. The sleeve has a toothed ring 8 which is co-acting with a toothed wheel located on the drive shaft. This wheel has a width equal to the length of the sleeve 9 thanks to which the continuity of the meshing is ensured during the sliding and moving the sample surface towards the counter-sample.

The counter-sample 12 is replaceable. This solution makes it possible to mount counter-samples made of various materials in the plate holder 13.

In the stationary head 6, a heater spiral is embedded in the ceramic mass the purpose of which is to maintain the set temperature during tribotests.

The engine speed value is monitored by a tachometer 4 located in the drive system.

4.1.65. The measuring system of frictional resistance of the test rig for testing sliding friction in a temperature-controlled lubricant according to the patent PL 132 896

The measuring system according to the invention number PL 132 896, created by Tadeusz Łubiński, Olgierd Olszewski, Krzysztof Druet and Zbigniew Gadomski, is designed to determine the value of the sliding friction resistance in a temperature-controlled lubricant.

This measuring system, shown in Figures 4.1.65.1, 4.1.65.2 and 4.1.65.3, consists of the lower holder 1 for holding the sample 12. The holder is connected by means of pins 2 with two strain gauge beams 3 through a two-arm lever 4. On these pins mounted are slidably stirrups 5 which are connected by pre-tensed springs 6 with the cantilever 7 connected to the bearing sleeve 8 of the piston 9 embedded in the body 10.

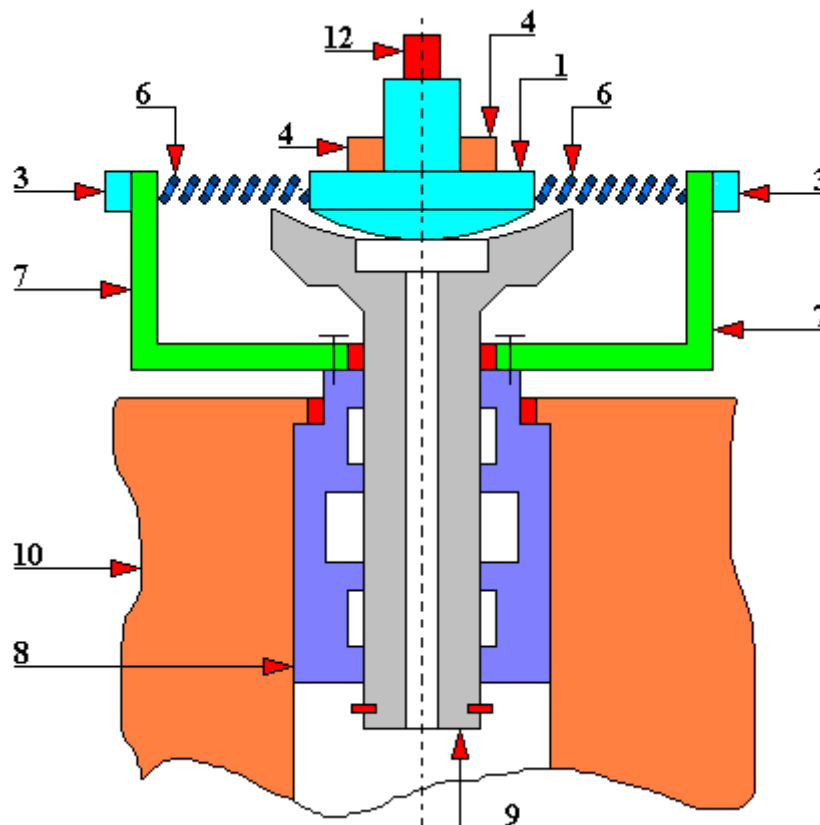


Fig. 4.1.65.1. A general diagram of the measuring system designed for determining the sliding friction resistance value in a temperature-controlled lubricant according to the patent PL 132 896 in an axial cross-section.

1 - lower holder for mounting the sample, 3 - two strain gauge beams, 6 - spring, 7 - cantilever, 8 - bearing sleeve, 9 - piston, 10 - body, 12 - sample

The essence of the operation of the system is as follows. A moment of friction arises between the mating surfaces of the sample 12 (fixed in the lower handle 1) and the counter-sample (fixed in the upper handle, not shown in these drawings) mounted in the rotating spindle. This moment is balanced by a pair of forces resulting from the change in the tension of the springs 6 which deflect the strain gauge beams 3. Strain gauges 13 connected to the measuring system are glued to these beams. The electronic system generates a signal depending on the value of the moment of friction.

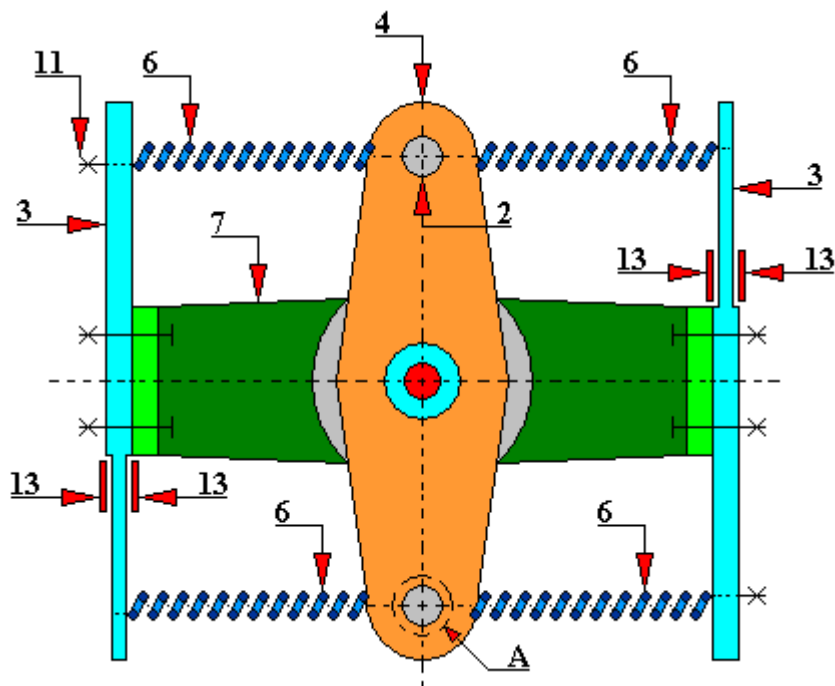


Fig. 4.1.65.2. A general diagram of the measuring system designed to determine the sliding friction resistance value in a temperature-controlled lubricant according to the patent PL 132 896 in top view.

2 - pin, 3 - two strain gauge beams, 4 - two-arm lever, 6 - spring, 7 - cantilever, 11 - screw, 13 - strain gauge transducer, A - detail on how to fasten the springs

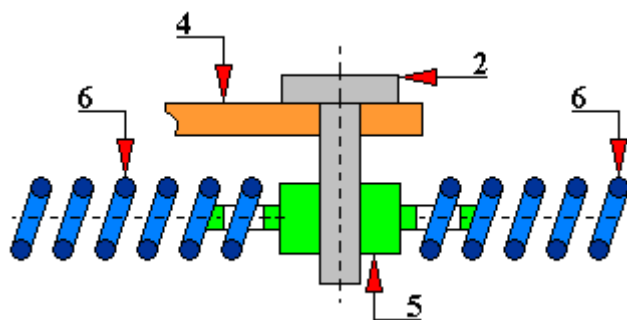


Fig. 4.1.65.3. Detail A from Figure 138.2 (not to scale).

2 - pin, 4 - two-arm lever, 5 - sliding stirrups, 6 - spring

4.1.66. Automatic unit designed to test the friction contact according to the patent RU 2165 077

An automatic unit for testing the friction contact enables testing both in static and dynamic conditions. Authors of this constructions are Buchanczienko S.J., Łarnonow S.A., Puzskarienko A.B. (Tomsk Polytechnic University, Tomsk, Russia). This test rig is presented in the patent database of the Russian Federation (Ruspatentu) with the number: RU 2165 077 C2.

The automatic test unit, shown in Figures 4.1.66.1 ÷ 4.1.66.5, is designed to test friction and wear of the roller-block friction contact in both static and dynamic conditions. It enables testing both lubricants and construction materials for building friction contacts. It includes a test rig for testing samples (friction test rig) 1 filled with the tested lubricant and equipped with mechanisms for fixing the tested samples 10, 11.

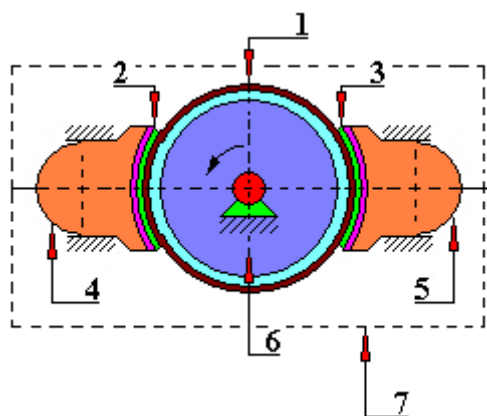


Fig. 4.1.66.1. Test chamber of the automatic test unit, a mechanical part.

1 - counter-sample, 2 - tested sample, 3 - tested sample, 4 - articulated support, 5 - articulated support, 6 - shaft, 7 - test chamber

This test rig is technically very advanced. It has, among others, programmable controllers, hydraulic and control units, etc. The main goal of such a high degree of technical advancement of this test rig is to increase the efficiency and reliability of the obtained test results and to bring the test conditions closer to the actual conditions existing in the operated friction contacts of test rigs and mechanisms.

The friction test rig has a test chamber connected to the circulation, filtration and thermoregulation system of the tested lubricant, allowing achieving inter alia the following set parameters:

- pressure in the test chamber,
- degree of purification of the tested lubricant,
- thermoregulation of the operating parameters of the tested friction contact according to various test conditions.

This test rig, thanks to the control and monitoring system of the given friction conditions allows to set and monitor the load forces of the tested friction contact.

The drive of the main motion of the counter-sample is transferred by a programmable DC electric motor that enables speed changes with simultaneous registration of the moment of friction occurring between the tested friction contacts.

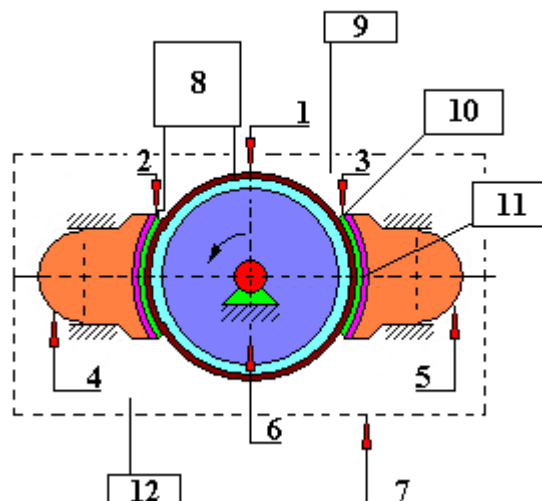


Fig. 4.1.66.2. Measurements of the test chamber of an automatic testing unit.

1 - counter-sample, 2 - tested sample, 3 - tested sample, 4 - articulated support, 5 - articulated support, 6 - shaft, 7 - test chamber, 8 – sensor of electro-resistance, 9 - thermocouple, 10 - thermocouple, 11 - thermocouple, 12 - thermocouple

In addition to the test chamber filled with the tested lubricant and tested samples, this automatic test unit includes mechanisms for fixing the test samples, electric motor of the working motion drive, servo-hydraulic systems for loading the tested samples which include a source of hydraulic energy, control elements, actuating mechanisms, pressure sensors, a sensor of total linear wear of the tested tribological system, a measurement and control unit with a computer as the central unit.

The test chamber contains a pressure gauge, a dynamic pressure sensor connected with an analog-digital relay of a microcontroller of the control system, a counter-sample mounted on a roller to which the tested samples - blocks are pressed. These blocks are positioned in counter-position in spherical handles that can rotate freely.

In the main motion control circuit installed is a test rig recording the moment of friction occurring in the tested friction contact. The source of the working drive is an electric motor connected to an analog-to-digital converter of the control system microcontroller.

The servo-hydraulic control system of the tested samples is additionally equipped with a pressure source stabilization block. The stabilization block is made of a pneumohydraulic accumulator connected to the pressure main of the entire test unit. It contains a manometer and a test rig recording the value of the applied pressure.

In the circuit controlling the load system applied is the programming and control equipment with proportional control, consisting of three autonomous units mounted on a common control panel with the possibility of separately connecting each of them depending on the load conditions of the tested samples (blocks). When switching on the first independent unit, represented by a programmable-control throttling hydraulic distributor with proportional control, two variants of its connection to work are possible:

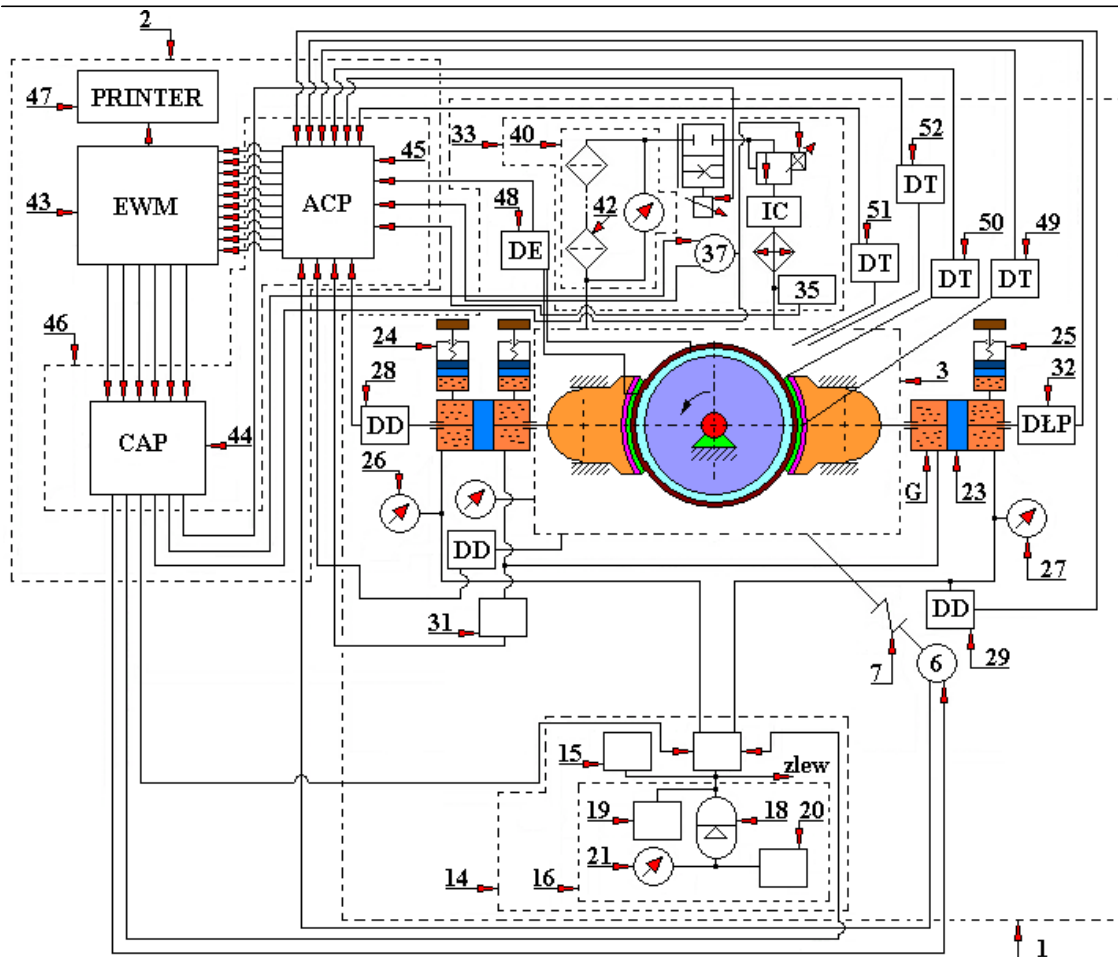


Fig. 4.1.66.3. Automatic unit designed to test the friction contact for static and dynamic conditions.

1 - friction test rig, 2 - control system, 3 - test chamber, 4 - pressure gauge, 5 - dynamic pressure (DD) sensor, 6 - programmable drive motor, 7 - clutch, 8 - shaft, 9 - counter-sample, 10, 11 - tested samples (blocks), 12, 13 - articulated supports, 14 - load system, 15 - hydraulic energy source (IGE), 16 - load level stabilizing block, 17 - programmer (GPU), 18 - pneumatic accumulator, 19 - hydraulic valve overflow, 20 - hydraulic energy source (IPE), 21 - pressure gauge, 22, 23 - a pair of plungers, 24, 25 - manual weights, 26, 27 - pressure gauges, 28, 29 - dynamic load sensors (DD), 30 - manual load, 31 - dynamic load (DD) sensor, 32 - photoelectric linear displacement sensor (DŁP), 33 - lubricant circulation, filtration and thermoregulation system, 34 - lubricant with a circulation sensor (IC), 35 - liquid purity control unit (PKCzRz), 36 - cooler, 37 - programmable DC motor, 38 - control programmer, 39 - control valve with a control heater, 40 - filter block, 41 - differential pressure gauge, 42 - main conduits filters, 43 - computer (EWM), 44 - digital-to-analog converter (CAP), 45 - analog-to-digital converter (ACP), 46 - microcontroller, 47 - printer, 48 - electro-resistance sensor (DE), 49, 50, 51, 52 - temperature sensors (DT)

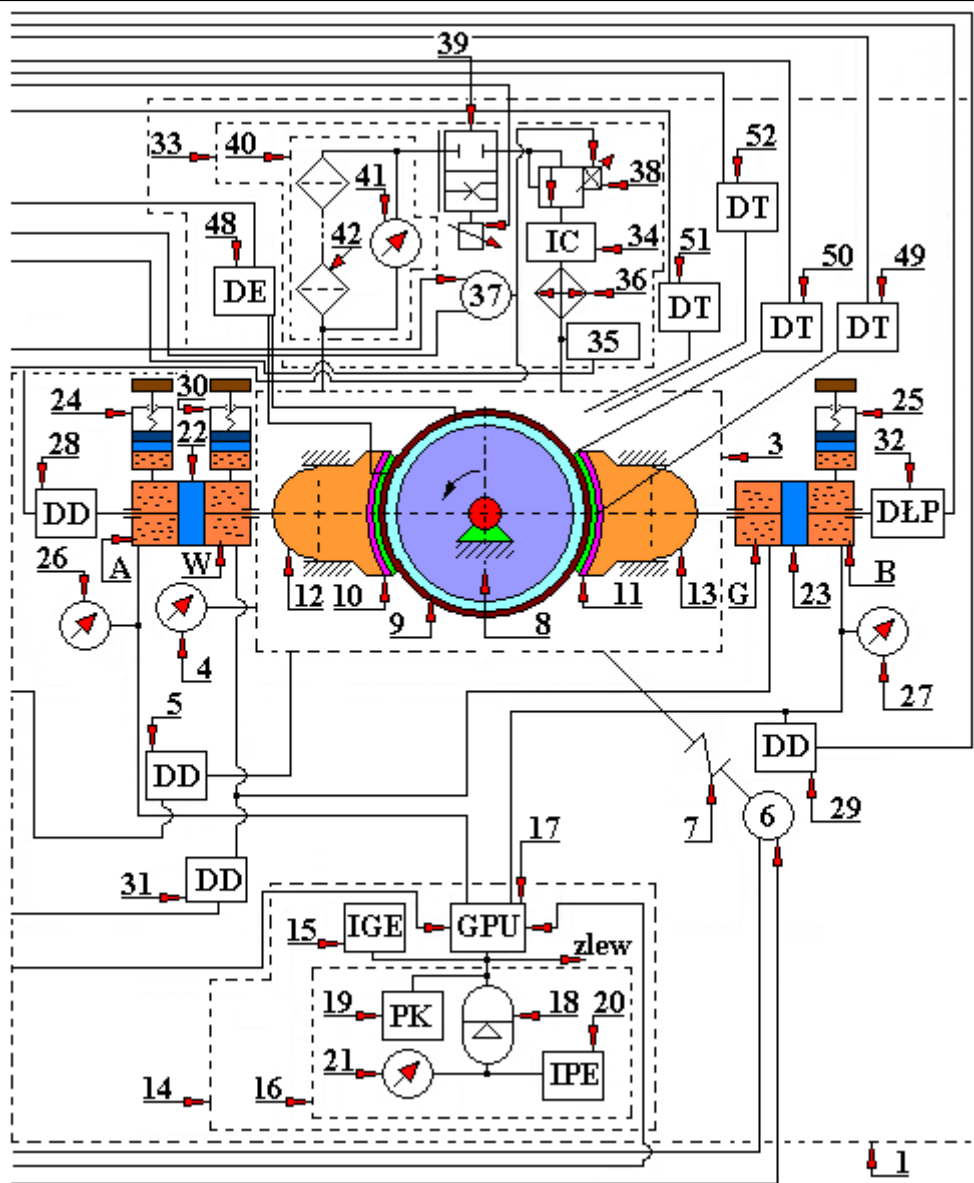


Fig. 4.1.66.4. An automatic test unit, a friction test rig (basic part)

1 - friction test rig, 3 - test chamber, 4 - pressure gauge, 5 - dynamic pressure (DD) sensor, 6 - programmable drive motor, 7 - clutch, 8 - shaft, 9 - counter-sample, 10, 11 - tested samples (blocks), 12, 13 - articulated supports, 14 - load system, 15 - hydraulic energy source (IGE), 16 - load level stabilizing block, 17 - programmer (GPU), 18 - pneumatic accumulator, 19 - hydraulic overflow valve, 20 - source hydraulic energy (IPE), 21 - pressure gauge, 22, 23 - pair of plungers, 24, 25 - manual weights, 26, 27 - pressure gauges, 28, 29 - dynamic load sensors (DD), 30 - manual load, 31 - dynamic load sensor (DD), 32 - photoelectric linear displacement sensor (DŁP), 33 - lubricant circulation, filtration and thermoregulation system, 34 - lubricant with a circulation sensor (IC), 35 - liquid purity control unit (PKCzRz), 36 - cooler, 37 - programmable DC motor, 38 - control programmer, 39 - control valve with a control heater, 40 - filter block, 41 - differential pressure gauge, 42 - main conduits filters, 48 - electro-resistance sensor (DE), 49, 50, 51, 52 - temperature sensors (DT)

- a) the first variant - one of its control channels was connected to two pressure channels of the double-acting plunger pairs, while its other control channel was connected to the release.
- b) the second variant - its control channels were connected to the respective pressure channels of each of the double-acting plunger pairs.

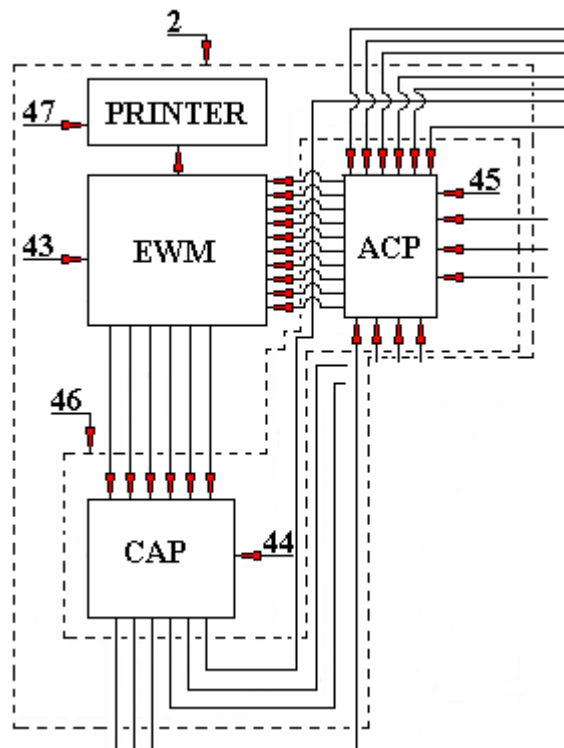


Fig. 4.1.66.5. Control system layout and its input / output ports for the automatic friction contact test unit
 2 - control system, 43 - computer (EWM) 44 - digital-to-analog converter (CAP), 45 - analog-to-digital converter (ACP), 46 - microcontroller, 47 - printer

When switching on the second independent unit, consisting of two programmable-control hydraulic safety valves with a proportional control, the control channel of each valve was connected to the corresponding pressure channel of only one of the double-acting plunger pairs.

When switching on the third independent unit, consisting of two programmable-control throttling valves, the control channel of each of the throttling valves was connected to the corresponding pressure channels of one of the double-acting plunger pairs.

A programmable-control hydraulic equipment is connected to the source of hydraulic energy, a block of its stabilization, and to a digital-to-analog converter of the control system microcontroller. This equipment enables simultaneous application of identical or different loads on the test samples / blocks.

The executive mechanisms are two double-acting plunger pairs mounted as opposing. The pressure applied to them can be set by means of a program or manually by means of two manual regulators. These plungers have two manometers, two dynamic pressure sensors connected to the ports of analog-to-digital converter of the microcontroller of the control system.

On the face of one of the plunger pairs fitted is a tip of photoelectric linear displacement sensor connected to the ports of analog-to-digital microcontroller of the control system.

Generally, one can say that the automatic unit for tribological tests consists of two basic systems: friction test rig 1 and control system 2 (Fig. 4.1.66.3). The friction test rig 1 comprises a sliding test chamber 3 mounted on a bearing unit (not shown in the drawings) in which mounted is a pressure gauge 4 with a dynamic pressure sensor (DD) 5. The test chamber unit 3 includes a programmable-controlling DC electric motor 6 which controls the main motion (its rotation frequency ranges from 0 to 6000 rpm with a torque value from 0.5 Nm to 2 Nm). At the end of the motor shaft 6, the shaft 8 and the counter-sample 9 were mounted on the tensioning conical rings (not shown in the drawing) by means of a rigid muff 7. A counter-sample 9 co-acts with test samples/blocks 10 and 11 mounted as opposing in a self-aligning ball supports 12 and 13.

The load system 14 (Fig. 4.1.66.3) of the tribological pair consists of a hydraulic energy source (IGE) 15, a pressure main which is connected to the stabilization block 16 of the pressure supply level (inlet) and a programmable-control hydraulic test rig with a proportional control (GPU) 17. A programming-controlling test rig with a proportional control 17 consists of three independent units:

- a program-control throttle valve of the hydraulic distributor with a proportional control 17 (Fig. 4.1.66.6 and Fig. 4.1.66.7); two program-control hydraulic safety valves 17 (Fig. 4.1.66.8);
- and two program-control hydraulic throttle valves with a proportional control 17 (Fig. 4.1.66.9) mounted on one panel (not shown in the drawing).

The use of these high-quality independent units extends the range of possibilities of variants of the programmed load of the tested samples/blocks 10 and 11. The pressure source level stabilization block 16 has a pneumo-hydroaccumulator 18 (Fig. 4.1.66.3), a hydraulic cavity which is connected to the pressure main of the hydraulic energy source 15 and to the hydraulic overflow valve (PK) 19. And its pneumatic cavity is connected to the pressure main of the hydraulic energy source (IPE) 20 and to the pressure gauge 21.

The pressure cavities A and B of the plunger pairs 22 and 23 are designed to provide loading pressure, and are connected to manual loads 24 and 25, pressure gauges 26, 27 and dynamic pressure sensors (DD) 28 and 29. And in the W and G cavities mounted are measuring surfaces of the total linear wear of the tested friction contact. The surfaces (cavities) W and G of the plunger pairs 22 and 23 are connected to each other and filled with a working fluid (lubricant) with its predetermined physico-chemical parameters. The sensitivity of the measuring unit for measuring the total linear wear of the tested samples depends to some extent on the quality of the tested lubricant. The cavities W and G are connected to a manual load 30 and to a dynamic pressure sensor (DD) 31.

A photoelectric linear displacement sensor (DŁP) 32 rests on the front surface of the plunger pair 23 with its measuring tip. The control channels of the program-control hydro-machine with a proportional control 17 are connected to the load cavities A and B of the double-acting plunger pairs 22 and 23.

The lubricant circulation, filtration and thermoregulation system 33 includes a circulation source (IC) of the tested lubricant 34, in the suction part of the main where installed is a liquid purity control unit (PKCzŻ) 35 and a radiator 36, cooling with a programmable-control DC electric motor 37 (rotational speed from 0 to 1000 rpm and torque from 0 to 2 Nm), mounted at the required (desired) distance from it, depending on the programmed temperature of the tested lubricant and connected with the test chamber drain 3.

The pressure part of the main of the circulation source of the tested lubricant 34 is connected to a hydraulic control safety valve 38, at the outlet of which a hydraulic heating throttle for the tested lubricant 39 and a filtration block 40 are mounted.

The filtration block 40 contains a differential pressure gauge 41 whose one measuring tip is connected to the hydraulic line (main) at its inlet to the filtration block (on the pumping) 40, while the other tip - at the outlet from this filtration block, and arterial filters 42 mounted in series. These filters have different granulation, i.e. they are characterized by a different degree of purification of the tested lubricating liquid. Their number can be selected depending on their characteristics and the desired degree of purification, and the pressure of the tested lubricant supplied by the circulation source 34.

The control system 2 comprises a computer (EWM) 43 connected by its I/O ports to a digital-to-analog converter (CAP) 44 and to an analog-to-digital converter (ACP) 45, which are included in the micro-controller unit 46. Computer I/O ports 43 are also connected to the printer 47.

The outputs of the digital-to-analog converter 44 are connected to:

- inputs of the programmable-control DC electric motor 6 of the main motion drive;
- inputs of the programmable-control hydro-machine with a proportional control 17;
- a programmable-control input of a DC electric motor 37;
- a programmable-control hydraulic safety valve input with a proportional control 38;
- input of programmable-control hydraulic throttle valve with a proportional control 39.

And the inputs of analog-to-digital converter 45 are connected to:

- dynamic pressure sensor outputs (DD) 5, 28, 29 and 31;
- the output of the programmable-controlling DC motor 6;
- the output of the linear displacement sensor (DLP) 32;
- the output of a programmable-controlling DC motor 37;
- the output of the liquid purity control unit (PKCzŻ) 35;
- an output of the electrical resistance sensor (variable resistance resistor) (DE) 48;
- temperature sensor outputs (DT) 49, 50, 51 and 52.

The electric resistance sensor (DE) 48 is mounted in such a way that one of its measuring tips is connected to the tested sample (block) 10, while its other measuring tip is connected to the counter-sample surface 9.

The measuring tip of the temperature sensor (DT) 49 was placed in the center (middle) of the tested sample (block) 11.

The measuring tip of the temperature sensor (DT) 50 is attached to the counter-sample 9 directly at the exit from the friction zone.

Temperature sensors 51 and 52 are positioned at the desired distance from the friction zone opposite to each other.

Also, this test rig can be equipped with optional hydraulic energy sensors (IGE) 15, tested lubricant circulation sensors (IC) 34, pumps or pump center units, pneumatic energy sensors (IPE) 20, pneumatic pumps (compressors) or center units of these pumps, arterial filters 42 of any design (mesh, magnetic, scheelite, plunge and others).

The automatic unit (set) for tribological tests works as follows:

1. Before starting the test we put the roller (disc) 8 on the outgoing end of the drive shaft on which the counter-sample 9 is mounted, while the tested samples/blocks 10 and 11 are mounted in self-adjusting ball holders 12 and 13.
2. After mounting the counter-sample 9 and samples 10 and 11, the test chamber 3 is sealed (air-tight sealing). The process of sealing is validated (a report is generated). If the report is negative, the computer will not allow further steps.
3. Next, in the control system 2, the initial and boundary conditions for carrying out the test are formulated (determined) by means of a computer (EWM) 43 according to, among others, the degree of filtration of the tested lubricant, the pressure in the contacts of the

- load system, the character of tests (static/dynamic test conditions), temperature values of the tested lubricant, rotational speed of the counter-sample, etc.
4. Before starting the test rig, all units are checked - the computer "polls" all units under its control. If the test result is negative, the test rig will not start up. The process of checking the efficiency of all units is generally supervised by the control system 2 via the computer (EWM) 43 which in turn provides the supply voltage to all control units via a digital-to-analog converter 44. The feedback signals from these instruments are converted, amplified and routed to the computer (EWM) 43 via an analog-to-digital converter 45. All information about the course of the experiment is mapped in the form of tables and graphs, both on the desktop of the computer monitor (EWM) 43 and on the printout presented by the printer 47.
 5. After determining the operating conditions, the test rig starts up. As the first one switched on is the system of circulation, filtration and thermoregulation 33 of the tested lubricant, as a result of which the lubricant with the circulation source (IC) 34 is supplied under constant pressure to the programmable-control hydraulic safety valve 38 which changes its pressure according to a set program and supplies the lubricant to the hydraulic throttle valve 39. From the throttle valve, the lubricant is fed to the filtration block 40 where it is purified to the required degree of purity in the arterial filters 42; the contamination of filters is determined on the basis of the indications of the differential pressure gauge 41. In this way, the heated and purified tested lubricant is fed to the test chamber 3 which when leaving it is directed to the cooler 36 cooled by a programmable-control DC electric motor 37 to a preset temperature. The pressure in the test chamber 3 for static test conditions is determined by the pressure gauge 4. And the value of the pressure in the test chamber 3 for variable/programmable test conditions is determined by the dynamic pressure sensor (DD) 5. The degree and intensity of wear of the tested parts/samples is determined by the liquid purity control unit (PKCzŻ) 35.
 6. When the lubricant temperature reaches the programmed value, the programmable-control DC electric motor 6 of the main (working) motion drive is started which transmits the rotational motion to the counter-sample through the rigid muff 7 and the load system 14 at idle speed.
 7. If all previous steps of this algorithm have been successful, the experiment begins.

The load of the tested friction contact may take place in two variants: statically or dynamically.

The static load on the tested samples/blocks 10 and 11 is achieved by applying equal or different pressures to the cavities of the loading surfaces A and B using manually adjustable load regulators 24 or 25. We learn about the size of the set values of the load regulators on the basis of the values of manometers 26 and 27.

The dynamic load conditions are achieved by means of the load system 14 which operates as follows. The source of hydraulic energy (IGE) 15 generates the pressure of the working fluid which is stabilized by the stabilization block 16 of the pressure supply level and transmitted to the programmable-control hydraulic machine with a proportional control 17, achieving programmed load conditions of the tested friction contact in the load cavities A and B of plunger pairs 22 and 23.

The hydraulic equipment includes, among others, three independent units:

- program-control throttle valve of the hydraulic distributor with a proportional control;
- two programmable-control hydraulic safety valves with proportional control;
- two programmable-control throttle valves with proportional control.

Activation of each of these units or their combination enables to obtain a different character of the friction contact operation, and thus a different course of the experiment.

When the first independent unit is put into operation, namely the programmable-control throttle valve of the hydraulic distributor with proportional control, when one of its control channels is simultaneously connected to two load cavities A and B of the double-acting plunger pairs 22 and 23, while the second control channel is connected to the release (the drain) (Fig. 4.1.66.6), we then obtain the alternate load of the tested samples/blocks 10 and 11, both for the same and for different load conditions. However, when each of its control channels is connected to the appropriate load cavities A and B of one of the double-acting plunger pairs 22 and 23 (Fig. 4.1.66.7), then we obtain the simultaneous load of the tested samples/blocks 10 and 11 for the same load conditions.

When switching on the second independent unit, namely two programmable-control hydraulic safety valves with proportional control, when the control channel of each valve is connected to the appropriate cavity A or B of one of the double-acting plunger pairs 22 and 23 (Fig. 4.1.66.8), then we obtain the simultaneous load of the tested samples/blocks 10 and 11 both for the same and for different loading conditions.

When the third independent unit is switched on, namely two programmable-control throttles with proportional control, when the control channel of each throttle valve is connected to the appropriate cavity A or B of one of the double-acting plunger pairs 22 and 23 (Fig. 4.1.66.9), obtained is a simultaneous load on the tested samples/blocks 10 and 11 for both the same and different load conditions.

The stabilization block 16 equalizes the level of pressure feeding the programmable-control hydro machine with a proportional control 17 by means of a pneumohydraulic accumulator 18 connected to a pneumatic cavity the pressure of which is supplied by means of a pneumatic energy source (IPE) 20 and recorded by a pressure gauge 21.

In order to measure the total linear wear of the tested friction contact, the cavities (surfaces) W and G of the plunger pairs 22 and 23 are used, previously filled with the working medium under the initial pressure, depending on the amount of the expected total linear wear of the friction contact and the load manually set on the manual regulator 30 which is recorded by the dynamic pressure sensor 31. And directly for the measurement of the total linear wear of the counter-sample 9 and the tested sample/block 11 used is the linear displacement sensor (DŁP) 32.

During the course of the experiment, the temperature is continuously recorded on the automatic unit designed to test the friction contact:

- in the friction zone - with a temperature sensor (DT) 49;
- directly at the exit from the friction zone - with a temperature sensor 50

on the basis of the difference we can determine the size and speed of temperature changes in the friction zone. In addition, the temperature field around the friction zone is recorded with the temperature sensors 51 and 52. According to the temperature value of the sensor 52, the control system 2 turns on/ off the cooling or heating of the tested lubricant by giving an appropriate signal either to the hydraulic throttle valve with proportional control 39 or to the DC electric motor 37.

The electrical resistance in the friction zone between the counter-sample 9 and the tested sample/block 10 is recorded by an electrical resistance sensor (DE) 48.

After completion of the test, the control system 2 transmits a control signal to disconnect all controllers and power sources of control units which is followed by a washing phase and a change of the type of tested lubricant, as well as the tested counter-sample 9 and samples/blocks 10 and 11, formulation of new initial and boundary test conditions and the process repeats itself.

In this design solution the use of an automatic tribological programmable-control unit of a DC electric motor 6 of the main motion drive, hydraulic machine with proportional control 17, a DC electric motor 37, a hydraulic safety valve with proportional control 38, a hydraulic throttle valve also with proportional control 39, a filtration block 40 of the tested lubricant allows to bring the test conditions as close as possible to the actual conditions prevailing in the friction contacts

of test rigs and mechanisms, with the possibility of shortening the time of testing and reducing their labor consumption to a minimum.

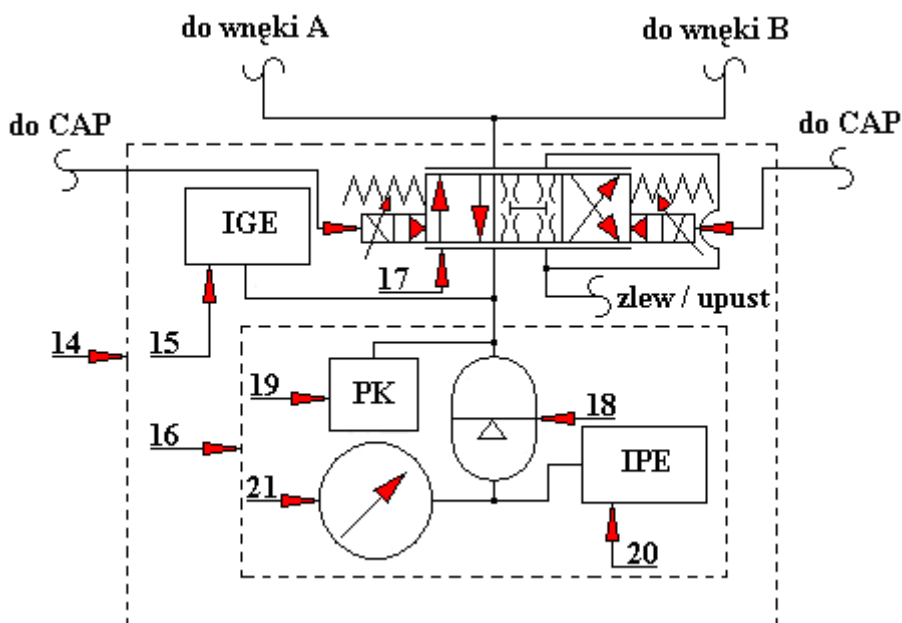


Fig. 4.1.66.6. A program-control system of the hydraulic distributor throttle valve with proportional control (the first independent unit of hydraulic machine). Connections for both the same and different load conditions

14 - load system, 15 - hydraulic energy source (IGE), 16 - load level stabilization block, 17 - programmer (GPU), 18 - pneumatic accumulator, 19 - hydraulic overflow valve (PK), 20 - hydraulic energy source, 21 - manometer, CAP (44) - digital-to-analog converter

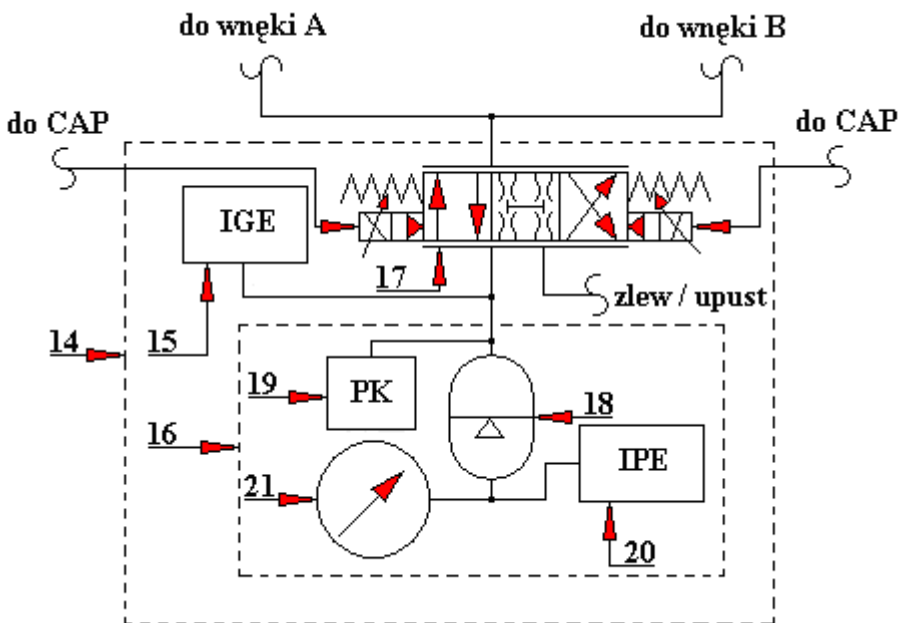


Fig. 4.1.66.7. A program-control system of the hydraulic distributor throttle with proportional control (the first independent unit of the hydraulic machine). Connection for equal load conditions

14 - load system, 15 - hydraulic energy source (IGE), 16 - load level stabilization block, 17 - programmer (GPU), 18 - pneumatic accumulator, 19 - hydraulic overflow valve (PK), 20 - hydraulic energy source, 21 - manometer, CAP (44) - digital-to-analog converter

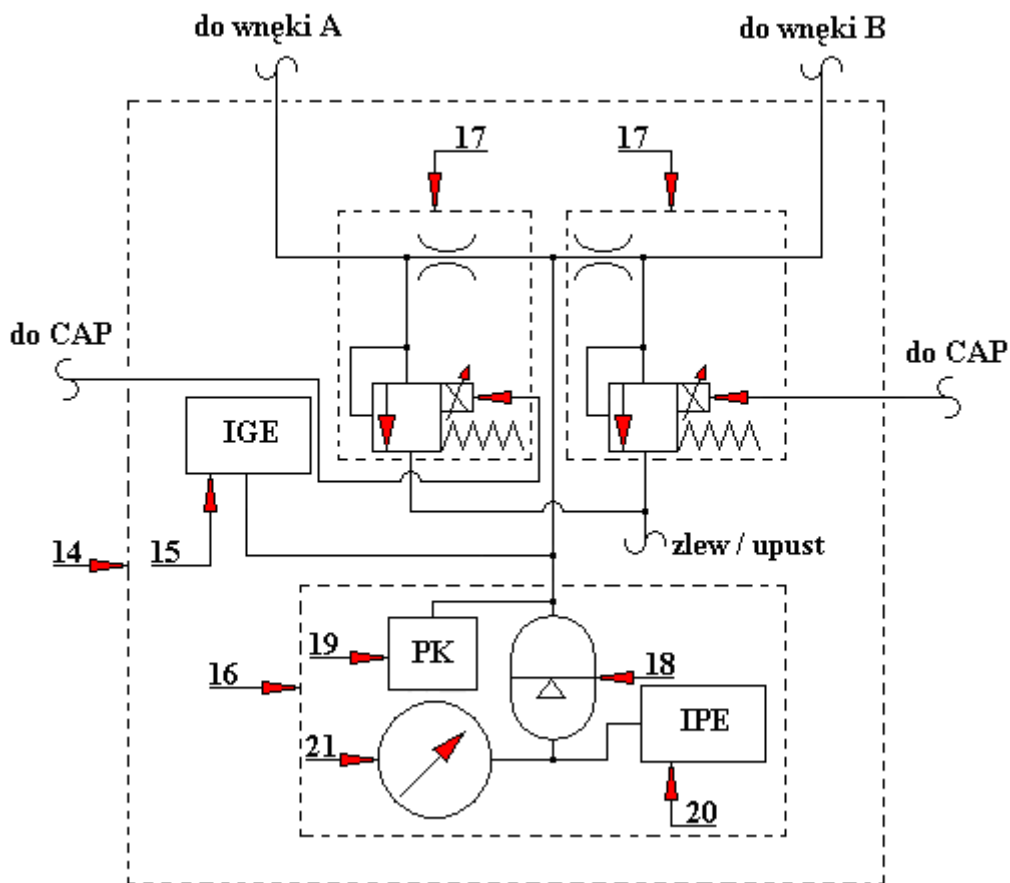


Fig. 4.1.66.8. A system of two programmable-control hydraulic safety valves with proportional control (second independent unit of the hydraulic machine)

14 - load system, 15 - hydraulic energy source (IGE), 16 - load level stabilization block, 17 - programmer (GPU), 18 - pneumatic accumulator, 19 - hydraulic overflow valve (PK), 20 - hydraulic energy source, 21 - manometer, CAP (44) - digital-to-analog converter

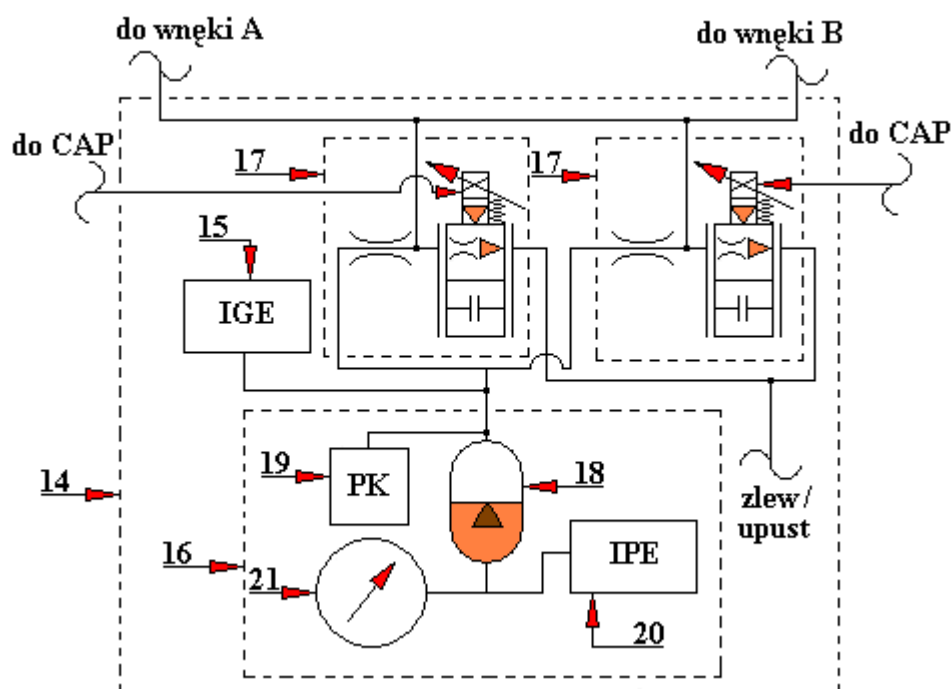


Fig. 4.1.66.9. A system of two programmable-control throttle valves with proportional control (the third independent unit of the hydraulic machine)

14 - load system, 15 - hydraulic energy source (IGE), 16 - load level stabilization block, 17 - programmer (GPU), 18 - pneumatic accumulator, 19 - hydraulic overflow valve (PK), 20 - hydraulic energy source, 21 - manometer, CAP (44) - digital-to-analog converter

4.1.67. Test chamber of a friction test rig with a ring-block friction contact according to the patent RU 2163 013 C2

The test chamber shown below in Fig. 4.1.67.1 and 4.1.67.2 of the friction test rig is designed to test liquid lubricants and to control and record the sum/total linear wear of the tested friction contact without its dismantling. The authors of this construction are Buchanczienko S.J., Łarnonow S.A., Puzskarienko A.B. (Tomsk Polytechnic University, Tomsk, Russia). This test rig is presented in the patent database of the Russian Federation (Ruspatentu) with the number: RU 2163 013 C2.

The test chamber of the friction test rig has a vertical structure and is mounted on a bearing contact 1 on which its body 2 is set containing the load block 3. The outer surface of the bearing contact 1 is realized by a tapered-threaded surface that co-acts with the inner tapered-threaded surface of the connector. In the holders (not shown in the drawings) of the bearing contact 1 there is a drive shaft 4, the input end of which is connected to the electric motor 5 of the main drive by means of a rigid muff 6 on tensioning conical rings (not shown in the drawings). And on the other end of this drive shaft 4, its output end, the shaft 7 is conically mounted. Counter-sample 10 is attached to the shaft 7 by means of a nut 8 and a spring washer 9.

A bearing contact 1, a body 2 and an electric motor 5 are rigidly mounted on the frame 11 of the friction test rig. In load block 3, two large plungers 12 and 13 and two small plungers 14 and 15, each double-acting, are mounted and rigidly tightened with nuts 16 and 17. The large plungers 12 and 13 rest on the small plungers 14 and 15, at the ends of which are mounted self-aligning ball holders 18 and 19 (Fig. 4.1.67.2) allowing free rotation in the prismatic guides 20 and 21 of the tested samples/blocks 24 and 25. The tested samples/blocks 24 and 25 are mounted in self-aligning ball holders 18 and 19 by means of cylindrical pins 22 and 23.

There is a resistance stub 26 in the nut 16, and a pressure sensor 27 in the nut 17. The frontal surfaces A and B are connected to each other by a rigid pipe 28 and to manual load regulators 29 and 30.

A system for recording the sum (total) linear wear of the tested friction contact was installed in the load block. It includes, among others, inter-plunger surfaces W and G (entering the load block 3 composed of an appropriate combination of large and small plungers: 12 to 14 and 13 to 15 and connected to the manual output override pressure regulator 31, pressure gauge 32 and dynamic pressure sensor 33 by means of a rigid tubular element 34 and connection ports 35 and 36).

In the outer part of the load block 3, a transparent cover 37 is mounted using a nut 38.

In order to feed the tested lubricant into the testing chamber of the friction test rig, a hole D was made, and in order to remove the lubricant from the chamber - a release/drain stub 39.

According to this design solution, the test chamber of the friction test rig works as follows:

At the output end of the drive shaft 4 fixed is a shaft/roller 7 made of a dielectric material characterized by both a low coefficient of thermal conductivity and a low coefficient of thermal expansion. The counter-sample 10 is placed on this shaft and secured against displacement by means of a nut 8 and a spring washer 9.

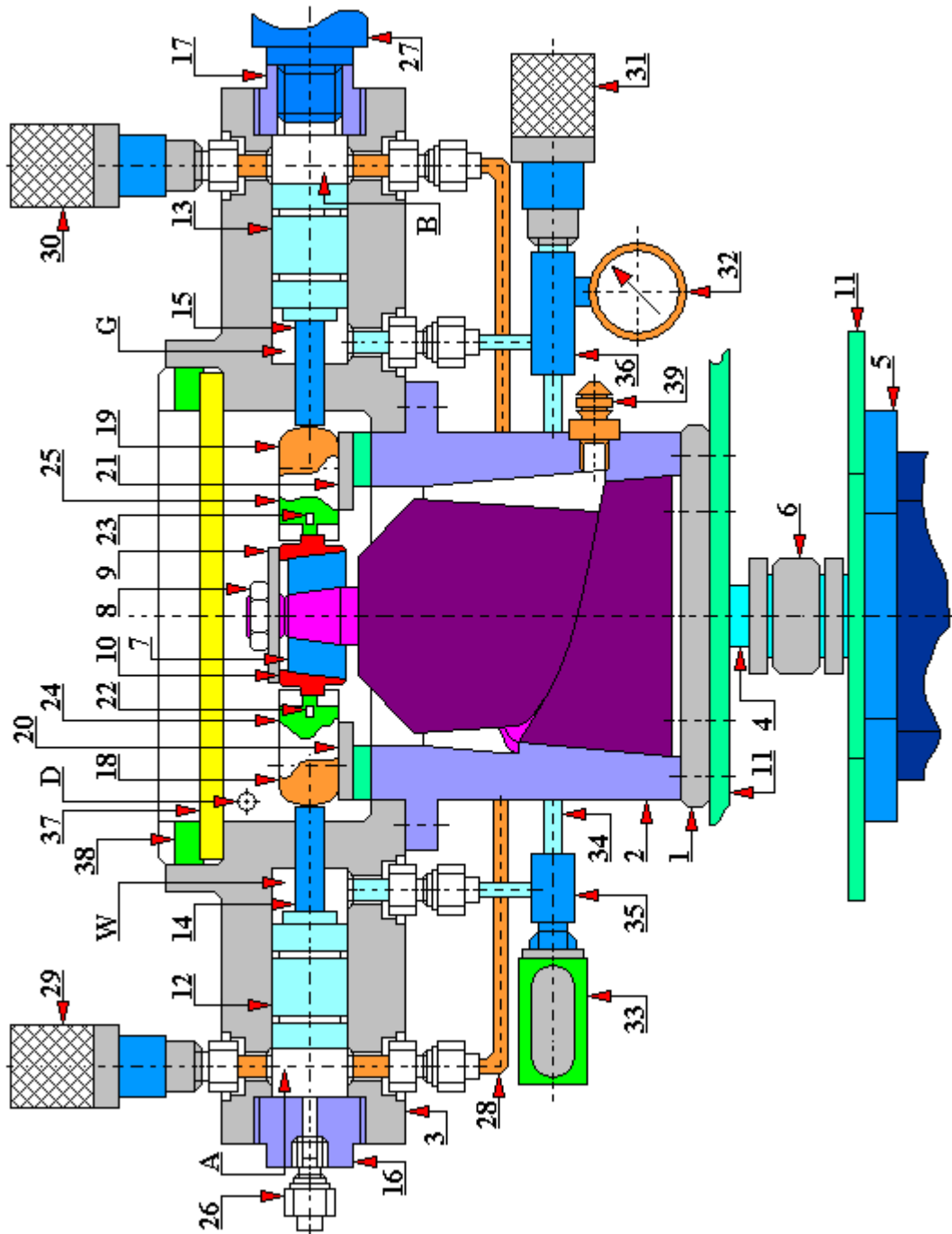


Fig. 4.1.67.1. The design of the testing chamber of a friction test rig with a ring-block friction contact according to the patent RU 2163 013 C2.

1 - bearing contact, 2 - body, 3 - load block, 4 - drive shaft, 5 - electric motor, 6 - rigid coupling, 7 - shaft, 8 - nut, 9 - spring washer, 10 - counter-sample, 11 - test rig frame 12 - large double-acting plunger, 13 - large double-acting plunger, 14 - small double-acting plunger, 15 - small double-acting plunger, 16 - nut, 17 - nut, 18 - self-adjusting articulated ball support (Fig. 4.1.67.1.), 19 - self-adjusting articulated ball support (Fig. 4.1.67.2.), 20 - guide, 21 - guide, 22 - parallel pin, 23 - parallel pin, 24 - sample/block, 25 - sample/block, 26 - pressure connector, 27 - pressure sensor, 28 - rigid pipeline 29 - manual (hand) load regulator, 30 - manual (hand) load regulator, 31 - manual (hand) output override pressure regulator, 32 - manometer, 33 - dynamic pressure sensor, 34 - rigid pipeline, 35 - connection stub, 36 - connection stub, 37 - transparent cover, 38 -

nut, 39 – release/drain connection, A- front face, B - front face, D - hole, W – inter-plunger area, G – inter-plunger area

The tested samples/blocks 24 and 25 are placed in self-aligning ball holders 18 and 19 which are free to rotate and move in prismatic guides 20 and 21. Samples 24 and 25 are attached to self-aligning ball holders 18 and 19 by roller pins 22 and 23.

After placing the tested samples in the ball holders, the transparent cover 37 is closed by means of a nut 38 and the chamber is sealed. The lubricant feeding hole D and the drain stub 33 are connected with the source of circulation of the tested lubricant and maintain its flow rate in the test chamber under the necessary pressure.

The electric motor 5 of the main motion drive is then started, rotating the counter-sample 10 by means of a rigid muff 6.

If the load on the tested samples/blocks 24 and 25 is achieved by means of a manual regulator, then a stopper (plug) is attached to the pressure stub 26 and the load on the friction contact is achieved by means of manual load regulators 29 and 30, thus creating override load pressure on annular surfaces A and B of large plungers 12 and 13. This pressure is applied to self-aligning ball holders 18 and 19 by small plungers 14 and 15. The amount of the loading pressure during the test is recorded by the pressure sensor 27.

When applying a dynamic load to the test samples/blocks, the pressure stub 26 connects to the pressure surface of the program-control servo element (not shown in the drawings).

During the running-in of the tested friction contact, the system of recording the sum (total) linear wear is filled with the tested working fluid. There is a relationship between the compressibility of the tested lubricant and the amount/volume of the loss of the mating friction contact. This dependence is used by the recording system of the linear wear. As a result, it is possible to determine with a certain accuracy the volume of loss of the friction contact without its dismantling. When testing in static conditions the total linear wear of the tested frictional pair is recorded according to the indications of the manometer 32. And in dynamic tests, the total linear wear is recorded according to the indications of the dynamic pressure sensor 33. Achieved in this way, both for dynamic and static tests, the initial override pressure of the lubricant outflow from the test chamber at the beginning of the test will show an absolute zero, i.e. indicate the beginning of the wear process of the counter-sample 10 and tested samples/blocks 24 and 25. According to the measure of how the wear process of the tested friction contact will proceed, the volume of the inter-plunger surfaces W and G will decrease. The intensity of this wear process can be determined simultaneously by measuring the surface diameters W and G and the compressibility of the tested working fluid. A greater intensity of the wear process causes a greater reduction in the pressure recorded by the pressure gauge 32 or the pressure sensor 33.

There are lubricant compositions in which there is no pressure reduction during the wear process, either on the pressure gauge 32 or on the sensor 33. On the contrary, there is a slight increase in pressure. However, there are not many such lubricants. Then, however, with this design solution of the friction test rig it is necessary in such cases to either increase the diameters of the large plungers 12 and 13 or reduce the diameters of the small plungers 14 and 15. There is also a third possibility - to change the tested lubricant so that its compressibility (pressure) is smaller.

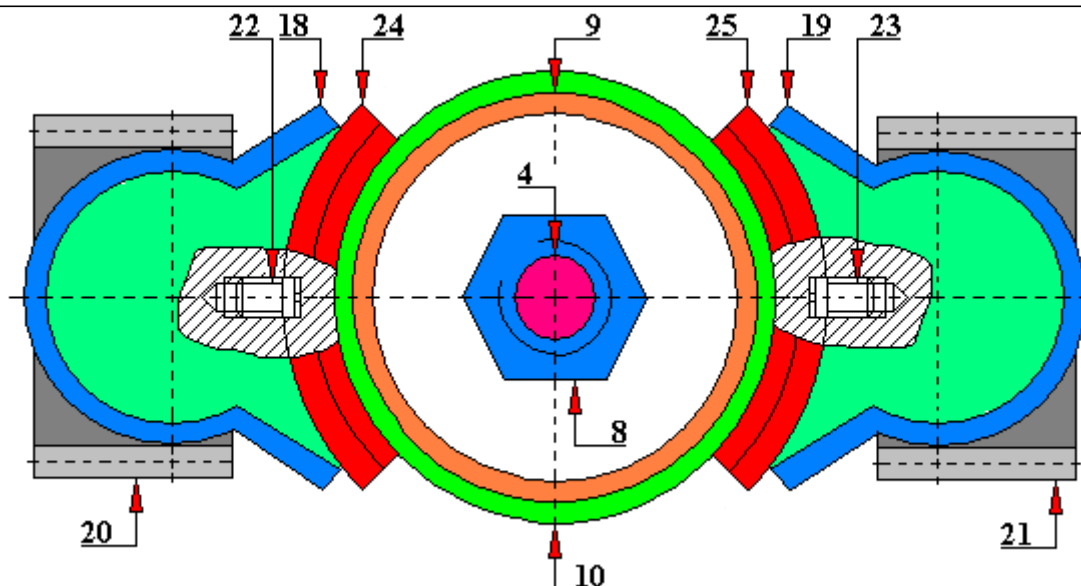


Fig. 4.1.67.2. Design of the self-adjusting articulated ball support of the friction test rig with a ring-block friction contact according to the patent RU 2163 013 C2.

4 - drive shaft, 8 - nut, 9 - spring washer, 10 - counter-sample, 18 - self-adjusting articulated ball support, 19 - self-adjusting articulated ball support, 20 - guide, 21 - guide, 22 - cylindrical pin, 23 - cylindrical pin, 24 - sample/block, 25 - sample/block

The use of a rigid muff 6 on the tapered tension rings and the use of fixation of the counter-sample 10 on the conical surfaces provides the transmission of the rotational motion of the counter-sample 10 with the lowest radial run-out in the tested friction mating. Vertical positioning of the test chamber allows a visual observation of the tested friction process or its monitoring (filming) through a transparent cover 37.

As the tested lubricant enters the test chamber tangentially to the inner cylindrical surface of the load block 3, a vortex stream is formed which entrains the abrasive particles formed in the friction process and removes them together with the tested lubricant from the test chamber by means of conical-threaded stub. The conical shape of the threaded stub makes it impossible for the formed abrasive particles to accumulate in one or more places but to keep them suspended inside the tested lubricant. The shape of this stub also ensures that these abrasive particles do not adhere to the wall of the body 2, even though the particles are pressed against it by a centrifugal force.

Due to the above-described effect, the abrasive particles formed during the wear process are all the time in the suspension of the tested lubricant and continuously escape from the inner surface of the test chamber.

The use of plunger pairs 12 and 14 as well as 13 and 15 as executive elements of the load block allows not only to achieve the required intensity and transmission of the hydraulic load signal of the tested friction contact but also to achieve minimal wear of the mating elements caused by friction in the plunger pairs themselves which is very important for creating real load conditions of the friction contact of test rigs and mechanisms. In this design solution the plunger pairs 12 and 14 as well as 13 and 15 were made as differential hydraulic cylinders allowing in parallel with the loading process to continuously record the total linear wear of the tested friction contact.

The use of self-adjusting ball holders 18 and 19 with pin mountings of the tested samples/blocks 24 and 25 allows to ensure the maximum possible tightness of their adherence to

the counter-sample surface 10, avoid their skewing when applying a load and limit the necessary maximum moment of frictional for the tested friction contact.

In order to increase the accuracy and credibility of the registration of the total linear wear of the tested friction contact, the pressure change of the tested lubricant was used.

4.1.68. Test rig for tribological tests of materials according to the patent SU 1219962 A

This test rig is intended for both tribological tests of construction materials and for tribological tests of lubricants (Fig. 4.1.68.1). This test rig was registered in the Patent Office of the Soviet Union under the number SU 1219962 A. Its inventors form a research team composed of: Prokopenko A. K., Garkunow D. N., Żigajło B. G., Bystrow W. N., Francjew W. N., Znajew W. A., Poljanin B. A. and Panfilow E. A.

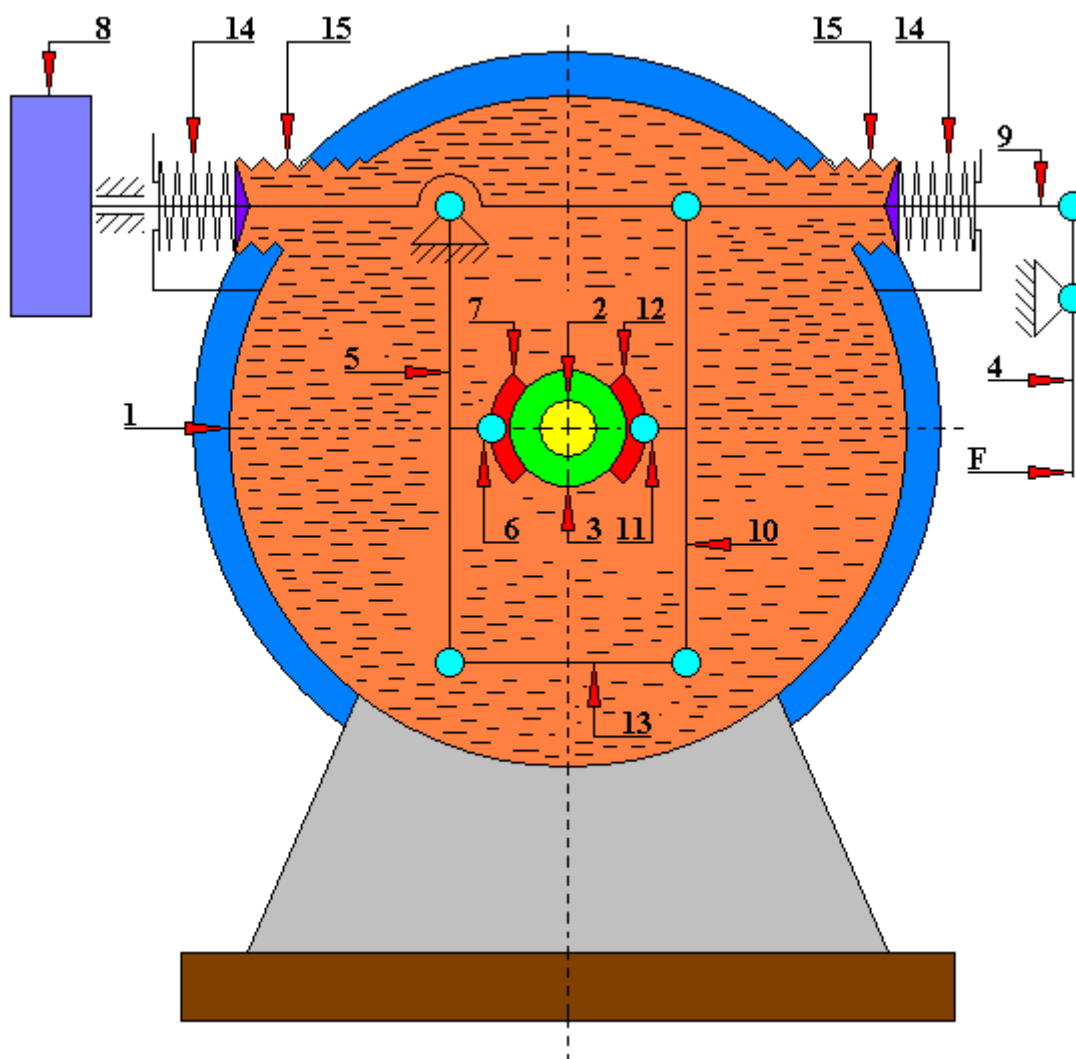


Fig. 4.1.68.1. A diagram of a test rig for tribological testing of materials according to the patent SU 1219962 A

1 - working chamber, 2 - drive shaft intended, among others, for fixing the sample, 3 - sample, 4 - load contact, 5 - first lever, 6 - counter-sample holder, 7 - first counter-sample, 8 - wear registration block, 9 - shaft, bar, 10 - second lever, 11 - counter-sample holder, 12 - second counter-sample, 13 - connector, 14 - spring, 15 - aneroid (syphon bellows)

The test rig for tribological testing of construction materials and lubricants includes a working chamber 1 in which there is a rotating shaft 2 for mounting the sample 3. Additionally, this test rig comprises a load contact 4 connected with a first lever 5 which is pivotally fixed in the

test chamber 1 and equipped with a holder 6 for securing the first counter-sample 7. And the second lever 10 together with the handle 11 is designed to fix the second counter-sample 12. The load contact 4 through the bar 9 is connected with the wear recording block 8. The connector 9, as shown in Figure 4.1.68.1, is articulated to the second lever 10 and then linked to the first lever 5 by a connector 13.

In order to increase the inertia of the connector 9 and increase its resistance to vibrations, the construction of the test rig uses springs 14 which are connected to the working chamber 1 and the connector 9 and placed outside the test rig to facilitate the regulation of their tension.

The test chamber 1 has aneroids (syphon bellows) 15 intended for its hermetization and damping the vibrations.

The test rig works as follows:

The tested sample 3 is mounted on the drive shaft 2, while counter-samples 7 and 12 are mounted in the handles 6 and 11. Then, the test chamber 1 is filled with the tested lubricant or lubricant composition and is hermetically sealed. By means of the load contact 4, a defined and controlled load of the tested friction contact is applied through a bar 9 kinematically associated with the first 5 and the second 10 lever provided with holders 6 and 11 for securing the counter-samples 7 and 12. The patent does not describe the method of applying the load. We do not know how it was applied, whether by means of a hydraulic system or by means of a sliding bolt/nut. The next step is to turn on the drive of the shaft 2 which is continuously variably regulated by an electric motor (not shown in the drawing). During the testing process, the total linear wear of co-acting elements is continuously recorded by means of the wear recording block 8. The wear recording block 8 may include a resistance sensor for the electrical resistance existing between sample 3 and counter samples 7 and 12. It is used mainly for metallic materials due to the need to conduct electricity.

The authors of this design solution ensure that the radial run-out of the shaft 2 does not affect the results of the measurements obtained from the wear recording block 8.

4.1.69. A tribometer for mandrel-disc fretting tests according to the patent application 396512

In the database of the Patent Office of the Republic of Poland there is a description of the construction of the tribometer with the application number 396512, which was not granted exclusivity rights. Yet, this test rig is an interesting technical solution intended for carrying out fretting tests which are technically difficult tests. The inventors of this construction are: Dudarew A., Dąbrowski J. R., Kulesza E., Sidun J. This test rig (Fig. 4.1.69.1) uses a mechanical system forcing the oscillating motion between a moving sample (disc) 7 and a stationary sample (mandrel) 8. In this kinematic pair, a conformal contact was used. The test rig is equipped with a commutator electric motor 3 with a cylindrical gear 4 which drives the system realizing the variable load of the sample and the motion forcing system. The load in this system is caused by the double-acting diaphragm actuator 2 co-acting with the spring 9. The applied load can be both constant and variable. The load is transferred to the contact point by means of the lever 1 and the sample 8 attached to it. The change of amplitude of the oscillating motion is made by changing the position of the joint on the arc lever 1 and it ranges from ± 0.01 [rad] to ± 0.06 [rad]. The permissible change of the friction radius (the distance between the mandrel and the table center) is from $0 \div 30$ [mm].

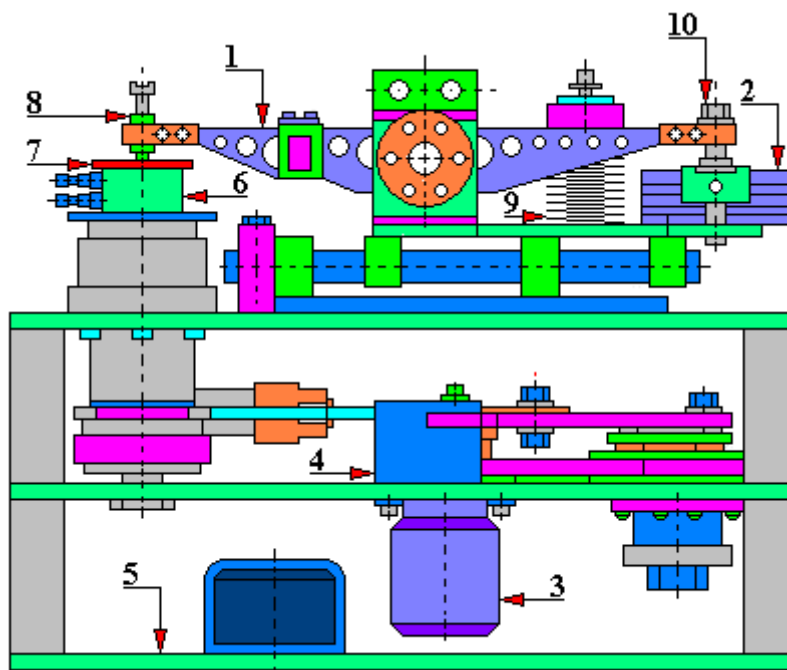


Fig. 4.1.69.1. A general design scheme of a tribometer for the mandrel-disc fretting tests, according to the patent application No. 396512

1 - lever, 2 - double-acting diaphragm actuator, 3 - electric motor, 4 - gear, 5 - test rig frame, 6 - replaceable rotary table, 7 - moving sample (disc), 8 - stationary sample (mandrel), 9 - spring, 10 - bolt fixing diaphragm actuator 2 to the lever 1

4.1.70. SKMR-2 fatigue test rig

The SKMR-2 fatigue test rig is an original non-commercial test rig built by the Laboratory of the Department of Machine Design and Operation at Gdańsk University of Technology (Fig. 4.1.70.1). It is intended, inter alia, to study the effect of load cycle asymmetry on the fatigue strength of the sliding layer/layers in bearing liners in various environments of lubricating oils or in the air.

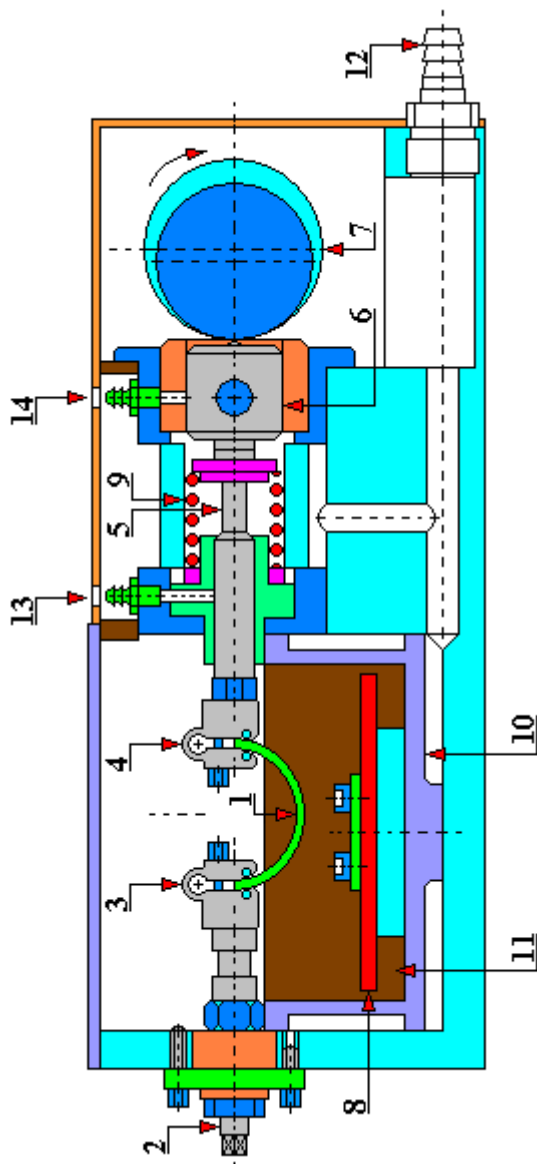


Fig. 4.1.70.1. General scheme of SKMR-2 test rig [186]

1 - tested sample, 2 - adjusting screw, 3 - stationary sample holder, 4 - movable sample holder, 5 - pusher, 6 - roller with a guide, 7 - eccentric, 8 - heater, 9 - spring, 10 - test chamber, 11 - tested lubricant, 12 - connection stub, 13 - pusher lubrication supply, 14 - roller lubrication supply with guide

This test rig has a test chamber with a controlled temperature of the lubricant thanks to which it is possible, for example, to conduct tests according to the ISO 7905-4 standard. The tested sample 1 (usually a thin-walled bearing shell) is placed in the air or in the lubricant 11 of

the test chamber 10. The test rig is driven by an electric motor which, by means of an eccentric 7 and pusher 5, causes cyclically changing bending stresses with an adjustable amplitude and average value in the tested layers of sample 1. The eccentric of the disc 7 has a radius that is adjustable in a certain range thanks to which it is possible to set the amount of kinematic excitations. The settings of excitations are made before the main test - at the stage of fitting the sample 1. Also the handle 3, which also functions as a dynamometer, has an adjustable position. This test rig has a built-in hydraulic system with an ultrathermostat enabling automatic regulation of the temperature of the lubricant or other liquid with an accuracy of 1°C.

The standard value of the load cycles performed on this tester is 3.6×10^6 . By means of a frequency converter, it is possible to regulate the rotational speed of the shaft with an eccentric disc. The values of excitations are set in the assembly conditions (at a temperature of approx. 25°C). Then, on the basis of the calibration characteristics of the measuring system of the test rig, the test results are converted into the value of stresses corresponding to the excitations with the given values at the temperature of carried out measurements.

4.1.71. Test rig for tribological tests with acoustic emission signals recording

A tribological test rig with acoustic emission signal recording consists of a 'ball-flat surface' friction contact and an acoustic emission measurement system. The authors of this design solution are Anna Piątkowska and Jacek Jagielski (Fig. 4.1.71.1).

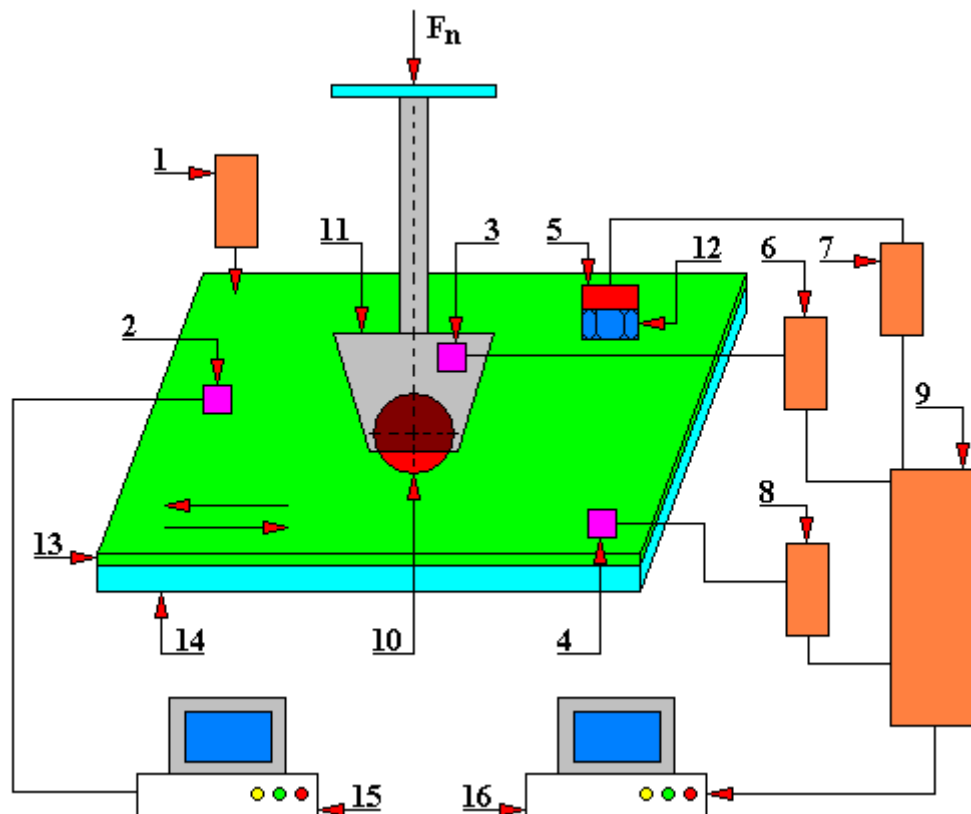


Fig. 4.1.71.1. A diagram of the test rig with acoustic emission signals recording [164]

1 - friction control system controlling the movement of rubbing objects, 2 - piezoelectric sensor for friction force measurement, 3 - high-frequency acoustic emission sensor, 4 - high-frequency acoustic emission sensor, 5 - accelerometer, 6 - conditioner, 7 - acoustic emission signal amplifier, 8 - emission signal amplifier acoustic emission, 9 - acoustic emission measurement card, 10 - ceramic ball (sample), 11 - ball holder, 12 - special intermediate nut, 13 - chrome coating (counter-sample), 14 - glass pane, 15 - computer designed to measure the friction force, 16 - computer designed to measure acoustic emission, F_n - pressing force

The acoustic emission measuring system of this test rig is made of a high-frequency sensor 3, a high-frequency sensor 4 and an accelerometer 5.

The measurement results of the acoustic signals, which are measured during friction, are recorded and analyzed using the FlexPro software on the computer 15. This program enables inter alia to determine the frequency and time descriptors characterizing the types of surface damage occurring during the friction process, e.g. cracking, accumulation of wear products, and separation of the layer from the substrate, abrasion.

In the presented test rig, the friction contact is made of a ceramic ball 10 and a chromium layer 13 with a thickness of 2 μm on a glass substrate 14.

During the friction process, vibroacoustic signals and acoustic emissions are emitted by the co-acting elements. These signals contain information about the course of the tested friction

process. Different types of friction contacts are likely to emit different vibroacoustic signals, as their character of operation is often different. The analysis of recorded acoustic signals can inform the user of the test rig or machine about processes occurring during the friction process, e.g. damage to friction surfaces, deformation processes, phase changes, micro-bumps of roughness peaks, chemical reactions. The area of knowledge in this field is currently little known. The signals generated during friction may simultaneously come from several/a dozen or so sources, overlap and partially distort/modify the obtained results. However, the authors of this rig predict that it will be possible to collect information on the initiation and development of damage as well as determine its size and type on the basis of the analysis of vibroacoustic signals.

During the mating of the ceramic ball 10, the sliding friction occurs over the chrome layer 13 with the reciprocating motion of the rubbing elements. The pressure force F_n is applied to the ball holder 11. The ball holder 11 and thus the ceramic ball 10 do not perform a rotational motion. The value of the contact force F_n may be constant or variable. The authors of this test rig carried out tests with the following force values F_n : 0.8 [N], 1.6 [N] and 2.4 [N]. Then the surface pressures obtained during friction were of the order of approx. 1 [GPa].

Probably due to numerous pieces of information received from the sensors installed on the test rig and the need to isolate the measurement paths, the authors of this design decided to use two independent measurement paths recording the received data on two different computers 15 and 16. The first path is intended only for recording changes in the friction force. And the second one is used to measure vibroacoustic signals and acoustic emission. The test rig is also equipped with its own system that controls the motions of the friction contact by means of a third computer (not shown in the figure). Thanks to this it is possible to program such displacement parameters as:

- acceleration,
- travelling time,
- rubbing speed,
- the number of cycles of reciprocating motion,
- stopping time in terminal (extreme) positions.

The following were used as executive elements:

- piezoelectric sensor 2 for measuring the friction force, type M209C12 PCB, incorporated into the sample holder 11, recording the friction force with a frequency of 10 measurements per second, VS550-Z high-frequency sensor 3 of acoustic emission with a frequency range of 400 ÷ 700 [kHz] mounted in a holder 11 of the ceramic ball 10,
- VS700-D high-frequency sensor 4 of acoustic emission with a frequency range of 60 ÷ 1950 [kHz] mounted directly on the surface of the ceramic ball 10,
- M352A60 type accelerometer 5 with the range of measured vibroacoustic frequencies 6 [Hz] ÷ 60 [kHz] attached to the ceramic surface of the ball 10 by gluing a special intermediate nut,
- a conditioner 6, type PA-1000, with a gain of 90 [dB] intended for amplification and compensation of vibroacoustic signals,
- acoustic emission signal amplifier 7, type AEP3, with a variable gain of 34 ÷ 49 [dB],
- acoustic emission signal amplifier 8, type AEP3, also with a variable gain of 34 ÷ 49 [dB],
- measuring card 9, manufactured by Energocontrol, with four analog input channels and equipped with a 24-bit converter operating with a maximum sampling frequency of 2 [MHz/channel].

At this test rig, multicycle tests can be carried out (reciprocating motion of co-acting elements takes place in a multiply repeated displacement cycle) or a single test can be performed. Measurements of acoustic emission signals were performed in 60-second intervals.

The following parameters were selected for the analysis of the acoustic emission signal by the authors of this test rig:

- changes in the amplitude of signals as a function of frequency (time-frequency characteristics STFT - Short-Time Fourier Transform),
- changes in the amplitude of the acoustic emission signal as a function of time (number of impulses above the assumed discrimination level, duration of impulses with maximum amplitude, maximum amplitude value, and time intervals between pulses).

The authors of the structure presented here state that this test rig enables the detection and recording of vibroacoustic signals related to microfriction, measurement of impulse signals, determination of the initiation and development of friction contact damage and determination of its type.

4.1.72. Test rig for accelerated wear testing of the piston-cylinder group of combustion engines

This test rig (Fig. 4.1.72.1 and 4.1.72.2) was developed by the Engine Testing Laboratory of Rzeszów University of Technology and is intended for qualification tests and tribological tests in conditions of increased dustiness of the combustion engine air.

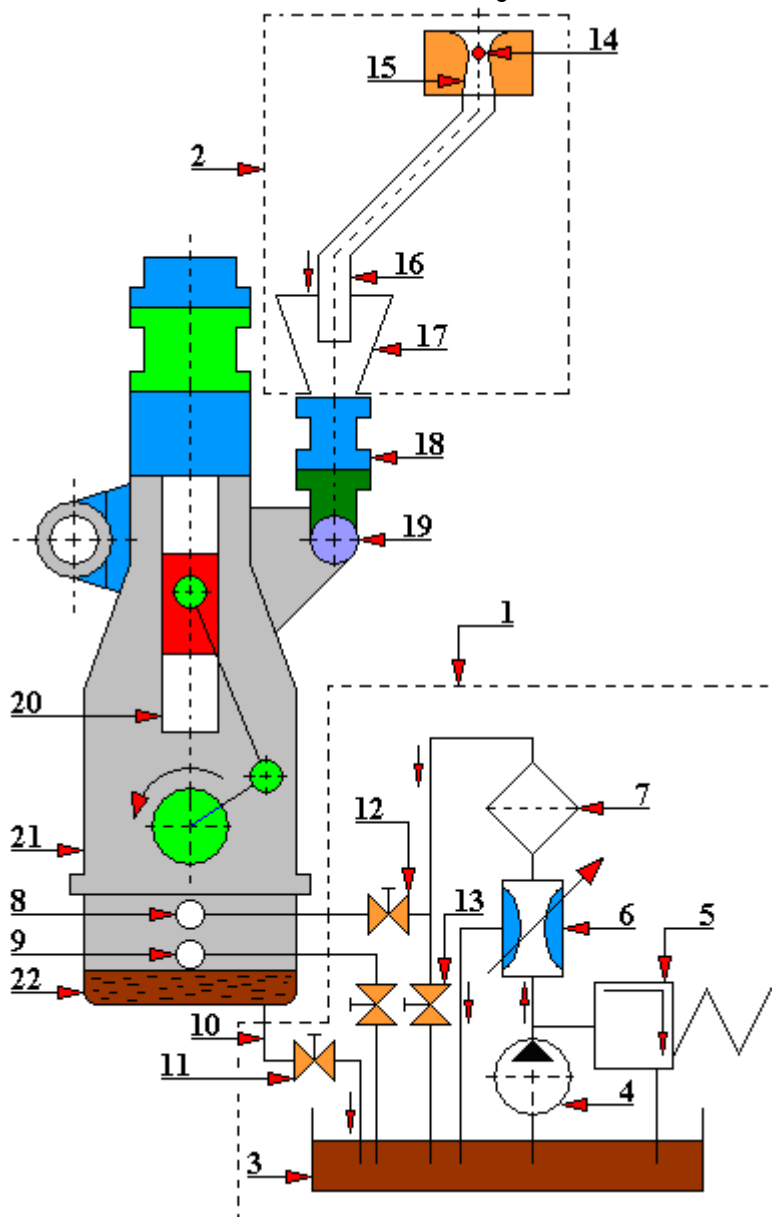


Fig. 4.1.72.1. A diagram of the test rig for accelerated wear testing of the piston-cylinder group of combustion engines [117]

1 - hydraulic system of additional oil cleaning, 2 - dusty material feeding unit, 3 - oil tank, 4 - oil pump, 5 - reducing valve, 6 - flow regulator, 7 - additional oil filter, 8 - inflow connector, 9 - drain connector, 10 - drain hose, 11 - shut-off valve, 12 - shut-off valve, 13 - shut-off valve, 14 - unit for accurate dispensing and spraying of dust, 15 - de Laval convergent-divergent nozzle, 16 - dust supply pipe, 17 - convergent nozzle, 18 - suction manifold, 19 - carburetor, 20 - piston-cylinder group, 21 - crankcase, 22 - oil pan

The equipment of this test rig includes a liquid brake (hydraulic) and control (not shown in the figures), road dust feeding and spraying system, lubricating oil fine filtration system, fuel supply system and air cooling system and lubricating oil cooling system (not shown in the drawings). The principle of operation of this test rig is as follows. Before fitting a given engine to be tested, all metrological measurements of the piston-cylinder system are performed which include the measurement of, among others:

- clearance of the pins in the piston holes,
- the height of the ring grooves in the pistons,
- piston diameters,
- clearances in locks,
- cylinder diameters in two sections and at several heights,
- the width and height of the piston rings.

After taking the measurements and re-fitting the engine, it is mounted on the wear test rig. Additionally, sensors for monitoring the process of its work are connected to it. Then, tests are carried out according to the developed test program. This test rig allows controlling the contamination of the inlet air to the combustion chamber. However, different requirements are necessary for example for aviation piston engines, and different for piston compressors, so the character of the test course is different for different drive units, depending on their intended use. After completing the tests, the tested engine is disassembled in order to perform metrological measurements again. On the basis of obtained results, conclusions are drawn in order to, for example, modernize the structure.

The piston-cylinder system is present, among others, in such piston operating machines as:

- combustion engines,
- compressors,
- pumps.

The tribological analysis of this system usually includes a cylinder liner, piston and rings. The factors determining the durability of the combustion engine are the friction conditions and the related wear of the mating elements of the piston-cylinder system [Priest M., Taylor C.M. 2000]. Along the piston travel there is a varying thickness of the oil film. As a result, we have different lubrication conditions, from boundary, mixed, to hydrodynamic lubrication in the middle section of the piston travel. As the main types of cylinder wear, the authors of [45, 116, 117] list:

- abrasive (dominant),
- corrosion,
- adhesive,
- fatigue,
- cavitation.

The test rig for accelerated wear testing of the piston-cylinder group of combustion engines enables to carry out qualification tests in the field of checking the technical characteristics and properties as well as economic and technical usability assessment, as well as to assess and determine the durability and reliability of a given combustion engine.

Figure 4.1.72.2. presents a diagram of a dust dispenser used on the test rig for accelerated testing of the piston-cylinder group of combustion engines. The principle of its work is as follows. In the sleeve 7 there is a dust 9 of known granulation which is acted on by the piston 8. This piston pushes the dust through the nozzle 14. The dust from the nozzle goes to de Leval chamber 10 which houses the disc 11. This disc additionally grinds and doses the dust material 9. De Leval nozzle 10 is powered by air 18. The broken up dust material 9 is directed to the tested combustion engine through the outlet 19. The operation of the piston 8 is controlled by a stepper motor 1 which by means of a gear transmission and contact, screw 5 - nut 6, moves the arm 20 of

the piston 8 by a preset value. The disc 11 has an independent drive, separate from the electric motor 13.

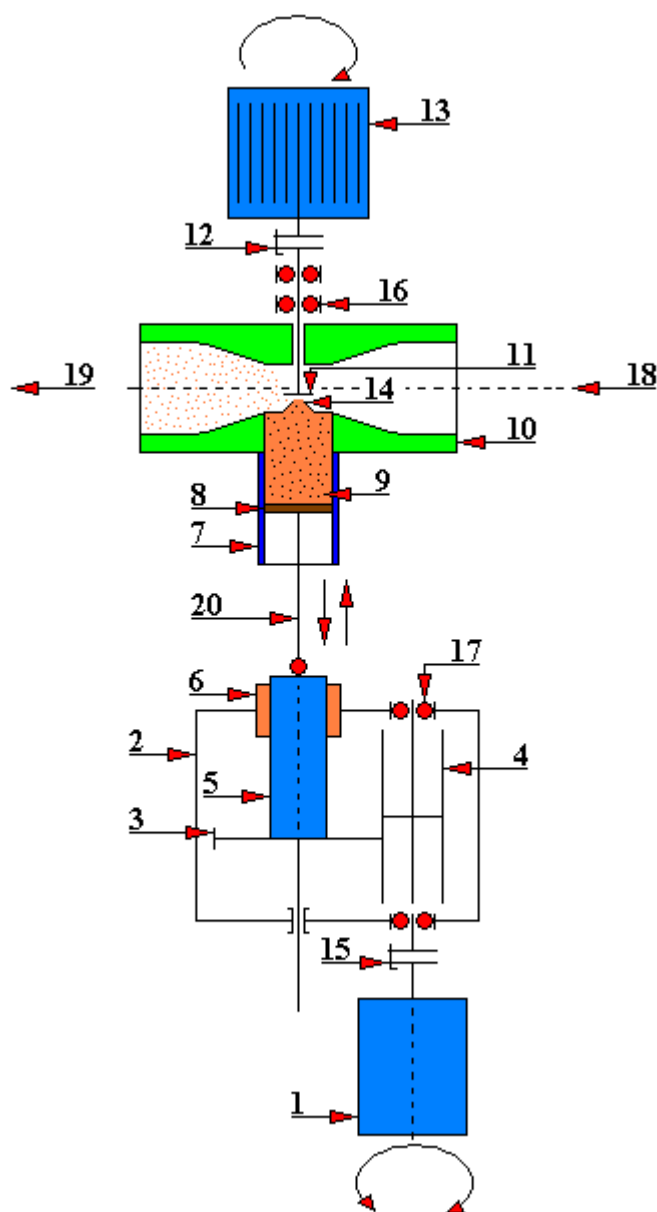


Fig. 4.1.72.2. A diagram of a dust dispenser for a test rig intended for accelerated wear testing of a piston-cylinder group of combustion engines [117]

1 - stepper motor, 2 - body of mechanical transmission, 3 - cylindrical gear, 4 - cylindrical gear, 5 - piston drive screw, 6 - nut, 7 - sleeve, 8 - piston, 9 - dust material, 10 - convergent-divergent de Laval nozzle, 11 - grinding disc, 12 - flexible coupling, 13 - electric motor, 14 - nozzle, 15 - flexible coupling, 16 - bearing, 17 - bearing, 18 - clean compressed air inlet, 19 - outlet of compressed air contaminated with dust material, 20 - piston arm

4.1.73. T-07 abrasion test rig

A test rig with the symbol T-07 is a commercial test rig manufactured by the Institute of Sustainable Technologies in Radom and it is designed to assess the wear resistance of metal materials or coatings when rubbing against loose abrasive. A general diagram of the test method used to test the abrasive wear resistance is shown in Figure 4.1.73.1. The abrasive is fed from the hopper to the area of the friction contact mating, i.e. a sample of the tested material and a rotating rubber roller. The pressing force is usually exerted by a sample of the tested material being most often steel. It is possible to adjust both the pressing force of the tested sample and the number of revolutions of the rubber roller.

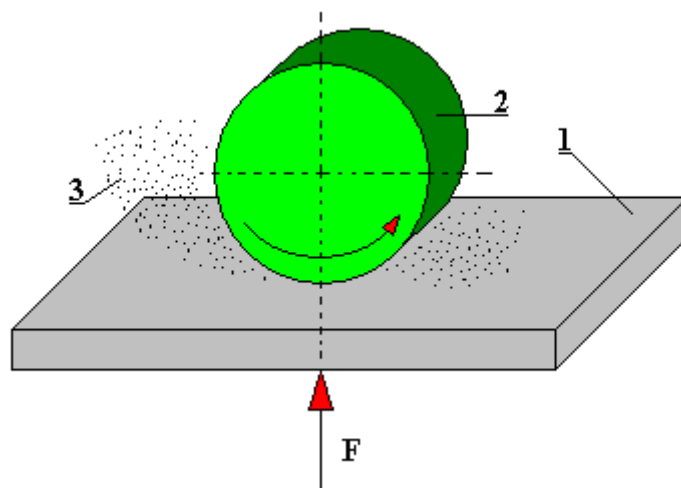


Fig. 4.1.73.1. The principle of operation of the T-07 abrasion test rig with the contact of mating elements of the roller-plane type

1 - sample of the tested material, 2 - rubber roller, 3 - abrasive, F - pressing force of the sample against the counter-sample

The basis for the development of the T-07 tribotester is a test rig for testing the abrasion of construction materials according to the patent PL 160596 whose authors are Jan Wulczyński and Witold Piekoszowski. The design solution provided in this patent application is presented in more detail in [Mikołajczyk J. 2018].

Fig. 5.1.73.2 shows the diagram of the T-07 test rig in a front view. This tribotester consists of three units:

- drive unit,
- loading unit,
- abrasive feeding unit.

The drive unit consists of: an electric motor 10 that drives the main shaft 5 through a toothed belt transmission 9 and a single-stage gear transmission 8. The shaft is seated in the body 12 by means of two cone bearings 6. A counter-sample 2 is attached to the other end of the main shaft 5. This counter-sample is in the shape of a roll and its outer part is made of a suitable type of rubber. This rubber is vulcanized to the steel hub. The structure of the counter-sample 2 used in the T-07 abrasion test rig is shown in Fig. 4.1.73.10.

The sample 1, shown in more detail in Fig. 4.1.73.11, is pressed against the counter-sample 2 by means of a loading unit. This assembly consists of a lever 6 (Fig. 4.1.73.13), a hanger 17, weights 7 and a clamping ring fixing the sample 1. The lever 6 (Fig. 4.1.73.3) in this design solution is supported on two needle bearings. The hanger 17 is designed to put a given load. The shape of steel weights used in the T-07 test rig is shown in Fig. 4.1.73.12.

The abrasive feeding unit (Fig. 4.1.73.3) consists of a reservoir for abrasive material 13 and a dosing rotary valve 15. The used abrasive is directed through the trough 8 to the reservoir 3. The dosing rotary valve 15 has an opening, with adjustable diameter, located near the tested friction contact. The movement of the abrasive towards the friction contact is made under the influence of gravity.

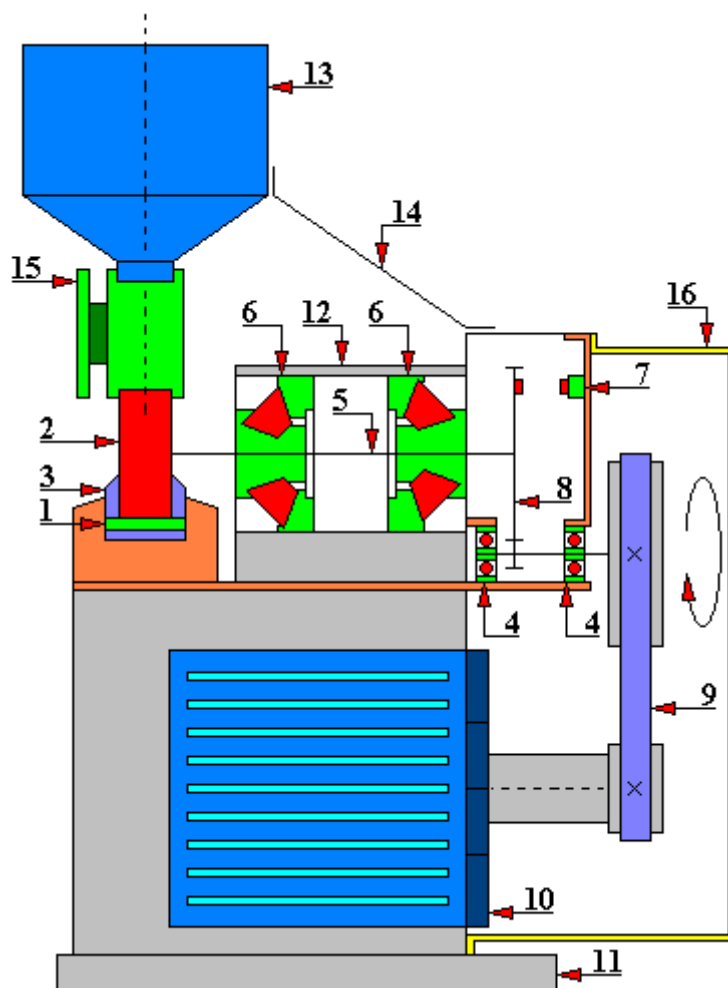


Fig. 4.1.73.2. A diagram of the T-07 abrasion test rig. Front view

1 - tested sample, 2 - counter-sample, 3 - clamping ring fixing the sample, 4 - single-row ball bearing, 5 - main shaft, 6 - cone bearing, 7 - rev counter sensor, 8 - single-stage gear transmission, 9 - toothed belt transmission, 10 - electric motor, 11 - base, 12 - body, 13 - reservoir for abrasive material, 14 – reservoir stiffening for abrasive material, 15 - dosing rotary valve, 16 - drive cover.

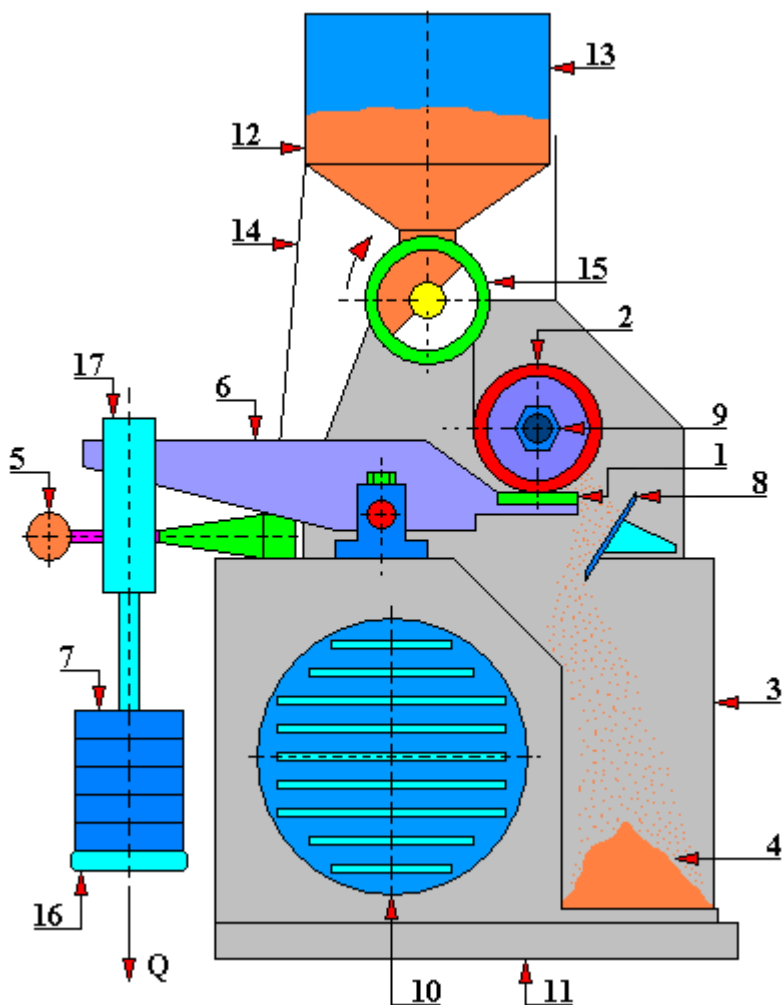


Fig. 4.1.73.3. A diagram of the T-07 abrasion test rig View from the side of the load contact
 1 - tested sample, 2 - counter-sample, 3 - reservoir for used abrasive material, 4 - used abrasive material, 5 - loading lever lock, 6 - loading lever, 7 - weights, 8 - used abrasive discharge trough, 9 - nut fixing the counter-sample, 10 - electric motor, 11 - base, 12 - abrasive material, 13 - reservoir for abrasive material, 14 - reservoir stiffening for the abrasive material, 15 - dosing rotary valve, 16 - hanger base, 17 - hanger, Q - preset load.

The following figures show:

- view of the test rig from the side of the friction contact (Fig. 4.1.73.4),
- view from the drive side (Fig. 4.1.73.5),
- view from the side of the load unit (Fig. 4.1.73.6),
- the way of mounting the sample in the tribotester (Fig. 4.1.73.7),
- diagram of mating of the friction contact: roller (counter-sample) - flat surface (sample) after mounting it in the clamping ring (Fig. 4.1.73.8),
- method of fixing the counter-sample (Fig. 4.1.73.9),
- structure of the counter-sample (Fig. 4.1.73.10),
- tested sample (Fig. 4.1.73.11).



Fig. 4.1.73.4. T-07 abrasion test rig View from the side of the load contact



Fig. 4.1.73.5. T-07 abrasion test rig. Serial number T-07/118/04 from 2004. View from the drive side



Fig. 4.1.73.6. T-07 abrasion test rig. Serial number T-07/118/04 from 2004. View from the side of the load unit

Fig. 4.1.73.7 shows the method of mounting the sample in the T-07 abrasion test rig. The tested sample 1 should be placed between the clamping ring 2 and lever 3. Then tighten with the bolt 4. When replacing the sample with a new one you must perform the above-mentioned steps in the reverse order. Both during the fixing of sample 1 and its removal it is necessary to disassemble the trough discharging the used abrasive to the reservoir for used abrasive.

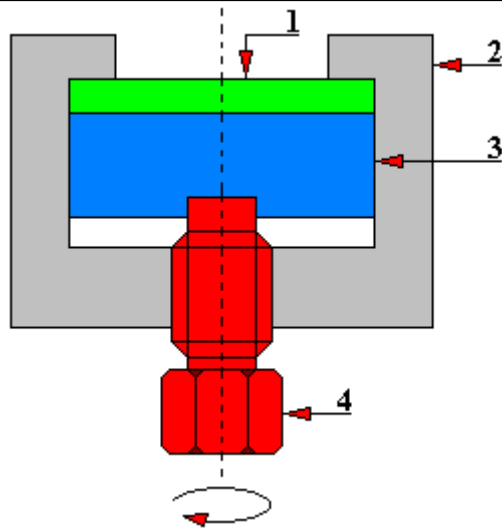


Fig. 4.1.73.7. The method of fixing the sample in the T-07 abrasion test rig
1 - test sample, 2 – clamping ring, 3 - loading lever, 4 - bolt

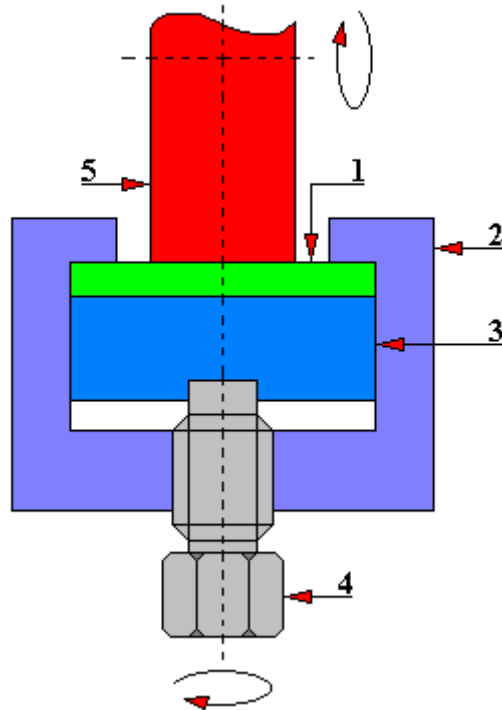


Fig. 4.1.73.8. A diagram of mating of the friction contact in the T-07 abrasion test rig
1 - tested sample, 2 – clamping ring, 3 - loading lever, 4 – bolt, 5 - rotating counter-sample in the form of a rubber disc

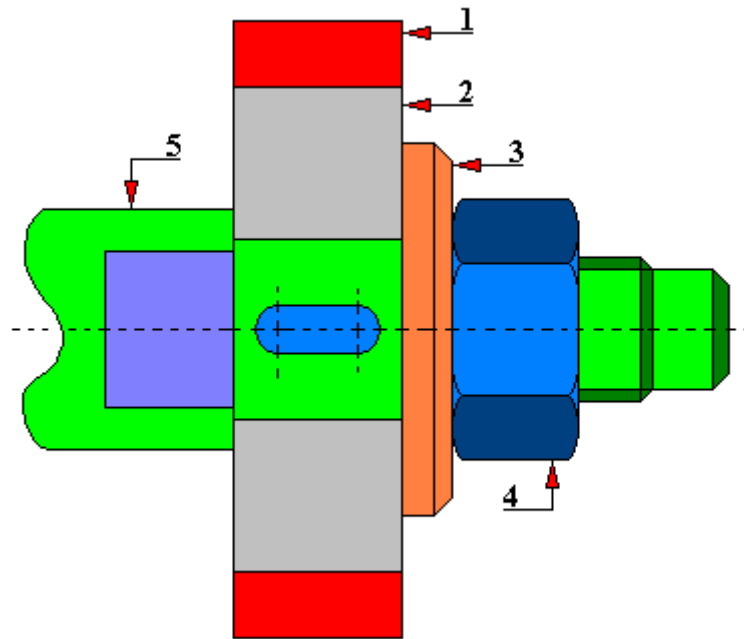


Fig. 4.1.73.9. The method of fixing the counter-sample in the T-07 abrasion test rig
 1 - counter-sample (part of the rubber disc), 2 - counter-sample (part of the steel hub), 3 - steel pressure washer, 4 - nut, 5 - main shaft

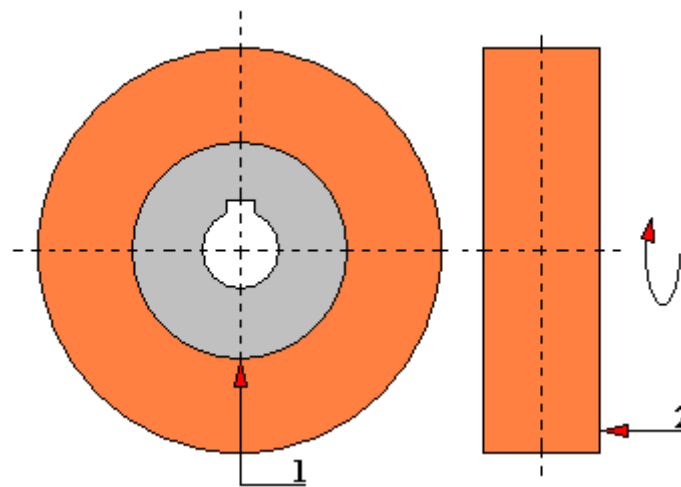


Fig. 4.1.73.10. The structure of the counter-sample applied in the T-07 abrasion test rig
 1 - steel hub, 2 - outer part of the counter-sample made of rubber with appropriate properties

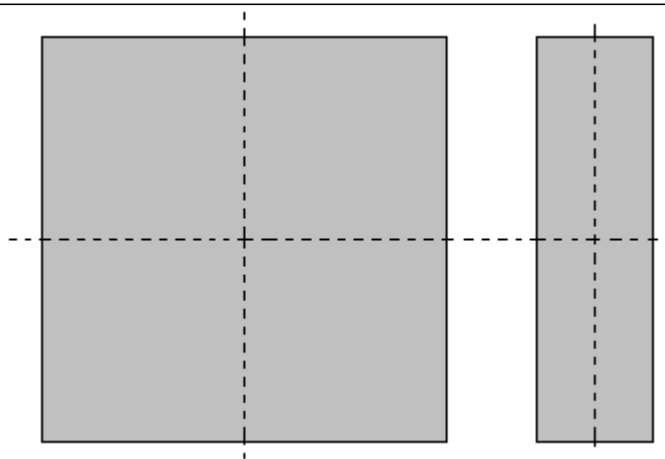


Fig. 4.1.73.11. The tested sample (most often steel) with dimensions of 30x30x3 [mm] used in the T-07 abrasion test rig

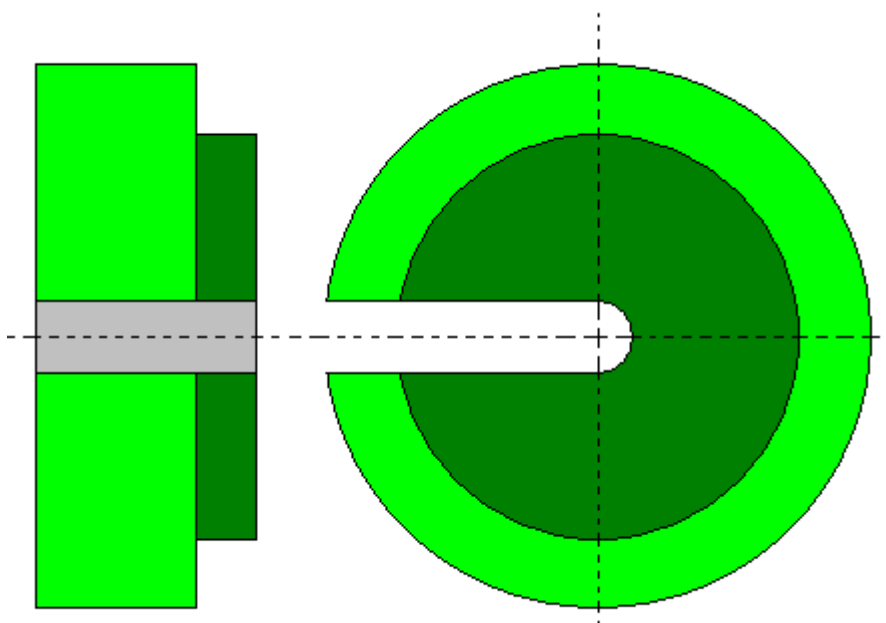


Fig. 4.1.73.12. The shape of steel weights used in the T-07 abrasion test rig

This tribotester is additionally equipped with a control and measurement system (Fig. 4.1.73.13) for counting the number of counter-sample revolutions and for switching off the drive motor after performing the set number of revolutions. The role of this system is played by the PS-2 Controller consisting of a pulse amplifier, a digital readout panel, an interface and a computer interface.

The principle of the test carried out with the T-07 tribotester is that the same operating conditions (load and speed) are applied to the friction of samples made of the tested and reference material. Abrasive particles are supplied to the friction contact zone and pressed

against the sample with a rotating rubber roller. The measurement consists in comparing the wear of samples - the reference one and the one from the tested material.

This test rig has only one rubber roller (counter-sample) included in the set. So the counter-sample is only of one type. This limits to some extent the field of application of this test rig. The hardness of tested materials or metal coatings must, therefore, be less than 1400 HV and the difference in hardness at a depth of 0.3 [mm] should not exceed 10%. When using porous materials as samples the grain size of the tested abrasive must not exceed 0.1 [mm].



Fig. 4.1.73.13. The PS-2 Controller is used to program the operating parameters of the T-07 abrasion test rig

The undeniable advantages of the T-07 test rig include:

- the possibility of carrying out tests with a wide range of abrasive types,
- with different sample materials (or coatings),
- with samples after virtually any heat, thermo-chemical or surface treatment,
- in various temperature and humidity conditions,
- simple construction,
- reliable operation,
- easy-to-use.

The disadvantages of this test rig include:

- the number of counter-sample rotations limited to six digits of the PS-2 Controller display, thus this number may not exceed the value of one million,
- the ability to perform tests only under static conditions, i.e. constant rotational speed of the counter-sample and a constant amount of abrasive material supplied.

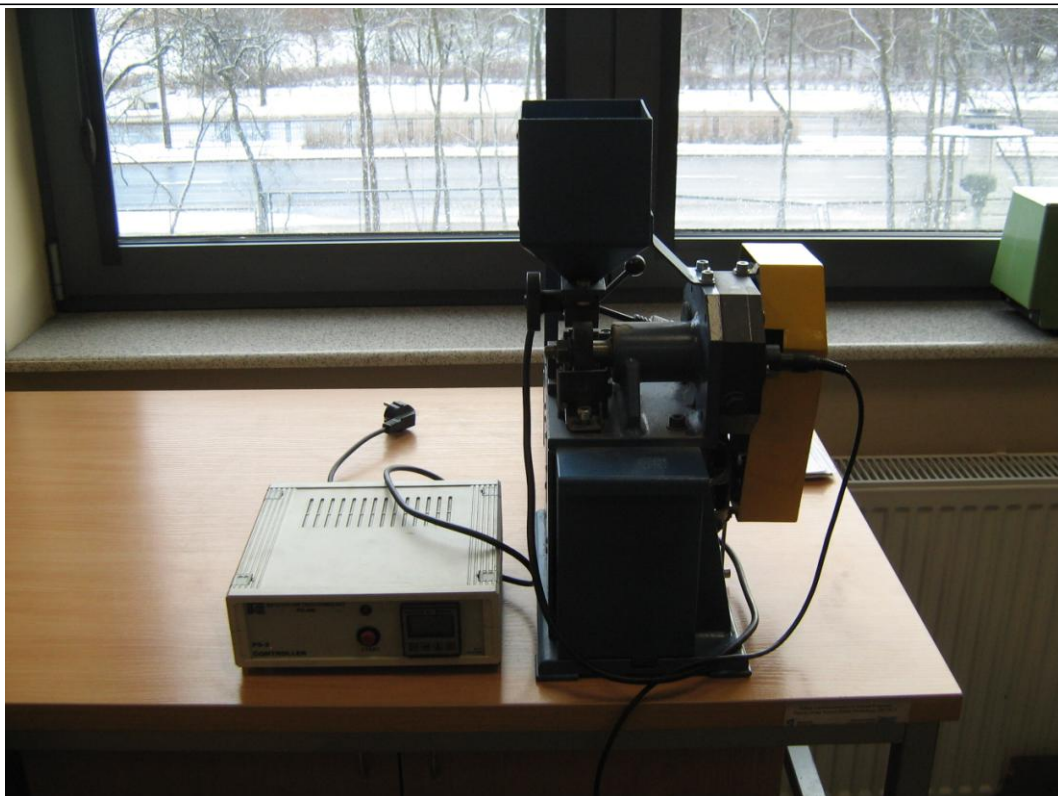


Fig. 4.1.73.14. The tribotester T-07 prepared for testing

Abrasive wear resistance tests carried out with the T-07 tribotester using loose abrasive are performed in accordance with the requirements of the *Ensuring of wear resistance...* standard GOST 23.208-79.

Fig. 4.1.73.15 shows the method of connecting the PS-2 Controller and T-07 tribotester to the electric grid. The PS-2 controller compares the pulses received from the RPM sensor installed in the tribotester with the preset RPM value by counting the pulses received from the RPM sensor. As soon as these values are equal, it disconnects the power supply from the test rig. The driving unit of this tribotester is an electric motor with a brake in it. As soon as the voltage is applied, the brake is released. The brake will operate as soon as there is no voltage. This solution is similar to that used in cranes in production halls (when the electric voltage is cut off, the weight suspended on the crane's slings is not dropped). This design solution means that as soon as the PS-2 Controller disconnects the voltage the counter-sample roll stops immediately. Otherwise, it might still rotate for some time due to inertial forces. Thus, the number of revolutions would or could be different even for the same abrasive used / tested. Such a design solution is beneficial even for the sake of accuracy of tests carried out.

Figures 4.1.73.16 and 4.1.73.17 show two types of methods of dosing the abrasive to the friction area in the abrasion test equipment. In both solutions, the abrasive moves by gravity.

The counter-sample rubber roller used in the T-07 tribotester has a diameter of $\varnothing 50$ [mm] and a width of $\neq 15$ [mm]. The hardness of the outer rubber coating is $78 \div 85$ [°ShA].

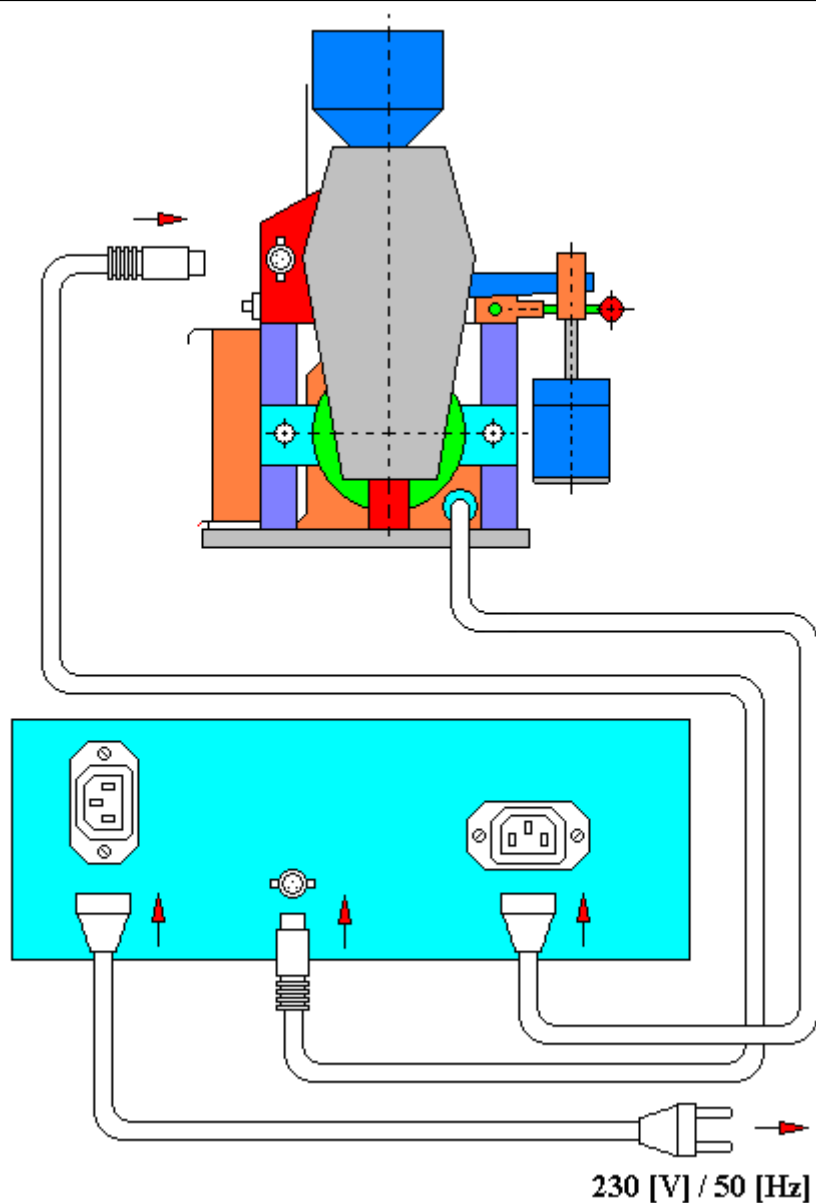


Fig. 4.1.73.15. The method of connection of voltage supply to the PS-2 Controller and T-07 tribotester

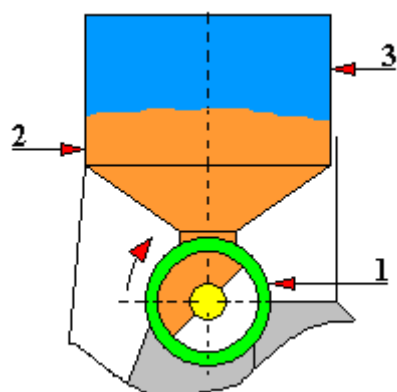


Fig. 4.1.73.16. The method of dosing the abrasive material used in the T-07 test rig
1 - rotary dosing valve, 2 - abrasive, 3 - abrasive reservoir

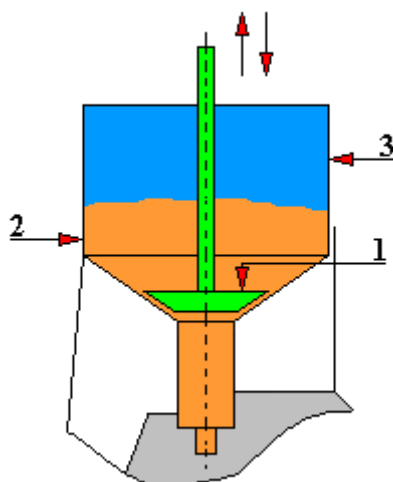


Fig. 4.1.73.17. A method of abrasive dosing solution used in other tribotesters intended for abrasion testing

1 - abrasive dosing head, 2 - abrasive, 3 - abrasive reservoir

4.1.74. T-20 ball-disc tribotester

The test rig with the symbol T-20 is a commercial test rig manufactured by the Institute of Sustainable Technologies in Radom. This test rig enables the testing of abrasive wear resistance of construction materials and coatings applied to test rig elements being in friction, in accordance with the method specified in the PN-EN 1071-6: 2008 standard. In particular, with the aid of this test rig, the resistance to abrasive wear can be determined by the ball-cratering method, depending on:

- rotational speed,
- the presence and type of abrasive,
- path of friction,
- set load.

The following parameters can be determined with the T-20 ball-disc tribotester: coating wear rate factor K_c ,

- substrate wear rate coefficient K_s ,
- thickness of the tested anti-wear coating,
- wear characteristics of the tested friction contact,
- frictional characteristics of the tested mating of materials.

This test rig is characterized by the following parameters of the friction contact:

- a) constant contact load during the test (from 0.1 [N] to 25 [N]),
- b) type of motion: permanent sliding during the test with continuously adjustable speed in the range $0 \div 0.4$ [m/sec],
- c) type of contact: spherical surface-flat surface, formed by a sample (disc) pressed against a rotating counter-sample (ball).

The diameter of the counter-sample (ball) used in the T-20 tribotester is $\varnothing 25.4$ [mm], and the diameter of the sample (disc) is $\varnothing 25.4$ [mm]. This test rig is a modern design solution that enables continuous measurement and recording of the following measured parameters:

- friction force,
- displacement,
- path of friction (number of revolutions),
- ambient temperature of the friction contact.

The discussed test rig (Fig. 4.1.74.1) consists of three independent units:

- a) tribotester T-20,
- b) controller BT-20,
- c) amplifier Spider 8.

The element that integrates these three units is the computer system with the T-20 software. Optionally, this test rig can be additionally equipped with a system for feeding abrasive slurry of any composition, mixed with the use of a magnetic stirrer and fed to the friction zone with the use of a pump.

Figures 4.1.74.2 and 4.1.74.3 show a general structure scheme of the discussed T-20 tribotester. Its structure includes:

- a) base 1 made in the form of a plate to which measuring sensors, auxiliary equipment and other units of the test rig are attached;
- b) a drive unit consisting of a DC motor 9, a flexible form coupling 10, a drive shaft 7 and a drive cantilever 2 fastened to the base 1 by means of screws, in which there are rolling bearings constituting the bearing of the drive shaft 7;

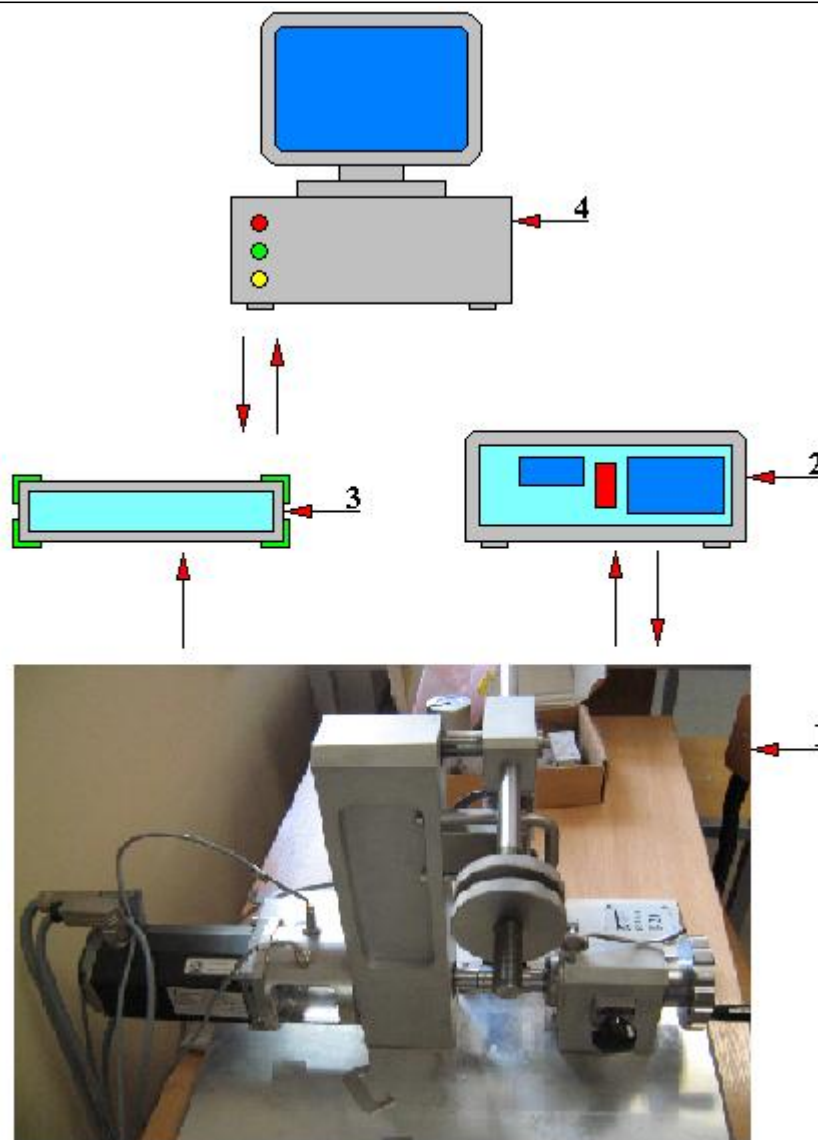


Fig. 4.1.74.1. A general scheme of the ball-disc test rig
 1 - tribotester T-20, 2 - BT-20 controller, 3 - Spider 8 amplifier, 4 - PC computer with T-20 software

- c) a pressure unit consisting of a pressure bracket 3, a pressure knob 11 connected by a screw mechanism to the pressure bracket 3 and a shaft 8 mounted in the pressure knob 11 by rolling bearings; the pressure unit is designed to fix the counter-sample;
- d) a loading lever unit consisting of a lever 4 which is rotationally mounted on a pin 20 which in turn is secured in the drive cantilever 2; balancing weights 21 are mounted on the right threaded part of the lever 4, and on the left part of the lever 4, a hanger 19 with a pan for putting weights 12 is mounted in a special groove, weights exert pressure on the tested friction contact; the loading lever unit is intended for free movement of the sample unit in the horizontal and vertical planes and for zeroing the pressure with unloaded contact;
- e) a sample holder unit consisting of a holder 22, a pressure plate 23 which is fastened to the holder 22 by means of a screw and a linear ball bearing 24 allowing the holder to be moved in the direction of the friction force; the sample (disc) mounting unit is placed on the lower part of the lever 4;

- f) a slurry feed unit (optional), consisting of a slurry reservoir 18, a slurry feed tube 13 connected thereto, and a slurry reservoir 17 for used slurry; the slurry feed unit is designed to feed the abrasive slurry to the friction zone to be tested;

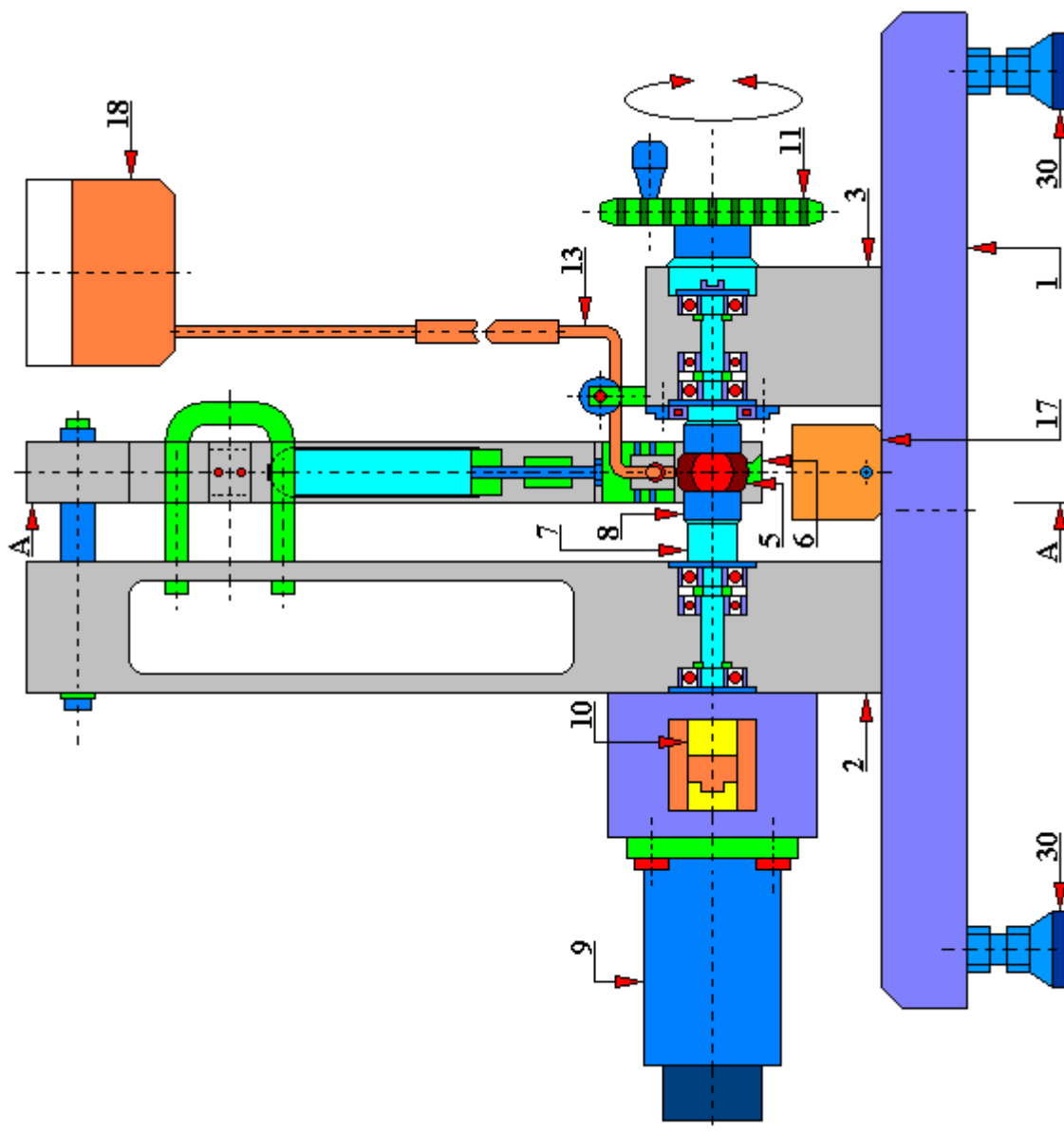


Fig. 4.1.74.2. A general structure scheme of the T-20 ball-disc tribotester
 1 - base, 2 - drive cantilever, 3 - pressure bracket, 5 - counter-sample, 6 - sample, 7 - drive shaft, 8 - shaft roller bearing, 9 - DC motor, 10 - flexible form coupling, 11 - pressure knob, 13 - slurry inlet tube, 17 - used slurry reservoir, 18 - slurry reservoir, 30 - adjusting leg

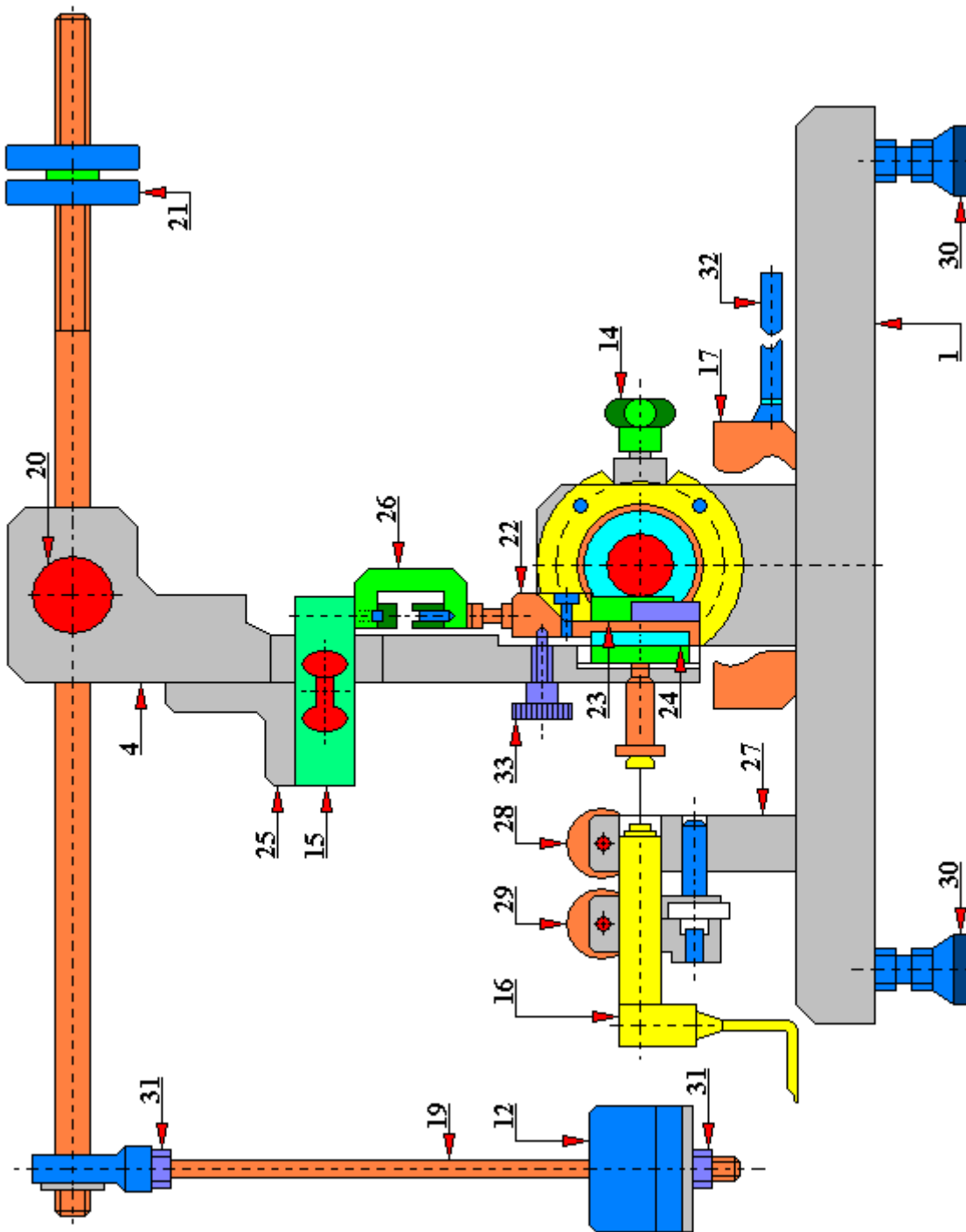


Fig. 4.1.74.3. A general structure scheme of the T-20 ball-disc tribotester for section A-A
 1 - base, 2 – drive cantilever, 3 – pressure bracket, 4 - lever, 5 - counter-sample, 6 - sample, 7 - drive shaft, 8 - shaft roller bearing, 9 - DC motor, 10 - flexible form coupling, 11 - pressure knob, 12 - weights, 13 - slurry inlet tube, 14 - blocking, 15 - strain gauge force transducer, 16 - inductive displacement sensor, 17 – used slurry reservoir, 18 – slurry reservoir, 19 - hanger with a pan, 20 - pin, 21 - balancing weights, 22 - handle, 23 - pressure plate, 24 - linear ball bearing, 25 - bracket, 26 - pusher, 27 – clamping ring, 28 - locking knob, 29 - transducer clamp knob, 30 – adjusting leg, 31 - nut, 32 - handle of the used slurry reservoir, 33 - knurled fixing screw

- g) a friction force sensor unit consisting of a bracket 25, a strain gauge 16, and a pusher 26; the bracket 25 is mounted on the loading lever 4 by means of bolts, and the friction force

is transmitted from the friction contact through the pusher 26; the friction force sensor unit is designed for mounting the strain gauge 16 in the plane of friction force;

- h) a displacement transducer unit comprised of an inductive displacement transducer 16 mounted in a clamping ring 27 by a clamp knob 29; the clamping ring 27 also has a locking knob 28 designed to secure the position of the displacement transducer after it has been precisely positioned; the displacement transducer unit is used to measure the displacement caused by wear of elements of the tested friction contact.

Figure 4.1.74.4 shows the ball-disc test rig consisting of a set of units: BT-20 controller, Spider 8 amplifier and T-20 tribotester, and Fig. 4.1.74.5 shows the tribotester T-20 in the view from the side of the load contact. The ball-disc friction contact used in the T-20 tribotester is shown in Fig. 4.1.74.6.



Fig. 4.1.74.4. A test rig of the ball-disc type consisting of a set of units: BT-20 controller, Spider 8 amplifier and T-20 tribotester



Fig. 4.1.74.5. T-20 tribotester (the view from the side of the load contact)

BT-20 controller (Fig. 4.1.74.11 and 4.1.74.12), included in the measurement and control system of the T-20 test rig, enables:

- a) counting the number of revolutions with the Impulse Counter pulse sensor;
- b) display of the current rotational speed;
- c) starting the test run from the level of controller after turning off the PC Control function (Start/Stop buttons);
- d) setting the spindle rotational speed using the Speed Adjustment regulator;
- e) automatic shut-down of the test rig drive when the preset number of revolutions is reached.

The BT-20 controller allows, as mentioned above, to set the number of revolutions and the rotational speed of the test disc. The number of revolutions is calculated according to the formula:

$$N = \frac{S}{\pi \cdot d}$$

where: N - number of revolutions,
 s – path of friction [m],
 d - ball diameter [m], $d = 0.0254$ [m]

For example, the following number of revolutions corresponds to the path of friction of 1 kilometer:

$$N = \frac{1000}{3.14 \cdot 0.0254} = 12538$$

However, the rotational speed is calculated according to the formula:

$$n = \frac{60 \cdot v}{\pi \cdot d}$$

where: n – rotational speed [rpm],
 v – rubbing speed [m/sec],
 d - ball diameter [m], $d = 0.0254$ [m]

For example, assuming that the set rubbing speed is 0.1 [m/sec], the rotational speed will be equal to:

$$n = \frac{60 \cdot 0.1}{3.14 \cdot 0.0254} = 75 \text{ [rpm]}$$



Fig. 4.1.74.6. The ball-disc friction contact used in the T-20 tribotester

The overall dimensions (width x height x depth) of the test kit are as follows:

- | | |
|------------------------|------------------|
| a) controller BT-20, | 225x85x200 [mm], |
| b) amplifier Spider 8. | 330x75x270 [mm], |
| c) tribotester T-20, | 440x350x510 [mm] |

The weight of the T-20 test rig is 25 [kg], and that of Spider 8 amplifier: 2.75 [kg], and that of BT-20 controller: 1.8 [kg].

The results of the abrasive wear rate of the coating K_c and the wear rate of substrate K_s at a given rotational speed, load and variable path of friction are calculated based on PN-EN 1071-6 standard.

The equation used as the basis for determining the wear in the case of abrasion of the coating is as follows:

$$S \cdot N = \frac{V_c}{K_c} + \frac{V_s}{K_s}$$

where: S – ball slide path,
 N - normal load,
 V_c - volume of the removed coating,
 V_s - volume of the substrate removed,
 K_s - abrasive wear rate of the substrate,
 K_c - the rate of abrasive wear of the coating.

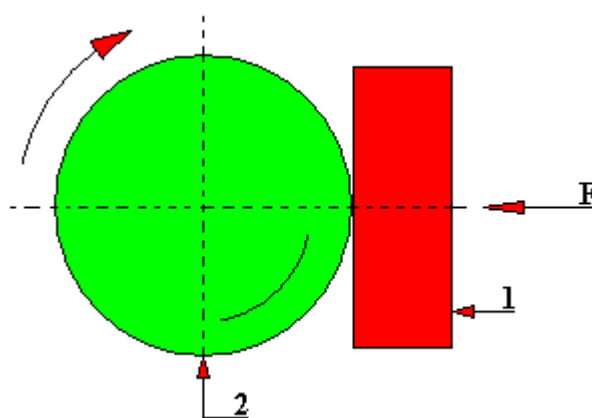


Fig. 4.1.74.7. A diagram of the friction contact of the T-20 test rig
 1 - stationary tested sample in the form of a disc, 2 - rotating counter-sample in the form of a ball,
 F - force acting on the sample

Within the 5th Framework Program of the European Union, there was an initiative to develop a testing method called ball-cratering [Gee et al. 2003]. This is the so-called coulotest (Fig. 4.1.74.8) which is used for determining the thickness of coatings by measuring the diameter of craters generated by the ball (counter-sample) in the presence of abrasive slurry. The thickness of coatings is determined taking into account the possibility of changes in both the sliding velocity and changes in the load and control of the abrasive slurry. The counter-sample (ball) 1 rotates on the sample surface (stationary disc) 2. The tested and controlled abrasive slurry is supplied to the friction zone through the feed line 8. Following the conducted test, a spherical cavity (crater) is obtained and is measured. If the tested coating applied to the sample (disc) surface is not abraded during the test, then the coating wear factor K_c is determined. If, however, during laboratory tests, the coating applied to the sample (disc) is abraded, then one may calculate the coating wear factor K_c and the substrate wear factor K_s .

This idea was written in the form of a draft of the European standard PN-EN 1071-6: 2008 and is being developed in many research centers, an example of which is discussed here T-20 tribotester of the Polish design which was developed on the basis of the idea of the ball-cratering method.

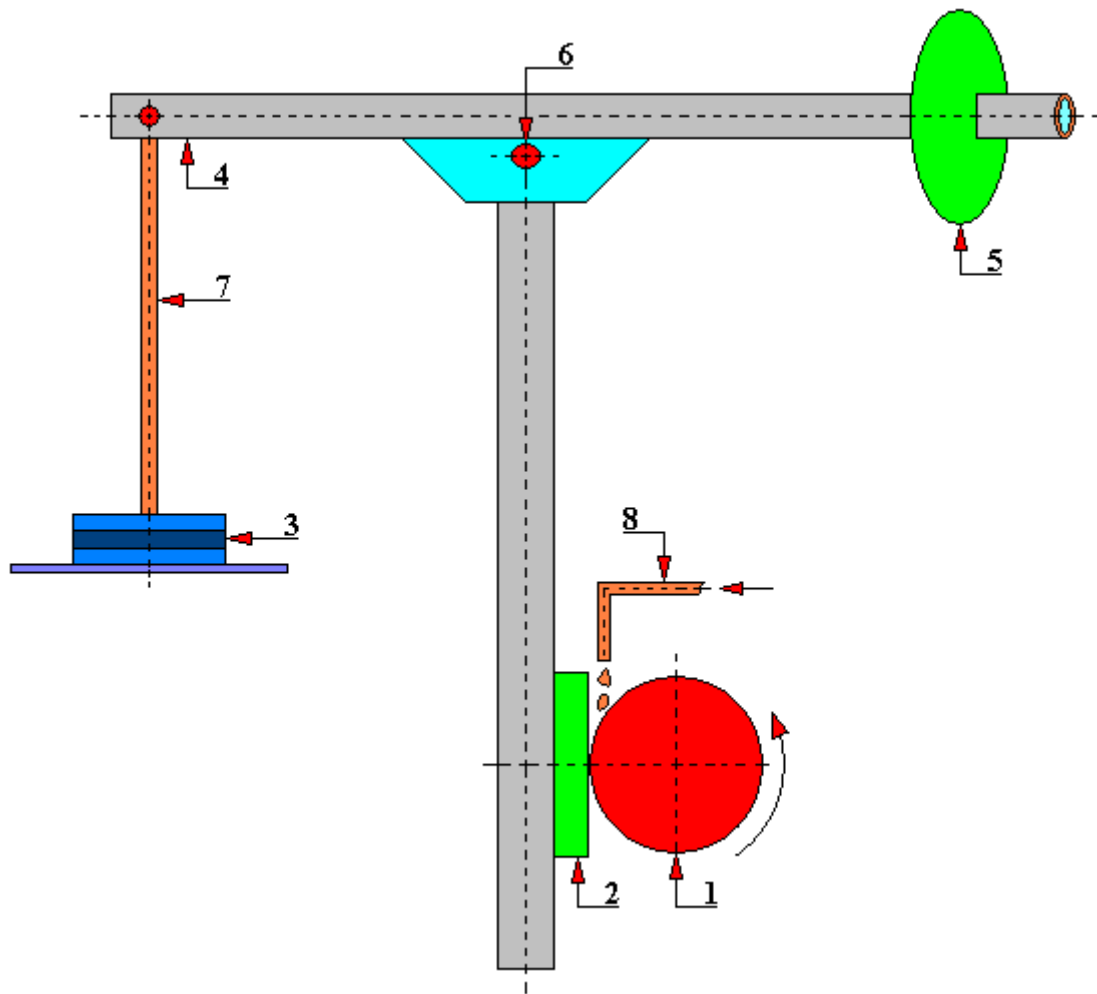


Fig. 4.1.74.8. A diagram of a test set for testing the abrasive wear of coatings using the ball-cratering method; the test can also be performed on the T-20 tribotester
1 - counter-sample (ball), 2 - sample (disc), 3 - weight, 4 - lever, 5 - counterweight, 6 - fulcrum, 7 - hanger of the load pan, 8 - conduit feeding the abrasive slurry to the friction area

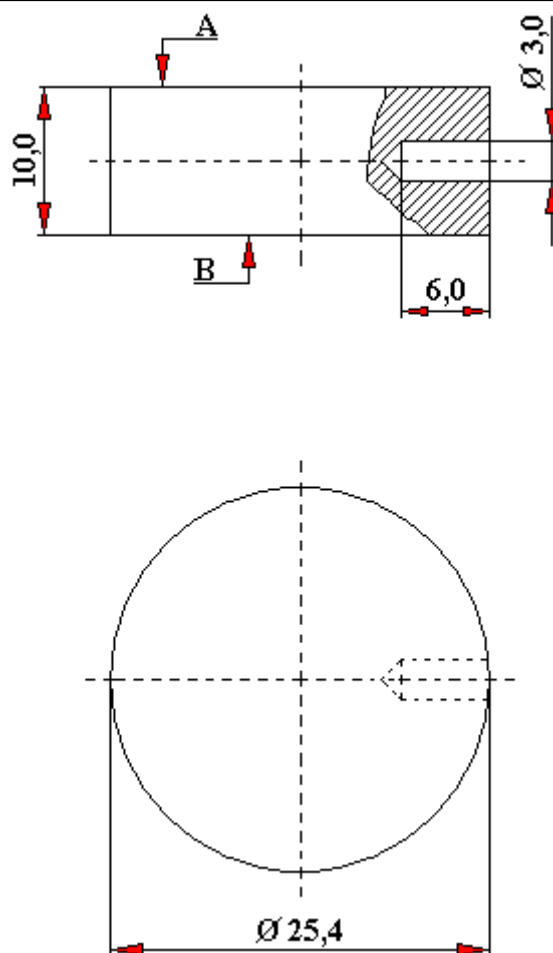


Fig. 4.1.74.9. The sample (disc) used in the T-20 tribotester
A, B – friction surfaces

After completing the tests the manufacturer of the T-20 tribotester recommends cleaning, with ethanol, the friction contact, test disc mounting points, the sample, its holder and places that have become dirty by the use of abrasive. An example of a test sample preparation procedure is shown below:

- a) degreasing in toluene for 5 ÷ 10 minutes, preferably in an ultrasonic cleaner,
- b) cleaning in hexane for 5 minutes (also in an ultrasonic cleaner),
- c) drying in a dryer for approx. 20 minutes in the temperature 110 ÷ 120 [°C].

The manufacturer of this test rig clearly indicated in the technical and operational documentation to use cotton gloves when touching the test samples. However, before using the test samples, they should be stored in a desiccator. Taking care of apparently little things can have a significant impact on the results of obtained tests.

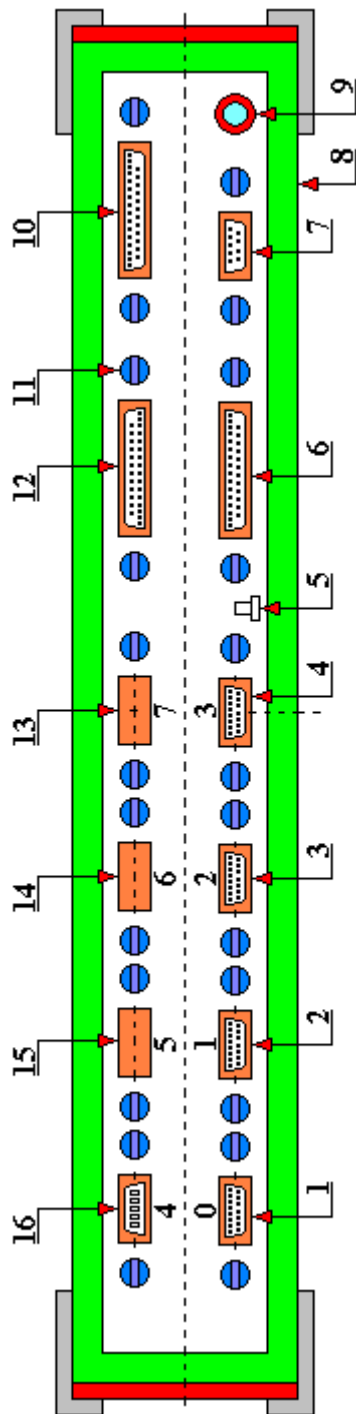


Fig. 4.1.74.10. Spider 8 measuring amplifier rear panel
 1 - 15-pin port number 0 (dedicated to the speed sensor), 2 - port number 1 (for the displacement transducer), 3 - 15-pin port number 2 (for the friction force transducer), 4 - 15-pin port number 3 (free), 5 - ground terminal, 6 - PC/Master twenty-five-pin port (dedicated to the computer), 7 - RS 232 port (free), 8 - amplifier housing, 9 - amplifier power socket 12 V DC, 10 - Digital I/O socket (intended for the BT-20 driver), 12 - printer input socket, twenty-five-pin, 13 - port free, 14 - port free, 15 - port free, 16 - port for thermocouple

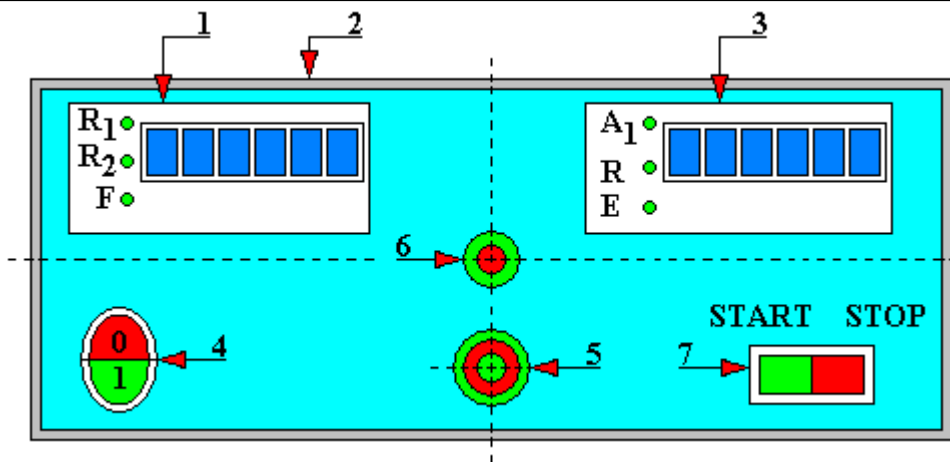


Fig. 4.1.74.11. Front panel of the BT-20 controller

1 - pulse counter indicating the number of rotations of the counter-sample (ball), 2 - housing, 3 - tachometer indicating the rotational speed of the counter-sample (ball) in rpm, 4 - power switch, 5 - potentiometer knob for setting the rotational speed of the counter-sample (ball), 6 - gauge showing how the test run was started (when engaged: start from the software level, when turned off: start from the level of the BT-20 controller, 7 - a button for starting/ending the test run from the controller level (first turn off the indicator No. 6)

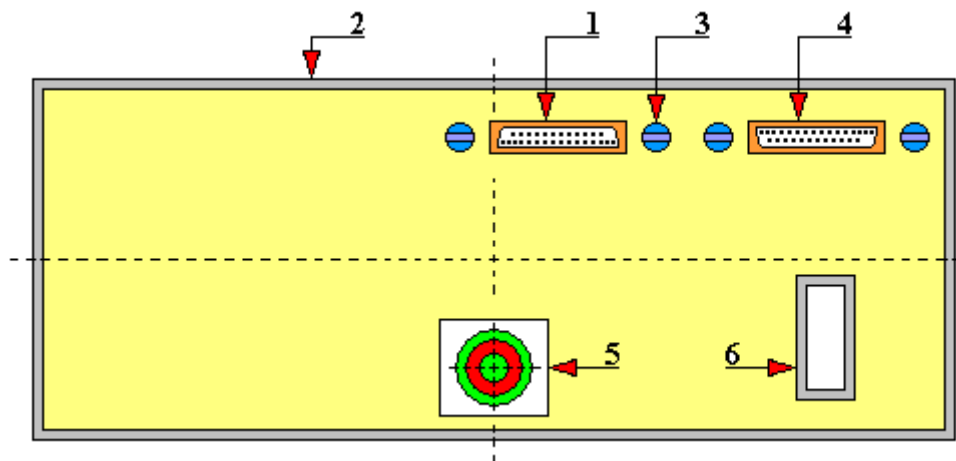


Fig. 4.1.74.12. Rear panel of the BT-20 controller

1 - socket to which Spider 8 amplifier is connected, 2 - housing, 3 - socket fixing screw, 4 - socket connected to the impulse sensor, 5 - power and control socket for the T-20 tribotester drive, 6 - AC 230 V/50 Hz power socket

4.1.75. 'Rotating bowl' test rig for testing wear in soil

Test rigs of the 'rotating bowl' type are intended mainly for testing the wear of agricultural machinery components operating in various types of soil with different moisture content. These test rigs are large in dimensions - the diameter of the bowl is even more than one meter; and are large in weight - the weight of the soil itself can be even several hundred kilograms. Discussed below are two variants of the test rig designed and built at the Faculty of Technical Sciences of the University of Warmia and Mazury in Olsztyn. Originally, this test rig (Fig. 4.1.75.1) was built of a frame 1 to which an electric motor 2 was attached driving the rotating bowl 4 by means of a belt transmission 3. The tested soil was put inside the bowl. To the fixed stationary frame 1 there are mounted as opposing forks 9 (two pieces) for loosening the soil, rollers 6 (also two pieces) for packing the soil and sample holders 8 (two pieces). A soil moisture sensor was placed inside the bowl.

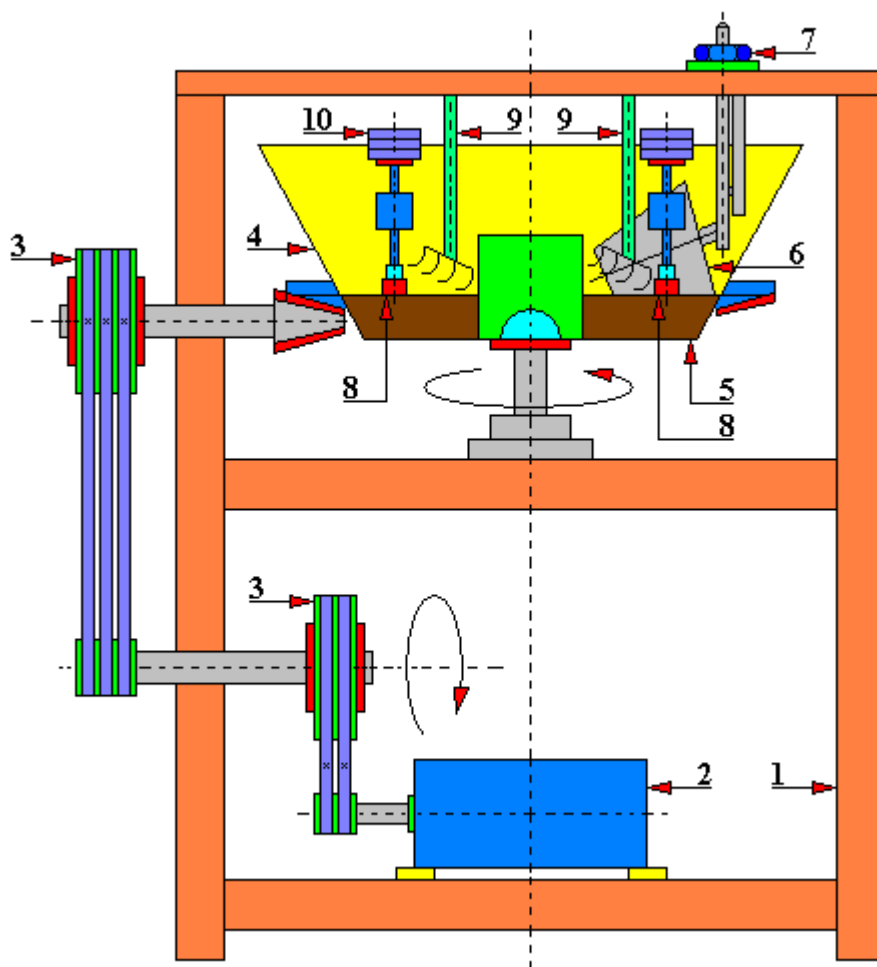


Fig. 4.1.75.1. A diagram of the 'rotating bowl' type test rig designed for testing wear in soil
 1 - frame, 2 - electric motor, 3 - belt transmission, 4 - rotating bowl, 5 - soil, 6 - packing roller, 7 - roller pressure, 8 - sample holder, 9 - loosening forks, 10 - sample weights

Considering its advantages (simple structure, operational reliability, ease of use, easy replacement of the steel samples tested, repeatability of the obtained results), this test rig has been modernized and extended. The expansion covered, inter alia, the use of the system of visualization and archiving of data obtained as a result of conducted tests, the system controlling

the operation of the bowl, the soil moistening system, introducing the oscillation mechanism of the motion of steel samples and the system of controlling this motion (Fig. 4.1.75.2 and 4.1.75.3).

In this tribotester samples were used (two pieces mounted as opposing) constituting cuboids with dimensions 30x25x10 [mm]. The material of the samples (Fig. 4.1.75.6) can be practically any, however, on this test rig, tests were mainly carried out for steel 38GSA which is commonly used in Poland for the production of plowshares. In order that temperature does not interfere with the material structure of samples, they were cut out with water cutters. The friction plane was mounted at an angle of $2^\circ \div 3^\circ$ in relation to the processed surface. Two independent sections are used to mount the tested samples, mounted on a fixed frame on a trailing suspension arm with the possibility of measuring the friction force. Each of these sections has mechanisms for loosening and compacting the surface of the material (soil) after passing of a foot with the tested sample to ensure the conditioning of the soil material.



Fig. 4.1.75.2. View of the modernized 'rotating bowl' test rig intended for testing wear in soil (in the foreground control cabinets with inverters and software, in the background the mechanical part of the test rig)

The modernization of this test rig allowed, among others, to:

- measure and register friction forces independently for both working sections,
- select the type of motion (without or with oscillation),
- control the moisture of the abrasive mass (soil),
- measure and record the moisture of the abrasive mass,
- measure and record the temperature of the abrasive mass,
- measure and record the traveled path of friction,
- set the path of friction,
- set the linear speed of abraded samples,

- set the oscillation speed,
- set the moisture content in the tested soil.

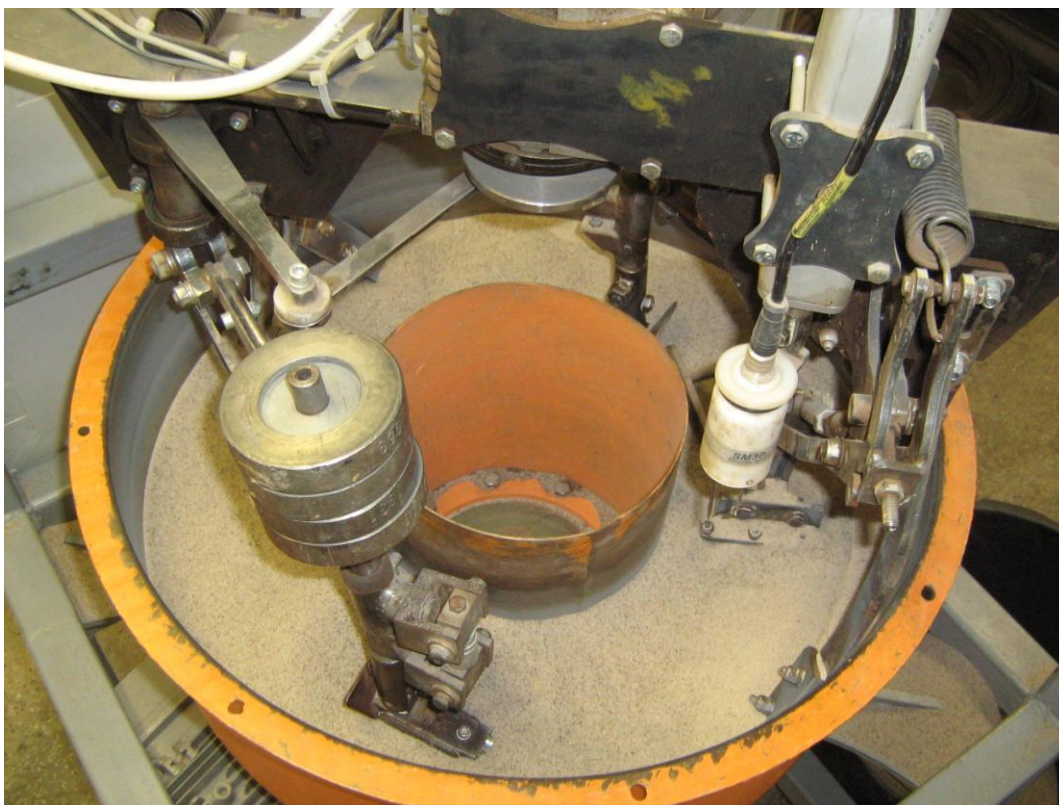


Fig. 4.1.75.3. A view of main elements of the 'rotating bowl' type test rig designed for testing wear in soil

The main element of the data visualization and archiving system (Fig. 4.1.75.4) of the 'rotating bowl' test rig is the V350-35-R2 PLC controller supplied with the output voltage of 24 [V] by means of RS-150-24 power supply. The controller communicates via the EX-A1 module with the IO-LC3 weighing module that supports friction force sensors for sections 1 and 2. For practical reasons, strain gauges of EMS20-200N type were used here.

To the voltage input of PLC V350-35-R2 controller connected is via an amplifier a moisture sensor of the SM300 type, equipped with a temperature transducer. In order that the moisture sensor used in this construction solution indicates the correct measurement it is necessary to completely immerse its electrodes in the soil. This operation is carried out by means of LAS4-2-1-250-24-EI linear actuator which is also connected to the PLC.

If, during tests, soil moisture is lower than the set value, then the controller periodically switches on the water pump. It performs this operation until the set and measured moisture values are equal.

The PCID-4RP sensor was used to measure the value of the bowl spinning, and thus the rate of samples wear. The setting of the oscillation mechanism was realized by the signal generated by the sensor of position of the oscillation mechanism, type PCIN-5.

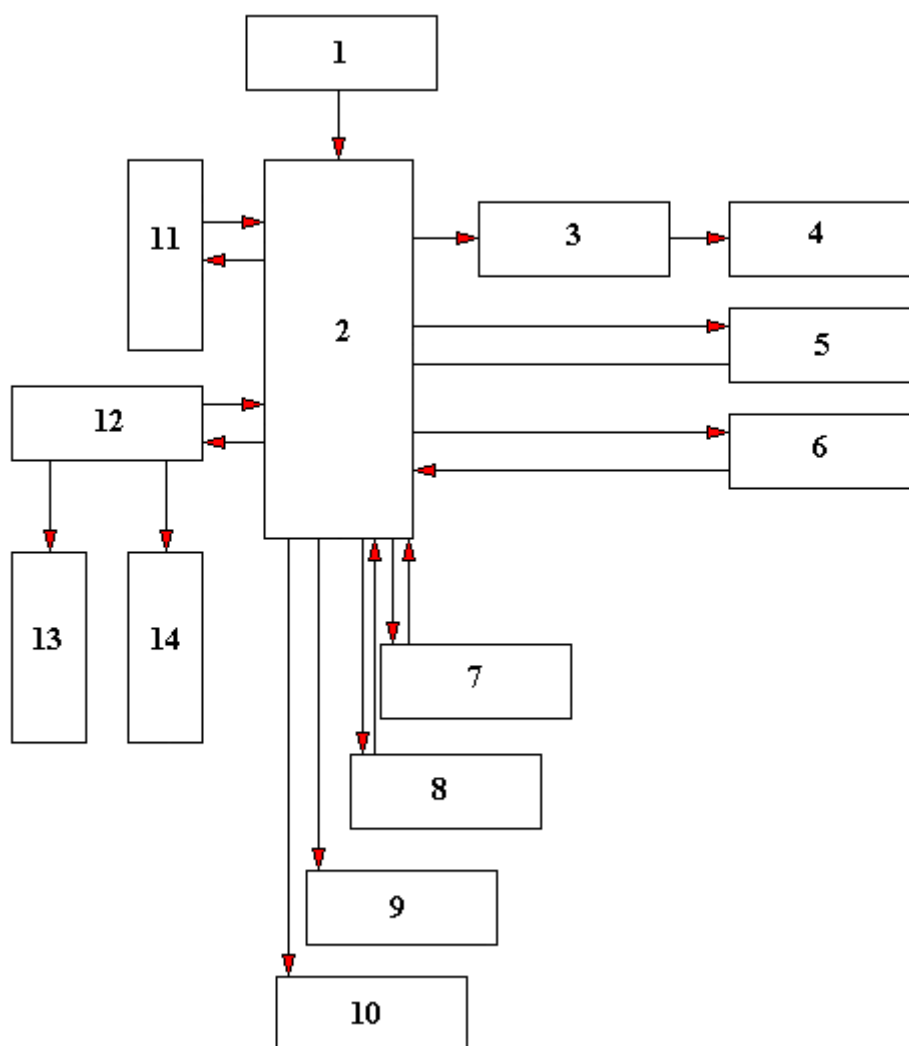


Fig. 4.1.75.4. A block diagram of the control and monitoring system for the operating parameters of the 'rotating bowl' type test rig designed for testing wear in soil

1 - RS-150-24 power supply, 2 - V 350-35-R2 controller, 3 - amplifier, 4 - SM 300 moisture and temperature sensor, 5 - PCID-4RP bowl spin speed sensor, 6 – sensor of position of the oscillation mechanism type PCIN-5, 7 - frequency converter of the SV015IC5-1F type supplying the bowl drive gear motor, 8 - frequency converter of the SV004IC5-1F type supplying the oscillation drive gear motor, 9 - linear position actuator, type LAS4-2-1-250-24-EI, of moisture and temperature sensor, 10 - water pump, 11 - EX-A1 module, 12 - IO-LC3 module, 13 - force sensor type EMS20-200N for section No.1, 14 - force sensor type EMS20-200N for section No.2

LS inverters were used to regulate the speed of the bowl's rotation and oscillating motion. They enable virtually any speed adjustment (in the range from 0 Hz to 50 Hz), both in manual or programmable mode, whether from the inverter menu level or from the PLC level. An inverter of the SV015IC5-1F type was used to adjust the speed of the bowl spinning, and SV004IC5-1F inverter was used to adjust the speed of the oscillating motion. The bowl is driven by a gear motor with a rated power of 1.5 [kW]. The PLC controller has built-in RS 232 communication ports that enable data exchange with a computer.

A program called 'Abrasive consumption' is used to operate the PLC controller and all units subordinate to it, which contains two working menu windows named 'Monitoring and supervision' and 'Moisture measurement'.

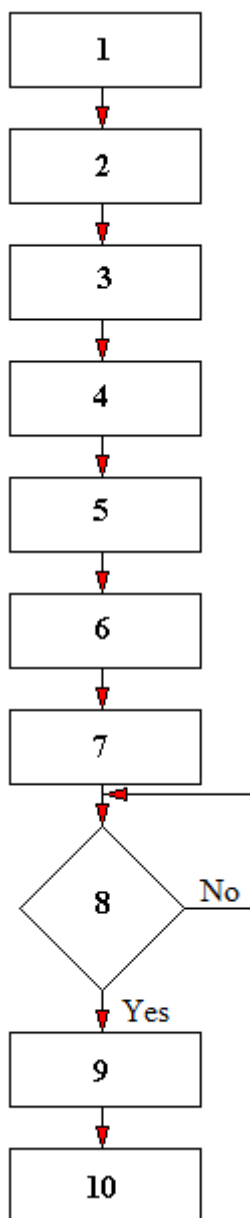


Fig. 4.1.75.5. Algorithm of operation of the 'rotating bowl' type test rig designed for testing wear in soil

1 - assembly of tested samples (2 pieces) in the holders, 2 - starting the PLC V350-35-R2 controller, 3 - determining/setting the value of moisture and the type of abrasive mass (soil), 4 - starting the automatic measurement of abrasive mass (soil) moisture, 5 - determining/setting the value of the friction speed, 6 - determining/setting the path of friction and the type of motion (with or without oscillation), 7 - starting the wear process, 8 - conditional block: comparison of the set path of friction with the actual path, 9 - export, for example to a computer, of data collected from the test rig during the course of the experiment, 10 - disassembly of used samples holders, possible replacement of the abrasive material, preparatory work for the next test

Figure 4.1.75.5 shows the algorithm for the operation of this test rig, and Fig. 4.1.75.7 diagram of the modernized test rig – a mechanical part. The frequency of data sampling

(moisture, temperature, bowl rotational speed, speed of oscillation motion, path of friction) taken from the test rig for the PLC controller used is 1 [Hz].

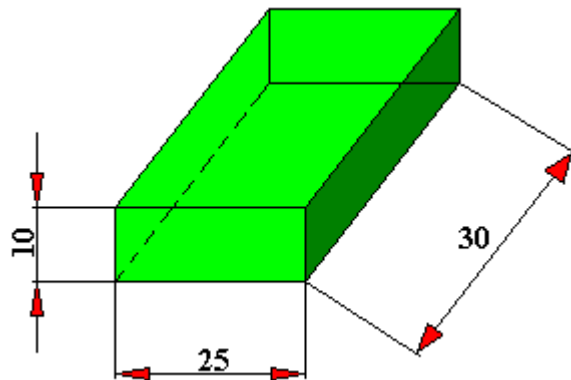


Fig. 4.1.75.6. A sample of steel 38GSA used for wear tests on a 'rotating bowl' type test rig. When changing the type of sample holders, it is possible to mount samples of a different shape.

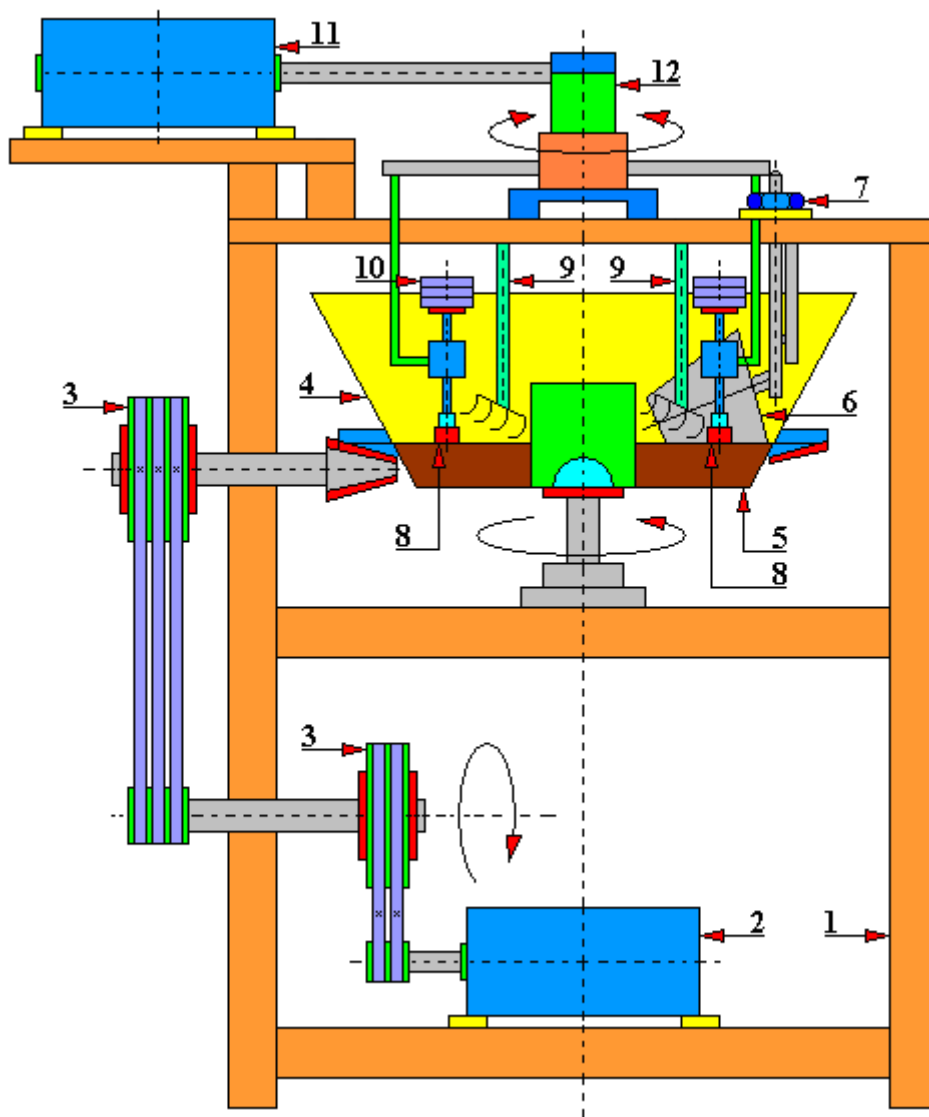


Fig. 4.1.75.7. A diagram of the modernized 'rotating bowl' type test rig designed for testing wear in soil (without a control system)

1 - frame, 2 - electric motor of the main motion drive (of the rotating bowl), 3 - belt transmission, 4 - rotating bowl, 5 - soil, 6 - packing roller, 7 - roller pressure, 8 - sample holder, 9 - loosening forks, 10 - sample weights

4.1.76. A test rig for testing the wear of working elements in soil using the 'ground tunneling' method

This test rig, presented in Fig. 4.1.76.1, is designed to test the wear of working materials working on the soil during deep penetration. Then, during e.g. deep ploughing, soil structure fractions vary depending on the depth of the working tool. Also the ambient moisture and pressure can have high values. These parameters can and do influence the durability of the main working elements of agricultural tools.

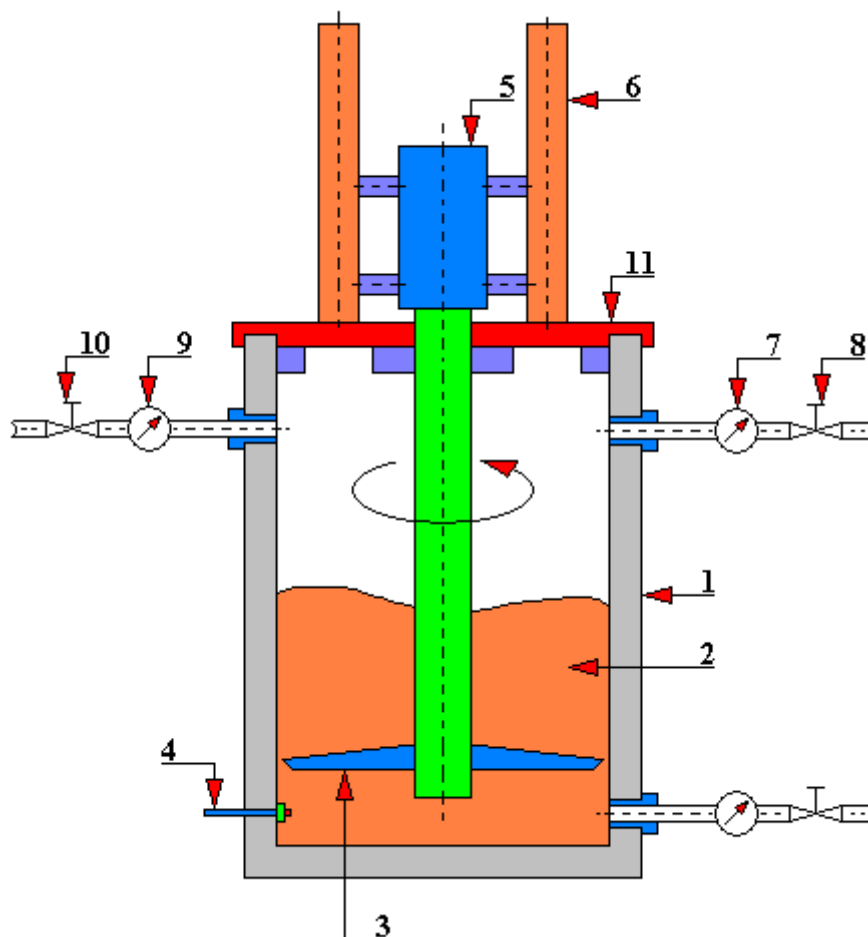


Fig. 4.1.76.1. A diagram of the construction of the ground tunneling test rig intended for testing the wear of working elements in soil

1 - cylinder, 2 - soil, 3 – test blade with samples, 4 - soil pressure sensor, 5 - drive engine, 6 - pressure system, 7 - air pressure gauge, 8 - air pressure valve, 9 - water pressure gauge, 10 - water pressure valve, 11 - cylinder cover

This test rig is made of a cylinder 1 inside of which located is the tested soil. In soil 2 there is a rotor 3 with sample holders. The rotor is driven by a speed-controlled motor 5. Parameters such as pressure and moisture inside the cylinder can be adjusted and monitored. Thanks to this, the analysis of the results obtained on the basis of such tests is easier and more accurate, and the set working conditions inside the cylinder reflect the conditions prevailing in real conditions.

4.1.77. A test rig with an abrasive cloth

A test rig with an abrasive cloth (Fig. 4.1.77.1) is intended for testing samples subject to abrasive wear, impacts and stresses arising in the tested materials while moving in an arc.

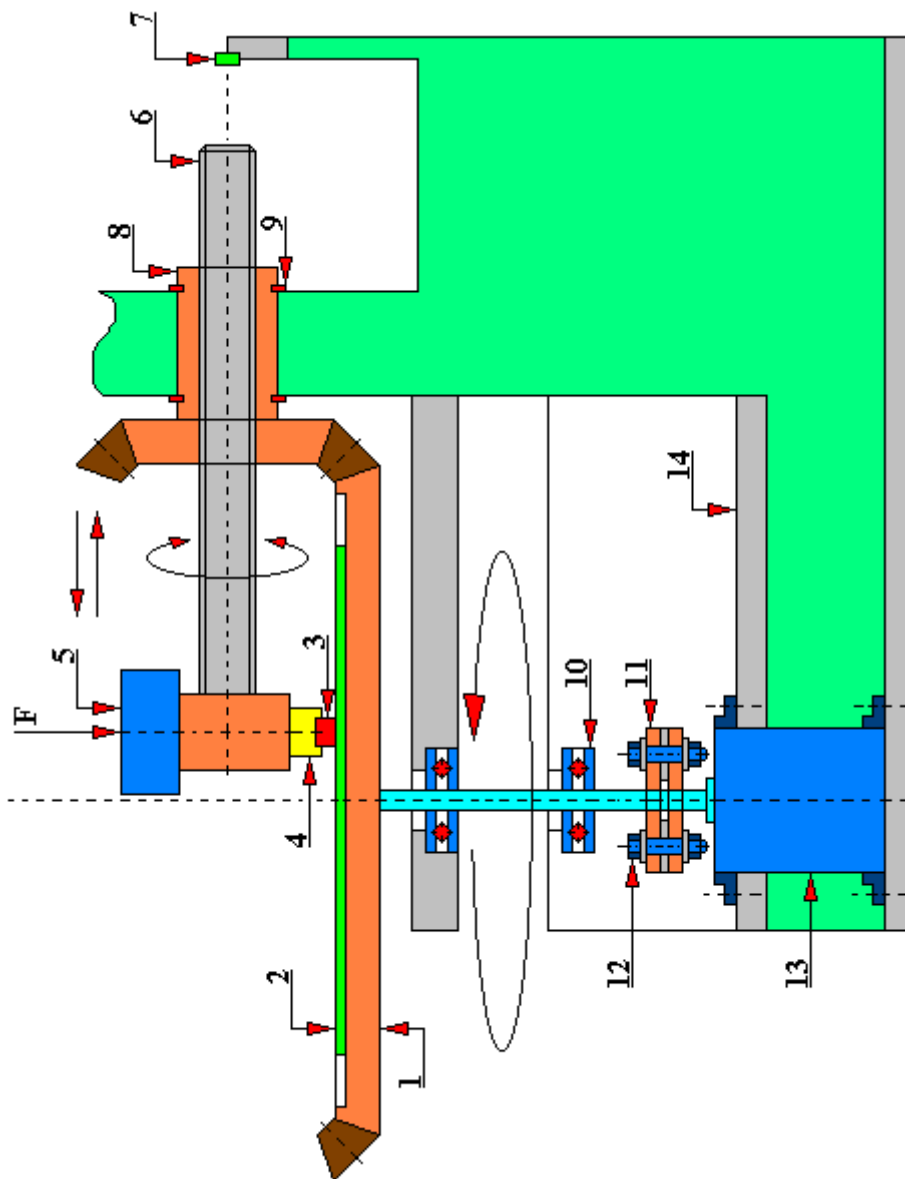


Fig. 4.1.77.1. A diagram of the test rig with an abrasive cloth

1 - rotating plate with conical teeth notched, 2 - abrasive cloth, 3 - tested sample, 4 - test sample holder, 5 - test sample loading mass, 6 - screw mechanism of radial travel of the tested sample, 7 - limit sensor, 8 - bevel gear acting as a nut, 9 - snap ring, 10 - thrust bearing, 11 - flexible coupling, 12 - screw fastening flexible clutch discs, 13 - drive motor, 14 - test rig body, F - force loading the tested sample

The tested sample 3, during the rotation of the plate 1, is moved from the central position to the edge of the abrasive disc 2 and back. The abrasive disc 2 in the form of an abrasive cloth with a certain granulation is attached to the rotating plate 1. As a result of combining the rotational motion of the plate 1 and the reciprocating motion of the sample 3 placed in the holder 4, when looking at the surface of the cloth 2, an arc motion is obtained. Depending on the relationship

between the rotational speed of the plate 1 and the speed of travelling of the sample 3, the arc (spiral) motion is more or less 'concentrated', and the resulting composite motion ensures continuous contact of the sample surface with the abrasive cloth. This test rig is based on ČSN 01 5084 *Determination of metal material...*

The path of motion of the tested sample, outlined on the surface of the abrasive cloth with a specific granulation, will be an Archimedes spiral (Fig. 4.1.77.2)

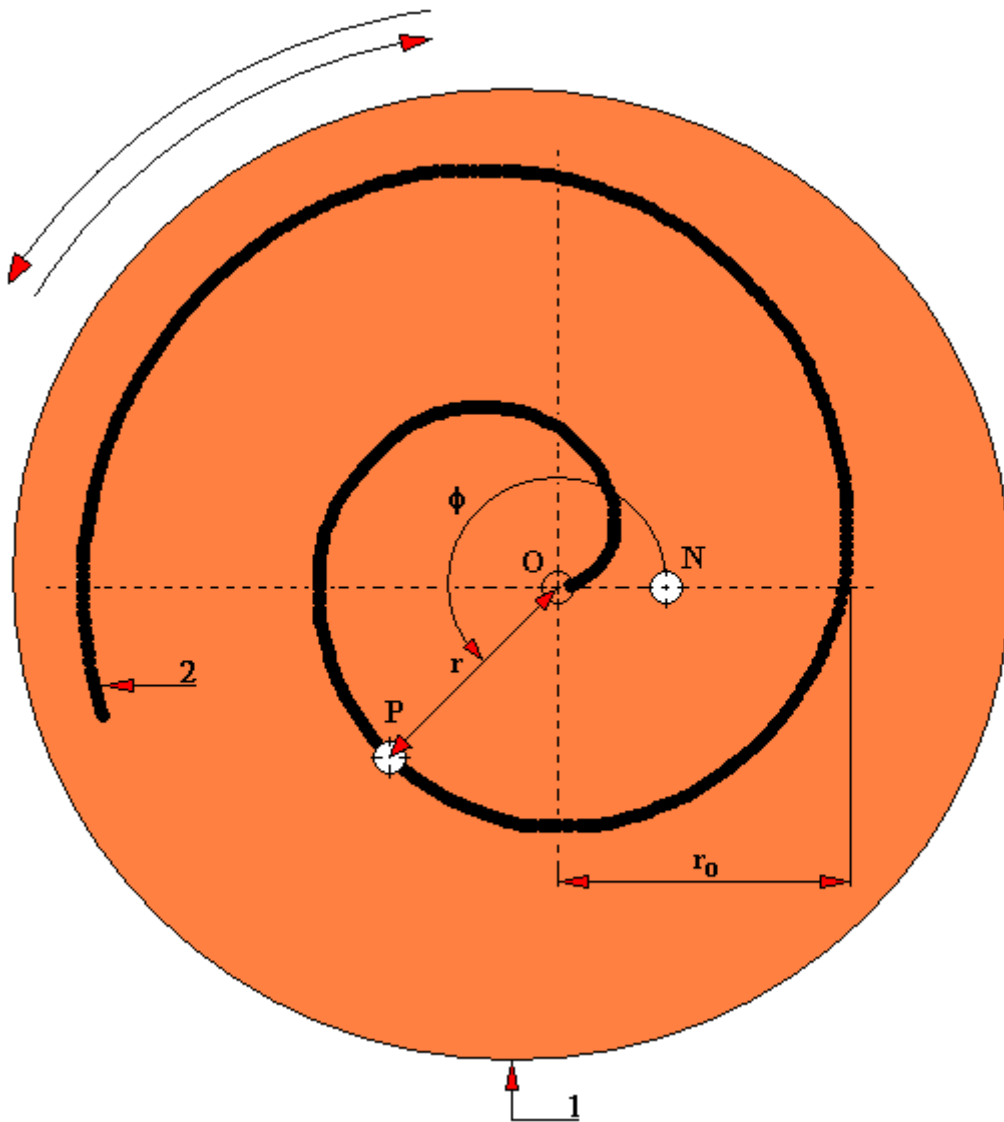


Fig. 4.1.77.1. The path of the sample on the surface of a circular abrasive cloth which is attached to the rotating plate of the test rig
 1 - abrasive cloth, 2 - the path of the sample during the test

If the point P (in our case the surface of the sample co-acting with the surface of the abrasive cloth) moves uniformly along a radius rotating with a constant angular velocity around the pole O of the abrasive cloth attached to the rotating plate, then its path will be the spiral of Archimedes.

If we denote the path OP by r , and the angle of rotation from the initial position by ϕ , then the polar equation of the spiral of Archimedes will be as follows:

$$\mathbf{r} = \mathbf{k} \cdot \boldsymbol{\varphi}$$

where: k - proportionality coefficient

If by r_0 we denote the length of the leading ray corresponding to a full revolution, i.e. an angle equal to 2π , then the spiral of Archimedes equation will be as follows:

$$\mathbf{r} = \frac{\mathbf{r}_0}{2 \cdot \pi} \cdot \boldsymbol{\varphi}$$

If, at the moment of starting the motion, the point (in our case the tested sample) was in position A away by a from the center, then the spiral of Archimedes equation will take the form:

$$\mathbf{r} = \mathbf{k} \cdot \boldsymbol{\varphi} + \mathbf{a}$$

The spiral of Archimedes crosses any radius originating from point O infinitely many times; the distances of points of intersection from the pole increase arithmetically [Poradnik mechanika, WNT, Warszawa 1972]. A variation of the spiral of Archimedes is the logarithmic spiral which can also be obtained on this test rig, but then it is necessary to modernize the drive of the radial motion of the sample so that the radial speed of the sample increases, and the rotational speed of the rotating plate remains constant during the test.

4.1.78. A test rig for high-temperature abrasive tests of HT-ET type

The HT-ET test rig (Fig. 4.1.78.1) is intended for testing the erosion of solid particles in a four-channel centrifugal accelerator. The abrasive material 3 placed in the reservoir 4 moves by gravity towards the centrifugal thrower 5 (accelerator). This thrower gives the abrasive particles a high kinetic energy directing them towards the samples 1 fixed in the holders 2. The samples 1 are placed at different angles around the accelerator. Thanks to this design solution it is possible to "bombard" the surface of the tested samples 1 with an abrasive material 3 being most often quartz sand.

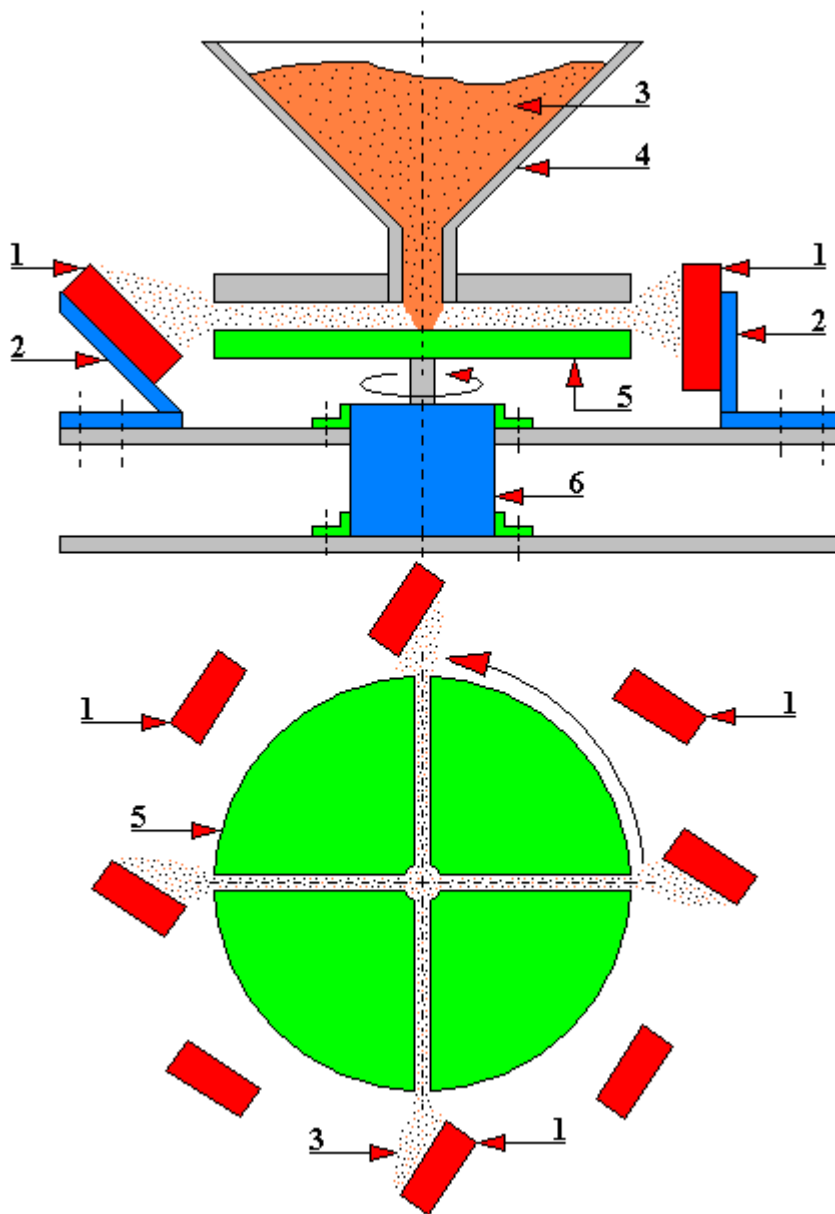


Fig. 4.1.78.1. A test rig for high-temperature abrasive tests of HT-ET type
 1 - tested sample, 2 - sample holder, 3 - abrasive mass, 4 - reservoir for abrasive mass, 5 - centrifugal thrower, 6 - drive motor

4.1.79. The test rig built on the basis of the Haworth method

Many authors (e.g. Napiórkowski J. 1994, Zwierzycki W. 1990) have already noticed the influence of the type of abrasive mass, the abrasive agent, on the course and wear values depending on the given experimental situation, which was aimed at creating a certain standardization, normalization of test rigs intended for testing friction and wear in the abrasive mass. Currently, the most commonly used media for testing engineering plastics include, among others:

- corundum grains,
- silicon carbides,
- quartz sand or natural sand fractions,
- soil mass.

The test rig, for which the testing method called the Haworth method was developed by the American Society for Testing and Material (ASTM), is presented below.

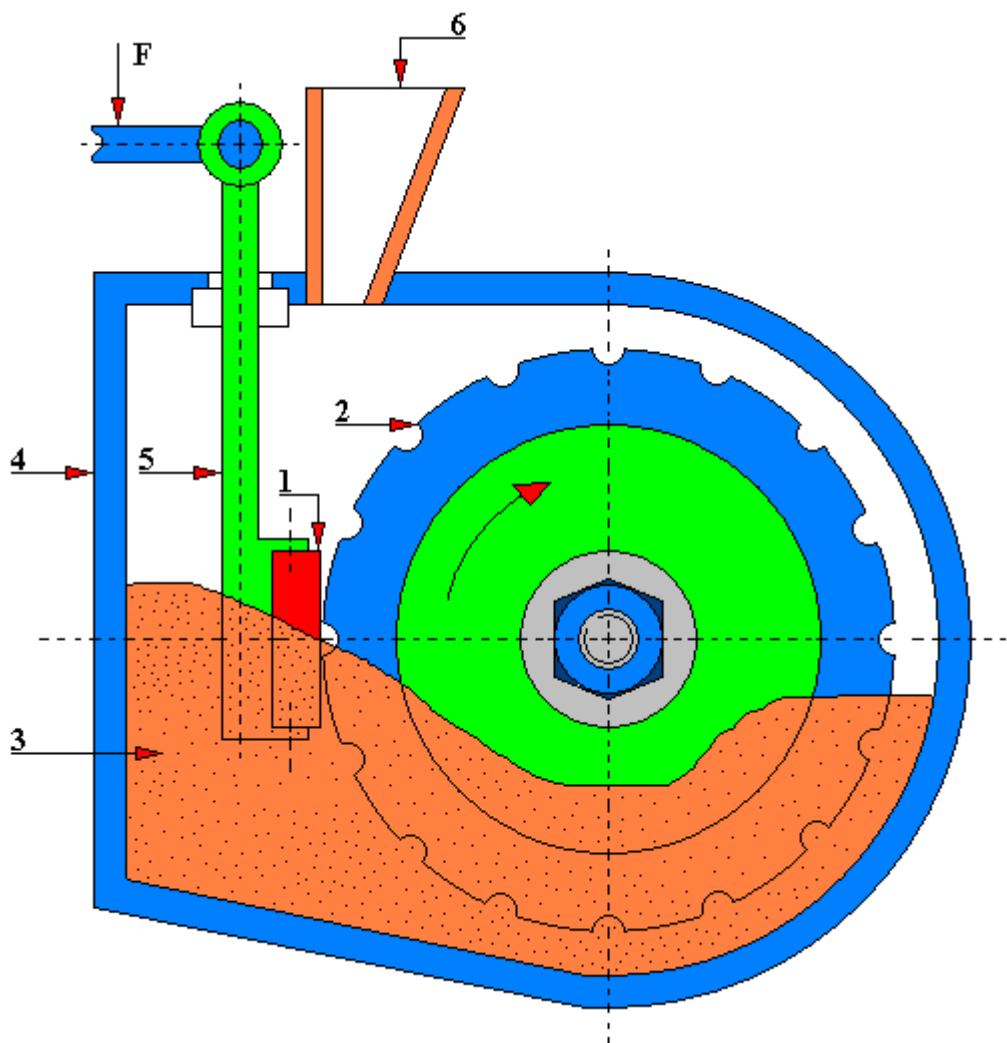


Fig. 4.1.79.1. A diagram of the Haworth-ZIS 116 test rig
 1 - tested sample, 2 - rubber disc, 3 - abrasive, 4 - body of the test rig, 5 - sample holder, 6 - charging hopper, F - force acting on the sample holder arm

The test rig for carrying out the Haworth tests (Fig. 4.1.79.1) consists of the body 4, which acts as the abrasive reservoir, and on the drive shaft in that body 4 mounted is a rotating rubber disc 2. This disc acts as a conveyor of the abrasive 3 which can be, for example, fine-grained quartz sand (according to the Standard test method ASTM G65) or other material with a loose and fine-grained structure. A rotary rubber disc 2 co-acts with the tested sample 1 fixed in the holder 5. The volume of force pressing the sample 1 against the surface of the rotating rubber disc 2 can be adjusted by the load F applied to the end of the lever unit which fixes sample 1. The abrasive 3 of known granulation is supplied to the inside of the body 4 by means of a hopper 6; the abrasive is continuously supplied by means of a rubber wheel 2 onto the surface of the tested sample 1. The purpose of tests carried out on this test rig is to quantify the wear of the tested sample material in conditions similar to the actual operating conditions.

Fig. 4.1.79.2 presents a modernized test rig for testing abrasibility with dry/wet loose abrasive equipped with a frequency inverter. This test rig is characterized by the fact that it enables the testing of various aggregates with different moisture for a variable set load and for a variable set rotational speed of the rubber wheel 14.

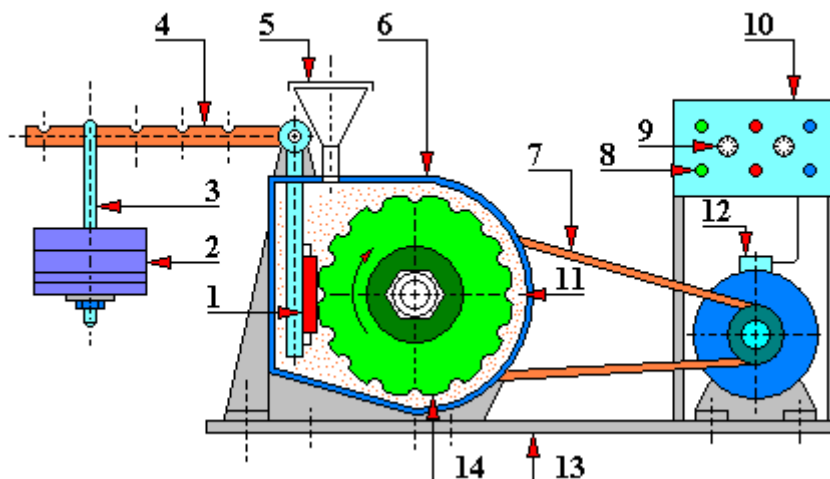


Fig. 4.1.79.2. A test rig for testing abrasion with dry/wet loose abrasive equipped with a frequency inverter

- 1 - tested sample, 2 - weights, 3 - load hanger, 4 - load arm, 5 - abrasive hopper, 6 - housing, 7 - drive belt, 8 - inverter operation controls, 9 - potentiometer, 10 - inverter (frequency converter), 11 - loose abrasive, 12 - electric motor, 13 - base, 14 - rubber wheel

4.1.80. Miller test rig

The Miller test rig is intended for conducting comparative tests of abrasive wear resistance of various groups of alloys, e.g. cast iron, composites, cast steels under abrasion conditions of metal-mixture SiC and water according to the method recommended by the American Society for Testing and Materials (ASTM), (Fig. 4.1.80.1). In this test rig the sample 6, fixed in the holder 8, moves in a reciprocating motion in a trough (working chamber) with a U-shaped section. Thanks to this it is possible for the SiC/water mixture to flow into the bottom of the trough after each working stroke of the sample 6. The speed of motion of the tested sample 6 is constant and it is 0.254 [m/sec], and the frequency of motion of this sample is equal to 0.8 [Hz]. The tilting guide arm 9 enables an easy exchange of the abrasive mass 10 and water with wear products.

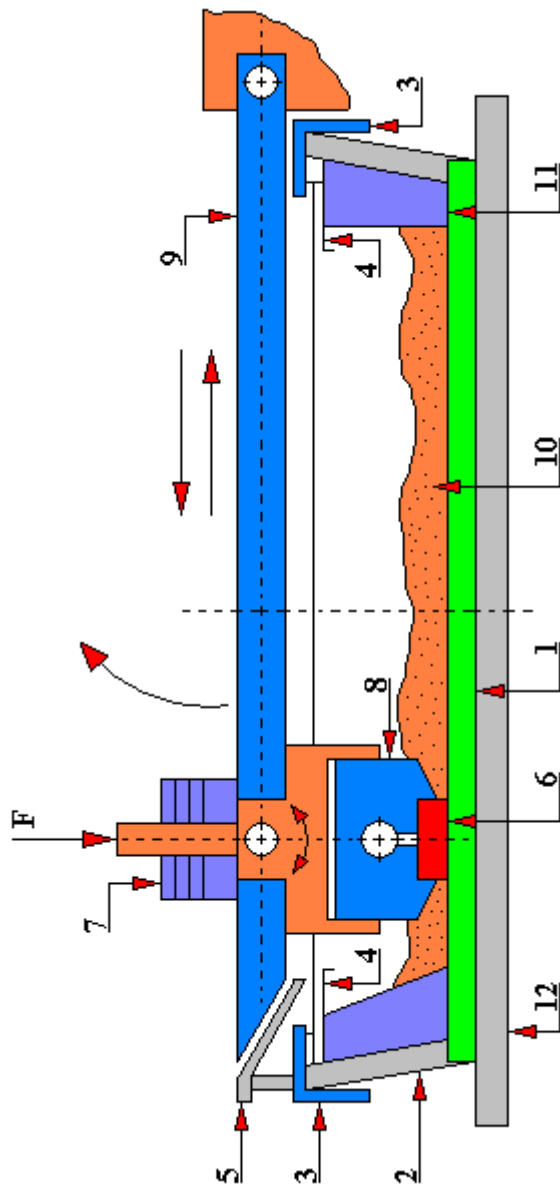


Fig. 4.1.80.1. A general diagram of the construction of the Miller test rig
 1 - washer, 2 - housing, 3 - clamping bar, 4 - protective plate, 5 - arm lift, 6 - tested sample, 7 - weights, 8 - sample holder, 9 - guide that also serves as a tilting arm of the test rig, 10 - mass abrasive, 11 - insert inside the working chamber of the test rig, 12 - base, F - force acting on the sample holder arm

4.1.81. Test rig for measuring the abrasive wear resistance using MWT method

The test rig shown in Fig. 4.1.81.1 is designed for carrying out tests of the abrasive wear resistance of materials using the Micro Wear Test (MWT) method. In this test rig, a portion of the abrasive in the form of a slurry of powdered quartz, flint or other mineral is applied to the surface of the rotating cast iron disc 4. A rotating holder 2, in which attached are test samples 1 (usually three samples), is pressed against this disc by a force F . The measure of resistance of the tested material to abrasive wear is the amount of reduction in mass of the sample/samples on the path of friction.

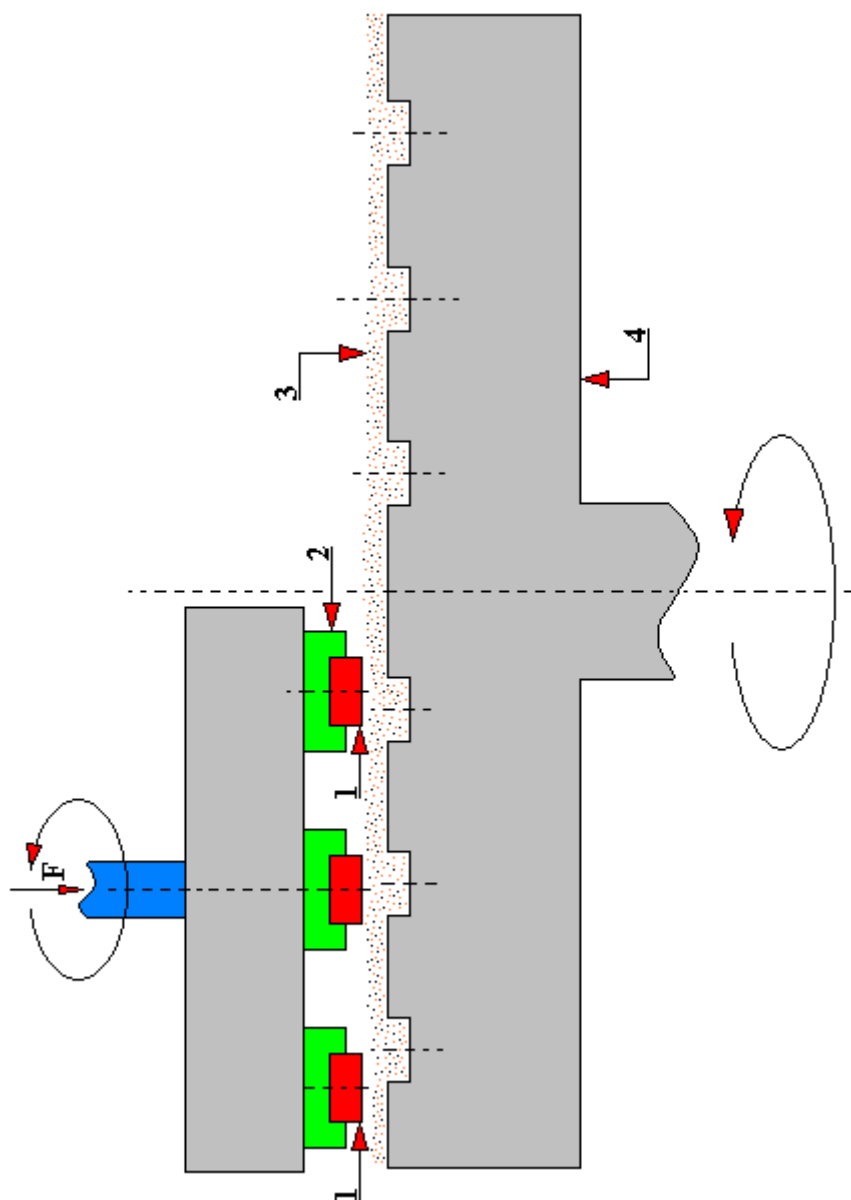


Fig. 4.1.81.1. The scheme of operation of the test rig for measuring the abrasive wear resistance using MWT method

1 - tested sample, 2 - sample holder, 3 - abrasive, 4 - cast iron disc

4.1.82. CIAT type tribotester

For the continuous abrasion test, the test rig shown in Fig. 4.1.82.1 was developed for experimental tests of the interaction of materials in the form of tool-workpiece. This test rig is built of a slowly rotating outer drum 1 inside of which the rotor 2 rotates quickly in the opposite direction to the drum rotation direction. A tool 4 (single or multi-knife) is attached to the rotor. The outer drum 1 is filled with a specified amount of test samples 3 and/or additional abrasive material. During rotation, the tool 4 co-acts with the surfaces of samples inside the drum 1. The rotational speed of the inner rotor 2 and the outer drum 1 in this test rig is regulated by two independently operating frequency converters. The range of rotational speed of the inner rotor 2 is from 60 to 650 [rpm], and that of the outer rotor 1 to 10 [rpm].

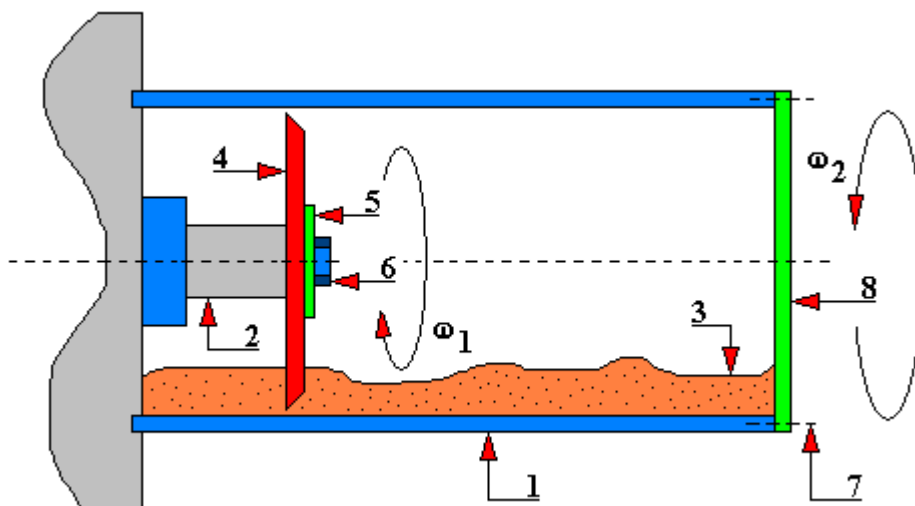


Fig. 4.1.82.1. A diagram of CIAT tribotester operation

1 - outer drum, 2 - rotating rotor, 3 - tested samples and/or additional abrasive, 4 - tool (rotating knife), 5 - washer, 6 - tool mounting screw, 7 - drum cover bolts fixing point, 8 - cover of the drum, ω_1 - angular velocity of the rotor 2, ω_2 - angular velocity of the drum 1



Fig. 4.1.82.2. A general view of the CIAT tribotester after removing the outer drum

The tribotester of the type of High Temperature Cyclic Impact Abrasion Test (HT-CIAT) was developed and produced by the Austrian Competence of Center for Tribology in Wiener Neustadt (Austria). In this test rig, the abrasive material of a given granulation acts on the tested

material through compressed air. A general view of the test rig is shown in Fig. 4.1.82.3. The abrasive and compressed air are directed parallel to the surface of the tested sample whose surface is inclined at an angle of 45° to the level. On this test rig one may carry out tests in a wide range of temperatures of the order of $500^\circ\text{C} \div 750^\circ\text{C}$ and the flow of abrasive agent in the range of a few grams/sec. Abrasive granulation from $\varnothing 0.4$ to $\varnothing 0.9$ [mm].



Fig. 4.1.82.3. A general view of the HT-CIAT tribotester
1 - test chamber, 2 - control cabinet, 3 - abrasive tank, 4 - thermal insulation, 5 - compressed gas medium supply unit

In the tank 3 there is prepared abrasive, which is fed by gravity to the tee, its one end is connected to the compressed pressure regulation unit 5, and the other to the test chamber 1 placed in a chamotte cylinder with wound heating spirals. The whole unit is placed in a thermal casing 4. The set temperature, the volume of compressed air pressure (optionally another gaseous medium) and the amount of abrasive supplied are regulated, and their data is archived by a computer system.

4.1.83. Soil bin type tribotester

The 'soil bin' type test rig is essentially similar to that of the 'rotating bowl' type test rig, except that the size of the test rig and its weight make it difficult to set its working elements in the rotational motion. In addition, setting such a large mass of soil (about several tons) in motion could cause a certain segregation of its particles (due to the centrifugal force), and thus affect the obtained test results. It is difficult to determine whether these results would differ, and possibly to what extent, from the results obtained in real conditions (e.g. on a specific area of an arable field).

In the 'soil bin' rig shown in Fig. 4.1.83.1 the stationary bin is placed on a concrete floor. This bin is formed by walls 2 built of two coaxial rings with a height of ca. 1200 [mm]. The outer ring has a diameter of ca. 4000 [mm], and the inner one is ca. 2000 [mm]. Both are usually of the same height, or the inner ring (due to the test rig's equipment including installed sensors, moisturizing system, motion mechanisms, etc.) may be lower than the outer ring by ca. 200 [mm]. Between these rings there is soil mass of up to several tons. Test samples 6 are placed in a rotary mechanism mounted above the bin with the soil. The drive system is driven by an electric motor of the main rotational motion with a power of approx. 40 [kW]. The rotational motion drive motors of sample holders have a power of approximately a few kilowatts. This test rig is also equipped with a hydraulic control system (not shown in the drawing) that simulates the operation of the installed working tools during their self-sinking into a given soil. The rotary holder of tested samples allows to mount the tested samples in a wide range of dimensions.

This test rig may have several arms (from 2 to 6) to which mounted are power transmission systems of the rotary holders 5 of samples 6 - depending on their design. The instrumentation frame and the frame 11 of the test rig are most often made of steel of ordinary quality. In extreme cases, when soil reagents are strongly alkaline or strongly acidic (depending on its origin), working elements which have a direct contact with the tested soil may be made of stainless or acid-resistant steels in order to increase their useful life.

After completion of tests, the soil mass is changed, the used samples are disassembled, the test rig is cleaned and prepared for further tests.

Fig. 4.1.83.2 shows the top view of the 'soil bin' test rig, and Fig. 4.1.83.3 shows a diagram of the test rig when the inner wall of the soil bin is lower than the outer wall (the most frequently used design).

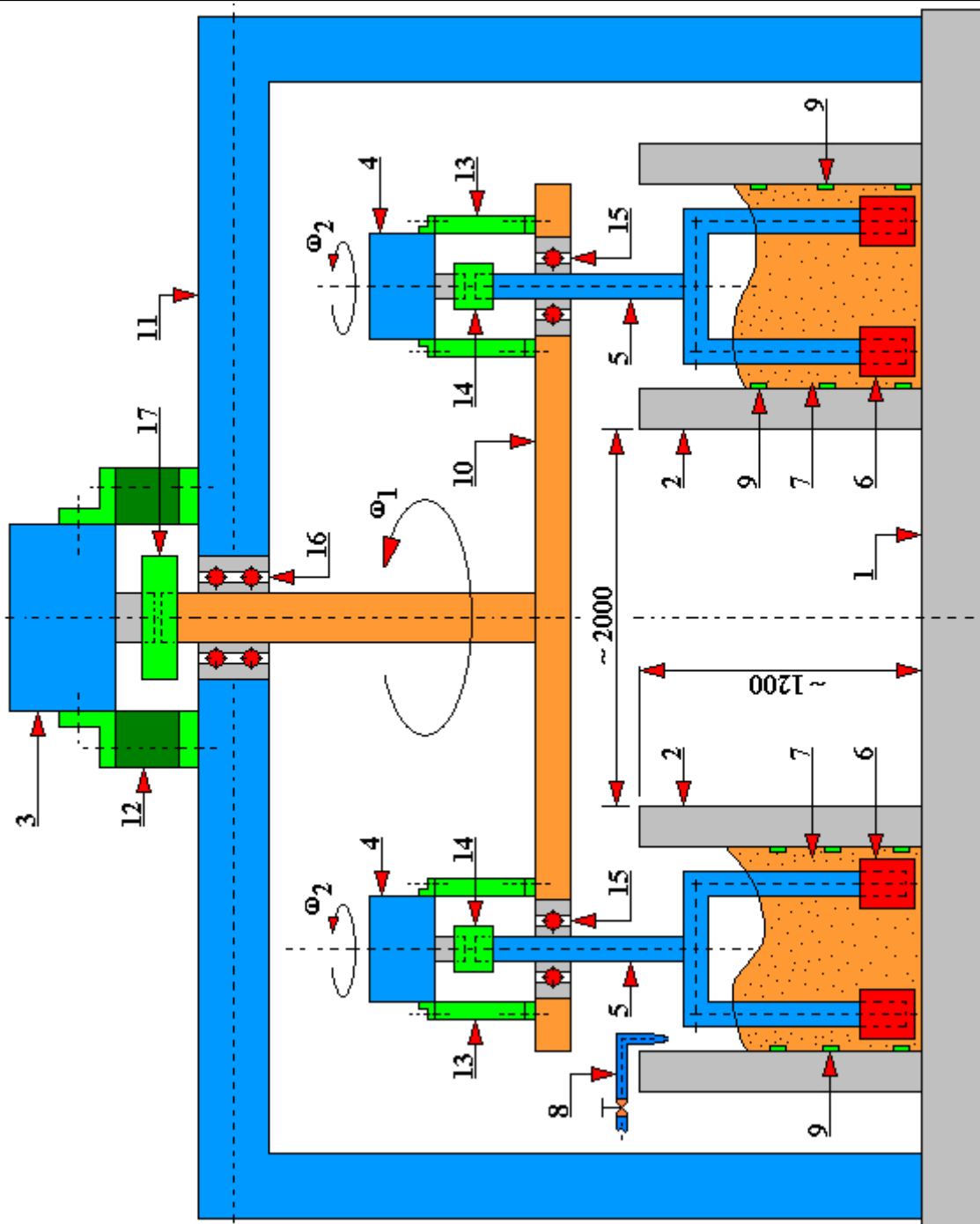


Fig. 4.1.83.1. A diagram of the test rig of the 'soil bin' type
 1 - concrete floor, 2 - bin walls, 3 - main rotation motor, 4 - sample holder rotation motor, 5 - rotating sample holder, 6 - tested sample, 7 - soil, 8 - water dosing system, 9 – soil moisture sensor, 10 - main rotary arm, 11 - test rig frame, 12 - flange fastening the motor 3 to the frame 11, 13 - steel flange fastening the motor 4 to the main rotary arm, 14 – coupling of the motor shaft 4 and sample holder 5, 15 – bearing of the rotary holder of samples 5, 16 - bearing of the main rotary arm 11, 17 – coupling of the motor shaft 3 of the main rotational motion and of the shaft of rotary arm 10, ω_1 - angular velocity of the main rotational motion motor, ω_2 - angular velocity of the rotational motion of the sample holder

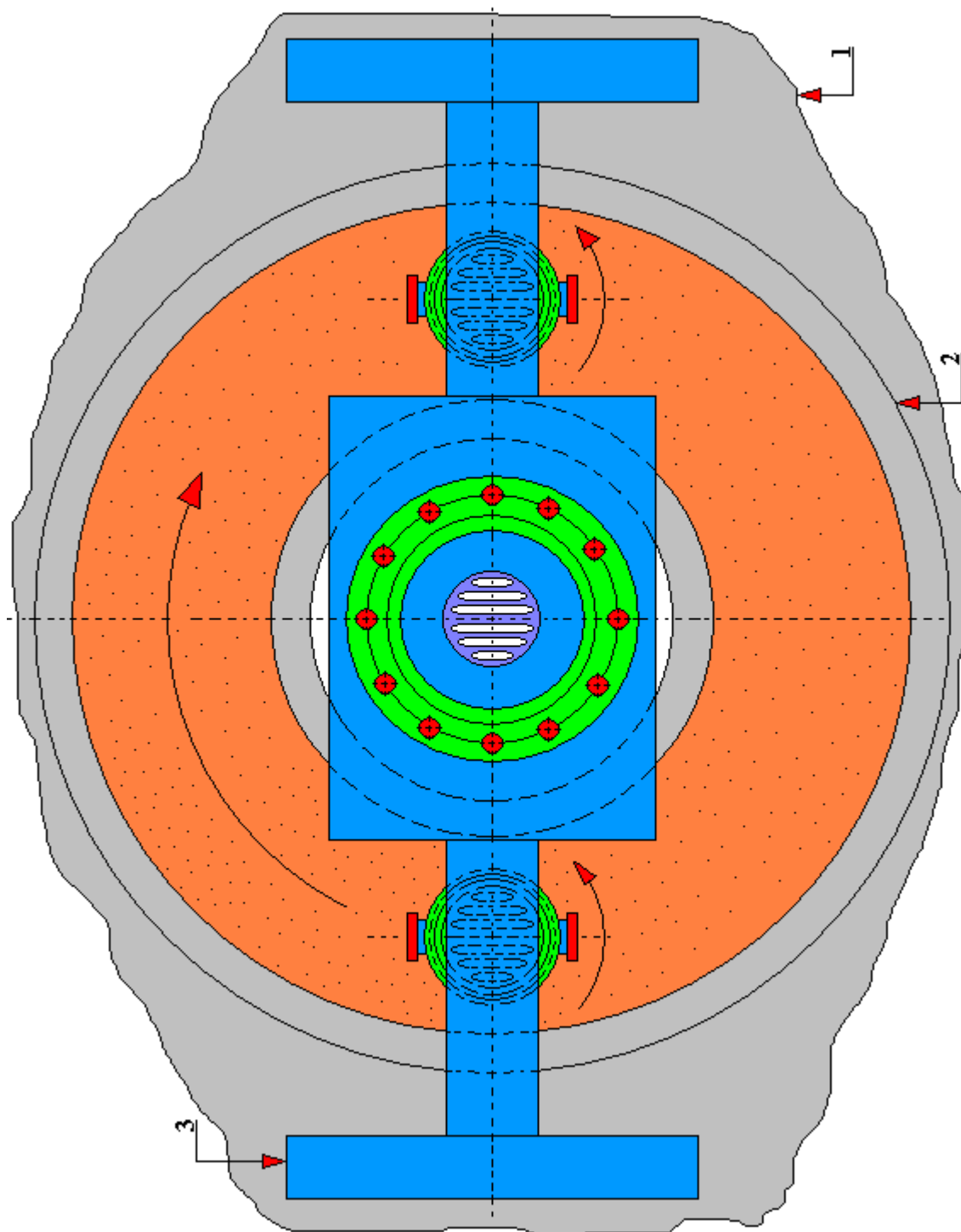


Fig. 4.1.83.2. Top view of the 'soil bin' type test rig
1 - concrete floor, 2 - external wall of the bin, 3 - frame (body) of the test rig

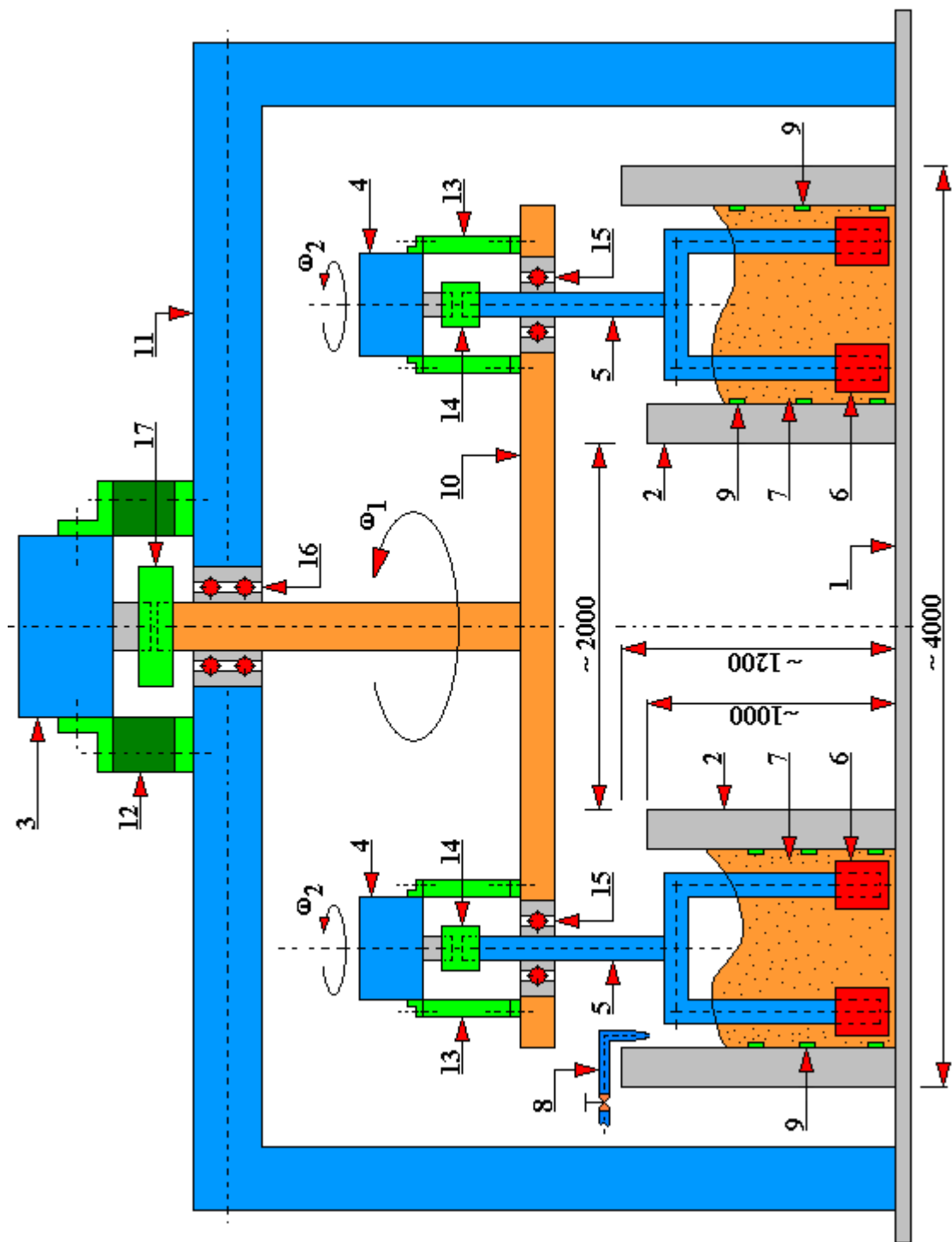


Fig. 4.1.83.3. A diagram of the 'soil bin' test rig with the inner wall of the bin lower than the outer one

1 - concrete floor, 2 - bin walls, 3 - main rotation motor, 4 - sample holder rotation motor, 5 - rotating sample holder, 6 - tested sample, 7 - soil, 8 - water dosing system, 9 – soil moisture sensor, 10 - main rotary arm, 11 - test rig frame, 12 - flange fastening the motor 3 to the frame 11, 13 - steel flange fastening the motor 4 to the main rotary arm, 14 – coupling of the motor shaft 4 and sample holder 5, 15 – bearing of the rotary holder of samples 5, 16 - bearing of the main rotary arm 11, 17 – coupling of the motor shaft 3 of the main rotational motion and of the shaft of

rotary arm 10, ω_1 - angular velocity of the main rotational motion motor, ω_2 - angular velocity of the rotational motion of the sample holder

4.1.84. Centrifugal particle accelerator

A centrifugal particle accelerator is an example of a sandblasting, shot blasting or glass beads blasting test rig for measuring wear. A simple design ensures repeatability of test results, stability of its operating parameters, in particular pressure and flow efficiency of the medium (abrasive) and a constant distance of the rotary arm nozzle (rotary arms) from the tested samples (Fig. 4.1.84.1). The nozzles are usually interchangeable with different diameters. Centrifugal force is used to impart kinetic energy to the abrasive particles. As a result, loose abrasive is thrown through the channel from the center (axis of rotation) to the outside. Inside the tubular arm (channel) the abrasive particles are accelerated. The maximum discharge velocity is at the end of the arm. The distances of samples from the nozzle exit and their inclination α can be adjusted as needed.

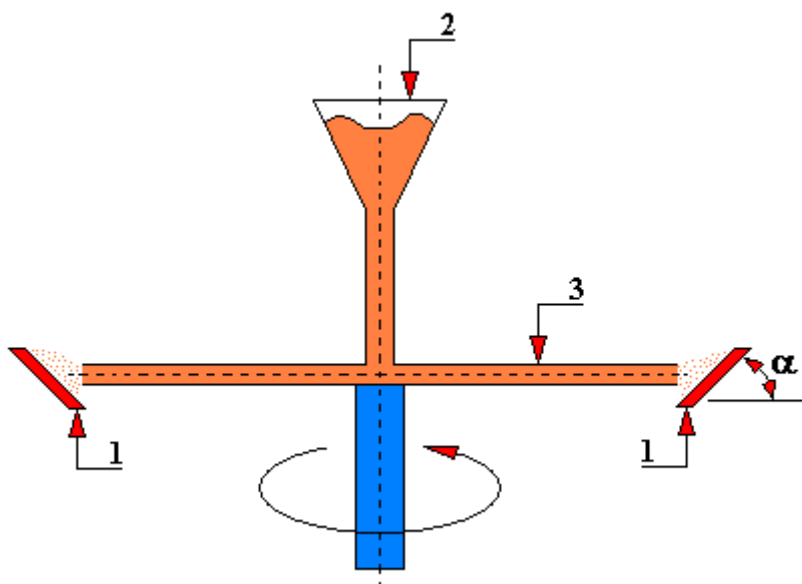


Fig. 4.1.84.1. A general diagram of a centrifugal accelerator of abrasive particles [38]
1 - tested samples, 2 - abrasive tank, 3 - rotating arm in the form of a tube, α - angle of inclination of the tested samples in relation to the direction of the outflow of the abrasive

4.1.85. Tribotester with a friction contact: piston ring-cylinder liner surface

This tribological test rig simulates the operation of elements of a piston group in the combustion engine or in a reciprocating compressor (Fig. 4.1.85.1). Sample 2 is a piston ring section and the counter-sample 1 is a cylinder liner section. Counter-samples are attached to the guide 3. The guide is mounted on one side in the piston head driven by a connecting rod from the crankshaft. The other end of the guide is led in a plain bearing. In this way the counter-sample makes a reciprocating motion. The samples mounted in bar-shaped force transducers 5 with glued strain gauges 6 are pressed against the counter-sample by means of hydraulic actuators 7 through articulated pushers 8. The pair can be lubricated with oil mist injected directly onto the sliding surface from two nozzles (not shown in the drawing). This test rig enables a continuous registration of friction forces and temperatures of the friction contact.

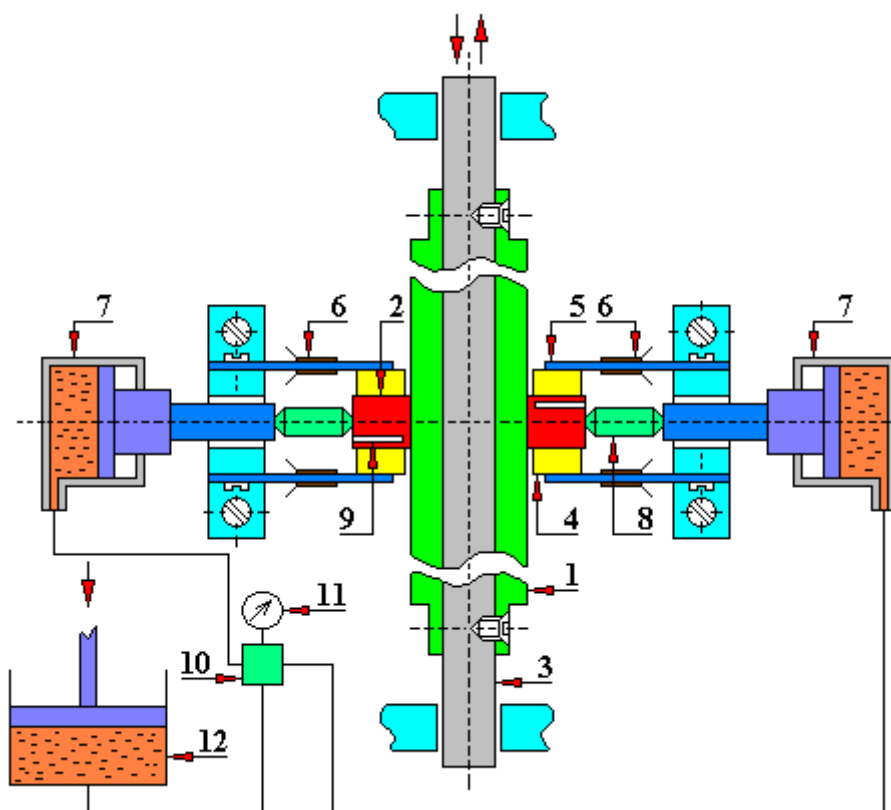


Fig. 4.1.85.1. A diagram of the test rig for tribological tests with the mating of piston ring and cylinder liner surface [173]

1 - counter-sample, 2 - sample, 3 - guide, 4 - sample holder mounted as articulated on the force transducer, 5 - force transducer, 6 - full bridge extensometer, 7 - hydraulic actuator, 8 - articulated pusher, 9 - thermocouple hole, 10 - hydraulic distributor, 11 - pressure gauge, 12 - hydraulic pump

4.1.86. Krauss tribotester

The Krauss test ring (Fig. 4.1.86.1) is designed for:

- determining the value of the mass wear of the friction material (sample) on the basis of which the volumetric wear is calculated;
- determining the value of linear wear.

The above-mentioned test rig is equipped with a high-power DC motor 6 (136 kW) which is the source of drive for it. The drive from the DC motor 6 is then transmitted via a gear transmission 7 to the active (drive) shaft 9. The brake disc 14 - most often cast iron - is mounted on this shaft. The brake disc 14 co-acts with brake shoes 15 which are samples of the friction material. This test rig allows to perform tests with a constant braking torque up to 981 [N m] and with a constant speed (the so-called *drag test*).

The structure of this tribological test rig also includes a cooling system consisting of two fans: blow 5 and exhaust 2. In addition, air conditioning is installed in the cooling air intake system. The force of pressure of the brake shoes 15 against the cast-iron brake disc 14 comes from the hydraulic system 1 which enables the pressure to be changed in the range of 0 ÷ 9 [MPa]. The archiving and visualization system of data collected from the test rig during the tests enables:

- measuring the rotational speed of the brake disc 14;
- measuring the pressure in the hydraulic (brake) system;
- measuring the temperature on the surface of the brake disc 14;
- measuring the braking torque.

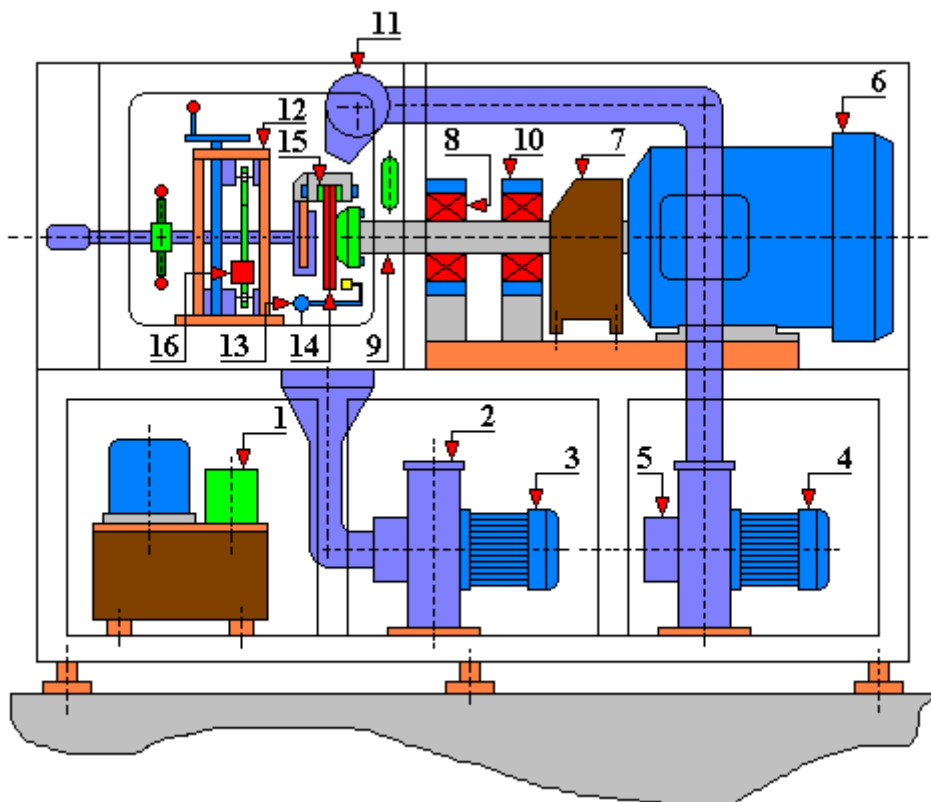


Fig. 4.1.86.1. A general diagram of the test rig for Krauss tribological tests

1 - hydraulic system, 2 - ventilation system, 3 - ventilation system drive motor, 4 - cooling system drive motor, 5 - cooling system, 6 - DC motor, 7 - gear transmission, 8 - bearing, 9 - active (drive) shaft, 10 - bearing housing, 11 - cooling system outlet (air supply), 12 - bracket, 13 - temperature sensor, 14 - brake disc, 15 - brake shoe, 16 - braking torque converter

The tested brake is mounted on the Krauss test rig as described in the ECE Regulation 90 (Annex 9, point 3.1.1.) [Regulation 90 of the United Nations Economic Commission for Europe (UNECE) - Uniform conditions for the approval of replacement brake lining assemblies and replacement drum brake linings for power-driven vehicles and their trailers]. The tests of friction materials can be carried out according to various tests [1. Metoda badawcza nr 17 firmy Lumag: Badanie współczynnika tarcia na stanowisku typu Krauss RWDC 136B; 2. Nosal S., Orłowski T.: Wpływ temperatury na właściwości tribologiczne skojarzenia: modyfikowany materiał czarny – żeliwo szare, Tribologia 2005, nr 3, s. 257÷265, 3. Nosal S. Tribologia – Wprowadzenie do zagadnień tarcia, zużycia i smarowania, wydanie 2 rozszerzone, Wydawnictwo Politechniki Poznańskiej, Poznań 2016].

Diagrams of the tested friction contacts are shown in Figures 4.1.86.2 and 4.1.86.3.

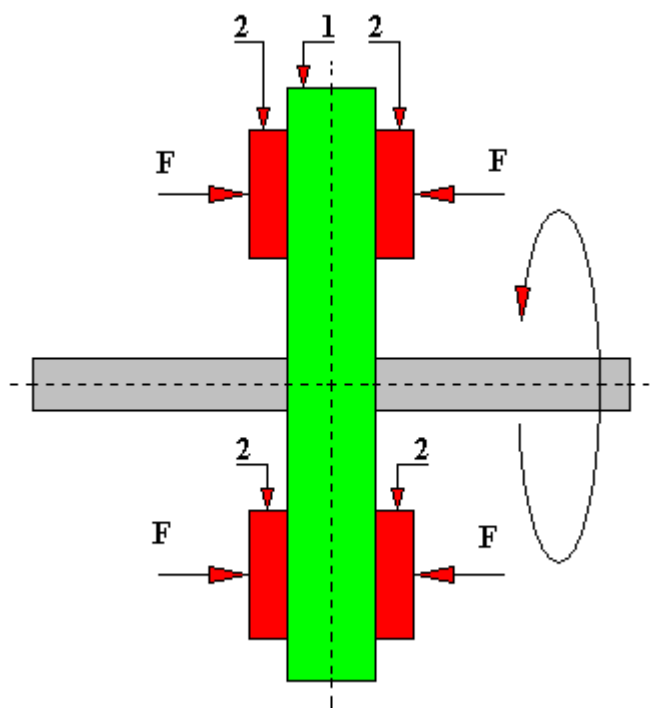


Fig. 4.1.86.2. A diagram of the mating of the friction contact: brake disc - brake shoes; version with two pairs of brake shoes

1 - brake disc (most often cast iron); 2 - brake shoes (samples of the friction material)

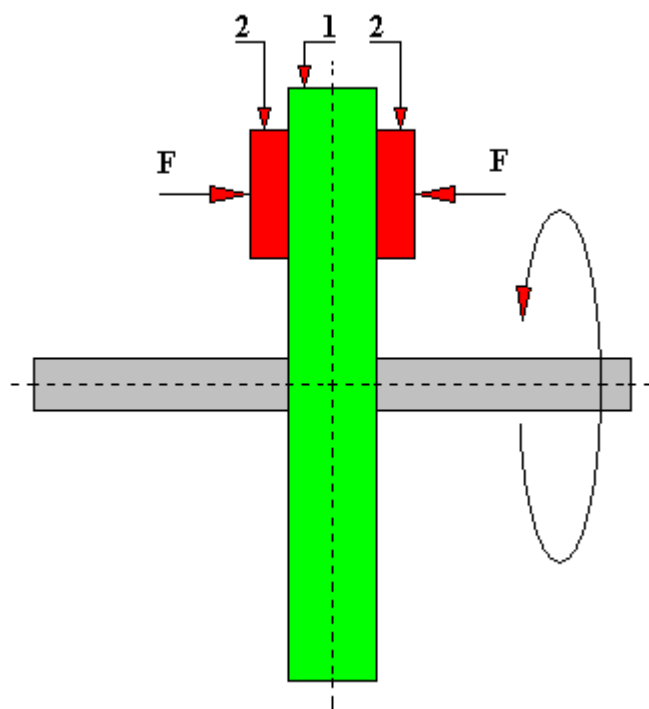


Fig. 4.1.86.3. A diagram of the mating of the friction contact: brake disc - brake shoes; version with one pair of brake shoes
 1 - brake disc (most often cast iron); 2 - brake shoes (samples of the friction material)

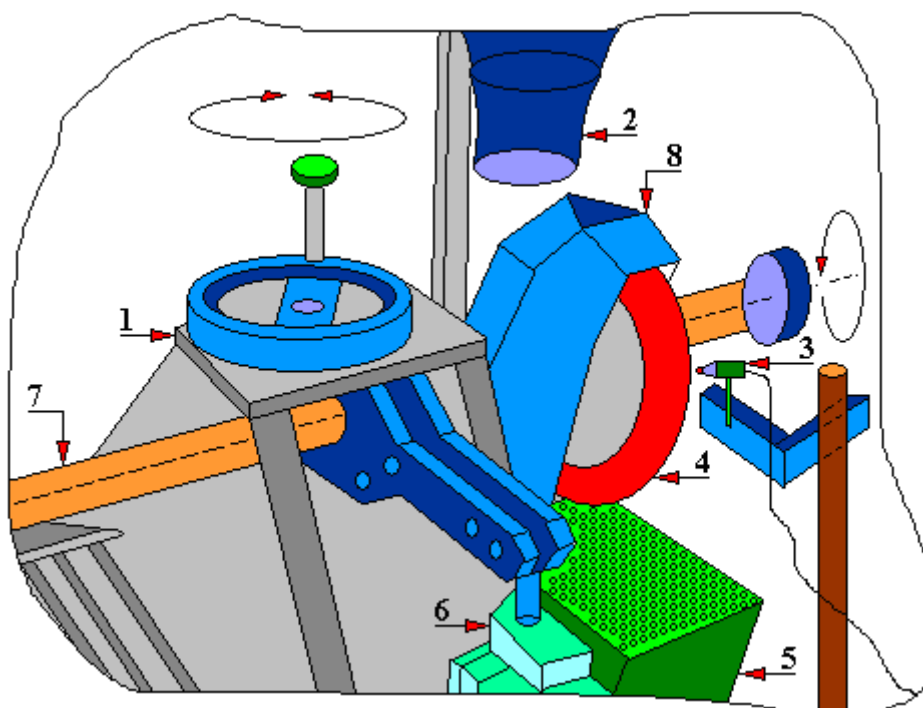


Fig. 4.1.86.4. A general view of the brake on the Krauss RWDC 136B test rig
 1 - bracket; 2 - cooling system (air supply); 3 - temperature sensor; 4 - brake disc; 5 - ventilation (exhaust) system; 6 - braking torque converter; 7 - rotary shaft; 8 - brake caliper

4.1.87. Tribotester for inertial testing TecSA TT 2400EL

On the inertia test rigs, the test conditions are similar to the actual working conditions of the brakes in vehicles. When building this type of rigs, the following basic factors influencing the operation of the brakes are taken into account:

- vehicle speed as reflected by the rotational speed of the wheels;
- the mass of the braked vehicle.

An example of the TecSA TT 2400 EL inertia rig is presented below (Fig. 4.1.87.1). The inertia wheels 4 mounted therein simulate a wheel load corresponding to the transported masses (loads). The motor 3 gives the inertia wheels 4 the set rotational speed. During the tests on this test rig, braking takes place, during which the following are measured:

- brake actuator stroke;
- brake system pressure;
- disc temperature;
- temperature of brake shoes;
- braking torque;
- velocity;
- braking distance.

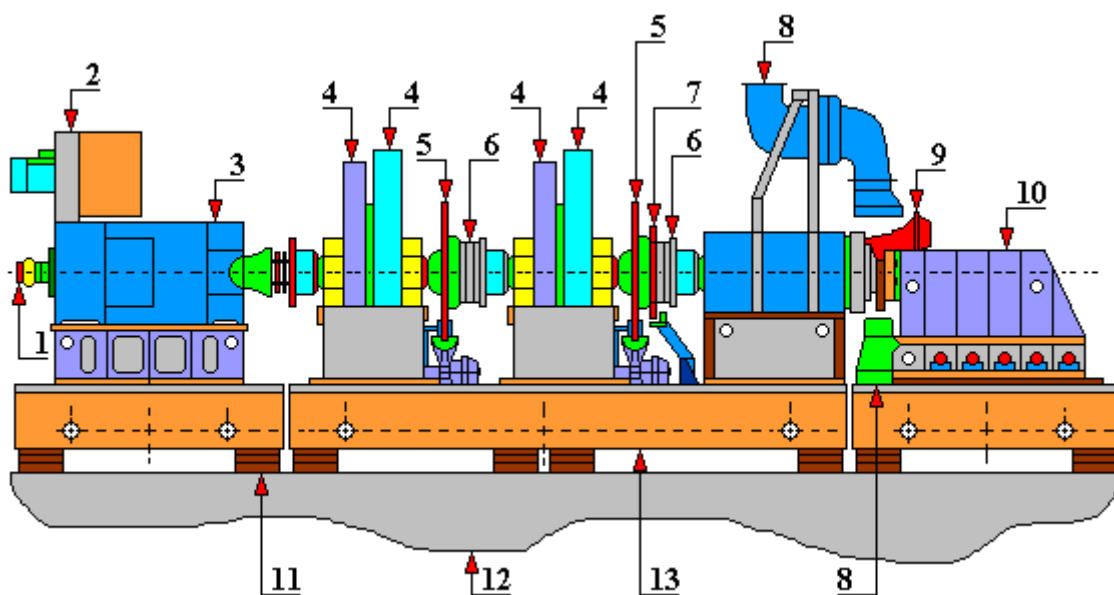


Fig. 4.1.87.1. A general diagram of the test rig for testing brakes TecSA TT 2400EL
 1 – tachometer (rev counter); 2 - electrical box; 3 - engine; 4 - inertia wheel; 5 - safety brake;
 6 - clutch; 7 - torque meter; 8 - ventilation; 9 - tested brake with a brake disc; 10 - trolley for
 mounting the brake or axle of the vehicle; 11 - adjustable legs; 12 - foundation; 13 - base

The above test rig is characterized by the following parameters: moment of inertia range:
 100÷2600 [kg·m²];

- maximum speed: 1500 [rpm];
- air pressure in the brake system: 0÷10 [bar];
- maximum braking torque: 40 000 [Nm];

- drive with a direct current motor with a power of 440 [kW];
- the possibility of installing a complete axle or just a brake;
- temperature measurement: 0÷1000°C;
- possibility of installing a fan simulating the wind;
- possibility of installing brake sprinklers simulating rain.

4.1.88. FAST tribotester

The FAST test rig (Fig. 4.1.88.1) is an example of a test rig designed to determine the tribological properties of the pair: friction material-raceway, i.e. the value of the friction coefficient, its stability during braking and wear resistance. The FAST tribotester is mainly used to determine the friction coefficient as a function of temperature at constant speed and changing pressure in order to obtain a constant friction force throughout the duration of the experiment. The test rig was developed at Ford factories.

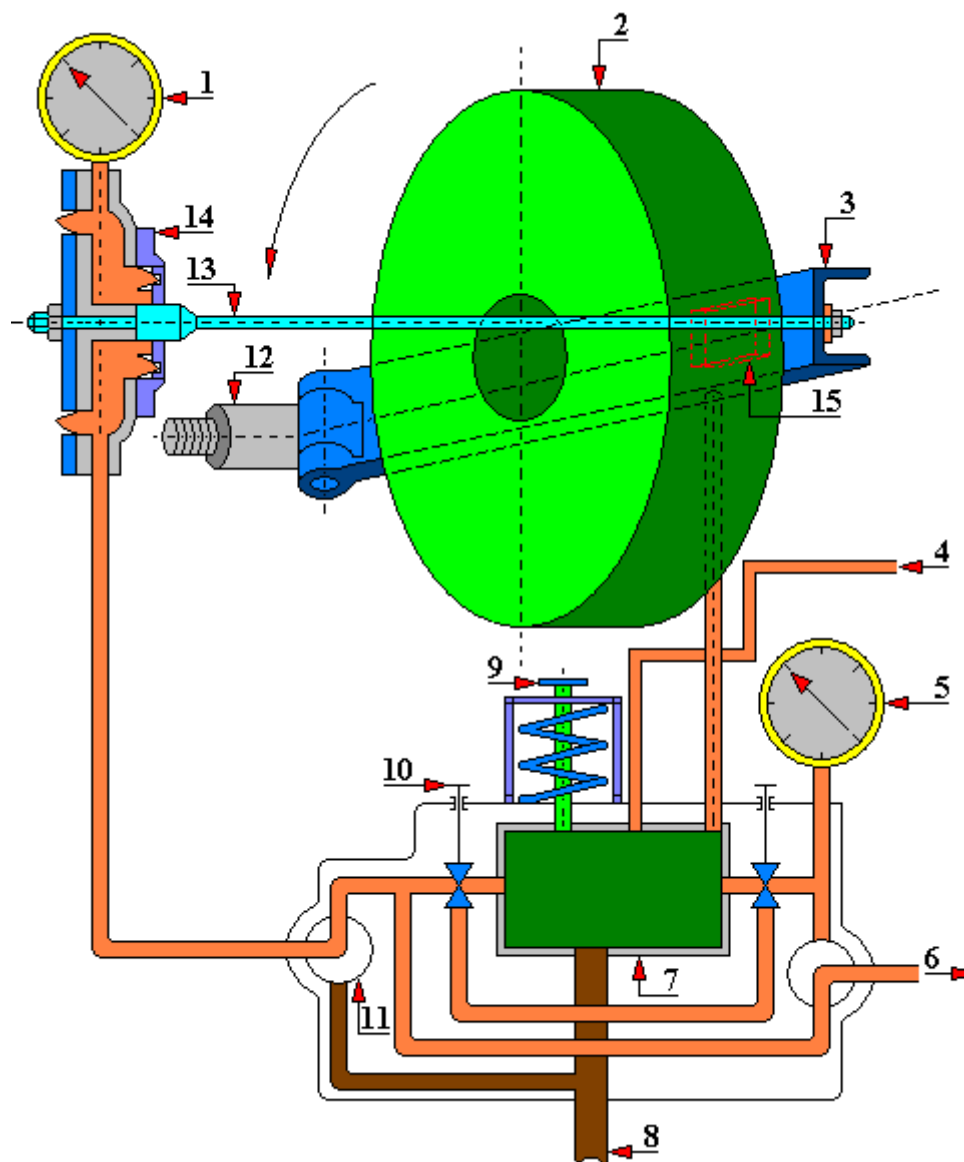


Fig. 4.1.88.1. A general A diagram of the FAST tribotester

1 - pressure force sensor; 2 - brake disc; 3 - sample holder arm; 4 - oil pump duct; 5 - manometer; 6 - actuator feed; 7 - valve island (working elements - slide valves); 8 - outflow to the reservoir; 9 - manual load regulation; 10 - needle valve; 11 - distribution valve; 12 - joint; 13 - rod; 14 - force exerting actuator; 15 - tested sample (12.7x12.7x3.18 mm)

4.1.89. Test rig for testing the degree of wear of hydraulic elements or systems according to the patent PL 187 552

The test rig, according to the patent PL 187 552, the author of which is Edward Lisowski, is designed to test the degree of wear resulting from friction of co-acting moving parts in elements of hydraulic systems operating in various test rigs.

The course of the wear process of co-acting elements due to friction is well known. In the first stage there is lapping of co-operating surfaces and the machining irregularities are removed as a result of which various filings and small turnings are emitted into the oil. As the surface is smoothed, the amount of turnings decreases and a small amount of fine particles of contamination is formed in the second step. In the last, third stage, wear increases rapidly and the amount and size of impurities increases. For each element, you can develop a wear chart that shows the amount of impurities depending on the degree of wear of this element.

The test rig for testing the degree of wear of hydraulic elements or systems according to this design solution has a four-way, two-position, hydraulically controlled distributor. The working input of the distributor is connected to the supply connection located on the drain line from the tested element. The drainage outlet of the distributor is connected to the outflow connection leading to other system elements or directly to the oil tank.

One working outlet of the distributor is connected by a conduit to the first filter chamber, and its second identical chamber is connected by a conduit to the second outlet of the distributor. The internal shapes of both chambers are made in such a way that they do not stop and deposit contamination particles contained in the oil flowing through the filter in any direction.

The filter has got a filter element in the form of a metal mesh with small dimensions of the filtering surface.

In the output position of the distributor, the supply connection is connected to the first chamber of the filter, the second chamber of which is connected to the outflow connection. After reversing the distributor, the second filter chamber is connected to the supply connection, and the first one to the discharge connection, as a result of which the direction of oil flow through the filter is changed.

From the conduit connecting the working outlet of the distributor with the first filter chamber, there is a branch leading to the overflow valve. From the output of this valve there is a line on which an adjustable throttle valve is mounted with the output connected to the outflow connection. From this line, between the overflow valve and the throttle valve, a branch leads to the control element of the distributor.

A counter is mounted on the control element of the distributor, which records the number of reversals of this distributor.

The task of the overflow valve is to send an impulse causing the distributor to reverse, because as a result of clogging the mesh with impurities, the oil flow resistance through the filter will increase.

The throttle valve is used to set the sensitivity of the operation of this test rig.

The advantage of this test rig is its small external dimensions, therefore it can be installed even in a hard-to-reach place in the system. The amount of contaminants involved in a one-time clogging of the mesh is constant for a specific test rig. Assuming the number of reversals recorded by the meter, it is possible to precisely determine the amount of impurities released into the oil by the tested element. A small mesh is quickly clogged with a small amount of contaminants, which results in a high switching frequency, increasing the accuracy of the average measurement result. This accuracy is used to assess the degree of wear of the element, on the basis of which the repair of the tested element can be predicted.

This test rig can be installed in the system in parallel in such a way that the contaminated oil flows through the filter in an appropriate proportion to the entire outflow of oil from the tested

element. As a result, this small test rig can be used to test items having a much higher throughput than the above test rig.

The number of switching operations compared with an appropriately scaled graph shows the place on the wear curve for a given element. An appropriately prepared table may be used instead of a graph.

The test rig can be used on test rigs inter alia to prepare wear curves.

The essence of the operation of the test rig is as follows (Fig. 4.1.89.1). In the initial position of the distributor slider 3, the oil from the tested element flows through port 1, distributor 3, line 4, first filter chamber 5, mesh 6, second filter chamber 5, line 7 and through the distributor 3 to port 2. At the same time, through the line 8, oil is led to the overflow valve 9 which is closed.

Impurities accumulate on the mesh 6 and they clog this mesh 6 causing an increase in the flow resistance, as a result of which oil begins to flow through the overflow valve 9 and through the line 10 through the throttle valve 12 to the drain port 2. At the same time, a signal is sent from the line 10 to the control element 11, causing the distributor 3 to reverse, which is recorded by the counter 13. Then the oil flows through the filter 5 in the opposite direction and very quickly removes impurities from the mesh 6, which, together with the oil, flow through the line 4 through the distributor 3 to the drain port 2 and further to the tank.

After cleaning the mesh 6, the flow resistance through the filter 5 decreases, as a result of which the overflow valve 9 closes and the distributor slider 3 returns to its original position. The oil begins to flow through the line 4 to the filter 5 and the whole cycle repeats itself until the operation of the tested system is interrupted.

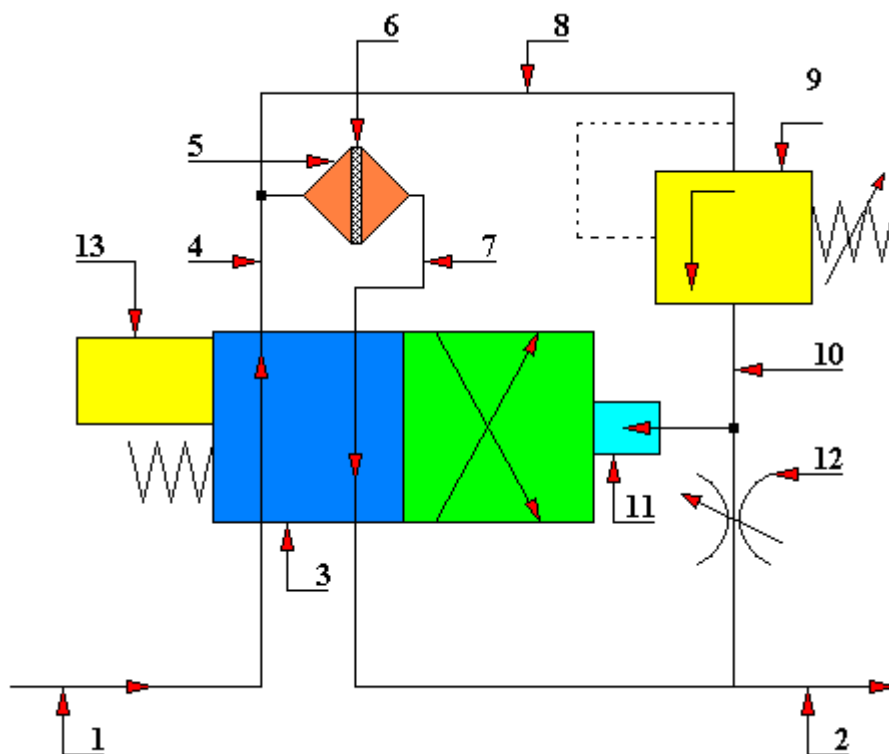


Fig. 4.1.89.1. A diagram of a test rig for testing the degree of wear of hydraulic elements or systems according to the patent PL 187 552

1 - port; 2 - port; 3 - distributor slider; 4 - line; 5 - filter; 6 - mesh; 7 - line; 8 - line; 9 - overflow valve; 10 - oil flow line; 11 - control element; 12 - throttle valve; 13 – counter

4.1.90. Test rig for testing high-speed headstocks according to the patent PL 55 370

The test rig, according to the patent PL 55 370, the author of which is Wit Werys, is intended for testing high-speed headstocks, especially grinding ones under load. In this design, the rolling bearing has been eliminated, making it possible to test the headstocks at the speed of 50,000 or more revolutions per minute. So at rotations that ordinary rolling bearings cannot withstand. Excessive heating of the tension member and the headstock tip due to friction has also been eliminated.

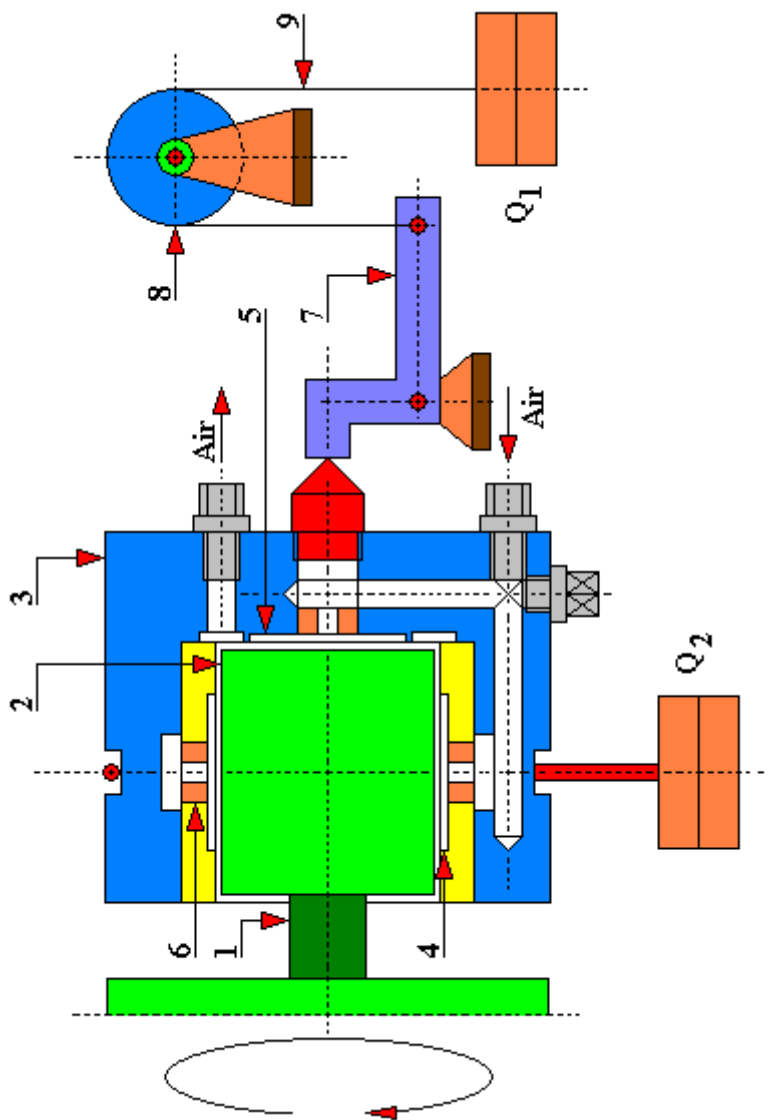


Fig. 4.1.90.1. A diagram of a test rig for testing a headstock according to the patent PL 55 370
 1 - tested headstock; 2 - headstock tip; 3 - non-rotating sleeve; 4 - radial air chamber; 5 - longitudinal air chamber; 6 - chokes; 7 - two-arm lever; 8 - pulley; 9 - line / tension member; Q₁ - longitudinal force; Q₂ - lateral force

The essence of the operation of this structure is as follows (Fig. 4.1.90.1). The tip 2 is attached to the tip of the tested headstock 1, onto which a non-rotating sleeve 3 is placed loosely. This sleeve has radial 4 and longitudinal 5 air chambers to which compressed air is supplied through chokes 6.

When testing headstocks, the sleeve 3 is loaded with external forces: longitudinal Q_1 and transverse Q_2 .

The values of the forces are determined by the size of the weights used, and a two-arm lever was used to change the vertical gravity force Q_1 into a longitudinal force acting on the system. This lever acts with one arm on the tusk embedded in the non-rotating sleeve 3, while its other arm is affected by the force of gravity of the weights through a line thrown through the pulley.

And the non-rotating sleeve 3 acts on the tip of the headstock 2 via the air cushions formed in the radial 4 and longitudinal 5 chambers by supplying these chambers with compressed air.

The non-rotating housing, with the headstock tip, forms an aerostatic bearing.

4.1.91. Test rig for testing impact and grinding wear according to the patent PL 210 732

The test rig, according to the patent PL 210 732, the authors of which are: Tadeusz Hejwowski, Andrzej Weroński and Jerzy Kielbiński, is designed for impact and grinding wear testing.

The wear test with the use of this test rig consists in measuring the loss of mass of the tested sample along the selected friction path of the roller driven by the gear motor. This roller acts as a counter-sample and is in contact with the surface of the test sample. And the sample is fixed in the arm holder and pressed against the roller (counter-sample) by means of a loading system.

The load system consists of a spring deformed by a slider connected through a force sensor to a second slider on the lever side. Both sliders move along a pair of mutually parallel guides.

The slider on the lever side is driven by a gear motor with an adjustable eccentric mounted on the output axis. This eccentric is connected via a link (a connector with adjustable length) to a lever arm with a fixed axis of rotation. The second arm of the lever with a fixed axis of rotation is connected with the slider by means of a connector of adjustable length.

The amplitude of the reciprocating motion is set by means of an eccentric with an adjustable radius (arm).

The initial displacement of the sliders is set using connectors with adjustable length.

The abrasive of known granulation from the abrasive reservoir is fed to the contact area of the roller (counter-sample) and the sample.

This test rig makes it possible to load the friction contact with known force waveforms and to continuously measure the values of these forces. In addition, its design allows to accurately model the working conditions of industrial elements subjected to wear and to carry out tests on the issues of material wear.

The essence of the operation of this test rig is as follows (Fig. 4.1.91.1). Measurement of the loss of the tested sample 1 is made along the selected friction path of the roller (counter-sample) 2 driven by the gear motor 3. The generator of a roller (counter-sample) 2 touches the surface of the tested sample 1. This sample is attached to the arm 4 and pressed against the roller (counter-sample) 2 with a variable force exerted by the load system.

The load system consists of a spring 5 deformed by a slider 6 connected through a force sensor 7 to a second slider 8 on the side of the lever 13. Both sliders (6 and 8) move along a pair of mutually parallel guides 9.

Slider 8 on the side of the lever 13 is driven by a gear motor 10 with an adjustable eccentric 11 mounted on the output axle.

An adjustable eccentric 11 is connected via a connector 12 of adjustable length to a lever arm 13 with a fixed immobile axis of rotation. The second arm of the lever 13 is connected by means of a connector 14 (with adjustable length) to the slide 8 on the side of the lever 13.

The amplitude of the reciprocating motion is set by moving the axis 15 of the eccentric 11 relative to the output axis of the gear motor 10.

The initial displacement of sliders 6 and 8 is inflicted by the change of length of connectors 12 and 14.

The value of the pressing force of the sample 1 exerted by the spring is measured with the force sensor 7.

The abrasive from the reservoir 16 is fed at the selected rate into the contact area of the roller (counter-sample) 3 with the sample 1.

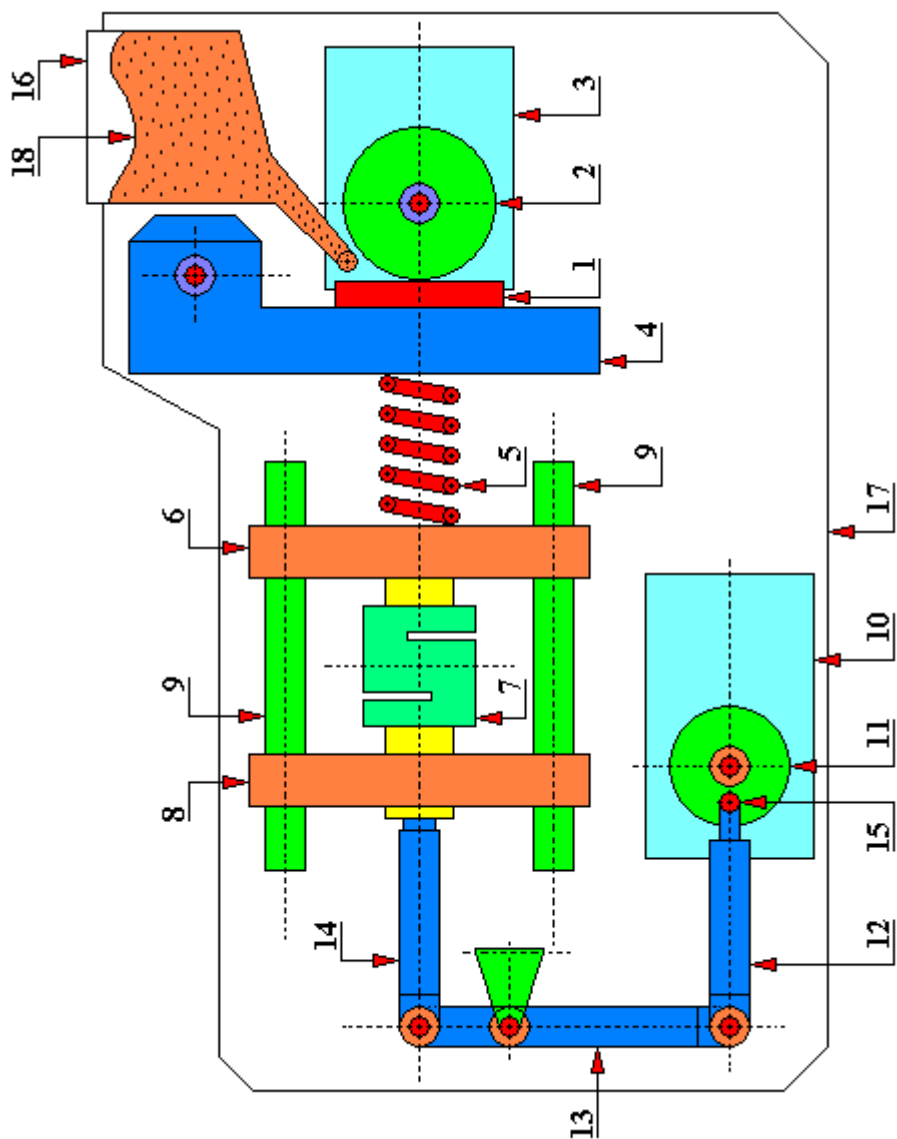


Fig. 4.1.91.1. A diagram of a test rig for the impact-abrasive wear test according to the patent PL 210 732

1 - tested sample; 2 - roller (counter-sample); 3 - gear motor; 4 - arm; 5 - spring; 6 - slider; 7 - force sensor; 8 - slider; 9 - a pair of guides; 10 - gear motor; 11 - eccentric; 12 - connector; 13 - lever; 14 - connector with adjustable length; 15 - axis of the eccentric; 16 - abrasive container 17 - test rig body; 18 - abrasive

4.1.92. Test rig for comparative testing of the wear resistance of friction materials according to the patent PL 123 756

The test rig, according to the patent PL 123 756, author of which is Aleksander Derkaczew, is intended for a comparative testing of the wear resistance of friction materials by triggering a controlled friction phenomenon and determining wear after a fixed operating time.

Comparative tests of the wear resistance of friction materials, both frictional and sliding, are used to ensure the proper selection of materials for friction contacts with specific wear durability requirements.

During comparative tests, a very important issue is to ensure the same possible friction conditions for various tested materials, and above all temperature on the friction surface, surface pressures and sliding velocity. Only then are the wear results of tests of individual materials comparable.

There are a large number of test rigs that allow only successive testing of individual friction materials at the same surface pressure and sliding velocity. However, maintaining the same temperature on the friction surfaces is very difficult for sliding materials, and practically impossible for high-abrasive materials. Because it depends primarily on the value of the friction coefficient, and this value is different for different friction materials. At the same time, the temperature on the friction surfaces has the greatest impact on the tested wear resistance.

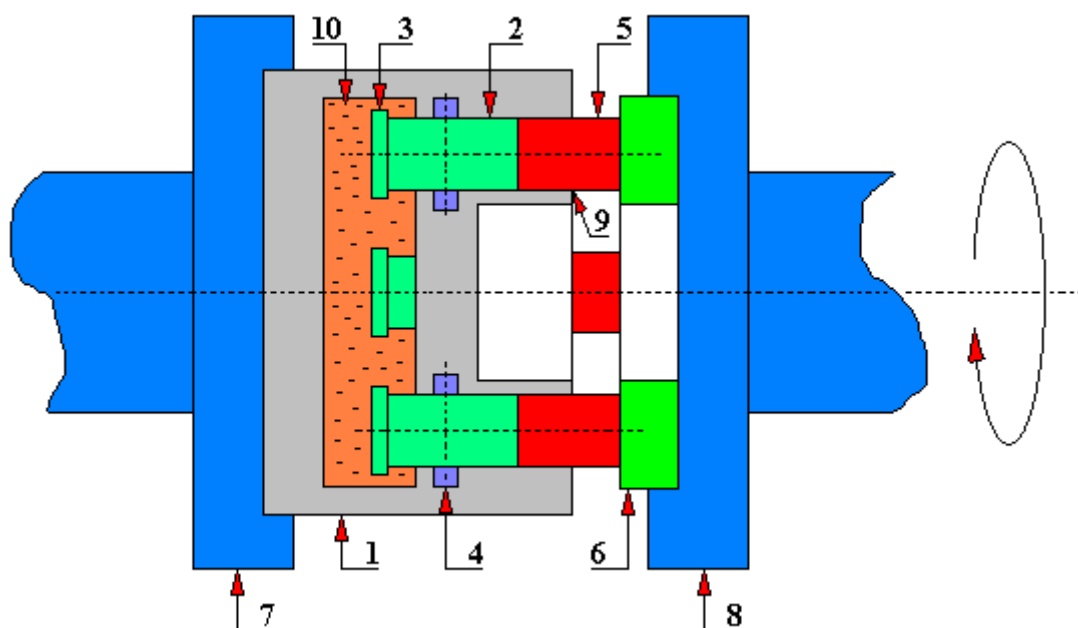


Fig. 4.1.92.1. A diagram of a test rig for comparative testing of the wear resistance of friction materials according to the patent PL 123 756

1 - body; 2 - pistons; 3 - safety flange; 4 - gaskets; 5 - tested samples; 6 - disc (counter-sample); 7 - head; 8 - head; 9 - openings in seats; 10 - oil

The essence of operation of this test rig is as follows (Fig. 4.1.92.1). In the body 1 there are openings 9, in which there are pistons 2 ended with safety flanges 3. These flanges prevent

the pistons 2 from slipping out. The pistons 2 are sealed in the body 1 by gaskets 4. The body 1 is filled with a liquid (oil).

In the sockets formed by the openings 9 and the front surfaces of the pistons 2, the test samples 5 are placed, which are pressed against the mating disc 6 (counter-sample) by the heads 7 and 8, or by a specific pressure applied to the inside of the body 1.

During the test one of the heads 7 or 8 rotates, causing the process of friction between the samples 5 and the disc 6. An uneven wear of individual samples 5 during the test causes different changes in the position of individual pistons 2, while maintaining the same pressure for pressing the samples 5 against the disc 6 (counter-sample).

The above drawing does not show how the oil is supplied to the body as it is irrelevant to this invention.

The above test rig allows four samples to be tested simultaneously. Of course, it is possible to redesign this test rig so that, for example, it is possible to test two, three, six, eight, etc. samples simultaneously, as needed.

4.1.93. Test rig for testing the wear of bodies in an abrasive mass according to the patent PL 150 471

The test rig, according to the patent PL 150 471, the author of which is Jan Sadowski, is intended for testing the wear of bodies in the abrasive mass under the variable conditions of displacement of the body and the abrasive mass.

This test rig (Fig. 4.1.93.1) was made as a container 1 filled with abrasive 4 with a set of displacement in relation to this abrasive of the tested body (samples) 6.

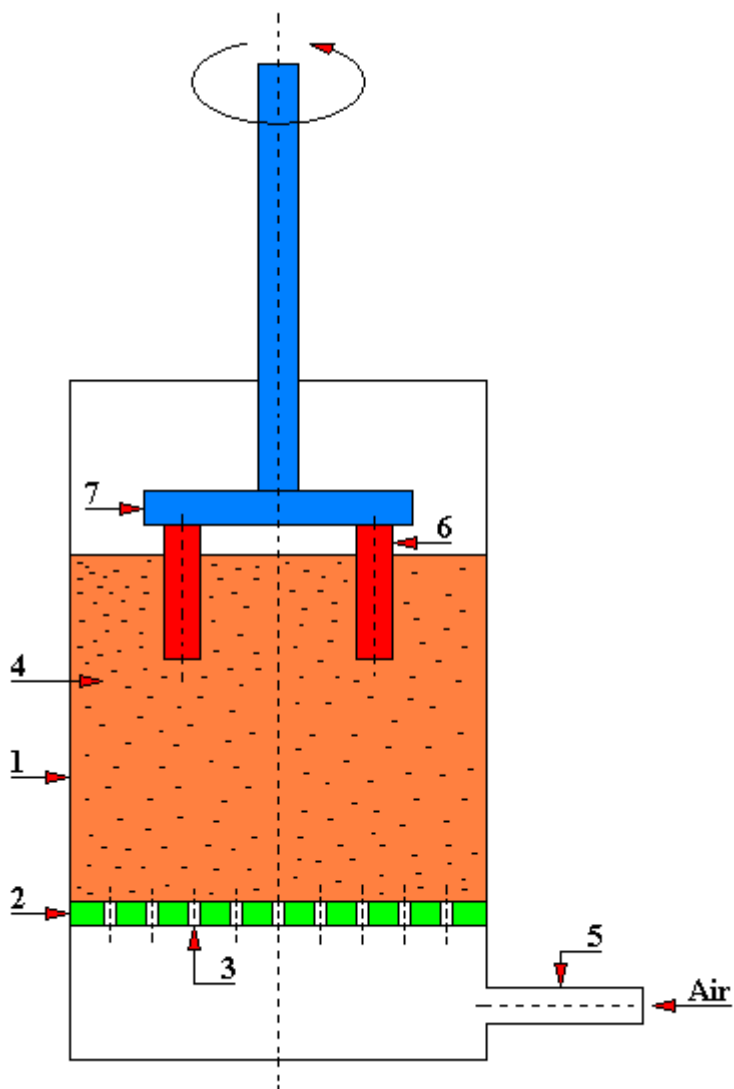


Fig. 4.1.93.1. A diagram of a test rig for testing the wear of bodies in abrasive mass according to the patent PL 150 471

1 - abrasive container; 2 - the bottom of the container; 3 - openings; 4 - abrasive; 5 - compressed air supply pipe; 6 - tested samples; 7 - sample holder

In the bottom 2 of the container 1, openings are made with a diameter smaller than that of the abrasive. A compressed air supply pipe 5 is connected with the openings below the level of the bottom 2. The test rig made in this way, when supplied with air under a certain pressure, allows the abrasive to be kept in a fluidized form in the container, so that the testing of the body (samples) rotating in this environment takes place practically without frictional resistance between the abrasive particles. Thanks to this, the supplied energy is not spent on overcoming the friction between the abrasive particles, but only on overcoming the friction between the tested body (samples) and the abrasive. Moreover, the change of abrasive mass properties can be obtained by changing the strength of the air stream or its temperature.

4.1.94. Test rig for testing the wear of bodies in an abrasive mass according to the patent PL 96 503

The test rig according to the patent PL 150 471, the authors of which are Józef Turczyński, Aleksander Karge, Maksymilian Zakrzowski, Rudolf Solik and Krzysztof Nowakowski, is designed to test the abrasion resistance of construction materials with the use of loose materials, in particular coal.

The essence of the operation of this test rig is as follows (Fig. 4.1.94.1). The test sample 7 is placed on the rotating drum 2. When testing the abrasion resistance the container 1 is filled with the abrasive material 8 (coal). If necessary, the abrasive material 8 is loaded with an additional weight 4 from above. The motor 3 is then turned on for a certain period of time. During the test, samples 7 are rubbed against the abrasive material 8. The abraded material from the sample 7 and from the abrasive material 8 falls into the container 6. After the determined friction time, the motor 3 is turned off, and then the samples 7 removed from the drum 2 are weighed. The percentage weight loss of the sample 7 determines the abrasion resistance.

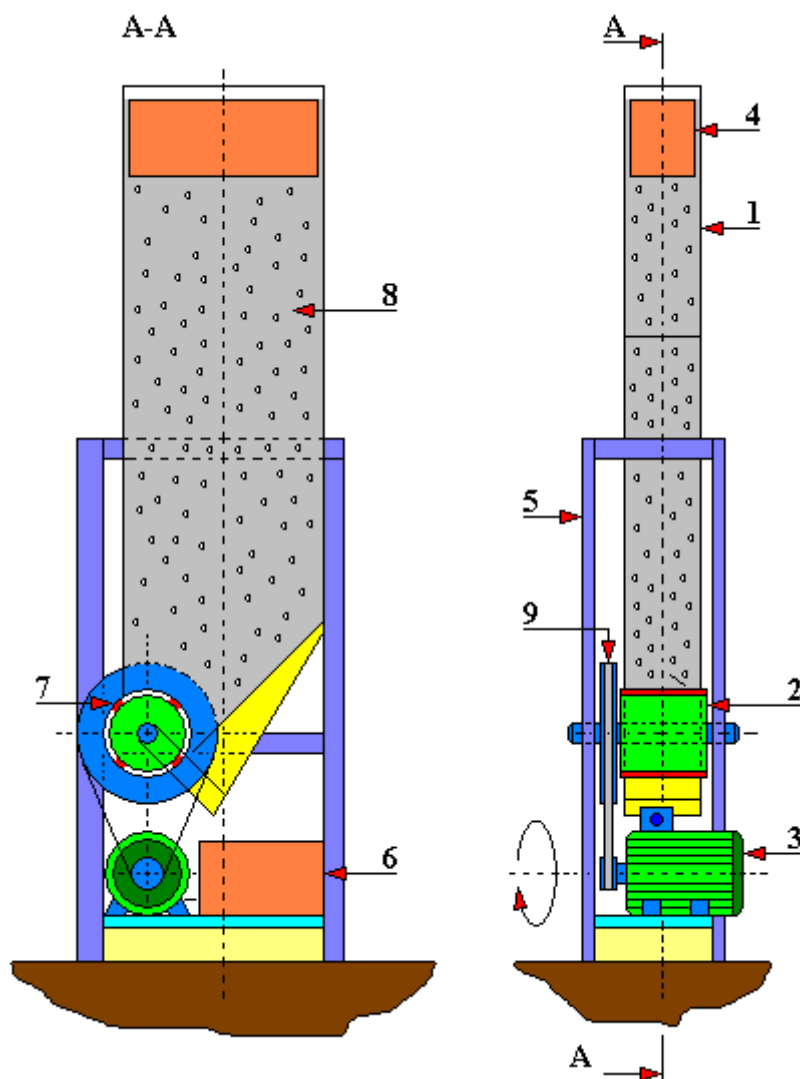


Fig. 4.1.94.1. A diagram of an abrasion resistance test rig according to the patent PL 96 503
 1 - abrasive (coal) container; 2 - drum; 3 - drum drive motor; 4 - additional weight; 5 - supporting structure; 6 - a container for used abrasive material; 7 - tested sample; 8 - abrasive material (coal); 9 - belt transmission

4.1.95. Test rig for testing the abrasion resistance of the material fold edges according to the patent PL 107 388

The test rig according to the patent PL 107 388, the authors of which are: Teresa Oberle, Mieczysław Jarczyński and Leon Malinowski, is designed to test the resistance of material fold edges to abrasion, especially the fold edges of complex textile products such as fabrics, knitwear, yarns, non-wovens, intended for clothing products.

There are a number of bends and folds in clothing products, such as the edges of sleeves, legs, hems of pockets and edges of the garment, and others. The fastest wear of a fabric in a clothing product as a result of abrasion occurs at the edges of the folds, while it is slower on the surfaces of the product. The fibers most exposed to abrasive forces are contained in the area of the outer edge of folds, and they are additionally stressed. In this case, further deformations caused by catching of these fibers on an uneven abrasive surface because the fibers to break in a much shorter time than breaking of fibers in a flat material.

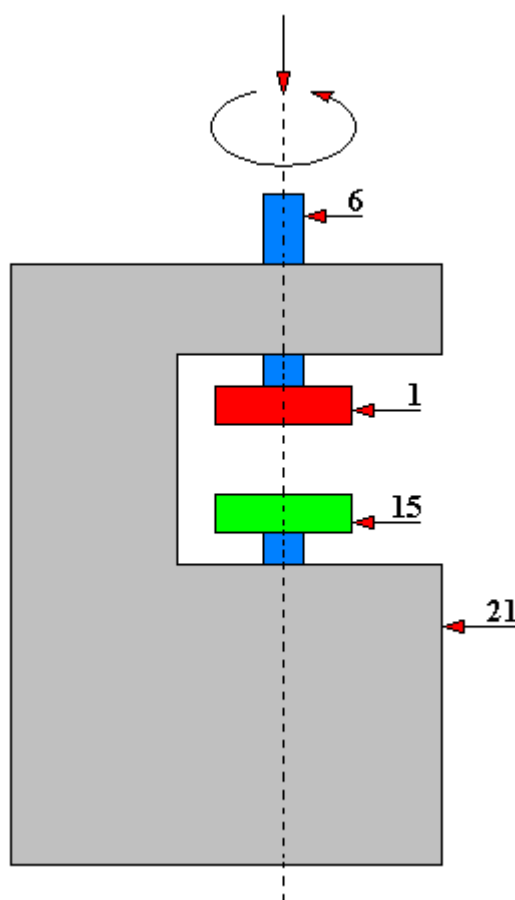


Fig. 4.1.95.1. A general diagram of the test rig for testing the abrasion resistance of fabric folds according to the patent PL 107 388

1 - upper head (rotating); 6 - spindle; 15 - lower head (fixed, non-rotating); 21 - test rig body

The fabric abrasion mechanism itself is a mixture of the abrasion phenomenon of monolithic surface of the fabric and yarn. During abrasion, loose ends of fibers are brought to the surface and are torn off by the unevenness of the abrasive surface. Also, those fiber arcs are deformed and broken on which caught are protrusions of the abrasive surface. The severity of this phenomenon is closely related to the pressure force and the structure of the abrasive

surface. Abrasion tests of textile materials are very important for improving the durability of clothing goods.

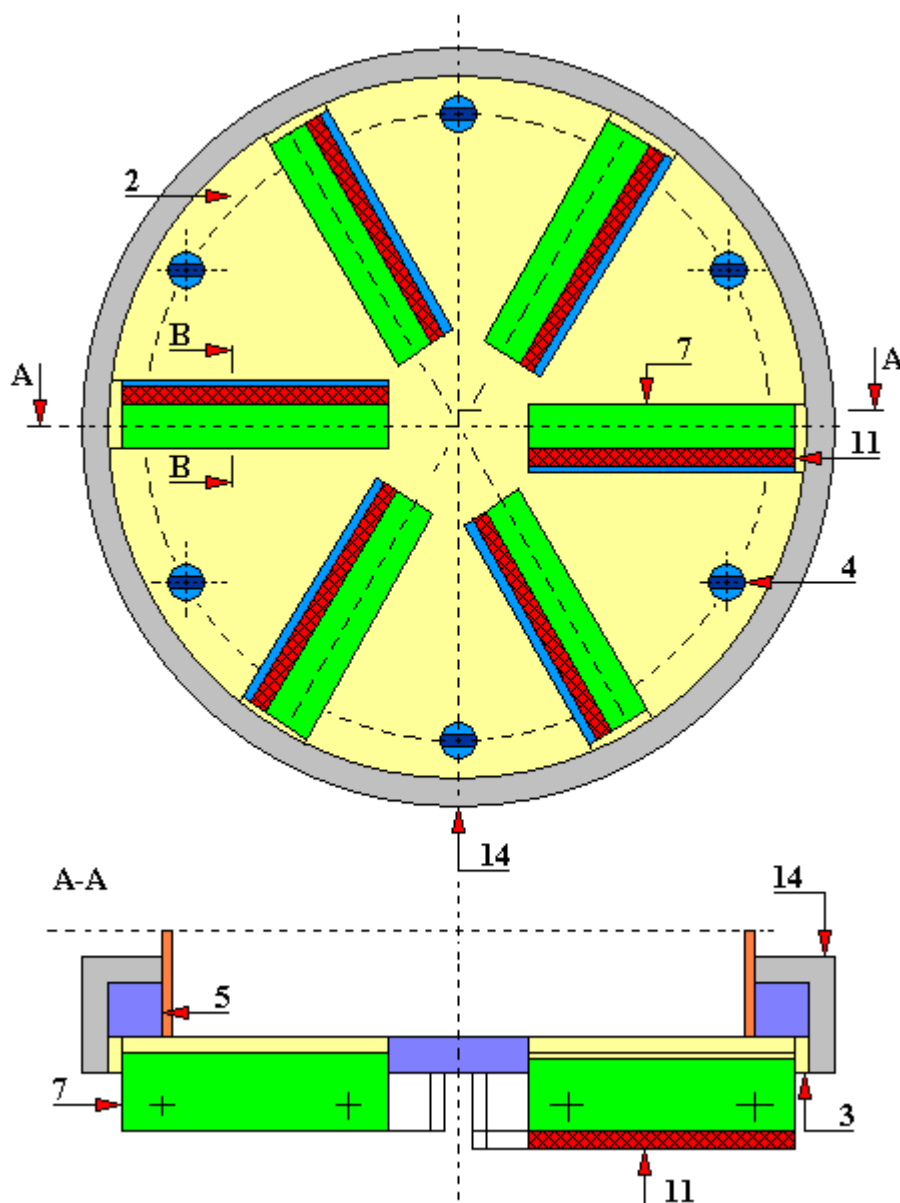


Figure 4.1.95.2. A test rig for testing the resistance of fabric folds to abrasion according to the patent PL 107 388. Upper head. Bottom view
 2 - disc; 3 - cutouts; 4 - screws; 5 - reduction sleeve; 7 - cube; 11 - rectangular sample; 14 - securing clip

The construction of this tribotester is as follows (Fig. 4.1.95.1÷4.1.95.4). The head of this test rig includes a disc with shaped cuts in which there are freely located cubes with a sample holder for the tested materials. These cubes have a socket for fixing a sample of the tested material and are detachably connected to a pressure plate by which the sample of the tested material is fixed. The cubes are free to move in such a way that the samples of the tested material are pressed against the abrasive medium only as a result of gravity force of the sample and cube. The disc has got a ring securing the cubes against falling out. And the second head (lower) contains a disc with a ring for mounting the abrasive medium.

The test rig allows you to test the resistance of fold edges of materials to abrasion in conditions very similar to natural ones, ensuring compliance of laboratory evaluation results with the results of the functional assessment of these materials. The test rig for testing the resistance of fabric folds to abrasion is adapted for co-working with the pillster test rig for testing the resistance of fabrics to pilling.

The essence of operation of the test rig according to the patent PL 107 388 is as follows. The upper head 1 of the test rig comprises a disc 2 with six shaped cutouts 3 located radially. This disc is connected by screws 4 to a reduction sleeve 5 attached to the spindle 6 of the pillster test rig. The spindle 6 is driven from the driving system of the pillster test rig by a rotary motion with a various direction of rotation. In the cutouts 3 of the disc 2 there are cubes 7 with a vertical clearance 8 provided. The cubes 7 have protrusions 9 and sockets 10 in which attached are half-folded rectangular samples 11 of the tested fabric, a spring washer 12 and screws 13. The disc 2 has a clamp 14, protecting the cubes 7 against falling out.

The lower head 15 of the test rig includes a disc 16 with two bolts 17 on which an abrasive medium 19 is mounted with a ring 18. The disc 16 is located on the plate 20 of the head 15 and is fixed in place by locating pins 17.

During the operation of the test rig, the head 1 with samples 11 of the tested fabric is set at such a distance from the head 15 with the abrasive medium 19 so that the fabric samples 11 would touch the working surface of the lower head. The force of pressing the edges of fabric samples 11 against the abrasive medium 19 is small and depends only on the weight of the fabric sample 11 and the weight of the cube 7. The movements of the heads 1 and 15 and the pressure force between the rubbing surfaces of the edges of the fabric sample 11 and the abrasive medium 19 are so chosen so that the conditions for measuring the abrasion resistance of the edges of fabric folds are similar to those occurring during normal use of the fabric in a garment product.

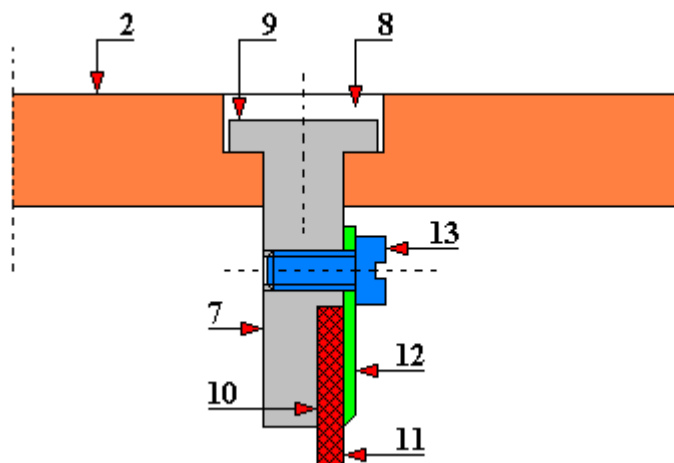


Figure 4.1.95.3. A diagram of a test rig for testing the abrasion resistance of fabric folds according to the patent PL 107 388. Upper head. Cross section B - B

2 - round disc; 7 - cube; 8 - vertical clearance; 9 - cube protrusion; 10 - socket; 11 - rectangular sample; 12 - spring washer (pressure plate); 13 - screw

It is worth mentioning here that the material of the cube 7 does not have to be steel. And it is the weight of the cube that mainly determines the value of the pressure of the tested material

(fabric) on the abrasion medium 19 (of course, it should be remembered that there is also the weight of the screws 13, spring washer 12 and rectangular samples 11). The force of gravity is simply at work here. Therefore, in order to reduce this pressure, for instance aluminum or even plastic cubes can be used here.

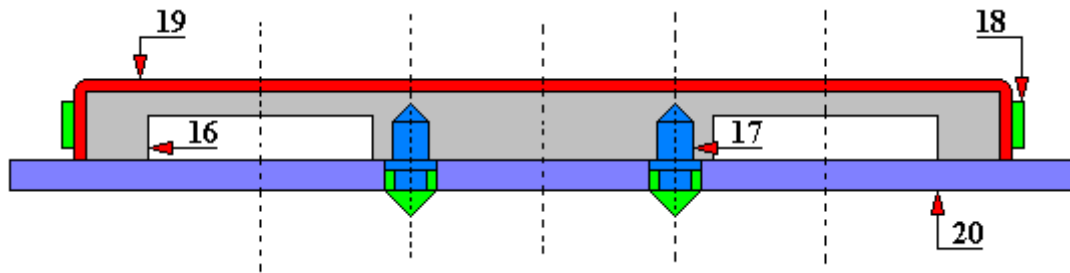


Figure 4.1.95.4. Lower head in a cross-section. A test rig for testing the abrasion resistance of fabric folds according to the patent PL 107 388
16 - disc; 17 - pin; 18 - ring; 19 - abrasion medium; 20 – plate

4.1.96. Test rig for testing elements in sliding interactions according to the patent PL 215 116

The test rig according to the patent PL 215 116, author of which is Tomasz Klepka, is designed to test elements, especially polymer ones in sliding interactions, with one-sided contact of elements, one of which moves in a sliding motion.

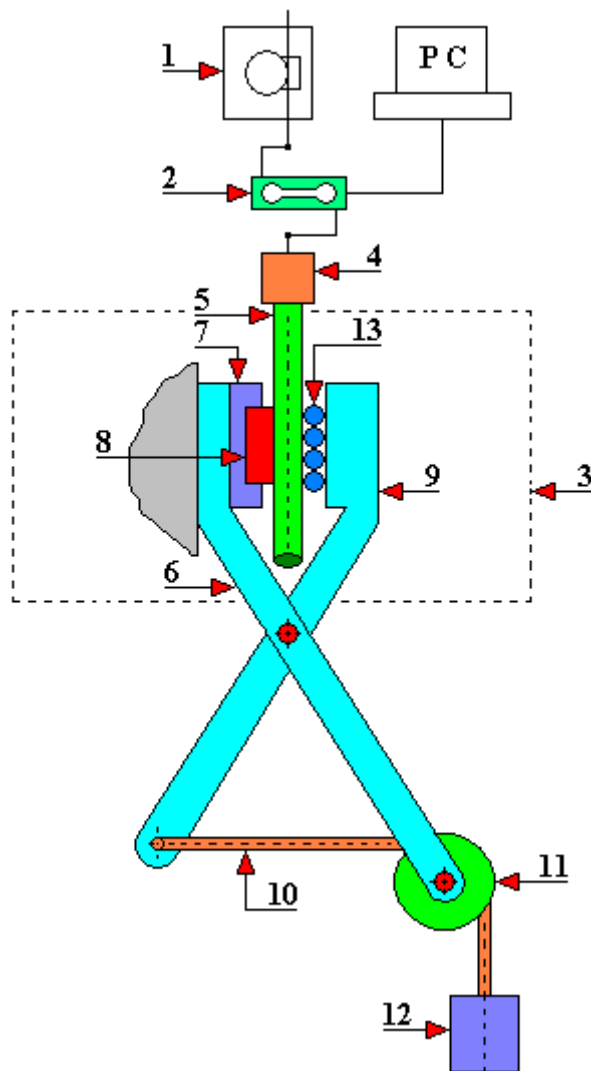


Fig. 4.1.96.1. General diagram of a test rig for testing elements in sliding interactions according to the patent PL 215 116

1 - drive system; 2 - strain gauge system; 3 - cover; 4 - hook for attaching the counter-sample; 5 - counter-sample; 6 - fixed lever arm; 7 - sample holder; 8 - sample; 9 - movable lever arm; 10 - tension member; 11 - pulley; 12 - weight; 13 - roller bearing; PC - computer

The above test rig consists of the following elements (Fig. 4.1.96.1):

- drive system 1;
- a strain gauge system 2 for force measurement, connected to a PC;
- covers 3;
- a hook 4 for fixing the counter-sample 5;

- a fixed arm of the lever 6 ended with a holder 7 for fixing the sample 8;
- a movable arm of the lever 9 ended with the mounting of the tension member 10;
- a pulley 11 through which the tension member passes;
- a weight 12 of variable mass;
- the roller bearing 13 leading the counter-sample 5 against the sample 8 during the tests.

The way it works is that the test sample 8 is mounted in the holder 7 of the fixed arm of the lever 6. Then the sample 8 is brought into contact with the counter-sample 5 and is attached to the drive system 1 ensuring a uniform sliding motion. The counter-sample 5 moves in a steady sliding motion in a vertical upward direction at a constant linear speed. The sample 8 and the counter-sample 5 touch each other one-sidedly with a constant pressure, at a given force from the weight 12. The contact area of the sample and counter-sample is isolated from the environment by means of cover 3.

4.1.97. Test rig for determining frictional resistance

The test rig for determining the frictional resistance was constructed at the Institute of Metal Forming and Welding of Częstochowa University of Technology. This test rig is designed to analyze changes in the friction force at high pressure values. This test rig (Fig. 4.1.97.1 and 4.1.97.2) consists of a clamping ring 2, which is attached to the base plate 1. Gripping jaws are fixed to this plate: permanent ones 4 and 5 and movable ones 6 and 7. Cuboid-shaped samples are mounted in the jaws. Normal pressure is exerted on samples by means of a set screw 9 and a pin 8, between which a dynamometer is fixed.

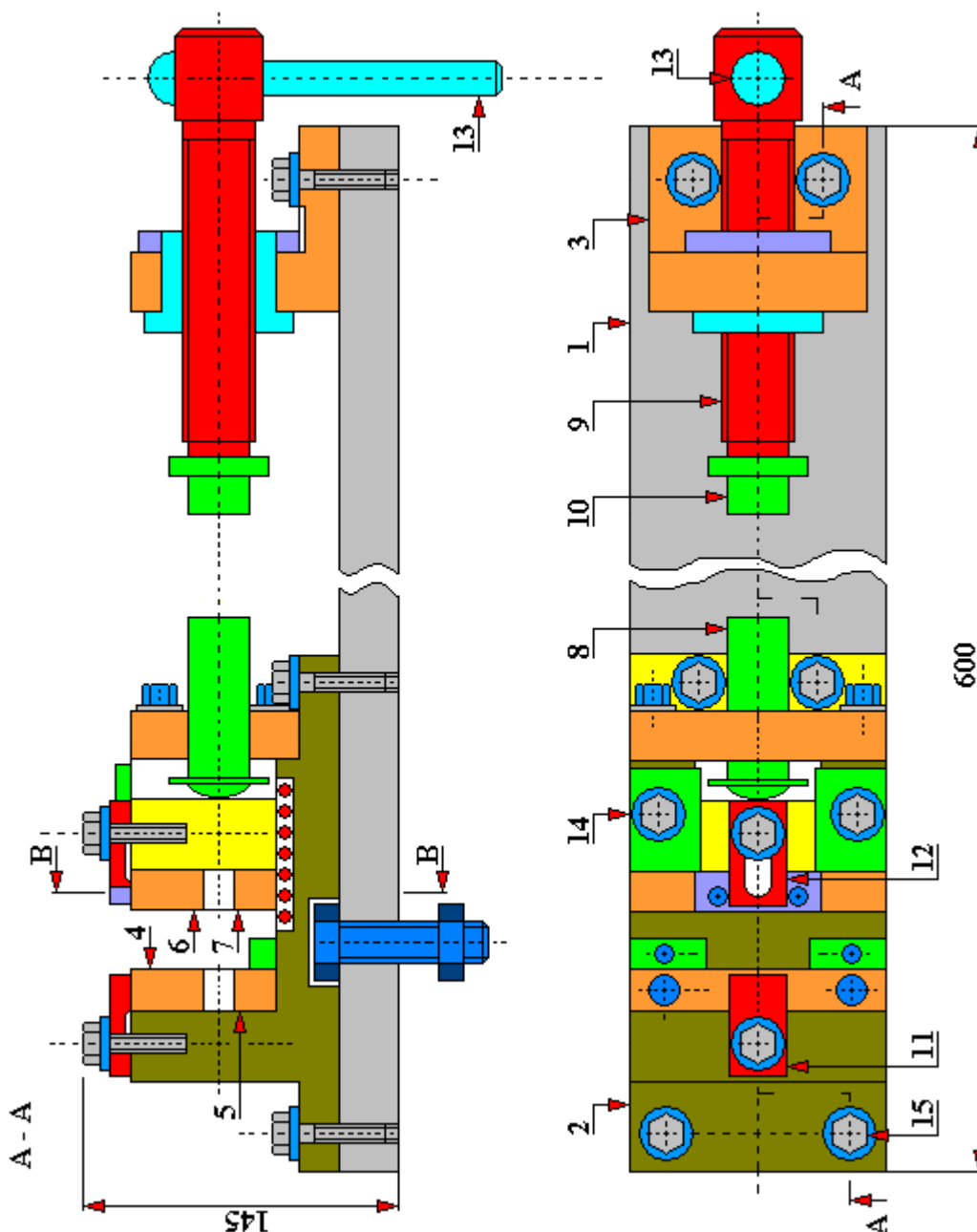


Fig. 4.1.97.1. A rig for determining the frictional resistance (top view and A-A section)

1 - base plate; 2 - body; 3 - bracket; 4 - fixed upper jaw; 5 - fixed lower jaw; 6 - upper movable jaw; 7 - lower movable jaw; 8 - pin; 9 - set screw; 10 - thrust pin; 11 - pressure pad of the thrust jaw; 12 - pressure pad of the movable jaw; 13 - knob; 14 - mounting pad; 15 - mounting screw

The travel of pin 8 (counter-sample) is performed by a test rig. This test rig enables the testing of frictional resistance under surface contact conditions, in one-way movement and at comparatively low relative speeds. Such a course of testing corresponds to a large extent to the conditions of carrying out plastic working processes. During these tests, the friction coefficient is determined on the basis of Amontons' law.

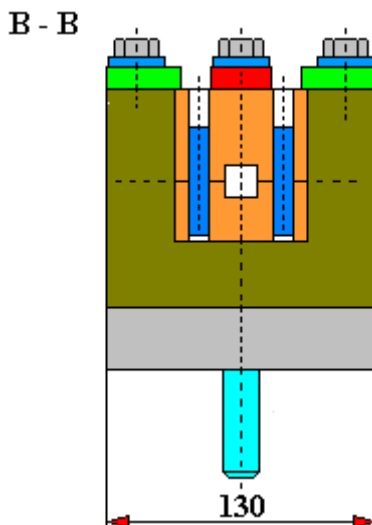


Fig. 4.1.97.2. A rig for determining frictional resistance. B-B section

The samples moved in relation to each other at high pressure values, after the completion of measurements on this rig, remained connected by adhesive forces. Therefore, the force needed to destroy the friction joint in the friction plane was also measured and this force according to [Monika Gierzyńska: „Tarcie, zużycie i smarowanie w obróbce plastycznej metali”; Wydawnictwa Naukowo-Techniczne, Warszawa 1983 r.], was called the force of normal adhesion. In order to measure this force, a special test rig was constructed shown in Fig. 4.1.97.3. After mounting samples (in the joined state), the instrument was mounted on a test rig which enabled the measurement and recording of the force needed to destroy the frictional joint. Fig. 4.1.97.4 shows a general view of the rig for determining the frictional resistance.

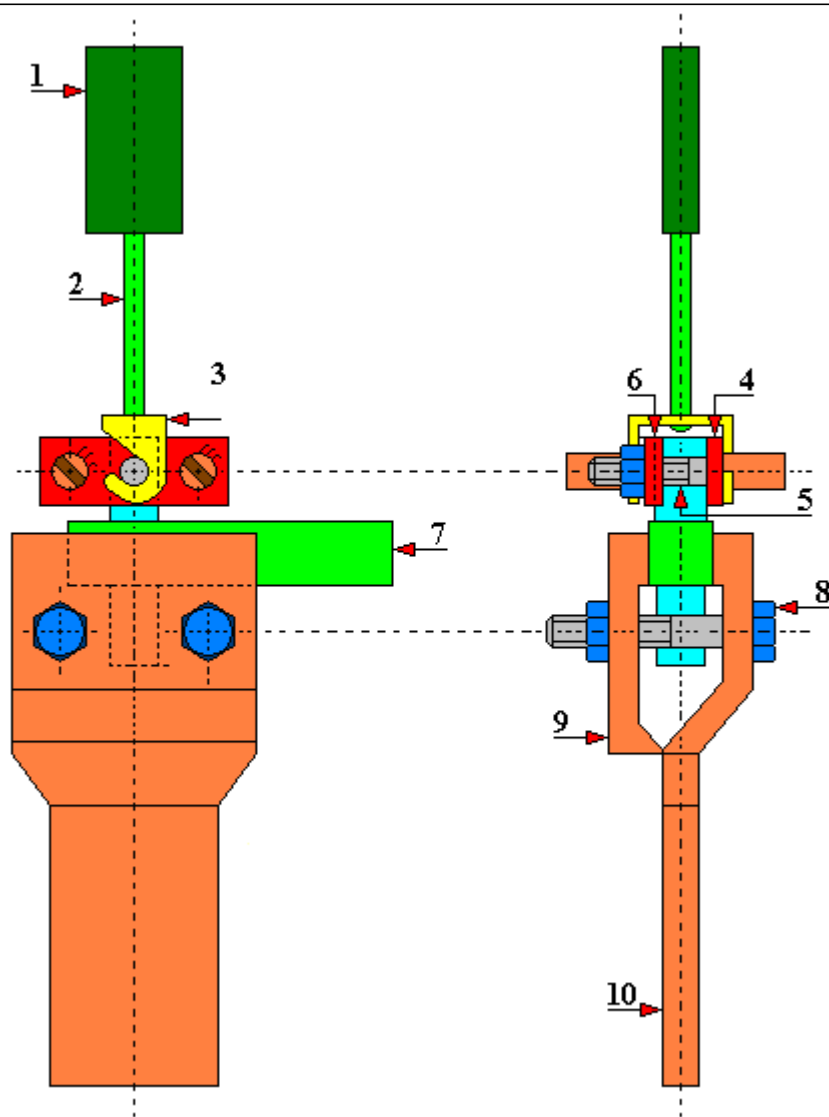


Fig. 4.1.97.3. Instrument for measuring normal adhesion forces

1 - mounting plate; 2 - steel line; 3 - catch; 4 - put-on yoke; 5 - a screw with a lens head; 6 - guiding yoke; 7 - sample; 8 - set screw; 9 - cover plate; 10 - fixing lens

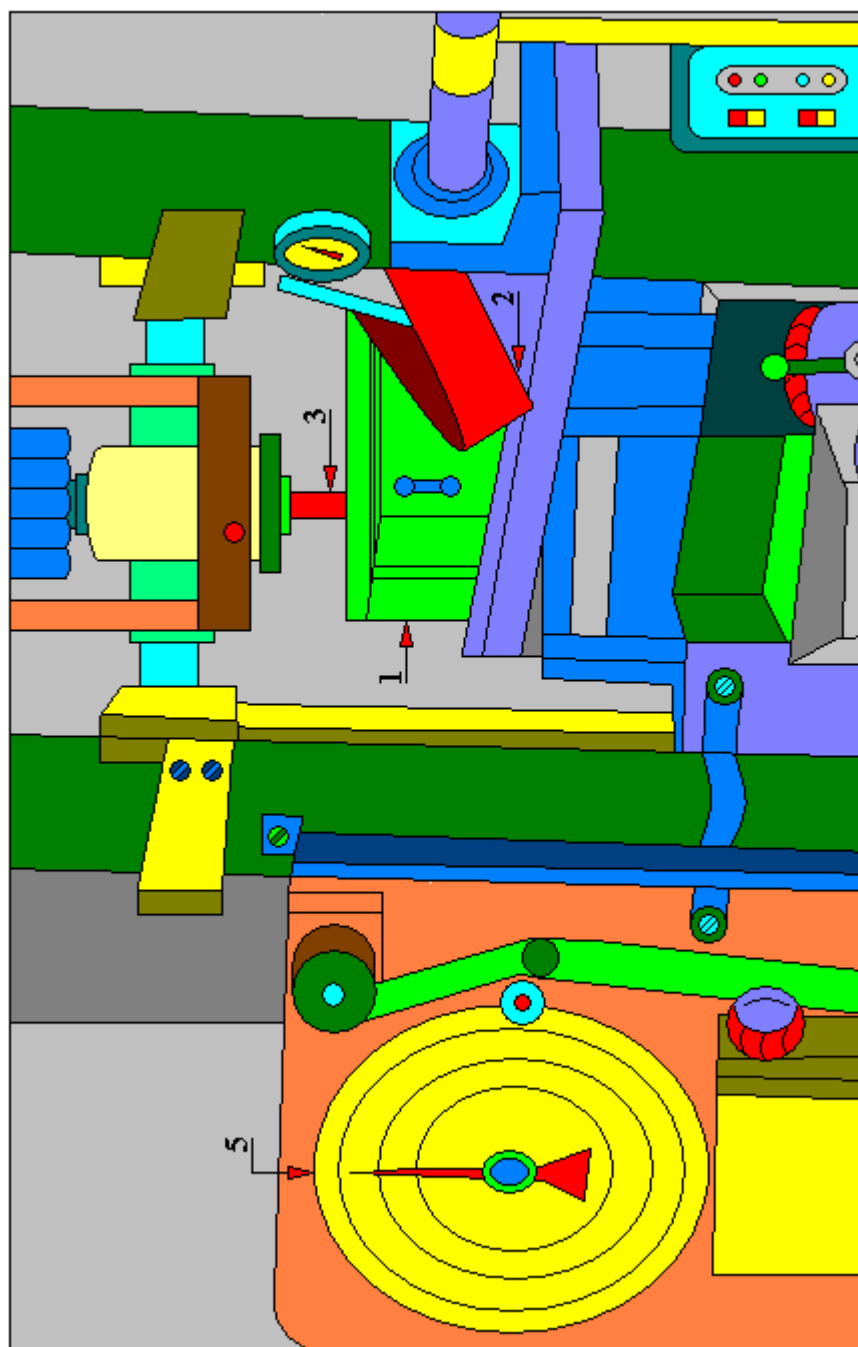


Fig. 4.1.97.4. A general view of the rig for determining the frictional resistance
1 – clamping ring; 2 - dynamometer; 3 - counter-sample; 4 - printer; 5 - counter-sample load manometer

4.1.98. Test rig for determining frictional resistance in the stamping process according to F. Tychowski and Z. Wiśniewski

The measurement of friction in conditions similar to the sheet metal stamping process can be performed based on the rig presented in Fig. 4.1.98.1. The rig for determining the frictional resistance and method of its determination have been presented in the work [205]. This rig consists of a steel ring (machined to a hardness of 62 HRC and diameter $d = \emptyset 170$ mm) on which slides a strip of steel tape cut from the tested metal sheet. Weights of known weight G_1 and G_2 are attached to the ends of the tape. It is a system corresponding to a tension member sliding on a circular ring with the wrapping angle α . The coefficient of friction μ is determined from the following formula:

$$G_1 = G_2 \cdot e^{\alpha \cdot \mu}$$

hence:

$$\mu = \frac{1}{\alpha} \cdot \ln \frac{G_1}{G_2}$$

where: α – wrapping angle;
 G_1, G_2 – heaviness of weights

The advantages of this measurement method include a simple construction of the rig. The disadvantages, however, include the lack of representation of the actual conditions present in the sheet metal stamping process. Although the sliding of the sheet on the drum in a way models the displacement of the sheet on the punch, the main disadvantage of this method is that the sheet material does not experience plastic deformation, so it is a measurement under the conditions of elastic, not elastic-plastic contact. Moreover, the state of stress and deformation occurring in the process of sliding the tape over the drum is different from the state of stress and deformation occurring in the actual stamping process.

If, however, we are not looking for an analogy of this method to the conditions prevailing during the stamping process, and we are only interested in determining the friction coefficient, then this method is inventive.

It is curious, however, that there is no element in the above formulas concerning the possible use of a lubricant. Also, another two important questions arise:

- for what maximum steel sheet thickness the above formula can still be used?
- for which grades of steel sheet does the above formula apply?

Nowadays, however, it is very easy to implement the above formula into a computer program (e.g. a simple Visual Basic program or even to Excel) in order to determine the friction coefficient. The only variables that should be introduced are the wrapping angle and heaviness of weights.

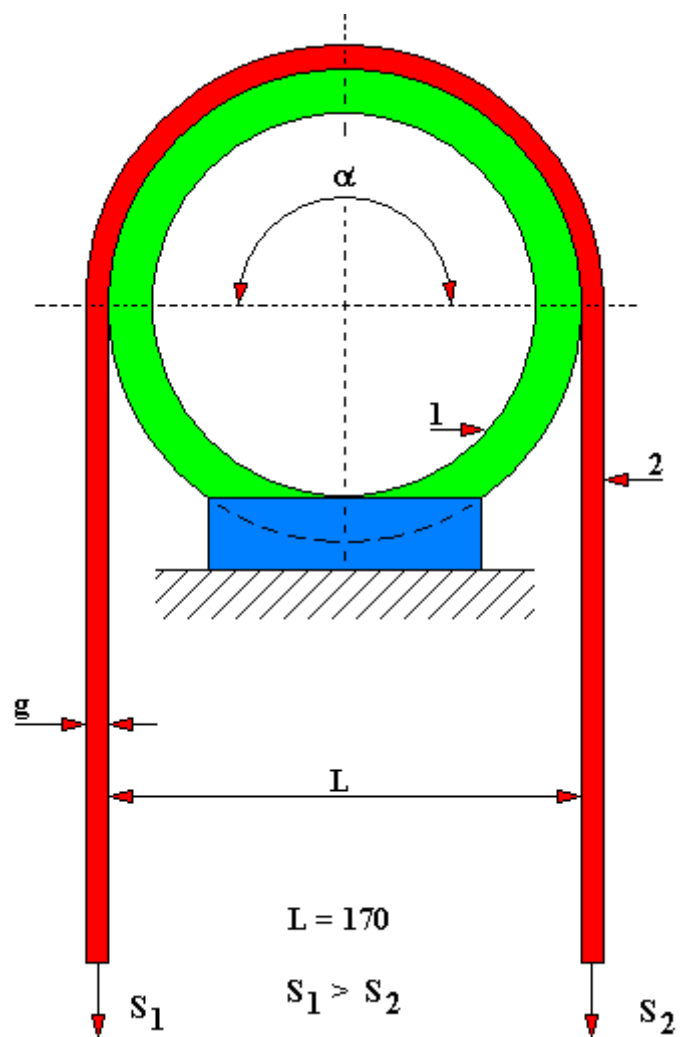


Fig. 4.1.98.1. A general view of the rig for determining frictional resistance during sheet metal forming according to F. Tychowski and Z. Wiśniewski [205]
 1 - steel ring; 2 - steel tape strip; g - thickness of the tape sheet; α - wrapping angle

4.1.99. Test rig for determining the coefficient of friction occurring between the punch and the deformed sheet according to Ju. P. Kazakov

The work [52] presents the rig and method of determining the friction coefficient occurring between the punch and the deformed sheet. It is a very precise method that involves stretching a strip of sheet metal with a punch of a cylindrical working surface. Fig. 4.1.99.1 shows the shape and dimensions of the sample used in this method.

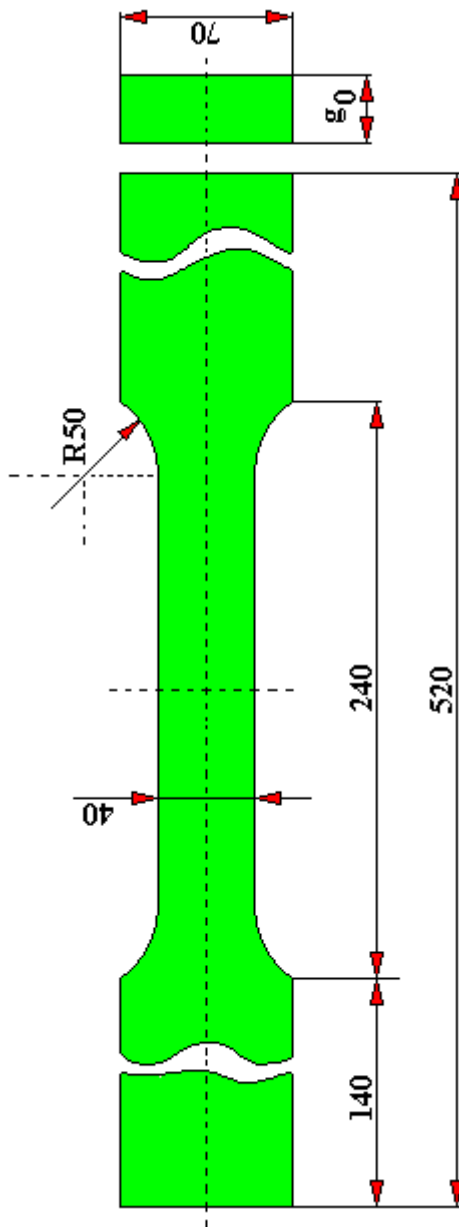


Fig. 4.1.99.1. The shape and dimensions of the sample for determining the frictional resistance in the stamping process according to Ju. P.Kazakov [52]
 g_0 – initial thickness of the sample

With a sample width to thickness ratio of 25, the non-uniformity of deformation (width) does not exceed 2.5%. Therefore, it can be omitted in the calculations.

The sample 6 (Fig. 4.1.99.2) is placed on the test rig consisting of the plate 7 on which the die block 2 with the blankholder is mounted. The tested sample 6 is rigidly fixed by the blankholders 3 and 5 and then drawn by pressing the roller 1 fixed in the holder 4. The process of loading the sample is carried out until the maximum deformation force is reached.

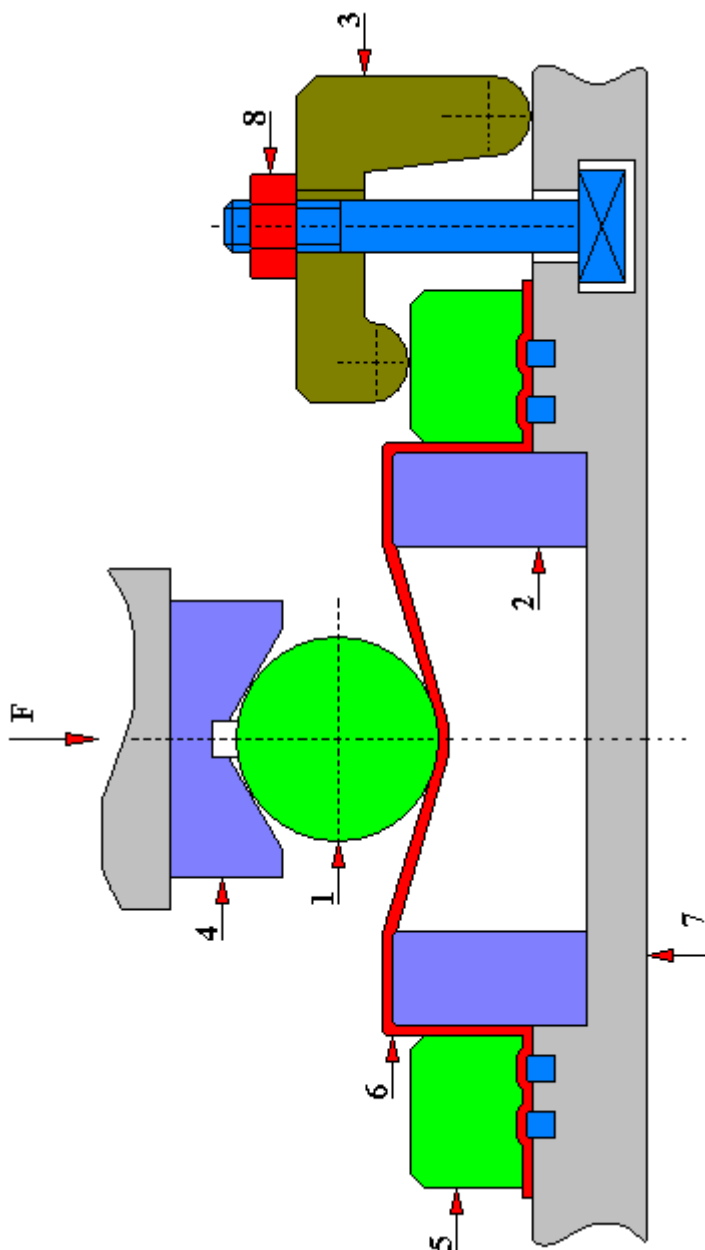


Fig. 4.1.99.2. A rig for determining the coefficient of friction between the deformed sheet and punch according to Ju. P. Kazakov [52]

1 - roller with a diameter of $\text{Ø}120$ mm; 2 - die block; 3 - blankholder; 4 - roller handle; 5 - blankholder; 6 - sheet metal strip (sample); 7 - mounting plate; 8 - nut; F - loading force

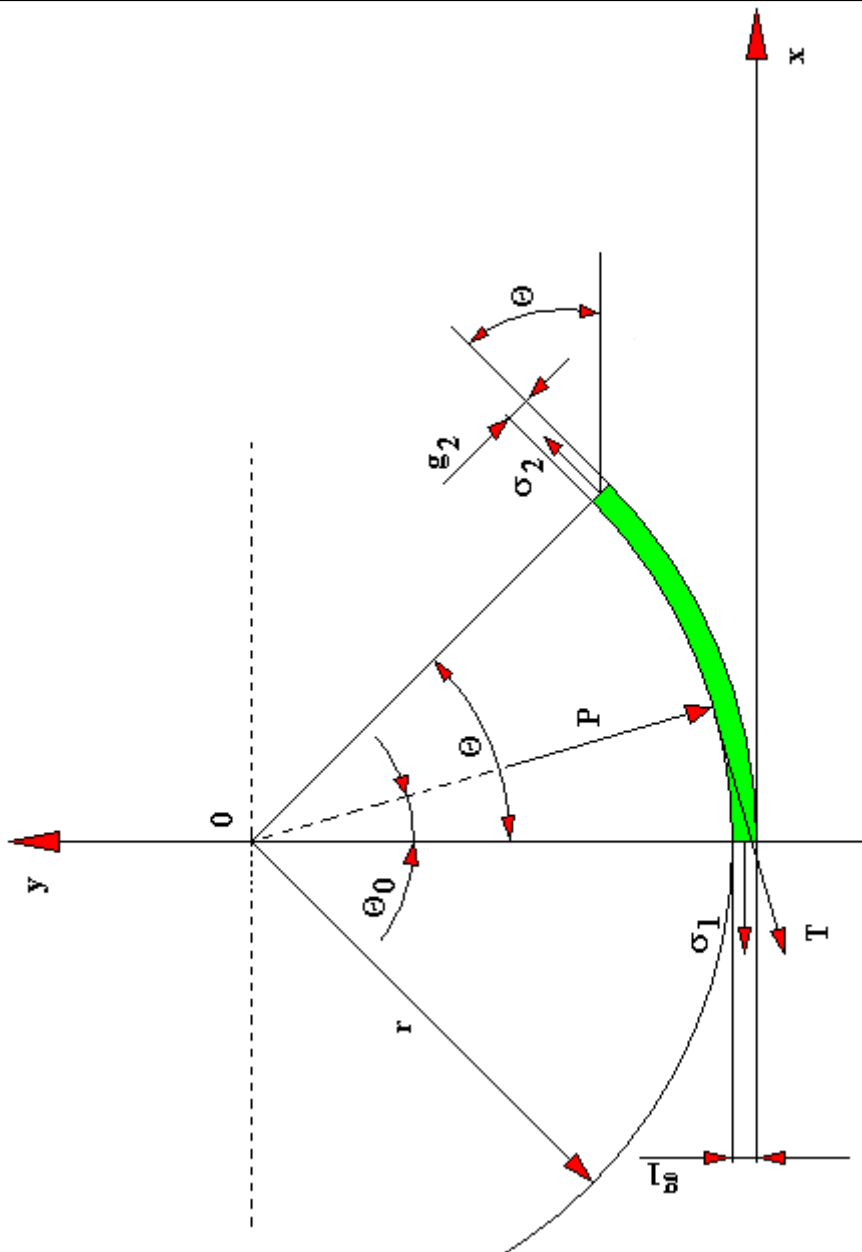


Fig. 4.1.99.3. A diagram of the action of forces on a deformed sheet metal strip according to Ju. P. Kazakov [52]

The values of forces T and N are determined from the equations of equilibrium of the sum of projections of forces on the x and y axis and the moments' equilibrium equation. Considering the sheet metal strip element shown in Fig. 4.1.99.3, the following is obtained:

$$\Sigma P i_x = g_2 \cdot \sigma_2 \cdot \cos Q - g_1 \cdot \sigma_1 - T \cdot \cos Q_0 + P \cdot \sin Q_0 = 0$$

$$\Sigma P i_y = g_2 \cdot \sigma_2 \cdot \sin Q - T \cdot \sin Q_1 - P \cdot \cos Q_0 = 0$$

$$\Sigma M_0 = g_2 \cdot \sigma_2 - g_1 \cdot \sigma_1 - T = 0$$

where:

g_1, g_2 – sheet metal thickness at the ends of the element under consideration;

g_0 – sheet thickness before deformation;

Θ – half of the wrapping angle;

σ_1, σ_2 – normal stresses which are determined from the diagram depending on the degree of deformation;

The friction force can be determined from the equation of moments:

$$\mathbf{T} = g_2 \cdot \sigma_2 - g_1 \cdot \sigma_1$$

And the angle Q can be determined from the conditions of the equilibrium of forces. Determining:

$$\mathbf{A} = g_2 \cdot \sigma_2 \cdot \cos Q - g_1 \cdot \sigma_1$$

$$\mathbf{B} = g_2 \cdot \sigma_2 \cdot \sin Q$$

and putting into the equation for

$$\Sigma P i_x$$

and

$$\Sigma P i_y$$

you will get:

$$\mathbf{A} - \mathbf{T} \cdot \cos Q_0 + \mathbf{P} \cdot \sin Q_0 = 0$$

$$\mathbf{B} - \mathbf{T} \cdot \sin Q_0 - \mathbf{P} \cdot \cos Q_0 = 0$$

and after solving the equations, the following was obtained:

$$\sin Q_0 = \frac{\mathbf{BT} \pm \sqrt{2(g_1 \cdot \sigma_1) \cdot (g_2 \cdot \sigma_2) \cdot (1 - \cos Q)}}{\mathbf{A}_2 + \mathbf{B}_2}$$

The force P is given by the equation:

$$P = g_2 \cdot \sigma_2 \cdot \frac{\sin Q_0}{\cos Q_0} - T \cdot \frac{\sin Q_0}{\cos Q_0}$$

And the friction coefficient is determined from the relationship:

$$\mu = \frac{T}{P}$$

4.1.100. A rig for determining the friction coefficient based on the principle of forcing a semicircular punch into a sheet metal strip according to Bilgin

The work [Kaftanöglu Bilgin: Determination of coefficient of friction under condition of deep-drawing and stretch forming. Wear, 1973, No 2] presents the rig and the method of determining the coefficient of friction based on the principle of forcing a semicircular punch into a metal sheet mounted in a tool with a blankholder (Fig. 4.1.100.1).

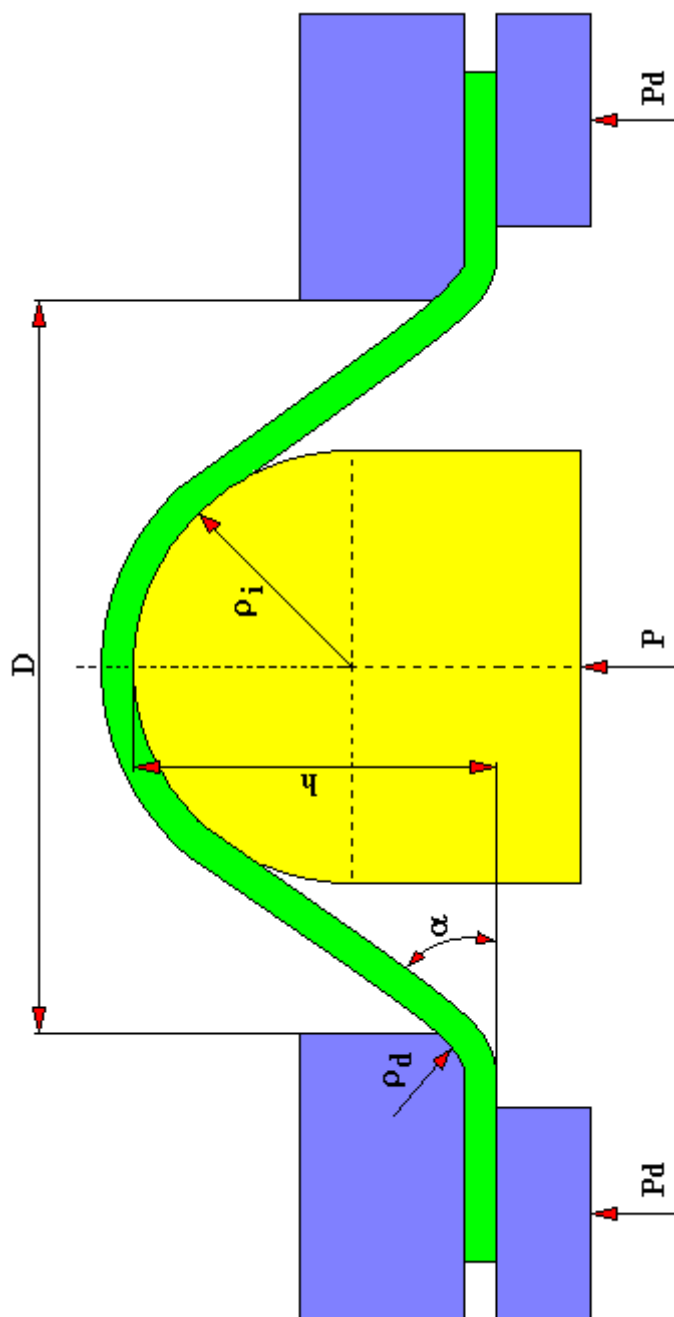


Fig. 4.1.100.1. Rig for determining the friction coefficient based on the method of forcing a semicircular punch into a sheet metal strip according to Bilgin
 P - pressure on the punch; P_d - clamping force; h - stamping depth;

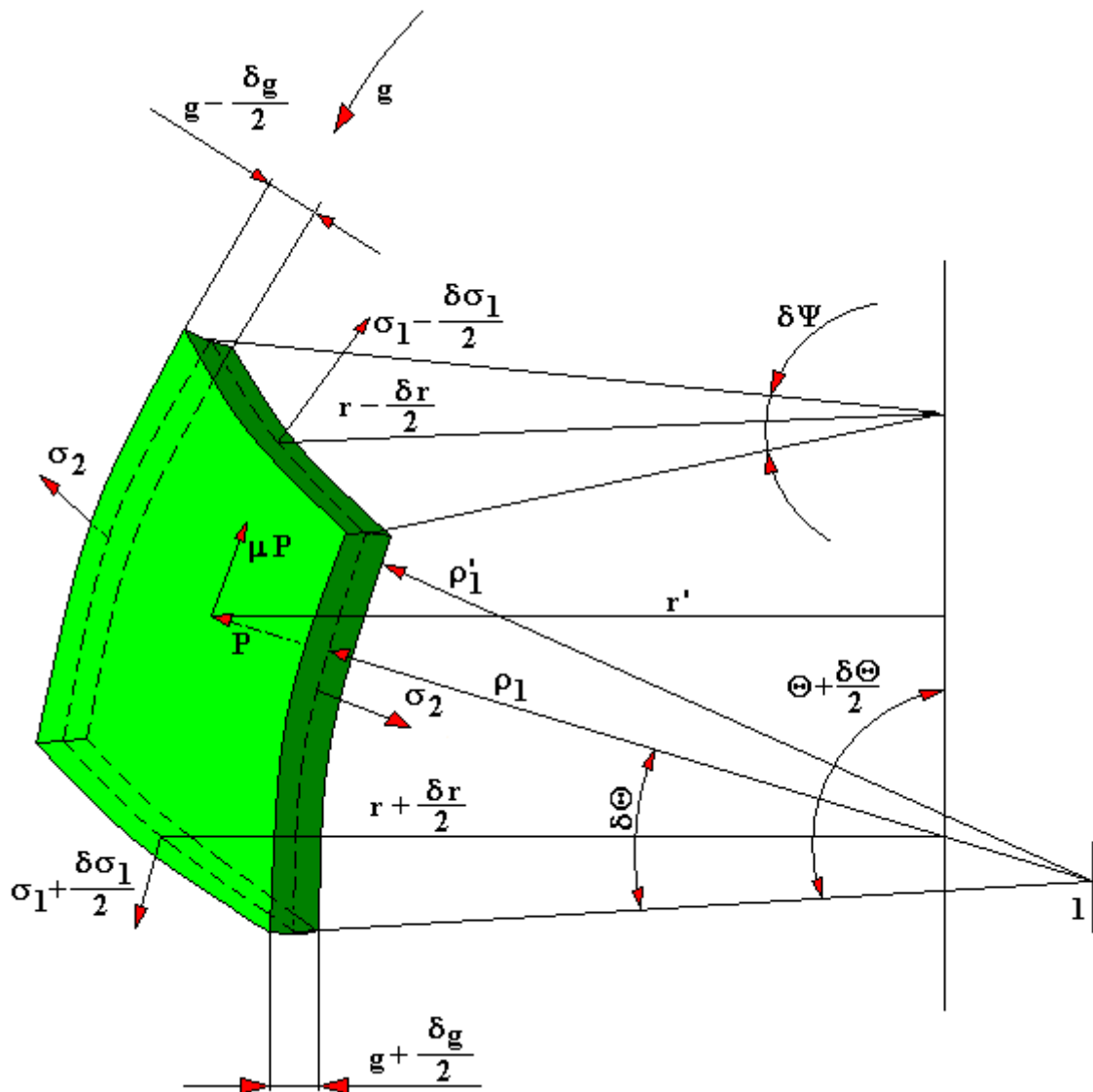


Fig. 4.1.100.2. Distribution of forces acting on the deformed element during the pressing of a semicircular punch into the sheet metal strip according to Bilgin

Considering the equilibrium equations of the deformed element shown in Figure 5.1.100.1, the relation on the friction coefficient was obtained in the form:

$$\mu = \frac{\delta P \cdot \text{ctg } \alpha}{2 \cdot \delta P d + \delta P}$$

where:

P - pressure on the punch;

Pd - clamping force

The relationship between the stamping depth h and the angle α can be described in the form of equation:

$$h = \left(\frac{D}{2} + \rho_d \right) \cdot \operatorname{tg} \alpha - (\rho'_1 + \rho'_d + g_0) \cdot (\sec \alpha - 1)$$

In order to determine the coefficient of friction the punch pressing process should be carried out with a different value of the clamping force P_d . As a result of changing the clamping force by the amount of δP_d , the force on the punch will also change by δP . From the experimental curves of the relationship of the force in punch P on the punch hollow h , the value δP , corresponding to different values of the punch hollow h , can be determined, and then the angle α can be determined. And describing the equilibrium equations of the spherical bowl element, the stresses σ_1 and σ_2 can be determined in the form of relationship:

$$\sigma_1 = \frac{P \cdot \rho_1}{2 \cdot g_t} \left[1 + \frac{\mu}{\sin \Theta} \cdot \left(\frac{\Theta}{\sin \Theta} - \cos \Theta \right) \right]$$

$$\sigma_2 = \frac{P \cdot \rho_1}{g_t} - \sigma_1$$

where:

σ_1, σ_2 - radial and circumferential stresses;

p - unit pressure between the punch and sheet metal;

g_t - instantaneous sheet thickness;

ρ_1 - mean radius of wall curvature.

If the stress ratio is denoted by k_x , then we get:

$$k_x = \frac{\sigma_2}{\sigma_1} = 1 - \frac{2 \mu \cdot (\Theta - \sin \Theta \cdot \cos \Theta)}{\sin^2 \Theta + \mu \cdot (\Theta - \sin \Theta \cdot \cos \Theta)}$$

hence

$$\mu = \frac{(1 - k_x) \cdot \sin^2 \Theta}{(1 - k_x) \cdot (\Theta - \sin \Theta \cdot \cos \Theta)}$$

finally

$$\mu = \frac{(1 - k_x) \cdot \sin^2 \Theta}{(1 - k_x) \cdot \left(\Theta \cdot \frac{1}{2} \sin^2 \Theta \right)}$$

The coefficient of friction is determined from the equation using the curve describing the relationship $K_x = f(\Theta)$, according to the equation:

$$K_x = \frac{d\varepsilon_2 \cdot (2 \cdot K_m - 1) + d\varepsilon_3 \cdot (K_m + R)}{d\varepsilon_2 + d\varepsilon_3 \cdot (R + 1)}$$

$$K_m = \frac{\sigma_3}{\sigma_1}$$

$$K_m = \frac{g_t}{2\rho_1 \cdot r} \cdot \left(r + K_x \cdot \rho_1 \cdot \sin \Theta \right)$$

$$\sigma_3 = \frac{1}{2} P$$

where:

R - constant that takes into account the anisotropy of the material;

$\varepsilon_2 = \ln(r/r_0)$ – sheet metal thickness determined experimentally;

$\varepsilon_3 = \ln(g/g_0)$ – at various points

The deformation distribution can be determined by means of coordination grids applied to the sheet before deformation. This method of determining the coefficient of friction is complex. In addition, it requires experience and the use of electronic computing techniques. Another disadvantage of this method is that it does not fully model the complex friction conditions occurring in various areas of stamping (in the blankholder or on the draw edge), between the stamping wall and die block, and between the punch and stamping. It only reflects the conditions occurring in a certain area of stamping, allowing to calculate the mean value of the friction coefficient. However, the frictional resistance, and therefore the friction coefficient between the deformed material and die block, as well as between the deformed material and punch, is different.

4.1.101. A tribological rig for testing the stick phase and slip phase

One of the basic reasons for the formation of a specific type of wear, called the corrugation of the wheels of a wagon wheelset, the corrugation of the raceways of the roller bearing rings is the formation of the reverse friction phase during the friction process. Such a case, for example, also occurs during the mating of the friction contact - the block brake. Fig. 4.1.101.1 shows a general diagram of the test rig (it is a mechanical model) for testing the stick phase and slip phase during the friction of two mutually mating elements. And Fig. 4.1.101.2 presents a pictorial diagram of the occurrence of the above-mentioned phases.

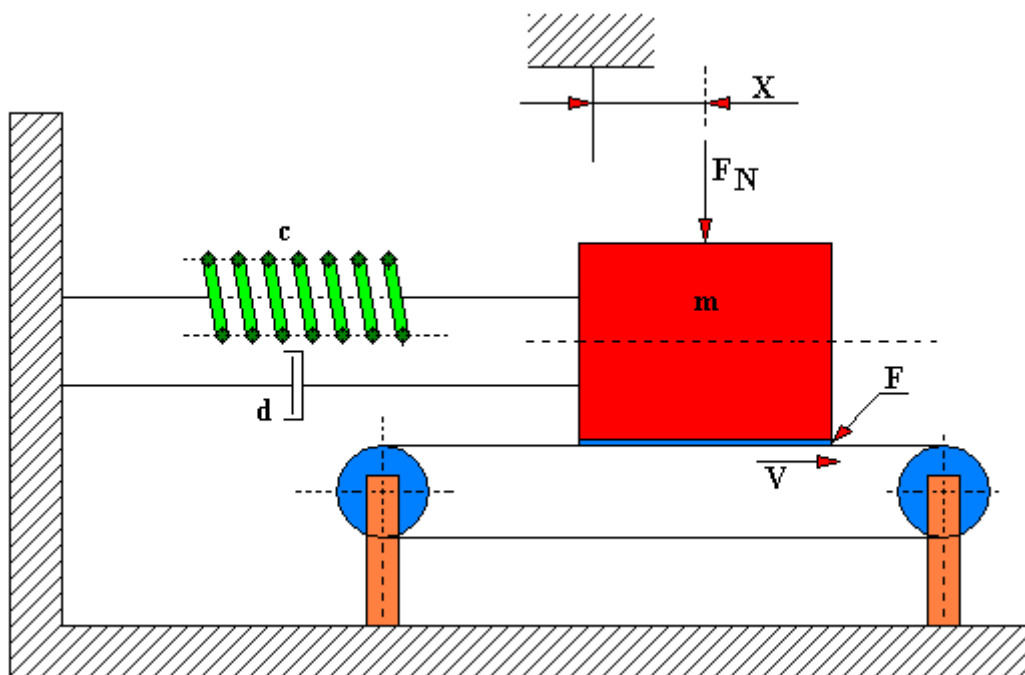


Fig. 4.1.101.1. A general diagram of the rig for stick and slip phase testing
 m - concentrated mass; d - damping coefficient; c - spring constant; F_N - normal force (perpendicular to the surface); V - tape feed speed; X - mass shift

The description of the movement of a block with a mass m in relation to the wheel (tape) during braking, under given initial conditions, can be made on the basis of the solution of the following differential equation:

$$\mathbf{m \cdot \ddot{x} + d \cdot \dot{x} + c \cdot x = \mu \cdot F_N \cdot (x - V)}$$

The speed of the wheel (tape) V is implicit in this equation. It is hidden in the expression for the coefficient of friction.

The work [165] shows that the process of formation of the stick phase can be influenced by appropriate selection of characteristics of the friction coefficient. For a certain limitation speed V_{gr} , the stick phase does not occur, which is consistent with the results of the work [206].

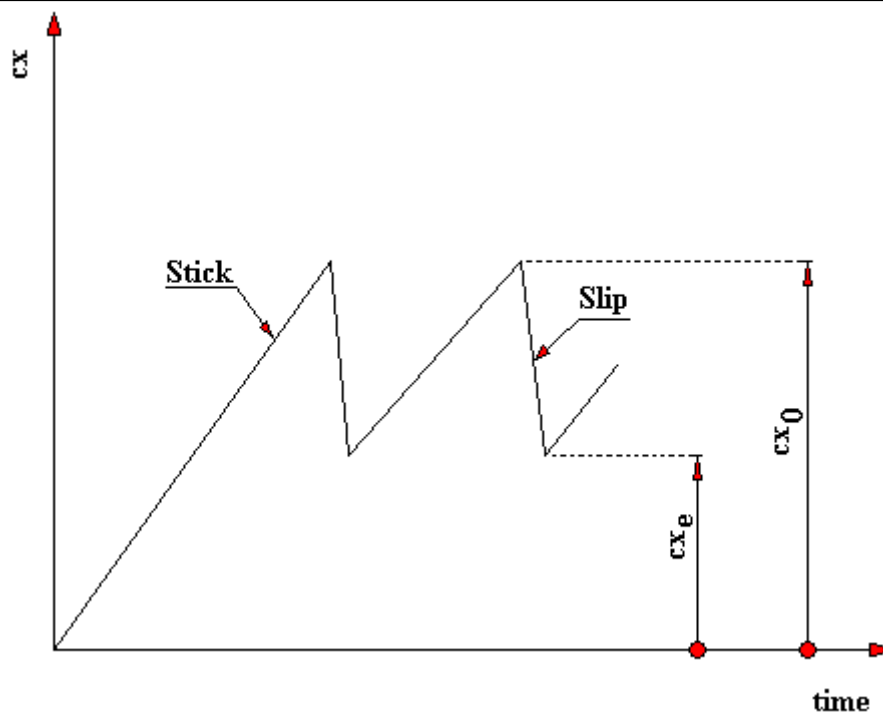


Fig. 4.1.101.2. A pictorial diagram of the occurrence of stick and slip phases

4.2. Group 2 (rolling pairs)

4.2.1. Amsler friction test rig

The Amsler friction test rig (Figures 4.2.1.1, 4.2.1.2 and 4.2.1.3) is designed for testing friction and wear. The moment of sample friction (4) against the counter-sample (5) is balanced by the driving torque of the electric motor (12) increased by the planetary gear (15) with which the swing lever (3) is connected. Counterweights are placed on the lever, the weight of which depends on the measured value of the moment of friction. The integrator lever is connected to the pivoting lever causing the displacement of the integrator counter wheel (1) to the appropriate disc diameter, corresponding to a given value of the friction moment.

The rotational speed of the disc is synchronized with the rotational speed of the counter-sample (5) by means of worm gears. A pen is placed on the lever which draws the course of the friction moment value. And the integrator integrates the work of friction. The integrator counter readings constitute the basis for calculating the coefficient of friction. The diagrams of friction moments are used to check the results of the calculation of the coefficients of friction.

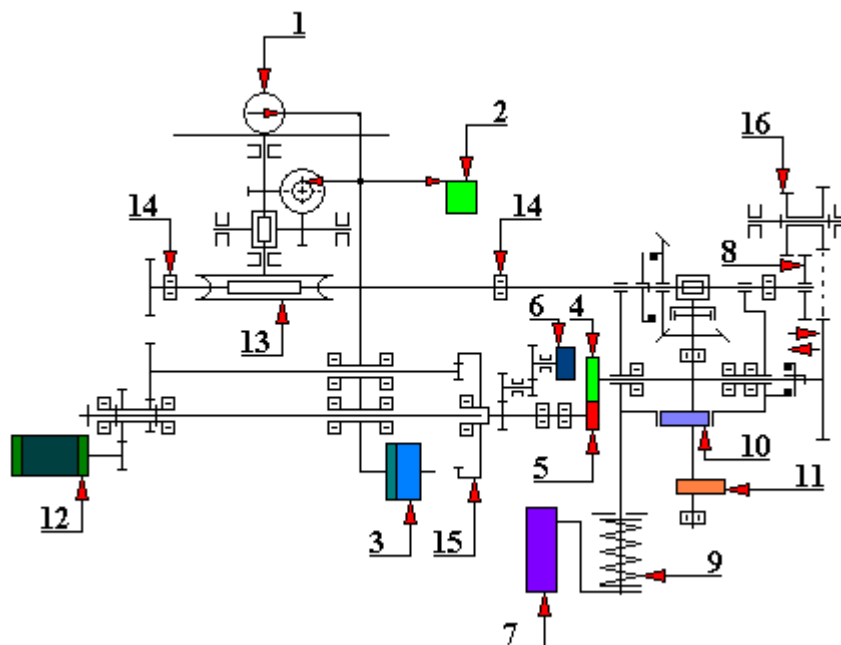


Fig. 4.2.1.1. Kinematic diagram of the Amsler test rig designed to test friction and wear [45]

1 - friction work recorder, 2 - moment of friction recorder, 3 - pendulum dynamometer load, 4 - sample, 5 - counter-sample, 6 - summing counter, 7 - load scale, 8 - rotation switch, 9 - spring burdening the counter-sample, 10 - eccentricity of horizontal motion, 11 - eccentricity of vertical motion, 12 - drive motor, 13 - worm gear, 14 - bearing, 15 - planetary gear, 16 - non-sliding 'two'

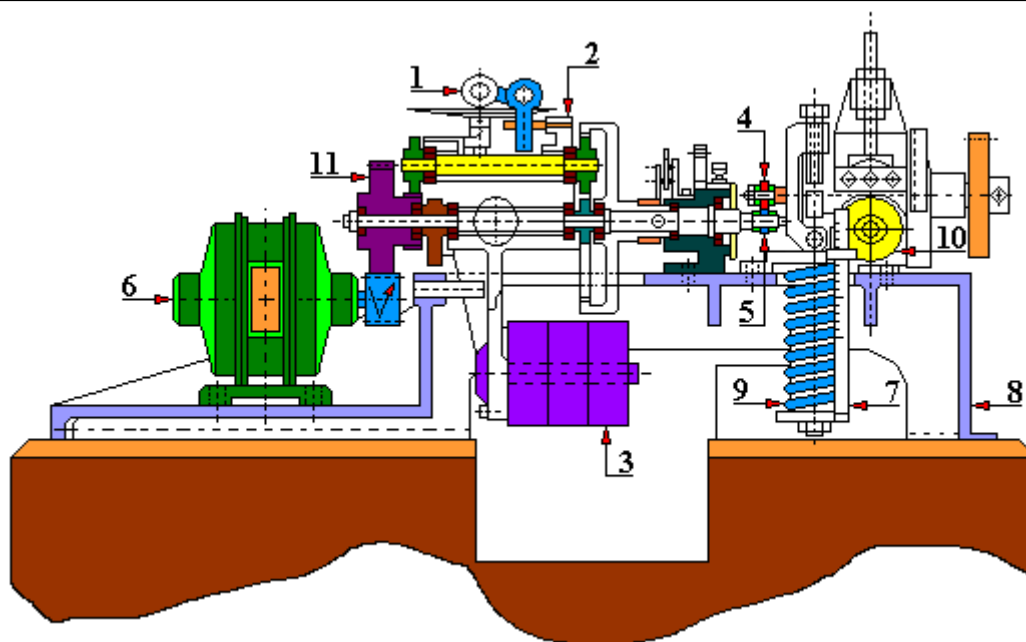


Fig. 4.2.1.2. Longitudinal section of the Amsler test rig designed to test friction and wear [45]
 1 - friction work recorder, 2 - moment of friction recorder, 3 - pendulum dynamometer load, 4 - sample, 5 - counter-sample, 6 - drive motor, 7- load scale, 8 - housing body, 9 - spring burdening the counter-sample, 10 – eccentricity of horizontal motion, 11 - non-sliding 'two'

The Amsler test rig is characterized by the following parameters:

- temperature measurement – with a thermocouple,
- sample width: 10 [mm],
- counter-sample width: 10 [mm],
- outer diameter of the sample from $\varnothing 30$ [mm] to $\varnothing 50$ [mm],
- outer diameter of the counter-sample from $\varnothing 30$ [mm] to $\varnothing 50$ [mm],
- sample rotational speed: 200 [rpm] or 400 [rpm],
- loading system - spring with pressing force $0 \div 250$ [N],
- load regulation - continuous,
- load characteristics - static,
- moment of friction measuring system - pendulum dynamometer,
- counter-sample rotational speed: $60 \div 120$ [rpm].

The seizure resistance test on the Amsler test rig is carried out according to the standard PN-88/H-04337.



Fig. 4.2.1.3. General view of the Amsler test rig

Modernization of the friction contact of the Amsler test rig (Fig. 4.2.1.4) consists in changing the disc-disc friction contact into a mandrel-disc type mating in a system of three samples (mandrels) and a counter-sample (disc). The reason for this modernization was the necessity to adapt the existing technical facilities to the testing needs. The authors of this construction are Klaudiusz Lenik, Krzysztof Dziedzic, Mariusz Barszcz and Mykhailo Pashechko.

Modernized

testing head (Fig. 4.2.1.4) is composed of the following elements:

- head disc,
- head arm (it acts as a resistance element preventing the head from rotating around its axis; at the same time, together with the strain gauge bridge placed on it, it creates a sensor that measures the friction force),
- the head holder for fixing the head in the tribotester body simultaneously transferring the load from the lever system to the friction contact of the counter-sample - sample.

Thanks to the use of a special basket it is possible to carry out tests of the tested friction contact in dry friction conditions or with the use of liquid lubricants and with the use of abrasive.

In the modernized friction contact of the Amsler test rig the tested samples have a shape of a cylinder or a cuboid, and the counter-sample has the shape of a disc. The moving element in this friction contact is the counter-sample. And samples (from 3 to 6 pieces) remain at rest and slidingly co-act with the counter-sample disc. The samples are mounted in the holder with a left-hand thread.

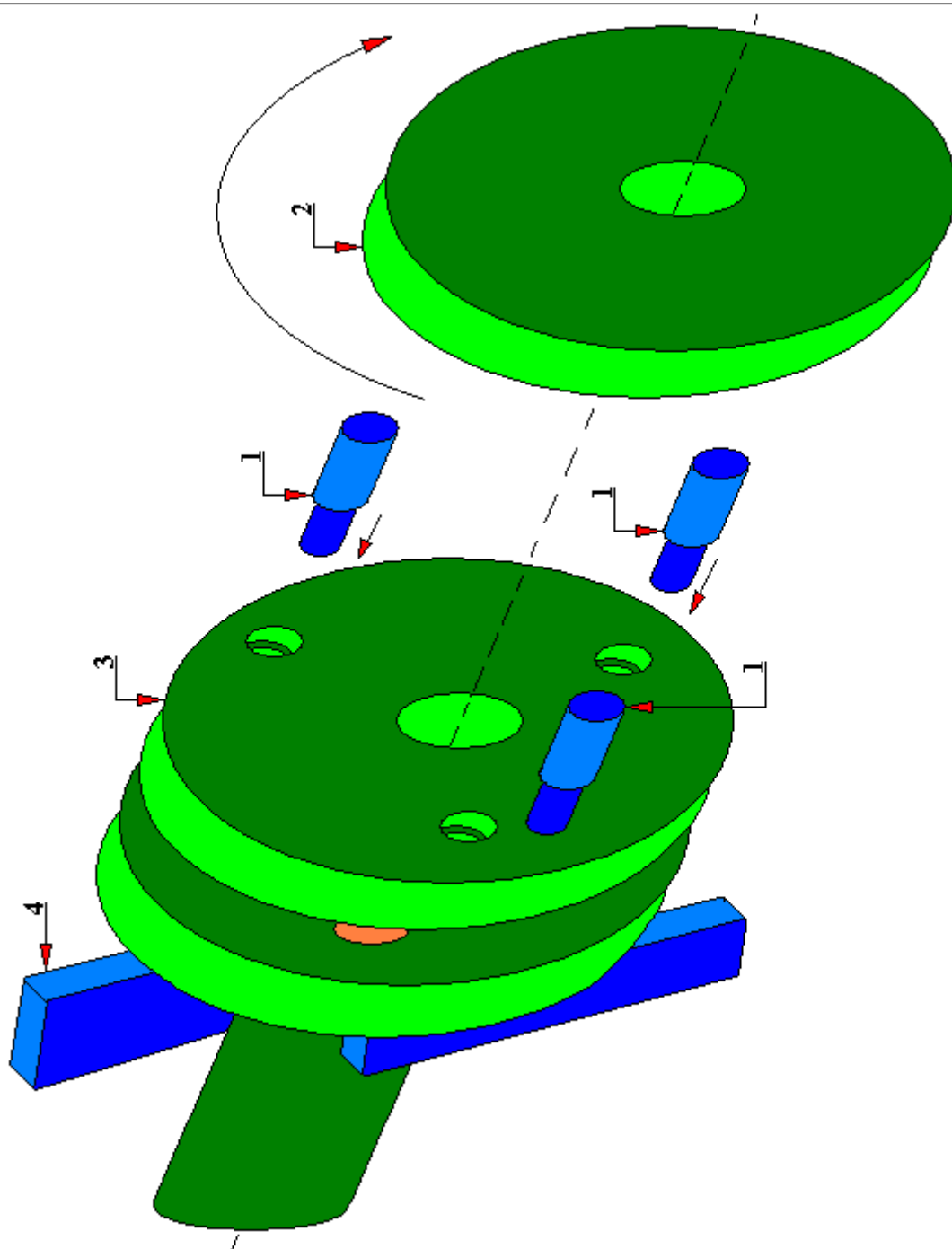


Fig. 4.2.1.4. A model of the modernized test head of the Amsler test rig [67]
1 - sample (mandrel), 2 - movable counter-sample (disc), 3 - sample holder, 4 - head arm

4.2.2. T-05 test rig

The T-05 test rig is a test rig with a friction contact identical to that in the Timken test rig but it is equipped with a controller and computer. Thanks to the application of a modern design and control system, tests on this test rig can be carried out in concentrated or conformal contact: dry or lubricated with the possibility of adjustment of slide and amplitude. Generally, one may say that the tests on this test rig consist in measuring the friction force, block temperature, lubricant temperature, loss of block mass and roller mass, and in determining the width of the wear marks on the block occurring during friction tests of the steel roller against the block at a given load. The T-05 test rig is a commercial test rig manufactured by the Institute of Sustainable Technologies in Radom.

Standardized parameters of tests on a roller-block test rig include: - assessment of the durability of a layer of grease [ASTM D 2981 - 71]; - assessment of wear properties of plastic greases [ASTM D 3704 - 78]; - comparative tests of construction materials [ASTM G 77 - 93].

Parameters which characterize the operation of the friction contact of T-05 tribotester include, among others:

- the ratio of the lever loading system: 10: 1 or 30: 1;
- oscillating frequency (adjustable in a continuous way): 40 ÷ 500 cycles/min;
- lubrication method: oil bath lubrication or single application of a sample of the tested lubricant prior to the test;
- type of contact: concentrated or conformal, created by a rotating roller and a block pressed against it;
- type of motion: sliding with a slip speed of 0.037 ÷ 5.5 m/sec corresponding to 20 ÷ 3000 rpm;
- oscillating motion angle continuously adjustable : 0° ÷ 90°;
- gradually adjustable contact load in the range from 150 [N] to 3150 [N].



Fig. 4.2.2.1. General view of the T-05 test rig



Fig. 4.2.2.2. Attachment for bath lubrication of test samples. T-05 test rig

4.2.3. Taber-Abraser test rig

Taber-Abraser test rig (Fig. 4.2.3.1) is designed to test the abrasion resistance of hard materials, e.g. thermally sprayed coatings. The flat sample 1 attached to the rotating table is in a rotating motion and is rubbed by two symmetrically arranged grinding wheels 2, usually made of silicon carbide, placed under an adjustable load F . The indicator determining the wear for this type of test rig is the loss of weight of sample 1 in the period of the so-called 'steady-state wear regime', i.e. the period during which the wear is stabilized at a constant level after every 1000 cycles of rotation, expressed in mg/1000 cycles. In order to carry out tests on this test rig it is necessary to suck off the abrasion products and keep a relative humidity of the atmosphere and temperature at a constant level.

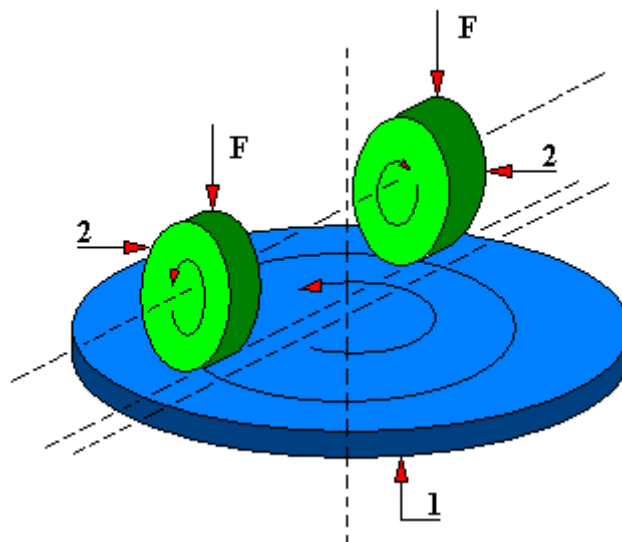


Fig. 4.2.3.1. General scheme of operation of the Taber-Abraser test rig
1 - flat sample; 2 - roller grinding wheel; F - load

4.2.4. STBL-02 tribological test rig

The essence of the operation of the friction contact of STBL-02 test rig is the co-action of one rolling element, e.g. NU309 (roller) with three inner rings. There is, thus, a certain analogy as regards the essence of operation between this tribological test rig and the four-ball test rig.

Figure 4.2.4.1 shows a general diagram of the friction contact of this test rig.

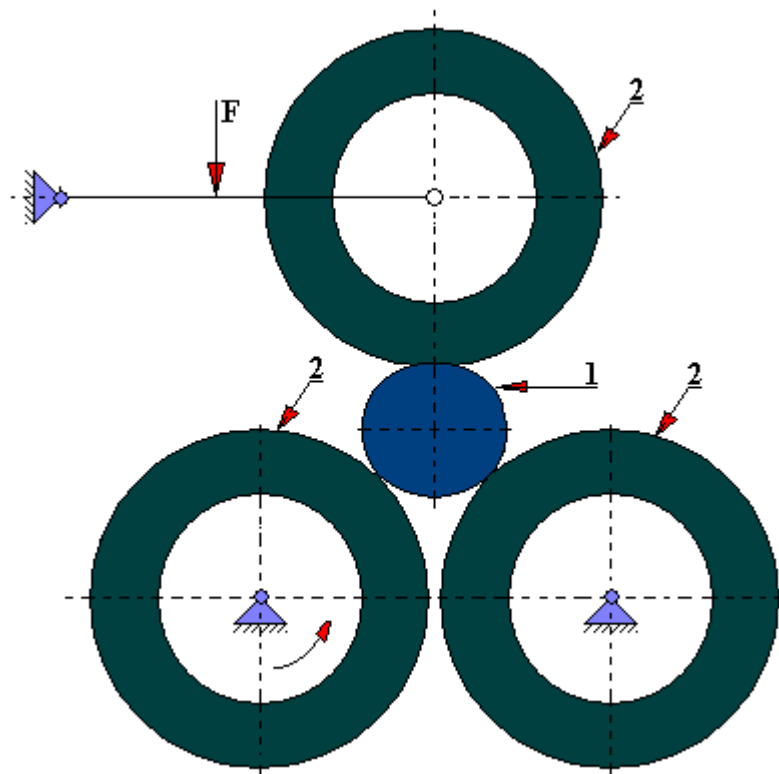


Fig. 4.2.4.1. General diagram of the friction contact of STBL-02 test rig
1 - given roller, 2 - inner rings of the bearing

4.2.5. Pavlov test rig for determining the frictional resistance during the rolling process using the forced braking method or clamping method

The above-mentioned test rig for determining the co-efficient of friction in the rolling process is presented in [162]. The measuring principle is based on the fact that the rolled material (strip) (Fig. 4.2.5.1) is mounted in a special holder with a pull 1 connected to a dynamometer 6 which enables the measurement of the friction force T . And the other end of the strip is fed onto the rolls. When the strip is nipped by rollers the chain is stretched, and the horizontal force is measured on the dynamometer. At the same time, the force of pressure on the rollers should be measured with a second dynamometer 3. From the equilibrium condition of the sum of projections on the X axis (Fig. 4.2.5.2) the following relationship is obtained:

$$\mu = \frac{T}{2 \cdot P_N \cdot \cos \alpha} + \operatorname{tg} \frac{\alpha}{2}$$

Knowing the value of the friction forces T and the rolls pressing force P_M it is possible to determine the friction factor μ .

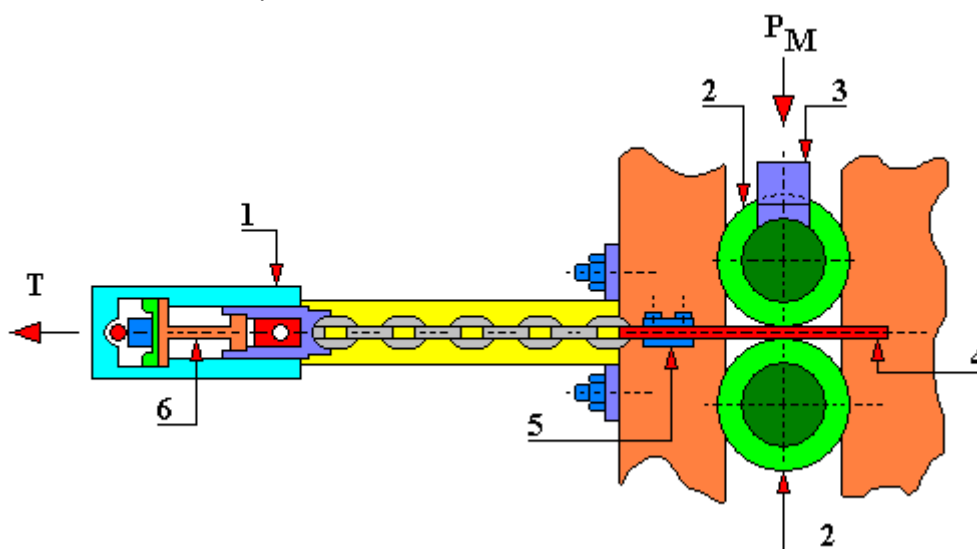


Fig. 4.2.5.1. Pavlov test rig for determining frictional resistance during the rolling process
 1 - pull; 2 - rollers; 3 - dynamometer for measuring the force of pressure on the rollers; 4 - rolled material (strip); 5 - strip holder; 6 - dynamometer for measuring the friction force; T - friction force; P_M - pressing force on rollers.

A similar distribution of forces (Fig. 4.2.5.3) is presented in [220]. When the metal (strip) comes into contact with the rollers, acting is the normal force N (perpendicular to the surface) resulting from the pressure of rollers, and the friction force T directed tangentially.

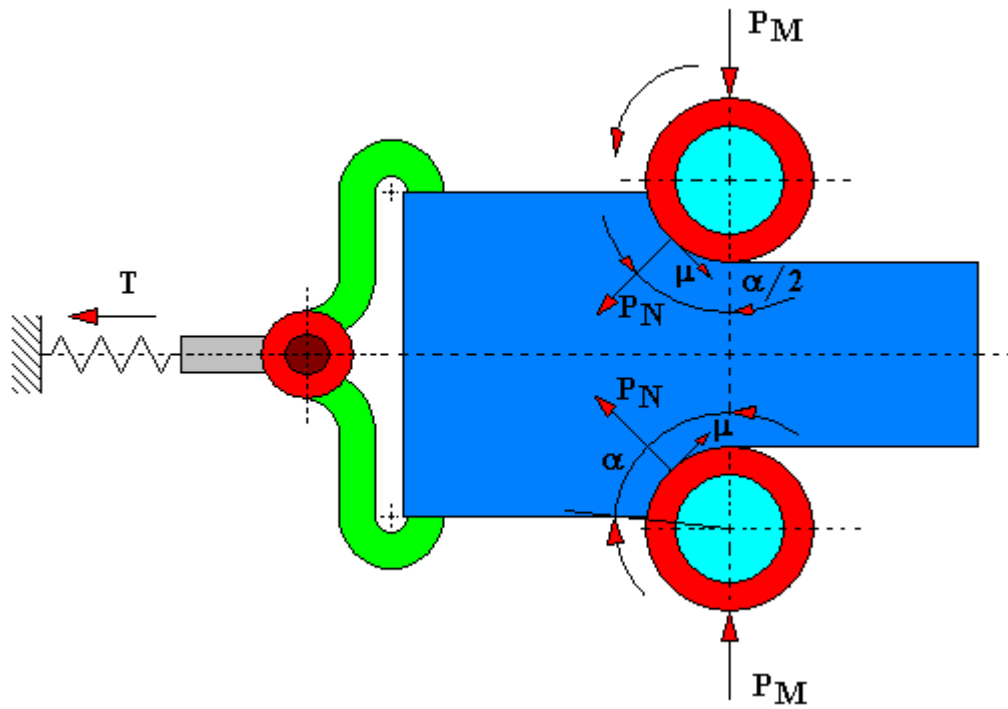


Fig. 4.2.5.2. Diagram of forces acting on the rollers T - friction force; P_M - pressing force on rollers; P_N - normal force (perpendicular to the surface); μ - coefficient of friction

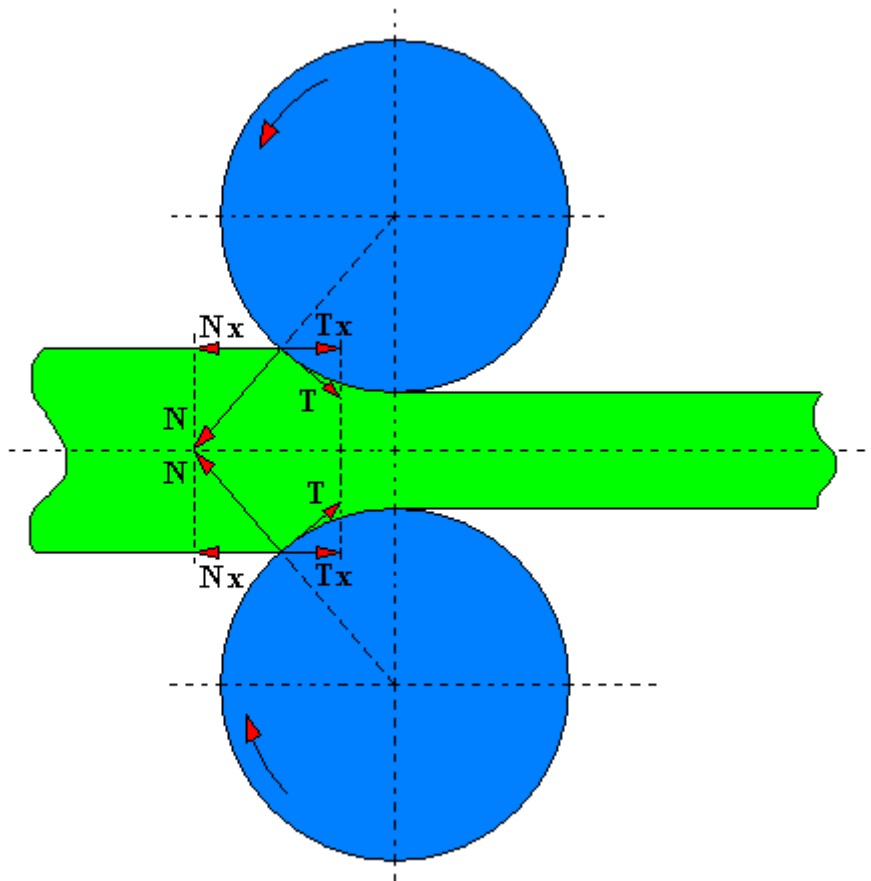


Fig. 4.2.5.3. The distribution of forces when the metal is gripped by rollers [220]

N - normal force; T - friction force; N_x - projection of the normal force onto the X axis; T_x - projection of the friction force T onto the X axis

4.2.6. T-02 four-ball test rig

The tribotester T-02 (figures 4.2.6.1 ÷ 4.2.6.5) is intended mainly for determining the anti-seize and anti-wear properties of oils, greases and their additives. This test rig allows to measure, among others:

- moment of friction,
- load,
- temperature of the tested lubricant,
- test run time.

The construction of the four-ball test rig includes, among others, measuring converters, digital measuring amplifier and a computer with a measuring and recording program. This tribotester is a commercial test rig manufactured by the Institute of Sustainable Technologies in Radom. Figure 4.2.6.1 shows a general diagram of this test rig.

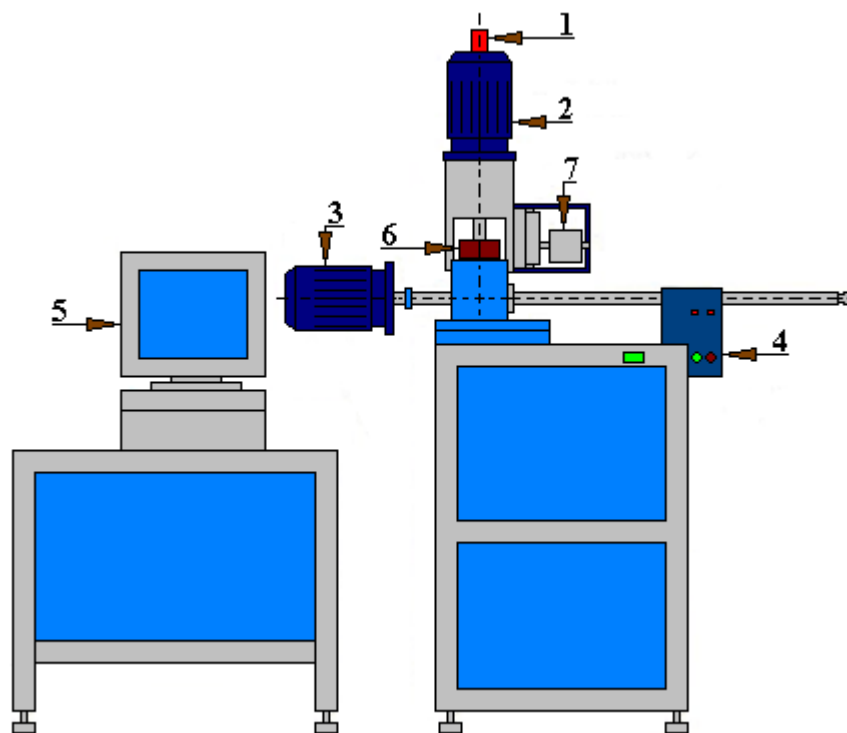


Fig. 4.2.6.1. General diagram of the four-ball test rig T-02

1 - encoder, 2 - main drive motor, 3 - lever load drive motor, 4 - weight, 5 - computer, 6 - friction contact with thermocouple, 7 - torque meter



Fig. 4.2.6.2. General view of the T-02 four-ball test rig

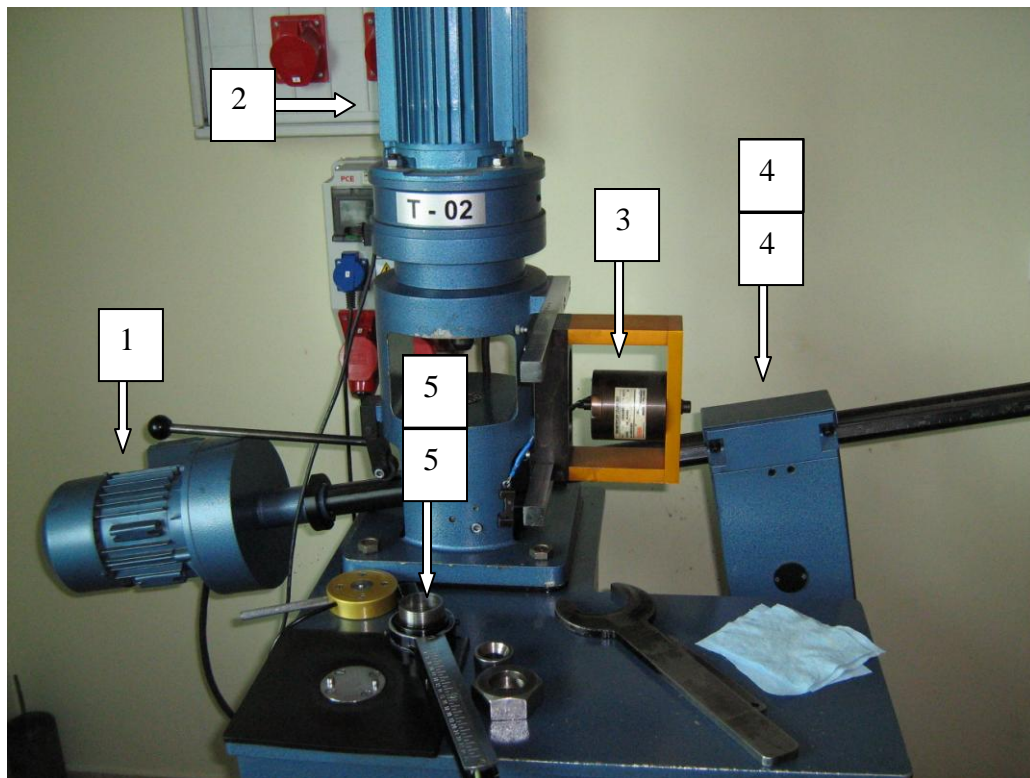


Fig. 4.2.6.3. View of the main components of the T-02 four-ball test rig
1 - lever load drive motor, 2 - working (main) drive motor, 3 - torque meter, 4 - lever load, 5 - friction contact socket



Fig. 4.2.6.4. View of the modernized T-02 four-ball test rig Visible change in the type of torque meter used. One of the military laboratories

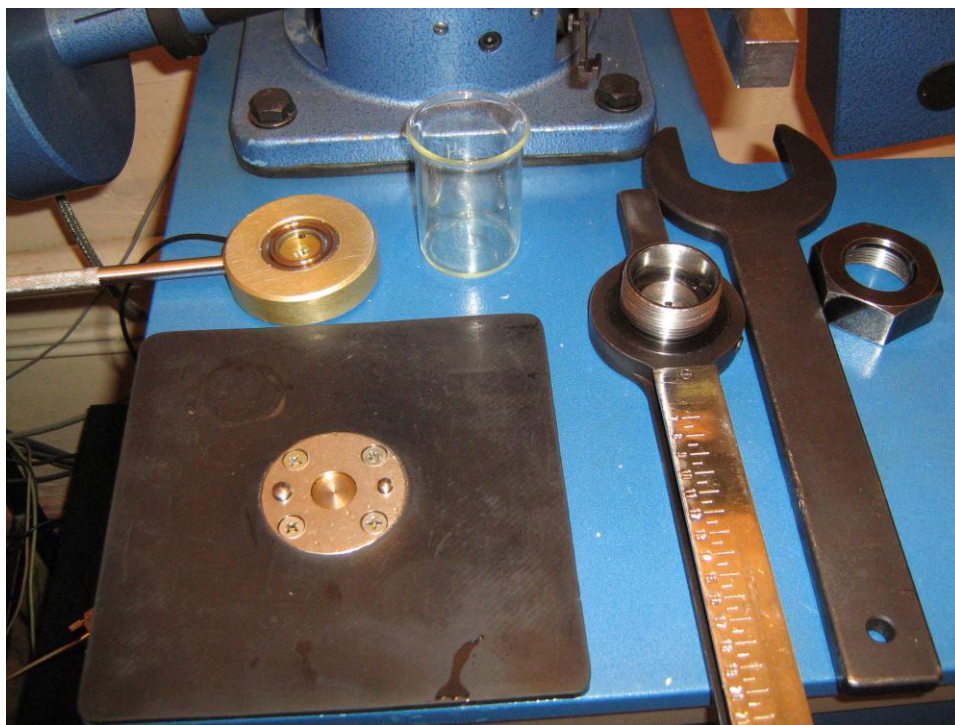


Fig. 4.2.6.5. View of the modernized T-02 four-ball test rig. Tool table. One of the military laboratories

4.2.7. T-03 four-ball test rig designed for testing the pitting

The tribotester T-03, whose contact diagram is shown in Figure 4.2.7.1, is a modification of the classic four-ball machine. The change of construction design consists mainly in modifying the friction contact. The three lower balls 2 are placed in a special raceway of the pan 3 which allows them to roll freely. In addition, this friction test rig is equipped with a set for controlling the temperature of the friction contact and for its measuring. In addition, this test rig has a built-in electronically controlled time clock to determine the test time and a vibration switch to identify the first onsets of pitting. All the above-mentioned sets included in T-03 tribotester are computer controlled. This tribotester is a commercial test rig manufactured by the Institute of Sustainable Technologies in Radom, Poland.

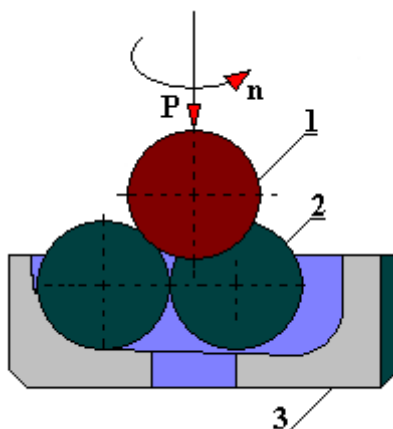


Fig. 4.2.7.1. Diagram of the friction contact of T-03 four-ball test rig for testing the pitting [Patent No. PL 177200-B1-G01N 3/56, *Aparat czterokulowy do badania wpływu środków smarowych na powierzchniowe zużycie zmęczeniowe (Four-ball test rig for testing the effect of lubricants on surface fatigue wear)*]; 1 – upper ball, 2 - three lower balls, 3 - pan with a special raceway.

Test studies of the effect of lubricating liquids on pitting on a modified four-ball test rig represent the subject of the British standard IP 300/82 *Rolling Contact Fatigue Tests for Fluids in a Modified Four-Ball Test rig*. According to this standard two test methods are possible:

- test at ambient temperature,
- test at elevated temperature.

These tests consist in carrying out a run of a set of four balls under the conditions specified by the standard (load, speed, temperature). All three lower balls roll in a special raceway of a pan in which the tested lubricant is put. The test is carried out until fatigue wear of the upper ball (pitting) occurs. During the test the symptom of the beginning of pitting is an increase in the vibration amplitude of the friction contact. The measure of the wear of these tests is the total running time of the friction contact until pitting occurs on the upper ball 1.

4.2.8. Test rig for measuring the resistance and coefficient of rolling resistance of motor vehicle wheels according to the patent PL 74 682

A test rig for direct measurement of pressing force, rolling resistance coefficient and rolling resistance force (Fig. 4.2.8.1) created by Stanisław Lipiński, Witold Mazurowski, Jerzy Morawski, Zdzisław Przybysz enables the above-mentioned measurements to be made while ensuring the continuity of recording the test results as a function of speed and force and the possibility of testing the variability of the rolling resistance coefficient depending on the tire tread and elasticity of the tire at every point of its circumference. The above-mentioned test rig is characterized by a simple structure and it does not require a special test rig, at the same time it allows the use of typical, commonly known electrical measuring equipment such as multi-channel strain gauge bridge and loop oscillograph.

Until now the technical resistance was determined in road samples of a motor vehicle as the towing force on the dynamometric hook of one-wheel trailer loaded with a specific method of weight testing. This type of measurement is burdened with an error occurring, among others, as a result of:

- lack of horizontal position of the hook;
- variable ventilation resistance;
- dependence of the rolling resistance on the type and condition of the road surface.

On the other hand, in test rigs, the existing stationary methods have been carried out on carousel or drum test rigs where the rolling resistance coefficient is measured by measuring the power or energy lost to overcome the rolling moments of the wheel or by measuring the rolling resistance moments. These measurements give intermediate results burdened with a number of errors, inter alia, such as:

- variability of the efficiency of test rigs;
- periodic need to calibrate/validate test rigs;
- measurement errors of the pressing force;
- errors in reading intermediate quantities used for calculating the rolling resistance coefficient, such as: • pressing force, rolling radius, rolling resistance force.

If the rolling resistance is specified with the letter P , the rolling resistance coefficient with the letter f and the wheel pressure, the so-called radial load, with the letter N , then we get:

$$P = f \cdot N$$

Since the rolling resistance coefficient f is a small value, ranging from 1% to 5% of the pressure of the tire N , its measurement accuracy was burdened with a large error due to the effects of friction occurring in the articulated elements of the suspension or wheel mounting in a motor vehicle or in a raceway test rig (carousel or drum). In order to minimize or eliminate the above-mentioned defects the present test rig was built whose essence of operation is presented below.

The wheel band 1 together with the tire 2 is mounted on a hub 3 with rolling bearings on the measuring axle 4 of a motor vehicle or a test rig for testing tires of motor vehicles. The measuring axis 4 has two flanges: front 5 and rear 6. The rear flange 6 has two pairs of fixed handles 7 and 8, while the front flange 5 has two pairs of sliding handles 9 and 10 with adjustable handwheels 11.

In opposite handles 7 and 9, plates 12 are mounted with affixed strain gauges for testing the pressing force of the tire. And in opposite handles 8 and 10, plates 13 are mounted with affixed strain gauges for testing the rolling resistance force. The plates 12 and 13 are made of a material with a low modulus of elasticity.

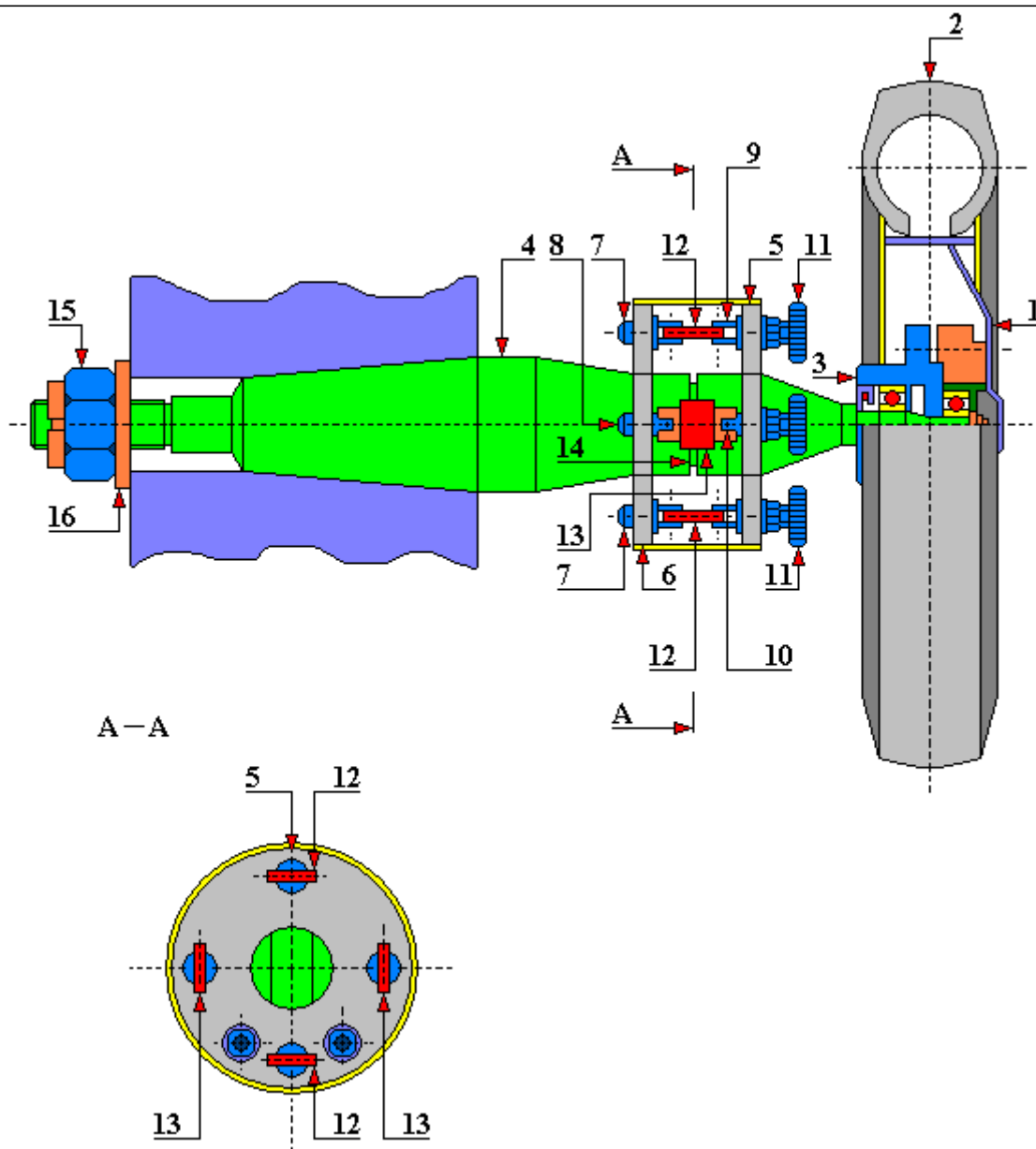


Fig. 4.2.8.1. General view of a test rig for measuring the resistance and coefficient of rolling resistance of motor vehicle wheels according to the patent PL 74 682

1 - band; 2 - tire; 3 – ball bearing hub; 4 - measuring axis; 5 - front flange; 6 - back flange; 7 - first pair of fixed handles; 8 - second pair of fixed handles; 9 - first pair of sliding handles; 10 - second pair of sliding handles; 11 - adjustment handwheels; 12 - plates with affixed strain gauges for testing the pressing force; 13 - plates with affixed strain gauges for testing the rolling resistance force; 14 - indentation (notch); 15 - nut; 16 - washer

In order to ensure the operation of strain gauges in a pure tension system, the initial stress of the plates 12 and 13 is adjusted with handwheels 11. The strain gauges of the plates 12 and 13 are electrically connected to a multi-channel strain gauge bridge and a loop oscillograph. In order to obtain the most accurate signals originating from elastic deformations of the plates 12 and 13 resulting from the bending of the measuring axis 4, and with the loaded forces P (rolling resistance) and N (radial load) an indentation (notch) of this measuring axis was made. This notch is between flanges 5 and 6. The shape of this notch is similar to a rectangular section. The longer sides of this cross-section are in the direction of the pressing force, and the shorter sides

are in the direction of the rolling resistance force. This ensures that the two pairs of plates 12 and 13 are equally deformed under axle load 4.

The plates 12 and 13 are mounted in the holders 7, 8, 9 and 10 at such a distance from the neutral axis that during the load on the axis 4 it is possible to obtain their elastic deformation ensuring a sufficiently strong electrical signal of the strain gauge co-acting with the measuring test rig, which would not be possible to achieve if the strain gauges were placed directly on the axis 4.

Based on the strength relationship:

$$\varepsilon = \frac{\delta}{E}$$

where:

ε - relative plate deformation;

δ - stress in the plate;

E - modulus of elasticity

by selecting the plate material and dimensions of its cross-section it is possible to obtain sufficiently large deformations ε which determine the generation of a sufficiently strong signal for the electrical reading apparatus.

4.2.9. MWO test rig (test rig with rotating load)

MWO test rig (Figures 4.2.9.1, 4.2.9.2 and 4.2.9.3) used to determine the ultimate durability of dynamically loaded radial slide bearings. It is a non-commercial original test rig built by the Laboratory of the Department of Construction and Operation of Machines of Gdańsk University of Technology.

This test rig is a bearing test rig with a rotating load. It is designed to test the fatigue strength of the sliding layer in multilayer thin-walled bearing bushings under the conditions of a full lubricating film.

This test rig consists of two tested bearings (1) placed in supports (4). The load of the tested bearings (1) is a dynamically unbalanced shaft (2) with masses (3). An unbalanced shaft is set in a controlled rotational motion. The bearing housings are attached to the stabilizer beam (6). This beam is supported on a ball joint (8) and four flexible supports (7). The bearings (1) are supplied with oil via a system of drillings in the shaft (2). The rotation of the load at each point of the sliding layer in a given bushing section causes theoretically identical variable stresses. The components of these stresses are, among others:

- alternating normal hoop stresses,
- pulsating radial stresses.

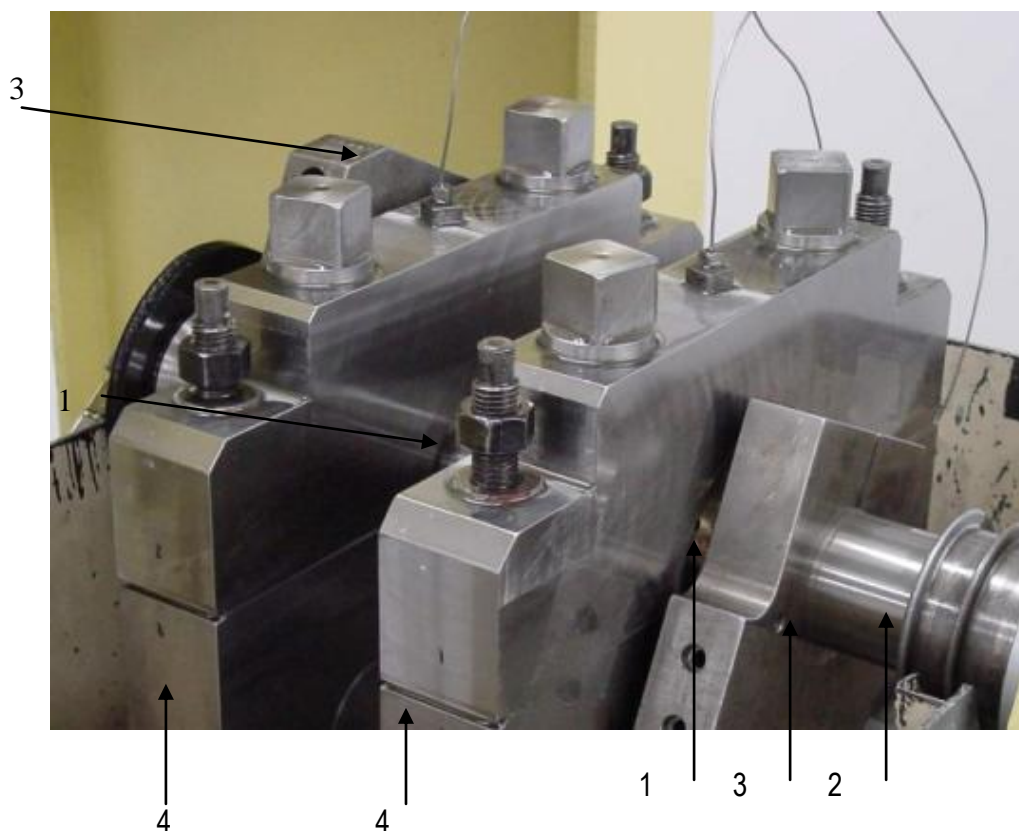


Fig. 4.2.9.1. MWO (test rig with rotating load) after removing the test head cover
1 - tested bearings, 2 - hollow shaft, 3 - rotating loading masses, 4 - bearing supports [based on a photo taken from: <https://mech.pg.edu.pl/web/katedra-konstrukcji-maszyn-i-pojazdow/mwo>]

Fatigue tests and the procedure of determining the rated fatigue strength index is based on a two-point strategy.

The technical data of the MWO test rig are as follows:

- bushing width: up to 50 [mm],

- rotational speed of the shaft: 300-4500 [rpm],
- standard bearing diameter: \varnothing 52.7 [mm],
- maximum surface pressure: up to 128 [MPa],
- maximum (rotating) bearing reaction: up to 120 [kN].

This test rig facilitates, among others, the testing of:

- shaft rotational speed,
- load quantities,
- supply oil pressure,
- bearing temperature,
- oil temperature on the upstream,
- the amount of oil supplied to the bearings.

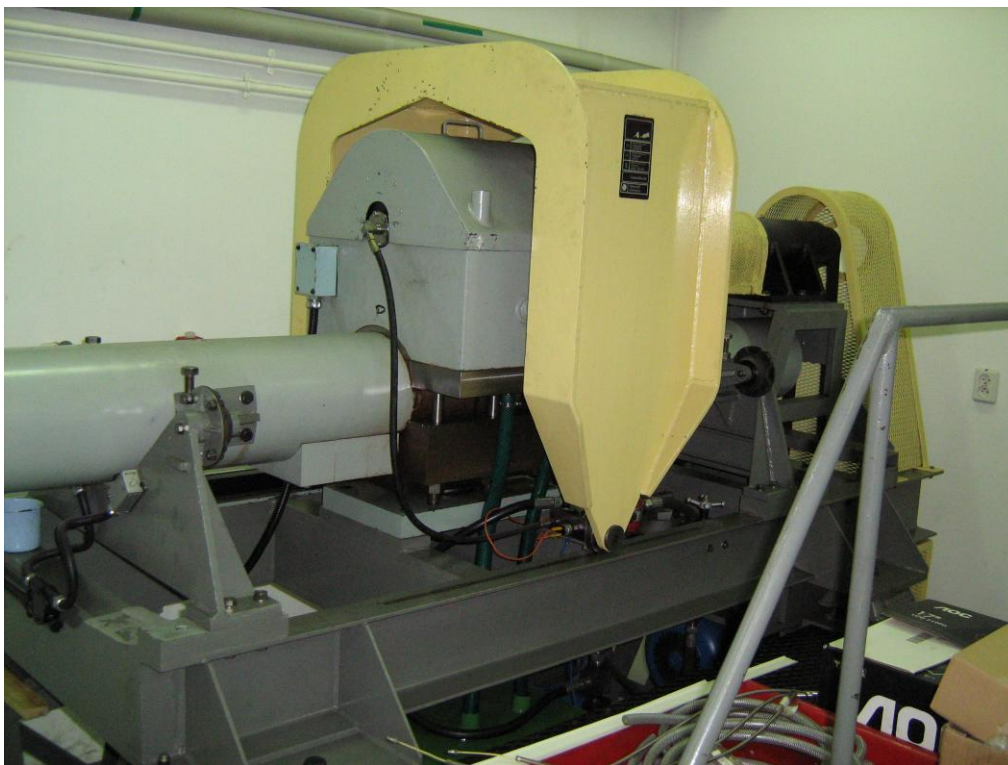


Fig. 4.2.9.2. MWO (test rig with a rotating load) with the test head cover fitted

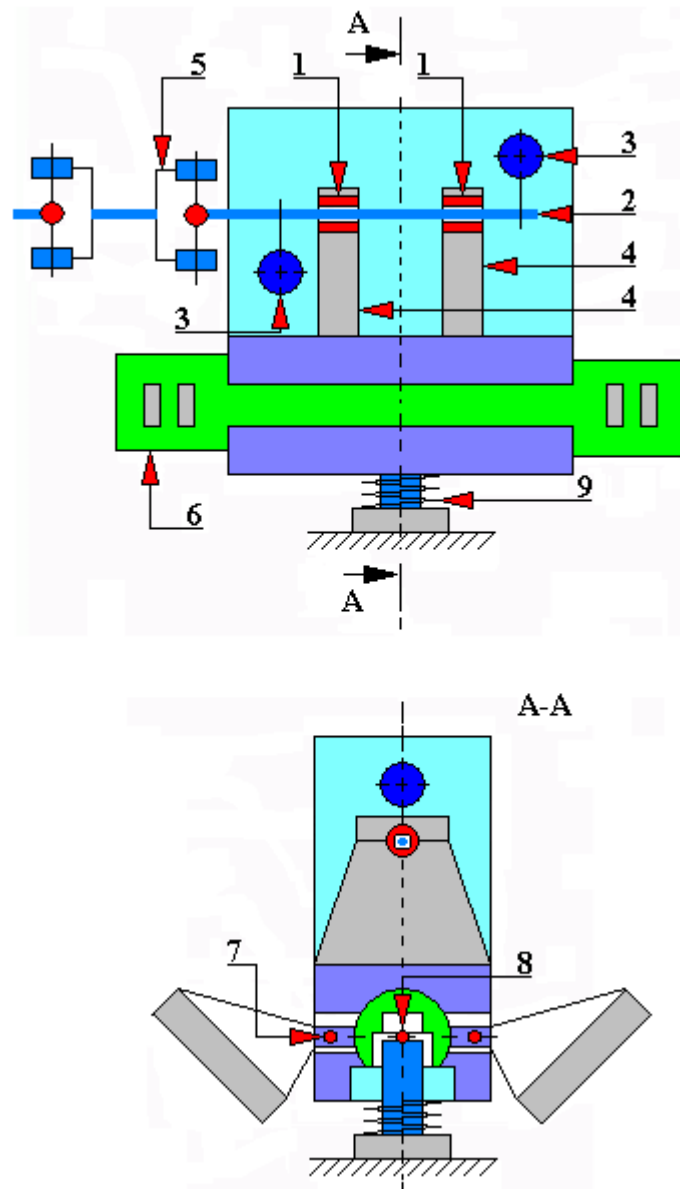


Fig. 4.2.9.3. MWO (test rig with rotating load). Construction scheme
 1 - tested bearings, 2 - hollow shaft, 3 - rotating loading masses, 4 - bearing supports, 5 - Cardan joint (clutch), 6 - stabilizing beam, 7 - flexible support, 8 - ball joint, 9 - spring.

4.2.10. Four-ball test rig according to the patent PL 160 591

This test rig (Figure 4.2.10.1), according to the patent No. PL 160 591, the authors of which are Witold Piekoszewski, Marian Szczerek, Stanisław Koziół, is intended for carrying out a four-ball test. In particular, this test rig is applicable to tribological tests according to the test methods contained in standards PN-76 / C-04147 (Polish standard) and IP300 (British standard). The test rig includes a drive unit to drive the upper ball holder, a lower holder with three stationary balls, a loading lever with a weight and counterweight. The drive from the motor (1) is transferred onto the spindle ending with the holder (4) of upper ball (5) directly through the clutch jaw (3) or indirectly through the two-stage belt transmission with toothed belts (2), and the handle (6) with fixed lower balls is pressed by a loading lever with one arm in the form of a toothed bar with a weight placed on it i.e. is a stepper motor (8) coupled with the toothed bar by a gear wheel (9) mounted on the motor shaft (8). The stepper motor (8) is controlled by the rotational speed of the spindle terminated with the upper ball holder by means of the controller (14) and the impulse sensor (13). And the strain gauge (7) is coupled with the lever (12) rigidly connected to the holder (6) of the fixed lower balls. This test rig has a control and measurement system for measuring and recording the moment of friction occurring between the movable upper ball and the fixed lower balls. This system consists of:

- strain gauge (7),
- amplifier (15),
- voltage-frequency converter (16),
- frequency counter (17),
- digital reading panel (18),
- interface (19),
- computer interface (20).

The handle with fixed lower balls is pressed by a loading lever with one arm in the form of a toothed bar with a weight placed on it in the form of a stepper motor.

The main drive motor is connected to the spindle via a clutch, and the lower balls are placed in a raceway mounted in the holder by a nut.

The unquestionable advantage of this test rig in this version is the ability to carry out tests at two different spindle rotational speeds depending on the clutch jaw engagement. This test rig does not have a multi-stage or variable transmission. Probably the reason for this state was the adaptation of this tribotester to the requirements of the above standards. No provision was made, for example, in the event when standards change and other spindle speeds are required. Of course today it is relatively easy to remedy this by using e.g. an inverter (frequency converter). In the patent description for this test rig there is no data regarding, among others: the type of the impulse sensor used, the controller, the amplifier, the voltage / frequency converter, the type of frequency counter used, the type of digital readout panel, the type of computer interface, the type of stepper motor or the type of strain gauge. This, of course, was not the essence of the invention. But it gives the user the option to conduct some modernization of this rig if there is such a need. The test rig is easy to use. There are no heating elements in the holder of the three immobile balls for possible temperature setting. The patent specification shows that the test rig is not equipped with a vibration pickup or thermocouples. Undoubtedly, this equipment would have a positive impact on the scope of tests carried out on this test rig.

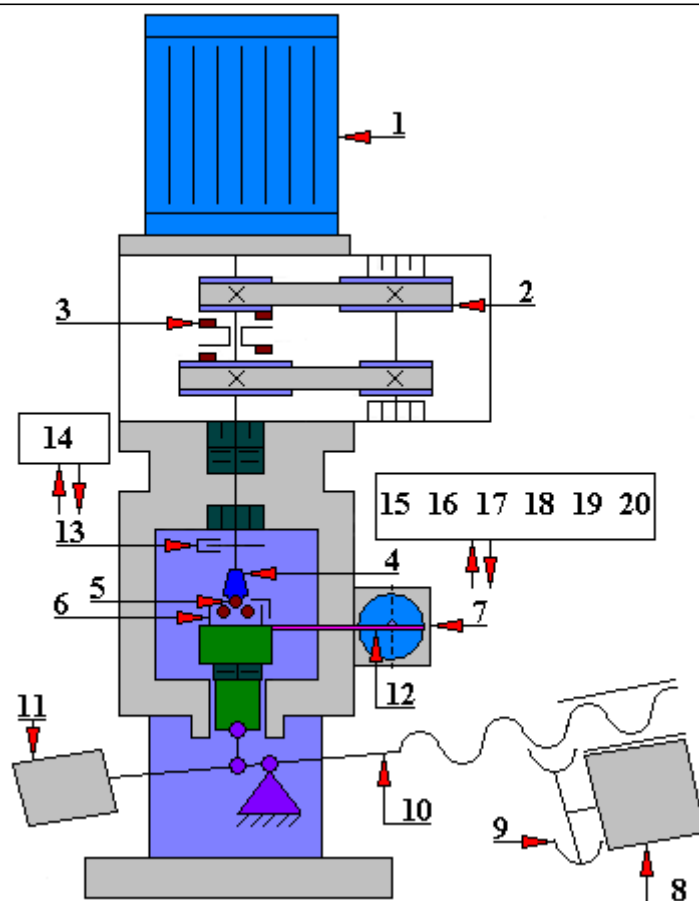


Fig. 4.2.10.1. A four-ball test rig according to the patent PL 160 591

1 - electric motor, 2 - two-stage belt transmission with cogbelts, 3 - clutch jaw, 4 - upper ball holder, 5 - upper ball, 6 - fixed lower balls holder, 7 - strain gauge, 8 - stepper motor, 9 - toothed wheel, 10 - loading lever arm, 11 - counterweight, 12 - lever, 13 - impulse sensor, 14 - controller, 15 - amplifier, 16 - voltage / frequency converter, 17 - frequency counter, 18 - digital readout panel, 19 - interface, 20 - computer interface [developed on the basis of the patent description]

4.2.11. Four-ball test rig according to the patent PL 160 592

The four-ball test rig (Figure 4.2.11.1), according to the patent No. PL 160 592, the authors of which are Witold Piekoszewski, Marian Szczerek, Stanisław Koziół, is intended for carrying out a fatigue tests. It is a technologically advanced machine. Its characteristic feature is that it has a very extensive control and measurement system. The test rig includes a drive motor which moves a spindle terminated in an upper ball holder, a raceway holder and a raceway of the movable three lower sample balls. The lower balls are pressed against the upper ball by means of a loading lever with weights and a counterweight. A vibration pickup (9) is attached to the holder (7) of the race (8) of the lower balls (3). This pickup or sensor turns off the main electric motor when pitting wear begins. This test rig has a control and measurement system consisting of three circuits: I, II and III. Circuit I measures the temperature of the sample and consists of:

- thermostat (10),
- the push-pull amplifier (11),
- voltage/frequency converter (12),
- frequency counter (13),
- digital reading panel (14),
- interface (15),
- computer interface (16).

Circuit II is used for measuring the vibrations of the test friction contact and for controlling the operation of the electric motor. This circuit consists of:

- vibration pickup (9),
- amplifier (17),
- threshold discriminator block (18)
- and the relay (19).

The task of the last third circuit is to count the time or revolutions of the spindle until the drive motor (1) is automatically tripped by the sensor (9) - the moment of starting pitting wear. Circuit III consists of:

- impulse amplifier (20),
- digital reading panel (21),
- interface (22)
- and the computer interface (23).

The control and measurement system consists of parallel circuits to measure the sample temperature, to measure the vibrations of the friction contact and to count the spindle revolutions. The electric motor drives the spindle which terminates in a handle that fixes the upper ball in a fixed position, and the lower balls are placed in a raceway fixed in the handle. The handle with lower balls is pressed against the upper ball by the pusher and sleeve by means of a lever with weights placed on the hanger. The lever on the left side has a counterweight fitted.

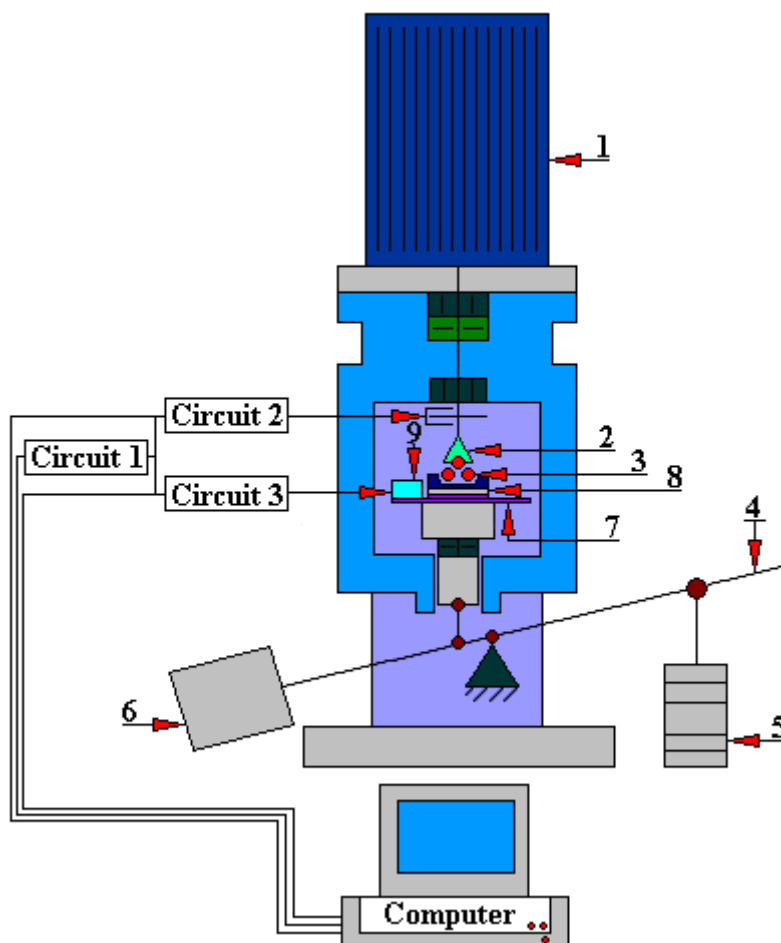


Fig. 4.2.11.1. A four-ball test rig according to the patent PL 160 592

1 - electric motor, 2 - upper ball holder, 3 - lower balls, 4 - loading lever, 5 - weights, 6 - counterweight, 7 - handle, 8 - raceway, 9 - vibration sensor.

Circuit 1 includes: 10 - thermostat, 11 - push-pull amplifier, 12 - voltage/frequency converter, 13 - frequency counter, 14 - digital readout panel, 15 - interface.

Circuit 2 includes: 9 - vibration sensor, 17 - amplifier, 18 - threshold discriminator block, 19 - relay.

Circuit 3 includes: 20 - impulse amplifier, 21 - digital reading panel, 22 - interface, 23 - computer interface

4.2.12. Four-ball test rig according to the patent PL 177200

A four-ball test rig (Fig. 4.2.12.1) according to the patent No. PL 177200, created by Witold Piekoszewski, Marian Szczerek, Stanisław Kozioł and Jan Wulczyński is designed to test the influence of lubricants on surface fatigue wear. This test rig has an electric motor (1) powered from the controller (30) which drives the spindle (15) through a clutch (16) with a damping insert. In the lower part of the spindle (15) there is a holder (2) that fixes the upper ball which, together with the lower balls placed in the raceway (4) fixed in the holder (5) with a special nut (3), creates a test friction contact. The handle (5) with lower balls and raceway (4) is pressed against the upper ball with the lever (6) with weights (7) placed on the hanger (8) by means of the pusher (9), sleeve (11) and test rig (12). A counterweight (10) is attached to the left side of the lever (6). The lower ball holder (5) in the lower cylindrical part has a thermocouple (14) placed centrally. A vibration pickup (13) is located on the side surface of the special nut (3).

This test rig has a control and measurement system consisting of five circuits: They are all connected in series with the interface (32) and the computer (33) via a computer interface connection (31). The circuit 1 is connected to the transducer (13) of the friction contact vibrations. This circuit consists of a charge amplifier (18), analog-to-digital converter (19) and impulse counter (20). Circuit 2 is connected to the rotation sensor (17). This circuit consists of a receiver (21), amplifier (22) and impulse counter (23). Circuit 3 is connected to the rotation sensor (17). This circuit consists of a receiver (24) and impulse counter (25). Circuit 4 is connected to a temperature converter (14), and it comprises an amplifier (26), analog-to-digital converter (27) and impulse counter (28). The last fifth circuit is the circuit which is controlling the operation of the main drive motor. Its input is connected in series with the interface (32) and computer (33) via a computer interface (31), and its output is connected to the drive motor (1). This circuit consists of a digital to analog converter (29) and a power supply controller (30).

Generally, circuit 1 is used to measure vibrations of the friction contact. Circuit 2 measures the rotational speed of the disc, circuit 3 measures the friction path by counting the counter-sample revolutions, and circuit 4 measures the temperature of the lubricant. And the last circuit 5 controls the operation of the drive motor of the four-ball test rig.

The above-mentioned test rig is technically very advanced, yet its operation is simple.

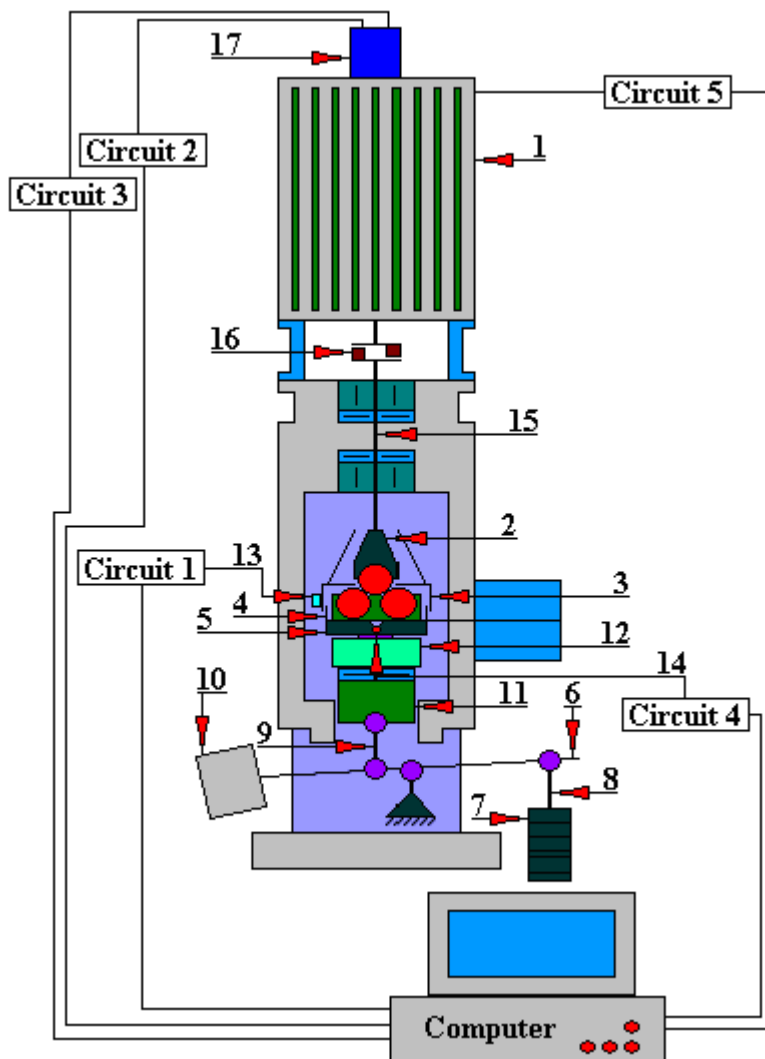


Fig. 4.2.12.1. A four-ball test rig according to the patent PL 177 200
 1 - electric motor, 2 - upper ball holder, 3 - special nut, 4 - raceway, 5 - holder, 6 - lever, 7 - weights, 8 - hanger, 9 - pusher, 10 - counterweight, 11 - sleeve, 12 - test rig, 13 - vibration sensor, 14 - thermocouple, 15 - spindle, 16 - clutch, 17 - rotation sensor. Circuit 1 consists of: vibration sensor (13), charge amplifier (18), analog-to-digital converter (19) and impulse counter (20). Circuit 2 consists of: receiver (21), amplifier (22) and impulse counter (23). Circuit 3 consists of: receiver (24) and impulse counter (25). Circuit 4 consists of: amplifier (26), analog-to-digital converter (27) and impulse counter (28). Circuit 5 consists of: digital-to-analog converter (29) and a power supply controller (30). The elements that bind the whole together are the interface, computer interface connections and the computer.

4.2.13. Four-ball test rig according to the patent 177203

A four-ball test rig (Fig. 4.2.13.1) according to the patent No. PL 177203, created by Witold Piekoszewski, Marian Szczerek, Stanisław Koziół and Jan Wulczyński, is designed to evaluate the tribological properties of lubricants. The test rig includes a friction test contact formed by four balls. The upper ball rotates, while the other three are stationary and they are pressed against the upper ball from below. In this tribotester the main drive motor (1) is powered by the controller (33). This motor drives - via a clutch with a damping insert (11) - the spindle (10), in the lower part of which there is a holder (2) which fixes the upper ball immobile in the spindle (10). The holder (4) with the lower balls is pressed against the upper ball by the lever (14) with a weight (16) by means of the pusher (8), sleeve (12) and test rig (3) in which the loading force transducer (18) is placed. On the left side of the lever (14), a counterweight (17) is attached to the flange of which the motor (9) is attached, the pin of which is connected to the power screw (6) supported on the bearing (15) inside the lever (14) and co-acting with the nut (7) permanently connected to the weight (16). The weight (16) moves along the outer surface of the lever (14). The lower ball holder (14) is also connected to the resistance to motion transducer (5) and has a centrally located thermocouple (19) in the lower cylindrical part.

This test rig has the following control and measurement systems: U1 and U2. U1 system consists of the circuits 1, 2, 3 and 4. And U2 system consists of circuits 5 and 6. The U2 system is the control system.

Circuit 1 is connected to the contact force transducer (18). Circuit 1 includes: amplifier (20), analog-to-digital converter (21) and impulse counter (22).

Circuit 2 is connected to the resistance to motion transducer (5). This circuit consists of an amplifier (23), analog-to-digital converter (24) and impulse counter (25).

Circuit 3 is connected to the rotation sensor (13). This circuit consists of a receiver (26) and impulse counter (27).

Circuit 4 is attached to the thermocouple. This circuit consists of an amplifier (28), analog-to-digital converter (29) and impulse counter (30).

Circuit 5 is connected to and controls the main drive motor (1). This circuit consists of a digital-to-analog converter (31) and a power supply controller (32).

Circuit 6 is connected to and controls the motor (9). This circuit consists of actuating (33) and protective (34) elements.

Generally, one can say that:

- C1 circuit is used to measure the value of the force loading the friction contact,
- C2 circuit is used to measure the resistance to motion,
- C3 circuit is used to measure the rotational speed of the spindle,
- C4 circuit is used to measure the temperature of the lubricant,
- C5 circuit is used to control the operation of the spindle drive motor,
- C6 circuit controls the operation of the friction contact loading motor.

A four-ball test rig according to the patent 177203 is characterized by:

- the possibility of stepless and continuous adjustment of the spindle rotational speed,
- the possibility of stepless loading of the friction contact,
- the possibility of measuring the frictional resistance,
- the possibility of measuring the temperature of the lubricant,
- the possibility of archiving measurements.

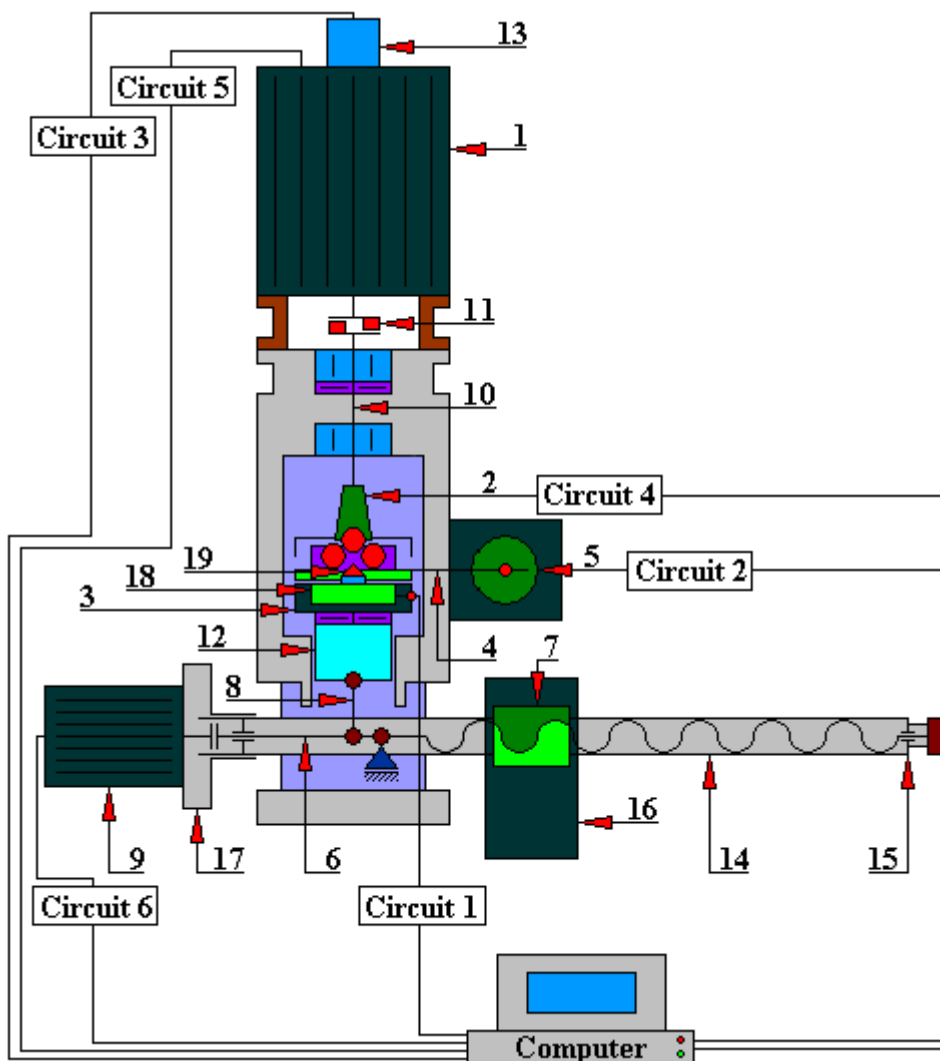


Fig. 4.2.13.1. A four-ball test rig according to the patent PL 177 203

1 - main drive motor, 2 - holder that fixes the upper ball immobile, 3 - test rig, 4 lower ball holder, 5 - resistance to motion transducer, 6 – power screw, 7 - nut, 8 - pusher, 9 - motor, 10 - spindle, 11 - clutch with a damping insert, 12 - sleeve, 13 - rotation sensor, 14 - lever, 15 - bearing, 16 - weight, 17 - counterweight, 18 - loading force transducer, 19 - thermocouple.

Circuit 1: amplifier (20), analog-to-digital converter (21), impulse counter (22).

Circuit 2: amplifier (23), analog-to-digital converter (24), impulse counter (25).

Circuit 3: receiver (26), impulse counter (27).

Circuit 4: amplifier (28), analog-to-digital converter (29), impulse counter (30).

Circuit 5: digital-to-analog converter (31), power supply controller (32).

Circuit 6: actuating (33) and protective elements (34)

4.2.14. Test rig for fatigue tests according to the patent No. PL 160595

A test rig (Fig. 4.2.14.1) according to the patent No. PL 160595, created by Witold Piekoszewski, Marek Wiśniewski, Marian Szczerek, Stanisław Koziół, is designed to test the resistance to surface fatigue wear of highly loaded friction elements, e.g. bearings. This tribological fatigue test rig consists of an electric drive motor (7) which - through a belt transmission with a toothed belt (6) - rotates a spindle with a test thrust ball bearing mounted at its end. The upper raceway of this bearing is mounted in housing (2) which is stationary and has a hole (8) for the oil supply. The housing (2) is pressed by the loading lever (3) with weights (4). On the spindle of the tested bearing (1) there is a pulse transmitter (5) of the revolution counter. In the drive system there is a belt transmission (6) between the main motor (7) and spindle.

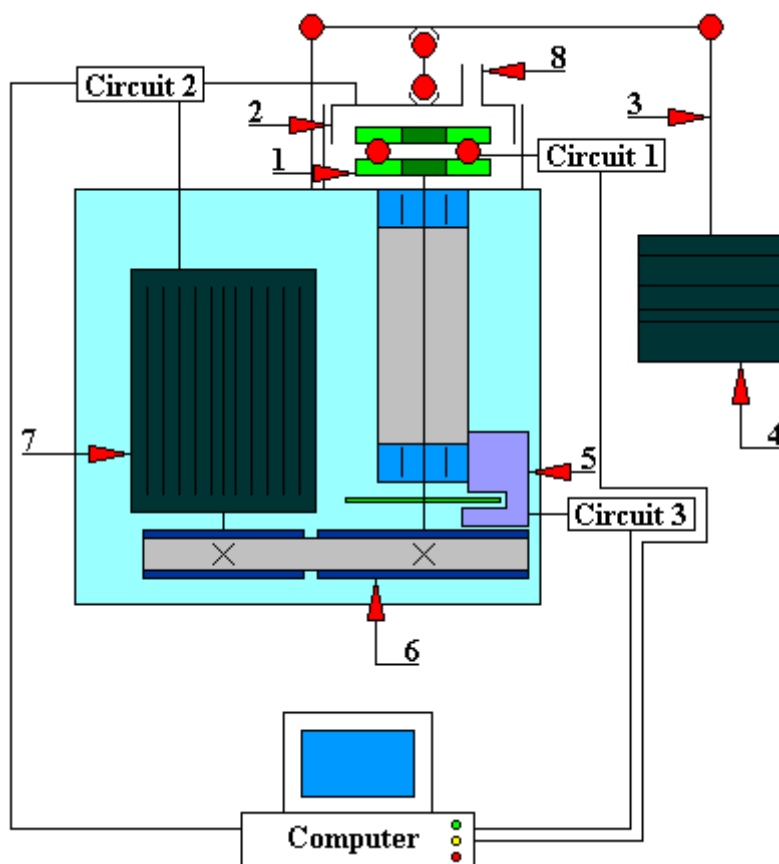


Fig. 4.2.14.1. The test rig for tribological tests of resistance to surface fatigue wear of highly loaded friction elements, e.g. bearings, according to the patent No. PL 160 595

1 - tested bearing, 2 - housing, 3 - loading lever, 4 - weights, 5 - revolutions counter pulse transmitter, 6 - belt transmission with a toothed belt, 7 - electric drive motor, 8 - oil supply hole.

Circuit 1 consists of: a thermostat (9), push-pull amplifier (10), voltage/frequency converter (11), frequency counter (12), digital readout panel (13), interface (14), a computer interface connector (15).

Circuit 2 consists of: a vibration sensor (16), amplifier (17), threshold discriminator block (18), relay (19).

Circuit 3 consists of: a pulse amplifier (20), digital readout panel (21), interface (22), computer interface (23).

This test rig has a control and measurement system consisting of three circuits: first, second and third.

The first circuit measures the sample temperature. It consists of a thermostat (9), push-pull amplifier (10), voltage/frequency converter (11), frequency counter (12), digital readout panel (13), interface (14) and a computer interface connector (15).

The second circuit is designed to measure the vibrations of the test friction contact and to control the trip of the drive motor (7). This circuit consists of a vibration sensor (16), amplifier (17), threshold discriminator block (18) and a relay (19).

The last, third circuit, is used to count the time or revolutions of the spindle until the drive motor is tripped automatically (7). This circuit consists of a pulse amplifier (20), digital readout panel (21), interface (22) and a computer interface (23).

This test rig is easy to use and simple in its construction. This is an undoubted advantage of this test rig. This makes it reliable in operation.

4.2.15. Four-ball test rig for tribological tests

The four-ball test rig presented below is a version produced before 1980 [45]. Therefore, its equipment does not have, among others, any data visualization or archiving system. It is designed to measure the durability of the oil layer between the rubbing rolling elements and to measure the value of the moment of friction between these elements. The test elements (Figures 5.2.15.1 and 5.2.15.2) are four balls with a diameter of $\text{Ø}12.7$ [mm], made of bearing steel with a hardness of 62.66 HRC. The three balls are permanently placed in the pan. And the fourth ball is fitted in the holder and pressed against the other balls with normal force. The ball fitted in the holder can only rotate with the speed of 1500 [rpm], which is also the rated speed of the induction motor. It is caused by - due to the simplicity of construction - the lack of gear or frequency converter (inverter) in the drive system. The rotational speed of 1500 [rpm] corresponds to the friction speed of 0.55 [m/sec]. The normal load pressing the balls may be up to 12 000 [N]. The measures of the quality of the tested oil are the diameters of the wear marks on the surfaces of three stationary balls during one minute - the duration of the test. The value of the normal load, at which the friction torque and the size of wear marks increase rapidly, is a measure of the lubricity of the tested oil. This four-ball test rig enables tests of oils at elevated (up to + 300°C) and low temperatures (up to - 40°C).

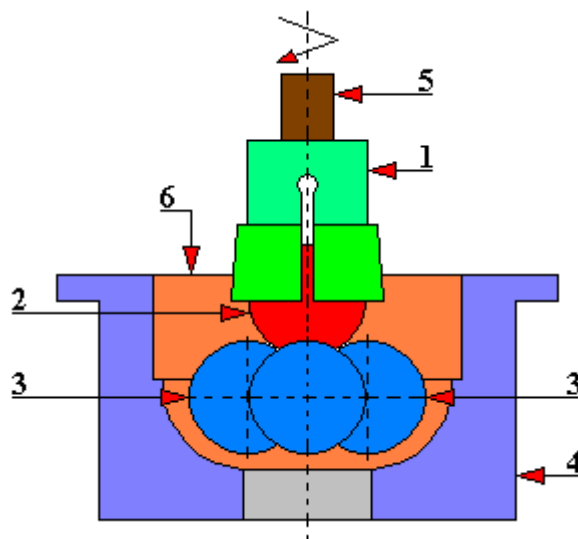


Fig. 4.2.15.1. A four-ball test rig for tribological tests. Friction mating - four balls in an oil pan [45]
 1 - upper ball holder, 2 - upper ball, 3 - three lower balls, 4 - pan, 5 - engine drive, 6 - tested oil

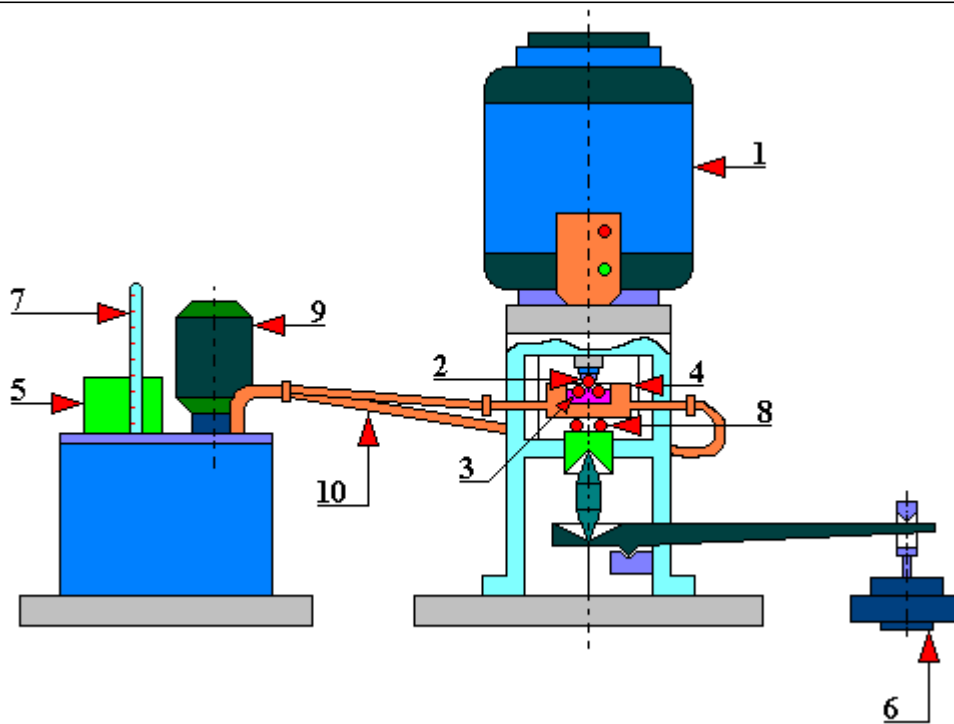


Fig. 4.2.15.2. A four-ball test rig for boundary friction testing equipped with a thermostat. Test rig diagram [45]

1 - electric motor, 2 - upper ball, 3 - three lower balls, 4 - pan, 5 - thermostat, 6 - preset load, 7 - thermometer, 8 - thrust bearing, 9 - circulating pump motor, 10 - suction/delivery lines of circulating pump

4.2.16. An older type of a four-ball test rig designed for tribological tests

This four-ball test rig presented below (Figures 4.2.16.1 and 4.2.16.2) is one of the first design solutions of this type. Therefore, its equipment does not have, among others, any data visualization or archiving system, a thermostat, frequency converter, etc. It is designed to measure the durability of the oil layer between the rubbing rolling elements and to measure the value of the moment of friction between these elements. The test elements here are, as in the model describe in point 90, four balls with a diameter of $\text{Ø}12.7$ [mm] made of bearing steel of a hardness of 62.66 HRC. The three balls are permanently placed in the pan. And the fourth ball is fitted in the holder and pressed against the other balls with normal force. The ball fitted in the holder can only rotate with the speed of 1500 [rpm], which is also the rated speed of the induction motor. It is caused by - due to the simplicity of construction – the lack of gear or frequency converter (inverter) in the drive system. The rotational speed of 1500 [rpm] corresponds to the friction speed of 0.55 [m/sec]. The normal load pressing the balls may be up to 1000 [N]. The measures of the quality of the tested oil are the diameters of the wear marks on the surfaces of three stationary balls during one minute - the duration of the test. The value of the normal load, at which the friction torque and the size of wear marks increase rapidly, is a measure of the lubricity of the tested oil. Oil tests carried out on this four-ball test rig may only be performed at ambient temperatures.



Fig. 4.2.16.1. An older type of a four-ball test rig designed to test the boundary friction. General view

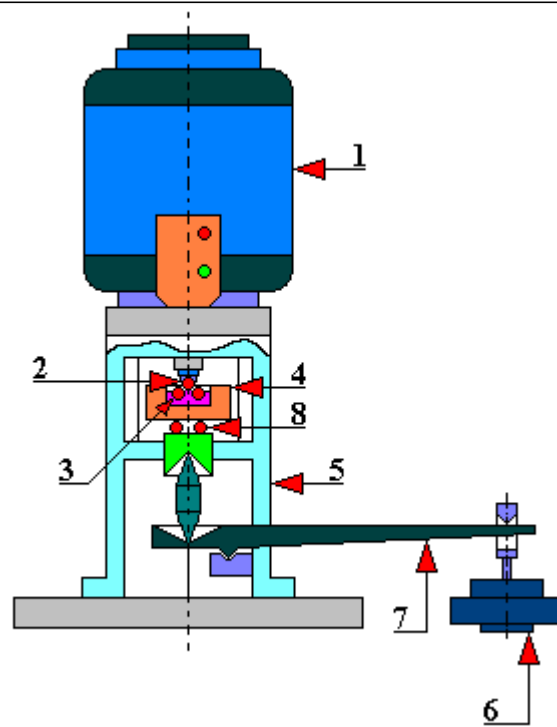


Fig. 4.2.16.2. A four-ball test rig designed to test the boundary friction. Test rig diagram
1 - electric motor, 2 - upper ball, 3 - three lower balls, 4 - pan, 5 - body, 6 - preset load, 7 -
loading lever arm, 8 - thrust bearing

4.2.17. Roller test rig (with cylindrical rollers) designed for testing pitting

This test rig consists of a pair of cylindrical rollers, or their multiple, constituting a convenient model replacing a pair of coating teeth. This design solution is used when examining the phenomena occurring on the side surfaces of gear teeth (Figures 4.2.17.1 and 4.2.17.2). In order to obtain the same load conditions for the surface layer of rollers and teeth in the contact zone of rollers, the same lubricant should be applied and the same kinematics parameters should be taken into account.

Tribological tests on roller machines are carried out in such a way that only one of the parameters influencing the wear is changed during the experiment. And the remaining parameters are treated as constant (unchangeable). Then the results of such tests allow detecting the influence of individual factors on wear, e.g. type of lubricant composition, lubrication efficiency, structure and texture of the surface layer, slip value, surface roughness, load value and others.

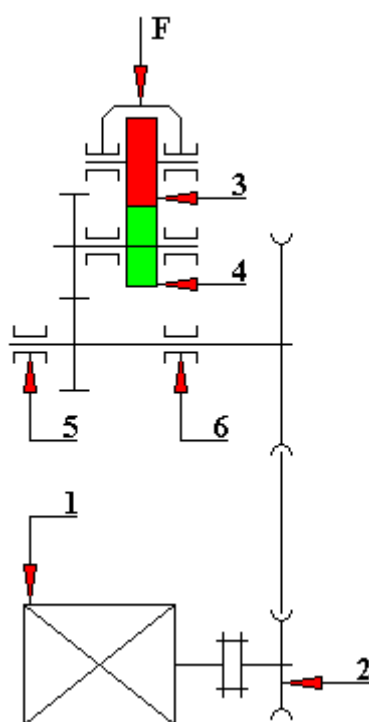


Fig. 4.2.17.1. Diagram of a single-contact test rig (built of one pair of cylindrical rollers) for testing pitting

1 - electric motor, 2 - belt transmission, 3 - passive cylindrical roller, 4 - active cylindrical (drive) roller, 5 - bearing, 6 - bearing

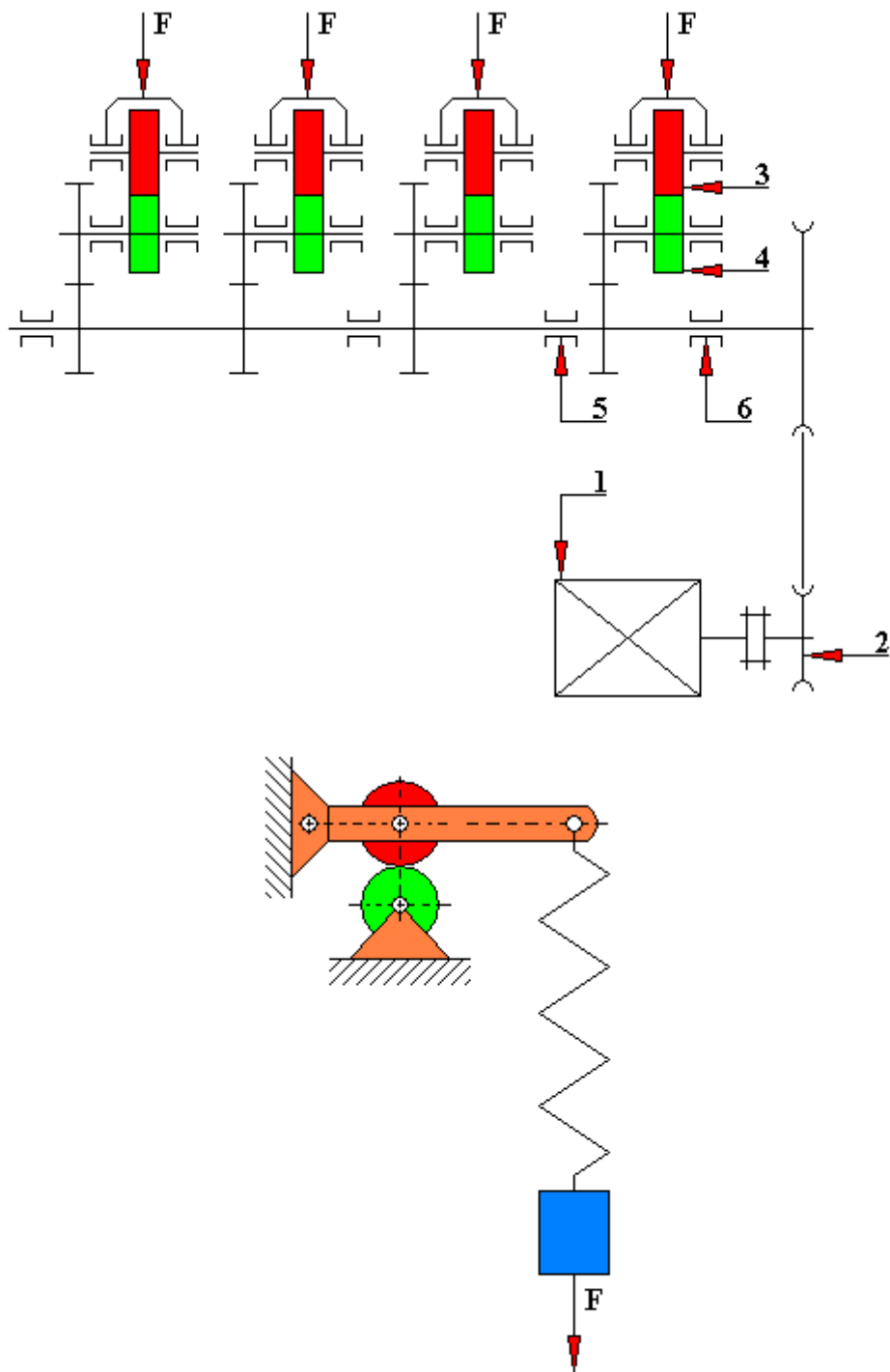


Fig. 4.2.17.2. Diagram of an extended single-contact test rig (built of four pairs of cylindrical rollers) for testing pitting [45]

1 - electric motor, 2 - belt transmission, 3 - passive cylindrical roller, 4 - active cylindrical (drive) roller, 5 - bearing, 6 - bearing

4.2.18. Roller test rig (with conical rollers) designed for testing pitting

This test rig belongs to the group of roller test rigs designed for testing pitting and scuffing. Its design consists of conical rollers in which the rolling and sliding conditions change along the generatrix of the cone (Figures 4.2.18.1, 4.2.18.2 and 4.2.18.3). The disadvantage of this type of test rigs is the appearance of frictional forces along the cone, which affects the stress distribution in the contact zone, and consequently the results of the tests.

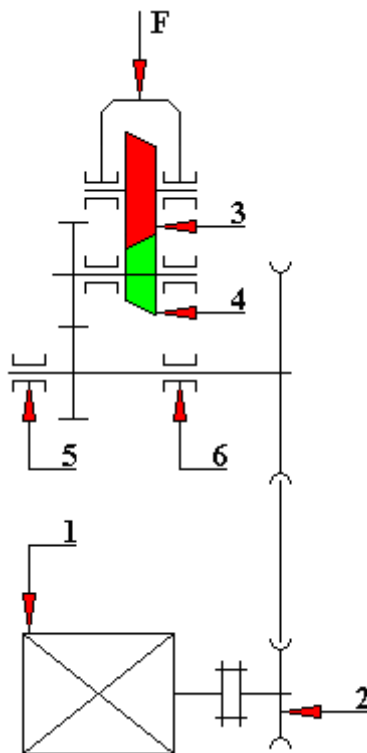


Fig. 4.2.18.1. A diagram of a single-contact test rig (built of one pair of conical rollers) for testing pitting

1 - electric motor, 2 - belt transmission, 3 - passive conical roller, 4 - active conical (drive) roller, 5 - bearing, 6 - bearing

Figure 4.2.18.3 shows a diagram of a roller test rig with rollers in the form of cones. On the generatrix of the cone, there are different slip values at different points. A conical roller 6 is mounted on the shaft 3, driven by an electric motor, which cooperates with the roller 7, mounted on the shaft 2. The roller 6 is driven by a pair of toothed wheels number 1 and 11. The load on the rollers is transmitted through the sleeve 8 and cone bearings 9. The cone bearing 4 transfers the load from the roller 6 to the test rig body 12. The shafts 2 and 3 are mounted in slide bearings 5 and 10. The average diameter of each roll is 100 [mm] (127 and 73 mm) and their width is 41.8 [mm].

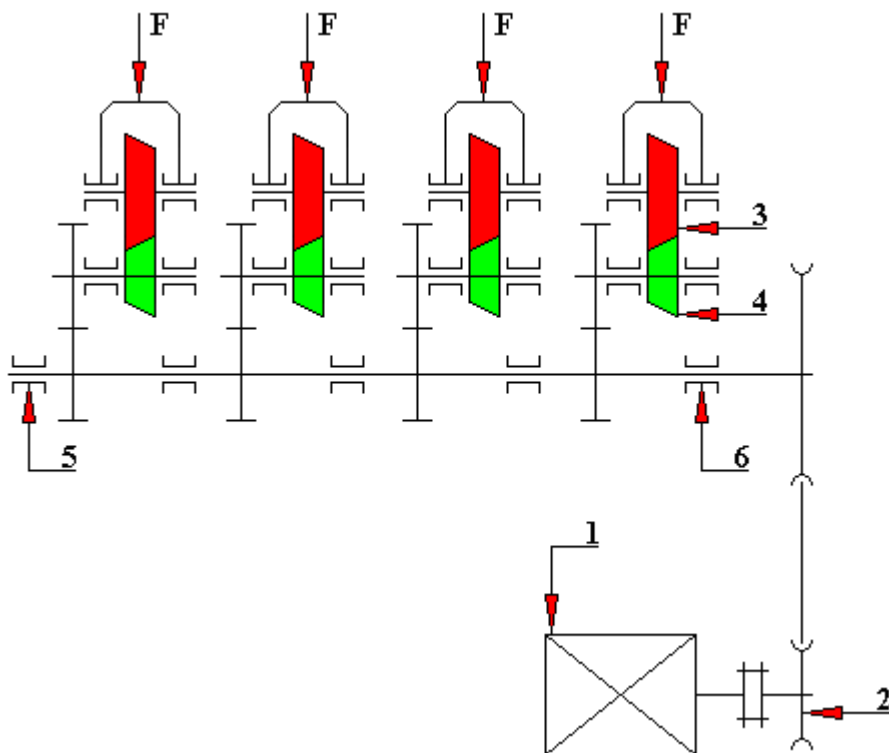


Fig. 4.2.18.2. A diagram of an extended single-contact test rig (built of four pairs of conical rollers) for testing pitting
 1 - electric motor, 2 - belt transmission, 3 - passive conical roller, 4 - active conical (drive) roller, 5 - bearing, 6 - bearing

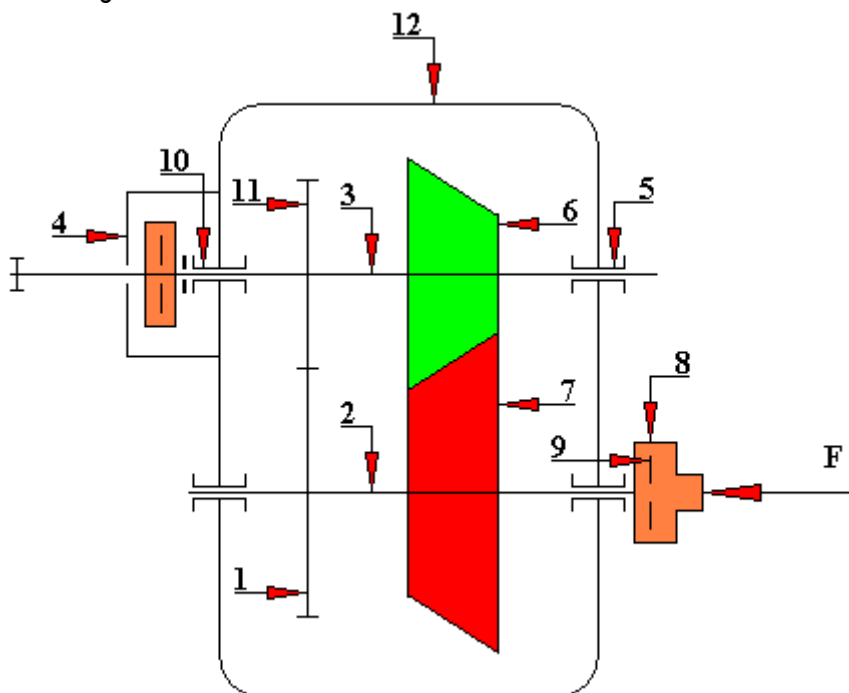


Fig. 4.2.18.3. A diagram of a conical roller test rig designed for testing pitting [45]
 1 – toothed wheel, 2 - idler shaft, 3 - live shaft (driven by an electric motor), 4 - cone bearing, 5 - slide bearing, 6 - conical roller, 7 - conical roller, 8 - sleeve, 9 - cone bearing, 10 - slide bearing, 11 - toothed wheel, 12 - test rig body

4.2.19. Three-contact test rig with a variable cyclic slip designed for testing pitting

This test rig also belongs to the group of roller test rigs designed for testing pitting and scuffing. In roller test rigs with variable cyclic slip (fixed during one roller/disc revolution) the working conditions of discs (rollers) are similar to the working conditions of toothed wheels. A design diagram of the test rig with a variable cyclic slip is shown in Figure 4.2.19.1. Rollers 1, 2 and 3 are pressure rollers (counter-samples). These rollers have a diameter of $\varnothing 50$ [mm], and their width is 10 [mm]. Roller axes 2 and 3 are fixed axes. And the roller axis 4 is mounted in the lever 1 to which the working load is applied. On the shaft of roller 4 there is an eccentric toothed wheel in gear with three toothed wheels also mounted eccentrically on the rollers 1, 2 and 3. The eccentricity of all toothed wheels is the same. The gear shafts are mounted in separate bearings. Their rotational motion is transmitted via rigid couplings.

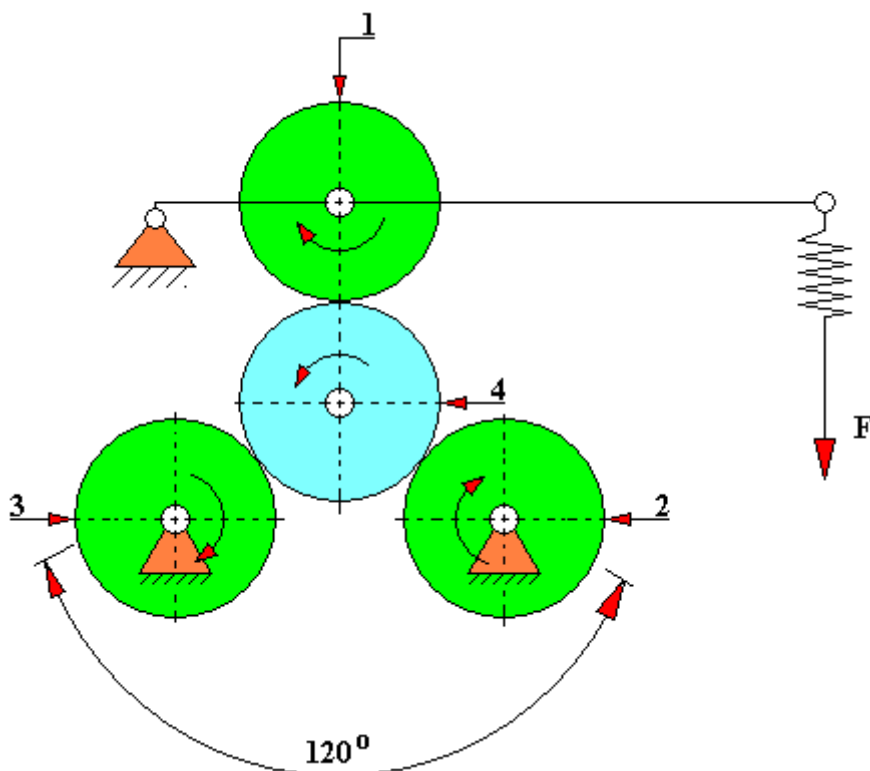


Fig. 4.2.19.1. A three-contact roller test rig with a variable cyclic slip designed for testing pitting [45]

1 - pressure roller, 2 - pressure roller, 3 - pressure roller, 4 - drive roller, F - load

4.2.20. Test rig with three rollers imitating the meshing of toothed wheels with straight and oblique teeth

This test rig is designed to assess the anti-scuffing, anti-pitting and anti-wear properties of gear oils (Figure 4.2.20.1).

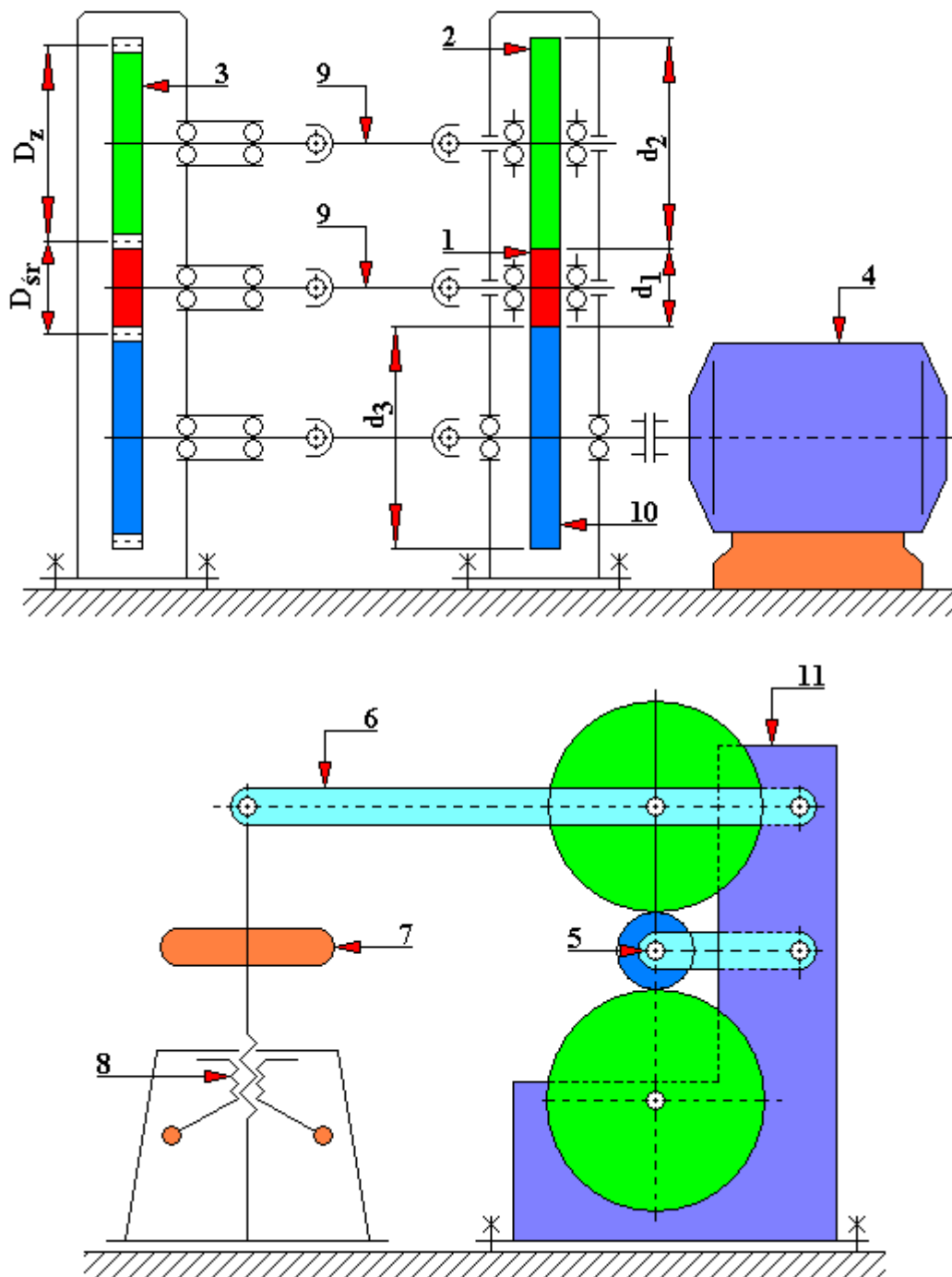


Fig. 4.2.20.1. A diagram of a roller test rig with three rollers for friction and wear testing [45]
 1 - tested roller (middle), 2 - upper pressure roller, 3 - closing gear, 4 - electric drive motor, 5 - rocker arm, 6 - loading lever, 7 - dynamometer, 8 - screw tensioning mechanism, 9 - clutch shaft, 10 - lower pressure roller, D_{sr} , D_z - pitch diameters, d_1 , d_2 , d_3 - diameters of friction wheels

The test sample is the middle roller 1. It is placed in the rocker arm 5. The tested roller 1 is pressed against the lower roller 10 and against the upper roller 2 which is placed on the lever 6. The levers are loaded by means of a bow dynamometer 7 and a screw tensioning mechanism 8. The rollers are driven by a DC motor 4 by a closing gear 3 and three coupling shafts 9. In the toothed gear 3 it is possible to replace the toothed wheels in order to achieve different slip on the middle tested roller 1. The tested lubricant is supplied to the contact area of the middle roller and the top roller.

The three-roller test rig has the following features:

- measurement of wear: isotope method or artificial bases,
- slip on the tested roller: 0÷90%,
- unit pressure in the contact area of rollers: 0÷2000 [MPa],
- force measuring system in the contact area of rollers: dynamometric,
- effective radius of curvature of the roller: 0.5÷2.5 [cm],
- moment of friction measuring system: strain gauge,
- rotational speed of the roller (infinitely variable speed control): 100÷3000 [rpm],
- roller rotational speed measurement system: frequency,
- system for measuring the temperature of the lubricant composition (oil) at the entry and exit from the contact area: with thermocouples.

4.2.21. Roller-disc test rig designed for tribological tests

A test rig of this type, shown in Fig. 4.2.21.1, reproduces the mating of a worm gear. It is designed to evaluate the anti-seize and anti-wear properties of the tested lubricant composition.

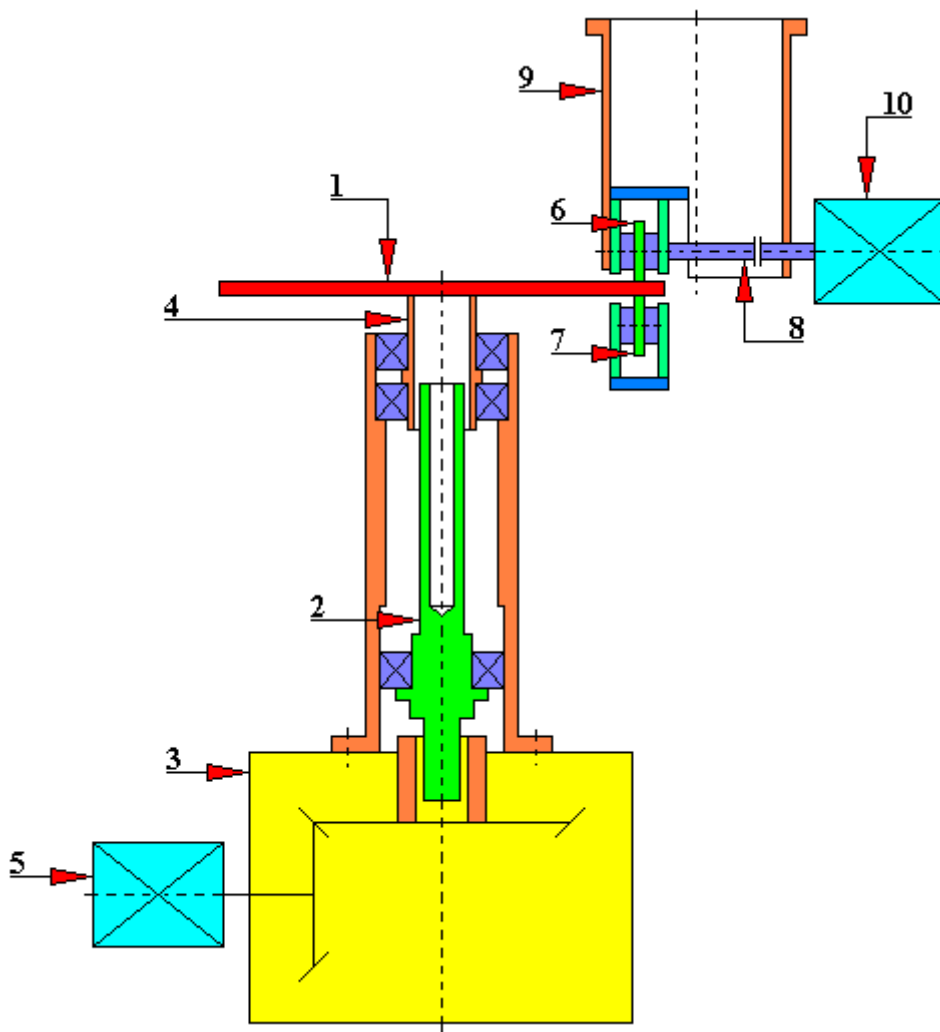


Fig. 4.2.21.1. A general diagram of the roller-disc test rig [45]

1 - disc, 2 - strain gauge shaft, 3 - gear (reducer or multiplier depending on the user's needs), 4 - disc mounting sleeve, 5 - electric drive motor of the disc, 6 - tested roller, 7 - supporting bearing, 8 - roller shaft, 9 - roller body, 10 - electric drive motor of the roller

The steel disc 1 is driven by a DC motor 5 by means of a bevel gear 3 and a strain gauge shaft 2. A roller 6, which has an independent drive from the DC motor 10, is pressed against the disc 1. And the roller 7 (support bearing) takes the load off disc 1. Roller 7 does not have its own drive (it is passive) and its speed direction is always perpendicular to the contact line. It is possible to 'skew' (no perpendicularity) of the test roller 6 with the body 9 in relation to the disc 1. Roller 6 and disc 1 can rotate as counter-rotating or co-rotating.

This test rig has the following features:

- measurement of wear: isotope method or artificial bases,
- moment of friction measuring system: strain gauge,
- disc velocity: 0,1÷40 [m/sec],

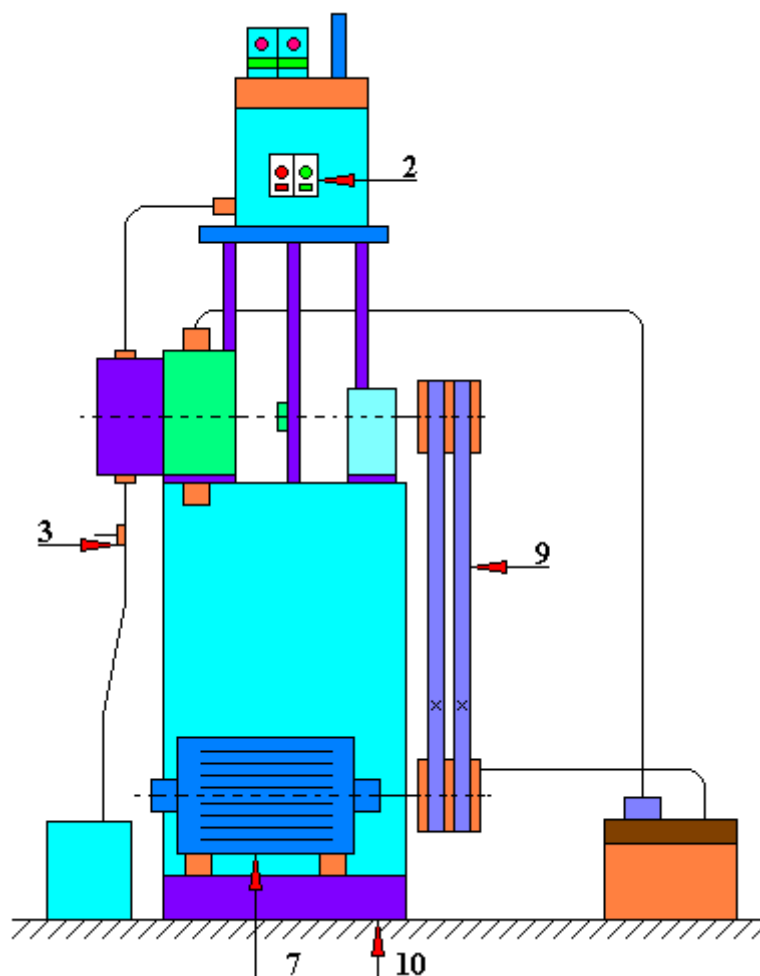
- roller angle of inclination: $0\div 90^\circ$,
- roller and disc revolutions measurement system: frequency,
- roller speed; $0,05\div 10$ [m/sec],
- roller diameter: $50\div 120$ [mm],
- unit pressure in the area of contact between the disc and the roller: $0\div 700$ [MPa],
- system for measuring the temperature of the lubricant composition at the entry and exit from the contact area: by thermocouples,
- force measuring system in the contact area between the roller and the disc: dynamometric.

4.2.22. SBOP type test rig designed for tribological tests

The SBOP test rig, shown in Figure 4.2.22.1, is designed to test the anti-wear and anti-seize properties of gear oils. They are built in a circulating power system. Both the closing gear 4 and the test gear 1 are housed in a common housing. Each of these gears (1 and 4) has a separate chamber and is individually lubricated. These gears are lubricated in a circulating system. The tested gear 1 is lubricated with the tested oil or oil composition which is fed from the ultrathermostat 2. The temperature of the oil flowing from the tested gear 1 is monitored by means of a thermometer 3. The torque measured at point 5 is introduced into the circulating power system by the tensioner test rig 8 and lever 6. The test rig is driven by an electric DC motor 7 with adjustable rotational speed.

The test rig of SBOP type has the following features:

- rotational speed measurement - frequency,
- active width of the teeth - 5 [mm],
- pinion rotational speed - $0 \div 1400$ [rpm],
- measurement of consumption - isotope method,
- torque measurement system - strain gauge,
- nominal module - couple I 5 [mm], couple II 3.5 [mm],
- number of teeth of tested wheels: couple I 14:20, couple II 21:30,
- rotational speed of the pinion: $100 \div 8000$ [rpm].



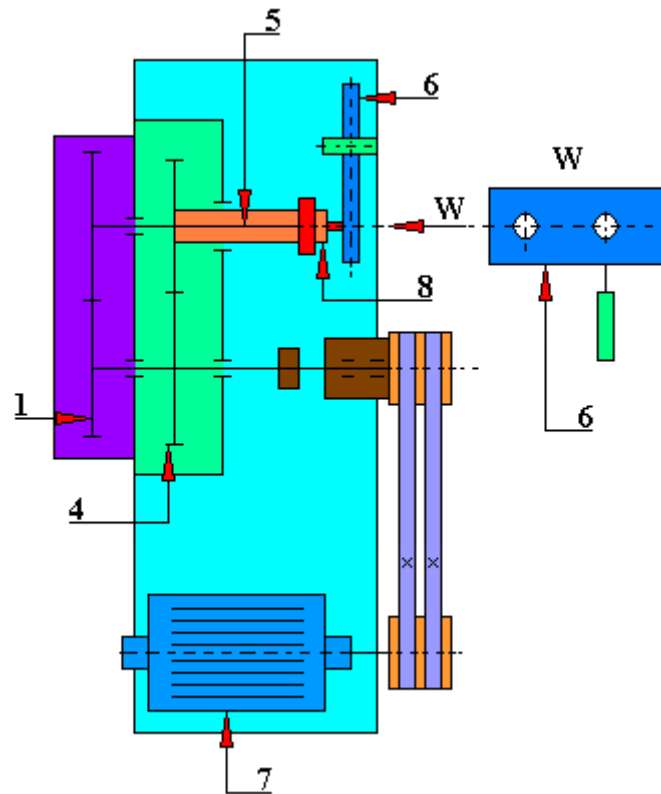


Fig. 4.2.22.1. General scheme of the SBOP test rig designed for testing the friction and wear [45]
 1 - tested gear, 2 - ultrathermometer, 3 - thermometer, 4 - closing gear, 5 - torque measuring point, 6 - closing lever, 7 - electric DC drive motor with adjustable rotational speed, 8 - tensioner, 9 - belt transmission, 10 - test rig base

4.2.23. The test rig designed to test slide bearings

This test rig, shown in Figure 4.2.23.1, is designed to test the properties of slide bearings of various designs and materials, the effect of the tested oil composition and its design features on the load capacity and friction torque. This test rig also enables to test the influence of the moment beveling the bearing on its load capacity. The test rig foundation is a plate 12 to which two bearings 2 are attached supporting the tested shaft 3. Between the support bearings 2 placed is the tested bearing 1.

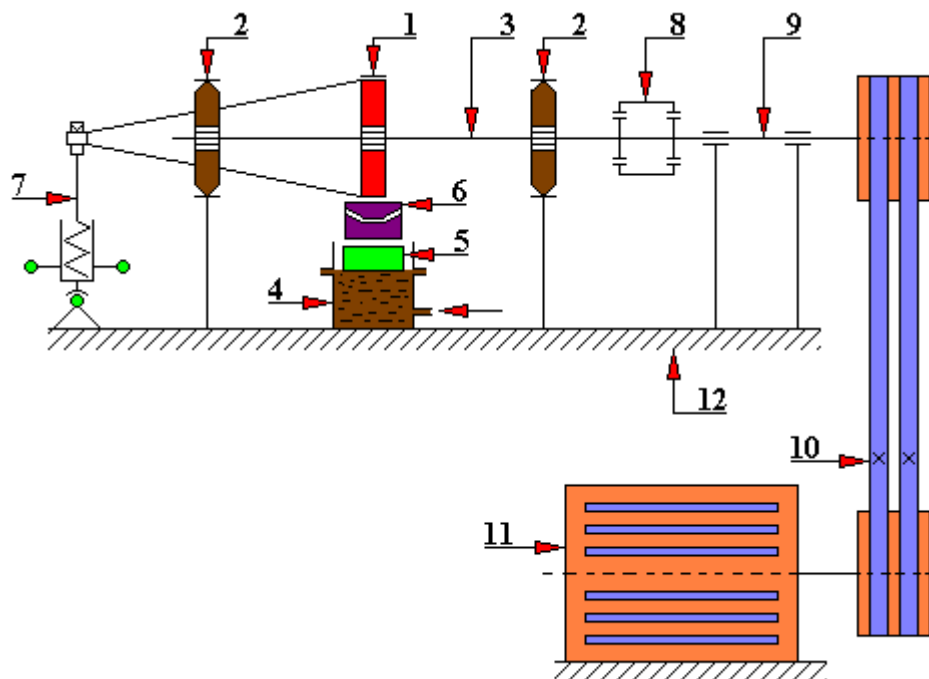


Fig. 4.2.23.1. General diagram of a test rig designed to test slide bearings [45]

1 - tested bearing, 2 - supporting bearings, 3 - tested shaft, 4 - hydraulic cylinder, 5 - hydrostatic support (flat hydrostatic bearing), 6 - radial load hydraulic system (spherical hydrostatic bearing), 7 - beveling moment loading system, 8 - flexible coupling, 9 - console (intermediate shaft), 10 - belt transmission, 11 - continuously adjustable DC drive motor, 12 - foundation

Between the tested bearing 1 and the hydraulic cylinder 4 there are two hydrostatic bearings: spherical 6 and plane 5. A continuously adjustable DC motor 11 by means of an intermediate shaft 9 and a flexible coupling 8 transmits the drive to the main shaft 3. The radial load is carried out by the hydraulic system 4, 5, 6, and the beveling load - by the system 7. The change of the support stiffness of the tested bearing is made by a discrete change in the spacing of the support bearings.

The test rig for tribological testing of slide bearings is characterized by the following features:

- the length of the tested bearing - up to 75 [mm],
- the diameter of the tested bearing: 30÷80 [mm],
- measurement of wear: by the method of artificial bases or isotope method,
- shaft rotational speed: 0÷6000 [rpm],
- the outer diameter of the tested bearing: up to \varnothing 100 [mm],
- friction environment: any oil composition,

- friction torque measuring system - strain gauge,
- oil pressure measuring system at the entrance to the bearing - with a manometer,
- temperature measuring system of the tested bushing - using a thermocouple,
- shaft rotational speed measuring system - frequency,
- radial force and beveling moment measuring system - using a manometer,
- load - static radial force $0 \div 15 \cdot 10^4$ [N], static beveling moment $0 \div 5.0$ [Nm],
- the outer diameter of the tested bearing – up to 100 [mm].

4.2.24. Test rig for testing the rolling resistance of discs according to the patent PL 223 986

The test rig was built according to the patent PL 223 986 shown in Figure 4.2.24.1, the authors of which are: Dariusz Woźniak, Lech Gładysiewicz, Monika Hardygóra, Damian Kaszuba, Waldemar Kisielewski and Ligota Wolczyńska is designed to measure the rolling of a sample that is a fragment of a belt, for various pressure forces which reflect the actual working conditions in belt conveyors used, for example, in the coal, ore, aggregate mines. During the operation of the conveyor, the excavated material is conveyed on the belt. The amount of energy required to move the belt is also determined by, among others, rolling resistance of the belt over pulleys, and this resistance can be tested on this test rig.

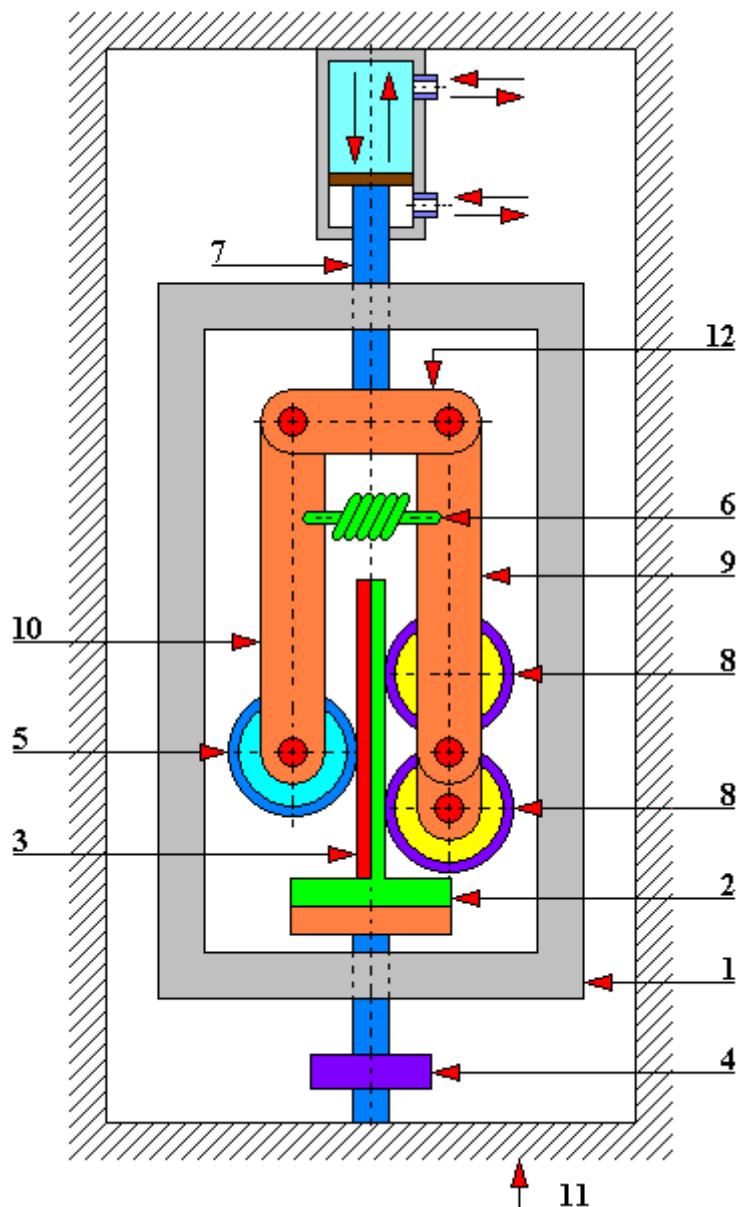


Fig. 4.2.24.1. A general diagram of the test rig for testing the rolling resistance of discs according to the patent PL 223 986

1 - thermal chamber, 2 - belt sample holder, 3 - tested belt sample, 4 - force sensor, 5 - main roller, 6 - tension spring, 7 - piston rod of the actuator, 8 - additional roller, 9 - arm, 10 - arm, 11 - body, 12 - frame

The measuring station is located inside the thermal chamber 1. This chamber allows you to set negative and positive temperatures. The sample of the tested belt 3, which is a section of the conveyor belt, is mounted in the holder 2. The prepared and mounted sample should stay for a specified time in a closed thermal chamber until the set temperature is stabilized. A force sensor 4 is mounted below the sample holder 2. The main roller 5 rolls over the tested sample of the belt section 3, and its pressure on the sample is realized by means of the tension spring 6. In order to compensate for the transverse forces transmitted by the force sensor 4 and onto the piston rod of the actuator 7, two additional rollers 8 are installed which always roll on the metal part of the handle 2. The main roller 5 and additional rollers 8 are articulated by the arms 9. The reciprocating motion is transmitted from the piston rod of the actuator 7 to the frame 10, then to the arms 9 and finally to the rollers: main 5 and additional 8. By setting the piston rod in motion, we determine the rolling resistance of the roller 5 along the section of the tested belt 3.

4.2.25. Test rig for modeling the friction process in needle bearings according to the patent PL 219 650 (SMT-1 test rig)

The test rig is built according to the patent PL 219 650, shown in Figure 4.2.25.1, the authors of which are: Jan Nachimowicz and Robert Korbut; it makes it possible to determine the slip in needle bearing, the impact on the wear of external factors (e.g. load, type of lubricant), and it also allows to determine the critical clearance.

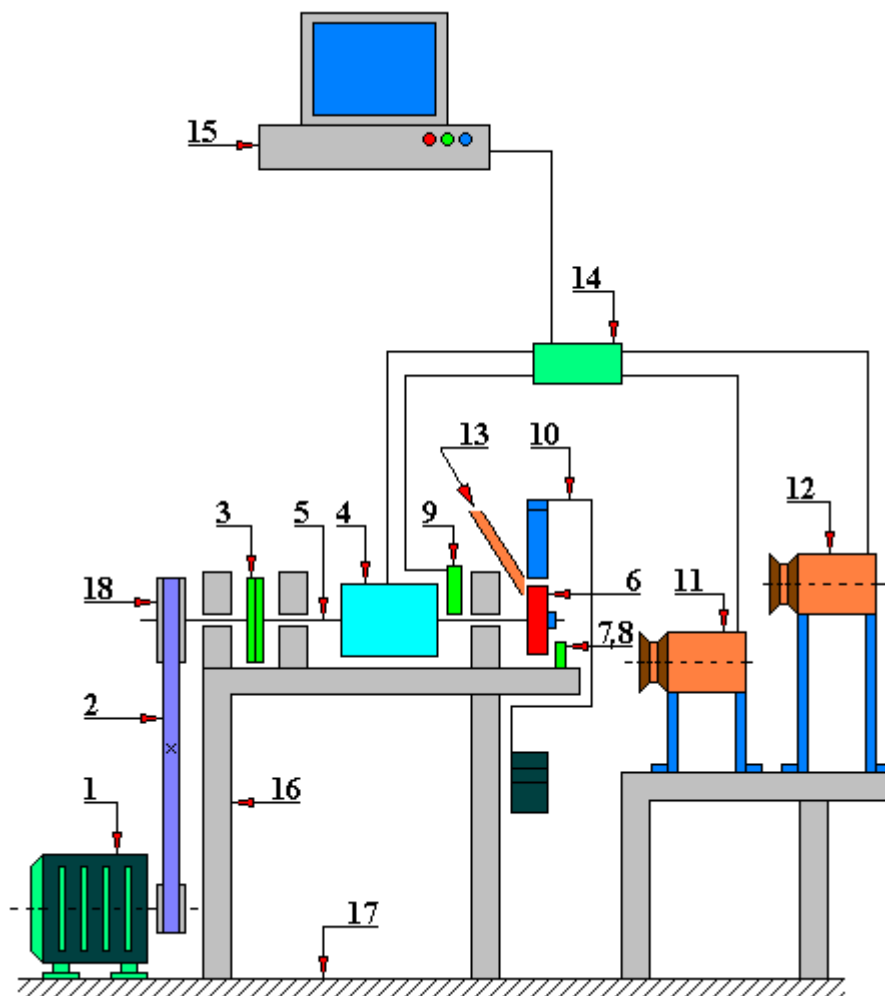


Fig. 4.2.25.1. A general diagram of the test rig for modeling the friction process in needle bearings according to the patent PL 219 650

1 - drive motor, 2 - V-belt, 3 - clutch, 4 - torque meter, 5 - shaft, 6 - tested sample (needle bearing), 7 – sensor of needle rotation around the shaft axis, 8 – sensor of needle rotation around its axis, 9 - shaft rotation sensor, 10 - arm, 11 - thermal imaging camera, 12 - optical camera, 13 - lubricant, 14 - transducer, 15 - PC computer, 16 - support frame of the station, 17 - foundation

The test rig is built of a drive motor 1 with a smooth adjustment of the rotational speed in the range $0 \div 1500$ [rpm]. The drive motor 1 transmits the drive to the shaft 5 by means of a belt transmission. The tested sample 6 (needle bearing) is mounted on this shaft. The tested samples (bearings) may have different internal diameters. Their assembly on the shaft 5 is possible thanks to the use of replaceable covers for the shaft end. The arm 10 makes it possible to apply load F onto the tested bearing. The attached equipment registers the rotational speeds of the shaft and

needles of the bearing, the moment of friction, and released heat. All data collected from the torque meter, cameras and rotation sensors are transmitted by the transducer 14 to the computer 15 and archived there. And Figure 4.2.25.2 shows the geometry of the system and the kinematics of the motion of rolling elements of this test rig.

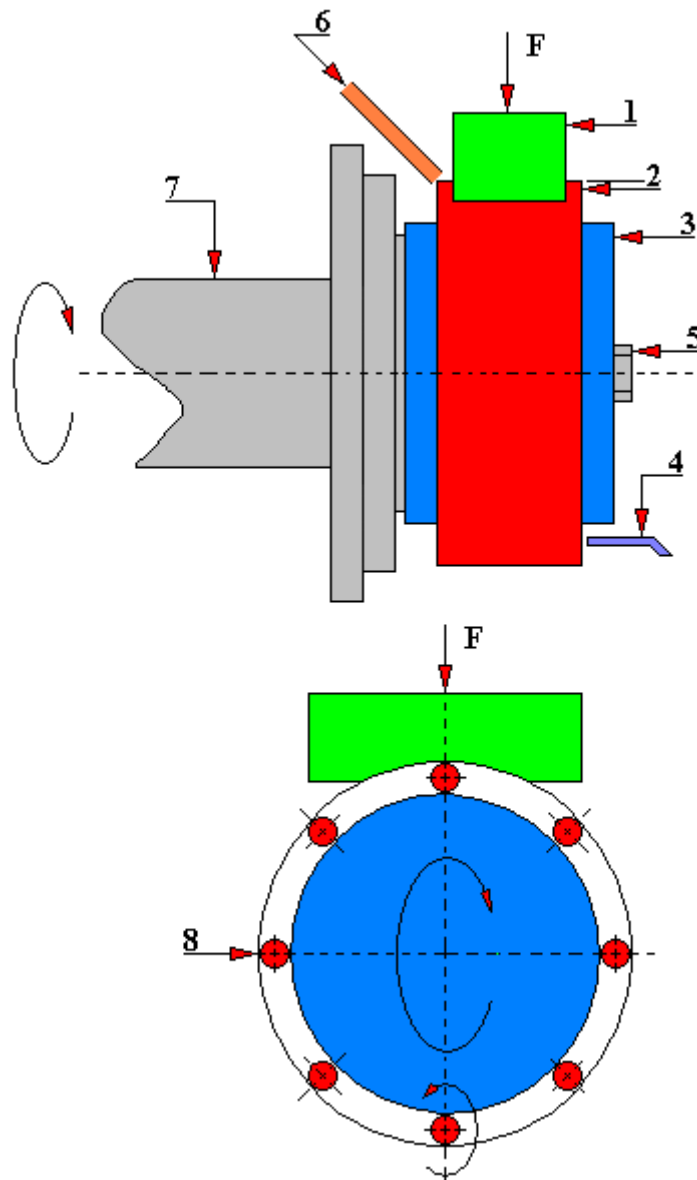


Fig. 4.2.25.2. The geometry of the system and the kinematics of the motion of rolling elements of the test rig for modeling the friction process in needle bearings according to the patent PL 219 650

1 - load F applied to the bearing, 2 - tested sample (needle bearing), 3 - replaceable cover, 4 – sensor of needle rotation around the shaft and its symmetry axis, 5 - nut, 6 - lubricant, 7 - drive shaft, 8 - bearing needle (bearing element)

It is worth mentioning here that this patent has become the basis for the construction of the test rig for testing needle bearings marked with the symbol SMT-1 the construction of which enables the study of the kinematics of motion and the moment of friction as a function of

rotational speed, load, geometric parameters of the bearing and in the presence of lubricants. A unique feature of the constructed test rig is the ability to track the rotation of the needle in relation to its axis of symmetry and around the axis of the shaft. These measurements are carried out using an optical camera with a capacity of up to 130,000. frames per second.

For the above-mentioned test rig a structurally interesting measurement system of the electric signal was adopted for testing the tribological properties of lubricants using the electric method (Fig. 4.2.25.3). The adopted test rig has four electrodes for measuring the conductivity of the boundary layer of the tested lubricant. Thanks to this, it is possible to determine the possible correlation between electrical parameters and the mechanical and frictional properties of the boundary lubricant layer.

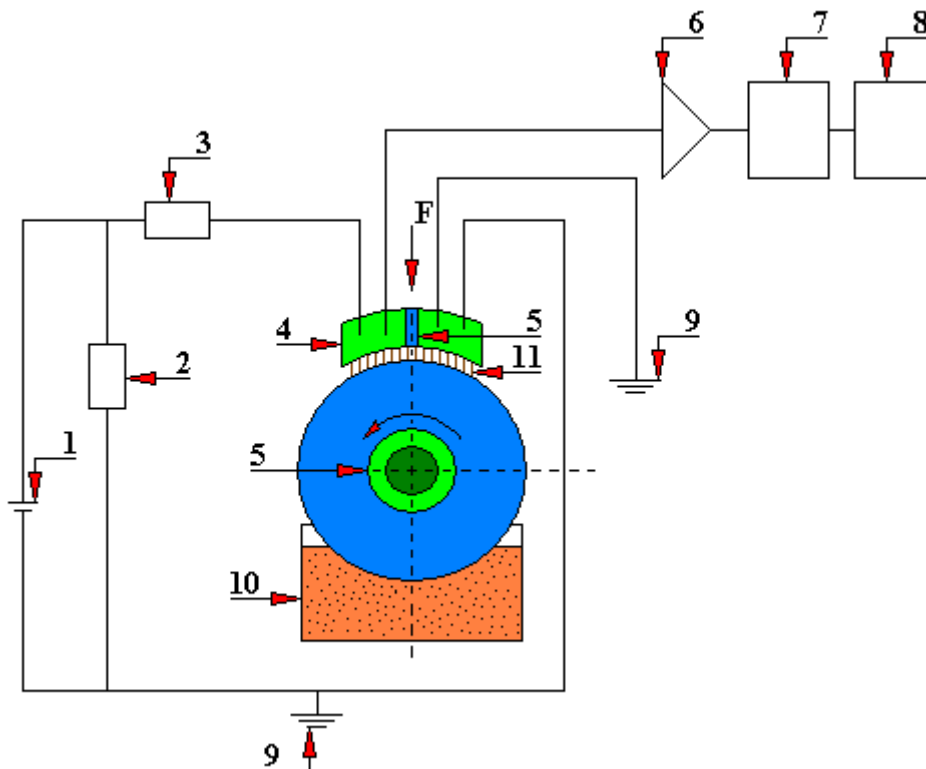


Fig. 4.2.25.3. The test rig scheme for an electro-physical sounding [26]
 1 – a voltage source E ; 2 – a calibrating resistance R_1 ; 3 – a resistance box R_2 ; 4 – a sample „the partial liner”; 5 – a dielectric; 6 - a differential amplifier; 7 – an analogue-to-digital converter; 8 – a personal computer PC; 9 – neutral phase; 10 – a tank with examined joint; 11 – a boundary lubricant layer

4.2.26. Test rig for testing journal bearings lubricated with a contaminated medium, according to the patent PL 103 942

The test rig, built according to the patent PL 103 942, for which construction diagrams are shown in Figures 4.2.26.1 and 4.2.26.2, and whose authors are: Jan Sikora, Antoni Neyman, Olgierd Olszewski, is designed for testing journal bearings.

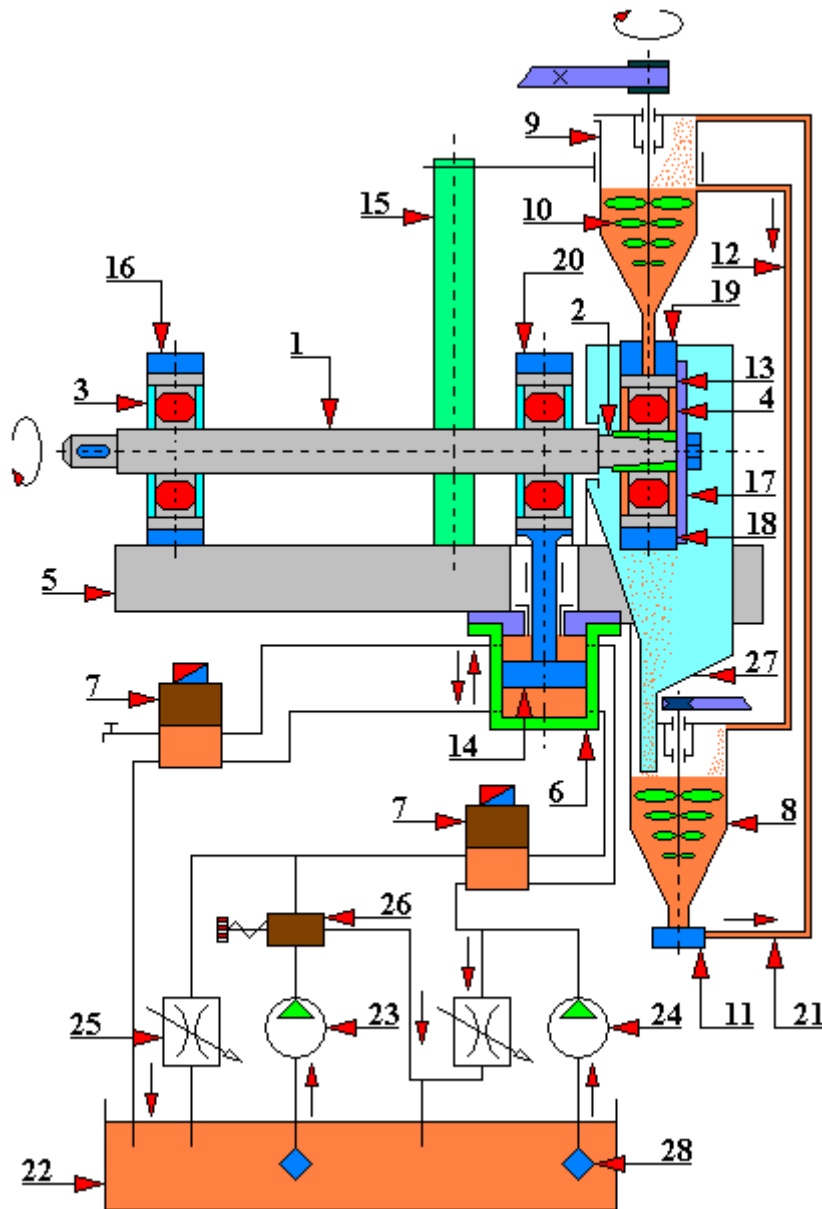


Fig. 4.2.26.1. Diagram of the test rig for testing bearings according to the patent PL 103 942
 1 - test shaft, 2 - test pin, 3 - support bearing, 4 - tested bearing, 5 - base, 6 - weight cylinder, 7 - oil distributor, 8 - lower oil tank, 9 - upper oil tank, 10 - agitator, 11 - pump, 12 - overflow pipeline, 13 - clamp, 14 - piston, 15 - upper tank holder cantilever, 16 - support bearing cantilever, 17 - washer, 18 - bridge, 19 - cover, 20 - load bearing cantilever, 21 - filling pipeline, 22 - oil tank, 23 - pump, 24 - pump, 25 - pressure release valve, 26 - overflow valve, 27 - housing, 28 - oil filter

A characteristic feature of this test rig is an easy replacement of both the pin and the tested bearing. In addition, the lubricant circulates in a closed system and contains hard impurities without sedimentation.

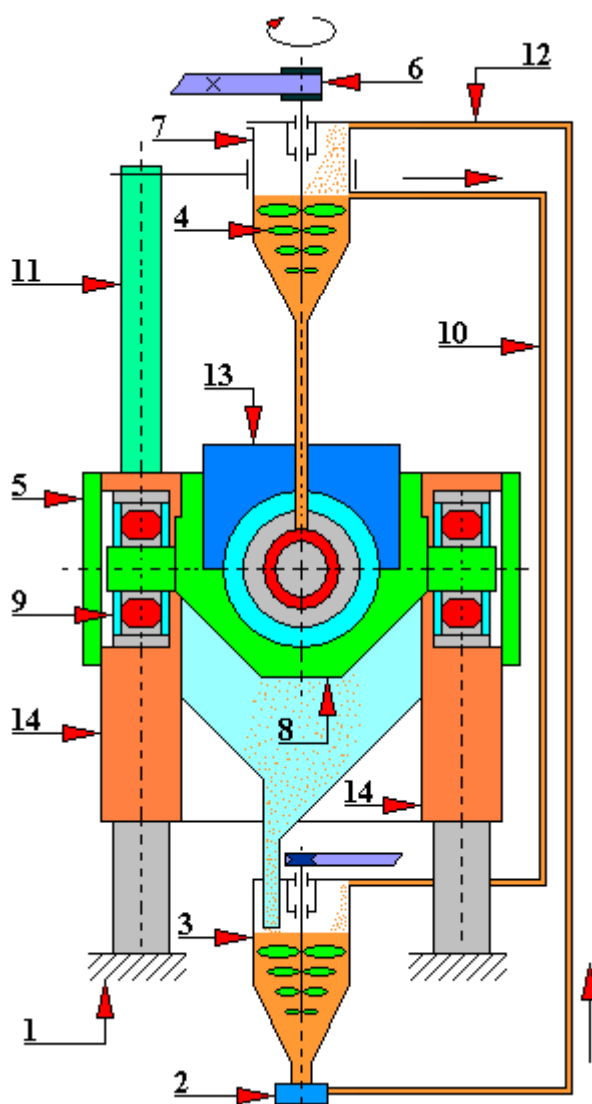


Fig. 4.2.26.2. A diagram of a bearing testing rig according to the patent PL 103 942 in the left side view

1 - foundation, 2 - pump, 3 - bottom oil tank, 4 - agitator, 5 - cover, 6 - agitator drive, 7 - top oil tank, 8 - bridge, 9 - barrel bearing, 10 - overflow pipeline, 11 - cantilever of upper tank handles, 12 - filling pipeline, 13 - cover, 14 - cantilevers

The tested bearing 4 (Figure 4.2.26.1), which is also one of the two bearings supporting the test shaft 1, is mounted on the test pin 2. The test pin is seated at the end of the test shaft by means of a frictional conical connection. The tested bearing 4 is mounted in a bracket placed between the bridge and the cover. The bridge is attached to the base 5 by means of two barrel bearings mounted in cantilevers. Between the bearing 4 and the second support bearing 3, a weight bearing is mounted on the shaft 1. The piston 14 of the double-sided hydraulic weight is attached to the housing of this bearing through a piston rod. The weight cylinder 6 is mounted to the base 5. The load on the tested bearing 4 is exerted by the oil supplied to the space above the

piston 14 from the oil tank 22 through the oil filter 28, the oil pump 24, the overflow valve 26 and the oil distributor 7. The value of the load oil pressure of the tested bearing 4 is regulated by the pressure release control valve 25. Under load, the space under the piston is connected to the overflow via a second oil distributor 7. The loading and unloading system of the double-sided hydraulic weight is controlled by the regulated pressure values and duration of the loading / unloading by the system of distributors 7.

The lubricant is supplied to the tested bearing 4 from a lubricating system consisting of an oil pump 11, an upper oil tank 9, a lower oil tank, a filling pipeline 21, an overflow pipeline 12 and agitators 10.

The upper oil tank 9 is equipped with a lubricant heater.

The overflow pipeline 12 protects against an excessive increase in the oil level in the upper tank 9.

The test shaft 1 is driven by a drive system with continuously variable rotational speed control.

The tested bearing 4 is separated from the remaining elements of the test rig by a housing 27.

4.2.27. Test rig for testing the meshing durability of an epicyclical cycloidal gear

K-H-V gearboxes (CYCLO gearboxes) are a type of special gears that enable a high gear ratio on one step. In terms of construction, they are rolling gears in which all the positively connected elements move in rolling motion. Thanks to this, it is possible to minimize the losses caused by friction, which is also associated with the reduction of power losses.

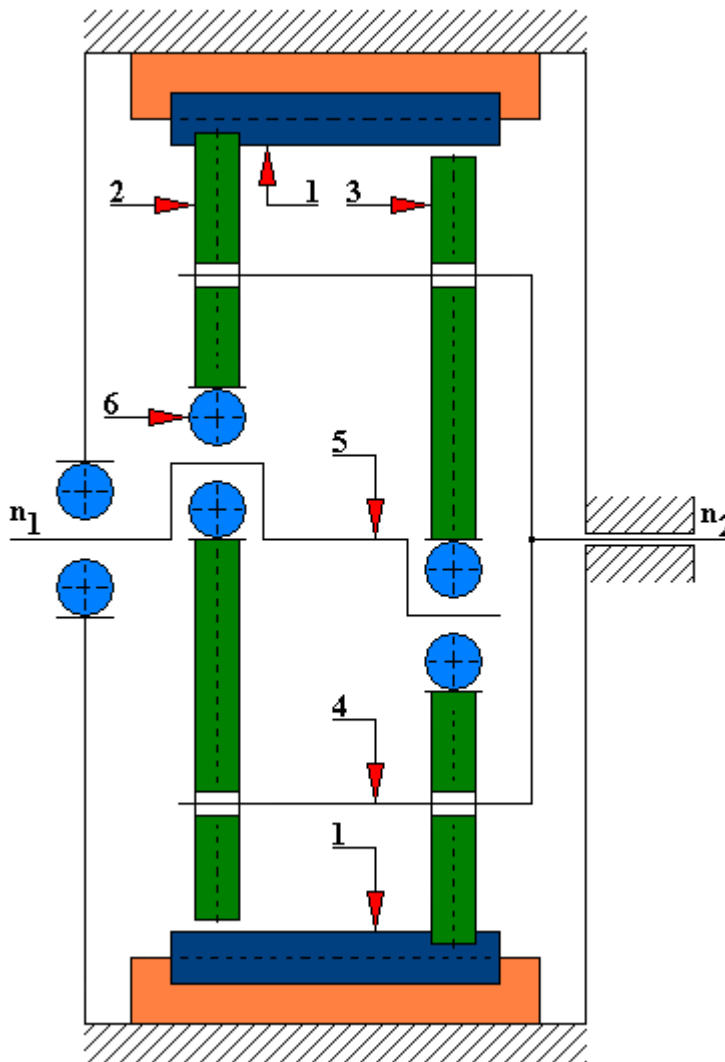


Fig. 4.2.27.1. Kinematic diagram of K-H-V type gear [180]

1 - rollers constituting the teeth (z_2) of a stationary wheel with internal tothing, 2 - first cam disc mounted on the driving shaft, 3 - second cam disc mounted on the driving shaft, 4 – straight-line mechanism, 5 - driving shaft, 6 - bearing

The principle of operation of this type of transmission is shown in Figure 4.2.27.1 and in Fig. 4.2.27.2. Mounted on the drive shaft 5 are two cam discs 2 and 3 which are offset eccentrically by half a turn. These discs co-act with rollers 1 constituting the teeth (z_2) of a stationary wheel with internal tothing. The number of curvatures on the cam discs is equivalent to the number of teeth (z_1) on the drive wheel. A gear of this type has pins and rollers (bushings) - not shown in the drawing - which are embedded with an appropriate clearance (usually a few millimeters) in the holes of both cam discs 2 and 3 which are also a part of the straight-line

mechanism 4. A straight-line mechanism is used for transmitting the rotational motion onto the driven shaft.

Figure 4.2.27.2 shows CYCLO type gears in which cam discs have 45 teeth (curves) and mesh with a stationary wheel with 46 teeth (rollers). The gear ratio in this transmission is therefore $i = 45$. If the shaft with cam discs is immobilized and the gear drive is transmitted through the housing together with the wheel with internal tothing, then the gear ratio $i = z_1/z_2 = 46/45 = 1.0222$.

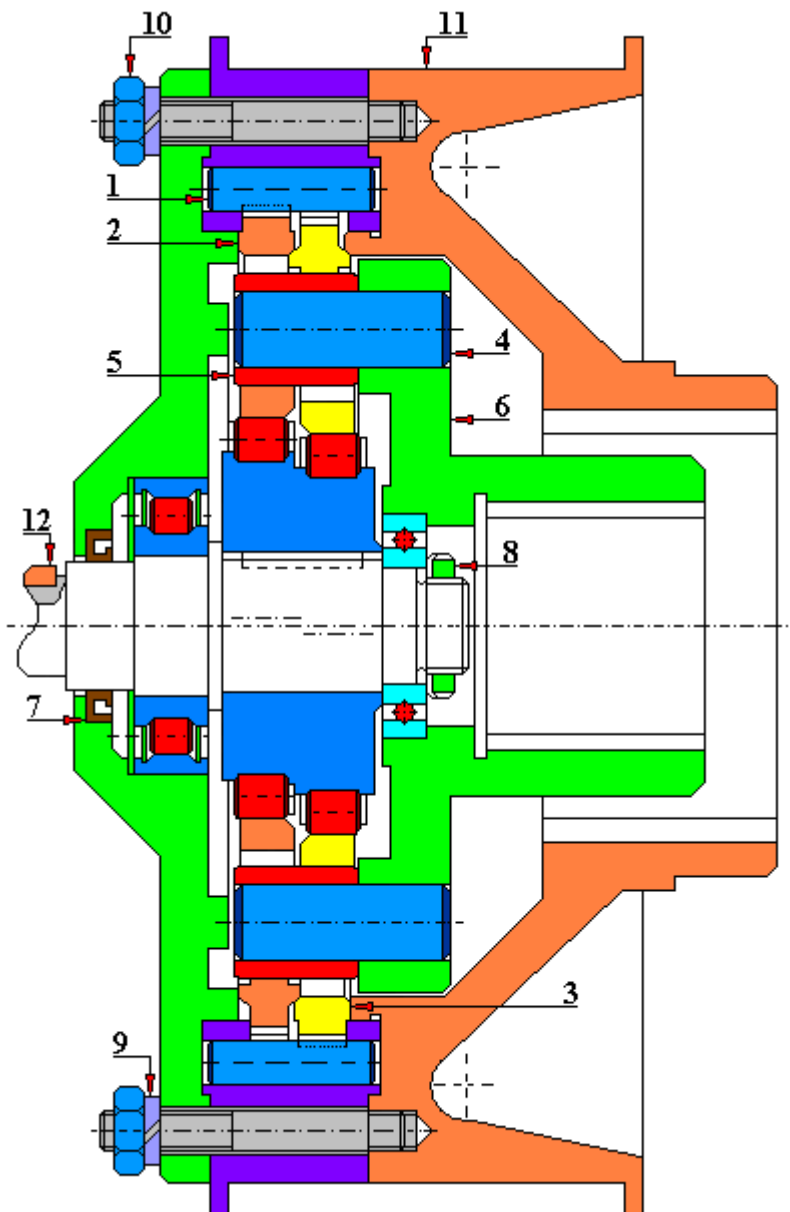


Fig. 4.2.27.2. CYCLO transmission [180]

1 - rollers, 2 - first cam disc, 3 - second cam disc, 4 - pins, 5 - rollers (sleeves), 6 –straight-line mechanism, 7 - lip seal of the drive shaft, 8 - nut securing the bearing, 9 - spring washer, 10 - hexagonal nut, 11 - gear body, 12 - key

There are also other design solutions of the CYCLO type transmission in which both the discs and stationary wheel are toothed, and their teeth have either an involute or cycloid contour properly adjusted to allow work with a different number of teeth in both mating wheels.

CYCLO gears are characterized by vibration-free operation in both directions of rotation, they are built to the minimum gear ratios $i = 9$ and the maximum gear ratios $i = 85$ (87) (*different authors provide different values*). The efficiency of these gears is very high reaching up to 0.98. The value of the transferred torques ranges from 15 [Nm] to 70 [Nm] with the power range from 0.12 [kW] to 110 [kW]. If we want higher gear ratios, then the CYCLO two-speed gearboxes should be used. These types of gears are used, among others, for driving machine tools, chain conveyors, construction machines, etc.

The test rig for testing the meshing durability of an epicyclical cycloidal gear was presented in the work of Bogdan Warda in the bimonthly Tribologia 6/2006. The load of the tested CYCLO type gear (Fig. 4.2.27.3) is provided by the mechanical coupling of two three-phase squirrel-cage induction motors: the braking 6 and driving 1. In addition the test system uses a two-speed belt transmission (items 7 to 16) the task of which is to increase the rotational speed obtained on the output shaft of the tested transmission to a value greater than the synchronous speed of the braking motor, which generates a torsional torque loading the tested transmission. This test rig is equipped with a data archiving and visualization system, including the temperature of the tested gear, the number of load cycles, torque values, and a vibration transducer designed to detect the appearance of fatigue failure to the mating surfaces. The following were used as executive elements:

- braking motor 6, type Sg 160L-8, 7,5 [kW], $n = 705$ [rpm];
- driving motor 1, type Sg 160M-6, 7,5 [kW], $n = 960$ [rpm];
- frequency converter 14, type SV 075 iG5A-4, power 7.5 [kW], supply voltage $u = 400$ [V] manufactured by LS Industrial System;
- torque meter 3 (type Mi10) operating on the principle of a torsion shaft;
- the tested epicyclical cycloidal gear 5;
- two-step belt transmission with toothed belts by OPTIBELT (items 7 to 16);
- flexible finger couplings 2 and 4 (two pieces in total).

And Figure 4.2.27.4 shows the general principle of operation of an epicyclical cycloidal gear. In order to enable the experimental verification of the model for forecasting the fatigue life of cycloidal meshing, the author of this test rig designed planet wheels with a reduced rim width from 14.5 [mm] to 6 [mm]. Then the expected life of the meshing of such a wheel is comparable with that of the central bearing (Figures 4.2.27.5 and 4.2.27.6). The planet wheels as well as rollers of the rack wheel are made of ŁH15SG bearing steel improved to the hardness of 63 HRC. The drive motor rotational speed is regulated by a frequency converter. The use of a braking motor allows reducing the gear ratio of the gear multiplying rotational speed and reducing its external dimensions. The construction of this test rig, however, makes it impossible to reverse the direction of load application.

In this design solution, the Mi10 torque meter co-works with the WT-1 torque indicator which has an analog meter for reading indications. The torque meter enables the measurement of slowly changing or static torques in the range $0 \div 100$ [Nm].

The presented test rig allows shortening the experiment time for fatigue tests dedicated to cycloidal gears.

Please note that when in the diagram shown in Figure 4.2.27.3. we replace the cycloidal gear with any other one, then we will get a universal test rig for practically every type of gear, if only the technical conditions allow it (Fig. 4.2.27.7).

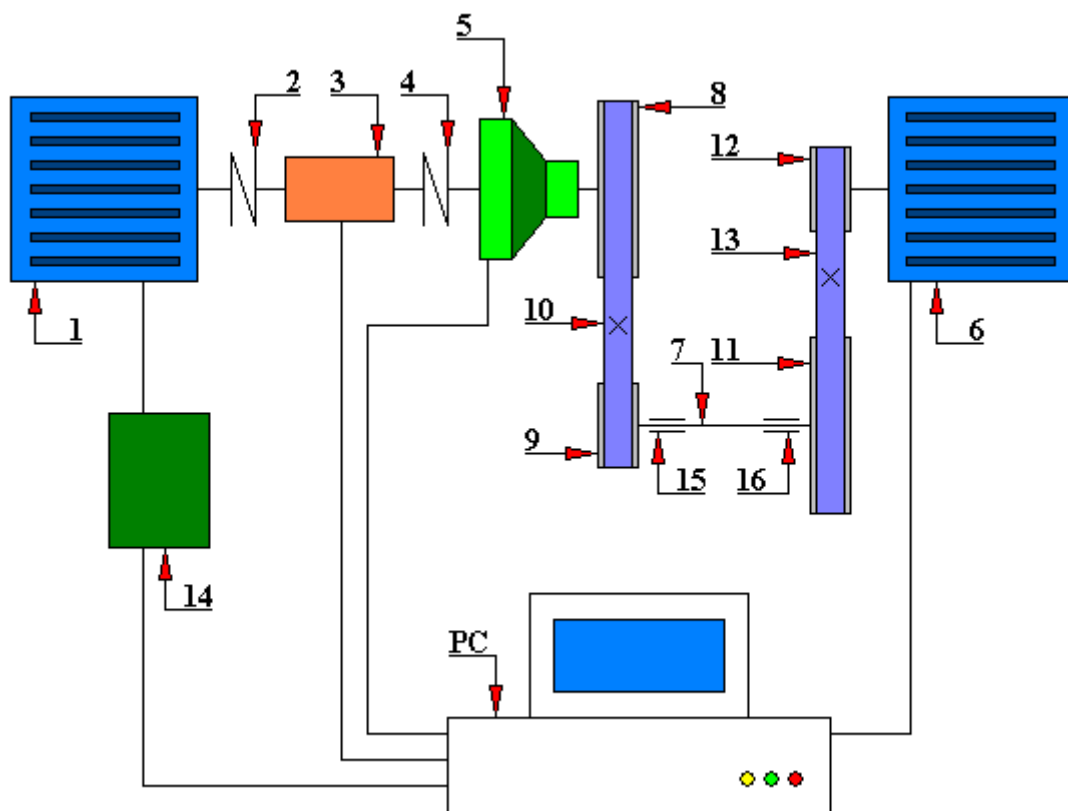


Fig. 4.2.27.3. General diagram of the test rig for testing the durability of rolling contacts of a cycloidal transmission

1 - drive motor, 2 - clutch, 3 - torque meter, 4 - clutch, 5 - cycloidal gear, 6 - braking motor, 7 - belt transmission shaft, 8 - gear wheel z_1 , 9 - gear wheel z_2 , 10 - toothed belt, 11 - gear wheel z_3 , 12 - gear wheel z_4 , 13 - toothed belt, 14 - frequency converter, 15 - support bearing, 16 - support bearing, PC - computer

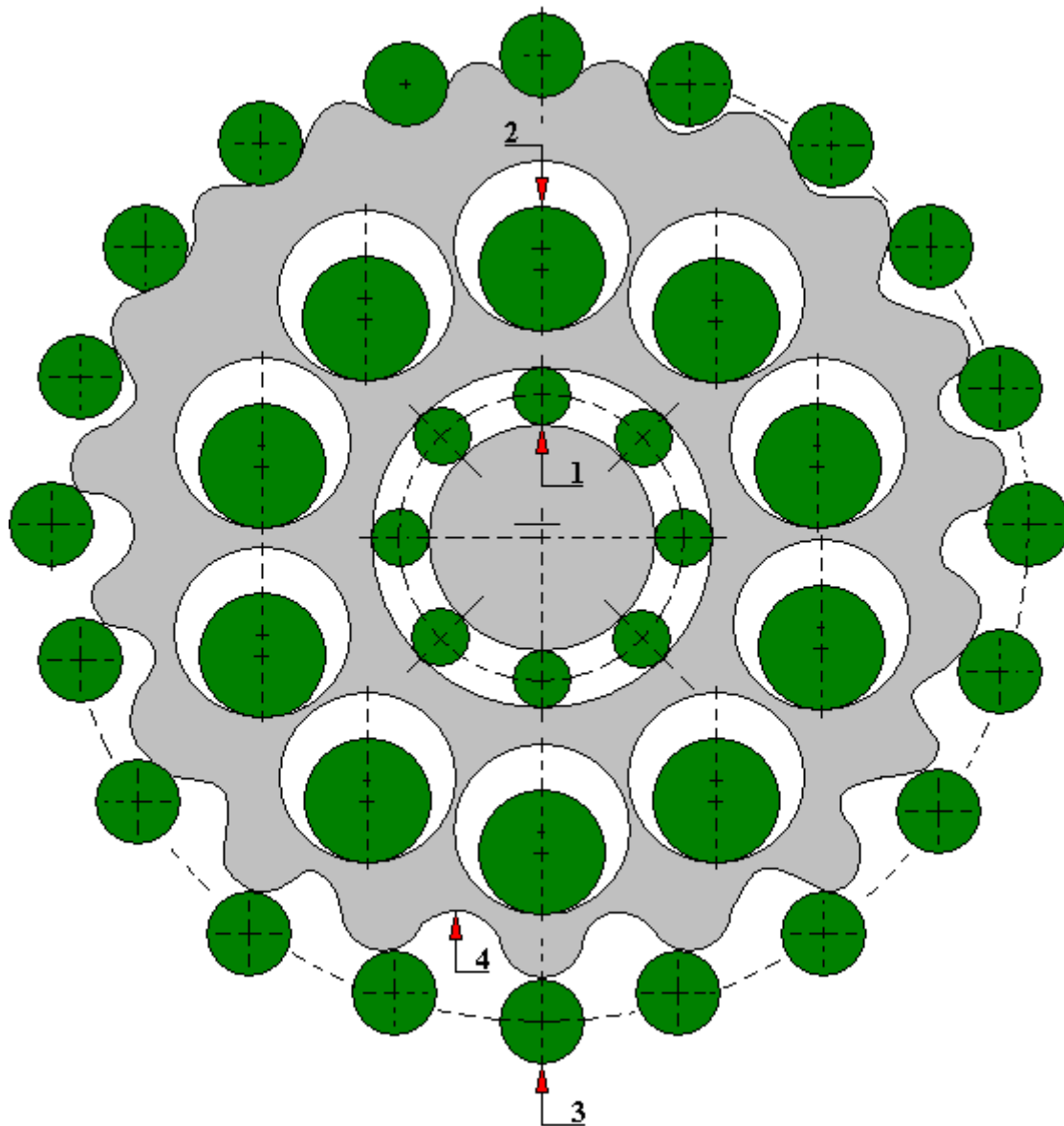


Fig. 4.2.27.4. A general principle of operation of an epicyclic cycloidal gear
 1 - cylindrical central bearing, 2 - set of rolling pins in the straight-line mechanism, 3 - special cycloidal gearing, 4 - planetary gear of cycloidal gear (first cam disc eccentrically moved by half a turn); the drawing does not show the second cam disc

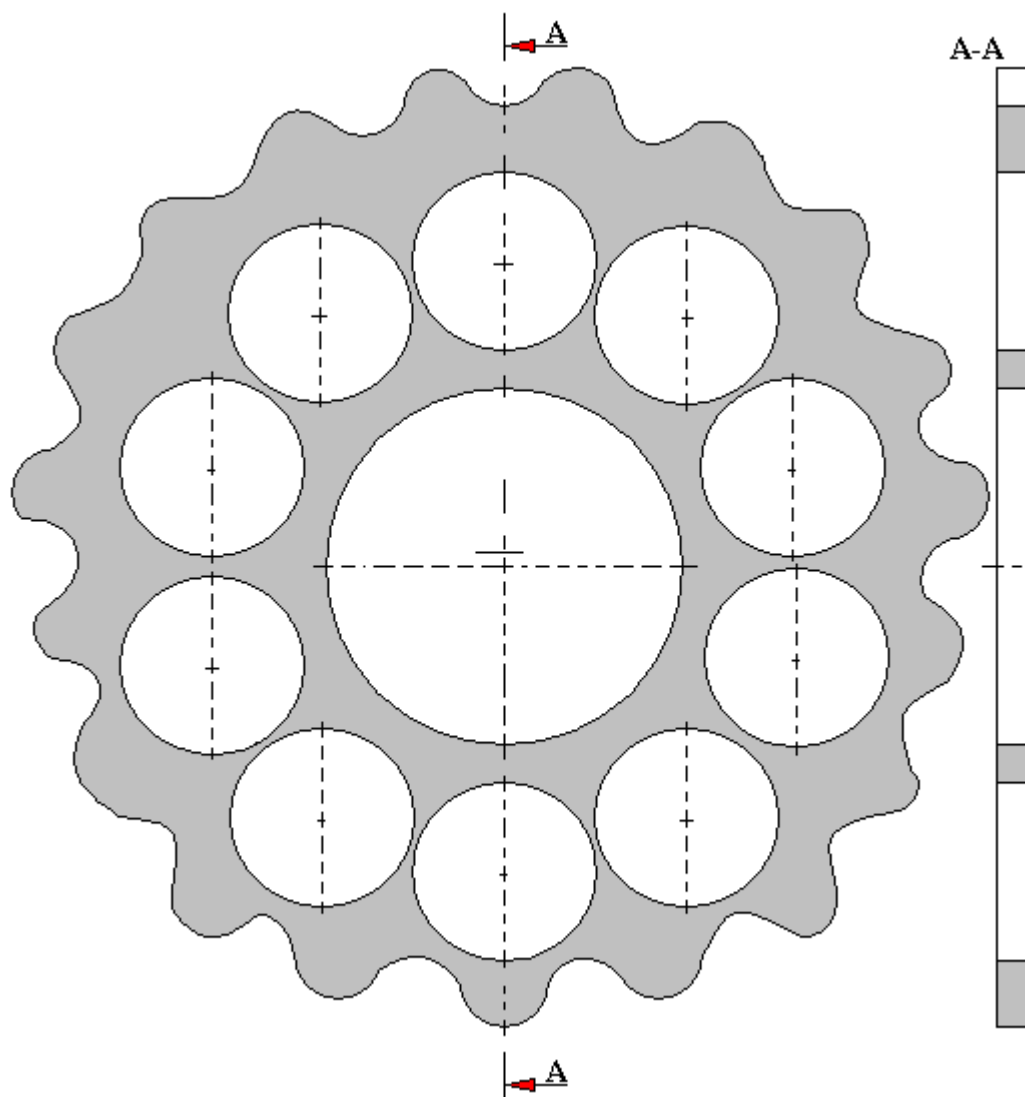


Fig. 4.2.27.5. A design of the standard planet gear of a cycloidal gear

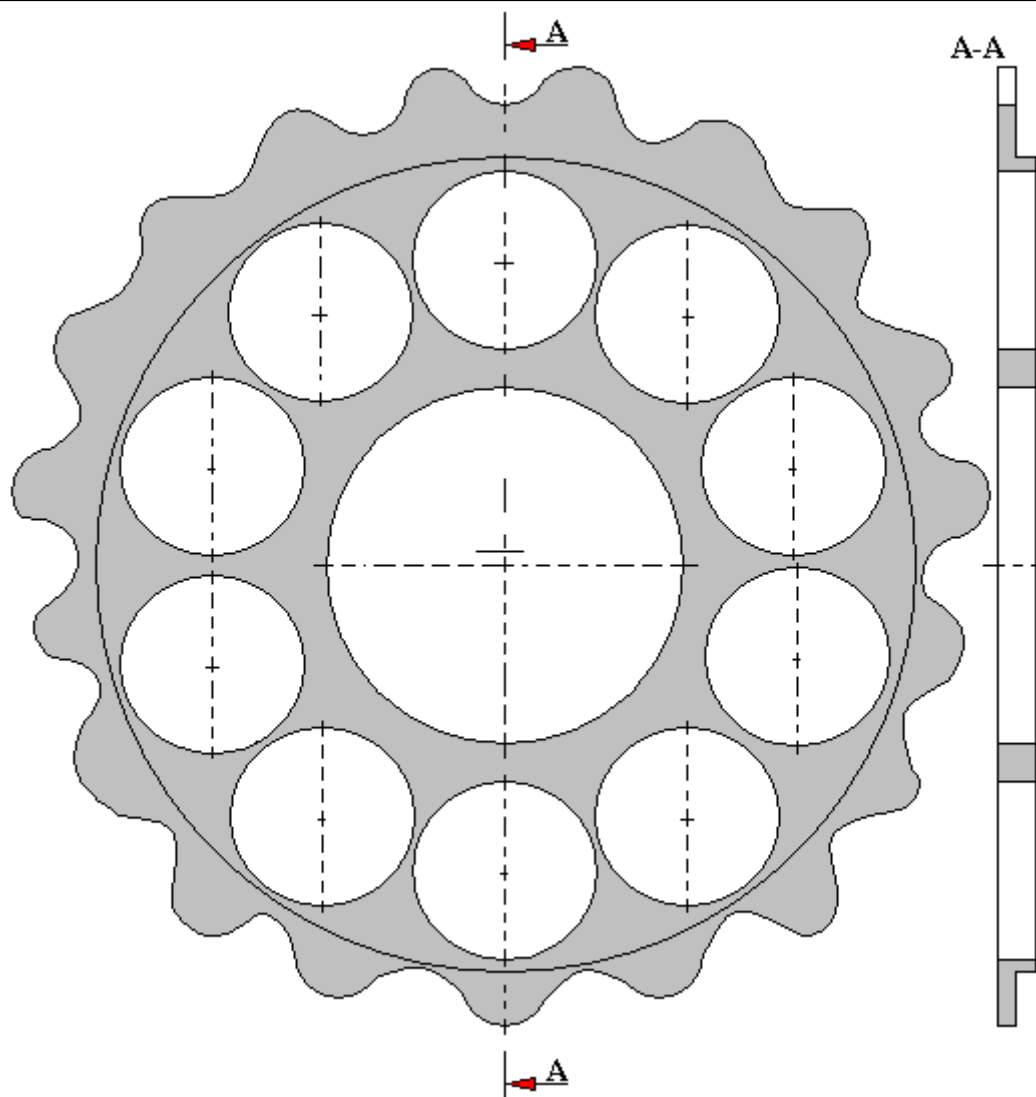


Fig. 4.2.27.6. The design of the planetary gear of a cycloidal gear intended for testing the meshing durability

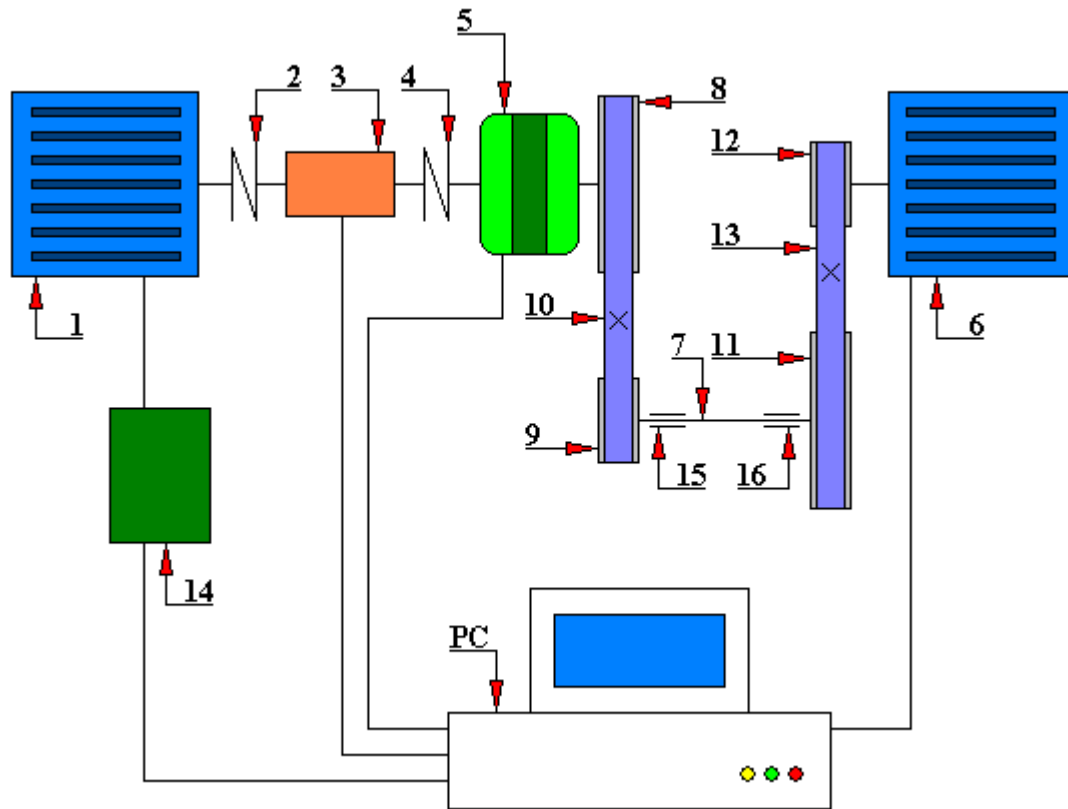


Fig. 4.2.27.7. A general diagram of a universal test rig for gear durability
 1 - drive motor, 2 - clutch, 3 - torque meter, 4 - clutch, 5 - any gear, 6 - braking motor, 7 - belt gear shaft, 8 - gear wheel z_1 , 9 - gear wheel z_2 , 10 - toothed belt, 11 - gear wheel z_3 , 12 - gear wheel z_4 , 13 - toothed belt, 14 - frequency converter, 15 - support bearing, 16 - support bearing, PC - computer

4.2.28. Test rig for tribological tests of materials, in particular lubricants, according to the patent SU 1670520 A1

This test rig is designed mainly for carrying out tribological tests of lubricants (Fig. 4.2.28.1). This test rig was registered in the Patent Office of the Soviet Union under the number SU 1670520 A1. Its inventors form a research team composed of: Kowalskij B.I., Tichonow W.I. and Dieriewiagina L.N. (State Design-Science-Research-Construction Institute "Krasnoyarskij Promstroj NII Projekt").

This test rig works as follows. Before starting the test, it is necessary to refill the lubricant reservoir tub 20 with the tested lubricant 21. Then, set the temperature value of the tested lubricant and the test duration using the adjusters 7 and 11. After these initial steps have been completed, the test rig is ready for operation.

At the beginning of operation, the control system heats the tested lubricant to the set temperature. For this purpose, power unit 1 is switched on which supplies voltage to control block 2 and to temperature controller 3. The temperature controller 3 turns on/off the heating element 4. Then, the tested lubricant 21 is heated to the set temperature value set with the temperature adjuster 7.

The temperature of the tested lubricant composition 21 is measured by a temperature sensor 6 placed in the lubricant 21, and its value is compared with the set value in the comparative block 5.

When the temperature of the lubricant 21 is below the set value, the indicator light of the temperature indicator 8 lights up. Then the start-up of the test rig is blocked. After reaching the set temperature value of the tested lubricant composition 21, the indicator light of the temperature indicator 8 goes out. A control signal is sent from the comparative block 5 to the bistable multivibrator 9 which controls the pulse generator of the test duration counter 10 via control block 2 by means of its output signals.

The control unit 2 also supplies voltage to sensors 14, 15, 16 for measuring the moment of friction force, wear and the conductivity of the friction contact.

Once the rotational motion is started, the counter-sample holder 22 operates without a load being applied thereto as long as the temperature of the lubricant 21 reaches a preset temperature value. During this phase of the operation cycle, the heated lubricant 21 releases some of its heat also into the counter-sample holder 22. Thereby it warms it up. The indicator light 8 lights up, and when the set temperature value is reached, it goes out. After this phase of the operation cycle, a load is applied to the holders 22 and 23 of the counter-sample and samples. At this point, all tribotechnical parameters of the friction process and wear of the tested friction contact are registered. The interlocking/locking block 12 supplies voltage to the recording units 17, 18, 19 and the signal for the test duration counter 10.

The signals obtained from the sensors of the moment of friction force 14, wear 15 and the conductivity coefficient of the friction contact 16 can be given either to the units recording the values of these sensors, i.e. to the units 17, 18 19 or given by the controller/microprocessor (not shown in the drawing) to the computer and processed there using a special program.

After the pre-set test duration, which was determined by the timer 11, the test duration counter 10 sends an appropriate signal to the control block 2 on the basis of which this block switches off the rotary drive 13, the current protection of sensors 14, 15, 16, and recording units 17, 18, 19 and the bistable multivibrator 9 returns to the neutral position. The operator manually turns off the power block 1.

After replacing the lubricant 21 in the reservoir 20 and tested samples and counter sample placed in holders 22 and 23, the testing process can be repeated.

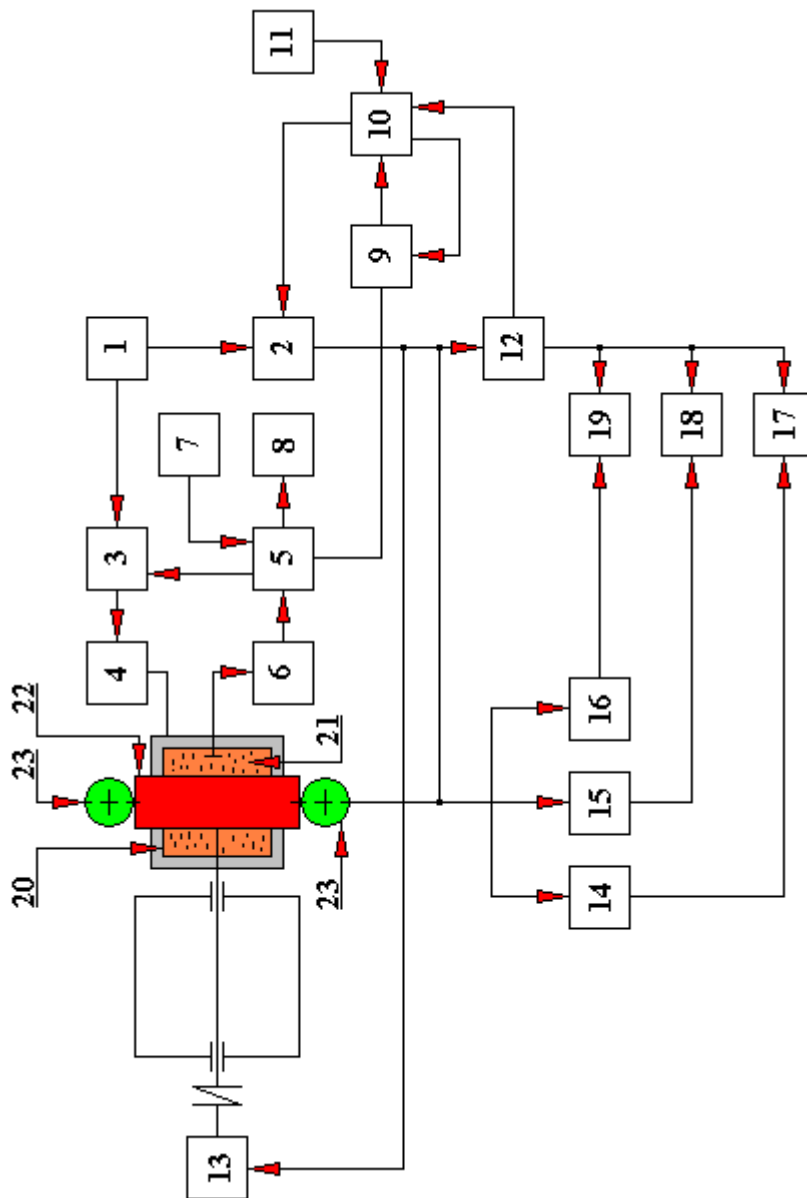


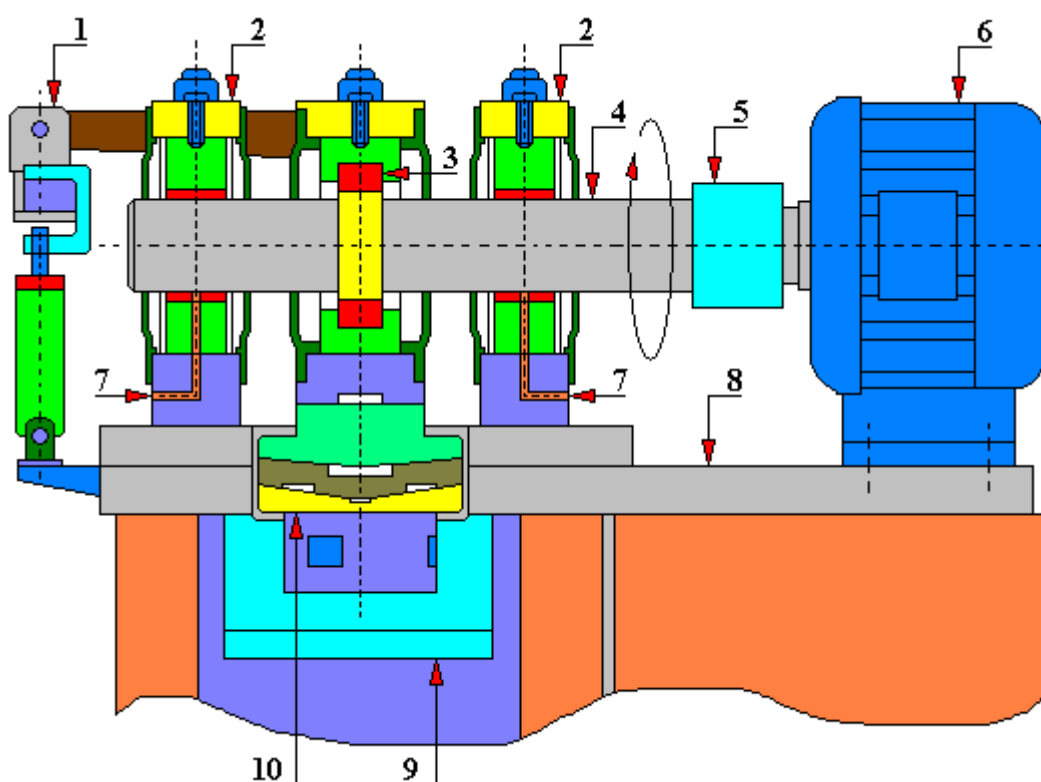
Fig. 4.2.28.1. A block diagram of a test rig for tribological testing of materials, in particular lubricants, according to the patent SU 1670520 A1

1 - power block, 2 - control block, 3 - temperature controller, 4 - heating element, 5 - comparative block, 6 - temperature sensor, 7 - temperature adjuster, 8 - indicator, 9 - bistable multivibrator, 10 - test time counter, 11 - test duration adjuster, 12 - locking block, 13 - rotation drive, 14 - sensor of the moment of friction force, 15 - wear sensor, 16 - friction contact conductivity coefficient sensor, 17 - moment of friction force recording unit, 18 - wear recording unit, 19 - a test rig recording the frictional conductivity, 20 - lubricant reservoir, 21 - tested lubricant, 22 - counter-sample holder, 23 - sample holder

4.2.29. Test rig for testing radial slide bearings PG 2 - 1Ł

A test rig for testing radial slide bearings PG2 - 1Ł (Fig. 4.2.29.1) was designed and constructed at the Department of Machine Construction and Operation at Gdańsk University of Technology. The above-mentioned rig is fully computerized, automatically controlled, which guarantees repeatability of tests. The course of the rotational speed of the journal and load can be of any character. The rig is additionally equipped with a patented friction measurement system thanks to which it is possible to test bearings with extremely low friction resistance and to load the tested bearings with a beveling moment. Data recording - digital. On the above test rig you can carry out, for example:

- testing of ecological foil bearings;
- testing of bearings supported on a spherical ball;
- testing of ceramic slide bearings;
- testing of combustion engine bearings.



Rys. 4.2.29.1. A general diagram of the test rig for testing PG-2 1Ł radial slide and rolling bearings

1 – a beveling system of the tested bearing; 2 – support bearing body; 3 – tested bearing; 4 – shaft; 5 – clutch; 6 – electric motor; 7 – supply of lubricating oil; 8 – frame; 9 – transverse load cylinder; 10 – hydrostatic bearing

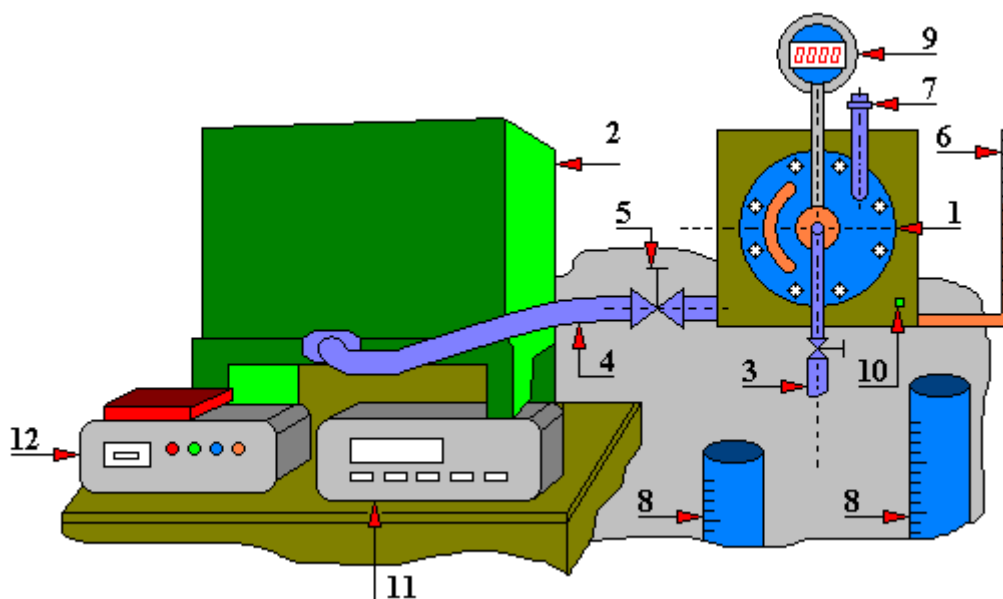


Fig. 4.2.29.2. Research system of PG 2-1L test rig [221]

1 – research head; 2 – expansion tank; 3 – oil outlet pipe; 4 – head supply oil pipe; 5 – control valve; 6 – oil level indicator; 7 – air pipe; 8 – measuring vessel; 9 – digital manometer; 10 – temperature sensor; 11 – temperature panel; 12 – rotational speed control panel

The above PG2-1L test rig also enables, among others, the testing of an individual feed system of a radial slide bearing, the operation of which is based on the co-acting of a permanent lubricating ring and a hydrodynamic guide.

So far, a frequently used solution for lubricating a radial bearing was the use of fixed ring co-acting with a scraper (Fig. 4.2.29.4). In this design (Fig. 4.2.29.3) instead of a scraper collecting oil and directing it to the bearing lubrication interspace, hydrodynamic guides are used. The idea behind this solution is to create a closed delivery channel in which the hydrodynamic effect is used for transporting the oil to the bearing. The idea behind this solution is to create a closed delivery channel in which the hydrodynamic effect is used for transporting the oil to the bearing. The channel is formed by the surfaces of the guide, feeding ring and bearing housing. As a result of the rotational motion of the fixed ring the channel is filled with oil and a flow is formed towards the outlet located at the top of the bearing. From there, the oil is drained through a channel to the bearing lubrication interspace.

The appropriate shape and position of the hydrodynamic guide in relation to the lubricating ring allows increasing the amount of oil supplied to the bearing compared to traditional methods of the ring lubrication. Due to the variable shape of the delivery channel and the associated hydrodynamic effect, it is possible to feed the bearing with oil at a slight pressure, which cannot be achieved with the previously used independent feed solutions.

The use of solid (Fig. 4.2.29.3 and 4.2.29.4) or loose lubrication rings (in both cases the rings are partially submerged in oil) is classified as the circulating lubrication.

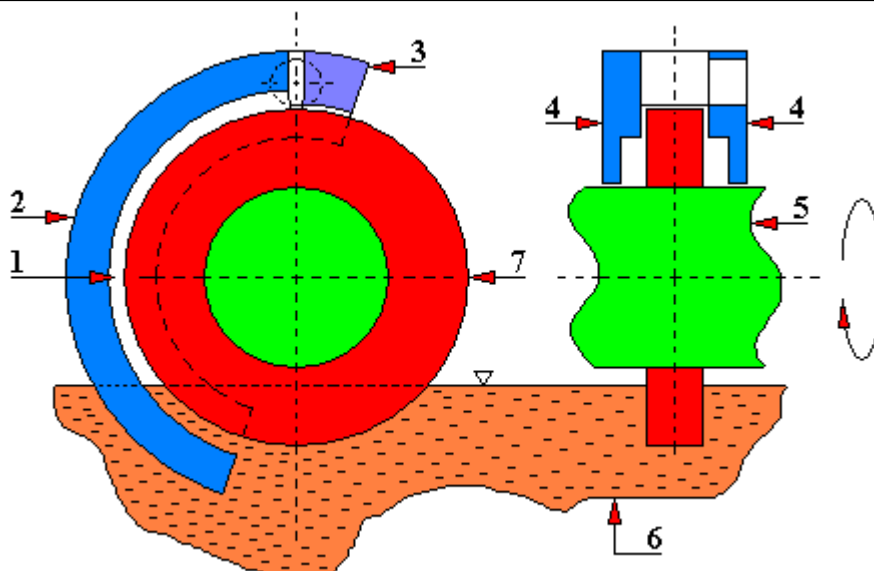
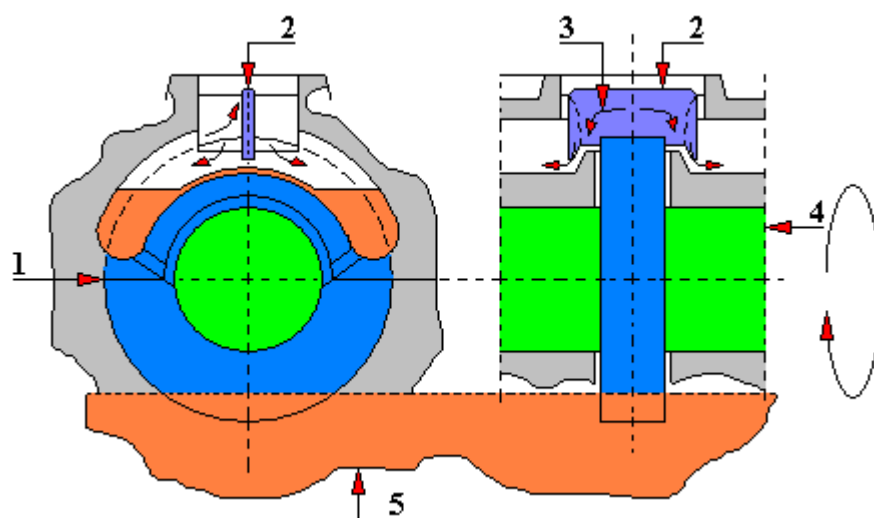
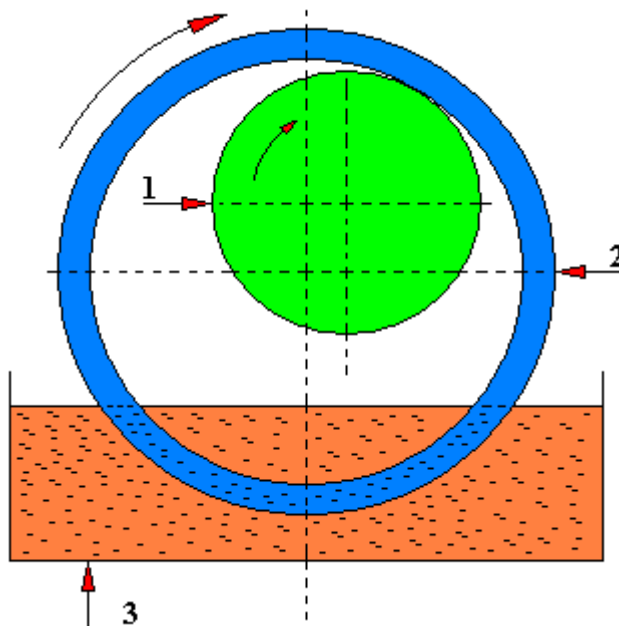


Fig. 4.2.29.3. Scheme of feed system including the feeder with step [221]
 1 – feeder; 2 – hydrodynamic guide; 3 – step of guide; 4 – covers; 5 – shaft (journal of bearing); 6 – oil; 7 – feeding disc



Rys. 4.2.29.4. A diagram of a design solution of a radial bearing lubricated with a fixed ring [180]
 1- fixed ring; 2 - scraper; 3 - oil flow direction; 4 - shaft; 5 - oil

a)



b)

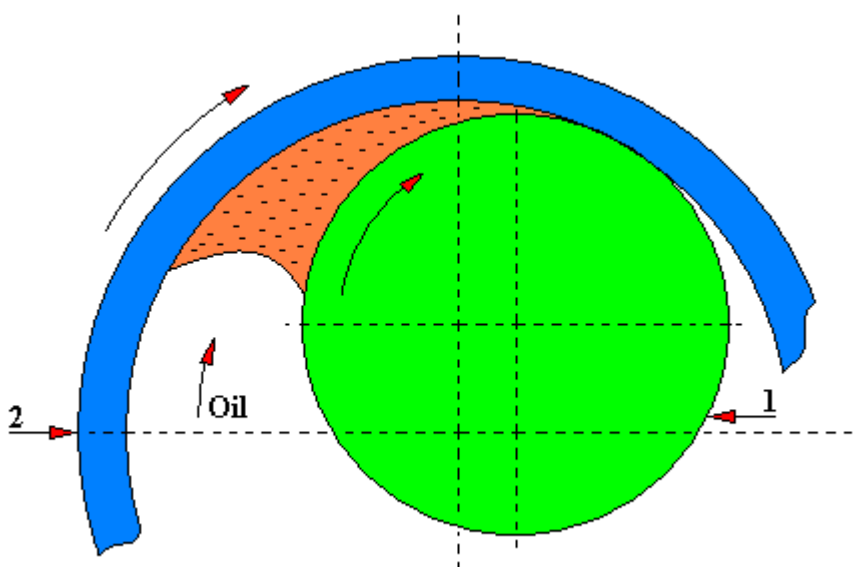


Fig. 4.2.29.5. A diagram of a design solution of a radial bearing lubricated with a fixed ring [180]
 1 - shaft, 2 - movable (loose) disc, 3 - oil (lubricant) reservoir

Also a free-standing slide bearing was tested on the PG2-1Ł test rig, according to the patent PL 117 430, the authors of which are: Olgierd Olszewski, Jan Sikora, Antoni Neyman, Aleksander Sidorczyk, shown in Fig. 4.2.29.6. In the bearing according to this patent, the bushings 1 (two pieces) forming the sliding sleeve are located in the body 2 which is also an oil reservoir closed on both sides by covers 3 (two pieces), sealed on the rotating shaft 4 with seals 5 and 6.

The bushings 1 are supported by means of a flexible element 7 through a stop 8. The flexible element is placed in the seat 9 of the body 2 and pressed to the stop 8 with a clamping ring 10. On the shaft 4 there is an oil carrier in the form of a hollow-bored ring 11, which has openings 12 distributed around the circumference by means of which the oil penetrates the outer surface of the ring 11. The oil filling the lower part of the body 2 also fills the concave part of the ring 11 in such a way that at a higher rotational speed the centrifugal force brings it to the upper position and through openings 12 pushes it out of the ring, and the scraper 13 directs it into the chamber 14 and onto the rubbing surfaces through the opening 15.

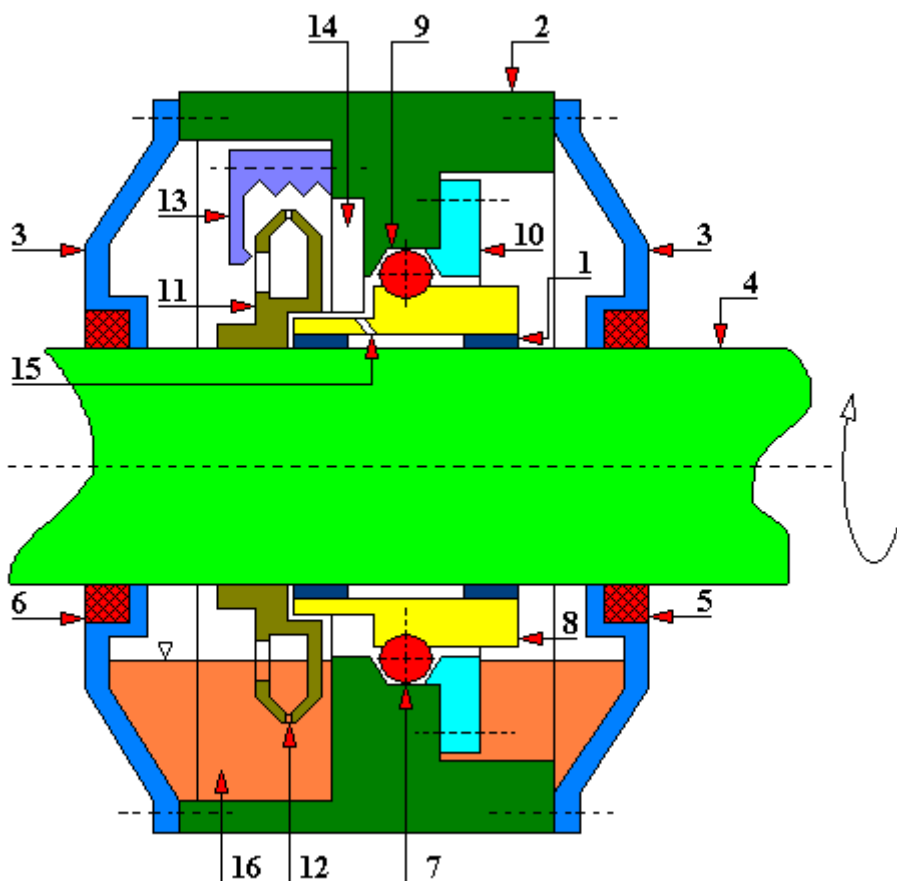


Fig. 4.2.29.6. A diagram of a free-standing slide bearing according to the patent PL 117 430
 1 - bushing (2 pieces); 2 - body; 3 - cover (2 pieces); 4 - rotary shaft; 5 - shaft seal; 6 - shaft seal;
 7 - flexible element supporting the bushing; 8 - stop; 9 - body seat; 10 - clamping ring; 11 -
 hollow-bored ring; 12 - openings; 13 - scraper; 14 - chamber; 15 - oil outlet opening; 16 - oil

Probably a modernized version of the above test rig is a testing test rig for radial slide bearings type PG-4 ŁA (B) which was also constructed at the Department of Fundamentals of Machine Design at Gdańsk University of Technology under the supervision of prof. dr. inż. K. Zygmunt (Fig. 4.2.29.7 and 4.2.29.8). The reason why this test rig was built was the initiative of the Wood Technology Institute in Poland to conduct tests on slide bearings with compressed wood bearing shells. This test rig has been well described in the following works [K. Zygmunt: Konstrukcja maszyn badawczych do łożysk ślizgowych i maszyn do badania zużycia na

próbkach. Problemy Tarcia, Zużycia i Smarowania, Zeszyt 6, 1964 r.; Jan Sikora, Alojzy Rigall: Badania łożysk z materiałów drewnopochodnych; Alojzy Rigall, Jan Sikora: Maszyna badawcza łożysk ślizgowych poprzecznych – typ PG-4 ŁA (B). Zagadnienia Tarcia, Zużycia i Smarowania, Zeszyt 8, 1970r.]

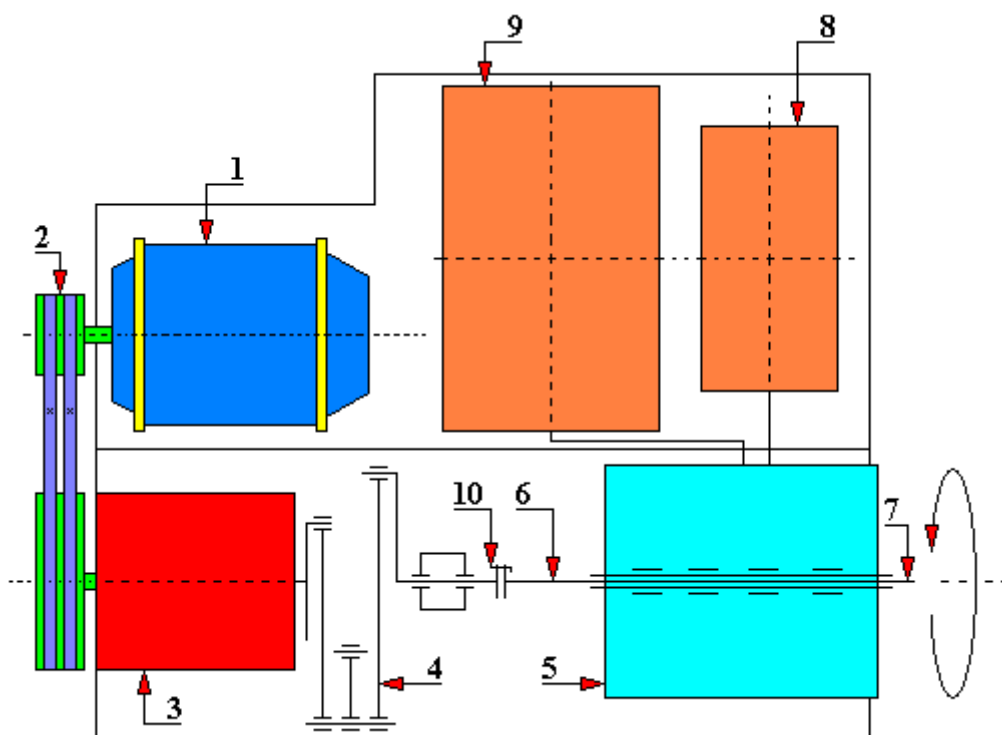


Fig. 4.2.29.7. A diagram of the test rig for radial slide bearings type PG-4 ŁA (B)
 1 - electric motor; 2 - belt transmission; 3 - gear transmission; 4 - attachment; 5 - test head; 6 - torsional roller; 7 - tested shaft; 8 - low pressure hydraulic system (lubrication system); 9 - high pressure hydraulic system (loading system); 10 – clutch

The structure of this test rig includes the following components:

- DC electric motor working in the Ward-Leonard system with the power:
 $N_1 = 13 \text{ kW}$ with $n_1 = 2800 \text{ rpm}$;
 $N_2 = 2.8 \text{ kW}$ with $n_2 = 350 \text{ rpm}$;
- belt transmission with a ratio of $i = 1.6$;
- gear transmission enabling to obtain two gear ratios $i_1 = 1$ and $i_2 = 5.62$, thus obtaining a stepless regulation of the peripheral speed in the range from 0.1 m/sec to about 4.6 m/sec;
- an attachment to convert a rotary motion into a swinging motion; it is an additional equipment for this test rig; the structure of the above-mentioned attachment is based on the principle of an articulated quadrilateral; it enables the testing of bearings with the swinging motion of the journal for two values of the amplitude of swings:

$$\varphi_1 = 22^\circ 30' \text{ oraz } \varphi_2 = 30^\circ$$

- test head;

- torsional roller; it plays a double role here, i.e. it plays the role of a flexible coupling connecting the tested shaft with the output shaft of the gear transmission and the role of a friction torque meter; at this point, the Authors of the design point out that a set of torsional rollers differing in diameter was used here in order to obtain the appropriate sensitivity of the measuring system at different values of the frictional moment;
- tested shaft;
- high pressure hydraulic system - used for exerting a load on the tested bearing;
- low pressure hydraulic system for the lubrication of tested bearings;
- overload clutch.

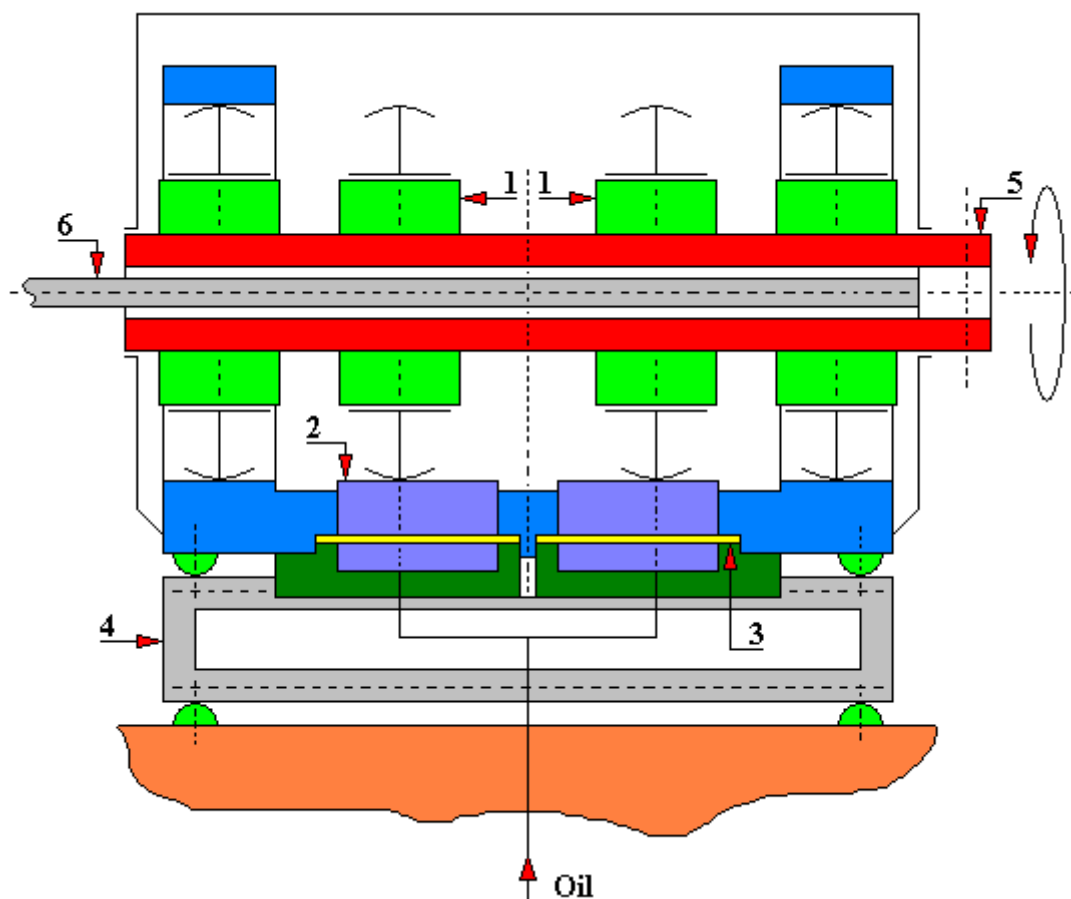


Figure 4.2.29.8. A diagram of a test head of a test rig for testing radial slide bearings type PG-4 ŁA (B)

1 - tested bearing; 2 - hydraulic weight piston; 3 - membrane; 4 - supporting channel (dynamometer); 5 - tested shaft; 6 - torsion shaft

This test rig was designed to carry out tests on the properties and sliding characteristic of bearings made of various materials, especially wood-based ones, lubricated with various lubricants. In principle, slide bearings operating in the range of mixed friction can be tested on this test rig during unidirectional rotary motion with a constant rotational speed and in swinging motion.

The tested bearings have an internal diameter $d = \text{Ø}50\text{mm}$ and the ratio of the length of the bearing to its diameter is $l/d = 1$. The peripheral speed range is $v = 0.1 \div \text{approx. } 4.6 \text{ m/sec}$.

The bearing load caused by the hydraulic loading system is static, continuously adjustable and allows achieving pressures p up to 150 kG/cm^2 . In the case of testing bearings with the ratio of the bearing length to its diameter $l/d = 0.4$ (and such testing on this test rig is possible), it is possible to obtain circumferential speeds of up to approx. 8 m/sec and p loads up to approx. 600 kg/cm^2 .

The test head (Fig. 4.2.29.8) was constructed in two variants. In the first variant, the self-aligning of the tested bearing is based on the rolling principle - a ball supported in a cylindrical seat. The second variant of the self-aligning support of the tested bearings was realized on the rolling principle with the use of swinging spherical roller bearings. The test head is the most important component of the PG-4ŁA (B) test rig. The four tested bearings are mounted in housings that enable them to be self-aligning in relation to the journal. The outer bearing housings are placed in the rigid body of the test head and secured against rotation. The middle bearing housings, also secured against rotation with respect to the body, rest on the pistons of the two hydraulic weights. The hydraulic weights are placed above the diaphragms closing the pressure chambers.

The load on the lower part of the middle tested bearings is caused, through pistons, by the pressure of the oil fed under the diaphragms. The reaction of this load on the tested shaft is perceived by the two extreme bearings, causing the upper half-shell bearings to be loaded. The loading forces in this case are therefore the internal forces of the test head system.

Pressurized oil is fed into the pressure chamber through a tube coiled in the shape of a helix to avoid disturbance during the friction torque measurement.

The lubricant (oil + possibly additives) is delivered to each bearing via a plastic conduit.

The test head is supported on two dynamometers, the stiffness of which has been selected to ensure the appropriate sensitivity of the measuring system with a minimum deflection from the position established during assembly. In Fig. 4.2.29.8 only one dynamometer is visible (visible from the front of the test rig). The other is behind him and supports the other end of the test rig. These dynamometers are designed to balance the frictional moment.

The measurement systems used in the PG-4 ŁA (B) test rig enable the measurements and registration of the following quantities:

- journal rotation speed;
- lubricant flow rate;
- lubricant pressure;
- load of the tested bearings;
- the moment of friction of the tested bearings;
- bearing shell temperature;
- temperature of the lubricant at the inflow and outflow from the tested bearing.

The measurement of the frictional moment on the PG-4 ŁA (B) test rig is performed as follows. The measured frictional moment is the sum of the frictional moments on the four tested bearings. The measurement of this total moment can be performed using three independent methods, described below.

The first method of measuring the frictional moment is to measure the response values on the dynamometers supporting the test head. These dynamometers are in the form of C-beams with shelves of high stiffness. Strain gauge transducers in a full-bridge summing system are glued to the walls of channels 4 (Fig. 4.2.29.8). Using this method, it is possible to measure the friction torque with an accuracy of approx. 1% at the expected highest frictional moments and with an accuracy of up to approx. 5% at the expected lowest frictional moments.

The second method of measuring the frictional moment also uses strain gauge transducers, which this time are glued in a full bridge summing system on the surface of the torsion bar 6 (Fig. 4.2.29.8). In this case, the measurement of the frictional moment is based on the measurement of the torsional moment transmitted by the torsion bar. Due to the fact that the

torsion bar 6 rotates, it is necessary in this method to use a head that collects the current from the rotating torsion shaft. The accuracy of this method roughly corresponds to that of the first method. Unfortunately, this method requires the use of replaceable torsion bars depending on the range of the measured friction torque. Moreover, it is possible here to register the obtained values of the frictional moment measurement.

The third method of measuring the frictional moment is similar to the second method. The indicator of the value of the frictional moment is the angle of relative torsion of the two discs, one of which is mounted on the tested shaft, and the other on the output shaft of the gear. The reading of the torsion angle of the torsion bar 6 (Fig. 4.2.29.8) is based on the use of the stroboscopic effect. Low torsional stiffness and a long length of the torsion bar allow for high torsion angles (up to approx. 25°). The advantage of this method is virtually no electronic equipment and the associated costs. Unfortunately, in this method, as in the latter, it is necessary to use replaceable torsion bars depending on the range of the measured frictional moment. Also, the continuous recording of the measured quantities is difficult. The accuracy of the measurement with this method is lower than the previous two. What is also important, the person measuring with this method must have good eyesight, otherwise the reading errors may be significant.

In the case of continuous recording of the value of the frictional moment, the Authors originally equipped the PG-4 ŁA (B) test rig with the following units:

- bridge-amplifier for strain gauge measurements and a tape recorder for measurements of moments of variable value with the frequency of changes f not exceeding 100 Hz;
- bridge-amplifier for strain gauge measurements and cathode or loop oscilloscope for measurements of variable frictional moments with the frequency of changes f greater than 100 Hz.

The first and third methods of measuring the frictional moment were used to measure the constant frictional moments. The second method of measuring the frictional moment was used in the case of measuring variable moments due to the low inertia of the tested shaft.

The load measurement of the tested bearings was carried out using an indirect method by measuring the oil pressure in the pressure chambers using a sensor with a resistance strain gauge transducer. This method of measurement allowed for continuous recording of the bearing load. In order to verify the indications of sensors with strain gauge transducers, additional control manometers were installed in the system.

The temperatures of the bushings and the lubricant were measured by means of thermocouples placed in special openings made in the bushing. At that time, the Authors used a tape recorder for the continuous recording of temperature measurements.

The lubricant flow rate was measured continuously with a rotameter.

The pressure of the lubricant was measured using manometers.

The rotational speed of the journal was measured using a tachometer or a strobe lamp.

Two independent oil systems were constructed to supply the test head of the PG-4 ŁA (B) test rig:

- hydraulic high pressure loading system (Fig. 4.2.29.9);
- hydraulic lubrication system - low pressure (Fig. 4.2.29.10).

The construction of the high pressure system (Fig. 4.2.29.9) includes, among others, the following parts:

- hand pump 1 with shut-off valve;
- oil pressure accumulator 5;
- stop valve 3;
- a small needle relief valve 4 intended for precise regulation of the oil pressure, i.e. the force loading the tested bearings.

The maximum permissible pressure of the hydraulic high pressure loading system is 150 kG/cm².

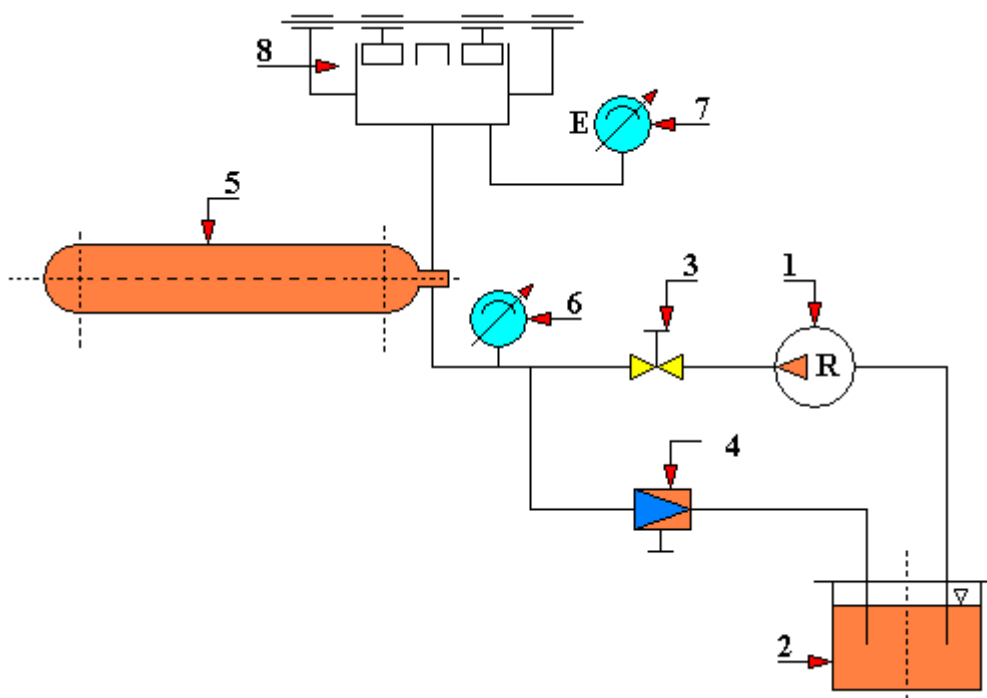


Fig. 4.2.29.9. A diagram of the hydraulic loading system of the test rig for testing radial slide bearings, type PG-4 ŁA (B)

1 - hand pump; 2 - oil tank; 3 - stop valve; 4 - needle valve; 5 - pressure accumulator; 6 - manometer; 7 - strain gauge manometer; 8 - test head

The low pressure system was designed in two variants depending on the type of lubricant.

When lubricated with oil (Fig. 4.2.29.10), the system is powered by a gear pump 1 with a nominal capacity of 6.3 l/min from an oil tank 2 with a capacity of approx. 60 liters. There is a water cooler 10 in the tank. Two filters (3 and 6), rotameter 7 and a lubricant distributor 8 for the four tested bearings were installed in the oil circuit. In order to regulate the oil flow, a throttle valve was used, located in the branch parallel to the test head. Closing the throttle valve 5 increases the flow resistance in this branch and increases the amount of oil flowing to the four tested bearings. From the tested bearings 9, the oil returns to the oil tank 2 again.

When the tested bearings are lubricated with water, then the lubricating circuit is an open circuit. In this case, the lubricating circuit is supplied from the water supply network through a cut-off valve, which simultaneously regulates the amount of flowing water. Then, in such a circuit, apart from the shut-off valve, only the rotameter and the distributor are included.

The adjustment of a uniform supply of the tested bearings with the lubricant is carried out by appropriate setting of the adjusting screws in the distributor.

This test rig is set on a concrete foundation. Whereas the reducer, the attachment for swing movements and the test head are attached to a cast iron plate screwed to a concrete block.

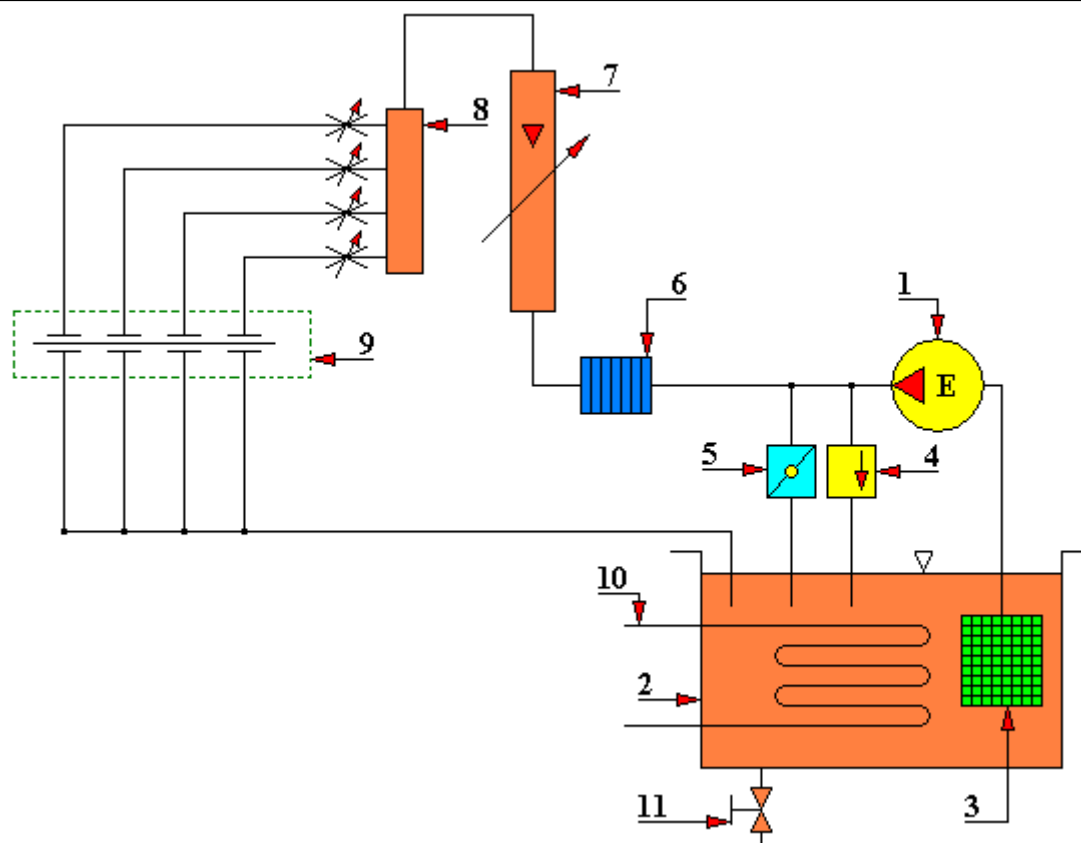


Fig. 4.2.29.10. A diagram of the hydraulic lubrication system of the test rig for testing radial slide bearings type PG-4 ŁA (B)

1 - gear pump; 2 - oil tank; 3 - mesh filter; 4 - safety valve; 5 - throttle valve; 6 - plate-slot filter; 7 - rotameter; 8 - distributor; 9 - tested bearings; 10 - oil cooler; 11 - oil drain valve

Among others, the testing of bearings made of wood-based materials was carried out at the above test rigs. The reason for conducting these tests was the necessity to search for substitute materials for the scarce non-ferrous metals and their alloys, which constitute a basic bearing material. Wood-based materials, including waste generated in wood industry plants, have become the object of interest of designers of this type of bearings. From a wide range of wood-based materials, the following were used for slide bearings:

- wood glued under pressure (so-called laminated wood);
- pressed and bent wood (so-called compressed wood)

The testing of slide bearings made of wood-based materials was carried out by the Department of Fundamentals of Machine Design at Gdańsk University of Technology under the supervision of prof. dr hab. K. Zygmunt, commissioned by the Gdańsk Shipyard. The initiator of the above-mentioned testing was the Wood Technology Institute in Poland. The results of the conducted tests allowed evaluating the laminated wood of Polish production as a full-value bearing material, equal to *lignum vitae*.

1 - steel sleeve; 2 - bearing's upper half-shell made of compressed wood; 3 - bearing's lower half-shell made of compressed wood; 4 - inner retaining ring (2 pieces)

Lignum vitae, a South American wood with high resin content, has been used very frequently as a material for the stern slide bearings of transatlantic passenger ship propellers and US submarines.

Similar comprehensive studies were carried out on compressed wood bearings (Fig. 4.2.29.11) predicting their operation in mixed friction conditions [185]. The bearing shells are made of two types of wood: birch and beech, saturated with machine oil.

The mechanical properties of compressed wood made of birch wood were as follows:

- compressive strength along the grain (perpendicular to the bearing surface): 500 kG/cm²;
- Brinell hardness inside the bearing shell: 16.4 kG/mm²;
- water absorption after 24 hours of soaking in water was: 21%;
- swelling parallel to the pressing direction after 24 h of soaking in water was: 9.8%.

The mechanical properties of compressed wood made of beech wood were as follows:

- compressive strength along the grain (perpendicular to the bearing surface): 526 kG/cm²;
- Brinell hardness inside the bearing shell: 16.2 kG/mm²;
- water absorption after 24 hours of soaking in water was: 13%;
- swelling parallel to the pressing direction after 24 h of soaking in water was: 6.8%.

For this testing, the above bearings were made by the Wood Technology Institute in Bydgoszcz.

Two compressed wood bearing half-shells were pressed into the steel sleeve and secured against axial displacement by means of retaining rings. The lubricant was supplied to the bearing through an opening in the upper part of the steel sleeve. Two openings were made in the lower part of the sleeve: one is radial at the edge of the bearing shell, the other is horizontal (in the middle section of the bearing shell, at a distance of approx. 1.5 mm from the sliding surface on the loaded side). Thermocouples were placed in these openings. The main dimensions of the bearing shells are shown in Figure 4.2.29.11. The diametral clearance ranged from 0.25 mm to 0.30 mm.

All the bearing shells had a similar microgeometry and surface smoothness corresponding to the class $\nabla 6 \div \nabla 7$. It was obtained by turning with the same turning knife made of high-speed steel at a cutting speed of $v=300$ m/min and a feed rate of $p=0.13 \div 0.20$ mm/rev. After treatment, birch bearing shells were smoother than the beech ones.

Before these tests, the bearings were stored in a state unprotected from external conditions.

After the tests, the bearings were stored in airtight plastic bags (in the case of bearing shells used for water lubrication tests, the bags were also filled with moistened cotton wool).

Shaft journals used for the tests were made of NZ 2 steel and 45 steel, surface hardened to a hardness of $48 \div 52$ HRC. The surface smoothness of journals corresponded to the class $\nabla 10$. The greatest height of unevenness on the journal surface R_{\max} did not exceed $0.5 \mu\text{m}$. The diameter of the journals was $d = \text{Ø } 51.25_{-0.01}$ mm.

The testing of properties of the compressed wood bearing shells was carried out with:

- water lubrication;
- lubrication with Lux 7 engine oil;
- lubrication with ŁT 4 solid lubricant;
- dry work.

During the test the following were measured, among others:

- bearing load (using strain gauges);
- frictional moment (using strain gauges);
- temperature of the lubricant at the inlet to the bearing (by means of a thermocouple);
- temperature of the lubricant at the outlet from the tested bearing (using a thermocouple);
- temperature on the load side of the bearing at a distance of approx. 1.5 mm from the sliding surface (using a thermocouple);
- pressure of the lubricant;
- amount of lubricant;
- journal rotational speed;
- linear wear (using a micrometer);
- bearing shell geometry before and after the tests (using a roundness error measuring unit according to doc. inż. T. Gerlach).

The results of the above-mentioned tests and a detailed program of preliminary tests are presented in the work [185].

According to the data provided by the Wood Technology Institute in Poland (Gluing Workshop in Bydgoszcz), compressed wood sleeves were used, for example, in the bucket chain joints of the KW-253 excavator prototype, where they turned out to be better than iron-graphite sleeves.

4.2.30. Pressure ring of the test rig for testing lubricating properties and friction phenomena according to the patent PL 125 950

The pressure ring according to the patent PL 125 950, the authors of which are Jerzy Korycki, Daniel Kujawski, Stanisław Radkowski, Zygmunt Świerczewski and Bogdan Wislicki, is installed in the test vessel of the test rig for testing the lubricity properties and oils and for testing friction phenomena.

According to a characteristic feature of the invention, at half of its height, the ring has radial openings with a diameter allowing free flow of the lubricant to be tested (Fig. 4.2.30.1). On its outer cylindrical surface, the ring has a recess (undercut) around its entire circumference, which serves to collect the lubricant flowing out of the described openings. The height of the ring is selected in such a way in relation to the diameter of the balls and the depth of the test vessel that its lower face surface can be used for mounting body flanges or various plates used in the testing of friction junctions in this vessel.

The ring according to this patent has a pressure function and function of a component part of the lubrication system allowing minimizing the dimensions of the test vessel and reducing the level of external disturbances.

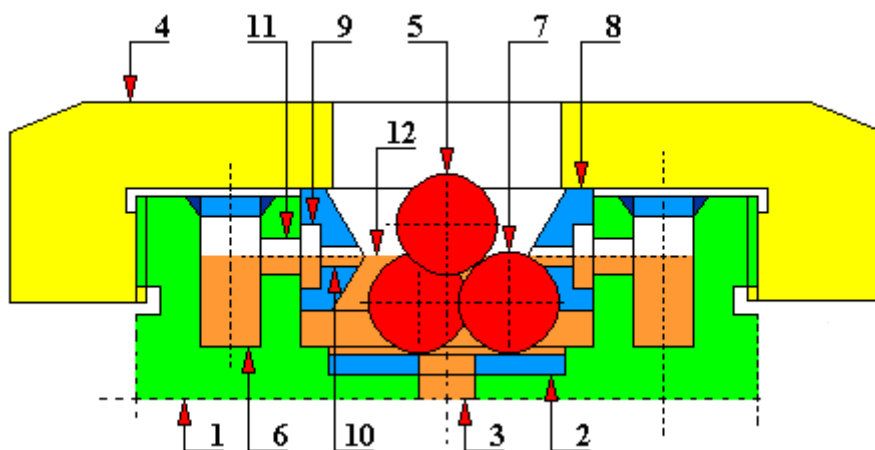


Fig. 4.2.30.1. Pressure ring of the test rig for testing lubricating properties and friction phenomena according to the patent PL 125 950

1 - test vessel body; 2 - hard plate; 3 - opening; 4 - nut; 5 - top ball; 6 - annular channel; 7 - three lower balls; 8 - pressure ring; 9 - recess (undercut) of the pressure ring; 10 - radial through openings; 11 - opening; 12 - tested lubricant

4.2.31. Test rig for testing rolling bearings according to the patent PL 129 957

The test rig, according to the patent PL 129 957, author of which is Adam Rozenau, is intended for testing rolling bearings under transverse load with relative rotational motion of the rings of the tested bearing.

The essence of the operation of this test rig is as follows (Fig. 4.2.31.1, 4.2.31.2 and 4.2.31.3). The tested bearing 1 is mounted on the journal 11 which ends the drive system 2. On the outer ring of the tested bearing there is a measuring pin 3, the end of which is supported in the measuring head body 4 by a ball joint 5 and springs 6. The two piezoelectric sensors 7 for testing the vibration level of the bearing are placed on the measuring pin 3. The loading system is a hydraulic cylinder 8 rotationally positioned around the longitudinal axis of the tested bearing. Spring elements 10 are put between the body of the measuring head 4 and the base of the test rig 9. It is possible to support the measuring pin 3 by means of an annular spring.

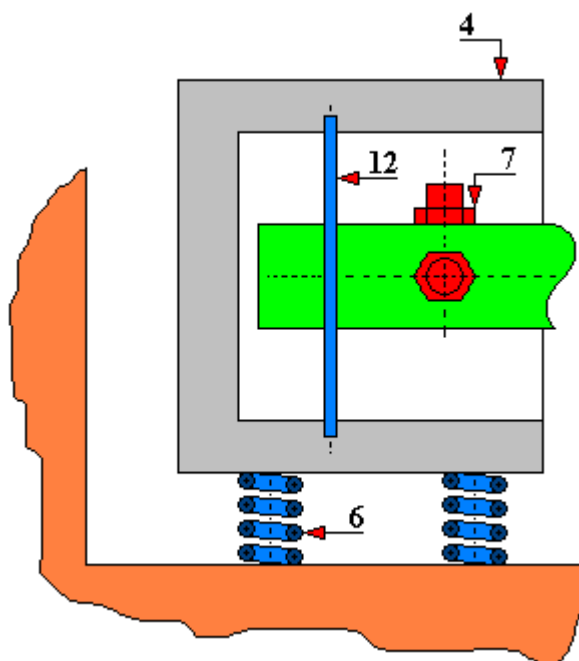


Fig. 4.2.31.1. Support for the measuring pin with an annular spring. A test rig for testing rolling bearings according to the patent PL 129 957

1 - tested bearing; 2 - drive system; 3 - measuring pin; 4 - body of the measuring head; 5 - ball joint; 6 - spring; 7 - piezoelectric sensor; 8 - hydraulic cylinder; 9 - test rig base; 10 - spring element; 11 - journal; 12 - annular spring (description applies to all drawings of this test rig)

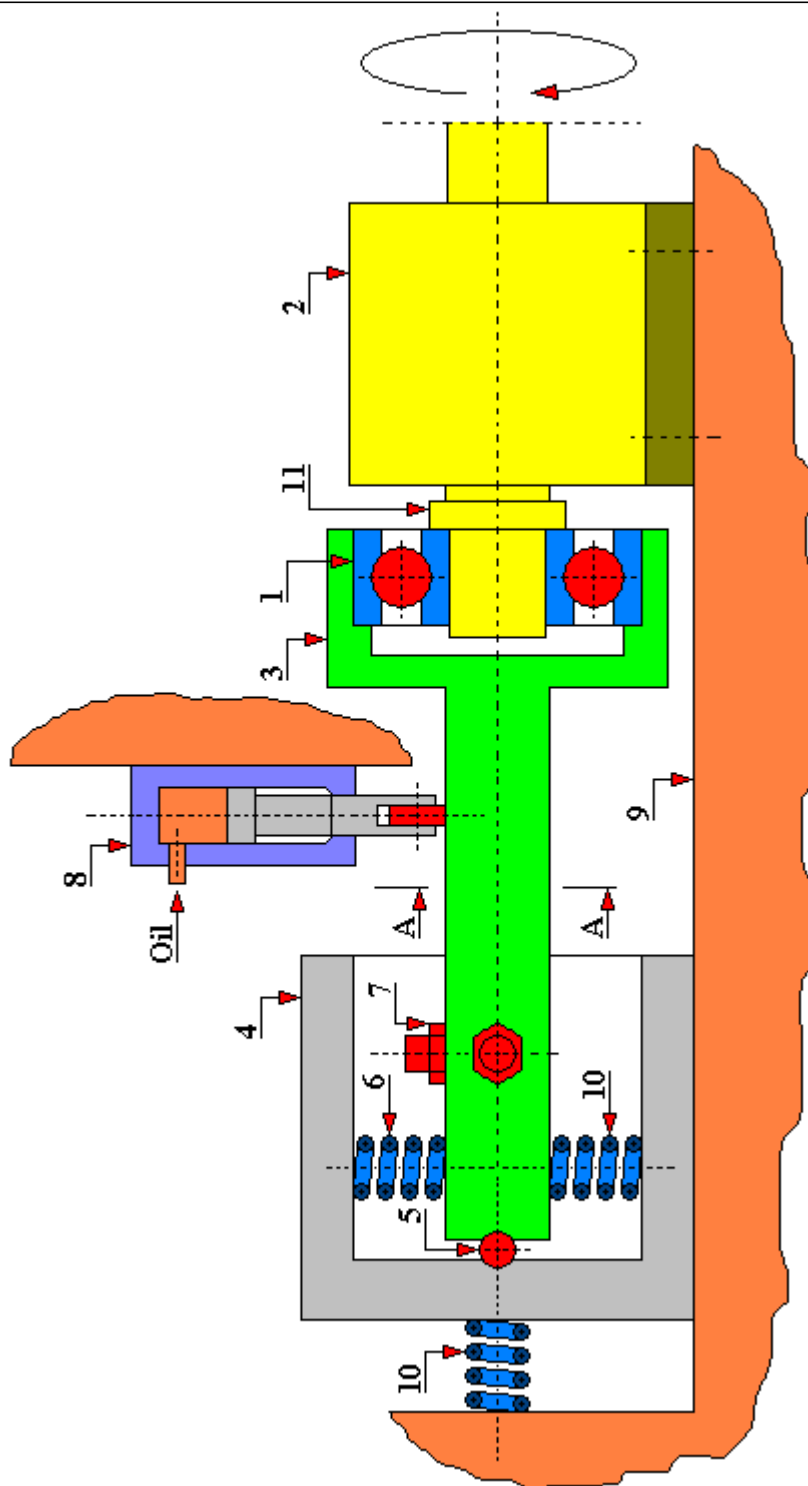


Figure 4.2.31.2. A diagram of a test rig for testing rolling bearings according to the patent PL 129 957

1 - tested bearing; 2 - drive system; 3 - measuring pin; 4 - body of the measuring head; 5 - ball joint; 6 - spring; 7 - piezoelectric sensor; 8 - hydraulic cylinder; 9 - test rig base; 10 - spring element; 11 - journal; 12 - annular spring (description applies to all drawings of this test rig)

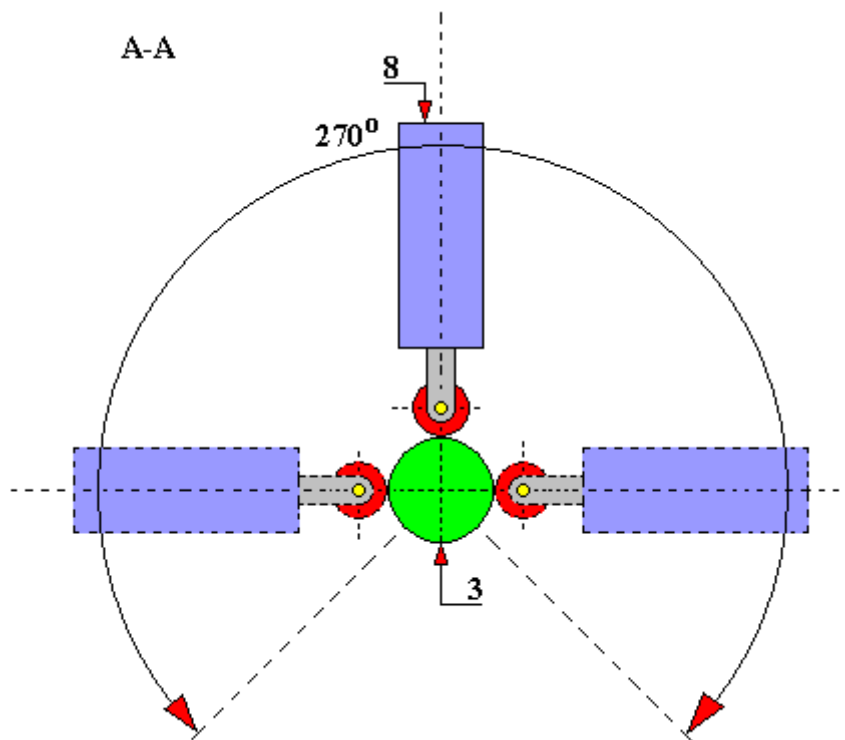


Fig. 4.2.31.3. A diagram of a test rig for testing rolling bearings according to the patent PL 129 957. A-A cross section

1 - tested bearing; 2 - drive system; 3 - measuring pin; 4 - body of the measuring head; 5 - ball joint; 6 - spring; 7 - piezoelectric sensor; 8 - hydraulic cylinder; 9 - test rig base; 10 - spring element; 11 - journal; 12 - annular spring (description applies to all drawings of this test rig)

4.2.32. Tribological rig for testing starter bearings

The durability of slide bearings directly depends on the course of their wear process. In conditions of a mixed friction which occurs e.g. in porous bearings, abrasive wear predominates. The intensity of abrasive wear depends, among others, on the conditions of mating between the friction surfaces of the journal and the shell occurring in a given bearing. Changes in the resistance to motion reflect the intensity of abrasive wear. These resistances depend on many factors, including the type and properties of the lubricant.

The values characterizing the resistance to motion may include:

- value of the moment of friction;
- coefficient of friction (coefficient of resistance to motion);
- size of vibrations;
- change of temperature value.

The work [16] presents a tribological rig for testing starter bearings - Fig. 4.2.32.1.

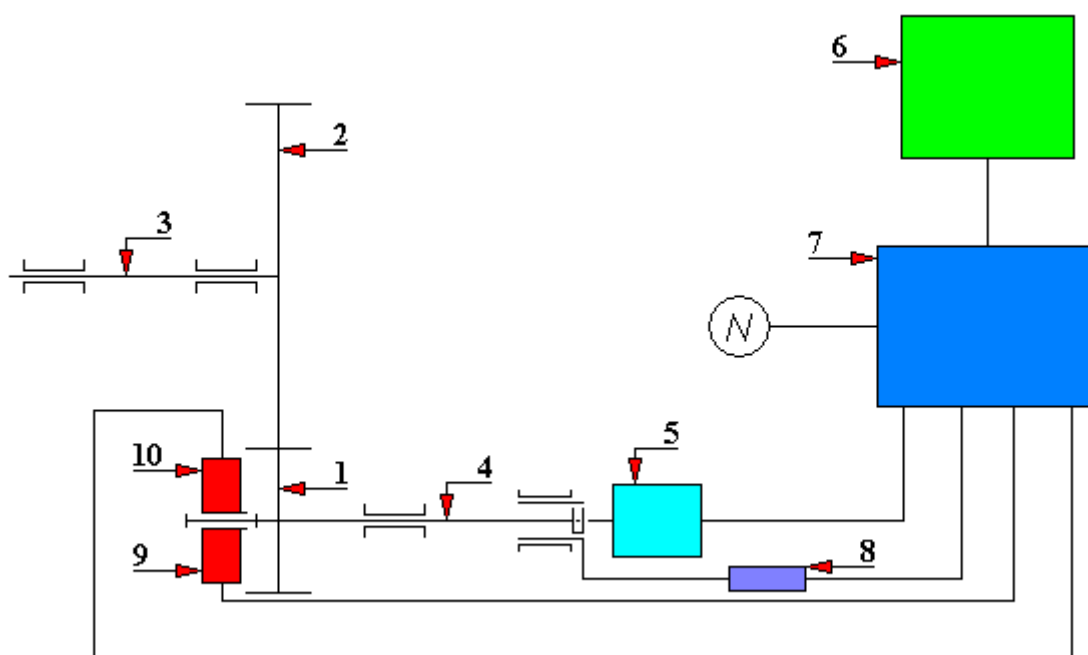


Fig. 4.2.32.1. A diagram of the rig for measuring the moment of friction, temperature and vibration level in the starter bearing system

1 - pinion; 2 - flywheel; 3 - engine crankshaft; 4 - starter shaft; 5 - rotational speed sensor; 6 - computer disc; 7 - control card cage; 8 - force sensor; 9 - thermocouple; 10 - vibration sensor

This test rig is characterized by the following construction. In the system of thrust slide bearings, a sensor is mounted to measure the moment of friction received from the bearing shell of the starter shaft. The value of the force generated by the moment of friction on the sensor lever arm is measured by a force sensor 8. The force sensor 8 is mounted on a tripod capable of positioning relative to the frame on which the motor rests. The rotational speed of the starter rotor is measured by a rotational speed sensor 5 connected to the rotor by means of an elastic clutch. The rotational speed sensor was attached to the stator of the starter with a special clamping ring. A vibration (acceleration) sensor 10 and a thermocouple 9 are mounted in the front cover.

Signals from sensors 5, 8, 9 and 10 are sent to the control card cage 7. The signals from the control card cage are transmitted to the computer disc and recorded.

4.3. Group 3 (universal rigs)

4.3.1. Four-ball test rig

This is a test rig which belongs to the group of machines used for testing, among others, a scuffing process - with a point contact. A general diagram of a four-ball friction contact is shown in Figure 4.3.1.1. This contact is made of four balls arranged in the form of a regular tetrahedron. This allows the forces to be evenly distributed in the contact. The fourth upper ball is pressed against the other balls under a given load and given rotational speed.

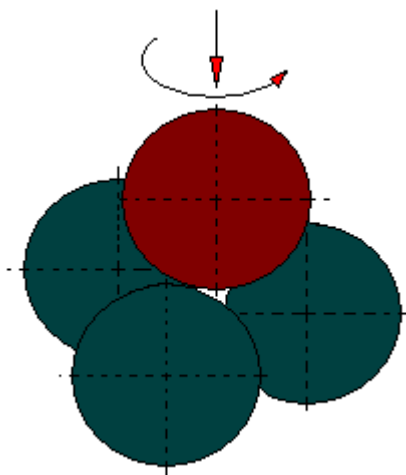


Fig. 4.3.1.1. General diagram of a four-ball friction contact

The standardized parameters of tests carried out on a four-ball test rig include:

- weld point;
- wear index;
- anti-wear properties;
- seizing load.

The above-mentioned parameters are precisely defined in the following standards: PN-76/C-04147, GOST 9490, DIN 51 350, ASTM D 2596, ASTM D 2783, ASTM D 2266, ASTM D 4172 in which the test parameters are presented. The friction contact of the four-ball test rig is a concentrated triple point contact formed by the surface of four balls of the diameter of 1/2". This feature of the four-ball test rig is also its disadvantage because we are limited only to a point contact and to one material of the contacting elements - bearing steel. An additional disadvantage of tests performed on this test rig is the method of assessing the suitability of lubricants based on the measurements of wear marks and the balls welding force. This necessity causes the application of high contact loads that may not be present in the actual pairs. These very high loads cause qualitative differences in the contact area compared to the contact area occurring in the actual, typical operating conditions of machines.

The friction test on the four-ball test rig can be performed according to the standard ASTM D 2783-82. *Measurement of Extreme-pressure Properties of Lubricating Fluids (Four-Ball Method)*.

Depending on the design of the lower three balls mounting, it is possible to recreate, under load and in motion, the conditions of sliding friction (Figure 4.3.1.2) or rolling friction conditions, ball by ball or, to be precise, balls on the groove-shaped raceway, formed during the tests on the upper ball (Figure 4.3.1.3).

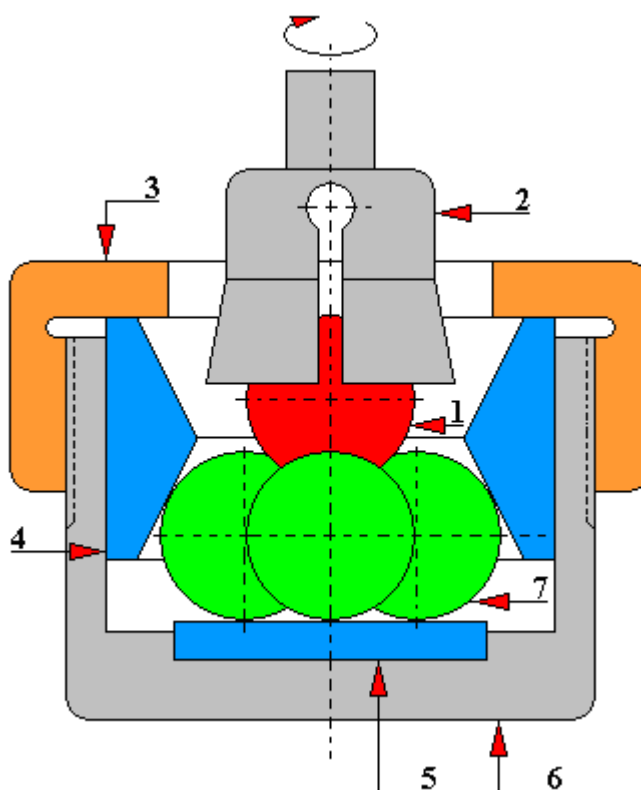


Fig. 4.3.1.2. Diagram of mounting the friction contact of the four-ball test rig for recreating the sliding friction conditions [175, 176]

1 - upper ball, 2 - upper ball holder, 3 - nut, 4 - inner ring, 5 - replaceable plate, 6 - cup, 7 - lower balls

On the above test rig it is also possible to carry out tests on the destruction of the surface of balls when running dry or with the use of a lubricant. When testing with the use of a lubricant (cooling agent), a rubber hose should be connected to the cup holder chamber through which the cooling agent (e.g. water) or lubricant is flowing. In order to regulate the temperature of the cooling agent (or lubricant), e.g. a Höppler thermostat can be connected to the system.

Changing the way of mounting the three lower balls as shown in Figure 4.3.1.3. results in rotations of the upper ball in relation to the axis of the handle, while the lower balls perform a complex rolling-rotary motion that cannot be easily determined from the conditions of motion. This nature of motion causes a continuous change of the contact surface of the lower balls with the upper one.

The ball arrangement in a four-ball test rig, as shown in Figure 4.3.1.2, is used for testing wear and lubricity, while the ball arrangement as shown in Figure 4.3.3 is used for testing anti-pitting properties.

In order to determine the slide that occurs at the contact point of the balls it was necessary to further redesign the cup of the four-ball test rig, as shown in Figure 4.3.1.4.

All balls shown in Figures 4.3.1.2, 4.3.1.3 and 4.3.1.4 are 1/2 " in diameter.

The apparent simplicity of the construction of the four-ball test rig holds the complexity of the ball movement, difficulties in determining the slides, the complexity of the variability of the stress field, the complexity of the destruction of the surface of the rolling elements, either with or without the use of a lubricant.

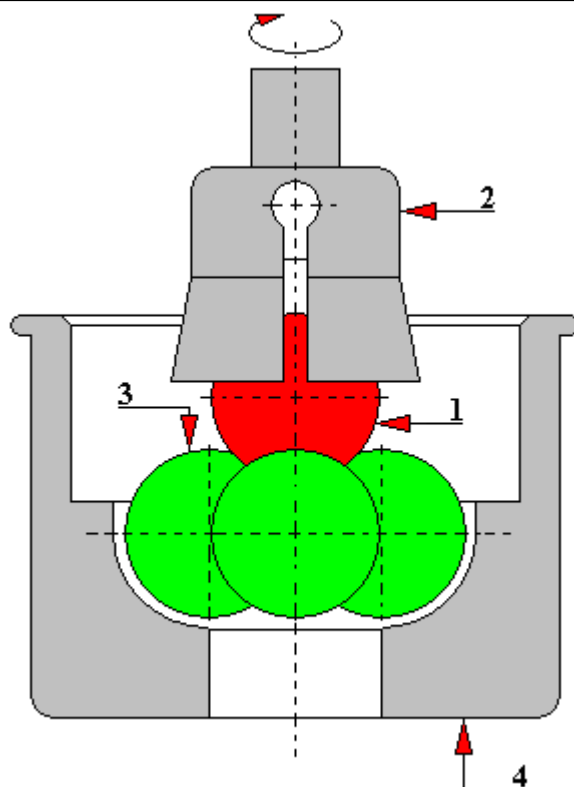


Fig. 4.3.1.3. Scheme of mounting the friction contact of the four-ball test rig to reproduce the conditions of rolling friction of a ball on ball, (more precisely, ball on a groove-shaped raceway) [175, 176]

1 - upper ball, 2 - upper ball holder, 3 - lower balls, 4 - cup

Another typical friction contact used in this type of test rigs is shown in Figure 4.3.1.5. The lower three balls were replaced in this case with three discs. The drive is transmitted to the upper ball which also exerts pressure on the three disc supports. The shape of the cup used allows testing with or without the use of a lubricant. A further development of this solution is to replace three discs with rollers as shown in Figure 4.3.1.6. Other solutions of typical friction contacts of the four-ball test rig are shown in the Figures: 5.3.1.7÷5.3.1.12.

Figure 4.3.1.13 shows an example of a four-ball test rig. It is designed to measure the durability of the oil layer between rubbing rolling elements and to measure the value of the moment of friction between these elements. The test elements are four balls with a diameter of $\varnothing 12.7$ [mm] made of bearing steel with a hardness of 62 ± 66 HRC. The three balls are permanently placed in the cup. And the fourth ball is fixed in the holder and pressed against the others with normal force. The ball fixed in the handle can only rotate at 1500 [rpm], which is also the rated speed of the induction motor. It is caused by – because of the simplicity of construction – lack of gear or frequency converter (inverter) in the drive system. The rotational speed of 1500 [rpm] corresponds to the friction speed of 0.55 [m/sec]. The normal load pressing the balls may be up to 1000 [N]. The measures of the quality of the tested oil are the diameters of the wear marks on the surfaces of three stationary balls during one minute – test time. The value of the normal load at which there is a sharp increase in the moment of friction and the size of wear marks is a measure of the lubricity of the tested oil. Oil tests on this four-ball test rig may only be performed at ambient temperatures. Figure 4.3.1.14 shows a general diagram of an exemplary four-ball test rig.

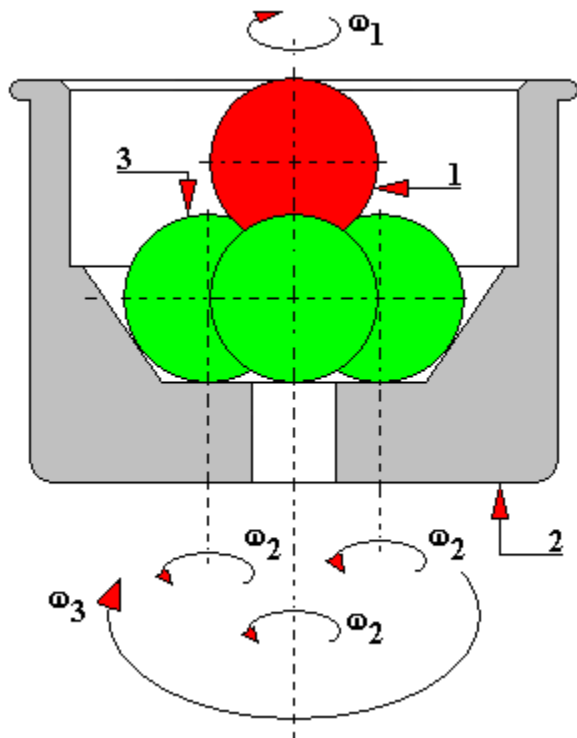


Fig. 4.3.1.4. Scheme of mounting the friction contact of the four-ball test rig for reproducing the conditions of rolling friction of a ball on ball proposed in the study by Biezborodko and Winogradow in order to determine the sliding values [5]

1 - upper ball, 2 - cup, 3 - three lower balls, ω_1 - angular velocity of the upper ball, ω_2 - angular velocity of the rotation of the lower balls, ω_3 - angular velocity of the rotary motion of the lower balls

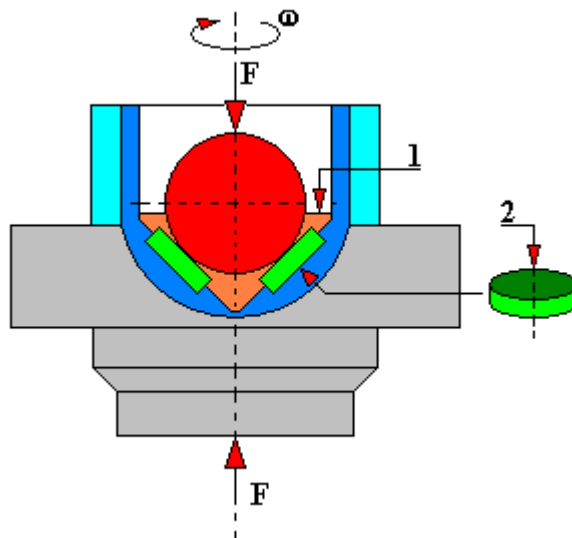


Fig. 4.3.1.5. Diagram of mounting the friction contact of a four-ball test rig consisting of three discs and a ball of 1/2 "or 1" in diameter [175, 176]

1 - lubricant, 2 - disc, F - pressing force, ω - angular velocity of the ball

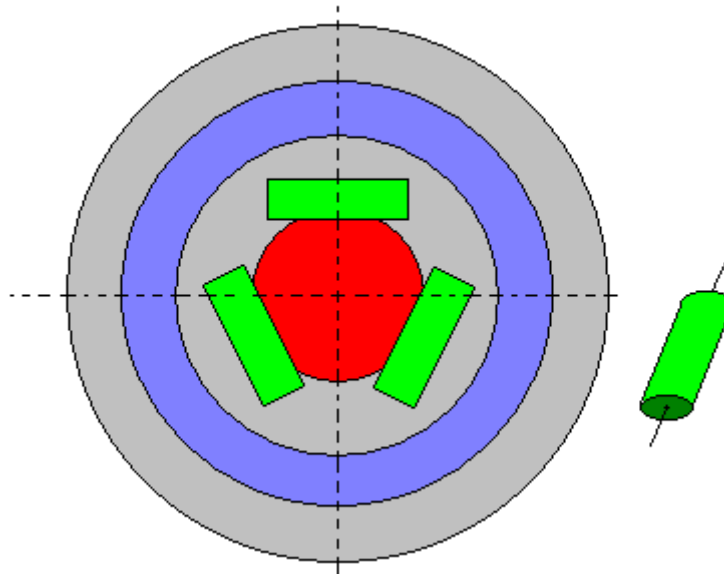


Fig. 4.3.1.6. Diagram of mounting the friction contact of the four-ball test rig consisting of three shafts and a ball with a diameter of 1/2 "or 1" [175, 176]

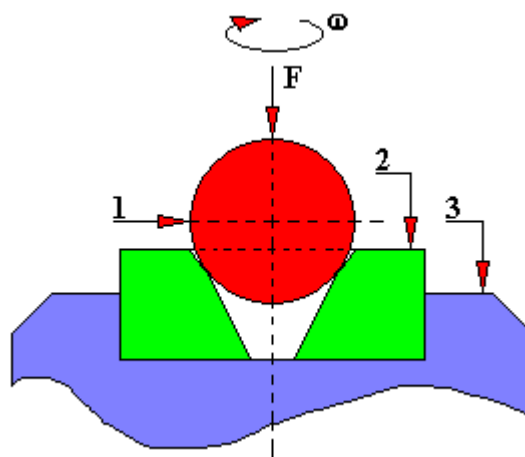


Fig. 4.3.1.7. Diagram of mounting the friction contact of the four-ball test rig consisting of a ring with an internal conical hole and a ball with a diameter of 1/2 " [175, 176]
1- rotating ball, 2 - ring, 3 - ring holder, F - pressing force on the ball, ω - angular velocity of the ball

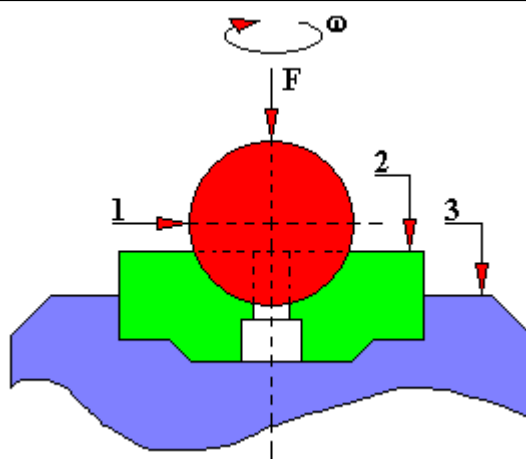


Fig. 4.3.1.8. Diagram of mounting the friction contact of the four-ball test rig consisting of a ring with an internal stepped hole and a ball with a diameter of 1/2 " [175, 176]
 1- rotating ball, 2 - ring, 3 - ring holder, F - pressing force on the ball, ω - angular velocity of the ball

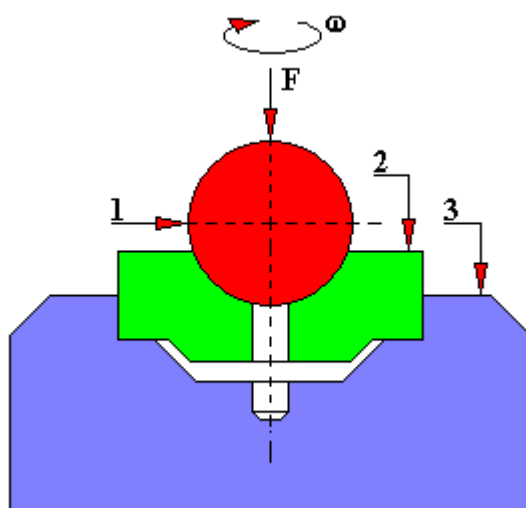


Fig. 4.3.1.9. Diagram of mounting the friction contact of the four-ball test rig consisting of a ring with an internal non-stepped hole and a ball with a diameter of 1/2 " [175, 176]
 1- rotating ball, 2 - ring, 3 - ring holder, F - pressing force on the ball, ω - angular velocity of the ball

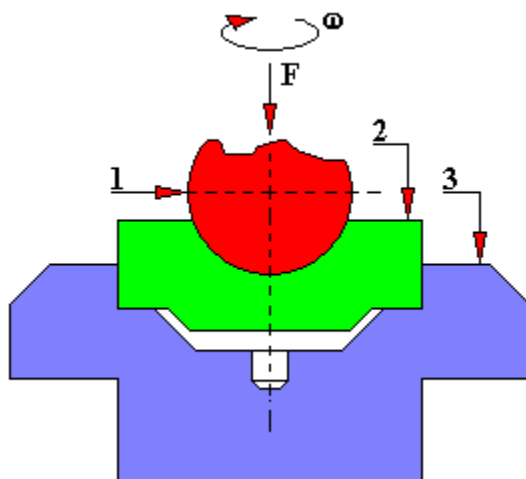


Fig. 4.3.1.10. Scheme of mounting the friction contact of the four-ball test rig consisting of a base with a spherical cap-shaped recess and a ball with a diameter of 1" [175, 176]
 1- rotating ball, 2 - base, 3 - base mounting holder, F - pressing force on the ball, ω - angular velocity of the ball

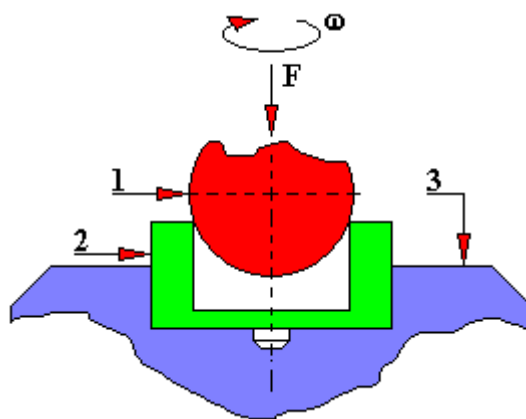


Fig. 4.3.1.11. Diagram of mounting the friction contact of a four-ball test rig consisting of a cylinder and a ball of 1" in diameter [175, 176]
 1- rotating ball, 2 - cylinder, 3 - cylinder mounting holder, F - pressing force on the ball, ω - angular velocity of the ball

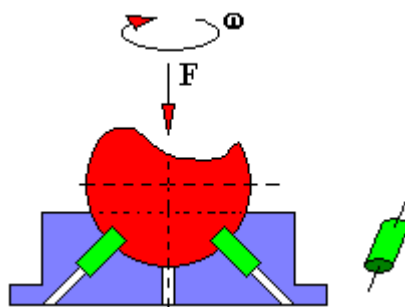


Fig. 4.3.1.12. Diagram of mounting the friction contact of a four-ball test rig consisting of three shafts and a ball with a diameter of 1" [175, 176]



Fig. 4.3.1.13. General view of an exemplary four-ball test rig with a friction contact as in Figure 4.3.1.2.

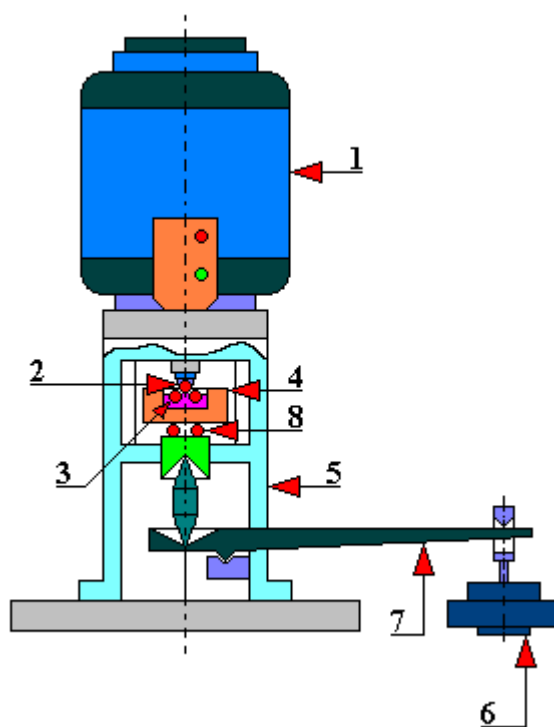


Fig. 4.3.1.14. General diagram of a four-ball test rig
1 - electric motor, 2 - upper ball, 3 - three lower balls, 4 - cup, 5 - body, 6 - given load, 7 - loading lever arm, 8 - thrust bearing.

4.3.2. Test rig for testing sliding and rolling friction of friction wheels TM 260.1

The above-mentioned test rig (Fig. 4.3.2.1) is a commercial test rig of the company 'Gunt'. It is designed to determine the effect of slip on the friction force and to determine the coefficient of friction depending on:

- load;
- type of lubricant;
- rotational speed;
- type of friction contacts.

This test rig is equipped with a force transducer designed to determine the friction force, and tachometers. In order to carry out tests on this test rig it is necessary to provide a drive, and for this purpose the TM 260 drive unit (Fig. 4.3.2.2) is used which provides a smooth change of velocity.

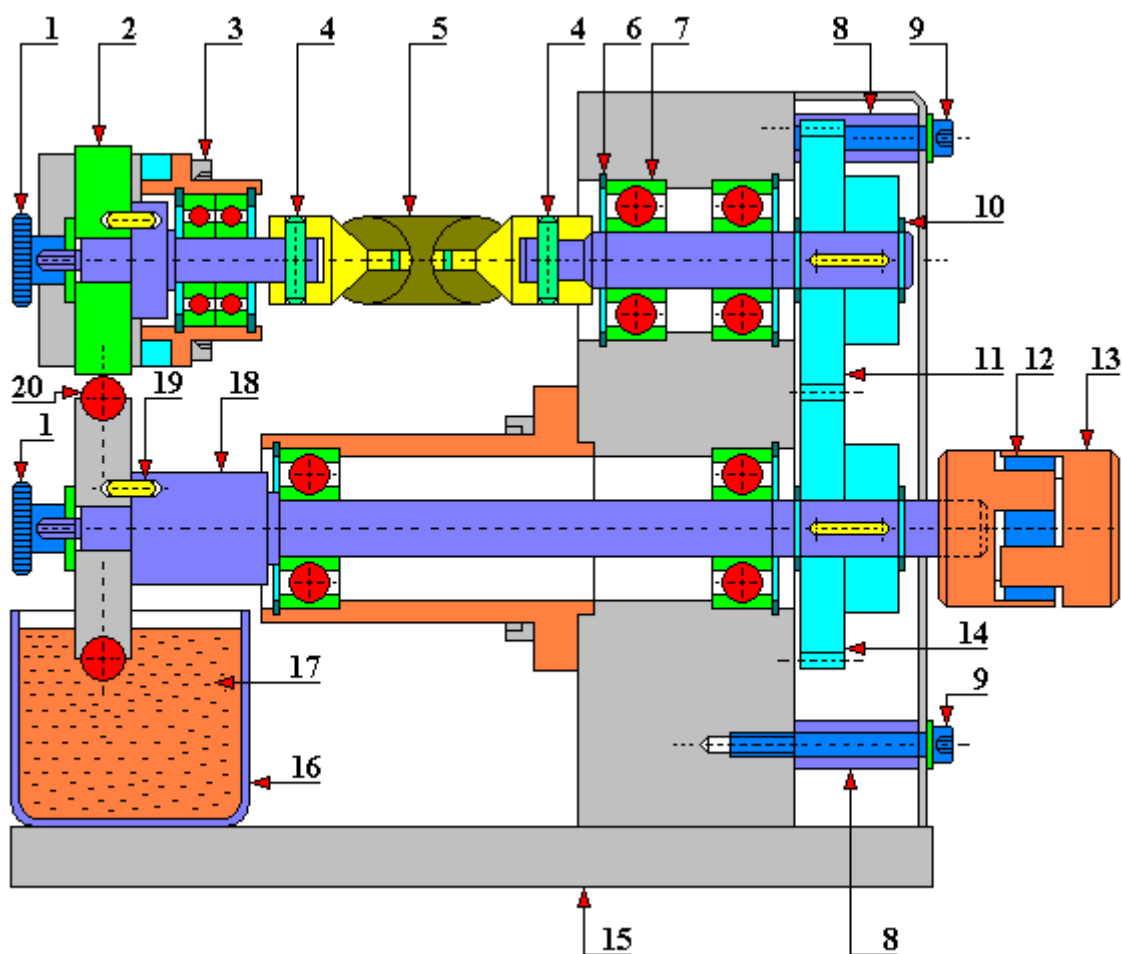


Fig. 4.3.2.1. General view of TM 260 test rig

1 - knurled nut; 2 - friction disc (counter-sample); 3 - nut; 4 - pin; 5 - ball joint; 6 - inner retaining ring; 7 - single row ball bearing; 8 - distance sleeve; 9 - mounting screw; 10 - outer retaining ring; 11 - gear wheel z_2 ; 12 - shock-absorbing clutch liner; 13 - drive connection; 14 - gear wheel z_1 ; 15 - base; 16 - lubricant container; 17 - lubricant; 18 - live shaft; 19 - pin; 20 - rubber ring (sample)

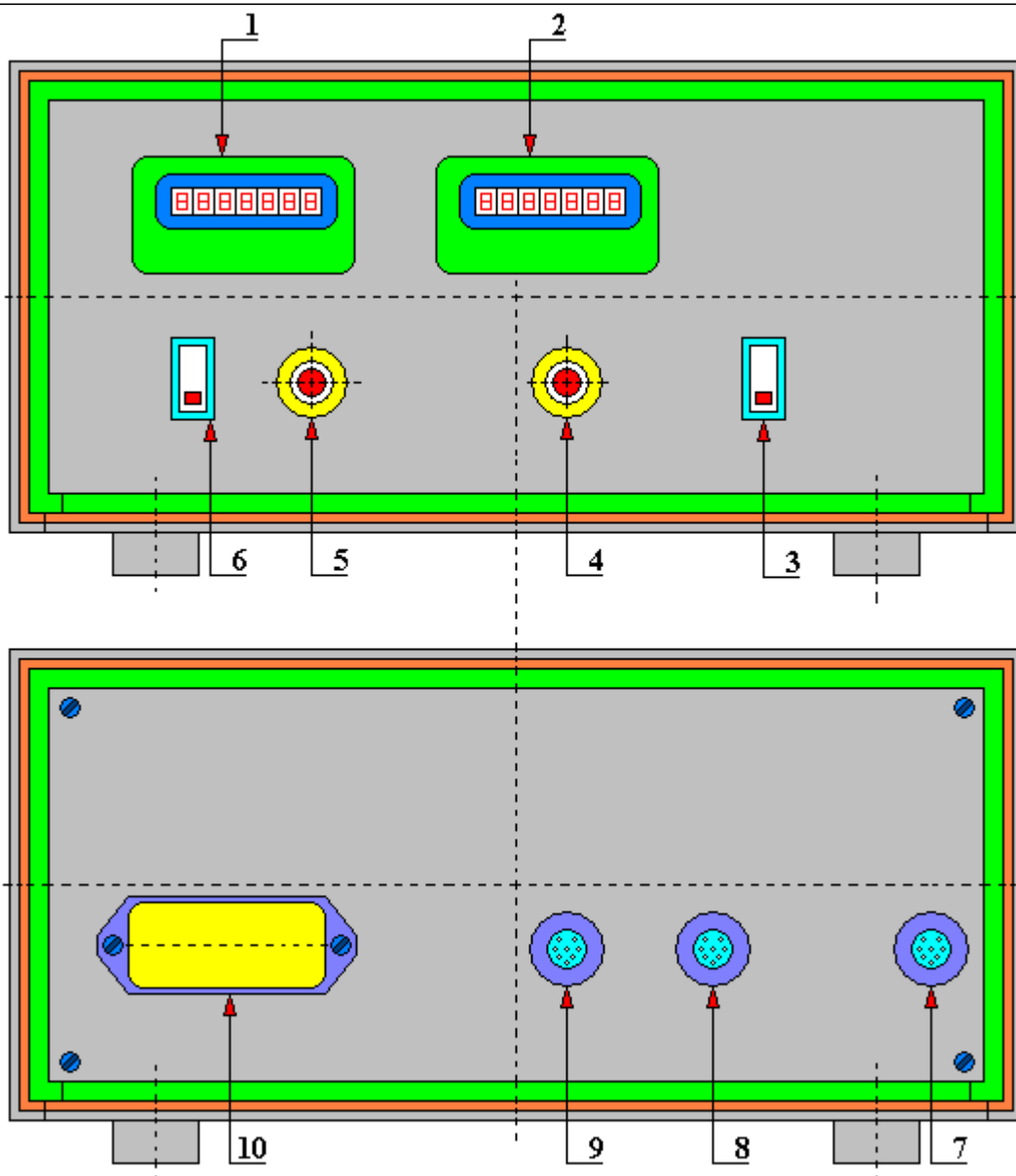


Fig. 4.3.2.2. TM 260 drive unit. General view

1 - RPM display; 2 - friction force display; 3 - lighting switch; 4 - force calibration potentiometer; 5 - rotational speed potentiometer; 6 - power switch; 7 - lighting socket; 8 - force transducer socket; 9 - engine connection socket; 10 - power grid socket

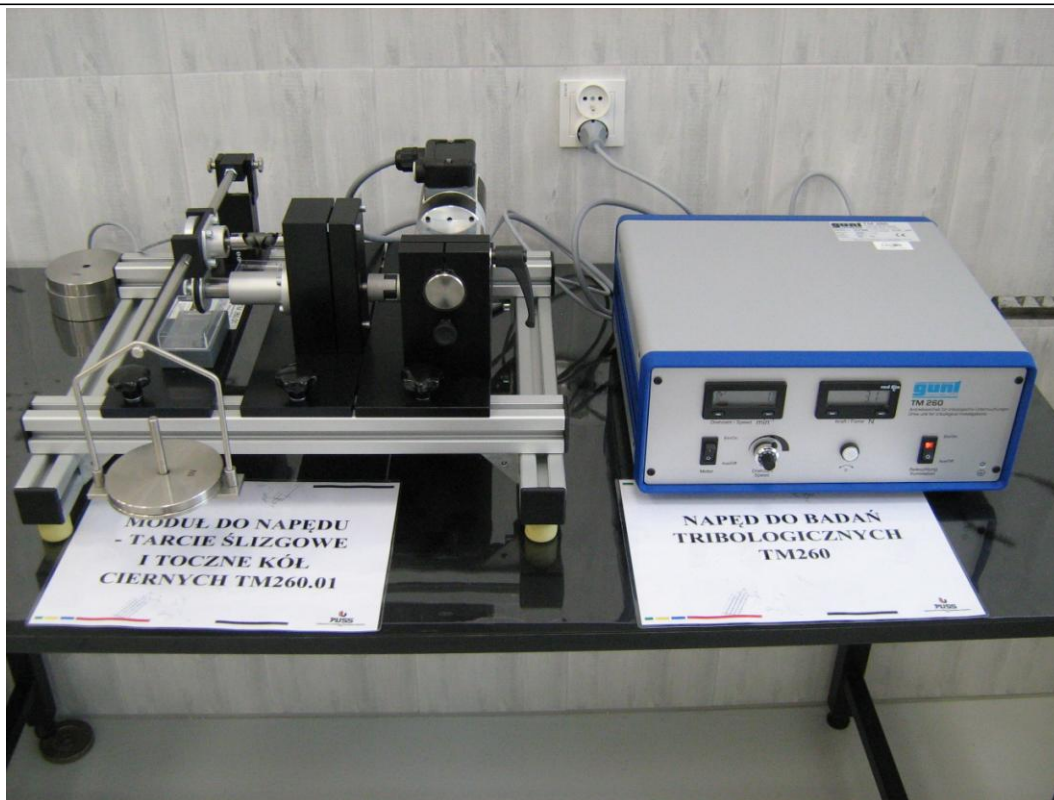


Fig. 4.3.2.3. General view of TM 260 test rig

4.3.3. CMI-2 (SMC-2) tribotester

The SMC-2 tribotester is designed to test materials for wear and determine their anti-friction properties in sliding friction and rolling friction at normal temperatures with pairs of disc-disc, disc-block and sleeve-shaft samples. This test rig is a development of an earlier design of the tribotester also of the Soviet production MI-1.

The specifications of this test rig are as follows:

- number of revolutions of the shaft of the lower sample: 300; 500; 1000 [rpm];
- the range of a permissible error of the number of revolutions of the lower sample shaft from the measured quantity: $\pm 10\%$;
- the acceptable error range of the measured sum (total) value of the revolutions of the lower sample according to the meter: ± 100 revolutions;
- maximum moment of friction: 150 [kg force · cm];
- maximum moment of friction for the shaft-sleeve and disc-block pair at 1000 rpm: 100 [kg force · cm];
- moment of friction measuring range: from 15 to 150 [kg force · cm];
- a relative spread (variation) indicated by the torque meter from the measured value should not be greater than 5%;
- a relative spread (variation) of the load scale indications from the measured value should not exceed 7%;
- electric power demand should not exceed 2.2 [kW];
- the torque meter sensitivity threshold in the working range should not exceed 1.5 [kg force · cm].

The overall dimensions of the test rig are as follows:

- length: 1130 [mm];
- width: 655 [mm];
- height: 1030 [mm].

The load measurement range [kg force] is:

- for round samples (disc type) and disc-block type: from 20 to 200 [kg force];
- for shaft-sleeve samples: from 50 to 500 [kg force].



Fig. 4.3.3.1. A general view of the SMC-2 test rig (on the left side a control panel with the printer of the moment of friction)

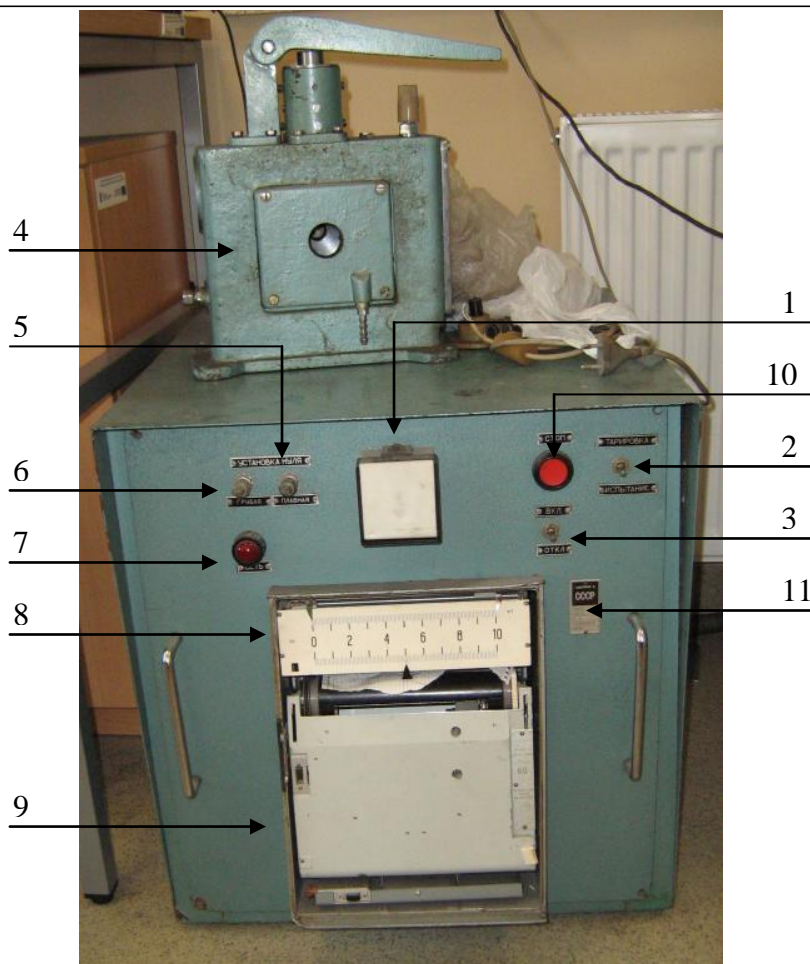


Fig. 4.3.3.2. A general view of the SMC-2 tribotester control panel with a printer of the moment of friction. At the top, instrumentation intended for determining indications of the load mechanism for the range of up to 500 kg of force
 1 - pulse counter, 2 – ‘Test/Tare’ switch, 3 - pulse counter switch, 4 - instrumentation for determining the load mechanism indications for the range up to 500 kg of force, 5 - zero setting (accurate), 6 - zero setting (rough), 7 - mains connection indicator, 8 - potentiometer (regulator), 9 - printer, 10 – ‘Stop’ button, 11 - rating plate.

The overall dimensions of the control panel are as follows:

- length: 590 [mm];
- width: 570 [mm];
- height: 550 [mm].

The weight of test rig is 500 kg.

The weight of the control panel is 75 kg.

The SMC-2 tribotester consists of the following main components:

- a) carriage mechanism;
- b) load mechanism;
- c) headstock of the lower sample;
- d) sensor;
- e) drive mechanism;
- f) control panel.

In order to carry out tests in low-viscosity lubricants with different samples this test rig was equipped with two test chambers with auxiliary units. The first exchangeable test chamber is

designed for disc-disc and disc-block samples. And the second is designed only for samples of the sleeve-shaft type. Fig. 5.3.3.1 shows a general view of the SMC-2 tribotester located at the Technical Faculty of the University of Warmia and Mazury in Olsztyn.



Fig. 4.3.3.3. A view of the carriage drive shaft after removing the cover. Visible pipes for cooling water supplied from the water supply system

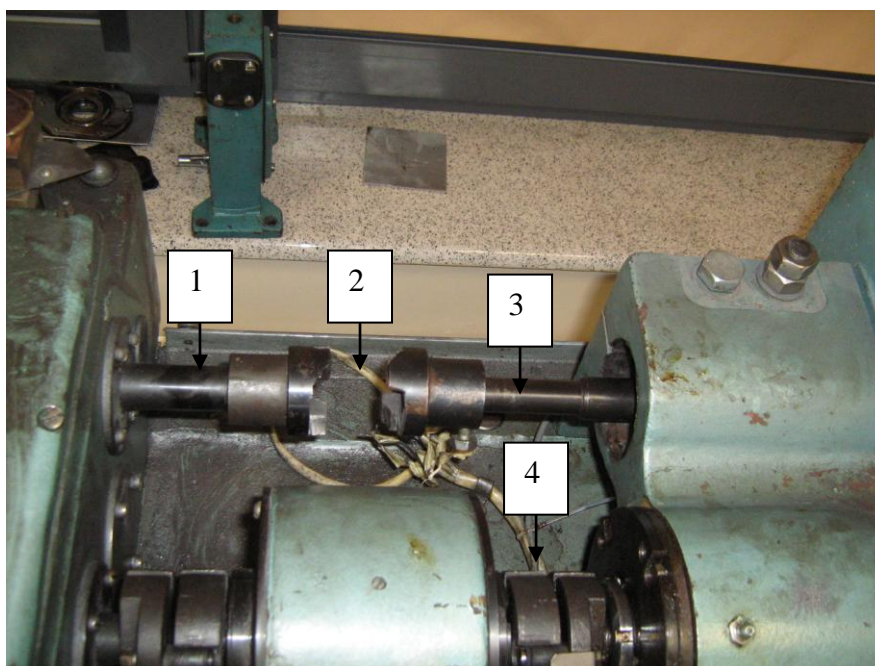


Fig. 4.3.3.4. A view (after removing the cover) of the place for the installation of the inductive sensor
1 - drive shaft on the reducer side, 2 - connection point of the inductive sensor, 3 - return shaft from the upper sample, 4 - carriage drive shaft



Fig. 4.3.3.5. The lower sample rev counter used in the original equipment of the SMC-2 tribotester



Fig. 4.3.3.6. In the foreground - a carriage drive shaft. In the far right - the lower sample drive shaft, on the left - the upper sample shaft

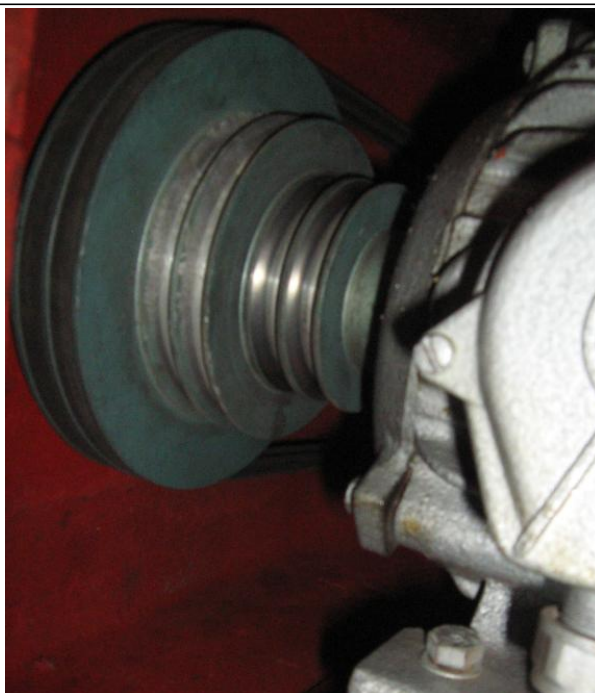


Fig. 4.3.3.7. A view of belt pulleys mounted on the shaft of the SMC-2 tribotester drive motor. There are two V-belts on each wheel step

The control panel (Fig. 4.3.3.2.) is a separate unit of the SMC-2 tribotester which can be put in a different place. The operator controlling the test rig can track the measured moment of friction on the potentiometer scale. On the front surface of the control panel there is also a counter that sums up the number of shaft revolutions of the lower sample. This counter receives electrical control pulses from a neodymium sensor located on the carriage drive shaft.



Fig. 4.3.3.8. Hoses of the carriage drive shaft cooling system and the lower sample headstock

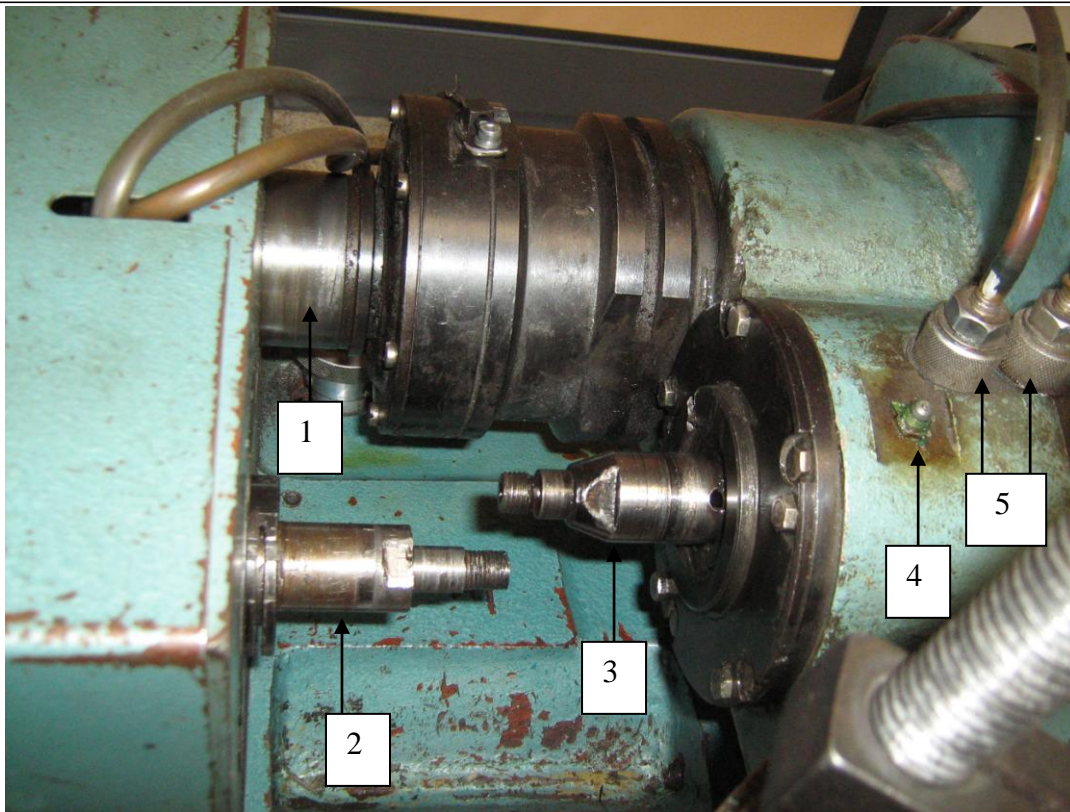


Fig. 4.3.3.9. A view of the working chamber after removal of covers
1 - carriage drive shaft, 2 - lower sample shaft, 3 - upper sample shaft, 4 - grease nipple, 5 - cooling water inlets



Fig. 4.3.3.10. Examples of disc-disc samples made of steel, intended for tribological tests on the SMC-2 test rig



Fig. 4.3.3.11. Examples of disc-disc samples made of abrasive material bonded with a binder, intended for testing on the SMC-2 tribotester

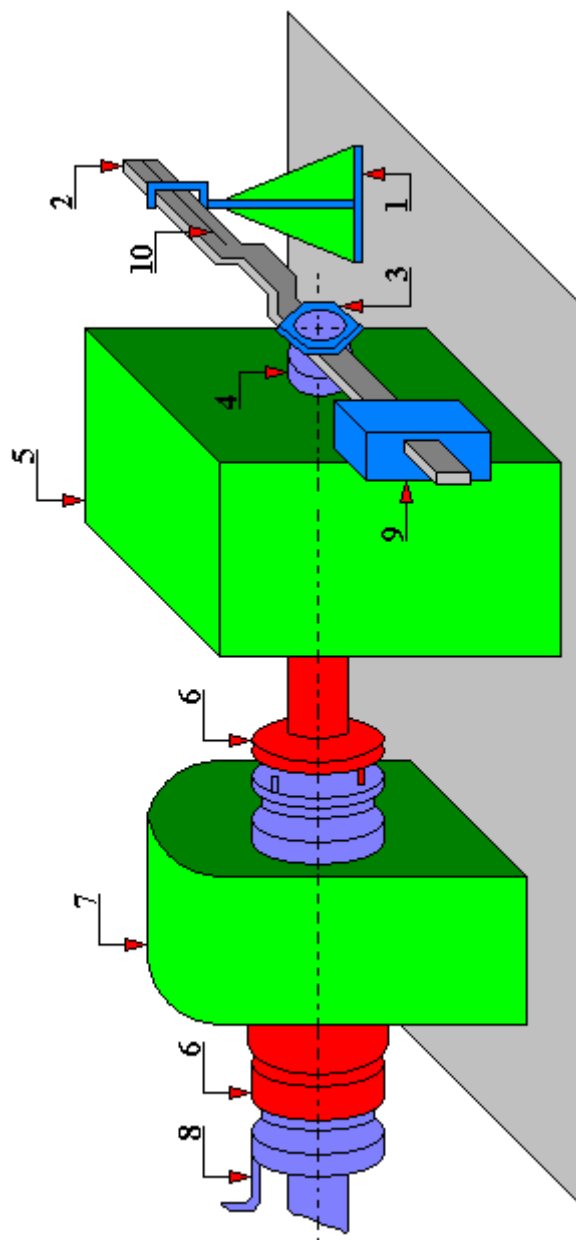


Fig. 4.3.3.12. Setting of the SMC-2 (SMC-2) test rig to control the measuring torque
1 - hanger, 2 - lever, 3 - nut, 4 - shaft, 5 - lower sample plate, 6 - disc, 7 sensor, 8 - retainer, 9 - load, 10 - control scratch

Table 4.3.3.1. Measured measuring torque values

Real moment [kg force · cm]	Motion to the right Graduation of the torque scale	Backward motion Graduation of the torque scale
15	9	9
30	18,5	----
45	28	28
60	37	37
75	46,5	46,5
90	51	51
105	65,5	---
120	73,5	73,5
135	83	83
150	96	96

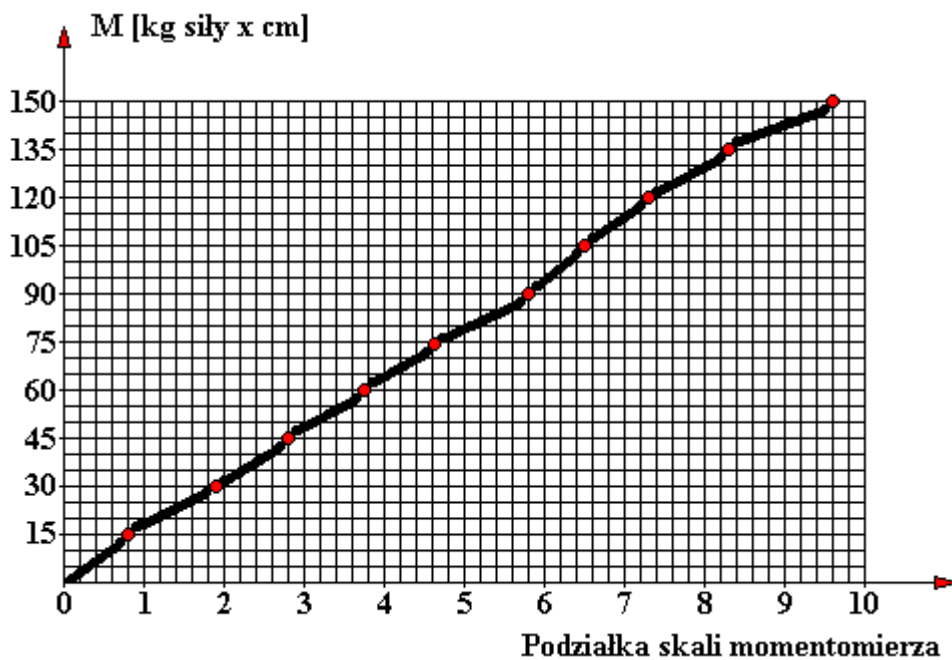


Fig. 4.3.3.13. Measured values of the measuring torque presented in the system: preset real moment M [kg force · cm] and the scale of the torque meter for motion in the right direction (developed on the basis of the measurement results from Table 4.3.3.1)

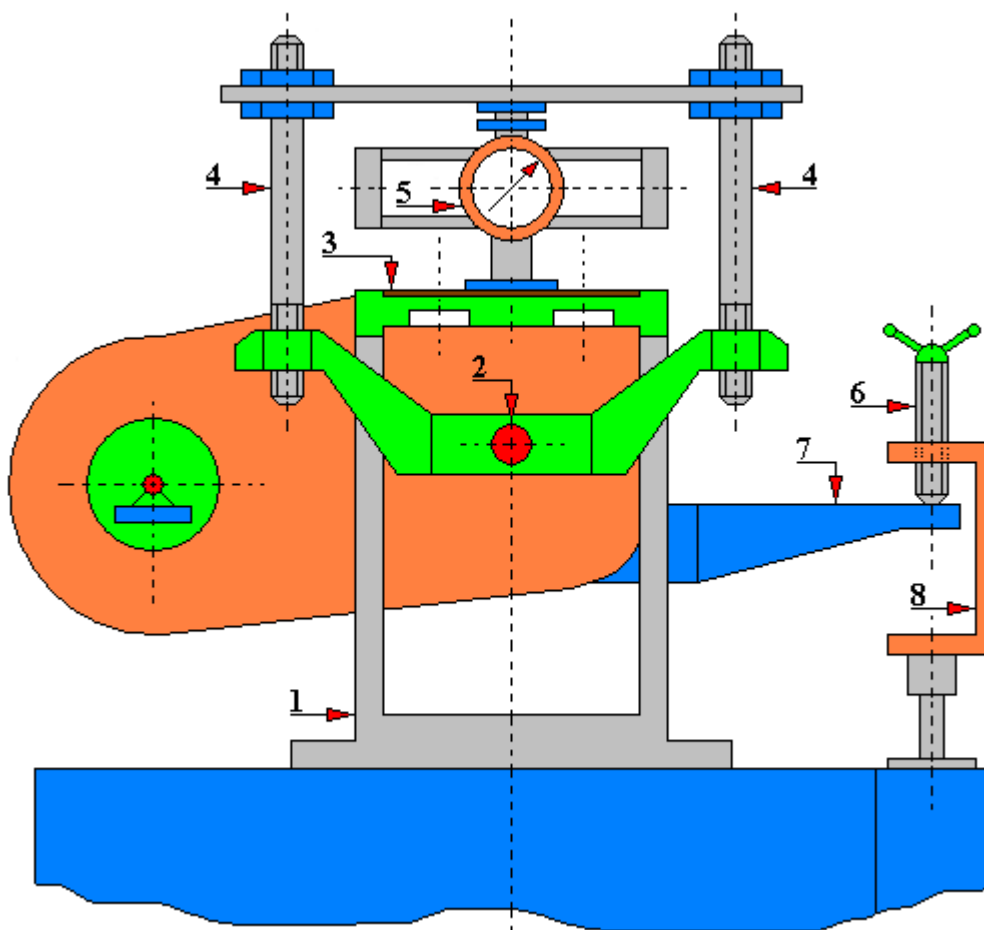


Fig. 4.3.3.14. Setting of the test rig for determining the error / deviation of an applied load up to 200 kg force

1 - body, 2 - main shaft, 3 - cover, 4 - test rig for taring according to a preset load, 5 – dynamometer, type ДОСМ-3-0.2, in accordance with GOST 5.1546-72, 6 - bolt, 7 - bracket, 8 - bail/clamp

Table 4.3.3.2. Measured values of indications of the load mechanism scale during the test up to 200 kg force

Real load [kg force]	Measurement 1	Measurement 2	Measurement 3	Average of measurements
20	11,0	10,0	9,0	10,0
40	42,5	42,0	41,0	41,8
60	81,0	76,0	75,0	77,3
80	105,0	106,5	105,0	105,5
100	---	138,5	137,5	138,0
120	---	182,0	169,0	175,5
140	---	222,0	212,0	217,0
160	---	271,0	260,0	265,5
180	---	310,0	306,0	308,0
200	---	---	---	---

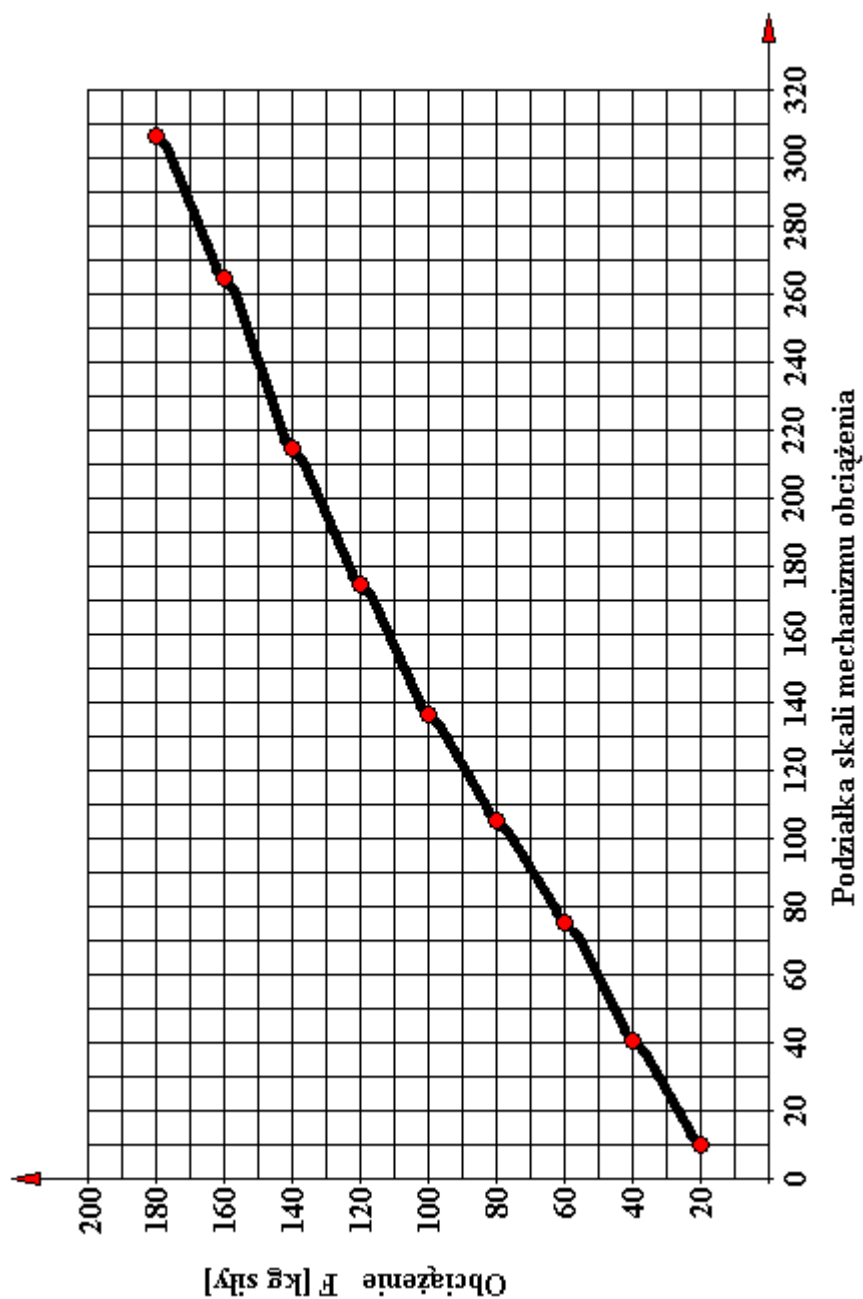


Fig. 4.3.3.15. Measured values of the load mechanism scale depending on the set load for the test up to 200 kg (graph for indications of the mean value from measurements 1, 2 and 3). Prepared on the basis of measurement results from Table 4.3.3.2]

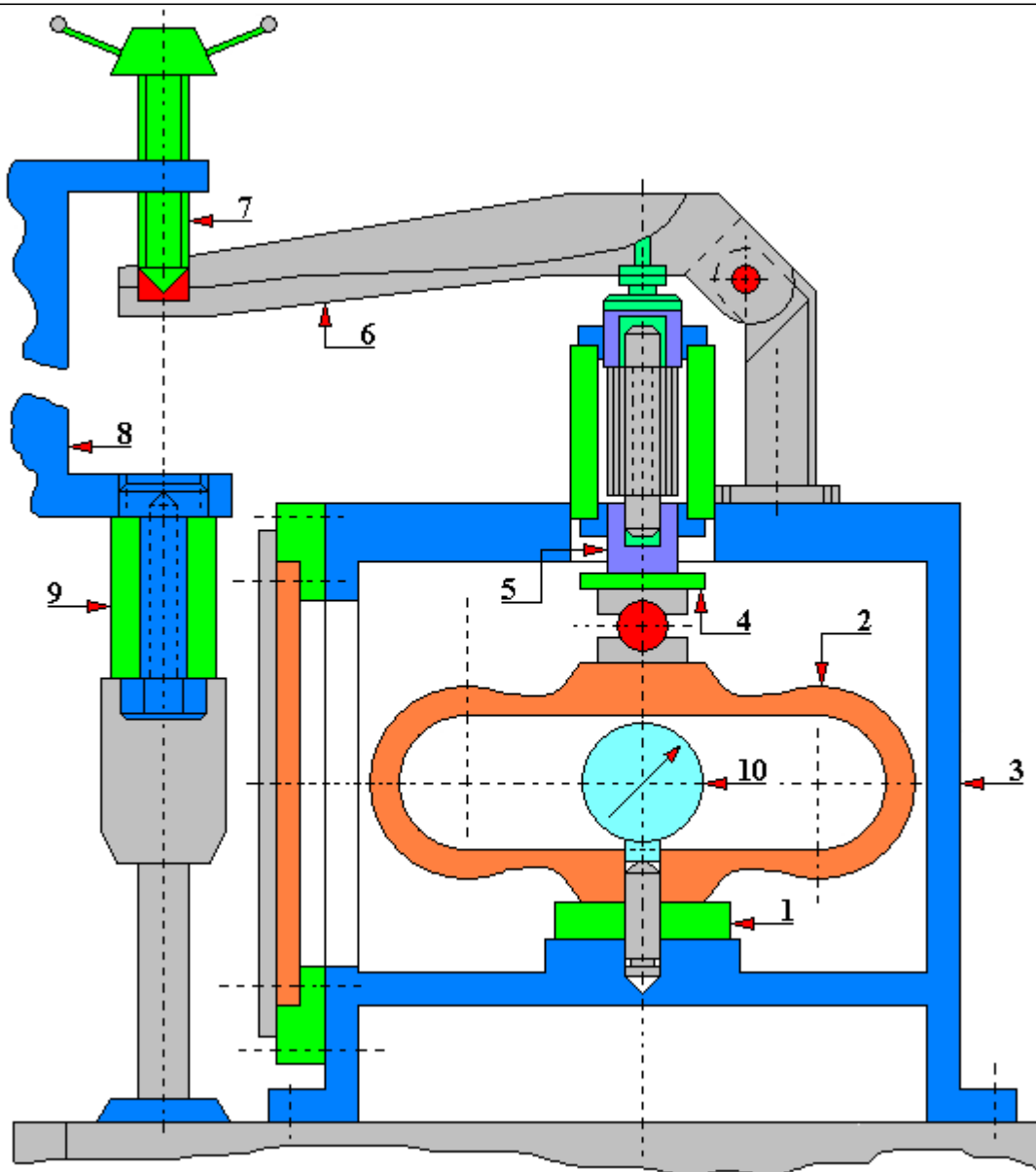


Fig. 4.3.3.16. Setting of the test rig for determining the error / deviation of an applied load up to 500 kg force

1 - plate, 2 - dynamometer type ДОСМ-3-1 in accordance with GOST 9500-60, 3 - chamber for testing samples of the 'sleeve-shaft' type, 4 - plate, 5 - support, 6 - lever, 7 - screw, 8 - bail/clamp, 9 - extension cord, 10 - dynamometer clock

Table 4.3.3.3. The measured values of indications of the load mechanism scale during the test up to 200 kg force

Real load [kg force]	Load mechanism scale indications
50	10
100	48
200	118
300	188
400	258
500	----

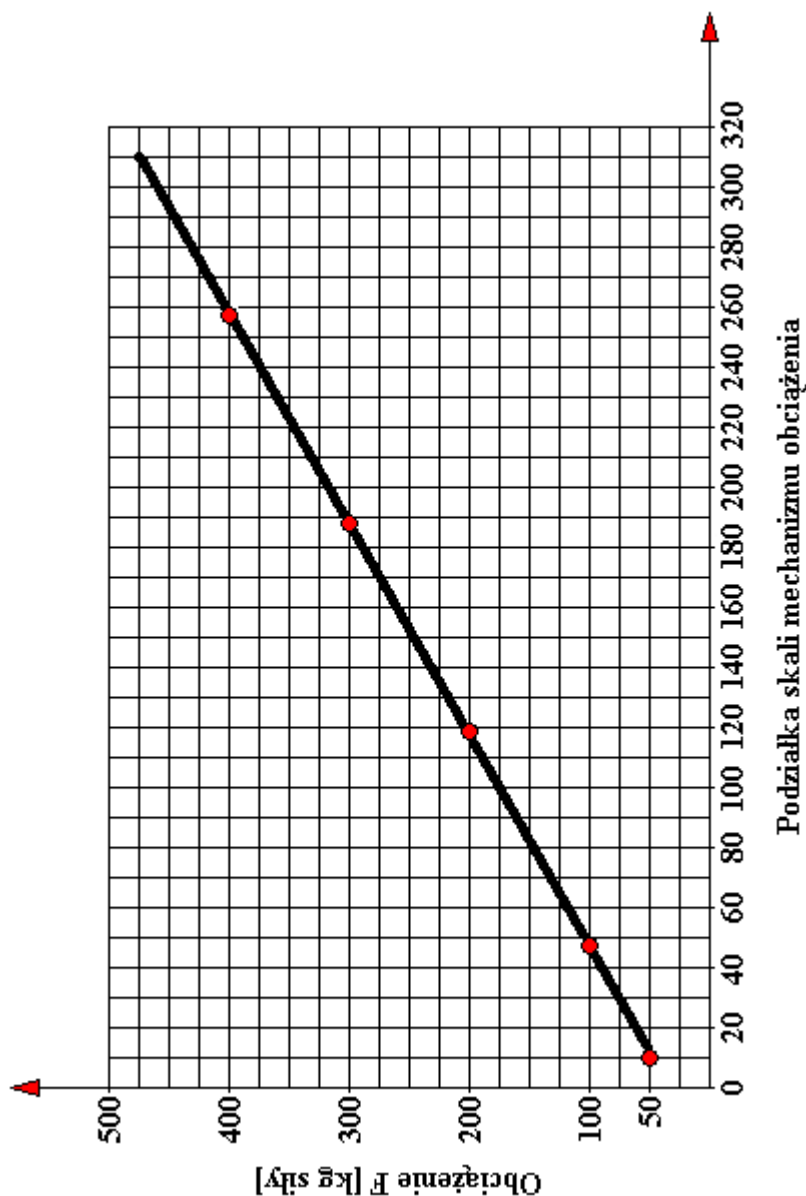


Fig. 4.3.3.17. Measured values of the load mechanism scale depending on the set load for the test up to 500 kg. Prepared on the basis of measurement results from Table 4.3.3.3

Figures 4.3.3.18, 4.3.3.19, 4.3.3.20, 4.3.3.21 and 4.3.3.22 show the types of samples that can be tested on the SCM-2 test rig. In particular, Fig. 4.3.3.18 shows the dimensions of the samples used during the rolling friction tests for the disc-by-disc kinematic pair. This pair can co-work either with or without lubricant. The samples can be made virtually of any material, therefore, in the technical and operational documentation the manufacturer did not specify the grade/grades they should be made of. The tribotester is intended to conduct research, and any restrictions, e.g. concerning the type of materials used for the friction contacts, could be detrimental to science. However, due to a certain dimensional regime, dimensional chain, it is necessary to make test samples so that they have given dimensions, deviations and a given shape.

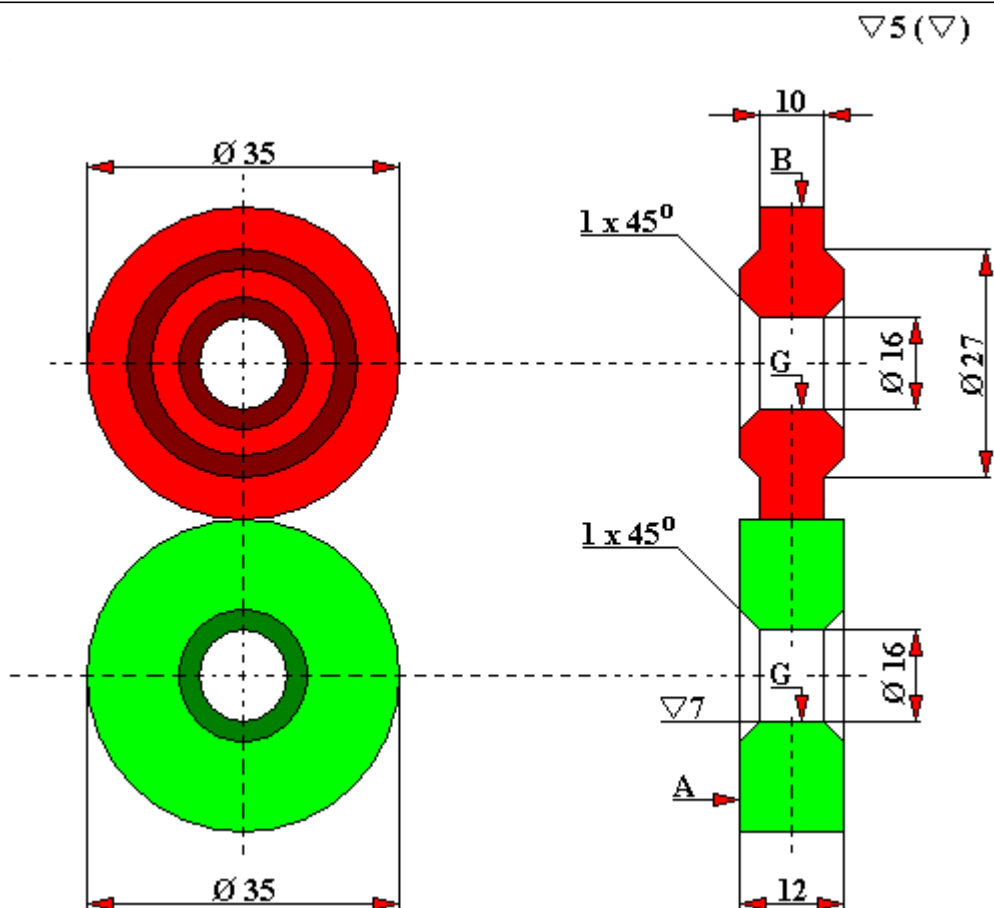


Fig. 4.3.3.18. Round samples (disc by disc)

Non-parallelism of surface A to surface B, maximum 0.02 [mm]. Front run-out of surface A in relation to surface G, maximum 0.02 [mm]. Radial run-out of surface B in relation to surface G, maximum 0.03 [mm].

Fig. 4.3.3.19 shows a mating diagram and dimensions of friction contacts for a disc-block friction contact. In this case there is a sliding friction. The shape of the sample 1 (block) in this case determines the type of contact between the mating surfaces. The shape of the sample 1 reflects the shape of the counter-sample 2, so the type of contact is conformal. The design solution of this tribotester enables testing for the above-mentioned samples both with and without lubricant. The tested sample 1 (block) is mounted in a special holder intended for both samples with conformal contact and with the Hertzian contact. This handle is shown in figures 4.3.3.33 and 4.3.3.34.

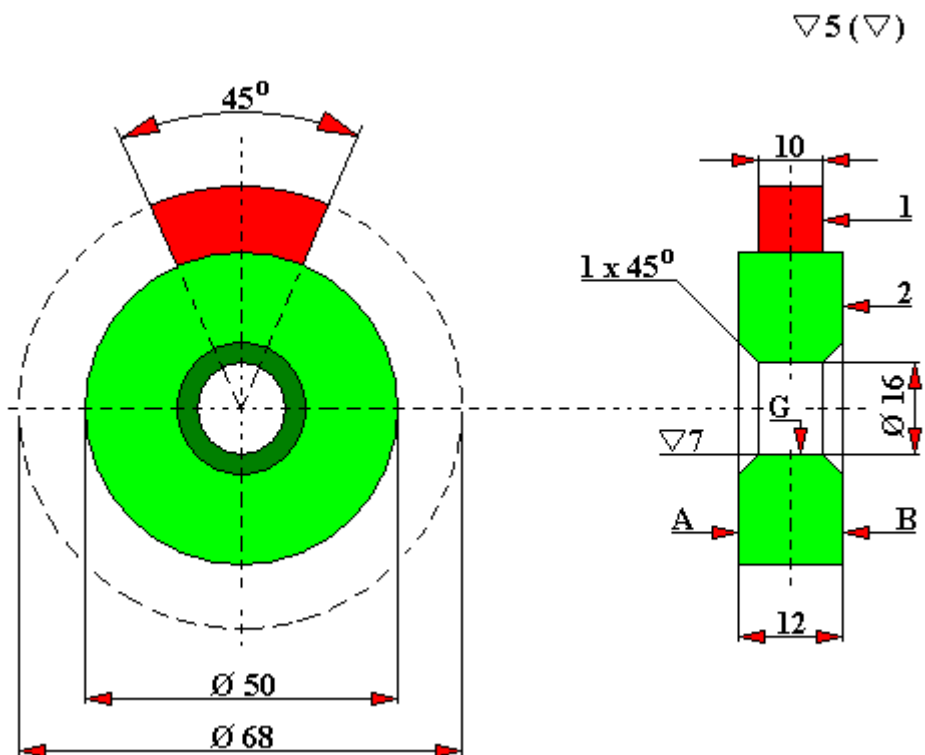


Fig. 4.3.3.19. A mating diagram of the friction contact: disc-block A conformal contact
1 – sample (block), 2 – counter-sample (disc)

Non-parallelism of surface A to surface B, maximum 0.02 [mm]. Front run-out of surface A in relation to surface G, maximum 0.02 [mm]. Radial run-out of surface B in relation to surface G, maximum 0.03 [mm].

Fig. 4.3.3.20 shows a mating diagram and dimensions of friction contacts for a disc-block friction contact for the Hertzian contact. The tested sample 1 has the shape of a cuboid with dimensions of 10x10x25 [mm]. And the geometrical dimensions of the counter-sample 2 are identical to the samples of the disc-block type with a conformal contact. The outer diameter of the counter-sample is $\varnothing 50$ [mm] with a chamfered inner hole of $\varnothing 16$ [mm] intended for mounting the counter-sample on the drive shaft. The thickness of the counter-sample disc is 12 [mm].

The following Figures 4.3.3.21 and 4.3.3.22 show the mating scheme and dimensions of friction contacts for the sleeve-shaft contact. The manufacturer of the SMC-2 tribotester mentions two cases regarding the load on the tested samples:

- up to 250 kg force;
- up to 500 kg force.

In these two cases the geometrical dimensions of both the shaft 2 and the sleeve 1 mating with it are different. These pairs can also mate with or without controlled lubricants.

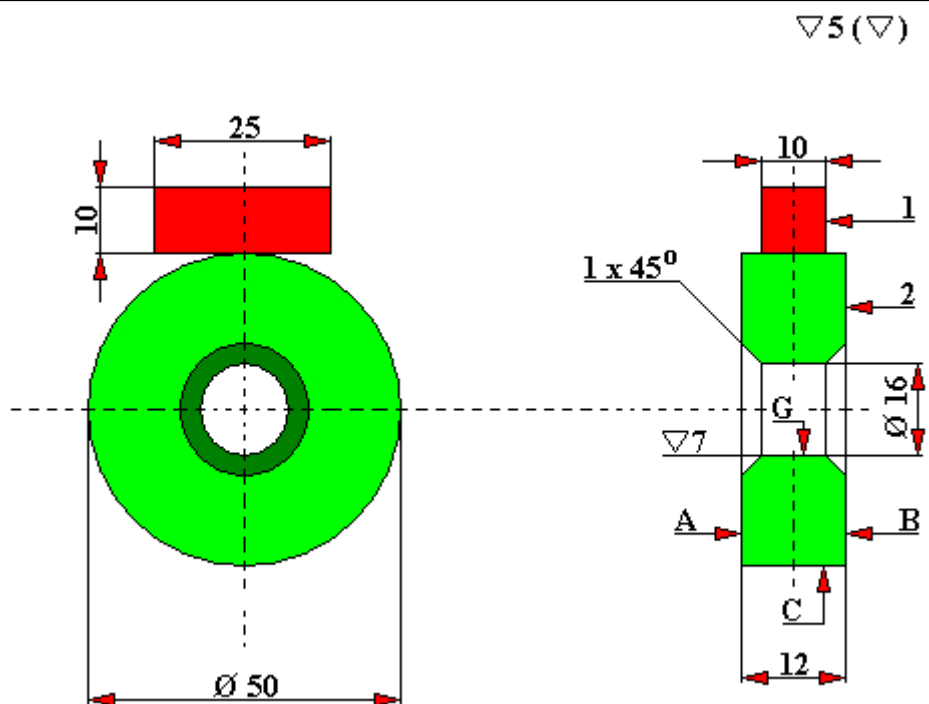


Fig. 4.3.3.20. A mating diagram of the friction contact: disc-block. Hertzian contact 1 – sample (block), 2 – counter-sample (disc). Non-parallelism of surface A to surface B, maximum 0.02 [mm]. Front run-out of surface A in relation to surface G, maximum 0.02 [mm]. Radial run-out of surface C in relation to surface G, maximum 0.03 [mm].

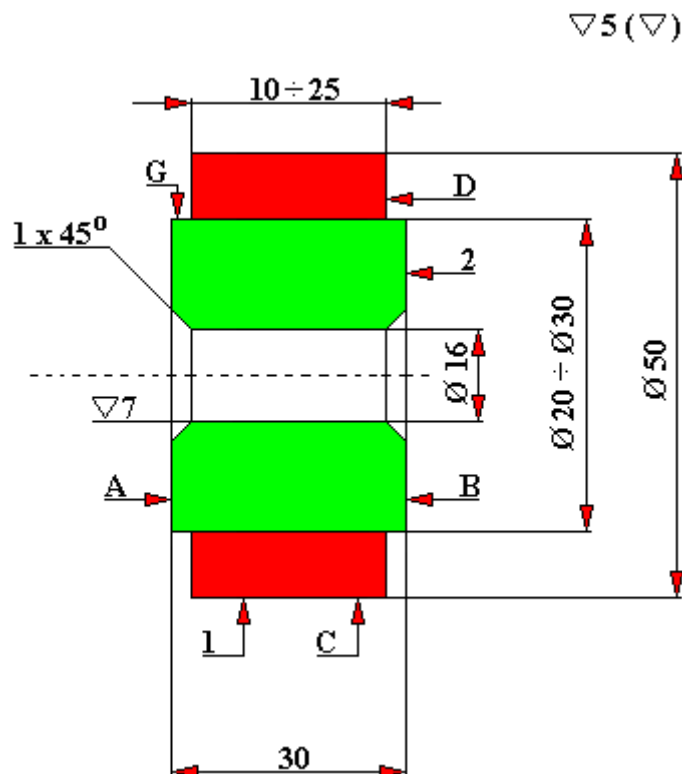


Fig. 4.3.3.21. A mating diagram of the sleeve-shaft friction contact. Load up to 250 kg of force 1 – sleeve, 2 – shaft. Non-parallelism of surface A to surface B and D maximum 0.02 [mm]. Front run-out of surface A in relation to surface B, maximum 0.02 [mm]. Radial run-out of surface A in relation to surface G and C maximum 0.03 [mm].

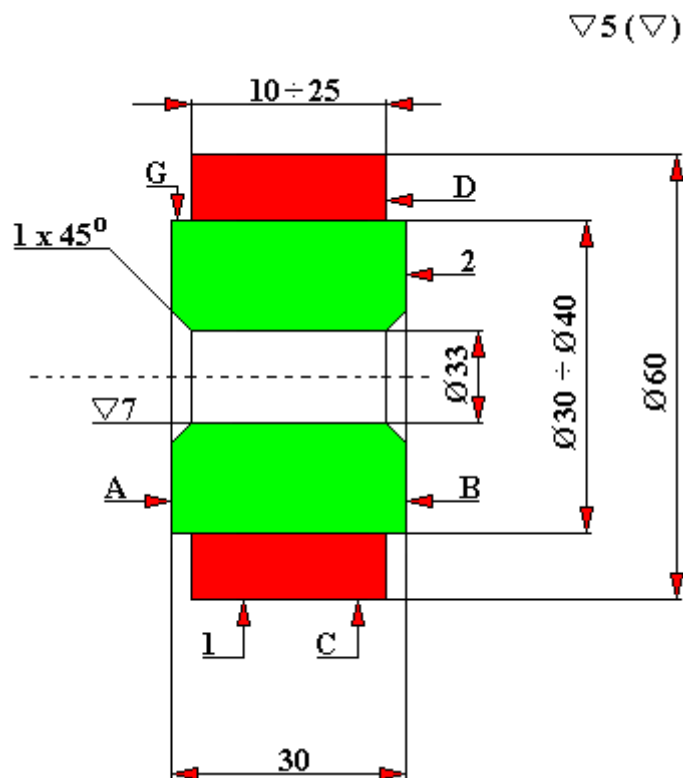


Fig. 4.3.3.22. A mating diagram of the sleeve-shaft friction contact used in the SMC-2 tribotester. Load up to 500 kg of force
 1 – sleeve, 2 – shaft. Non-parallelism of surface A to surface B and D maximum 0.02 [mm]. Front run-out of surface A in relation to surface B, maximum 0.02 [mm]. Radial run-out of surface A in relation to surface G and C maximum 0.03 [mm].

Fig. 4.3.3.23 presents a kinematic diagram of the SMC-2 tribotester. The test rig is driven by an electric motor 21; on its shaft mounted are stepped belt pulleys 1. These pulleys, via the V-belts 2, transmit the drive to the passive belt pulleys 5, which in turn via the clutch 26 transmit the drive to the reducer. In the reducer, in addition to the wheel assembly 3, 4 and again 3, there is a tachometer 6 and two output shafts 29 and 30. The shaft 29 through the clutch 9, the lower sample headstock 25 and the carriage 31 with interchangeable change wheels 12 and 13, drives the lower sample shaft 11. This sample co-works with the upper sample 14 which is connected, via a clutch, on the right side with the torsion shaft of the inductive sensor 10. And the other side of the torsion shaft of the inductive sensor is connected also by a coupling to the shaft 29. The inductive sensor, receiving the drive of the torsion shaft on both sides, determines the quantity of the twisting moment (and thus the moment of friction) between the mating samples 11 and 14. The headstock 25 of the lower sample is connected to the loading mechanism. In this way conducted are both the kinematic drive of the tribotester as well as setting of the loading force.

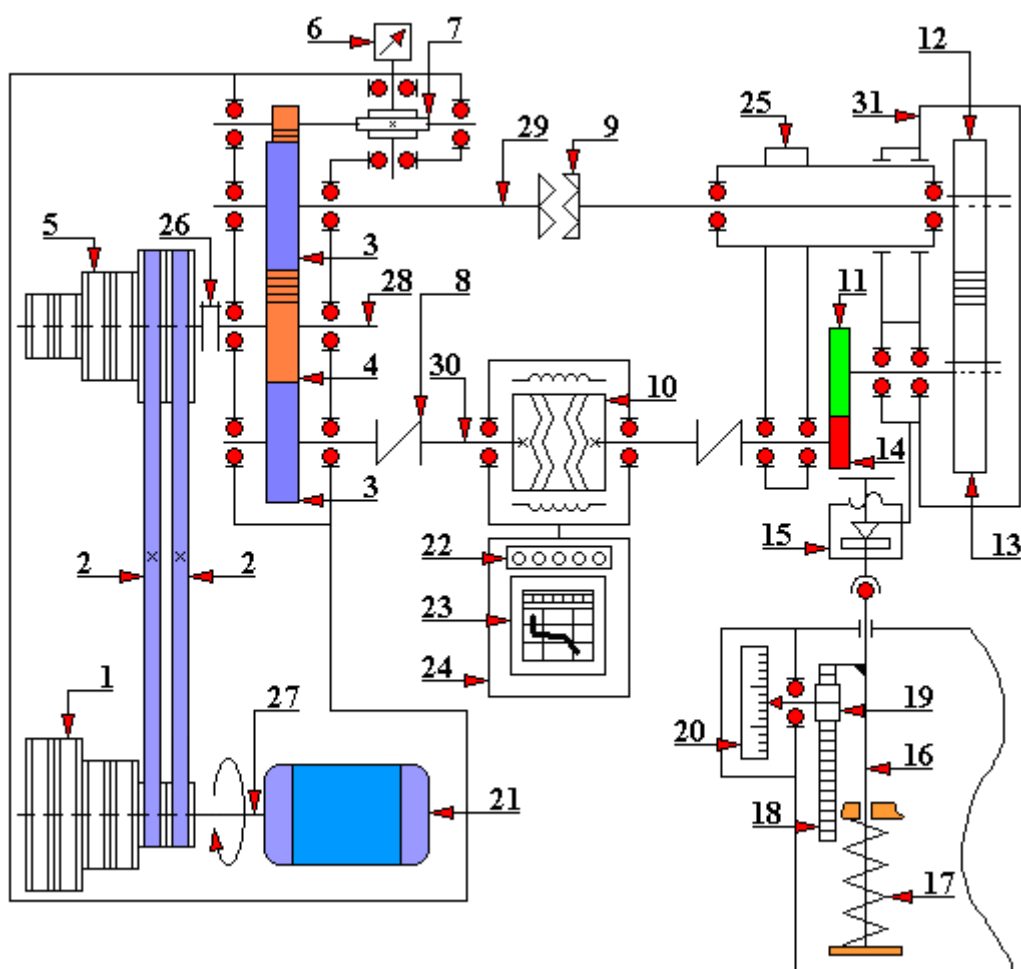


Fig. 4.3.3.23. Kinematic diagram of the operation of the CML-2 (SMC-2) tribotester
 1 - active/ drive pulley ($d_1 = \text{Ø}90 \text{ mm}$, $d_2 = \text{Ø}133 \text{ mm}$, $d_3 = \text{Ø}200 \text{ mm}$), 2 - V-belt (2 pieces), 3 - toothed wheel ($z = 45$), 4 - toothed wheel ($z = 45$), 5 - passive/ driven pulley ($d_1 = \text{Ø}276 \text{ mm}$, $d_2 = \text{Ø}245 \text{ mm}$, $d_3 = \text{Ø}184 \text{ mm}$), 6 - tachometer, 7 - reducer, 8 - clutch, 9 - overload clutch, 10 - inductive sensor, 11 - sample, 12 - carriage change wheel ($z_1 = 54$, $z_2 = 64$, $z_3 = 62$, $z_4 = 60$), 13 - carriage change wheel ($z_1 = 54$, $z_2 = 71$, $z_3 = 73$, $z_4 = 75$), 14 - counter-sample, 15 - bail/ clamp of the load mechanism, 16 - pin, 17 - spring of the load mechanism, 18 - toothed bar, 19 - toothed wheel ($z = 30$), 20 - drum scale, 21 - electric drive motor (type A-02-32/6 asynchronous, compact rotor - squirrel-cage, 3-phase, 2.2 kW, 950 rpm, 220/380 [V] in accordance with GOST 13859-68), 22 - meter, 23 - potentiometer, 24 - control panel, 25 - headstock of the lower sample (counter-samples), 26 - clutch, 27 - shaft I (electric motor), 28 - shaft II, 29 - shaft III, 30 - shaft IV, 31 - carriage.

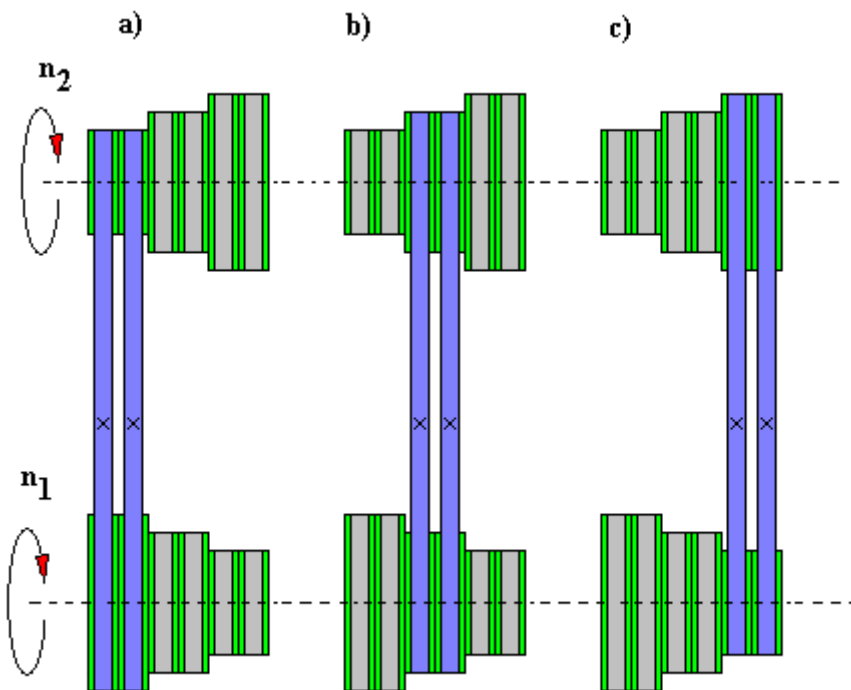


Fig. 4.3.3.24. Scheme of setting the V-belts of the sample headstock drive (speed n_2) for the following values:
 a) $n_2 = 1000$ [rpm], b) $n_2 = 500$ [rpm], c) $n_2 = 300$ [rpm]. The electric motor used for the drive has the following parameters: $N = 2.2$ [kW], $n_1 = 950$ [rpm].

Table 4.3.3.4. The use of change wheels depending on the type of tested samples

Type of samples	Type of friction	Percentage difference in the number of change wheel teeth	Applied toothed change wheels
	Rolling friction	0%	$z_1 = 54, z_2 = 54$
	Rolling friction	10%	$z_1 = 64, z_2 = 71$
	Rolling friction	15%	$z_1 = 62, z_2 = 73$
	Rolling friction	20%	$z_1 = 60, z_2 = 75$

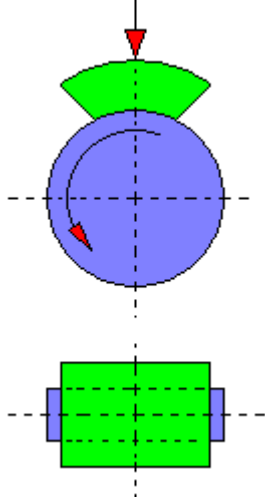
	<p>Sliding friction</p>	<p>100%</p>	<p>Toothed wheels can be unchanged providing that the clutch is disengaged</p>
---	-------------------------	-------------	--

Figure 4.3.3.25 shows the cooling system and lubrication points used in the SMC-2 tribotester. The cooling system of the mating friction contacts has been realized in such a way that tap water is supplied to the body, and its outflow is connected with the sewage system. The cooling water circuit is not closed. The amount of water flowing through the body can be regulated by the water supply valve.

Point lubrication of the places shown in the above drawing is performed with the use of manual grease guns.

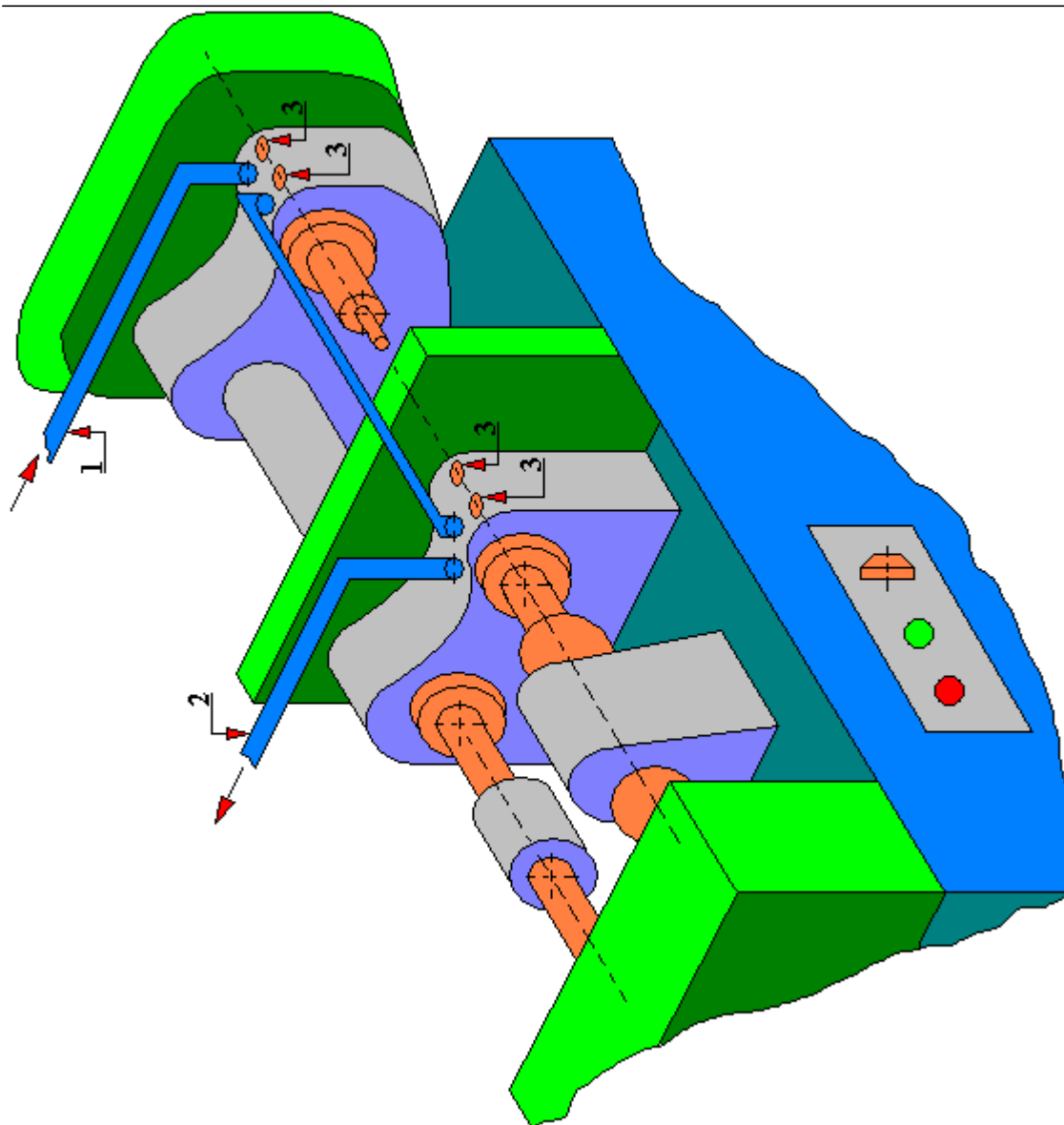


Fig. 4.3.3.25. A diagram of the CML-2 (SMC-2) tribotester head with an indication of the cooling system supply points and lubrication points
1 - cooling water supply, 2 - cooling water discharge, 3 - lubrication points of the test rig (prepared on the basis of the technical and operational documentation)

Figure 4.3.3.26 shows the sample loading mechanism. The principle of its operation is as follows. Rotary motion of the handwheel of the screw 2 resting with its end on the surface of the body of the SMC-2 tribotester causes the displacement up or down (depending on the direction of handwheel rotation) of the yoke (clamp) 1.

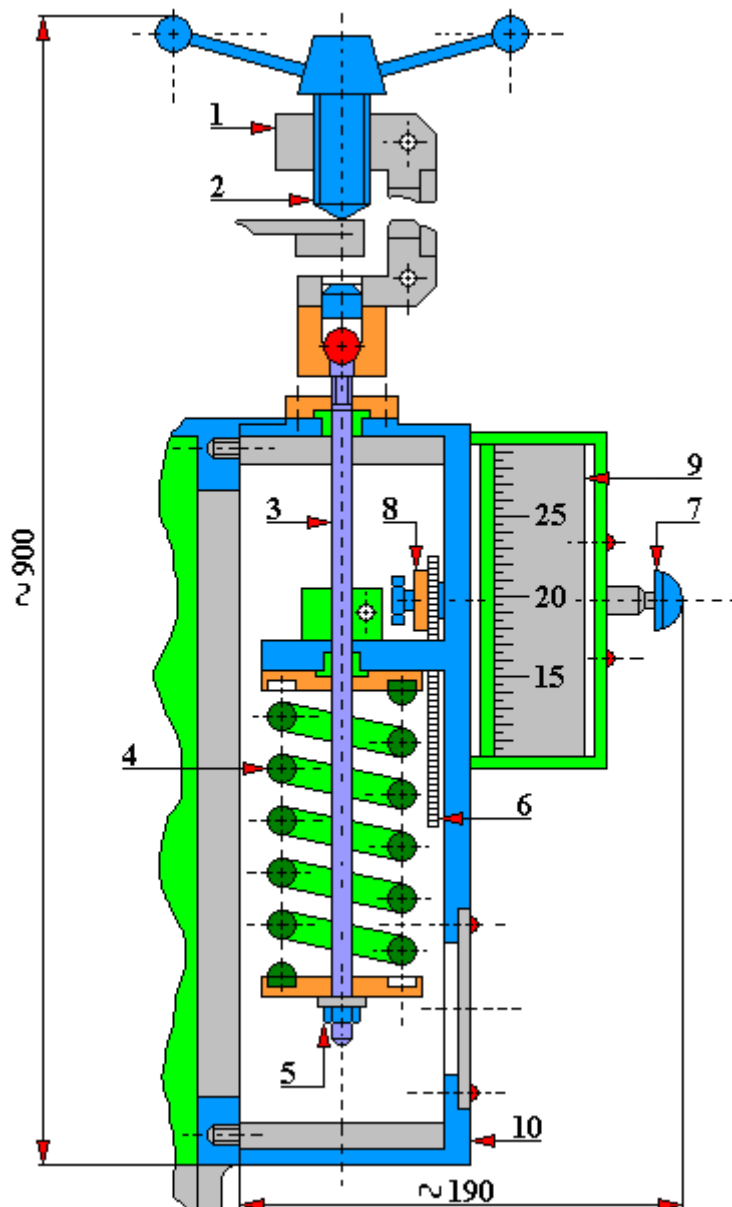


Fig. 4.3.3.26. The loading mechanism used in the CML-2 (SMC-2) tribotester
 1 - bail/ clamp - 2 screw, 3 - pin, 4 - compression coil spring, 5 - M8 nut in accordance with GOST 5927-70, 6 - toothed bar with straight teeth, 7 - handle, 8 - shaft, 9 - drum scale, 10 - body)

A pin 3 is mounted in the lower part of the yoke 1. On this pin there is a spring 4 secured against slipping out of the socket by means of a nut 5. The moving pin 3 deflects the spring 4. Depending on the size of the load, two types of springs with different characteristics are used. The first spring is used for the load range from 20 kg to 200 kg of force, the second - for the range from 50 kg to 500 kg of force. The sliding pin 3 is rigidly connected to a toothed bar 6 that moves with it. This bar co-works with the rack 8. The load scale drum 9 is mounted on the rack shaft 8. The sliding toothed bar 6 rotates the rack 8, thus the load scale drum 9 indicates the value of the load force of samples. The indications of the scale of the set load 9 are presented in Table 4.3.3.2 and 4.3.3.1 and on graphical charts made on their basis presented in Figures 4.3.3.15 and 4.3.3.17 respectively. The values of the drum scale on the graphs correspond to the value of the force measured with the dynamometer supplied with the SMC-2 tribotester. Tables 4.3.3.4 and 4.3.3.3 show the scale values for several values of preset forces (50, 100, 200, 300, 400 and 500 kg

force for one range and values 20, 40, 60, 80, 100, 120, 140, 160, 180, 200 kg load for the second force range). The user of the tribotester can develop their own table of indications of the scale of load mechanism (more or less accurate) depending on their own needs. On the basis of the data contained in the above-mentioned tables built were graphs (Figures 4.3.3.15 and 4.3.3.17) to facilitate the reading on the load mechanism drum scale corresponding to the set load value. Please note that the drum scale 9 has a conventional scale. Setting the scale to "0" is done by turning the handle 7 which must first be pressed. And the initial tension of the load spring is conducted by means of nuts 5.

In order to measure the moment of friction of tested samples on this tribological test rig a non-contact / no-touch inductive sensor was used, shown in Fig. 4.3.3.27. This sensor consists of two main parts:

- rotational rotor,
- stationary stator.

The main part of the rotor is the torsion bar 6 which engages in the load contact of the tribotester by means of switchable clutches (not shown in the drawing). Thanks to this, it is possible to measure the torsional moment coming during the samples testing. On the working length of the torsion bar 6 there are three rings (rims) on which the adjustable rings 7 are mounted. These rings are made of a paramagnetic material. Rings 8 made of soft magnetic steel are mounted on the adjustable rings 7. The side surfaces of the rings 8 are tooth-shaped. And the stationary stator is made in the shape of a cylinder consisting of a sleeve 2 and rings 3. The stator is attached to the body of the inductive sensor with screws 1. Power coils 4 and measuring coils 5 are placed in the grooves of the stator magnetic conductors. The stator magnetic conductors are made of soft magnetic steel.

The inductive sensor has two characteristic working air-gaps:

- S1 - radial air-gap between the movable rotor and stationary stator; this gap separates the rotor from the stator along its entire length and constitutes a resistance for the magnetic flux Φ ; the magnitude of the change in this working gap due to inevitable radial runout of the rotor against the stator can be disregarded as it is small; its value is in the order of hundredths of a millimeter;
- S2 - the gap in the rotor elements, initially 0.8 mm, may change due to the twisting of the bar 6.

The magnetic flux Φ of the stator created by the supply coil 5 is divided into two parts in the rotor and passes through the following elements:

stator → S1 radial gap → middle ring 8 → S2 working gaps on the right and left half of the rotor → end rings 8 → S1 radial gap → stator.

In the absence of torque moment, the working gaps S2 on the right and left parts of the rotor are equal and the magnetic flux Φ in the rotor is divided into two equal parts. Since the measuring coils 5 are surrounded by a magnetic flux of the same magnitude, electrodynamic forces (EMF) of equal magnitude appear therein. During the tests a moment of friction appears which twists the shaft of the lower sample. The other end of the shaft is connected to a torsion bar 6 of an inductive sensor. Under the action of this moment, the torsion bar 6 twists and the extreme rings 8 of the rotor move relative to the center ring 8 in different directions to equal angles. As a result, the working gaps S2 in the left and right parts of the rotor change (on one side of the rotor the gaps increase, and on the other - they decrease). The resulting magnetic flux Φ in the rotor splits with most of it passing through the part (half) where the working gaps S2 have decreased. Therefore, the EMF in one measuring coil increases just like the magnetic flux through which it is passed has increased. And in the other one it decreases so as the flux has decreased. In this way, the change in the EMF value in the measuring coils 5 is proportional to the changes in the working gaps S2 (fluxes) or proportional to the measured torque. Electrical signals from the measuring coils are transmitted to the comparison module, and then to the electronic

potentiometer which displays and records the value of the measured moment of friction occurring in the sample testing process for the given operating conditions of the friction contact.

The primary coil 5 of the inductive sensor is powered by a voltage stabilized ferroresonant voltage stabilizer (not shown). The measuring coils (two pairs of secondary coils 4) are connected with the resistors R3, R5 and the electronic potentiometer EP located inside the control panel. In the absence of a frictional moment the voltages on the measuring coils of the inductive sensor are equal (they are almost identical). Then the voltage value indicated by the electronic potentiometer is zero. In fact, in practice, it is not possible for both measurement coils to show absolutely zero (due to, among others, uneven gaps in the sensor, inhomogeneity in the material of the coils, stator, rotor, etc.).

Therefore, in the absence of a frictional moment, the voltages of the measuring coils of the left and right parts of the sensor are not equal to each other and the electronic potentiometer will show a small value. For balancing the measuring circuit resistors R2 (for rough adjustment) and R7 (for fine adjustment) are used by means of which the zero position of the EP electronic potentiometer display is set. Resistors R2 and R7 are also located inside the control panel. Under the operation of the measured moment of frictional the equilibrium point in the supply of the measuring coils of the inductive sensor is disturbed. The circuit comes out of the equilibrium point, and the unbalance signal, proportional to the measured torque value, is given to the input of the EP electronic potentiometer which records the value of the measured frictional moment. The exact algorithm for taring this tribotester is included in the technical and operational documentation attached to this tribotester and concerns mainly the operating personnel of this test rig. It is worth adding here, however, that the drive shaft of the inductive sensor is connected to the shaft on which the tested lower sample is mounted.

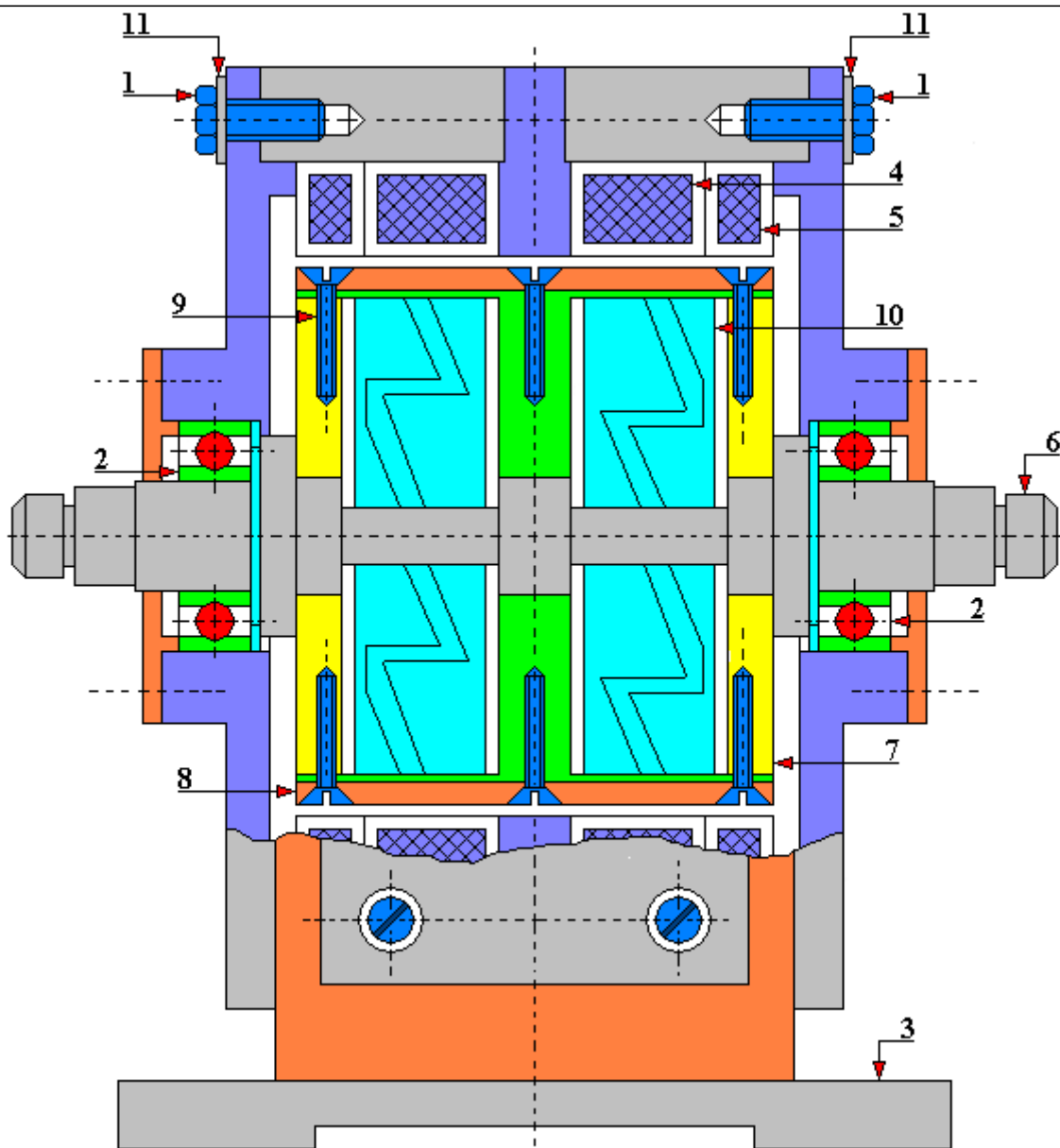


Fig. 4.3.3.27. Inductive sensor used in the CML-2 (SMC-2) tribotester

1 - M6x16 screw in accordance with GOST 1491-72, 2 - bearing, 3 - body, 4 - secondary winding coil, 5 - primary winding coil, 6 - drive shaft / torsion bar, 7 - ring, 8 - ring, 9 - ring fastening bolt, 10 - magnet, 11 - washer

Figures 4.3.3.28 and 4.3.3.29 show the headstock of the lower sample intended for mounting samples on shaft 9 with a special nut 10. The headstock has a complicated structure which is to ensure stiffness and certainty of mounting the tested samples. Its structure includes a shaft 7 mounted in radial bearings 6 which are located in the body 5. A labyrinth sealing of bearings was used to minimize friction in them which could cause additional error in the measurement of the moment of friction of the tested samples. Bearings 6 are lubricated by means of a grease nipple 3. The bearings are cooled by water circulating in the body system 5. The shaft 9 is designed to carry out tests with round samples of a disc-disc type and with disc-block type of samples. During the tests the shaft 9 is screwed with a threaded part into the shaft 7 which rests on the nut 11. This nut is attached to the bolt 8.

When conducting tests with samples of the shaft-sleeve type, the shaft 9 is replaced by shafts 11 - different for the diameter range from $\varnothing 24 \div \varnothing 30$ mm, and different for the diameter range from $\varnothing 30 \div \varnothing 40$ mm.

The carriage (car) is fixed in the headstock of the lower sample with a pin 1 (double-threaded bolt) which is locked with a nut 2. In order to facilitate the removal of the carriage from the headstock body the screw 4 was used.

The headstock of the lower sample is attached to the outer plane of the tribotester frame with bolts and fixed with pins.

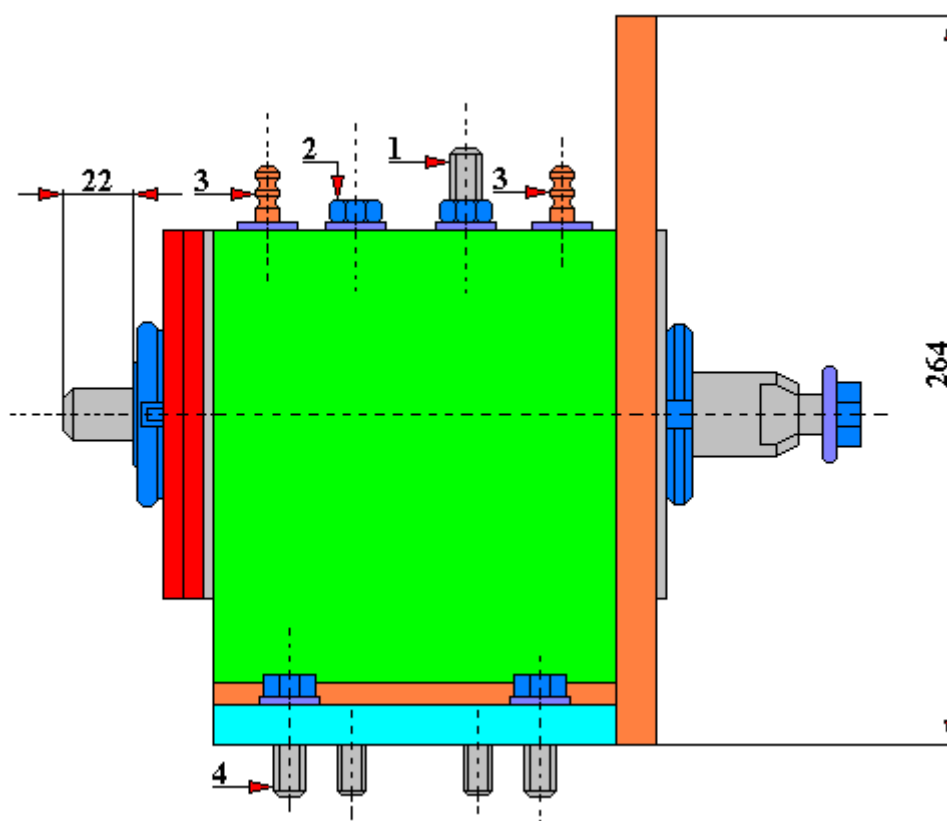


Fig. 4.3.3.28. General view (side) of the headstock of the lower sample of the CML-2 (SMC-2) tribotester

1 - stud bolt (double-ended) M16x80 according to GOST 11765-66, 2 - nut M16 according to GOST 5927-70, 3 grease nipple type I-W according to GOST 1303-56, 4 - screw, 5 - body, 6 - bearing II 210 in accordance with GOST 8338-57, 7 - shaft, 8 - M5x16 bolt in accordance with GOST 17475-72, 9 - shaft, 10 - nut, 11 - nut, 12 - sealing ring (the above description applies to Figures 4.3.3.28 and 4.3.3.29)

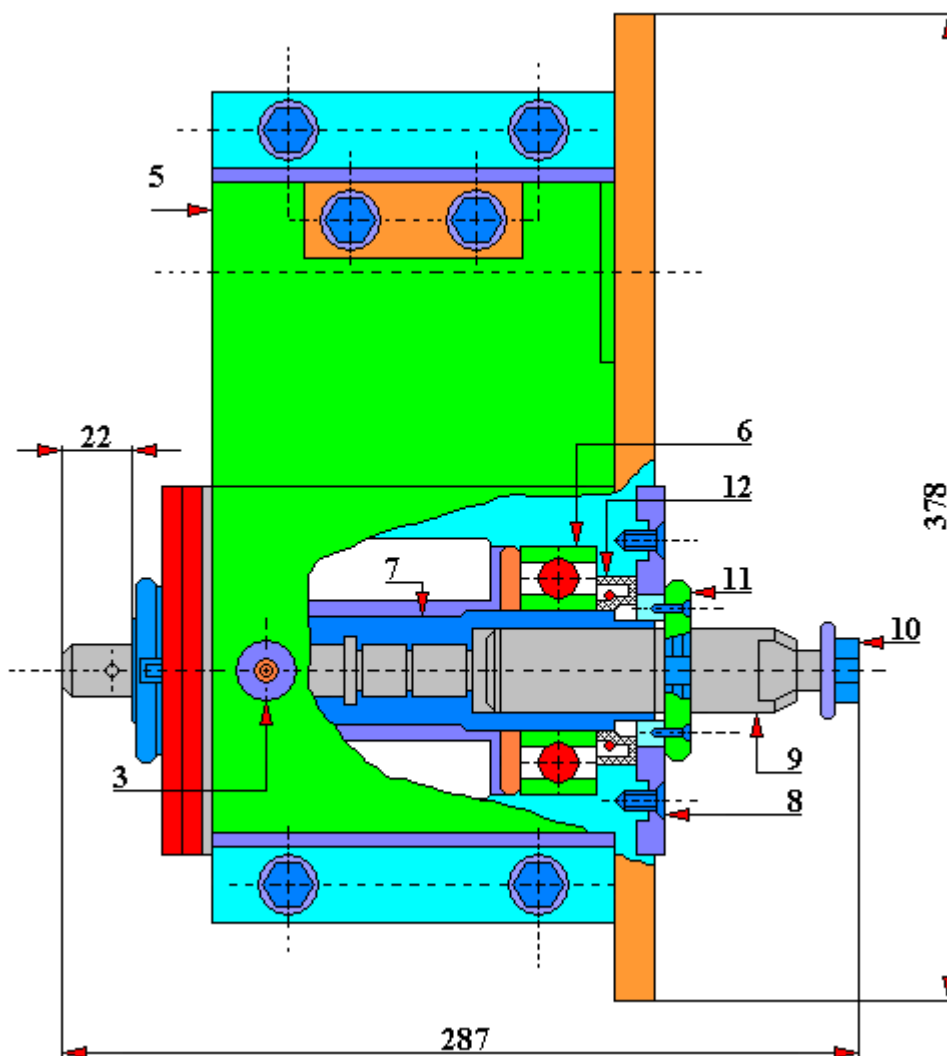


Fig. 4.3.3.29. Top view with a partial section of the headstock of the lower sample of the CML-2 (SMC-2) tribotester

1 - stud bolt (double-ended) M16x80 according to GOST 11765-66, 2 - nut M16 according to GOST 5927-70, 3 grease nipple type I-W according to GOST 1303-56, 4 - screw, 5 - body, 6 - bearing П 210 in accordance with GOST 8338-57, 7 - shaft, 8 - M5x16 bolt in accordance with GOST 17475-72, 9 - shaft, 10 - nut, 11 - nut, 12 - sealing ring (the above description applies to Figures 4.3.3.28 and 4.3.3.29)

Figures 4.3.3.30 and 4.3.3.31 show the chamber for testing round samples and disc-block samples. The chamber body is cast. The side wall of the chamber on the shaft side of the lower sample is closed with a cover 2. Screwed into this cover is a stub pipe 1 intended for draining of used lubricant flowing through the sealing gland. The side wall of the chamber on the shaft side of the upper sample is closed with a cover 6 and a cover 5 with a flange seal. Thanks to the possibility of sliding (within certain limits) of the cover 5, it is possible to apply a load to the upper sample and thus ensure constant contact between the mating lower and upper samples as they wear during the test process. The front part of the test chamber is closed with a cover 9 with a transparent window through which the course of the tested wear process of co-acting samples can be observed. The inner surface of the chamber is illuminated by the lamp 4.

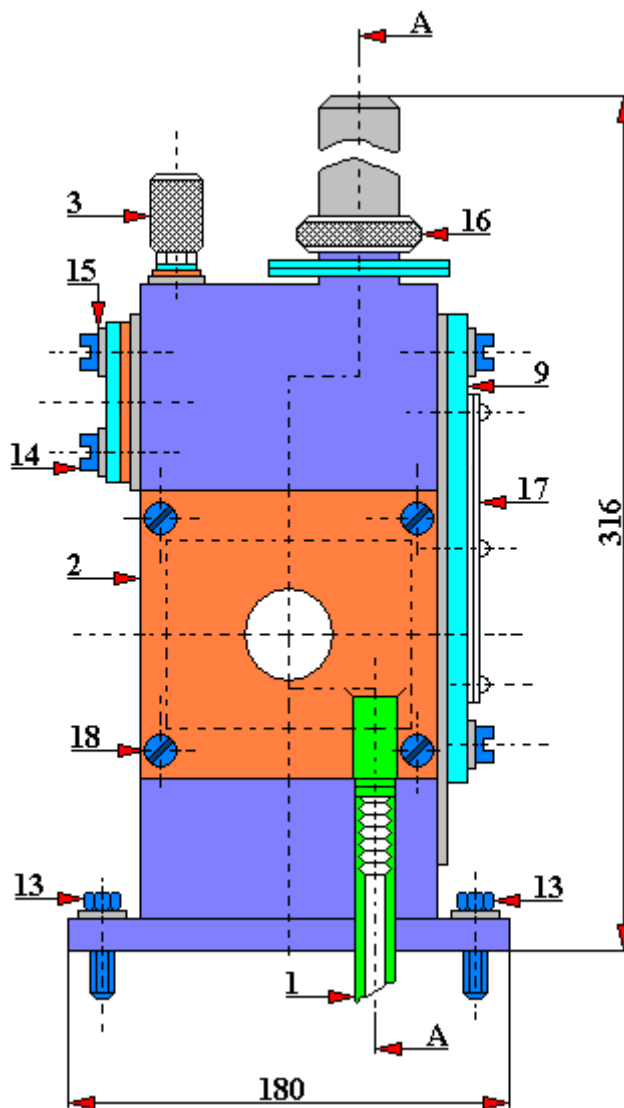


Fig. 4.3.3.30. A general view of the test chamber designed to perform tribological tests for round samples and samples of the disc-block type used in the CML₁-2 (SMC-2) tribotester
 1 - connector, 2 - cover, 3 - knurled pipe connector, 4 lamp bulb type MH 6.3 - 0.22 in accordance with GOST 2204-64 standard, 5 - cover, 6 - cover, 7 - body, 8 – lubricant drain valve, 9 - body, 10 - test chamber interior for the lubricant, 11 - test sample, 12 - counter-sample, 13 - bolt securing the chamber body to the tribotester body, 14 - bolt securing the test chamber cover, 15 - washer, 16 - knurled nut fixing the lamp inside the test chamber, 17 - plexiglass window, 18 – screw fixing the cover No. 2, 19 - electric cable powering the bulb, 20 - sealing ring, 21 - glass cover (the presented description applies to Figures 4.3.3.30 and 4.3.3.31)

Lubricant is fed to the test chamber by means of a pipe connector 3. And the drain of used lubricant from the chamber is done by means of a valve 8. There are no units for feeding the lubricant (suction and pressure pump installation) in this design solution of the test chamber.

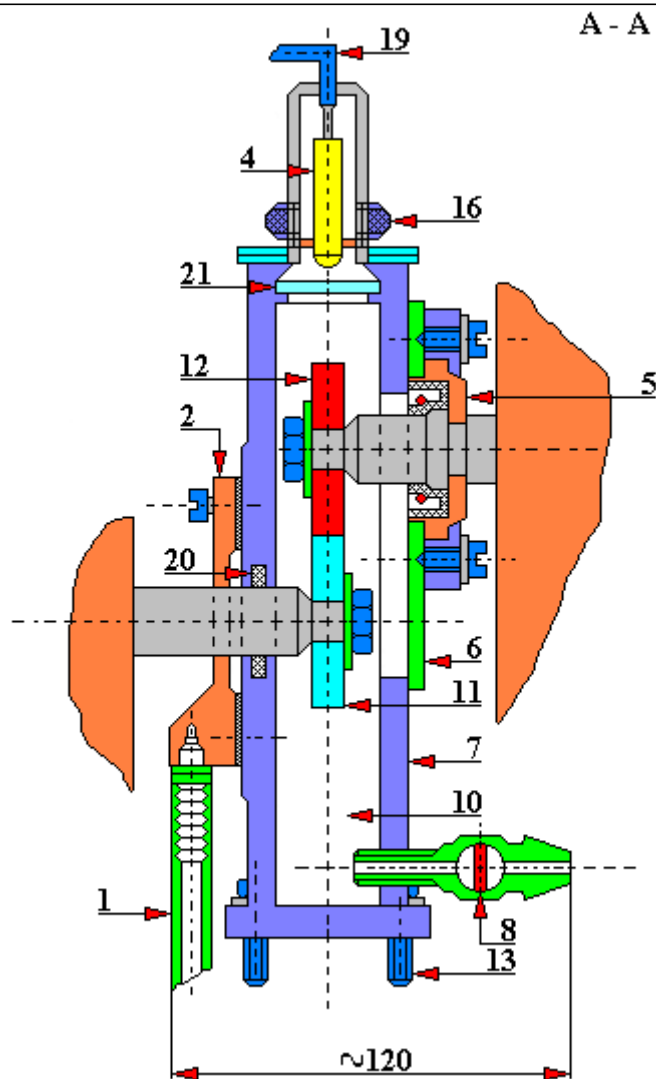


Fig. 4.3.3.31. A-A section of the test chamber designed to perform tribological tests for round samples and samples of the disc-block type used in the CML₂-2 (SMC-2) tribotester
 1 - connector, 2 - cover, 3 - knurled pipe connector, 4 lamp bulb type MH 6.3 - 0.22 in accordance with GOST 2204-64 standard, 5 - cover, 6 - cover, 7 - body, 8 – lubricant drain valve, 9 - body, 10 - test chamber interior for the lubricant, 11 - test sample, 12 - counter-sample, 13 - bolt securing the chamber body to the tribotester body, 14 - bolt securing the test chamber cover, 15 - washer, 16 - knurled nut fixing the lamp inside the test chamber, 17 - plexiglass window, 18 – screw fixing the cover No. 2, 19 - electric cable powering the bulb, 20 - sealing ring, 21 - glass cover (the presented description applies to Figures 4.3.3.30 and 4.3.3.31)

The test chamber is attached to the body of the SMC-2 tribotester with bolts.

Fig. 4.3.3.32 shows the chamber intended for sleeve-shaft tests. The body of this chamber is also cast. The side wall of the chamber on the shaft side of the lower sample is closed with a cover 16. A connector pipe 18 is screwed into this cover and it is intended for the drainage of used lubricant flowing through the flange packing. On the opposite side, the chamber is closed by a cover 21 with a bearing 20 mounted therein.

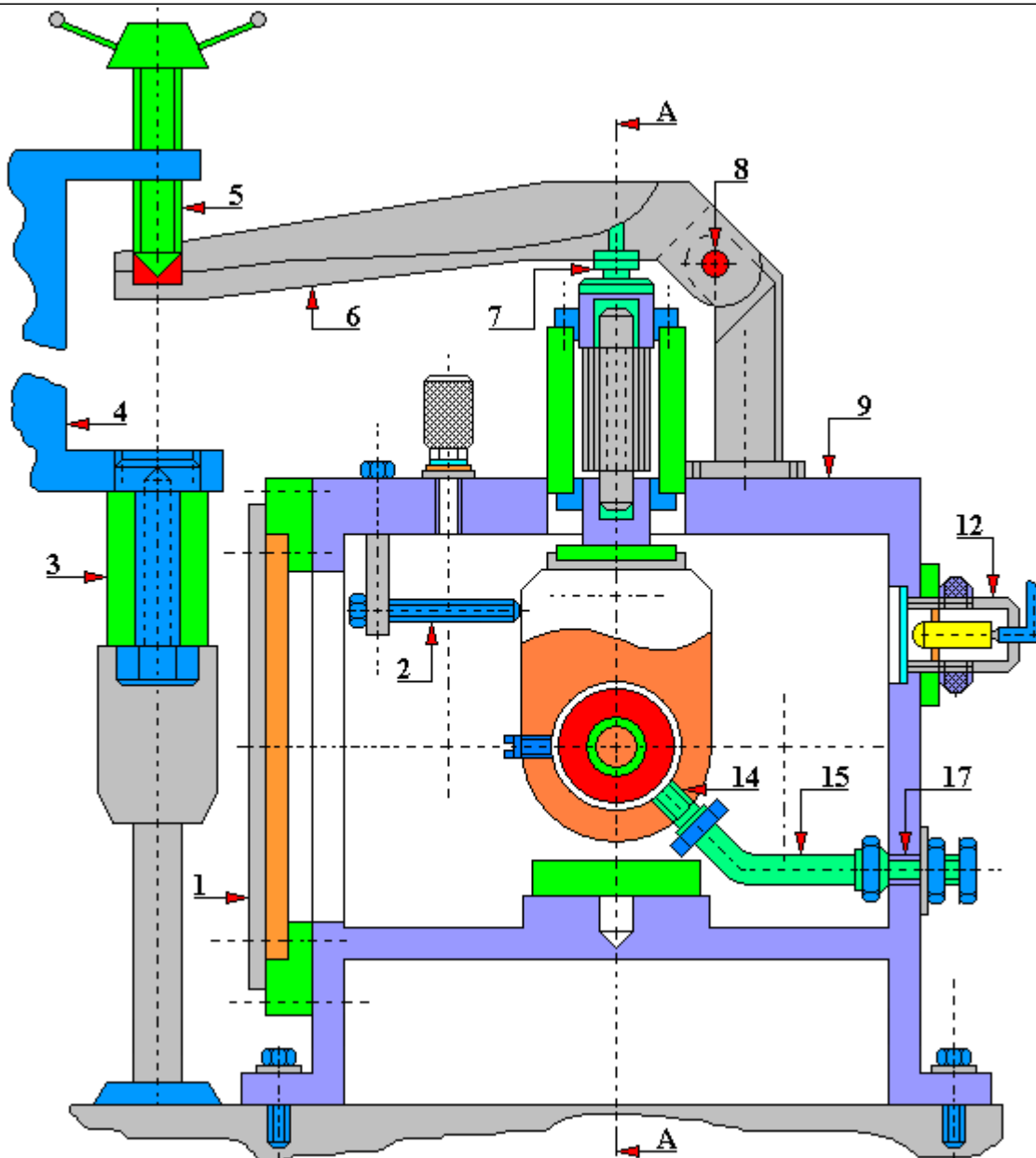


Fig. 4.3.3.32. A general view of the test chamber designed to perform tribological tests for samples of the shaft-sleeve type used in the CMLI-2 (SMC-2) tribotester

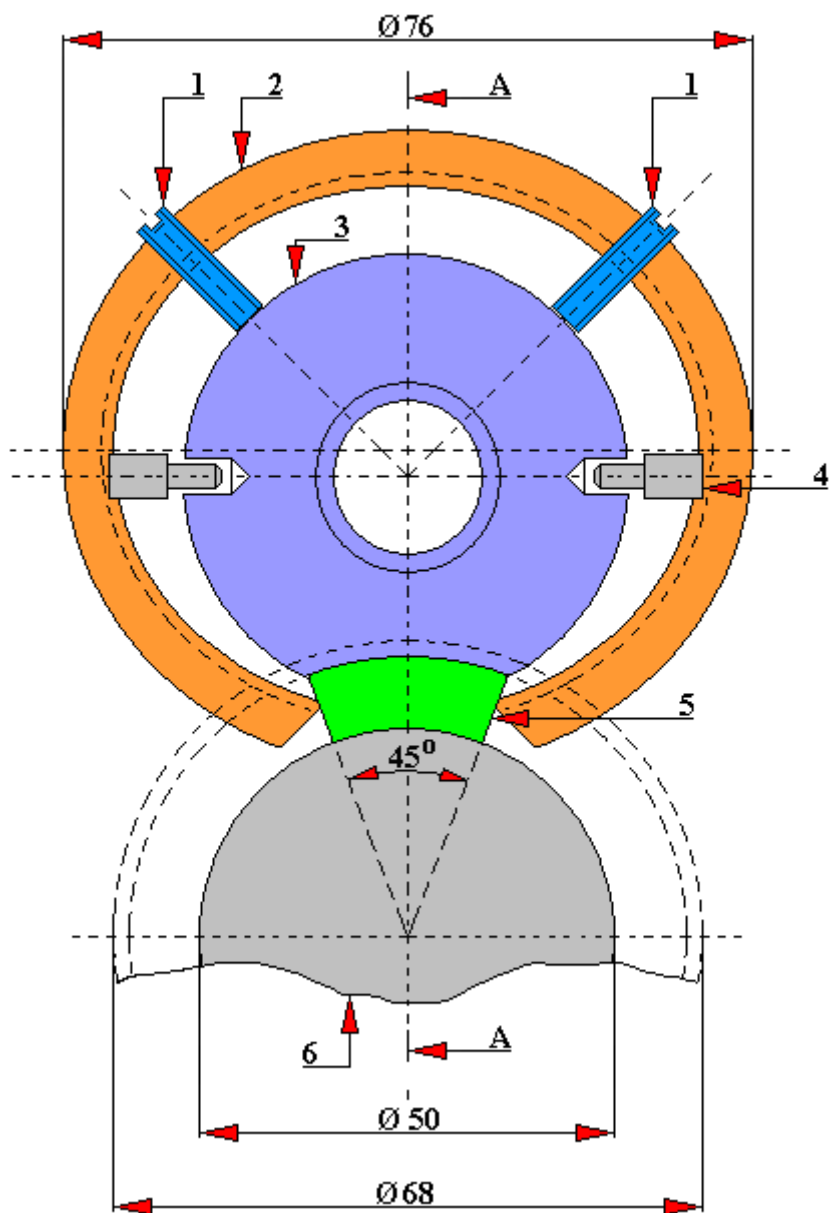
1 - cover, 2 - screw, 3 - extension cord, 4 - bow / clamp, 5 - screw, 6 - lever, 7 - support, 8 - bar, 9 - body, 10 - support, 11 – clamping ring / yoke, 12 - lighting lamp type MH 6.3-0.22 in accordance with the GOST 2204-69 standard, 13 - shaft, 14 – connector pipe (tube coupling), 15 - tube Б.230 - 6x0.3 type MPTY 6-05-919-63, 16 - cover, 17 –connector pipe (tube coupling), 18 – connector pipe (tube coupling), 19 - drain valve, 20 - bearing type 306 in accordance with GOST 8338-57, 21 - cover, 22 - nut (the presented description applies to the entire chamber research)

From the side of the load mechanism, through the extension of the clamp (bow) 3, clamp 4, bolt 5, lever 6, resistance (support) 7, bar 8 and resistance with a prism 10, it is possible to apply load to the upper sample - a sleeve fixed in the holder (clamping ring) for samples. During the tests, the clamping ring 11 is secured against rotation by means of a special screw 2. The rod 8 freely

moves in the ball handles. The lower sample is attached to shaft 13 with a nut 22. The shaft 13 and cover 21 in which one end of the shaft is mounted on the bearing is made in two versions:

- for work with samples with a shaft diameter from \varnothing 24 mm to \varnothing 30 mm;
- for work with samples with a shaft diameter from \varnothing 30 mm to \varnothing 40 mm;

Shaft 13 and cover 19 are replaceable. The front wall of the chamber is closed with a cover 1 with a transparent window designed to observe the process of wear. The interior of the chamber is illuminated by a lamp 12. The lubricant is supplied directly to the friction zone via the connector pipe 14, pipe duct 15 and connector pipe 17. The used lubricant is drained from the test chamber through the valve 19. This chamber is attached to the tribotester body with screws.



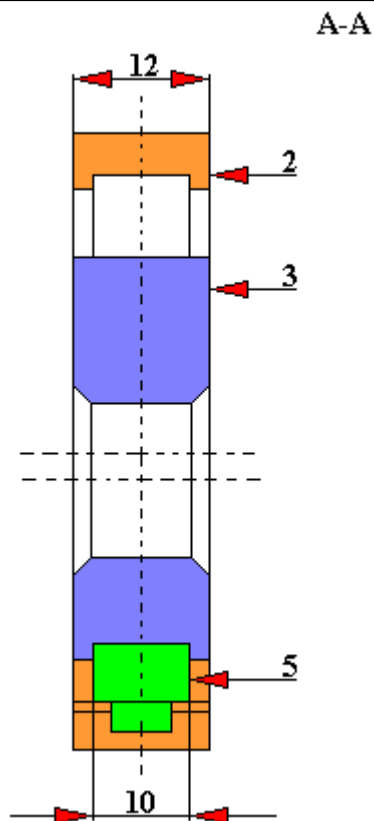


Fig. 4.3.3.33. The holder for block-type samples used in the CML₂-2 (SMC-2) tribotester
 1 - M5x20 screw in accordance with GOST 1477-64, 2 - yoke, 3 - ring, 4 - pin, 5 - block-type sample, 6 - counter-sample

Fig. 4.3.3.34 shows the electrical diagram for connecting the main drive motor of the tribotester to the power grid. The tribotester is powered by a three-phase asynchronous compact squirrel-cage motor, type A-02-32 / 6 (compliant with the GOST standard) with a power of 2.2 [kW] and speed of 950 [rpm]. The motor is protected against short-circuits with 16 [A] safety fuses. Stepped pulleys with the following diameters are mounted on the motor shaft: Ø 90 mm, Ø 133 mm, Ø 200 mm. Active pulleys co-act with passive pulleys with diameters: Ø 276 mm, Ø 245 mm, Ø 184 mm. Two V-belts are mounted on each stage of the belt transmission.

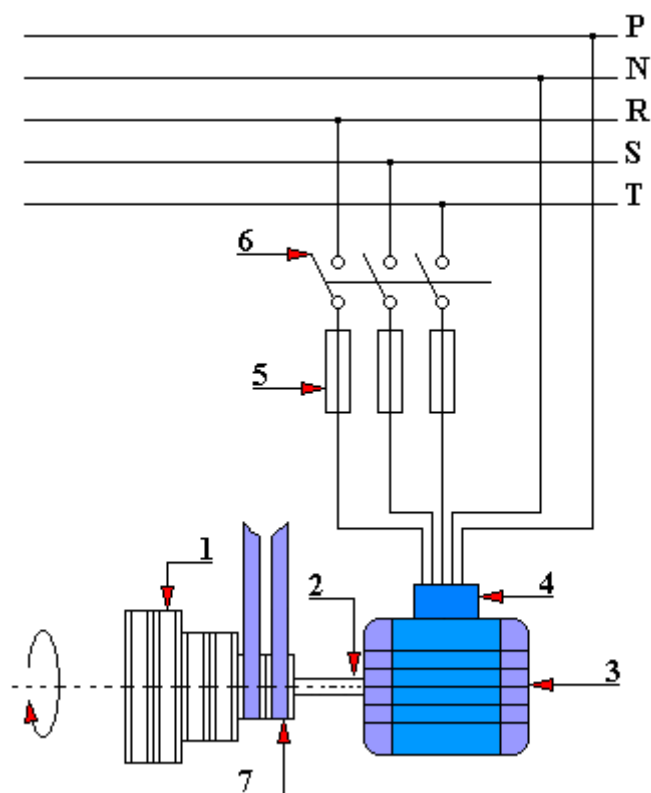


Fig. 4.3.3.34. A wiring diagram for connecting the CMLQ-2 (SMC-2) tribotester drive motor
 1 - pulley, 2 - electric motor shaft, 3 - drive motor type A-02-32 / 6 asynchronous, squirrel-cage rotor, 3-phase, 2.2 [kW], 950 [rpm], 220 / 380 [V] in accordance with GOST 13859-68, 4 - electric cable box, 5 – safety fuse 16 [A], 6 - main switch, 7 - V-belt, P - protective conductor, N - neutral wire, R (L1), S (L2), T (L3) - phase conductors

4.3.4. Universal test rig for testing wear and friction coefficient of MZiWT-1 type

This test rig, created by Franciszek Rudol, has been described in detail in the work [179]. The application for this test rig was also made to the Polish Patent Office.

The durability and performance characteristics of machines whose parts operate under friction conditions depend, among others, on:

- selection of appropriate materials for their production;
- application of the appropriate technological process;
- proper lubrication of mating surfaces;
- operating conditions.

As a result of friction of mating pairs of parts of machines or living organisms these parts wear out. That been said, different wear processes can take place here. For example, frictional wear in extreme cases results in the inability to continue operation of the test rig. In addition to frictional resistance, the wear can occur, for example, as a result of rolling resistance, rolling resistance with a slip, and a special process is the wear due to friction of bulk loose materials, which are suspended either in liquids or in gases.

Friction and associated wear is a very complex problem. That is why, for example, in laboratory tests, usually a precisely defined one of the simple friction mechanisms is adopted. These tests include, among others:

- scratching method;
- Brinell method (abrasion of the sample with grains of quartz sand);
- method of rubbing against abrasive cloth;
- sand friction method;
- method of jet friction;
- method of friction on the Amsler test rig, Skoda-Savine test rig, Khrushchev test rig and others.

Wear tests under friction conditions are such an important problem that in many countries the methodology of carrying out these tests is included in the relevant standards. For example, in Poland the first standards for wear testing under friction conditions were the following standards:

- PN-67/M-04301. Friction and wear processes in friction of solids. Division, names and terms. PN-67/M-04305.
- Determination of wear resistance on the Amsler test rig.
- PN-67/M-04306. Determination of wear resistance on the Skoda-Savine test rig.
- PN-67/M-04304. Determination of wear resistance with friction of cast iron bushings. The method of artificial bases.
- PN-70/M-04307. Friction materials. Determination of the dry friction coefficient.

At the Institute of Machine Technology and Metal Science of Cracow University of Technology an MZiWT-1 test rig was developed for:

- determination of the friction coefficient;
- tests of wear of mating materials with dry sliding friction or with lubrication in various liquid or gaseous media;
- boundary friction tests;
- rolling friction wear tests;
- rolling friction with slip wear tests.

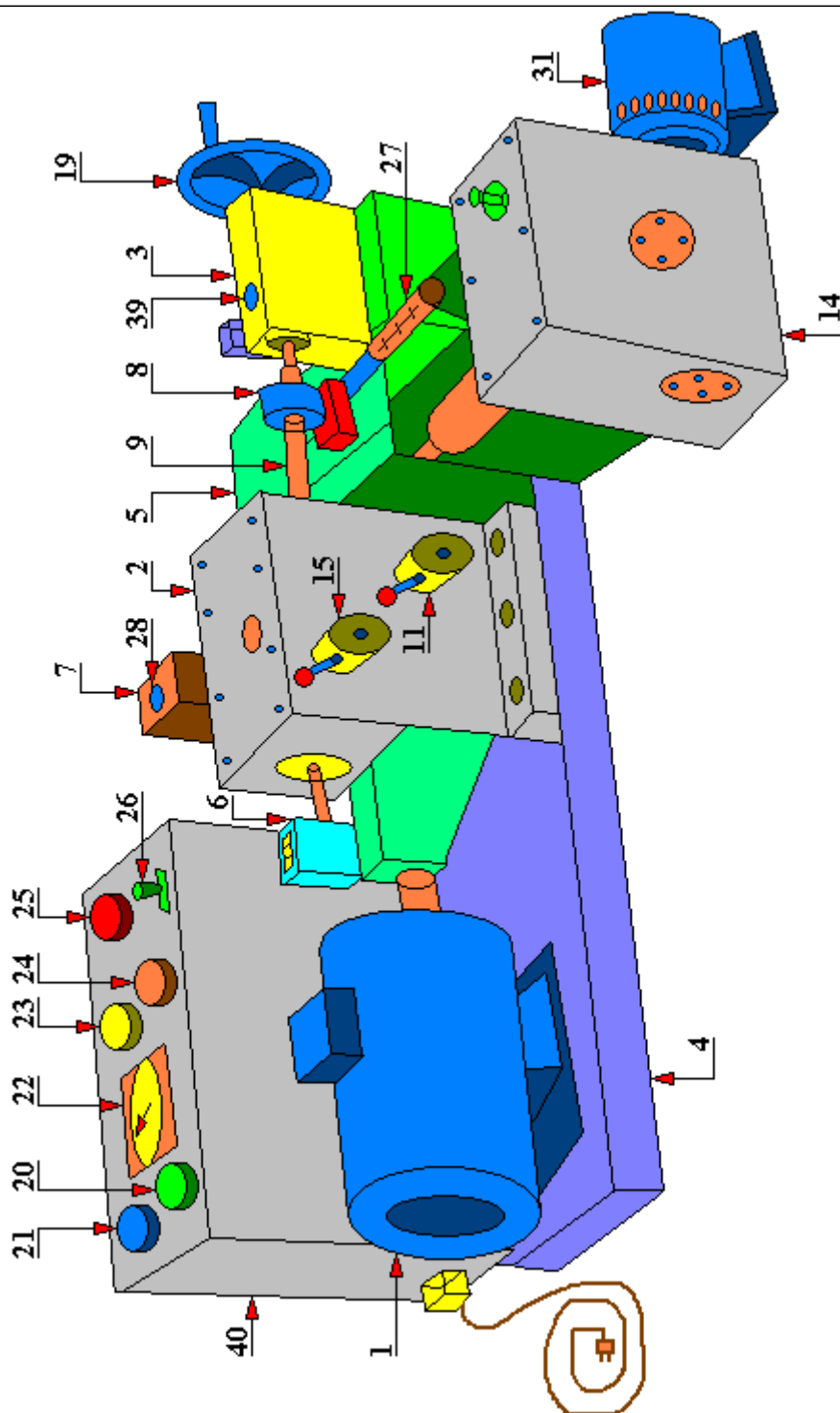


Fig. 4.3.4.1. A general view of the MZiWT-1 test rig [179]

1 - self-locking motor; 2 - drive box; 3 - turning tailstock; 4 - base; 5 - removable tub; 6 - revolution counter with an eraser; 7 - put and slidable weight; 8 - counter-sample; 9 - spindle; 11 - rotation change lever; 14 - drive box; 15 - declutch lever (spindle engaging/disengaging); 19 - handwheel; 20 - test rig switch on button; 21 - test rig switch off button; 22 - time relay; 23 - engine 31 start button; 24 - engine 31 rotation direction change button; 25 - indicator of the operation of the furnace with a thermoregulatory element; 26 - furnace switch; 27 - dynamometer; 28 - bolt securing the sliding weight 7; 31 - engine of a special test rig for testing the coefficient of friction; 39 - clamping screw fixing the position of the tailstock's jaw; 40 - electric control panel

The present test rig uses the principle of measuring the circumferential abrasion, which is obtained on the surface of a stationary sample when there is rubbing against it by the cylindrical surface of the counter-sample rotating at a predetermined speed. However, unlike the Skoda-Savine test rig, the stationary sample is pressed against the counter-sample which is mounted two-sidedly. This significant difference causes that the harmonic vibrations generated during the friction process are characterized by much smaller amplitude, which has a positive effect on reducing the spread of obtained results.

The MZiWT-1 test rig (Fig. 4.3.4.1) consists of a self-locking motor 1 of a special design, driving the spindle 9 through the change wheel located in the drive box 2. In this way, three different speeds are obtained on the spindle: 480; 900 and 1500 rpm. The change of rotation is obtained by setting the lever 11 to the appropriate position. And the lever 15 allows to release (disengage) the spindle 9. The jaw is fixed in the tailstock by means of a Morse taper No. 2. By using the handwheel 19 the jaw is pressed against the counter-sample holder 8, and then its position is fixed by means of the clamping screw 39.

On the common base 4 there is placed a removable tub 5 with a suitable handle which enables easy positioning and fixing of the tested samples. In place of tub 5, you can put a thermoregulatory furnace for testing at elevated temperatures (up to about 700°C) or a rolling plate for testing the coefficient of friction. The revolution counter 6 with the eraser enables an exact setting of the friction time with the assumed path of friction, for example 200 meters.

The load is exerted on the sample by means of a lever system and by means of a put and slidable weight 7. The desired amount of load is acquired by setting the weight 7 in the appropriate position of the lever. The range of loading forces is from 50 to 150 [N]. Of course, it can be extended if necessary by changing the weight 7 to another one. Such a combination allows a constant pressing of the test sample against the friction surface of the rotating counter-sample 8 throughout the whole friction process.

A special test rig is used for testing the friction coefficient, consisting of, among others, a drive box 14 and a motor 31 with a power of 0.016 [kW] and giving 1500 [rpm]. As already mentioned, instead of the tub 5, a special rolling plate with the test sample attached to it is now put on. This sample, as in the case of the previous description, is pressed with a suitable force against the counter-sample 8 mounted on the spindle of the test rig. The tested sample is disc-shaped (for rolling friction test) or cuboid-shaped (for sliding friction test). The drive from the drive box 14 sets the rolling plate with the sample, hooked by means of a catch on the tension member, in a sliding motion, and the dynamometer 27 measures the friction force, simultaneously recording it on a special tape wound on a rotating drum. This drum also has a sliding motion along the guide consistent with the motion of the dynamometer 27.

The MZiWT-1 test rig is electrically controlled from the control panel 40. The test rig is turned on and off by means of buttons 20 and 21. The time relay 22 enables the tests to be carried out "on time" with an automatic switch-off after a specified period of friction. The switch 20 is used for switching the test rig off, should the need or necessity arise, before the test rig is automatically switched off by means of a time relay. The button 23 is used to apply current to the motor 31 that starts the drive of the friction coefficient test rig and must be kept pressed for the whole duration of the test lasting less than a minute. The button must be released before reaching the extreme position. Newer versions of this test rig are equipped with mechanical or photocell/ photoresistor limit switches. The button 24 actuates the test rig in the opposite direction, allowing the test rig to be returned to its home position. The red lamp/ button 25 is used to control the operation of the furnace with a thermoregulatory unit. This test rig is turned on and off by a switch 26, and thermoregulation is conducted by means of an additional test rig with a thermocouple or contact thermometer.

The prototype MZiWT-1 test rigs were made in Poland by "PONAR-Tarnów" Mechanical Plant in Tarnów.

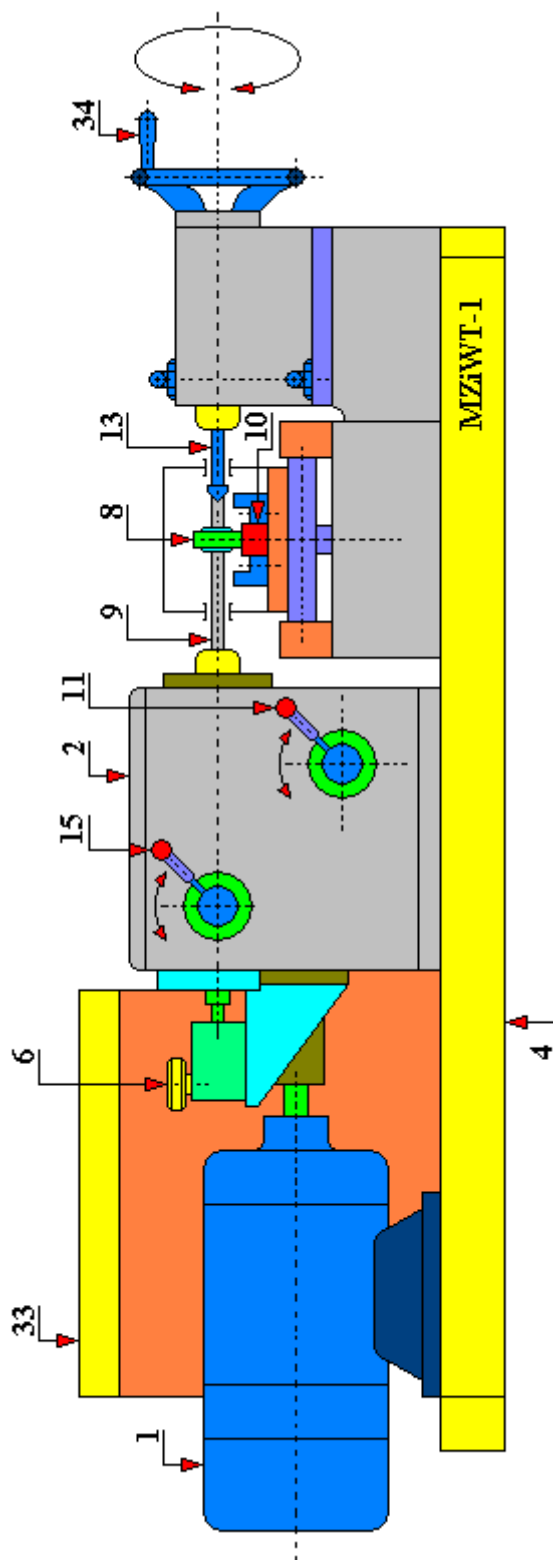


Fig. 4.3.4.2. A diagram of the construction of the MZiWT-1 test rig. Side view [179]
 1 - self-locking motor; 2 - drive box; 4 - base; 6 - revolution counter with eraser; 8 - counter-sample; 10 - tested sample; 11 - rotation change lever; 13 - tailstock; 15 - declutch lever (spindle engaging/disengaging); 33 - control panel; 34 - tailstock handwheel

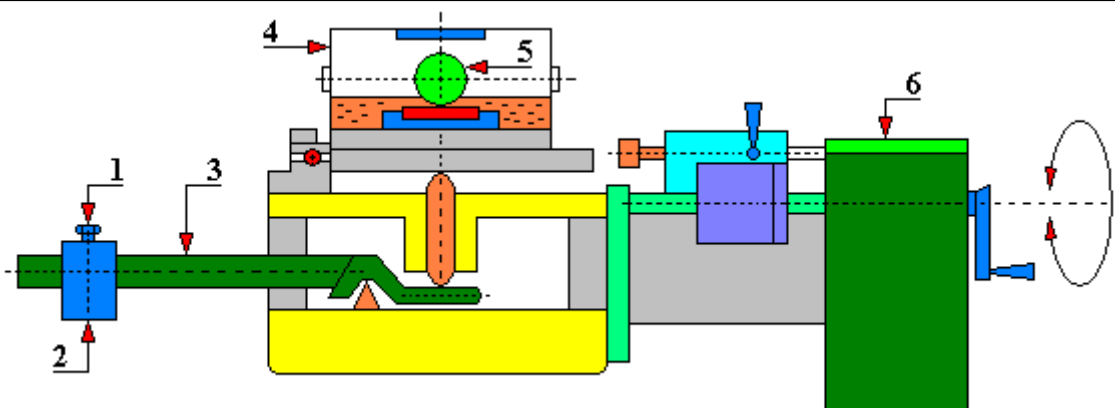


Fig. 4.3.4.3. A diagram of the construction of the MZiWT-1 test rig. View from the side of the lever [179]

1 - screw fixing the sliding weight; 2 - sliding weight; 3 - lever; 4 - tub; 5 -counter-sample; 6 - drive box

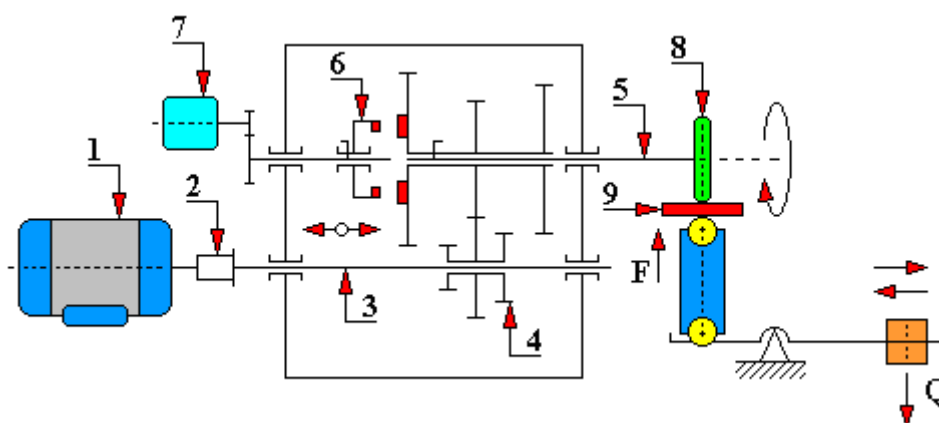


Fig. 4.3.4.4. A kinematic diagram of the MZiWT-1 test rig for a set allowing carrying out wear tests in sliding friction conditions [179]

1 - self-locking motor; 2 - clutch sleeve; 3 - intermediate shaft; 4 - sliding triple gear (so-called sliding triple); 5 - spindle; 6 – jaw clutch; 7 - revolution counter with eraser; 8 - counter-sample; 9 - tested sample

The MZiTW-1 test rig uses a car engine according to the idea of mgr ing. W. Ofiarowski (Fig. 4.3.4.5). It is an appropriately modified BZTr-24b motor in which the rotor shaft 1 and the bearing were changed so as to allow the rotor to move axially, and then the friction brake 2 and spring 3 were built in. Grooves have been cut on both the rotor and stator to generate an axial force during the current flow. This force, generated when the current is turned on, moves the brake friction disc 2 away from the matched and specially made cast iron cover. However, when the current is switched off, the previously compressed spring 3 now moves the rotor to the starting position by the axial force generated during the running of the motor, i.e. it pushes the friction plate 2 against the cast iron cover and brakes the rotor still rotating by inertia.

The BZTr-24b engine has the power of 0.4 [kW] and the rotational speed $n=1300$ [min^{-1}]. Its producer is Opolskie Zakłady Silników Elektrycznych "Brzeg" in Opole, Poland. It is a three-phase motor, $f=60$ [Hz]; 230/400[V].

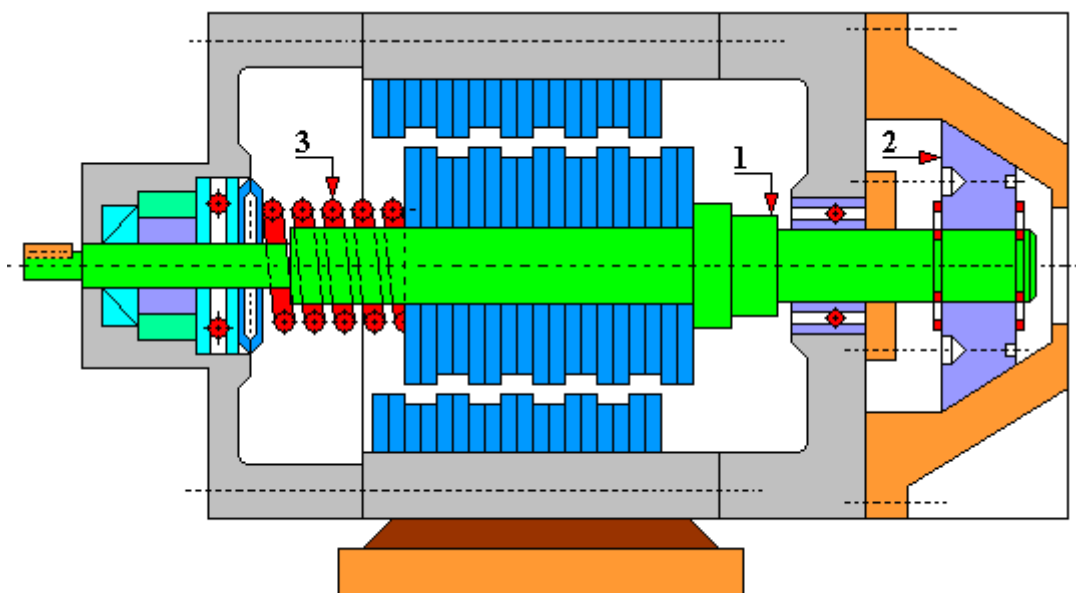


Fig. 4.3.4.5. A diagram of a self-locking motor used in the MZiWT-1 test rig [179]
1 - rotor shaft; 2 - friction brake; 3 - spring

In order to perform tests to determine the coefficient of friction (Fig. 4.3.4.6), in the MZiWT test rig, in place of a tub, the rolling plate 1 is mounted with pins 2. On balls 3, on the rolling plate 1, a second rolling plate can move with the appropriate holder 4 attached in which the test sample 7 is set and clamped with screws 5. The upper rolling plate is connected to the end of a dynamometer by means of a tension member 6. Before measurement, attention should be paid to the correct initial, i.e. extreme setting of the tested sample and dynamometer.

The provisions specified in PN-70/M-04307 can be partially used in these tests.

In order to measure the wear, a tub is placed on the test rig (Fig. 4.3.4.8). The tub is placed on the test rig by means of the articulated plate 1 and pressure is exerted on it from below by means of a pin 9 with a defined force F . A beam 4 is permanently attached to the plate 2 in the bottom of the tub to which the test sample is pressed by means of a second beam 5 and screws 6. In the case of a wear test for boundary or fluid sliding friction, a suitable lubricant is poured into the tub to a height of approx. 5 millimeters above the surface of sample 10.

During the tests, there is a self-circulation of the lubricating liquid, and therefore also the removal of wear products, cooling and lubrication. This fluid (lubricant) must be changed when its temperature rises beyond the permissible limits. The liquid is replaced using a siphon.

In the case of dry friction testing, water is poured to a level of approx. 3 millimeters below the level of the tested sample in order to cool it intensively.

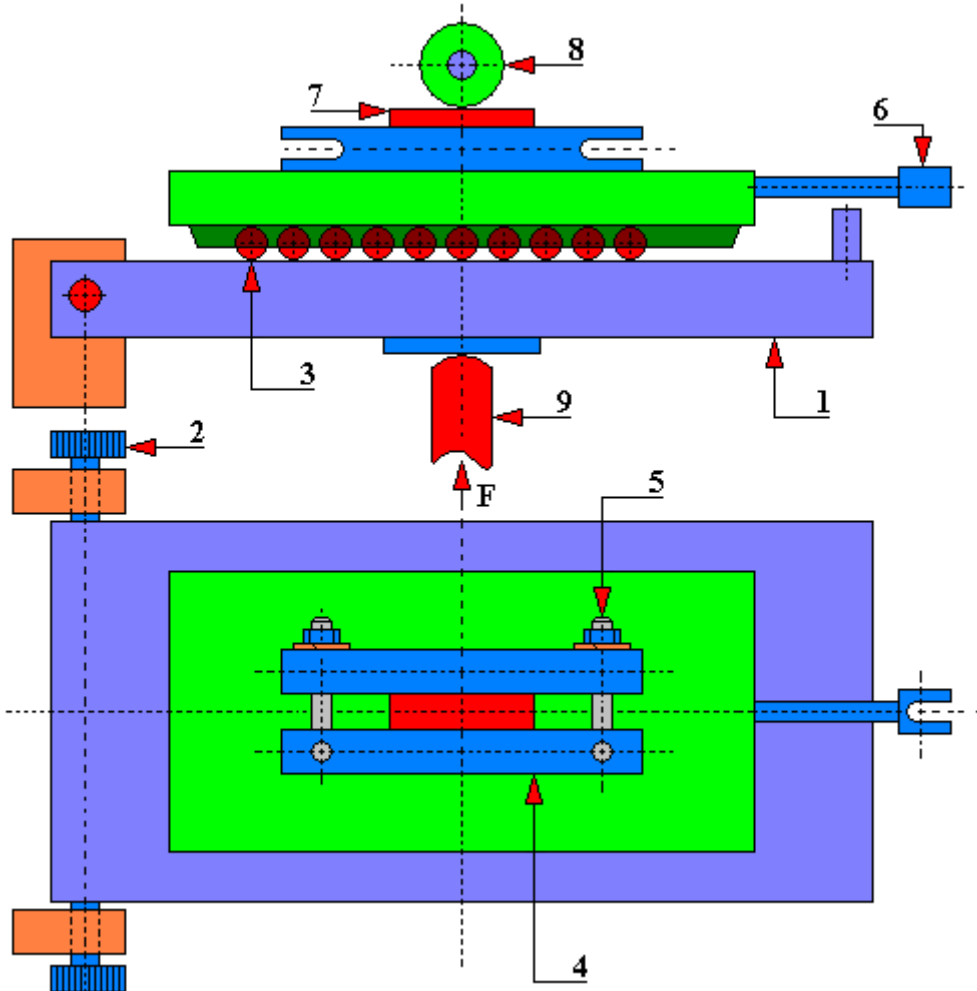


Fig. 4.3.4.6. A diagram of a rolling plate with a holder for testing the friction coefficient used in the MZIWT-1 test rig [179]

1 - rolling plate; 2 - bolt; 3 - balls; 4 - sample holder; 5 - screws; 6 - a tension member with a dynamometer tip; 7 - test sample; 8 - counter-sample; 9 - pin exerting force on the rolling plate; F - force acting on the plate mounted articulately

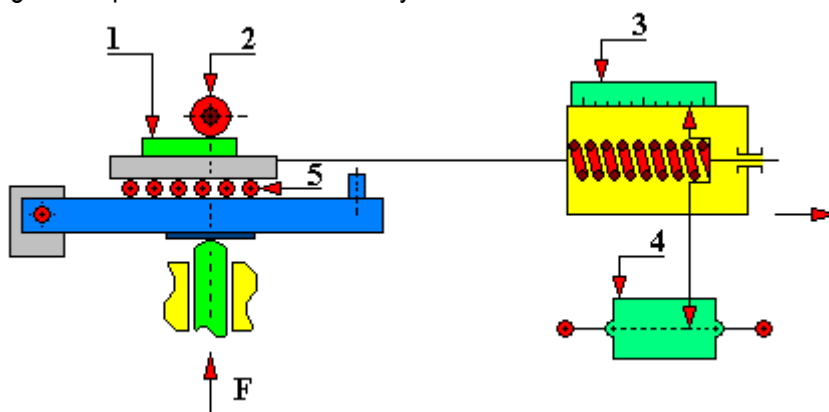


Fig. 4.3.4.7. A diagram of a set of test rigs for testing the friction coefficient used in the MZIWT-1 test rig [179]

1 - sample; 2 - counter-sample; 3 - dynamometer scale specifying the value of the friction force T; 4 - friction force T recorder; 5 - rollers enabling the handle to be moved; F - force acting on the plate mounted articulately

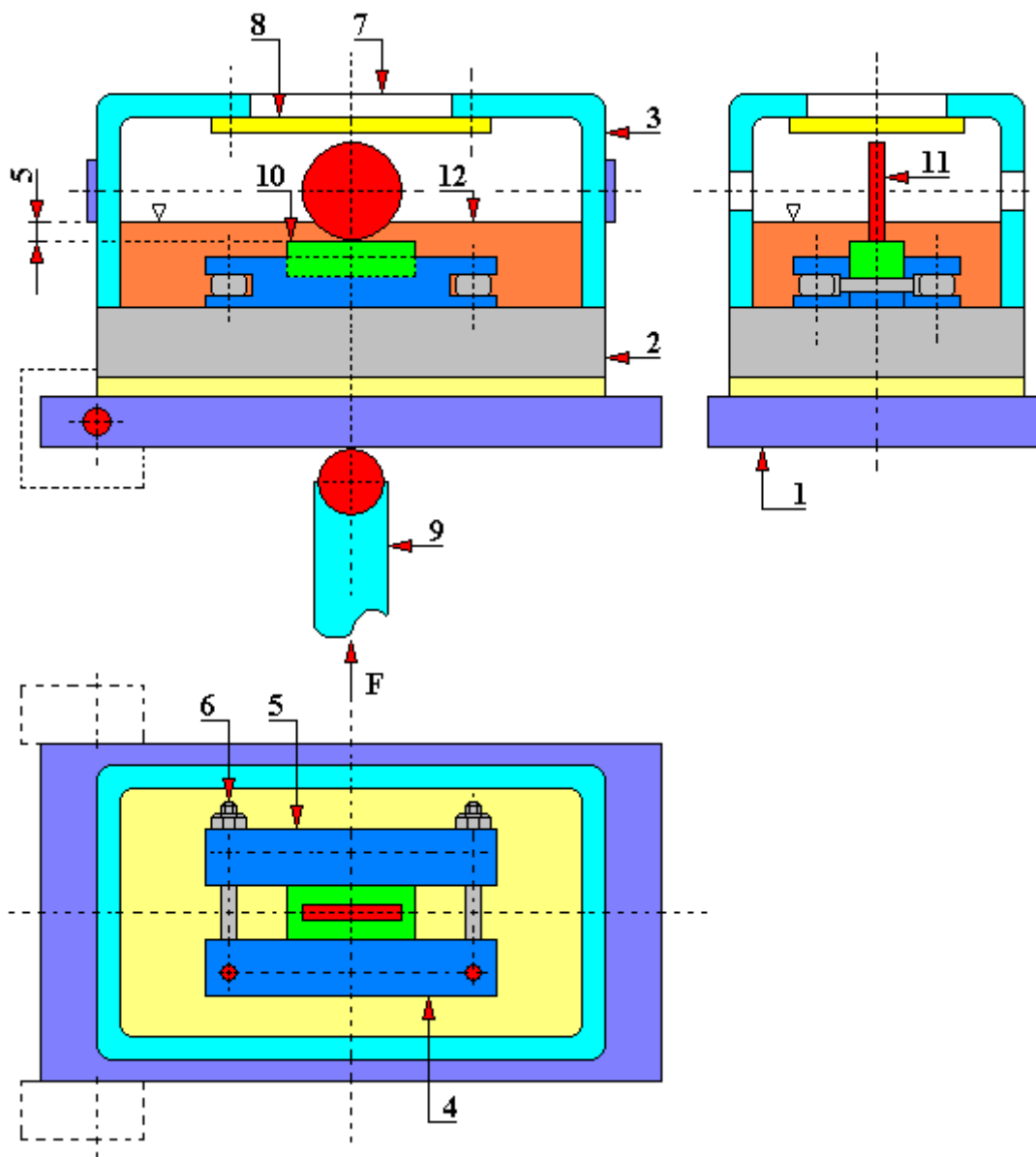


Fig. 4.3.4.8. A general view of the tub intended for wear testing in the conditions of boundary sliding friction, liquid or dry friction, used in the MZIWT-1 test rig [179]
 1 - articulated plate; 2 - tub bottom plate; 3 - cover; 4 - first beam; 5 - second beam; 6 - screw; 7 - opening; 8 - plexiglass; 9 - pin; 10 - sample; 11 - counter-sample; 12 - lubricant; F - force acting on the bottom of the tub

In order to carry out wear tests at elevated temperatures, the MZIWT test rig was equipped with a furnace (Fig. 4.3.4.9), enabling the wear measurements to take place at maximum temperatures up to approx. 700°C. The construction of the electric furnace is as follows. Thermal insulation 4 is provided on the plate 1 which is articulated to the test rig base, loaded with the force F from below. On this plate 1 there is also a water cooled tank (not shown). On the inside, the tank has a chamotte lining in which a heating spiral 7 is built-in. The furnace is

covered with a lid with insulated walls. The tested sample 8 is placed on a base with cut-outs enabling its repositioning in order to make subsequent abrasions. The sample has a protrusion that fits into the appropriate cut-out of the handle preventing it from moving.

The thermocouple or the contact thermometer is connected to a thermoregulatory test rig and placed in the furnace through the opening 5, and through the sight glass 6 abrasion process can be observed or lubricant can be periodically supplied. For longer periods of use, the furnace should be additionally cooled from the outside, e.g. by blowing with compressed air. Similarly, the spindle and the jaw should be cooled with water using for example a brush. Cooling of the spindle and the jaw is also required during the dry friction test.

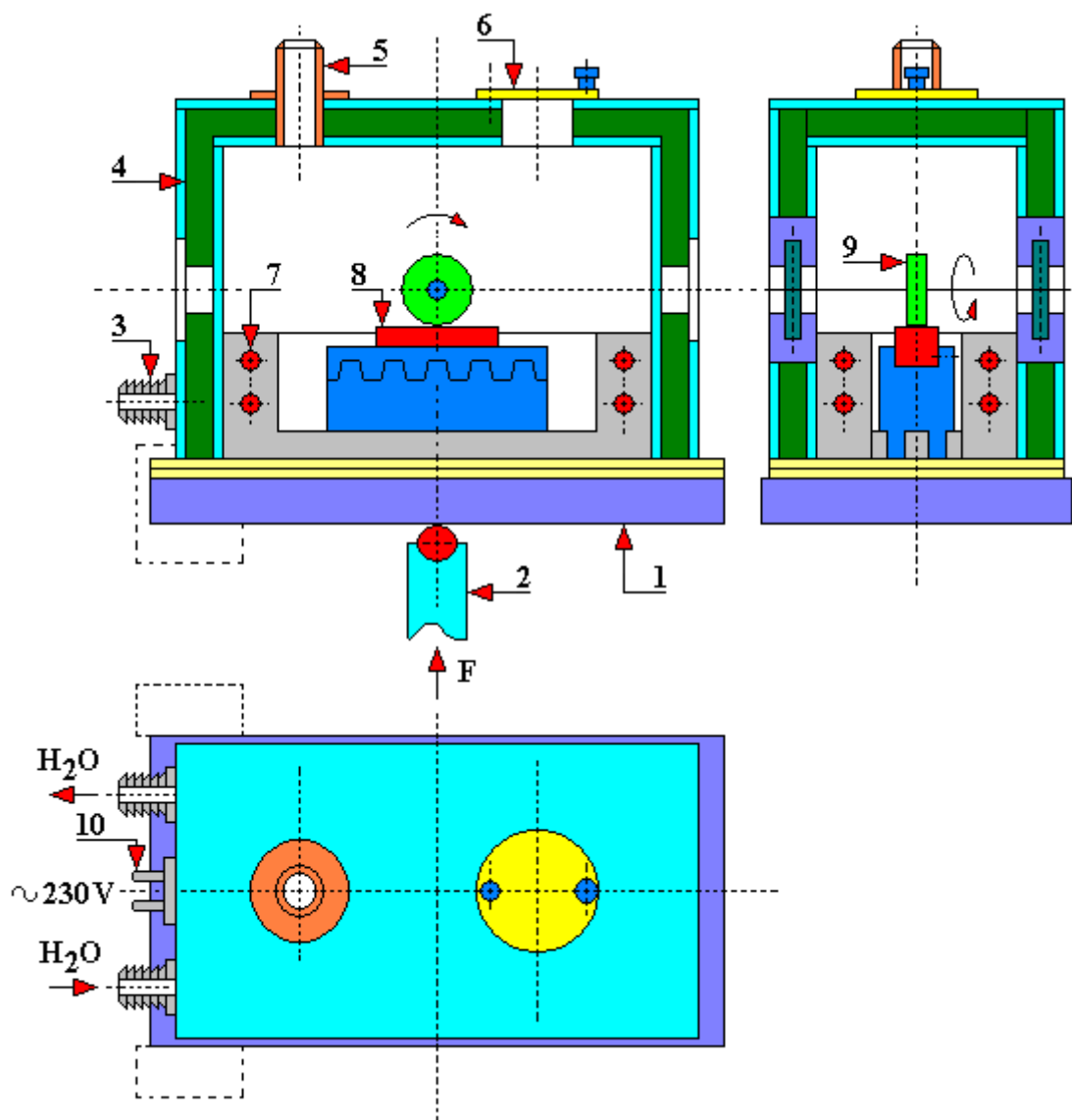


Fig. 4.3.4.9. A furnace for wear testing under conditions of sliding friction at elevated temperatures used in the MZIWT-1 test rig [179]

1 - articulated plate; 2 - pressure pin; 3 - stub pipe supplying water; 4 - thermal insulation; 5 - opening, e.g. for mounting a thermocouple; 6 - observation sight glass; 7 - heating spiral; 8 - tested sample; 9 - counter-sample; 10 - electric plug; F - force acting on the bottom of the articulated plate

In the case of carrying out wear tests according to standards, the amount of wear is determined by weighing or using the method of artificial bases. Determining the coefficient of friction consists in reading the size of the friction force from the obtained graph and then dividing it by the size of the applied loading force during the test. The amount of circumferential abrasion, which is the basis for determining the wear resistance under conditions of sliding friction, is measured, for example, with a microscope for measuring the diameter of impressions when measuring hardness using the Brinell method or with a workshop microscope.

The MZIWT-1 test rig is characterized by the following features:

- because the pressure on the mating materials is exerted by the tested sample on the rotating counter-sample, i.e. from the bottom and by the double-sided attachment of the counter-sample, the measurement accuracy was higher than on the Skoda-Savine test rig;
- a large range of possible different test variants was obtained, for example:
 - wear tests with the use of Durady-Poldi counter-sample;
 - wear tests with the use of a simplified shape of the counter-sample (different from Durady-Poldi), thanks to which the counter-sample can be made of virtually any material;
 - tests practically in any liquid or gaseous medium;
 - tests at elevated temperatures;
 - determination of the value of the friction coefficient;
 - testing the influence of the type of lubricant on the wear of the tested friction contact;
 - wear tests with constant pressure;
- in the case of the adopted method of circumferential abrasion, the tests are of short duration and allow to obtain the proper characteristics of the mating materials.

In the case of carrying out wear tests with rolling friction and rolling friction with a slip, a special handle is used (Fig. 4.3.4.10). On a plate articulated on the base of the test rig and loaded from below with a defined force F , the sample is fixed in a special jaw holder. In this case, the sample is made in the same way as the counter-sample, i.e. it is a disc with a diameter of $\varnothing 30$ mm and a thickness of 2.5 mm. This holder allows the sample to rotate under the influence of the rotating counter-sample.

For the rolling friction with a slip wear test, the jaw holder is set so that the sample has the axis of rotation set at a certain angle to the axis of rotation of the counter-sample, e.g. 45° (Fig. 4.3.4.11).

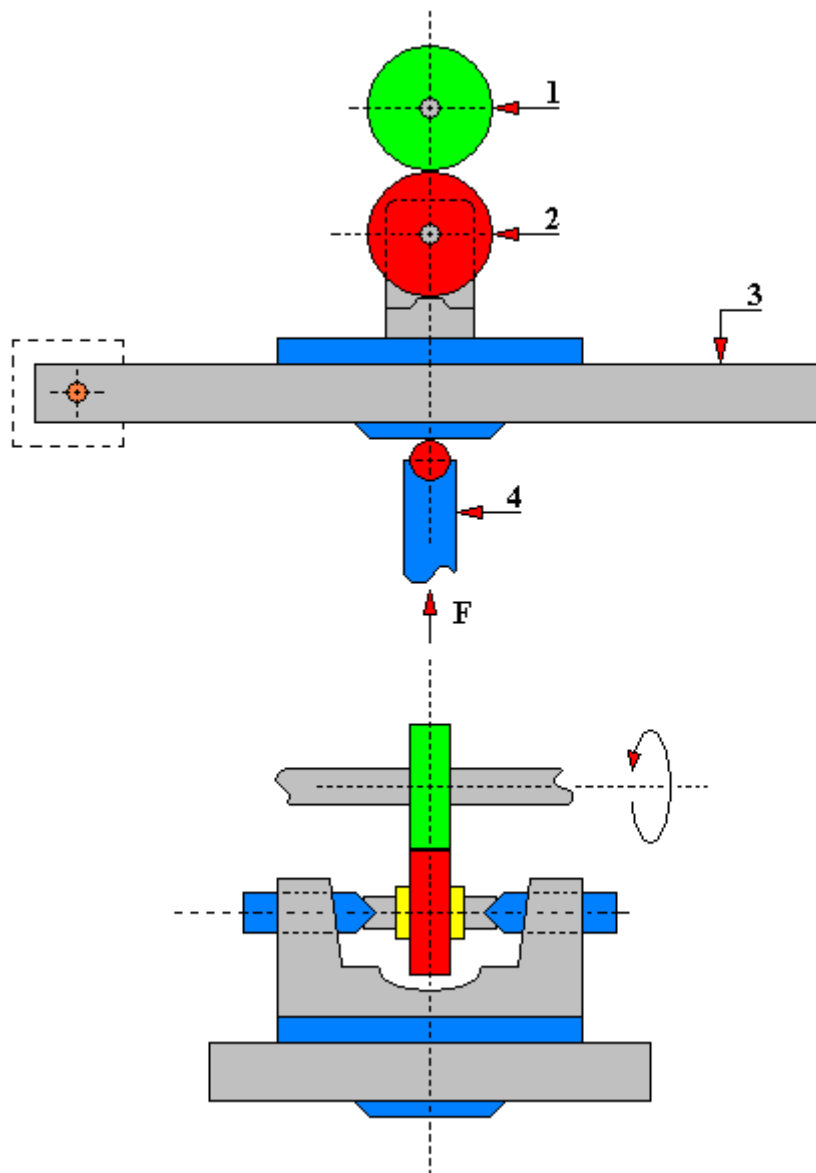


Fig. 4.3.4.10. Holder for rolling friction wear tests used in the MZIWT-1 test rig [179]
1 - counter-sample; 2 - sample; 3 - articulated plate; 4 - pressure pin; F - force acting on the bottom of the tub

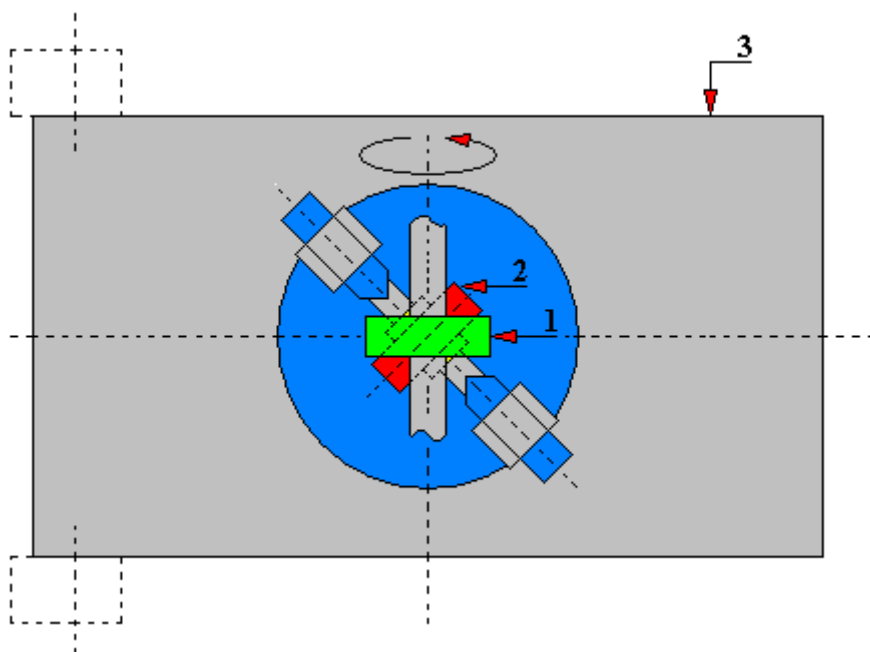


Fig. 4.3.4.11. Holder for rolling friction with a slip wear tests used in the MZIWT-1 test rig [179]
1 - counter-sample; 2 - sample; 3 - articulated plate

POSTSCRIPT

A collection of friction machines presented in this publication is an attempt to look holistically at the design solutions of friction machines employed, especially non-commercial ones. The reader will easily recognize and distinguish between older and newer solutions. These constructions that have worked well are still being modernized. Tribology and the construction of friction machines are developing very dynamically and the time that was devoted to writing this publication was only one year which is not much. The subject concerning the construction of tribological devices is very interesting. I trust that this book will be an inspiration for many young people to build new friction machines.

I sincerely thank Anna Szczerbiak for the effort she put in translating this publication into English.



dr inż. Jarosław Mikołajczyk

ORCID number: 0000-0001-9196-0039
Stanisław Staszic University of Applied
Sciences in Piła, Poland

e-mail: jmikołajczyk@puss.pila.pl

LITERATURE

1. Abbott E. J., Firestone F. A. 1993. Specyfing surface quality. [W:] Mechanical Engineering Nr 55, pp. 556÷572.
2. Алябьев А. Я., Ильинский И. И., Шевеля В. В.: „Практические задачи и методология испытаний материалов на фреттинг-коррозию.” Труды Меж. Научной Конф. „Трени, износ и смазочные материалы”, t. I, Ташкент, 22÷26 мая 1985, s. 395÷398. USSR.
3. Barre F., Lopez J., Mathia T. G. 1997. New methods for characterising the anisotropy of engineering surfaces. [W:] Trans. 7th International Conference on Metrology and Properties of Engineering Surfaces. Gothenburg, Sweden, pp. 479÷486.
4. Bartz W.J. 2012. Lubrication of industrial gears with synthetic gear oils. [W:] Symposium 2012 Tribologie und Mobilität, s. 37÷38. Wiener Neustadt, Austria.
5. Безбородко М. Д., Г. В. Виноградов: „Исследование противоизносных свойств смазочных материалов при трении качения.” Трение и Износ в машинах, Сборник XV, 1962
6. Bezjazyyczny V. F. 2002. Wpływ jakości warstwy wierzchniej po obróbce mechanicznej na właściwości eksploatacyjne części maszyn. [W:] Zagadnienia Eksploatacji Maszyn z. Nr 2, s. 7÷27.
7. Biszczad R., Cichosz P. 2002. Korelacja parametrów chropowatości z wybranymi modelami topografii powierzchni. Instytut Badań i Ekspertyz Naukowych, Gorzów Wlkp.
8. Boryczko A. 1987. Przemieszczenie narzędzia i przedmiotu a zakłócenia struktury geometrycznej powierzchni toczonych. [W:] Mechanik nr 5, s. 211÷214.
9. Burakowski T. 2004. Rozważania o synergizmie w inżynierii powierzchni. Wydawnictwo Politechniki Radomskiej, Radom.
10. Burakowski T. 1998. Rozwój inżynierii powierzchni a rozwój inżynierii eksploatacji. [W:] Tribologia nr 5, s. 829÷843.
11. Burakowski T. 2002. Znaczenie inżynierii powierzchni w tribologii. [W:] Tribologia nr 4, s. 1097÷1111.
12. Burakowski T. 2013. Areologia. Podstawy teoretyczne. Wydawnictwo Naukowe Instytutu Technologii Eksploatacji PIB. Radom.
13. Burakowski T., Marczak R. 1995. Eksploatacyjna warstwa wierzchnia i jej badania. [W:] Zagadnienia Eksploatacji Maszyn z. 3, s. 327÷337.
14. Burakowski T., Marczak R. 1999. Wybrane procesy konstituowania się eksploatacyjnej warstwy wierzchniej. [W:] Tribologia nr 6, s. 757÷765.
15. Burakowski T., Wierzchoń T. 1995. Inżynieria powierzchni metali. WNT, Warszawa.
16. Burcan J., Siczek K.: Wpływ wybranych dodatków środków smarnych na trwałość łożysk ślizgowych, Nowe tendencje w tribologii i tribotechnice, Politechnika Częstochowska, Konferencje , Zeszyt nr 21, Częstochowa 1997.
17. Burgdorf M.: Über die Ermittlung des Reibwertes für verfahren der Massivumformung durch den Ringstauchversuch Ind. Anz. 1967, No 39.
18. Cichosz P., Kowalski M. 2004. Modelowanie matematyczne topografii powierzchni płaskowierzchołkowych typu „plateau”. [W:] Zeszyty Naukowe Wydziału Mechanicznego nr 36. Wydawnictwo Uczelniane Politechniki Koszalińskiej, s. 195÷202, Koszalin.
19. Czarniecki H. 2005. Analiza teoretyczna wpływu stereometrii powierzchni na działanie pary tribologicznej. [W:] Tribologia nr 4, s. 19÷31.
20. Dąca J., Rudnicki Z., Warszyński M. 2003. Analiza wpływu topografii powierzchni na przebieg zjawisk tribologicznych. [W:] Materiały XXI Sympozjonu PKM, Bielsko–Biała, WNT tom 1, s. 213÷218, Warszawa.
21. Dagnall H. 1986. Exploring surface texture. Rank Taylor Hobson, Leicester.

22. De Chiffre L. 1999. Industrial survey on ISO surface texture parameters. [W:] Annals of the CIRP, 48/3, pp. 463÷466.
23. Dietrych J., Kocańda S., Korewa W., Kornberger Z., Zygmunt K.: Poradnik konstrukcji maszyn, cz. I, II i III. Warszawa WNT, 1969
24. DIN 4776. Kenngrößen Rk, Rpk, Rvk, Mr₁, Mr₂ zur Beschreibung des Materialanteils im Rauheitsprofil. Messbegingungen und Auswertverfahren.
25. DIN 4761. Oberflächencharakter. Geometrische Oberflächentextur Merkmale. Begriffe, Kurzzeichen.
26. Djuzhev A. A., Korotkevich S. V., Pinchuk V. G.: "Development of the electrical probing methods and criterions for estimation of properties of lubricating materials", Tribologia 2/2006, s. 61÷75.
27. Dobrucki W.: Zarys przeróbki plastycznej metali, Katowice, Śląsk 1965.
28. Dobrucki W., Odrzywołem E.: Analiza metod wyznaczania współczynnika tarcia między narzędziem i metalem w stanie plastycznym, opartych na procesie spęczania, Obróbka plastyczna 1979, No 4.
29. Dokumentacja techniczno-ruchowa urządzenia SMC-2.
30. Dong W. P., Sullivan P. J., Stout K. J. 1994. Comprehensive study of parameters for characterizing three-dimensional surface topography. III. Parameters for characterising amplitude and some functional properties. [W:] Wear, Vol. 178, pp. 29÷43.
31. Dong W. P., Sullivan P. J., Stout K. J. 1994. Comprehensive study of parameters for characterizing three-dimensional surface topography. IV. Parameters for characterising spatial and hybrid properties. [W:] Wear, Vol. 178, pp. 45÷60.
32. Druet K., Król M.: „Tribometr TPZ-1”, III Międzynarodowe Sympozjum INSYCONT, 25÷27 września 1990 Kraków, Wydawnictwo AGH, s. 617÷621.
33. Duś-Sitek M. 1999. „Doświadczalne stwierdzenie istnienia strefy nadpowierzchniowej warstwy wierzchniej – modyfikacja modelu warstwy wierzchniej.” [W:] Inżynieria Powierzchni nr 1, s. 29÷34.
34. Economou S., De Bonte M., Celis JP, Smith RW, Lugscheider E. (2000r.): „Tribological behaviour at room temperature and 550°C of TiC – based plasma sprayed coatings in fretting gross slip conditions.” Wear, Vol. 244.
35. Feld M., Konczakowski A. 1988. Analiza widmowa struktury geometrycznej powierzchni szlifowanych. Materiały XI Naukowej Szkoły Obróbki Ściernej, s. 109÷116, Łódź.
36. Fleischer G. 1999. Studie zur Energie- und Verschleißverteilung zwischen den Festkörper während der Reibung. Universität Otto von Guericke. Magdeburg.
37. Garkunow D.N. 1987. Effect der Verschleißlosigkeit – eine neue Etappe bei der Verbesserung des Verschleißlosigkeit von Maschinenelementen. [W:] Schmierungstechnik, nr 3.
38. Gierek Adam: Zużycie tribologiczne, Wydawnictwo Politechniki Śląskiej, Gliwice 2005.
39. Gierzyńska Monika: „Tarcie, zużycie i smarowanie w obróbce plastycznej metali”; Wydawnictwa Naukowo-Techniczne, Warszawa 1983 r.
40. Godet M. 1984. The third body approach: A mechanical view of wear. [W:] Wear, Vol. 100, pp. 437÷452.
41. Górecka R., Polański Z. 1983. Metrologia warstwy wierzchniej. WNT, Warszawa.
42. Gubkin S. I.: Пластическая деформация металлов. Москва, Металлургиздат 1961. USSR.
43. Guzowski Stanisław: „Analiza zużycia frettingowego w połączeniach wciskowych na przykładzie osi zestawów kołowych pojazdów szynowych”. Politechnika Krakowska, Kraków 2003r.
44. Handzel-Powierża Z. 1990. Warstwa wierzchnia i problemy jej identyfikacji. Wybrane problemy tribologii. PWN, s. 317÷326, Warszawa.
45. Hebda M., Wachal A. 1980. Trybologia. WNT, Warszawa.

46. Iwabuchi A., Kato K., Kayaba T. (1986r.): „Fretting properties of SUS 304 stainless steel in vacuum environment.” *Wear*, Vol. 110.
47. Janecki J., Hebda M. 1969. *Tarcie, smarowanie i zużycie części maszyn*. WNT, Warszawa.
48. Kaczmarek J., Klimczak T. 1986. Dwu- i trójwymiarowa charakterystyka mikronierówności powierzchni. [W:] *Zagadnienia Eksploatacji Maszyn*, z. 1, s. 39÷46.
49. Kaftanöglu Bilgin: Determination of coefficient of friction under condition of deep-drawing and stretch forming. *Wear*, 1973, No 2.
50. Kałdoński T. 1995. *Tribologia i płyny eksploatacyjne*, cz. II: Wybrane problemy tribologii. Wydawnictwo Wojskowe Akademii Technicznej, Warszawa.
51. Kałdoński T.J., Kałdoński T., Ozimina D. 2008. Wpływ napięcia powierzchniowego, kąta zwilżania i adsorpcji substancji smarnych na ich właściwości smarowości. [W:] *Tribologia* nr 2, s. 235÷246.
52. Kazakow Ju. P.: Sposób opriedielienija koeficjenta trienija pri plasticzeskom tieczieni listowych mietalłow. *Kuzniecno-stamp. Proizw.* No 9, Moskwa 1972, USSR.
53. Kedziora H.–J., Parsons F., Tabenkin A. 2004. Industrial problems with proliferation and expansion of surface finish parameters. *Proc. of XI Int. Coll. On Surfaces*, pt. 1, pp. 93÷100, Chemnitz.
54. Klaffke D. (1985r.): „Fretting wear of ceramic-steel: The importance of wear ranking criteriae. *Wear*, Vol. 104.
55. Kolman R. 1965. *Mechaniczne wzmacnianie powierzchni części maszyn*. WNT, Warszawa.
56. Kołodziej E., Skrzyniowski A. (2008r.): „Wpływ obróbki mechanicznej tarczy hamulcowej na właściwości tribologiczne przy współpracy z nakładką cierną.” *Czasopismo Techniczne* z. 8-M/2008, Wydawnictwo Politechniki Krakowskiej im. Tadeusza Kościuszki, s. 97÷108.
57. Konczakowska A., Konczakowski A. 1978. Badania struktury geometrycznej powierzchni metodami korelacji i widmowymi. [W:] *Mechanik* nr 6, s. 294÷296.
58. Kośła K., Cichomski M., Kozłowski W. 2012. Preparation and tribological characterization of the organosilanes on aluminium surface. *III Krajowa Konferencja Nano- i Mikromechaniki*, s. 141, Warszawa.
59. Kowalewski P., Wieleba W. (2009r.): „Stanowisko do badania współczynnika tarcia statycznego par trących typu metal-polimer.” *Czasopismo Techniczne Mechanika* z.3, 1-M/2009, Wydawnictwo Politechniki Krakowskiej im. Tadeusza Kościuszki, s. 191÷194.
60. Krause H., Schroelkamp Ch. 1981. Investigation into the reaction of metallic bodies in tribological system. *Proc. of Eurotrib'81*, pp. 324÷329, Warsaw.
61. Krawiec S. 2011. *Kompozycje smarów plastycznych i stałych w procesie tarcia stalowych węzłów maszyn*. Oficyna Wydawnicza Politechniki Wrocławskiej, Wrocław.
62. Laber S. 2001. *Preparaty eksploatacyjne*. Wydział Mechaniczny Instytutu Budowy Maszyn i Pojazdów, Uniwersytet Zielonogórski, Zielona Góra.
63. Laber S. 2003. *Badania własności eksploatacyjnych i smarnych uszlachetniacza metalu Motor Life Professional*. Uniwersytet Zielonogórski, Zielona Góra.
64. Latoś H. 1999. Podstawy doboru kierunkowości i struktury powierzchni o określonych właściwościach tarciovych. *Prace Naukowe Instytutu Technologii Maszyn i Automatyzacji Politechniki Wrocławskiej* nr 74, seria Konferencje nr 34, s. 117÷124, Wrocław.
65. Lawrowski Z. 2009. *Tribologia: tarcie, zużywanie i smarowanie*. Oficyna Wydawnicza Politechniki Wrocławskiej, Wrocław.
66. Legutko S., Nosal S. 2004. *Kształtowanie technologicznej i eksploatacyjnej warstwy wierzchniej*. Ośrodek Wydawnictw Naukowych PAN, Poznań.

67. Lenik K., Dzedzic K., Barszcz M., Pashechko M.: „Modernizacja wężła tarcowego maszyny Amslera z przystosowaniem do badań powłok z materiałów eutektycznych w układzie trzpień –tarcza” Tribologia 3/2008.
68. Lepiarczyk D., Tarnowski J., Gawędzki W. (2009r.): „Stanowisko do badania statycznego i kinetycznego współczynnika tarcia skojarzeń ciernych.” Tribologia nr 6-2009, str. 69÷79.
69. Li C. G., Dong S., Zhang G. X. 2000. Evaluation of the anisotropy of machined 3D surface topography. [W:] Wear, Vol. 237, pp. 211÷216.
70. Liszewski Mariusz, Krupicz Bazyli: „Badania odporności erozyjnej wybranych materiałów”. Tribologia 4/2010.
71. Lubimow W., Oczóś K. E. 1997. Wybrane zagadnienia kształtowania nierówności powierzchni w procesach obróbkowych. [W:] Mechanik nr 3, s. 81÷84.
72. Lubimow W., Oczóś K. E., Łabudzki R. 2000. Klasyfikacja struktur geometrycznych powierzchni (SGP) obrobionych ściernie. W: Oczóś K. E. (redakcja) Obróbka ścierna. Podstawy i technika. Oficyna Wydawnicza Politechniki Rzeszowskiej, s. 206÷211, Rzeszów.
73. Magiera Jerzy, Pieczarka Marian: „O pewnej metodzie określania trwałości filmu olejowego podczas współpracy czopa z panewką.” Czasopismo Techniczne Z. 10-M (161) 1972, Państwowe Wydawnictwo Naukowe, Warszawa-Kraków.
74. Male A. T., Cockroft M. G.: A method for the determination of the coefficient of friction of metals under conditions of bulk plastik deformation. I. Inst. Met. 1964÷1965, V. 93.
75. Marczak R. 1993. Postęp w badaniach zjawiska Garkunowa. Materiały konferencji „Problemy bezzużyciowego tarcia w maszynach.” Wydaw. WSI Radom.
76. Marczak R. 1955. Istota, model i możliwości wykorzystania zjawiska Garkunowa w technice. Materiały Konferencyjne NT. Problemy niekonwencjonalnych układów łożyskowych. Łódź.
77. Marczak R. et al.: Sprawozdanie Nr 1553/07/P, IEPiM, Wydział Mechaniczny PR, praca niepublikowana, Radom 1998.
78. Materiały informacyjne PUPH „MIND” Sp. z o.o., Łochowice, 86-005 Białe Błota.
79. Materiały informacyjne Zakładu „PLASTMAL” Sp. z o.o., Warszawa.
80. Matuszewski M., Mikołajczyk J. 2011. Konstrukcja i sterowanie stanowiska do badań tribologicznych. [W:] CAX’2010, Komputerowe Wspomaganie Nauki i Techniki, VII Warsztaty Naukowe, s. 35÷40, Wydawnictwa Uczelniane Uniwersytetu Technologiczno-Przyrodniczego, Bydgoszcz.
81. Mori M., Kumehara H. 1976. Replication of cutting edge roughness on the work surface. [W:] Bull. of Japan Soc. of Precision Engineering, Vol. 10, No. 1, pp. 171÷179.
82. Михеев В. А.: “Влияние вибраций на работу пластичных смазок в узлах с трением скольжения.” INSYCONT III Międzynarodowe Sympozjum, Materiały Konferencyjne, Wydawnictwo AGH, Kraków 25÷27 września 1990, s.717÷724.
83. Mikołajczyk J. 2009. Zestawienie porównawcze dodatków depresujących do olejów. [W:] Zaawansowana tribologia, s. 92÷100. XXX Ogólnopolska Konferencja Tribologiczna. Nałęczów.
84. Mikołajczyk J. 2009. Zestawienie porównawcze własności fizyko-chemicznych dodatków smarnych w oleju podstawowym SAE-30. VI Konferencja Naukowo-Techniczna TEROTECHNOLOGIA, s. 74÷79, Kielce.
85. Mikołajczyk J. 2012. System rejestracji i wizualizacji warunków pracy stanowiska do badań tribologicznych. [W:] CAX’2011, Komputerowe Wspomaganie Nauki i Techniki, VIII Warsztaty Naukowe, s. 13÷18, Wydawnictwa Uczelniane Uniwersytetu Technologiczno-Przyrodniczego, Bydgoszcz.

86. Mikołajczyk J.: System wizualizacji i archiwizacji danych stanowiska do badań tribologicznych; praca dyplomowa na Wydziale Elektrotechniki i Telekomunikacji Uniwersytetu Technologiczno-Przyrodniczego w Bydgoszczy, Bydgoszcz 2011.
87. Mikołajczyk J. 2012. Badanie wpływu preparatu eksploatacyjnego Mind M na zmianę własności smarnych oleju bazowego SN-150. [W:] Inżynieria i Aparatura Chemiczna nr 5, s. 235÷236.
88. Mikołajczyk J., Styp-Rekowski M., Matuszewski M., Musiał J. 2012. Einfluß der Kompositionen von Schmierzusätzen auf die Exploitations-Eigenschaften der Mischung mit Basisöl SN-150. Symposium 2012 Tribologie und Mobilität, s. 97÷104. Wiener Neustadt, Austria.
89. Mikołajczyk J., Styp-Rekowski M. 2012. The Influence of Mind M Preparation on the Lubricant Properties of Oil SN-150. 53. [W:] Tribologie-Fachtagung, Band I, Vortrag 18. Göttingen, Niemcy.
90. Mikołajczyk J.: Maszyny tarciove. Budowa, przeznaczenie. Wydawnictwo PWSZ w Piła Piła 2018.
91. Mikołajczyk J.: The effect of temperature lag on the value of power-temperature correlation for frictional pair of conformal contact. Developments in Mechanical Engineering. No. 15(8) 2020; ISSN: 2300-3383; s. 79÷86.
92. Mikołajczyk J.: Finding the correlation between wear of samples kinematic pair of conformal contact and electric power consumption. Developments in Mechanical Engineering No. 15(8) 2020; ISSN: 2300-3383; s. 59÷68.
93. Mikołajczyk J., Grabowska M., Piochacz A.: Attempt to use computed tomography CAT to analyze the anodized layer. Developments in Mechanical Engineering. No. 15(8) 2020; ISSN: 2300-3383; s. 25÷34.
94. Neyman Antoni (1993r.): „Studia nad frettingiem. Wpływ struktury węzła styku na zużycie.” Zeszyty Naukowe Politechniki Gdańskiej 501, Mechanika Nr LXIX.
95. Nittel J.: Neues Verfahren zur Schmierstoffprüfung in der Umformtechnik durch Reibwertmessung, Fert. Techn. und Betr., 1968, H. 5.
96. Nosal S.: Tribologia. Wprowadzenie do zagadnień tarcia, zużywania i smarowania. Wydawnictwo Politechniki Poznańskiej, Poznań 2012.
97. Nosal S.: Tribologia – Wprowadzenie do zagadnień tarcia, zużywania i smarowania, Wydanie 2 rozszerzone, Wydawnictwo Politechniki Poznańskiej, Poznań 2016.
98. Nosal S., Orłowski T.: Wpływ temperatury na właściwości tribologiczne skojarzenia: modyfikowany materiał cierny – żeliwo szare, Tribologia 2005, nr 3, s. 257÷265.
99. Nowicki B. 1980. Badania mikrostruktury geometrycznej powierzchni obrobionych i metod jej oceny. Prace Naukowe Politechniki Warszawskiej, [W:] Mechanika, z. 70, Warszawa.
100. Nowicki B. 1985. Multiparameter representation of surface roughness. [W:] Wear, Vol. 102, pp. 161÷176.
101. Nowicki B. 1991. Struktura geometryczna: chropowatość i falistość powierzchni. WNT, Warszawa.
102. Nowicki B. 1991. Wpływ struktury geometrycznej powierzchni na własności użytkowe części maszyn. [W:] Mechanik nr 4, s. 148÷149.
103. Nyc R. 2000. Możliwości zastosowania profilometrii skaningowej do interpretacji zużycia elementów maszyn. [W:] Problemy Eksploatacji nr 3, s. 183÷191.
104. Nyc R. 2001. Ocena zużycia współpracujących powierzchni elementów maszyn na podstawie krzywych nośności. [W:] Tribologia nr 3, s.349÷355.
105. Ocoś K. E., Lubimow W. 1998. Analiza w układzie 3D struktury geometrycznej powierzchni szlifowanych. W: Dąbrowski L., Marciniak M., Nowicki B. (redakcja): Badania podstawowe i techniczne obróbki ściernej, s. 116÷122. Warszawa.

106. Oczóś K. E., Lubimow W. 1999. Klasyfikacja struktur geometrycznych powierzchni (SGP). [W:] Prace Naukowe Instytutu Technologii Maszyn i Automatyzacji Politechniki Wrocławskiej nr 74, s. 149÷154. Wrocław.
107. Oczóś K. E., Lubimow W. 1998. Nowe aspekty trójwymiarowej (3D) analizy chropowatości powierzchni obrabianej. [W:] Mechanik nr 8/9, s. 471÷476.
108. Oczóś K. E., Lubimow W. 2003. Struktura geometryczna powierzchni. Oficyna Wydawnicza Politechniki Rzeszowskiej, Rzeszów.
109. Oczóś K. E., Lubimow W. 2008. Rozważania nad istotnością parametrów struktury geometrycznej powierzchni w układzie 3D. [W:] Mechanik nr 3, s. 132÷137.
110. Oczóś K. E., Lubimow W., Łabudzki R. 2001. Analiza porównawcza struktur geometrycznych powierzchni (SGP) po obróbce ściernej. Zbiór prac XXIV Naukowej Szkoły Obróbki Ściernej, s. 249÷260. Łopuszna.
111. Oczóś K. E., Lubimow W., Łabudzki R. 2001. Izotropowość i symetryczność SGP. Materiały VI Konferencji N–T „Kształtowanie materiałów niemetalowych”. Oficyna Wydawnicza Politechniki Rzeszowskiej, s. 293÷302. Rzeszów.
112. Oczóś K.E., Lubimow W. 2008. Rozważania nad istotnością parametrów struktury powierzchni w układzie 3D. [W:] Mechanik 6.
113. Ozimina D. 2000. Metody oceny oddziaływań tribochemicznych dodatków przeciwzatarciowych. [W:] Metrologia i Systemy Pomiarowe nr 1, s. 73÷87.
114. Ozimina D. (red.) 2013. Eksploatacja systemów tribologicznych, t. 2: Tarcie, zużycie, smarowanie wybranych węzłów tribologicznych. Wydawnictwo Politechniki Świętokrzyskiej, seria Monografie, studia, rozprawy, z. M49, Kielce.
115. Panicz A. 2000. Chropowatość powierzchni – co nowego?. [W:] Pomiary Automatyka Kontrola nr 5, s. 39÷47.
116. Pawlus P.: Topografia powierzchni: pomiar, analiza, oddziaływanie. Oficyna Wydawnicza Politechniki Rzeszowskiej, Rzeszów 2006.
117. Pawlus P., Michalski J.: „Metodyka badania grupy tłokowo-cylindrowej silników spalinowych”. Tribologia 3/2008.
118. Patent PL 55 370. Autor: Wit Werys.
119. Patent PL 74 682. Autor: Stanisław Lipiński, Witold Mazurowski, Jerzy Morawski, Zdzisław Przybysz.
120. Patent PL 95 008. Autor: Tadeusz Łubiński, Olgierd Olszewski, Jan Kłopotcki, Jerzy Pasiński
121. Patent PL 96 503. Autor: Józef Turczyński, Aleksander Karge, Maksymilian Zakrzowski, Rudolf Solik, Krzysztof Nowakowski.
122. Patent PL 103 942. Autor: Jan Sikora, Antoni Neyman, Olgierd Olszewski.
123. Patent PL 107 388. Autor: Teresa Oberle, Mieczysław Jarczyński, Leon Malinowski.
124. Patent PL 113 646. Autor: Lucjan Kocjan.
125. Patent PL 115 763. Autor: Franciszek Rudol, Elżbieta Elman, Alicja Maj.
126. Patent PL 117 430. Autor: Olszewski Olgierd, Sikora Jan, Neyman Antoni, Sidorczyk Aleksander.
127. Patent PL 119 178. Autor: Kazimierz Ziemiański.
128. Patent PL 123 756. Autor: Aleksander Derkaczew.
129. Patent PL 125 950. Autor: Jerzy Korycki, Daniel Kujawski, Stanisław Radkowski, Zygmunt Świerczewski, Bogdan Wislicki.
130. Patent PL 129 957. Autor: Adam Rozenau.
131. Patent PL 132 896. Autor: Tadeusz Łubiński, Olgierd Olszewski, Krzysztof Druet, Zbigniew Gadomski.
132. Patent PL 150 471. Autor: Jan Sadowski.
133. Patent PL 154 209. Autor: Edward Kołodziej, Władysław Śliwiński.

134. Patent PL 160 590. Autors: Marek Wiśniewski, Witold Piekoszewski, Marian Szczerek, Ryszard Reizer.
135. Patent PL 160 591. Autors: Witold Piekoszewski, Marian Szczerek, Stanisław Koziół.
136. Patent PL 160 592. Autors: Witold Piekoszewski, Marian Szczerek, Stanisław Koziół.
137. Patent PL 160 594. Autors: Stanisław Koziół, Marian Szczerek, Witold Piekoszewski.
138. Patent PL 160 595. Autors: Witold Piekoszewski, Marek Wiśniewski, Marian Szczerek, Stanisław Koziół.
139. Patent PL 160 596. Autors: Jan Wulczyński, Witold Piekoszewski.
140. Patent PL 160 597. Autors: Marek Wiśniewski, Witold Piekoszewski, Marian Szczerek, Ryszard Reizer.
141. Patent PL 170 088. Autors: Klaudiusz Lenik, Czesław Kajdas, Gabriel Borowski.
142. Patent PL 171 768. Autors: Jan Sadowski, Jan Ciecieląg.
143. Patent PL 176 145. Autors: Stanisław Koziół, Witold Piekoszewski, Marian Szczerek, Marek Wiśniewski.
144. Patent PL 177 192. Autors: Stanisław Koziół, Witold Piekoszewski, Marian Szczerek, Jan Wulczyński.
145. Patent PL 177 200. Autors: Witold Piekoszewski, Marian Szczerek, Stanisław Koziół, Jan Wulczyński.
146. Patent PL 177 201. Autors: Stanisław Koziół, Witold Piekoszewski, Marian Szczerek, Jan Wulczyński.
147. Patent PL 177 203. Autors: Witold Piekoszewski, Marian Szczerek, Stanisław Koziół, Jan Wulczyński.
148. Patent PL 177 205. Autors: Stanisław Koziół, Witold Piekoszewski, Marian Szczerek.
149. Patent PL 187 552. Autor: Edward Lisowski.
150. Patent PL 193 429. Autor: Tadeusz Hejwowski.
151. Patent PL 207 139. Autors: Andrzej Weroński, Andrzej Trzciniński.
152. Patent PL 210 732. Autors: Tadeusz Hejwowski, Andrzej Weroński, Jerzy Kielbiński.
153. Patent PL 211 447. Autors: Andrzej Weroński, Andrzej Trzciniński, Tadeusz Hejwowski.
154. Patent PL 215 116. Autor: Tomasz Klepka.
155. Patent PL 219 650. Autors: Jan Nachimowicz, Robert Korbut.
156. Patent PL 222 239. Autors: Wojciech Horak, Józef Salwiński, Włodzimierz Ochojski, Marcin Szczęch.
157. Patent PL 223 986. Autors: Dariusz Woźniak, Lech Gładysiewicz, Monika Hardygóra, Damian Kaszuba, Waldemar Kisielewski, Ligota Wołczyńska.
158. Patent RU 216 3013 C2. Autors: Buchanczenko S.J., Łarnonow S.A., Puszkarienko A.B. (Tomsk Polytechnic University, Tomsk), Russia.
159. Patent RU 216 5077 C2. Autors: Buchanczenko S.J., Łarnonow S.A., Puszkarienko A.B. (Tomsk Polytechnic University, Tomsk), Russia.
160. Patent SU 121 9962 A. Autors: Prokopienko A. K., Garkunow D. N., Żigajło B. G., Bystrow W. N., Francjew W. N., Znajew W. A., Poljanin B. A. and Panfilow E. A. USSR.
161. Patent SU 167 0520 A1. Autors: Kowalskij B.J., Tichonow W.J., Dieriewiagina Ł. N.
162. Pawłow I. M.: Teoria prokatki. Moskwa, Mietalurgizdat, 1950. USSR.
163. Peters J. 2001. Contribution of CIRP to the development of metrology and surface quality evaluation during the last fifty years. [W:] Annals of the CIRP, 50/2, pp. 471÷488.
164. Piątkowska Anna, Jagielski Jacek: „Opis stanowiska badawczego z rejestracją sygnałów emisji akustycznej” Tribologia 3/2008.
165. Piec P.: Analiza zjawisk kontaktowych typu stick-slip w miejscu styku koła z klockiem hamulcowym. Monografia 187. Politechnika Krakowska, 1995.

166. Piekoszewski W., Szczerek M., Wiśniewski M. 2000. Charakterystyki tribologiczne chropowatości powierzchni elementów maszyn. [W:] Zagadnienia Eksploatacji Maszyn, z. 3, s. 43÷69.
167. Pietrusewicz W. 1985. Parametry powierzchni i ich przydatność do określenia cech użytkowych przedmiotu. Materiały Konferencji N–T „Wpływ technologii na stan warstwy wierzchniej”. Poznań – Gorzów Wlkp.
168. PN – EN ISO 1302: 2004. Specyfikacje geometrii wyrobów (GPS). Oznaczanie struktury geometrycznej powierzchni w dokumentacji technicznej wyrobu.
169. PN – EN ISO 4287: 1999. Struktura geometryczna powierzchni: metoda profilowa. Terminy, definicje i parametry struktury geometrycznej powierzchni.
170. PN – 87/M – 04250: Warstwa wierzchnia. Terminologia.
171. Polański Z.: Metody optymalizacji w technologii maszyn. PWN, Warszawa 1977.
172. Polański Z. 1984. Planowanie doświadczeń w technice. PWN, Warszawa.
173. Posmyk Andrzej: „Kształtowanie właściwości tribologicznych warstwy wierzchniej tworzyw na bazie aluminium”, Zeszyty Naukowe Politechniki Śląskiej, Hutnictwo z. 82, Wydawnictwo Politechniki Śląskiej, Gliwice 2002.
174. Płaza S., Margielewski L., Celichowski G. 2005.: Wstęp do tribologii i tribochemia. Wydawnictwo Uniwersytetu Łódzkiego, Łódź.
175. Pytko Stanisław: „Badania mechanizmu niszczenia powierzchni tocznych elementów maszynowych” w „Elektryfikacja i mechanizacja górnictwa i hutnictwa” z. 25, Zeszyty Naukowe Akademii Górniczo-Hutniczej, Kraków 1967
176. Pytko Stanisław: Podstawy tribologii i techniki smarowania. Skrypty Uczelniane 1164, Wydawnictwo AGH, Kraków 1989
177. Rehbein W., Rigo J., Lange I. 2012. Prüfung des Stick-Slip-Verhaltens von Gleitbahnölen mittels Schwing-Reibverschleiss Tribometer (SRV). [W:] 53. Tribologie-Fachtagung. Vortrag 31, Band I. Göttingen. Niemcy.
178. Rigney D. A., Gleaser W. A. 1978. The significance of near surface microstructure in the wear process. [W:] Wear, Vol. 46, pp. 241÷250.
179. Rudol Franciszek: Uniwersalna maszyna do badania zużycia i współczynnika tarcia typ MZiWT-1, Czasopismo Techniczne, Z. 6-M (157)/1972.
180. Rutkowski Andrzej: „Części maszyn”, Wydawnictwa Szkolne i Pedagogiczne, Warszawa 1986.
181. Rybak Tomasz, Wiśniewski Tomasz, Magda Janusz, Wiśniewska-Weinert Hanna, Leshchynsky Volf: „Stanowisko do badań tribologicznych w wysokich temperaturach elementów łożysk z proszków spiekanych ze zmodyfikowaną warstwą wierzchnią”. Tribologia 4/2010.
182. Sadowski J. 2006. Nowa interpretacja i ocena zużycia tribologicznego. Wydawnictwo Politechniki Radomskiej, Radom.
183. Sadowski J. 1997. Termodynamiczne aspekty procesów tribologicznych. Wydawnictwo Politechniki Radomskiej, Radom.
184. Sadowski J. 2003. The thermodynamic theory of friction and wear . Wydawnictwo Politechniki Radomskiej, Radom.
185. Sikora Jan, Rigall Alojzy: „Badania łożysk z materiałów drewnopochodnych”. Zagadnienia tarcia, zużycia, smarowania. z. 8, 1970 r.; s. 77÷96.
186. Sikora Jan: „Wpływ asymetrii cyklu obciążenia i rodzaju oleju na wytrzymałość zmęczeniową stopu łożyskowego”, Tribologia 1/2007.
187. Stachowiak G. W., Batchelor A. W. 2001. Engineering tribology. Butterworth-Heinemann.
188. Starczewski L. 2002. Wodorowe zużywanie ciernych elementów maszyn. Wydawnictwo Instytutu Technologii Eksploatacji, Radom.

189. Stout K. J., Davis E. J., Sullivan P. J. 1990. Atlas of machined surfaces. Chapman and Hall, London.
190. Stout K. J., Dong W. P., Mainsah E. 1993. A proposal for standardisation of assessment of three-dimensional micro-topography – Part I. Surface digitisation and parametric characterisation. University of Birmingham.
191. Stout K. J., Sullivan P. J., Dong W. P., Mainsah E., Luo N., Mathia T., Zahouani H. 1993. The development of methods for the characterisation of roughness in three-dimensions. Commission of the European Communities.
192. Styp-Rekowski M. 1990. Geometrical constructional features of special rolling bearings against their exploitational properties. Proceedings of IVth Symposium INTERTRIBO '90, Vol. C, pp. 93÷96.
193. Styp-Rekowski M. 2001. Znaczenie cech konstrukcyjnych dla trwałości skośnych łożysk kulkowych. Wydawnictwo Naukowe ATR, seria Rozprawy, nr 103, Bydgoszcz.
194. Styp-Rekowski M., Mikołajczyk J. 2009. Smarowanie w eksploatacji maszyn. Seminarium pt. Twórczość Inżynierska dla Współczesnej Europy, s. 53÷58. Bydgoszcz-Białe Błota.
195. Styp-Rekowski M., Świerk K., Mikołajczyk J. 2010. Modyfikowanie cech środka smarującego za pomocą dodatków i komputerowe wspomaganie ich doboru. [W:] CAX'2009, Komputerowe Wspomaganie Nauki i Techniki, VI Warsztaty Naukowe, s. 15÷19, Wydawnictwa Uczelniane Uniwersytetu Technologiczno-Przyrodniczego, Bydgoszcz.
196. Styp-Rekowski M., Mikołajczyk J. 2012. Wpływ dodatku na własności smarowe oleju bazowego SN-150. [W:] Tribologia nr 4, s. 227÷232.
197. Styp-Rekowski M., Mikołajczyk J. 2012. Zmiana temperatury na drodze tarcia dla kompozycji olej bazowy SN-150-preparat eksploatacyjny Mind M. III Krajowa Konferencja Nano- i Mikromechaniki Instytutu Podstawowych Problemów Techniki Polskiej Akademii Nauk, s. 145÷146. Warszawa.
198. Szczerek M. 1997. Metodologiczne problemy systematyzacji eksperymentalnych badań tribologicznych. Wydawnictwo Instytutu Technologii Eksploatacji, Radom.
199. Szczerek M., Wiśniewski M. (redakcja) 2000. Tribologia i tribotechnika. Wydawnictwo Instytutu Technologii Eksploatacji, Radom.
200. Szulc L. 1965. Struktura i własności fizyko-mechaniczne obrobionych powierzchni metali. Zeszyt specjalny Politechniki Warszawskiej. Warszawa.
201. Szumniak J. 2001. Warstwa wierzchnia elementów trących. Budowa, własności i ich identyfikacja, wpływ na tarcie. Poradnik tribologii i tribotechniki (4–5), s. 11÷18.
202. Terry A.J., Broun C.A. 1997. A comparison of topographic characterisation parameters in grinding. [W:] Annals of the CIRP, 46/1, pp. 497÷500.
203. Tripp J. H., Ioannides E. 1990. Effects of surface roughness on rolling bearing life. Proceedings of the Japan International Conference. Japanese Society of Tribologists Nagoya, Vol. 2, pp. 797÷804.
204. Tsukada T., Kanad T. 1986. Evaluation of two- and three-dimensional surface roughness. [W:] Wear, Vol. 109, pp. 1÷4.
205. Tychowski F., Wiśniewski Z.: Badanie sił przy wyłaczaniu naczyń o podstawie kołowej, Obróbka plastyczna, Zeszyt 3, 1960.
206. Uetz H.: Tribologie – Verschleisskunde. Vorlesungsmanucript, Universitaet Stuttgart, 1980.
207. Vorburger T.V. at all. 1997. Characterisation of surface topography. [W:] Annals of the CIRP, 46/2, pp. 597÷615.
208. Walicka A. 2002. Reodynamika przepływu płynów nienewtonowskich w kanałach prostych i zakrzywionych. Wydawnictwo Uniwersytetu Zielonogórskiego, Zielona Góra.

209. Walicki E., Walicka A. 1998. Reologia wybranych płynów smarujących. Materiały Zebrania SPE KBM PAN, s. 137÷144, Zielona Góra.
210. Waterhouse R. B., Iwabuchi A. (1985r.): „The composition and properties of surface films formed during the temperature fretting of titanium alloys.” Proc. J. S. L. E., Int. Tribol. Conf., Tokyo, July 8÷10, Vol. 1.
211. Warburton J. (1989r.): „The fretting of mild steel in air.” Wear, Vol. 131.
212. Whitehouse D.J. 1978. Surfaces – a link between manufacture and function. Proc. Inst. Mech. Engrs., 192, pp. 179÷188.
213. Wieczorowski M., Cellary A., Chajda J. 1996. Charakterystyka chropowatości powierzchni. Politechnika Poznańska, Poznań.
214. Wieczorowski M., Cellary A., Chajda J. 2003. Przewodnik po pomiarach nierówności powierzchni czyli o chropowatości i nie tylko. Politechnika Poznańska, Poznań.
215. Williams J. 2005. Engineering tribology. Cambridge University Press, Cambridge.
216. Willis E. 1986. Surface finish in relation to cylinder liners. [W:] Wear, Vol. 109, pp. 351÷366.
217. Wiśniewski M. 2001. Parametry chropowatości powierzchni. Poradnik tribologii i tribotechniki (2), s. 5÷6.
218. Witaszek Kazimierz, Witaszek Mirosław: Ocena zmian właściwości tribologicznych złącz konektorowych przy wielokrotnym łączeniu i rozłączaniu, XXX Ogólnopolska Konferencja Tribologiczna – Zaawansowana Tribologia, Nałęczów 2009, p. 149÷156.
219. Wolf H. 1969. Analyse des Istprofils hinsichtlich der Verteilung der Riefen und Rillenamplituden zum Erkennen der einzelnen Bestandteile des Istprofils am Profilschnitt. VDI-Bericht Nr 133, s. 325÷331. Düsseldorf. Germany.
220. Wusatowski Z.: Podstawy walcowania. Katowice, Wydawnictwo Górniczo-Hutnicze, 1960.
221. Zariczny Piotr, Sikora Jan: „Experimental Investigation of Journal Bering Individual Feed System”, Tribologia 1/2007, s. 287÷298.
222. Zhu M. H., Zhou Z. R., Kapsa Ph., Vincent L.: „An experimental investigation on composite fretting mode.” Tribology Int. 34, 2001.